© 2015. Published by The Company of Biologists Ltd | Biology Open (2015) 4, 1024-1039 doi:10.1242/bio.012815

RESEARCH ARTICLE

Cooperation of the BTB-Zinc finger protein, Abrupt, with cytoskeletal regulators in *Drosophila* epithelial tumorigenesis

Nezaket Turkel[1,*,§], Marta Portela[1,#,§], Carole Poon[1,‡], Jason Li[2], Anthony M. Brumby[1] and Helena E. Richardson[1,3,4,#,¶]

ABSTRACT

The deregulation of cell polarity or cytoskeletal regulators is a common occurrence in human epithelial cancers. Moreover, there is accumulating evidence in human epithelial cancer that BTB-ZF genes, such as *Bcl6* and *ZBTB7A*, are oncogenic. From our previous studies in the vinegar fly, *Drosophila melanogaster*, we have identified a cooperative interaction between a mutation in the apico-basal cell polarity regulator Scribble (Scrib) and overexpression of the BTB-ZF protein Abrupt (Ab). Herein, we show that co-expression of *ab* with actin cytoskeletal regulators, *RhoGEF2* or *Src64B,* in the developing eye-antennal epithelial tissue results in the formation of overgrown amorphous tumours, whereas *ab* and *DRac1* co-expression leads to non-cell autonomous overgrowth. Together with *ab*, these genes affect the expression of differentiation genes, resulting in tumours locked in a progenitor cell fate. Finally, we show that the expression of two mammalian genes related to *ab*, *Bcl6* and *ZBTB7A*, which are oncogenes in mammalian epithelial cancers, significantly correlate with the upregulation of cytoskeletal genes or downregulation of apico-basal cell polarity neoplastic tumour suppressor genes in colorectal, lung and other human epithelial cancers. Altogether, this analysis has revealed that upregulation of cytoskeletal regulators cooperate with Abrupt in *Drosophila* epithelial tumorigenesis, and that high expression of human BTB-ZF genes, *Bcl6* and *ZBTB7A,* shows significant correlations with cytoskeletal and cell polarity gene expression in specific epithelial tumour types. This highlights the need for further investigation of the cooperation between these genes in mammalian systems.

KEY WORDS: *Drosophila*, Eye-antennal disc, Apico-basal cell polarity, Actin cytoskeletal regulators, BTB-ZF, Abrupt, RhoGEF2, Rac1, Src, Scribble

[1]Cell Cycle and Development Laboratory, Peter MacCallum Cancer Centre, Melbourne, Victoria 3002, Australia. [2]Bioinformatics Core Facility, Peter MacCallum Cancer Centre, Melbourne, Victoria 3002, Australia. [3]Sir Peter MacCallum Department of Oncology, Department of Anatomy and Neuroscience, Department of Biochemistry and Molecular Biology, University of Melbourne, Melbourne, Victoria 3010, Australia. [4]School of Molecular Sciences, La Trobe University, Melbourne, Victoria 3086, Australia.
*Present address: Department of Genetics and Bioengineering, Faculty of Engineering and Architecture, Yeditepe University, 26 Ağustos Campus, Kayisdagi Cad., Kayisdagi, Istanbul 34755, Turkey. ‡Present address: Cell growth and Proliferation Laboratory, Peter MacCallum Cancer Centre, Melbourne, Victoria 3002, Australia. #Present address: Department of Biochemistry and Genetics, La Trobe Institute of Molecular Sciences, La Trobe University, Melbourne, Victoria 3086, Australia
§These authors contributed equally to this work

¶Author for correspondence (h.richardson@latrobe.edu.au)

This is an Open Access article distributed under the terms of the Creative Commons Attribution License (http://creativecommons.org/licenses/by/3.0), which permits unrestricted use, distribution and reproduction in any medium provided that the original work is properly attributed.

Received 26 May 2015; Accepted 5 June 2015

INTRODUCTION

Cancer is a cooperative process involving many mutations that lead to the deregulation of the normal controls that regulate cell proliferation, survival, differentiation and migration, amongst other processes (Hanahan and Weinberg, 2011). Understanding the molecular events that occur during cooperative tumorigenesis is critical in order to develop therapeutics to combat cancer. The model organism, *Drosophila melanogaster* (vinegar fly), has proven to be an excellent model for the discovery of new tumorigenic genes and the dissection of their roles in tumour progression, and has proven relevance to human cancer (Brumby and Richardson, 2005; Cheng et al., 2013; Gonzalez, 2013; Rudrapatna et al., 2012; Stefanatos and Vidal, 2011).

Recently, the disruption of apical-basal cell polarity, which affects cell adhesion and signalling pathways and leads to an epithelial to mesenchymal transition (EMT), has been realized as a new hallmark of cancer (Elsum et al., 2012; Hanahan and Weinberg, 2011; Humbert et al., 2008). Central to cell polarity regulation are the Scribble module (Scribble (Scrib), Dlg and Lgl), the Crumbs module (Crumbs, Pals and Patj) and the Par module (Par6, Par3 and aPKC), which undergo positive or negative interactions in the establishment and maintenance of the apical and basolateral domains of an epithelial cell. Whole organism or tissue-specific depletion of genes in the Scribble module lead to a loss of cell polarity and aberrant signalling, leading to the formation of neoplastic tumour in *Drosophila* epithelial tissues (Elsum et al., 2012; Humbert et al., 2008). However, when *scrib, dlg* or *lgl* are mutated in patches of cells within the developing eye-antennal tissue, despite deregulation of signalling pathways and cell proliferation, tissue overgrowth does not ensue due to cell differentiation and Jun N-terminal Kinase (JNK)-mediated apoptosis (Brumby and Richardson, 2003; Doggett et al., 2011; Grzeschik et al., 2007, 2010; Igaki et al., 2006; Uhlirova and Bohmann, 2006; Uhlirova et al., 2005). In investigating cooperation between polarity loss and oncogenic pathways in epithelial tumorigenesis, we discovered that activation of the small GTPase, Ras ($Ras85D^{V12}$, referred to as Ras^{ACT} herein) or activated Notch ($Notch^{ICD}$, referred to as $Notch^{ACT}$ herein) cooperated with *scrib* loss-of-function to form massive invasive tumours (Brumby and Richardson, 2003). Subsequent analysis showed that cooperation depended upon activation of the JNK and downregulation of the Hippo negative tissue growth control pathways, thereby promoting tumour growth, inhibiting differentiation and promoting an invasive phenotype (Doggett et al., 2011; Igaki et al., 2006; Leong et al., 2009; Uhlirova and Bohmann, 2006; Uhlirova et al., 2005). This mechanism is conserved in mammalian cells and mouse models, where depletion or knockout of *scrib* leads to hyperplasia, and additional expression of the Ras oncogene ($Ha\text{-}Ras^{V12}$) cooperates with *scrib* loss-of-function to promote tumorigenesis (Dow et al., 2008; Elsum et al., 2013; Godde et al., 2014; Pearson et al., 2011). Moreover, similar to that observed in *Drosophila*, the expression of JNK is able to cooperate with

Downloaded from http://bio.biologists.org/ at La Trobe University on December 16, 2020

Biology Open (2015) 4, 1024-1039 doi:10.1242/bio.012815

Ha-Ras^{V12} to promote invasive growth in 3D matrigel cultures (Brumby et al., 2011).

To further investigate cooperative tumorigenesis, we carried out a screen for genes that when over-expressed in eye-antennal disc clones act similarly to *Ras^{ACT}* or *Notch^{ACT}* in cooperation with *scrib* loss-of-function (Turkel et al., 2013). In this screen, we identified *abrupt* (*ab*), which in cooperation with *scrib* loss-of-function promotes the retention of a progenitor-like cell state by blocking expression of differentiation genes, as well as promoting tumour growth and invasion. Abrupt encodes a Broad-Complex, Tramtrack, Bric-a-brac domain (BTB)-zinc-finger (ZF) transcription factor with roles in neuromuscular junction and dendrite morphogenesis, ovarian border cell migration and imaginal disc epithelial development (Grieder et al., 2007; Hattori et al., 2013; Hu et al., 1995; Jang et al., 2009). BTB-ZF transcription factors are a large family of proteins, with 47 human members, many of which have been shown to be associated with cancer (Costoya, 2007; Kelly and Daniel, 2006). The most well known of the BTB-ZF mammalian family members are Bcl6 and ZBTB7 (LRF/Pokemon), which function as proto-oncogenes in lymphomas, leukaemias and solid cancers (Hatzi and Melnick, 2014; Maeda et al., 2005). In solid cancers, Bcl6 is upregulated in breast, colorectal and squamous head and neck epithelial cancers, and contributes to their growth and progression (Sena et al., 2014; Walker et al., 2014; Worsham et al., 2012; Wu et al., 2014). ZBTB7A is upregulated in colorectal, bladder, breast, prostate, non-small cell lung cancer and liver cancers and reducing its expression blocks tumour development (Aggarwal et al., 2010, 2011; Guo et al., 2014; Jeon et al., 2008; Liu et al., 2012; Qu et al., 2010; Zhang et al., 2013; Zhao et al., 2013, 2008).

In a *Drosophila* genetic screen for Ras-cooperating genes (using *ey>Ras^{ACT}*, where expression of *Ras^{ACT}* is driven via the *eyeless* promoter throughout the developing eye), we identified the actin cytoskeletal regulatory genes, *RhoGEF2* and *DRac1* (Brumby et al., 2011). These genes enhanced the *ey>Ras^{ACT}* hyperplastic adult eye phenotype and also resulted in morphological and differentiation defects (Brumby et al., 2011). Furthermore, *RhoGEF2* and *DRac1* showed neoplastic growth in cooperation with *Ras^{ACT}* in a clonal context in the eye-antennal disc (Brumby et al., 2011). DRac1 (*Drosophila* Rac1) is a member of Rho/Rac/Cdc42 small-GTPase superfamily, key regulators of the actin cytoskeleton (Jaffe and Hall, 2005; Szczepanowska, 2009), and is involved in morphological cell shape changes during *Drosophila* development (Harden et al., 1995; Settleman, 1999; Van Aelst and D'Souza-Schorey, 1997). Indeed, constitutive activation of *Rac1* during tube morphogenesis of the *Drosophila* salivary gland causes changes in epithelial cell morphology, resembling an epithelial to mesenchymal transition (EMT) by mislocalization or loss of expression of the apical polarity regulators, Crumbs and aPKC, and the adherens junction proteins E-cadherin and β-catenin (Pirraglia et al., 2006; Pirraglia and Myat, 2010). It is therefore likely that these downstream effects of Rac1 also contribute to its cooperative effects with *Ras^{ACT}* in tumorigenesis in the eye-antennal disc (Brumby et al., 2011).

RhoGEF2 is a guanine nucleotide exchange factor (GEF) (Schmidt and Hall, 2002) that acts via activating the small GTPase, Rho1, in morphological cell shape changes during *Drosophila* development (Barrett et al., 1997; Häcker and Perrimon, 1998; Mulinari et al., 2008; Nikolaidou and Barrett, 2004; Padash Barmchi et al., 2005; Rogers et al., 2004). Consistent with RhoGEF2 functioning via Rho1, we also found that an activated allele of Rho1 (*Rho1^{V14}*) was also a *Ras^{ACT}* cooperating oncogene in epithelial tumorigenesis (Brumby et al., 2011). RhoGEF2 cooperates with *Ras^{ACT}* in tumorigenesis by activating the Rho1-Rok-MyoII-JNK pathway (Khoo et al., 2013). Interestingly, MyoII activity (pMRLC) is increased in *scrib^{-} Ras^{ACT}* eye-antennal disc clones and contributes to *scrib Ras^{ACT}* tumorigenesis (Kulshammer and Uhlirova, 2013), as does JNK activation (Igaki et al., 2006; Leong et al., 2009; Uhlirova and Bohmann, 2006).

Furthermore, in this genetic screen, we identified another cytoskeletal regulator, *Src42A,* a *Drosophila* homolog of the Src tyrosine kinase (Thomas and Brugge, 1997), but were unable to confirm its cooperative interaction with *Ras^{ACT}* with an independent transgene (Brumby et al., 2011). However, we found that overexpression of the second *Drosophila* Src family member, *Src64B,* using a transgenic line (Dodson et al., 1998), showed strong cooperation with *Ras^{ACT}* when expressed globally in the developing eye or in eye-antennal disc MARCM clones (C.P., A.B., H.R., unpublished data). *Src64B* also functions in regulation of the actin cytoskeleton and cell shape changes during development in *Drosophila* (Dodson et al., 1998; Guarnieri et al., 1998; Kelso et al., 2002; O'Reilly et al., 2006; Roulier et al., 1998; Strong and Thomas, 2011; Takahashi et al., 1996). Depending on the context, upregulation of *Src64B* or *Src42A* activity (via overexpression of the Src genes or Csk downregulation) can lead to either increased proliferation, or apoptosis and invasion (Pedraza et al., 2004; Read et al., 2004; Vidal et al., 2006, 2007). Recent studies have also shown that overexpression of *Src42A* or *Src64B* in *Drosophila* adult intestinal progenitor cells results in progenitor cell over-proliferation (Cordero et al., 2014; Kohlmaier et al., 2014). Furthermore, in the developing wing epithelium blocking apoptosis in tissues expressing *Src64B* results in overgrowth (Fernández et al., 2014), and in the eye-antennal epithelium *Src64B* or *Src42A* upregulation (or downregulation of the Src negative regulator, Csk) cooperates with *Ras^{ACT}* to result in neoplastic tumour formation (Enomoto and Igaki, 2013; Vidal et al., 2010, 2007).

Since *RhoGEF2, DRac1* or *Src* are cooperating oncogenes with *Ras^{ACT}*, and *ab* overexpression phenocopies *Ras^{ACT}* or *Notch^{ACT}* in cooperative tumorigenesis with *scrib* loss-of-function (Turkel et al., 2013), we sought to determine whether *ab* could also cooperate with *RhoGEF2, DRac1* or *Src64B* in tumorigenesis. Herein, we describe the effect of co-expression of *ab* with *RhoGEF2, DRac1* or *Src64B* in the developing eye-antennal epithelium. We show that co-expression of *ab* with *RhoGEF2* or *Src64B* results in neoplastic tumour formation, whereas *ab* and *DRac1* co-expression leads to non-cell autonomous overgrowth. We show that together with *ab* these genes affect the expression of differentiation genes. Finally, we investigate whether the expression of two mammalian genes related to *ab*, *Bcl-6* and *ZBTB7A*, which are oncogenic in mammalian cancer, are correlated with the upregulation of cytoskeletal genes or downregulation of apico-basal cell polarity neoplastic tumour suppressor genes in human epithelial cancers.

RESULTS

Cooperation of *abrupt* with *RhoGEF2*

To determine if *ab* cooperates with Ras-cooperative oncogene, *RhoGEF2,* to drive tumorigenesis, we generated clones expressing *ab* and *RhoGEF2* using the MARCM system (Lee and Luo, 1999), and compared tumour development to *scrib^{-} ab*-expressing clones in the *Drosophila* developing eye-antennal epithelium (Fig. 1). Our previous studies have shown that the overexpression of *ab* in otherwise wild-type eye disc clones promoted antennal disc overgrowth, but did not block photoreceptor differentiation. Mutation of *scrib* alone in clones results in cell morphology changes and disorganisation, but does not dramatically affect

Downloaded from http://bio.biologists.org/ at La Trobe University on December 16, 2020

Biology Open (2015) 4, 1024-1039 doi:10.1242/bio.012815

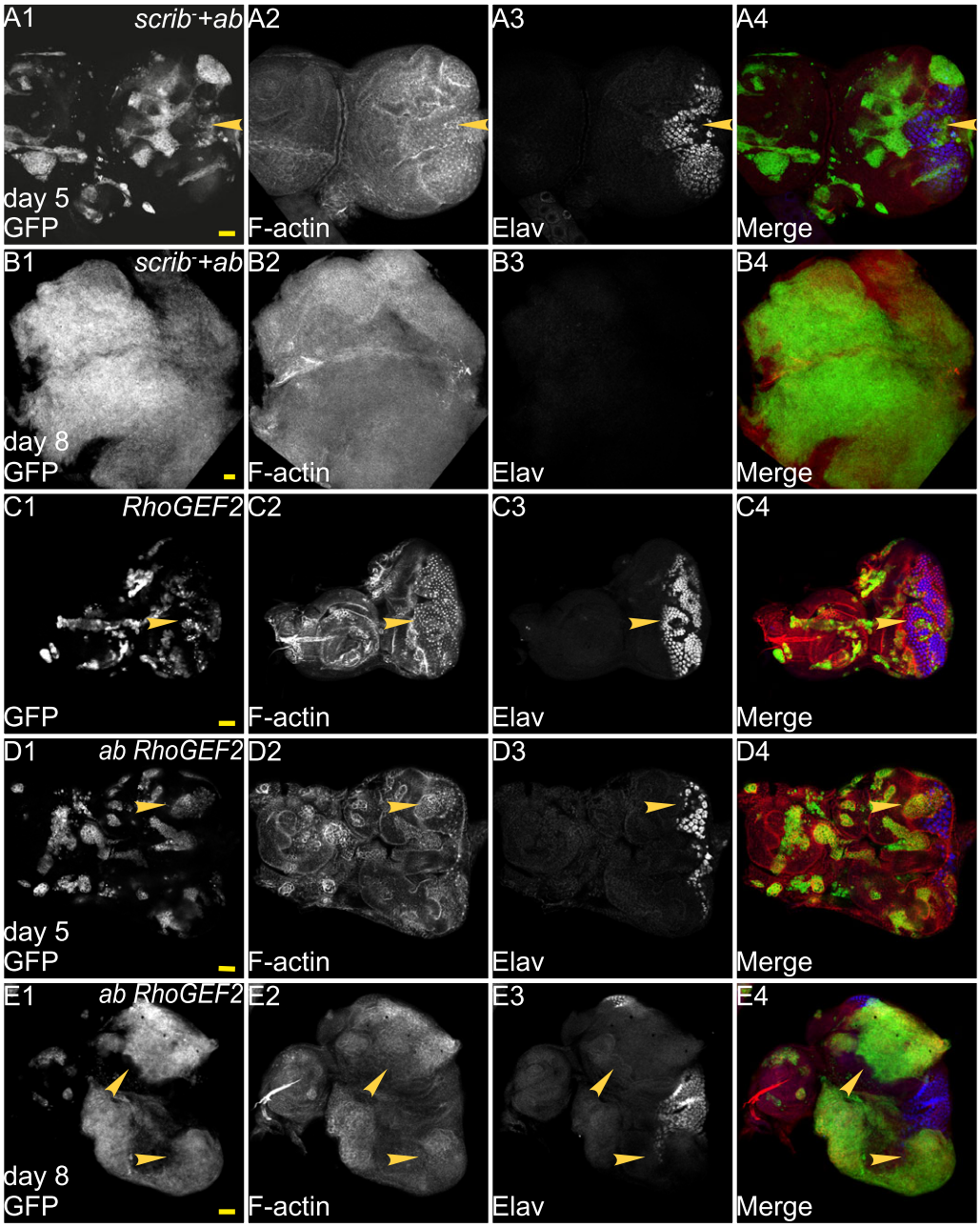


Fig. 1. *RhoGEF2* cooperates with *ab* to form large tumours. Confocal planar images of mosaic larval eye-antennal discs stained for F-actin (with Phalloidin, grey or red in merge) and Elav (grey or blue in merge); mutant clones are GFP^{+} and wild-type tissue is GFP^{-} (grey or green in merge). Eye-antennal discs are orientated with posterior to the left in this and all other figures. (A) *ab scrib*^{1} mosaic eye-antennal disc at day 5 AED. (B) *ab scrib*^{1} mosaic eye-antennal disc at day 8 AED. (C) *RhoGEF2* mosaic eye-antennal disc at day 5 AED. (D) *ab RhoGEF2* mosaic eye-antennal disc at day 5 AED. (E) *ab RhoGEF2* mosaic eye-antennal disc at day 8 AED. Arrowheads point to patches of mutant tissue showing differentiation defects. Genotypes: (A,B) *ey-FLP, UAS-GFP;; UAS-ab*^{55}*, FRT82B, scrib*^{1}*/tubGAL4; FRT82B, tubGAL80*. (C) *ey-FLP, UAS-GFP; UAS-RhoGEF2*; *FRT82B/tubGAL4; FRT82B, tubGAL80*. (D,E) *ey-FLP, UAS-GFP; UAS-RhoGEF2*; *UAS-ab*^{55}*, FRT82B/tubGAL4; FRT82B, tubGAL80*. Scale bars=50 µM.

differentiation as revealed by Elav staining or lead to tissue overgrowth and larvae enter pupariation normally at day 5/6 after egg deposition (AED) (Brumby and Richardson, 2003; Turkel et al., 2013). However, *scrib*$^{-}$ *ab*-expressing clones (marked by GFP) overgrow at the expense of the surrounding normal tissue (GFP negative) over an extended larval period and form massive tumours (Fig. 1A,B), which fuse with the surrounding tissue and invade into the brain (Turkel et al., 2013), similar to that observed for *scrib*$^{-}$ *Ras*^{ACT} tumours (Brumby and Richardson, 2003). *scrib*$^{-}$ *ab*-expressing clones showed cell morphology defects, as revealed by F-actin staining (Fig. 1A2,B2), and an inhibition of photoreceptor cell differentiation in the eye epithelium, as revealed by Elav staining (arrowheads, Fig. 1A1-A4).

RhoGEF2 expression in mosaic disc produced small clones with increased F-actin levels, and cell morphology and differentiation defects (arrowheads, Fig. 1C1,C3,C4) (Brumby et al., 2011; Khoo et al., 2013). At day 5/6 AED *ab RhoGEF2* co-expressing clones were smaller than the surrounding wild-type clones (Fig. 1D1,D4) and accumulated F-actin (Fig. 1D2). *ab RhoGEF2* mosaic discs also showed non-cell autonomous effects, as the surrounding wild-type

Downloaded from http://bio.biologists.org/ at La Trobe University on December 16, 2020

Biology Open (2015) 4, 1024-1039 doi:10.1242/bio.012815

tissue exhibited folding and distortion around the clonal tissue at day 5 (Fig. 1D2). At day 8/9 AED, *ab RhoGEF2* eye disc clones were overgrown relative to wild-type tissue (Fig. 1E), although folded wild-type tissue was present around clonal tissue. However, antennal disc clones did not overgrow and remained a similar size as day 5 clones. Differentiation as marked by Elav was reduced in eye disc clones throughout larval development (arrowheads, Fig. 1D1-D4,E1-E4). The effect of *ab RhoGEF2* cooperation led to a failure in pupation and the formation of giant larvae (not shown), similar to *RhoGEF2 Ras*^{ACT} cooperation (Khoo et al., 2013). However, in comparison to *scrib*$^{-}$ *ab* tumours, which exhibit fusion of the two eye-antennal discs that is associated with an invasive phenotype (Turkel et al., 2013), *ab RhoGEF2* did not show strong invasive properties, since the two eye-antennal discs did not fuse together (data not shown). Indeed, the cooperative tumorigenic effect of *ab RhoGEF2* was most similar to *Ras*^{ACT} *RhoGEF2* cooperation, with the exception of the effect on the antennal disc (Brumby et al., 2011; Khoo et al., 2013). Taken together, these data show that *RhoGEF2* is capable of cooperating with *ab* to produce overgrown, undifferentiated and amorphous tumours.

Cooperation of *abrupt* with *Src64B*

Since *Src64B* can cooperate with *Ras*^{ACT} (see introduction), we wished to determine if *ab* also cooperates with *Src64B*. When expressed alone, *Src64B* resulted in large clones in the antennal and the anterior portion of the eye disc, which showed high levels of F-actin accumulation (Fig. 2A2). Clones in the posterior differentiated region of the eye disc proper were very small and did not noticeably affect differentiation, although larger clones were observed in the overlying peripodial layer leading to the displacement of the underlying differentiated tissue (Fig. 2A1,A3,A4). *Src64B*-expressing mosaic larvae pupated normally, but were delayed in development and eclosed 1–2 days after their control counterparts (not shown). Co-expression of *Src64B* and *ab* resulted in large clones in the antenna and the eye discs, including the posterior region of the eye disc at day 5/6 AED (Fig. 2B1), however these were not significantly overgrown relative to the wild-type tissue. However at day 8/9 AED, *Src64B ab* eye disc clones were clearly overgrown relative to wild-type tissue. *Src64B ab* co-expressing clones had rounded-edges with high levels of F-actin at day 5/6 and day 8 AED (Fig. 2B2,C2). Differentiation, as revealed by Elav staining, was abolished in clones in the posterior region of the eye disc (arrowheads, Fig. 2B1-B4,C1-C4). The overall size of Day 8/9 *Src64B ab* mosaic eye-antennal discs were overgrown relative to wild-type mosaic eye-antennal discs, however there was slightly more wild-type tissue remaining at day 8/9 AED compared to *scrib*$^{-}$ *ab* mosaic discs (compare Fig. 2C with Fig. 1B). *Src64B ab* cooperation led to the formation of giant larvae and a failure of pupation (not shown), however they did not result in the fusion of the two eye-antennal discs (not shown), as occurs with *scrib*$^{-}$ *ab* tumours. Altogether, these data indicates that *ab* cooperates with *Src64B* to promote overgrown, undifferentiated and amorphous tumours.

Cooperation of *abrupt* with *DRac1*

Since *DRac1* and *Ras*^{ACT} cooperate to form invasive tumours in the eye-antennal epithelium (Brumby et al., 2011), we sought to investigate if *ab* and *DRac1* also cooperate in tumorigenesis.

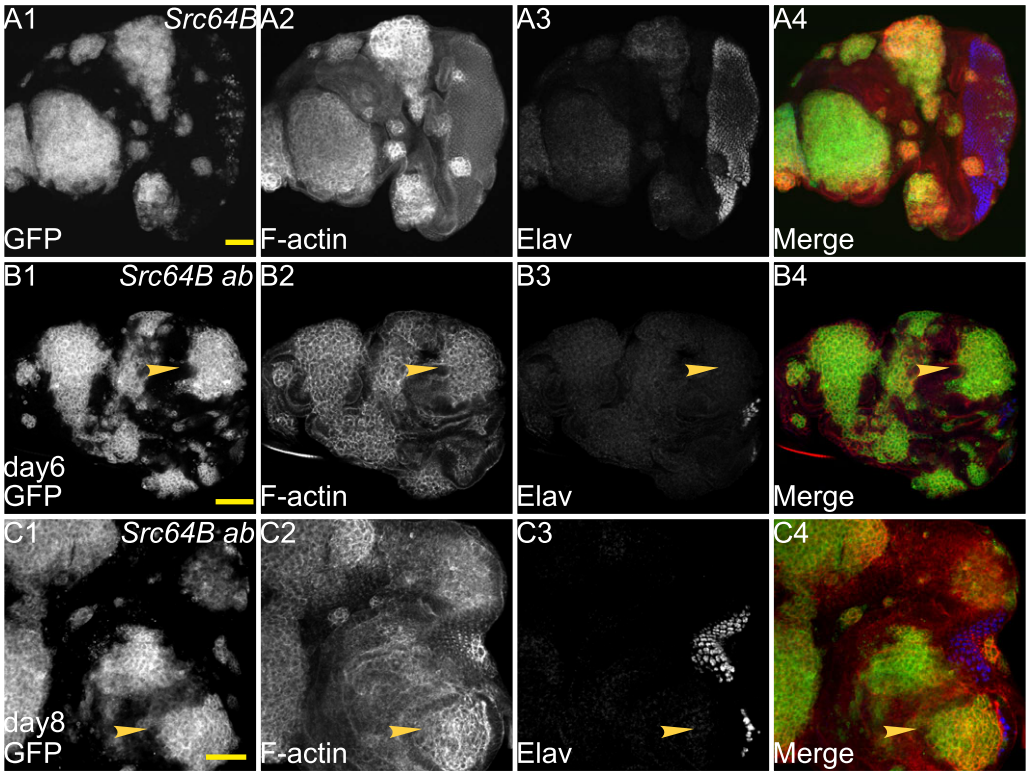


Fig. 2. *Src64B* cooperates with *ab* to form large tumours. Confocal planar images of mosaic larval eye-antennal discs stained for F-actin (with Phalloidin, grey or red in merge) and Elav (grey or blue in merge); mutant clones are GFP^{+} and wild-type tissue is GFP^{-} (grey or green in merge). (A) *Src64B* mosaic eye-antennal disc at day 5 AED. (B) *ab Src64B* mosaic eye-antennal disc at day 5 AED. (C) *ab Src64B* mosaic eye-antennal disc at day 8 AED. Arrowheads point to patches of mutant tissue showing differentiation defects. Genotypes: (A) *ey-FLP, UAS-GFP; UAS-Src64B; FRT82B/tubGAL4; FRT82B, tubGAL80*. (B,C) *ey-FLP, UAS-GFP; UAS-Src64B*; *UAS-ab*^{55}*, FRT82B/tubGAL4; FRT82B, tubGAL80*. Scale bars=50 µM.

Downloaded from http://bio.biologists.org/ at La Trobe University on December 16, 2020

Biology Open

Biology Open (2015) 4, 1024-1039 doi:10.1242/bio.012815

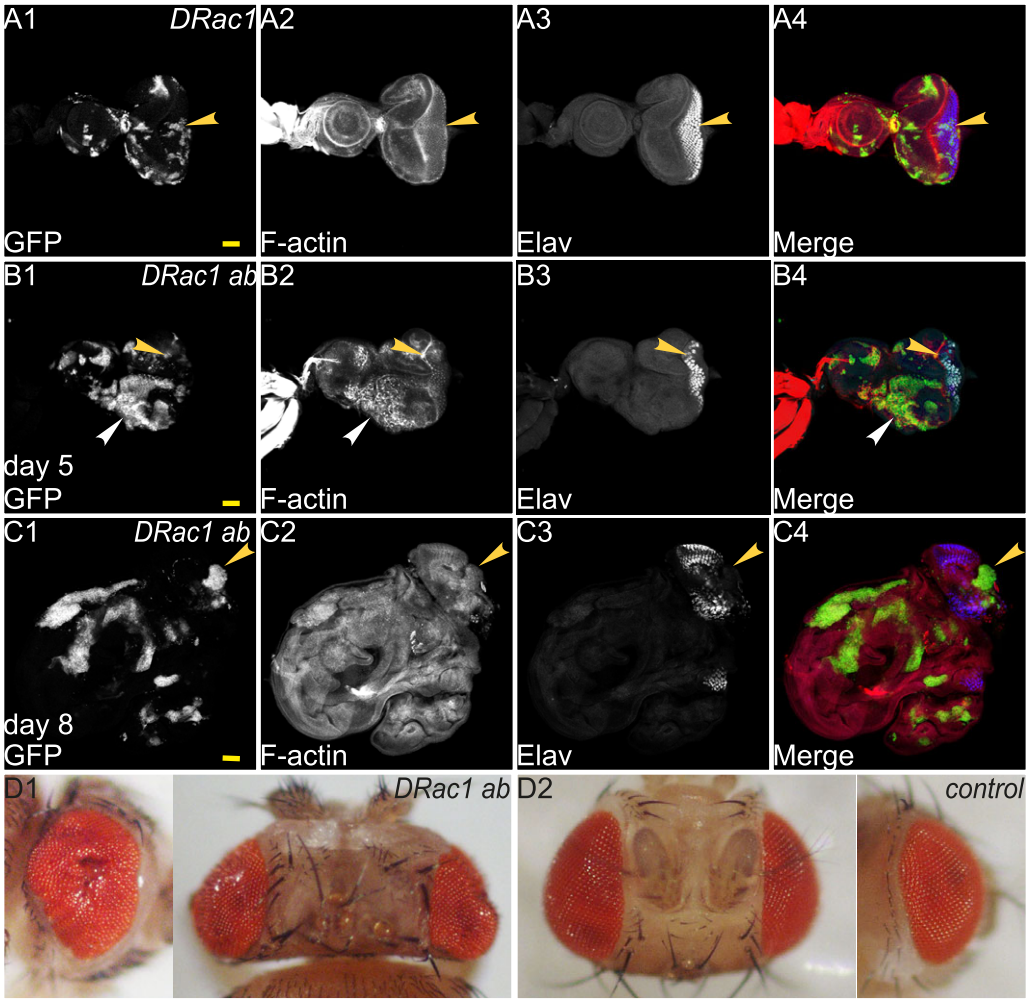


Fig. 3. Co-expression of *DRac1* with *ab* results in non-cell autonomous overgrowth. Confocal planar images of mosaic larval eye-antennal discs stained for F-actin (with Phalloidin, grey or red in merge) and Elav (grey or blue in merge); mutant clones are GFP^+ and wild-type tissue is GFP^- (grey or green in merge). (A) *DRac1* mosaic eye-antennal disc at day 5 AED. (B) *ab DRac1* mosaic eye-antennal disc at day 5 AED. (C) *ab DRac1* mosaic eye-antennal disc at day 8 AED. (D1) *ab DRac1* escaper adult fly heads, side and dorsal views. (D2) wild-type (control) adult fly heads, side and dorsal views. Yellow arrowheads point to patches of mutant tissue showing differentiation defects. Note that in panel C differentiation was observed in the wild-type tissue in the posterior region of the eye disc, but the highly folded nature of the wild-type tissue makes this difficult to image in a single Z section. White arrowheads point to an example of elevated F-actin. Genotypes: (A) *ey-FLP, UAS-GFP; UAS-DRac1; FRT82B/tubGAL4; FRT82B, tubGAL80*. (B,C,D1) *ey-FLP, UAS-GFP; UAS-DRac1*; *UAS-ab*^{55}, *FRT82B/tubGAL4; FRT82B, tubGAL80*. (D2) *ey-GAL4.* Scale bars=50 µM.

In mosaic eye-antennal discs at day 5 AED, *DRac1* over-expression produced small clones with cell morphology defects (although F-actin levels were only slightly increased, Fig. 3A2) and disrupted Elav expression (yellow arrowheads, Fig. 3A1-A4). Over-expression of *ab* with *DRac1* resulted in large clones mostly in the anterior region of the eye disc (Fig. 3B), although overall there was less mutant clonal tissue in the eye-antennal disc compared with the wild-type mosaic eye-antennal disc. At later times (day 8/9 AED), *DRac1 ab* co-expression resulted in strong non-cell autonomous effects, as indicated by the highly folded wild-type tissue surrounding the clonal tissue and greater representation of GFP^- tissue (Fig. 3C). *DRac1 ab* co-expression resulted in rounded clones with elevated F-actin levels at day 5 AED (white arrowheads, Fig. 3B1,B2,B4) although at day 8/9 AED F-actin appeared elevated throughout the tissue (Fig. 3C2). In the posterior region of the eye disc, *DRac1 ab* expressing clones showed reduced Elav expression (yellow arrowheads, Fig. 3B1-B4,C1-C4). *DRac1 ab* larvae were delayed in development and pupated 1–2 days after the wild-type controls (data not shown). Most died at the pupal stage, however the occasional adult emerged (~1/50 of expected numbers) with overgrown distorted eyes (Fig. 3D1) compared with the wild-type controls (Fig. 3D2). In summary, although *ab* cooperated with *DRac1*, this overgrowth was non-cell autonomous and the cooperation was not sufficient to form neoplastic tumours as observed with *DRac1 Ras*^{ACT} (Brumby et al., 2011).

Comparison of cooperative interactions relative to *scrib*$^-$ *ab* tumours

The comparative overgrowth at day 5/6 AED and day 8/9 AED for expression of the actin cytoskeletal genes with *ab* relative to *scrib*$^-$ *ab* is summarized in Fig. 4. To determine the relative overgrowth of the mutant tissue to wild-type tissue we quantified the volume of GFP^+ tissue to total eye-antennal disc volume for all genotypes at day 5/6 and day 8/9 (Fig. 4A,B). At day 5/6 AED the GFP^+ tumour volume relative to the total disc volume for *RhoGEF2 ab*, *Src64B ab* and *DRac1 ab* was similar to the *FRT* control, but *scrib*$^-$ *ab* clonal tissue was slightly reduced relative to wild-type tissue (Fig. 4A). However, at day 8/9 AED, *scrib*$^-$ *ab* GFP^+ tumours represented the

Downloaded from http://bio.biologists.org/ at La Trobe University on December 16, 2020

Biology Open (2015) 4, 1024-1039 doi:10.1242/bio.012815

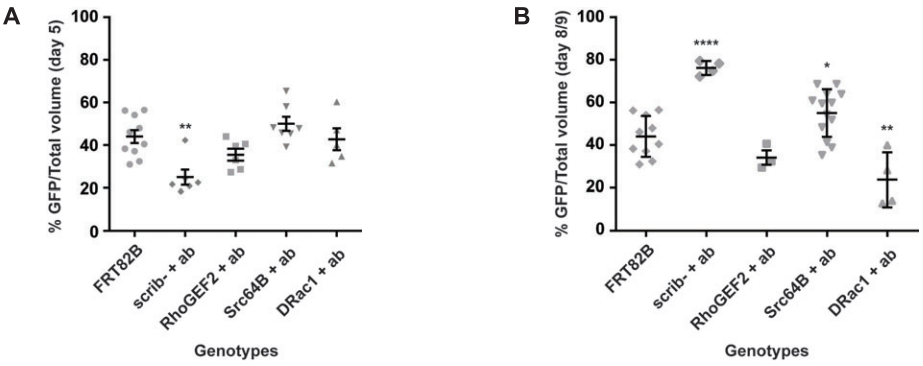


Fig. 4. Quantification of clonal overgrowth and summary of tumorigenic properties of *ab* with *scrib*$^{-}$, *RhoGEF2, Src64B* or *DRac1*.
(A) Quantification of Day 5/6 larval eye-antennal disc GFP^{+} clonal volume relative to total disc volume normalized to the Day 5 FRP control. (B) Quantification of Day 8/9 larval eye-antennal disc GFP^{+} clonal volume relative to total disc volume, normalized to the Day 5 FRT control. The volume of GFP^{+} clonal tissue relative to total disc volume was measured from confocal sections covering the whole eye-antennal disc of at least 3 samples per genotype. The data is presented as a percentage of GFP^{+} tissue versus total tissue volume. The data was compared using unpaired *t*-test (two-tailed with 99% confidence level); error bars represent standard error of the mean (s.e.m.). **P*<0.05, ***P*<0.007, and *****P*<0.0001. (C) Summary of the tumorigenic phenotypes in comparison with Ras^{V12}-driven tumours.

C

	Tumour Size					
	Antennal-disc	Eye-disc	Giant Larvae	Over-grown wild type tissue	Differentiation in clonal tissue	Similariy to Ras^{ACT} induced tumours
scrib^{-} *ab*	++++	++++	✓	–	–	✓
scrib^{-} *Ras*^{ACT}	++++	++++	✓	–	–	
ab RhoGEF2	+	+	✓	++	–	✓
RhoGEF2 Ras^{ACT}	+++	+++	✓	+	–	
Src64B ab	+++	+++	✓	+	–	✓
Src64B Ras^{ACT}	++++	++++	✓	–	–	
DRac1 ab	–	–	☒	++++	–	☒
DRac1 Ras^{ACT}	++++	++++	✓	–	–	

majority of the overgrown discs (Fig. 4B). *Src64B ab* GFP^{+} tumours were also more greatly represented relative to the wild-type tissue, however although the whole tissue was overgrown *RhoGEF2 ab* GFP^{+} tumours did not overgrow relative to the wild-type tissue (Fig. 4B). By contrast, *DRac1 ab* clones were underrepresented in the overgrown discs, suggesting that non-cell autonomous overgrowth had occurred (Fig. 4B). All cooperative interactions affected differentiation of photoreceptor development as judged by ELAV staining (Fig. 4C). Relative to *scrib*$^{-}$ *ab* cooperative tumorigenesis, co-expression of the cytoskeletal genes with *ab* resulted in less potent cooperative overgrowth at day 8/9 AED (Fig. 4A-C), which was correlated with non-cell autonomous tissue growth effects. Except for *DRac1 ab*, all cytoskeletal genes showed similar properties in cooperation with *ab* as with *Ras*^{V12} (Fig. 4C).

Cooperation of *abrupt* with *RhoGEF2, Src64B* or *DRac1* affects tissue growth via effects on cell proliferation and cell death

In order to assess how *ab* was cooperating with *RhoGEF2, Src64B* or *DRac1* relative to *scrib*$^{-}$ to affect tissue growth, we performed EdU labelling to reveal proliferating cells and TUNEL labelling to detect dying cells in mosaic eye-antennal discs from all genotypes at day 5/6 and day 8/9 (Figs 5 and 6). The EdU labelling experiment revealed that relative to the FRT control where cell proliferation ceases in the posterior region of the eye disc (Fig. 5A), *scrib*$^{-}$ *ab*, *RhoGEF2 ab,* and *Src64B ab* GFP^{+} clones showed increased numbers of EdU^{+} cells in the posterior region as well as throughout the eye-antennal discs at day 5 and day 8 AED (Fig. 5B,C,F-J), however *DRac1 ab* GFP^{+} clones showed a reduction in EdU incorporation relative to the surrounding wild-type tissue (Fig. 5D,E,J). The analysis of cell death, revealed that there were more dying cells in the wild-type tissue (GFP^{-}) in *scrib*$^{-}$ *ab*, *RhoGEF2 ab,* and *Src64B ab* mosaic discs at day 5 and day 8 AED (Fig. 6B,C,F-J) versus the FRT control that showed only low levels of TUNEL^{+} cells (Fig. 6A). Conversely, *DRac1 ab* GFP^{+} clones showed more dying cells relative to the wild-type tissue at day 8 AED (Fig. 6E,J), although similarly low numbers of TUNEL^{+} cells were present in the mutant tissue (GFP^{+}) versus wild-type tissue (GFP^{-}) at day 5 AED (Fig. 6D,J). Altogether, these results show that increased cell proliferation of the mutant tissue and increased cell death of the wild-type tissue occurs in *scrib*$^{-}$ *ab*, *RhoGEF2 ab,* and *Src64B ab* mosaic discs, whilst the opposite occurs in *DRac1 ab* mosaic discs. The EdU and TUNEL patterns are generally consistent with the tissue overgrowth data at day 8 (Fig. 4B), with the exception of *RhoGEF2 ab*, where the tumour did not overgrow relative to the wild-type tissue. Since EdU measures S phase cells, it is possible there might be delays in G2/M phase in the mutant tissue in this genotype to account for this effect. At day 5, the tumour volume was similar to wild-type for all samples, except for *scrib*$^{-}$ *ab* where mutant tissue was less represented (Fig. 4A), therefore the EdU and TUNEL data at day 5 does not reflect tumour volume at this stage, but predicts what occurs later in tumour development (i.e. day 8).

Cooperation of *abrupt* with *RhoGEF2, Src64B* or *DRac1* affects expression of critical eye and antennal differentiation genes

We have previously shown, by ChIP sequencing of Ab targets and expression array analysis, that Ab regulates the expression of eye-antennal cell fate genes and that this effect is enhanced or altered in *ab scrib*$^{-}$ tumours (Turkel et al., 2013). Since co-expression of *ab* with *RhoGEF2, Src64B* or *DRac1* also affects expression of the eye differentiation factor, Elav, we sought to determine whether other cell fate genes in eye and antennal development

Downloaded from http://bio.biologists.org/ at La Trobe University on December 16, 2020

Biology Open (2015) 4, 1024-1039 doi:10.1242/bio.012815

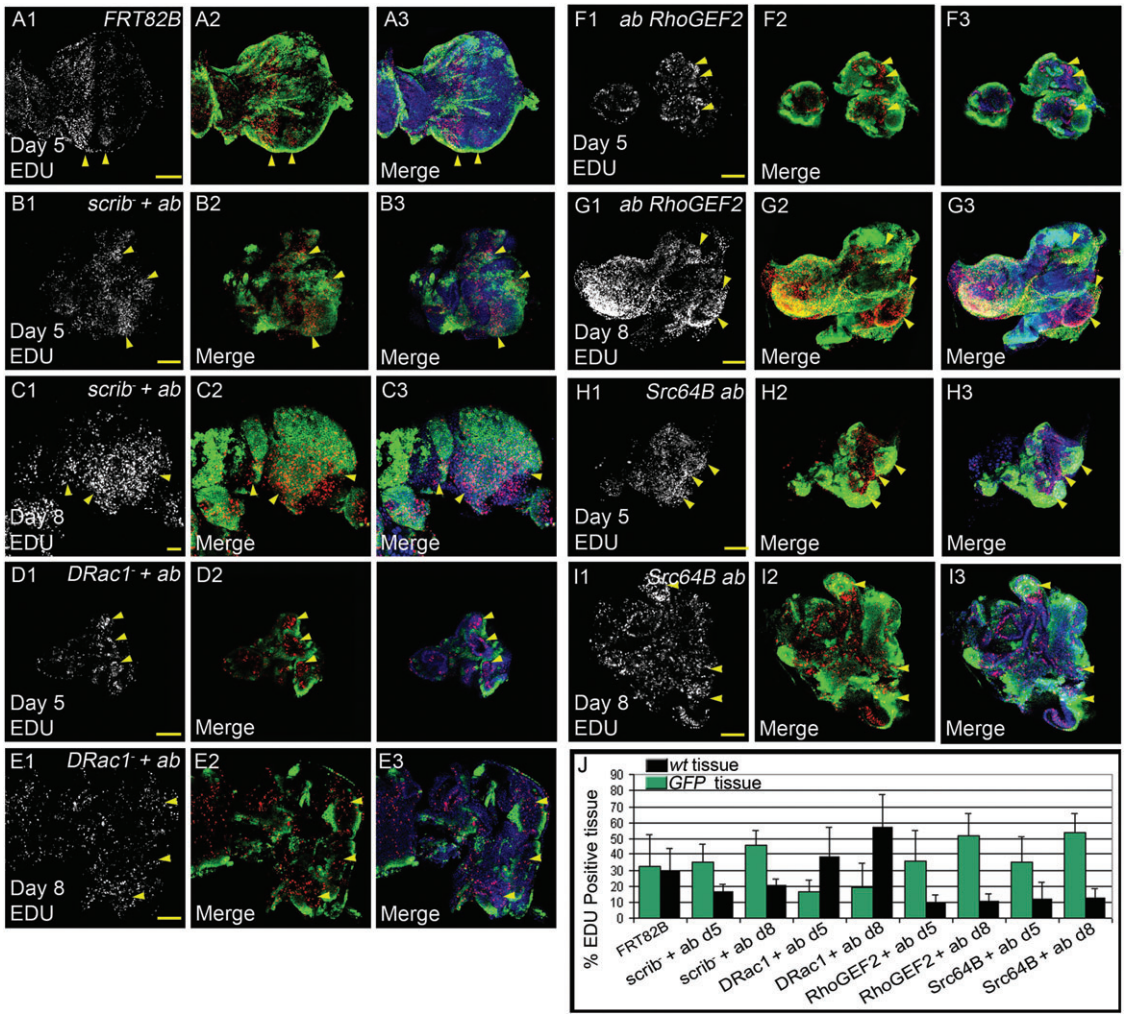


Fig. 5. Comparison of cell proliferation levels in *ab* with *scrib*^{1}, *DRac1, RhoGEF2* or *Src64B*. Confocal planar images of mosaic larval eye-antennal discs labelled with EdU for S-phases (grey or red in merge) and DAPI (blue in merge); mutant clones are GFP^{+} and wild-type tissue is GFP^{-} (green in merge). Arrowheads point to patches of tissue showing alterations in cell proliferation. (A) wild-type control clones. (B) *ab scrib*^{1} mosaic eye-antennal disc at day 5. (C) *ab scrib*^{1} mosaic eye-antennal disc at day 8. (D) *DRac1 ab* mosaic eye-antennal disc at day 5. (E) *DRac1 ab* mosaic eye-antennal disc at day 8. (F) *RhoGEF2 ab* mosaic eye-antennal disc at day 5. (G) *RhoGEF2 ab* mosaic eye-antennal disc at day 8. (H) *Src64B ab* mosaic eye-antennal disc at day 5. (I) *Src64B ab* mosaic eye-antennal disc at day 8. (J) Quantification showing the percentage of EdU positive tissue in wild-type versus mutant clones of the listed genotypes. Error bars represent s.e.m. Genotypes: (A) *ey-FLP, UAS-GFP; FRT82B/tubGAL4; FRT82B, tubGAL80*. (B-C) *ey-FLP, UAS-GFP;; UAS-ab*^{55}*, FRT82B, scrib*^{1}*/tubGAL4; FRT82B, tubGAL80*. (D-E) *ey-FLP, UAS-GFP; UAS-DRac1*; *UAS-ab*^{55}*, FRT82B/tubGAL4; FRT82B, tubGAL80*. (F-G) *ey-FLP, UAS-GFP; UAS-RhoGEF2*; *UAS-ab*^{55}*, FRT82B/tubGAL4; FRT82B, tubGAL80*. (H-I) *ey-FLP, UAS-GFP; UAS-Src64B*; *UAS-ab*^{55}*, FRT82B/tubGAL4; FRT82B, tubGAL80*. Scale bars=50 µM.

were also affected in these tumours. In eye development, Dachshund (Dac) is one of the earliest transcriptional regulators that drives cell fate determination in the developing eye (Chen et al., 1997; Shen and Mardon, 1997), and expression of Dac is blocked in *ab scrib*$^{-}$ tumours (Turkel et al., 2013). We therefore wished to determine if this was also the case in *ab* cytoskeletal gene cooperative tumours.

In wild-type eye-antennal discs, Dac is expressed in a broad band in the middle of the eye disc and also in a crescent in the antennal disc (Fig. 7A). *scrib*^{1} *ab* clones do not express Dac in the eye disc (arrowheads, Fig. 7B1-B4) or in the antennal disc. Dac expression is only slightly reduced in *scrib*^{1} clones and unaffected in *ab* overexpressing clones in the eye disc (Turkel et al., 2013). In *RhoGEF2 ab* clones in the eye disc, Dac expression was blocked (arrowheads, Fig. 7C1-C4). Similarly, Dac expression was blocked in *Src64B ab* clones (arrowheads, Fig. 7D1-D4) and in *DRac1 ab* clones (arrowheads, Fig. 5E1-E4). Dac expression was also blocked in the antennal disc in *ab RhoGEF2, ab Src64B* or *ab DRac1* co-expressing clones (Fig. 7C-E; data not shown). Thus, similarly to *ab scrib*$^{-}$ tumours, *ab* cytoskeletal gene tumours appear to be blocked in differentiation prior to Dac expression.

In antennal disc differentiation, initial expression domains of the transcription factors Homothorax (Hth), Cut (Ct) and Distal-less (Dll) during 2nd instar larval development establish the early proximo-distal axis of the antenna (Dominguez and Casares, 2005). We have previously shown that *scrib*$^{-}$ *ab* clones retain the expression of Dll within the growing tumour, but downstream regulated genes, such as Dac, are not retained (Turkel et al., 2013). We therefore tested if Dll was still expressed in *ab* cytoskeletal gene tumours.

In wild-type antennal discs, Dll is expressed in more distally destined cells in the antennae (Fig. 8A), and *scrib*$^{-}$ *ab* clones retain this expression (arrowheads, Fig. 8B1-B4). Co-expression of *RhoGEF2* with *ab* did not block Dll expression, and instead an enlarged Dll-expression domain was observed (arrowheads,

Downloaded from http://bio.biologists.org/ at La Trobe University on December 16, 2020

Biology Open

Biology Open (2015) 4, 1024-1039 doi:10.1242/bio.012815

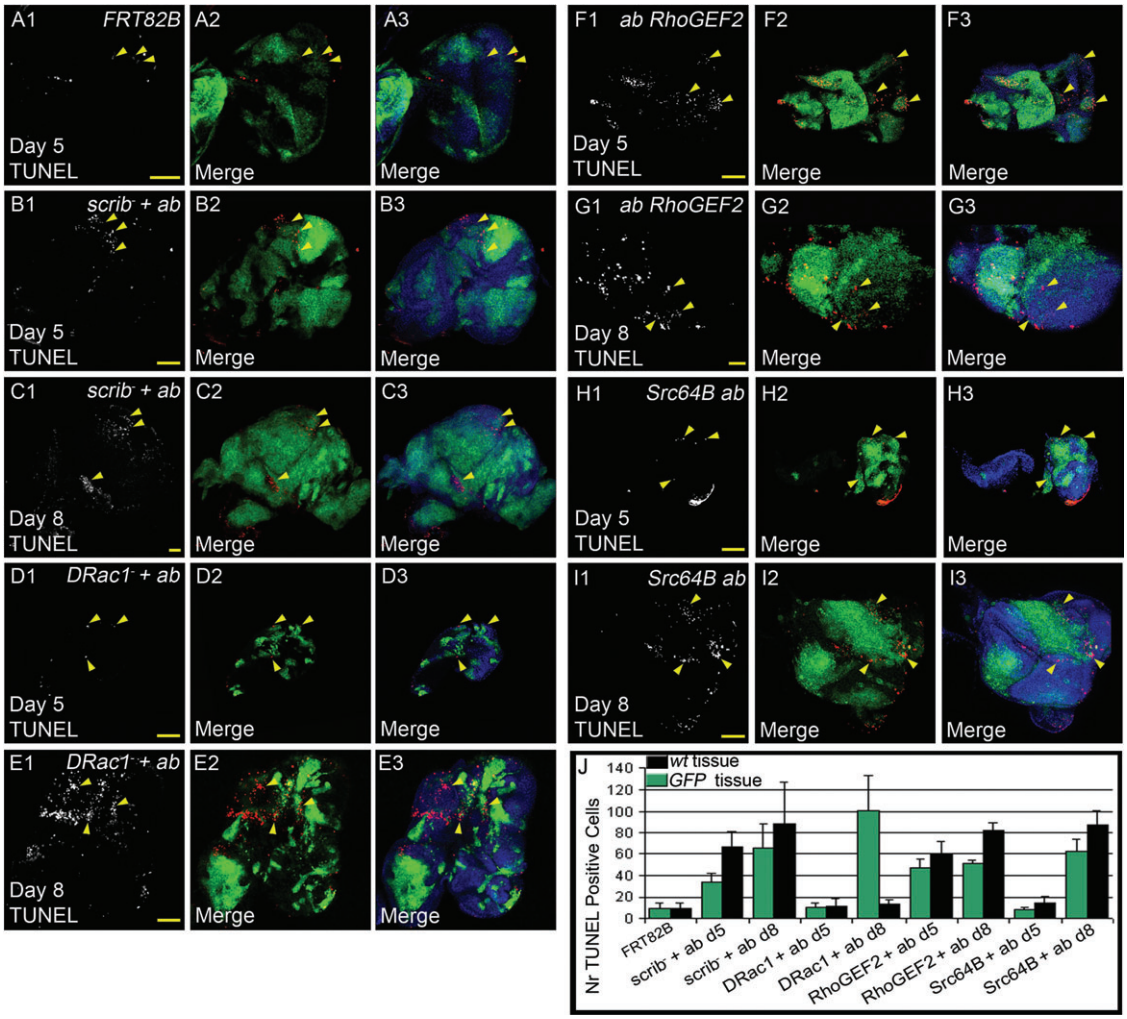


Fig. 6. Comparison of cell death levels in *ab* with *scrib*^{1}, *DRac1*, *RhoGEF2* or *Src64B*. Confocal planar images of mosaic larval eye-antennal discs labelled with TUNEL as an apoptotic marker (grey or red in merge) and DAPI (blue in merge); mutant clones are GFP^{+} and wild-type tissue is GFP^{-} (green in merge). Arrowheads point to patches of tissue showing alterations in cell death. (A) wild-type control clones. (B) *ab scrib*^{1} mosaic eye-antennal disc at day 5. (C) *ab scrib*^{1} mosaic eye-antennal disc at day 8. (D) *DRac1 ab* mosaic eye-antennal disc at day 5. (E) *DRac1 ab* mosaic eye-antennal disc at day 8. (F) *RhoGEF2 ab* mosaic eye-antennal disc at day 5. (G) *RhoGEF2 ab* mosaic eye-antennal disc at day 8. (H) *Src64B ab* mosaic eye-antennal disc at day 5. (I) *Src64B ab* mosaic eye-antennal disc at day 8. (J) Quantification showing the number of TUNEL positive cells in wild-type versus mutant clones of the listed genotypes. Error bars represent s.e.m. Genotypes: (A) *ey-FLP, UAS-GFP; FRT82B/tubGAL4; FRT82B, tubGAL80*. (B-C) *ey-FLP, UAS-GFP;; UAS-ab*^{55}*, FRT82B, scrib*^{1}*/tubGAL4; FRT82B, tubGAL80*. (D-E) *ey-FLP, UAS-GFP; UAS-DRac1*; *UAS-ab*^{55}*, FRT82B/tubGAL4; FRT82B, tubGAL80*. (F-G) *ey-FLP, UAS-GFP; UAS-RhoGEF2*; *UAS-ab*^{55}*, FRT82B/tubGAL4; FRT82B, tubGAL80*. (H-I) *ey-FLP, UAS-GFP; UAS-Src64B*; *UAS-ab*^{55}*, FRT82B/tubGAL4; FRT82B, tubGAL80*. Scale bars=50 µM.

Fig. 8C1-C4), probably due to a partial duplication of the antennae, which is sometimes observed in *ab*-expressing clones (Turkel et al., 2013). Surprisingly, *Src64B ab* clones showed reduced expression of Dll (arrowheads, Fig. 8D1-D4) and distortion of the antennal structures due to cell morphology changes (Fig. 8D2). In *DRac1 ab* clones, normal expression of Dll was also observed (arrowheads, Fig. 8E1-E4). Altogether, these results show that *RhoGEF2 ab* and *DRac1 ab* are similar to *scrib*$^{-}$ *ab* in cell fate status, however *Src64B ab* tumours are blocked at an earlier progenitor cell state than *scrib*$^{-}$ *ab* tumours (summarized in Fig. 9).

Correlation in expression of oncogenic BTB-Zinc finger genes, *Bcl6* and *ZBTB7A*, with apico-basal cell polarity and cytoskeletal genes in human epithelial cancer

Since we have shown here that *ab* cooperates with the cytoskeletal regulators, *RhoGEF2* and *Src64B,* to result in cooperative tumorigenesis, we wished to determine whether the expression of human homologs of these genes showed cooperation with BTB-Zn finger genes in human cancers. Since our previous studies had also shown that the cell polarity tumour suppressor, *scrib*, showed cooperative tumorigenesis with *ab* (Turkel et al., 2013), we also sought to determine whether human homologs of the Scribble module were downregulated in human tumours, showing high expression of BTB-Zn finger genes. Furthermore, since we have shown that the JNK signalling pathway was important in the invasive properties of these tumours and sufficient to cooperate with *Ras*^{ACT} in *Drosophila* and mammalian invasive tumour growth (Brumby et al., 2011), we wished to examine the correlation of expression of the human JNKK and JNK homologs with BTB-Zn finger genes in human cancer. Of the human BTB-Zn finger genes, there is greatest evidence for *Bcl6* and *ZBTB7A* as oncogenes in human epithelial cancer (see Introduction), so we focused our analysis on these genes. Using Oncomine, we analysed collections of human epithelial cancers for expression correlation with *Bcl6* or *ZBTB7A* and human *RhoGEF2*

Downloaded from http://bio.biologists.org/ at La Trobe University on December 16, 2020

Biology Open (2015) 4, 1024-1039 doi:10.1242/bio.012815

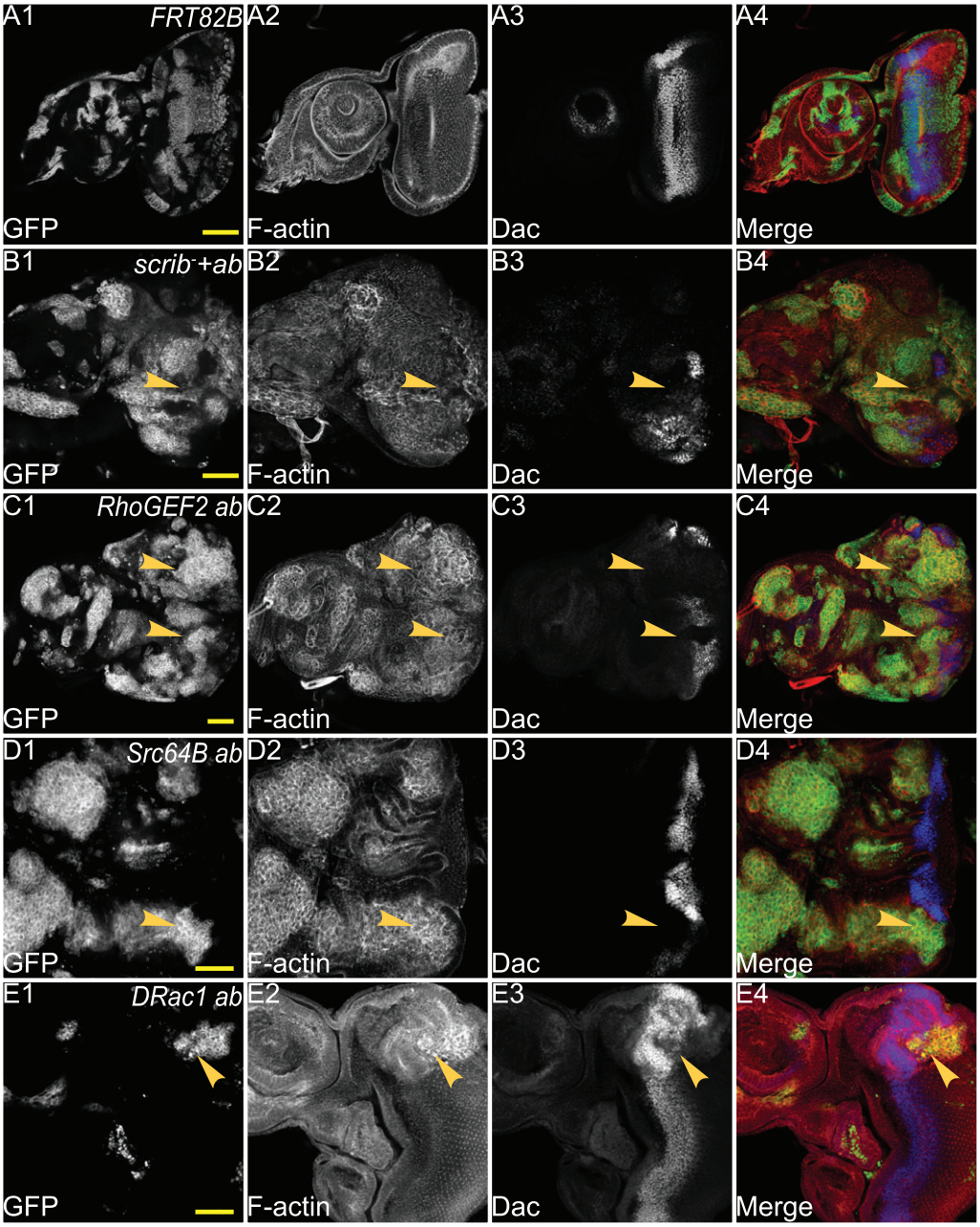


Fig. 7. Co-expression of *ab* with *scrib*$^{-}$, *RhoGEF2, Src64B* or *DRac1* prevents the expression of the eye cell fate gene, Dac. Confocal planar images of mosaic larval eye-antennal discs stained for F-actin (with Phalloidin, grey or red in merge) and Dac (grey or blue in merge); mutant clones are GFP^{+} and wild-type tissue is GFP^{-} (grey or green in merge). (A) wild-type control clones. (B) *ab scrib*^{1} mosaic eye-antennal disc at day 5 AED. (C) *RhoGEF2 ab* mosaic eye-antennal disc at day 5 AED. (D) *Src64B ab* mosaic eye-antennal disc at day 5 AED. (E) *DRac1 ab* mosaic eye-antennal disc at day 5 AED. Arrowheads point to patches of mutant tissue showing lack of Dac expression. Genotypes: (A) *ey-FLP, UAS-GFP; FRT82B/tubGAL4; FRT82B, tubGAL80.* (B) *ey-FLP, UAS-GFP;; UAS-ab*^{55}*, FRT82B, scrib*^{1}*/tubGAL4; FRT82B, tubGAL80.* (C) *ey-FLP, UAS-GFP; UAS-RhoGEF2*; *UAS-ab*^{55}*, FRT82B/ tubGAL4; FRT82B, tubGAL80.* (D) *ey-FLP, UAS-GFP; UAS-Src64B*; *UAS-ab*^{55}*, FRT82B/tubGAL4; FRT82B, tubGAL80.* (E) *ey-FLP, UAS-GFP; UAS-DRac1*; *UAS-ab*^{55}*, FRT82B/tubGAL4; FRT82B, tubGAL80.* Scale bars=50 µM.

homologs (*ARHGEF1, ARHGEF11, ARHGEF12*), *Src* homologs (*Src, Yes, Fyn*), Scribble module genes (*hscrib, llgl1, llgl2, dlg1, dlg2, dlg3, dlg4*), JNKK homologs (*MAP2K4, MAP2K7*) and JNK homologs (*MAPK8, MAPK9, MAPK10*). In this analysis, the cancer samples were compared with normal tissues where available. The correlation of expression of each of these polarity and cytoskeletal genes in each dataset revealed that there were significant correlations (P<0.05) for several cytoskeletal or polarity regulatory genes with *Bcl6* or *ZBTB7A* in several cancer types (Table 1; supplementary material Table S1 and supplementary data). Most interestingly, in the Gaspar Colon colorectal adenoma dataset (Gaspar et al., 2008) *Bcl6* expression was significantly positively correlated with *MAPK9, MAP2K4* and *Yes1*, and negatively with *Dlg2*, relative to normal intestinal mucosa (Fig. 10A, Table 1). The heatmap of individual samples, revealed a trend of high *Bcl6*, low *Dlg2* and high *MAPK9* in many colorectal carcinoma samples relative to the normal intestinal mucosa (Fig. 10A). Furthermore, in the Rohrbeck Lung (all-Lung, cancer only) dataset (Rohrbeck et al., 2008) *Bcl6* expression was positively correlated with *MAP2K4, Yes1* and negatively correlated with *Dlg2* and *Lgl1* (Fig. 10B, Table 1). Stratification of the Rohrbeck Lung cancers dataset into different stages showed that there were several samples of lung adenocarcinoma or lung squamous cell carcinoma having high *Bcl6* expression and high *MAP2K4* expression relative to normal lung (No value), whereas high *Bcl6* expression correlated with low *Dlg2* or *Llgl1* in some samples from all forms of lung cancers relative to normal lung (Fig. 10B). Also significantly positively correlated with a stronger trend compared with normal tissue were *Bcl6* and *MAP2K7* in the Boersma breast epithelial cancer dataset (Boersma et al., 2008) and *ZBTB7A* and *MAP2K7* in the Zhai cervical squamous carcinoma dataset (Zhai et al., 2007) (Table 1). Also significant was that in the Toruner Head-Neck all oral squamous carcinoma (cancer only) dataset (Toruner et al., 2004) positive correlations were seen between *Bcl6* and *MAPK10* and between *ZBTB7A* and *ArhGef12*, and in the Tomlins prostate carcinoma

Downloaded from http://bio.biologists.org/ at La Trobe University on December 16, 2020

Biology Open (2015) 4, 1024-1039 doi:10.1242/bio.012815

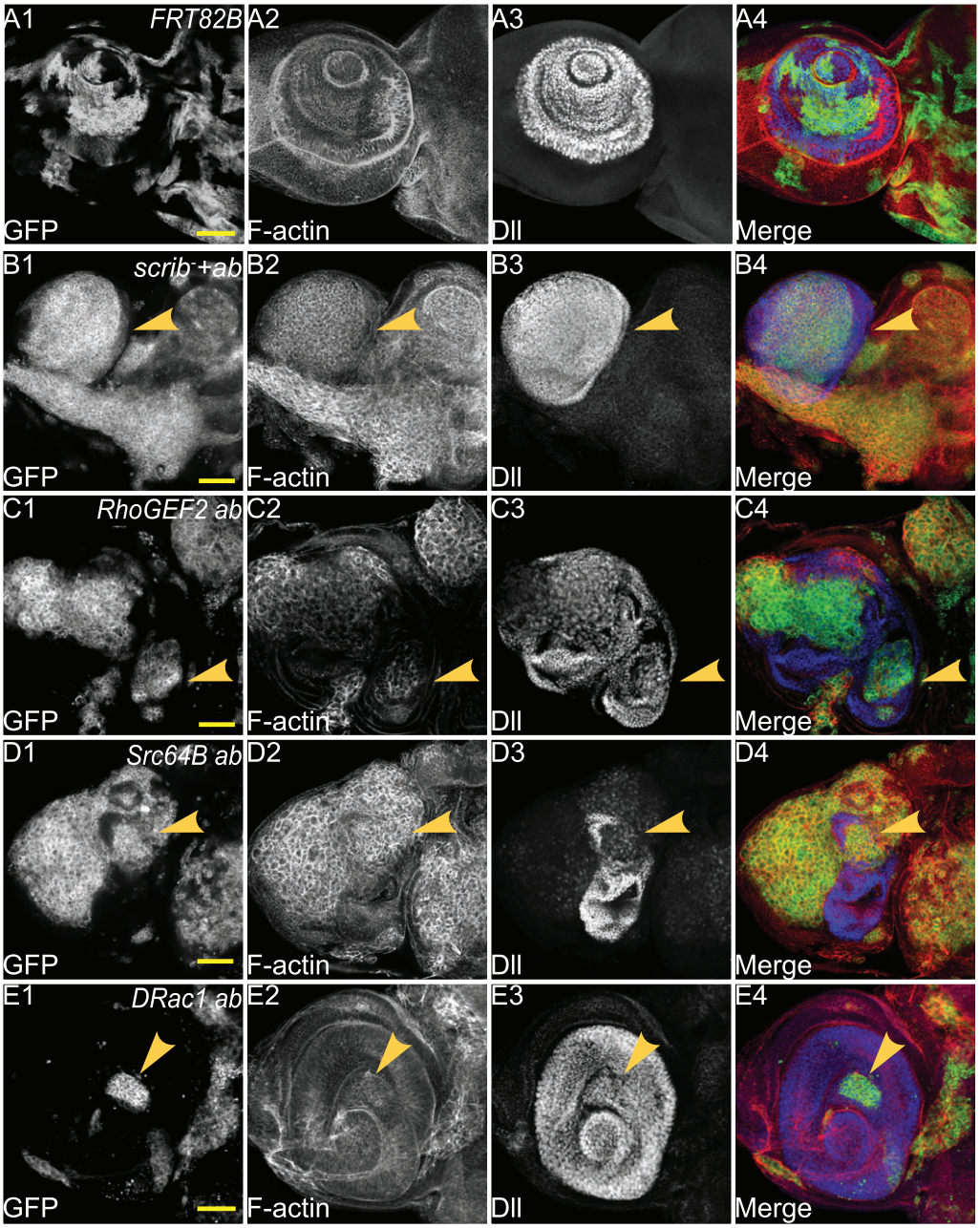


Fig. 8. Co-expression of *ab* with *Src64B* reduces expression of the antennal cell fate gene, Dll, but expression is retained in *ab scrib*$^{-}$, *ab RhoGEF2* and *ab DRac1* clones. Confocal planar images of mosaic larval antennal discs stained for F-actin (with Phalloidin, grey or red in merge) and Dll (grey or blue in merge); mutant clones are GFP^{+} and wild-type tissue is GFP^{-} (grey or green in merge). (A) wild-type control clones in the antennal disc at day 5 AED. (B) *ab scrib*^{1} mosaic antennal disc at day 5 AED. (C) *RhoGEF2 ab* mosaic antennal disc at day 5 AED. (D) *Src64B ab* mosaic antennal disc at day 5 AED. (E) *DRac1 ab* mosaic antennal disc at day 5 AED. Arrowheads point to Dll expression. Genotypes: (A) *ey-FLP, UAS-GFP; FRT82B/tubGAL4; FRT82B, tubGAL80*. (B) *eyFLP, UAS-GFP;; UAS-ab*^{55}*, FRT82B, scrib*^{1}*/tubGAL4; FRT82B, tubGAL80*. (C) *eyFLP, UAS-GFP; UAS-RhoGEF2*; *UAS-ab*^{55}*, FRT82B/tubGAL4; FRT82B, tubGAL80*. (D) *eyFLP, UAS-GFP; UAS-Src64B*; *UAS-ab*^{55}*, FRT82B/ tubGAL4; FRT82B, tubGAL80*. (E) *eyFLP, UAS-GFP; UAS-DRac1*; *UAS-ab*^{55}*, FRT82B/tubGAL4; FRT82B, tubGAL80*. Scale bars=50 µM.

dataset (Tomlins et al., 2007) Bcl6 expression was positively correlated with *ArhGef11* and *MAPK8* (Table 1). Significant positive correlations were also observed in the Collisson Pancreatic adenocarcinoma (cancer only) dataset (Collisson et al., 2011) between *ZBTB7A* and *Src* (Table 1). Furthermore, in the Grutzmann pancreatic ductal adenocarcinoma dataset (Grützmann et al., 2004), although of borderline significance, a positive correlation was observed between *ZBTB7A* and *MAP2K7* that showed a stronger trend compared with normal tissue (Table 1). Thus, taken together, these data show that in certain epithelial cancers the upregulation of *Bcl6* or *ZBTB7A* expression is significantly correlated with reduced expression of *Dlg2* or *Llgl1* cell polarity genes or high expression of *ArhGef11, ArhGef12, MAP2K4, MAP2K7, MAPK8, MAPK9, MAPK10, Src* or *Yes1* cytoskeletal genes. Based on our functional data in *Drosophila* and mammalian cells (this study; Brumby et al., 2011; Khoo et al., 2013; Turkel et al., 2013; C.P., A.B., H.R., unpublished data), we would expect the concordant expression of *Bcl6* or *ZBTB7A* with these genes should result in tumour growth, morphology changes, differentiation blockage and invasive properties.

DISCUSSION

In this study, we have shown that over-expression of the Ab BTB-ZF protein cooperates with upregulation of RhoGEF2 or Src64B in tumorigenesis, whereas Ab and DRac1 do not cooperate. Furthermore, we show that expression of Ab with each of these cytoskeletal regulators results in disruption to differentiation, in that the photoreceptor cell marker, Elav, and the early cell fate gene, Dac, are not expressed, although the antennal cell fate gene, Dll, is retained in all except *ab Src64B* co-expressing clones. Finally, we have found significant correlations in human epithelial cancer datasets between the high expression of BTB-ZF oncogenes, *Bcl6* and *ZBTB7A*, and low expression of *Dlg2* or *Llgl1* cell polarity genes or high expression of *ArhGef11*, *ArhGef12, MAP2K4,*

Biology Open

Downloaded from http://bio.biologists.org/ at La Trobe University on December 16, 2020

Biology Open (2015) 4, 1024-1039 doi:10.1242/bio.012815

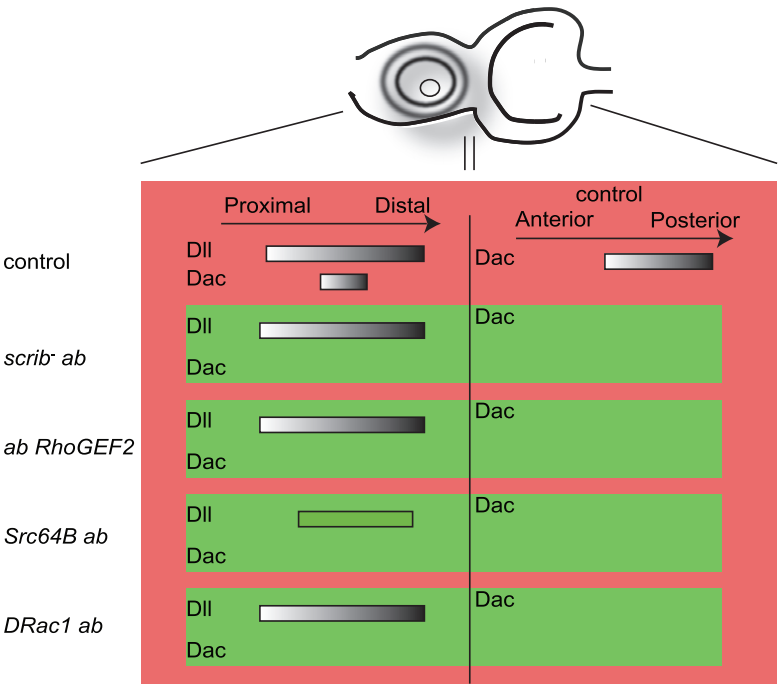


Fig. 9. Summary of the effects of *ab scrib*$^{-}$, *ab Src64B*, *ab RhoGEF2* and *ab DRac1* on Dac and Dll expression. A schematic of an eye-antennal disc showing the normal expression of Dac and Dll, and the effect of *ab scrib*$^{-}$, *ab Src64B*, *ab RhoGEF2* and *ab DRac1* on their expression patterns.

MAP2K7, MAPK8, MAPK9, MAPK10, Src or *Yes1* cytoskeletal genes. This data suggests that cooperation between these genes may occur in some human epithelial cancers.

Comparison of tumorigenic properties

RhoGEF2 ab or *Src64B ab* tumours showed overgrowth during an extended larval period resulting in giant larvae and loss of differentiation (Fig. 4C). However, unlike *scrib*$^{-}$ *ab* tumours there was also non-cell autonomous proliferation and the tumours did not appear to be as invasive as *scrib*$^{-}$ *ab* tumours, although a more detailed analysis of this is required. By contrast, co-expression of *DRac1* and *ab* did not result in cooperative tumorigenesis, but rather non-cell autonomous proliferation. Relative to the cooperation of these cytoskeletal genes with Ras^{V12} (Brumby et al., 2011; Khoo

Table 1 . Significant correlations in gene expression

Gene expression datasets	BTB-Zn gene	Polarity or cytoskeletal gene	*P* value	Pearson R	Notes
Positive Correlations					
Tomlins Prostate all	Bcl6	ARHGEF11	$5{,}60\times10^{-3}$	0.45	A
Tomlins Prostate Carcinoma	Bcl6	ARHGEF11	$1{,}40\times10^{-2}$	0.57	*, #
Toruner Head-Neck all oral squamous carcinoma (cancer only)	ZBTB7A	ARHGEF12	$1{,}70\times10^{-2}$	0.59	*
Toruner Head-Neck all oral squamous carcinoma (cancer only)	Bcl6	MAPK10	$1{,}10\times10^{-2}$	0.62	*
Tomlins Prostate all	Bcl6	MAPK8	$2{,}00\times10^{-2}$	0.46	A
Tomlins Prostate Carcinoma	Bcl6	MAPK8	$2{,}20\times10^{-2}$	0.57	*
Gasper colon all	Bcl6	MAPK9	$3{,}20\times10^{-13}$	0.71	A
Gaspar colorectal adenoma	Bcl6	MAPK9	$4{,}40\times10^{-9}$	0.69	*, #
Gaspar colon normal	Bcl6	MAPK9	$3{,}10\times10^{-6}$	0.82	N
Gaspar colorectal adenoma	Bcl6	MAP2K4	$6{,}80\times10^{-3}$	0.36	*, #
Rohrbeck all-Lung (cancer only)	Bcl6	MAP2K4	$2{,}50\times10^{-3}$	0.45	*
Boersma Breast epithelial cancer	Bcl6	MAP2K7	$2{,}30\times10^{-3}$	0.43	*, #
Grutzmann Pancreatic ductal adenocarcinoma	ZBTB7A	MAP2K7	$5{,}10\times10^{-2}$	0.6	*, #, §
Grutzmann Pancreas all (no met)	ZBTB7A	MAP2K7	$1{,}20\times10^{-2}$	0.52	A
Zhai Cervix Cervical squamous	ZBTB7A	MAP2K7	$1{,}30\times10^{-2}$	0.46	*, #
Zhai Cervix all	ZBTB7A	SCRIB	$3{,}40\times10^{-2}$	0.34	A
Collisson Pancreas all-adenocarcinoma	ZBTB7A	SRC	$3{,}10\times10^{-2}$	0.42	*
Gasper colon all	Bcl6	YES1	$1{,}60\times10^{-5}$	0.47	A
Gaspar colorectal adenoma	Bcl6	YES1	$1{,}40\times10^{-4}$	0.49	*, #
Gaspar colon normal	Bcl6	YES1	$3{,}40\times10^{-2}$	0.45	N
Rohrbeck all-Lung (cancer only)	Bcl6	YES1	$9{,}60\times10^{-3}$	0.4	*
Negative correlations					
Gasper colon all	Bcl6	DLG2	$2{,}20\times10^{-15}$	–0.75	A
Gaspar colorectal adenoma	Bcl6	DLG2	$7{,}40\times10^{-13}$	–0.79	*, #
Gaspar colon normal	Bcl6	DLG2	$8{,}40\times10^{-4}$	–0.66	N
Rohrbeck all-Lung (cancer only)	Bcl6	DLG2	$2{,}00\times10^{-2}$	–0.36	*
Rohrbeck all-Lung (cancer only)	Bcl6	LLGL1	$3{,}80\times10^{-3}$	–0.44	*

A, all (normal and cancer); N, normal; * Bcl6/ZBTB7 high and correlated as expected with the test gene; # trend is stronger in cancer compared with normal tissue; § borderline significance with positive correlation.

Downloaded from http://bio.biologists.org/ at La Trobe University on December 16, 2020

Biology Open (2015) 4, 1024-1039 doi:10.1242/bio.012815

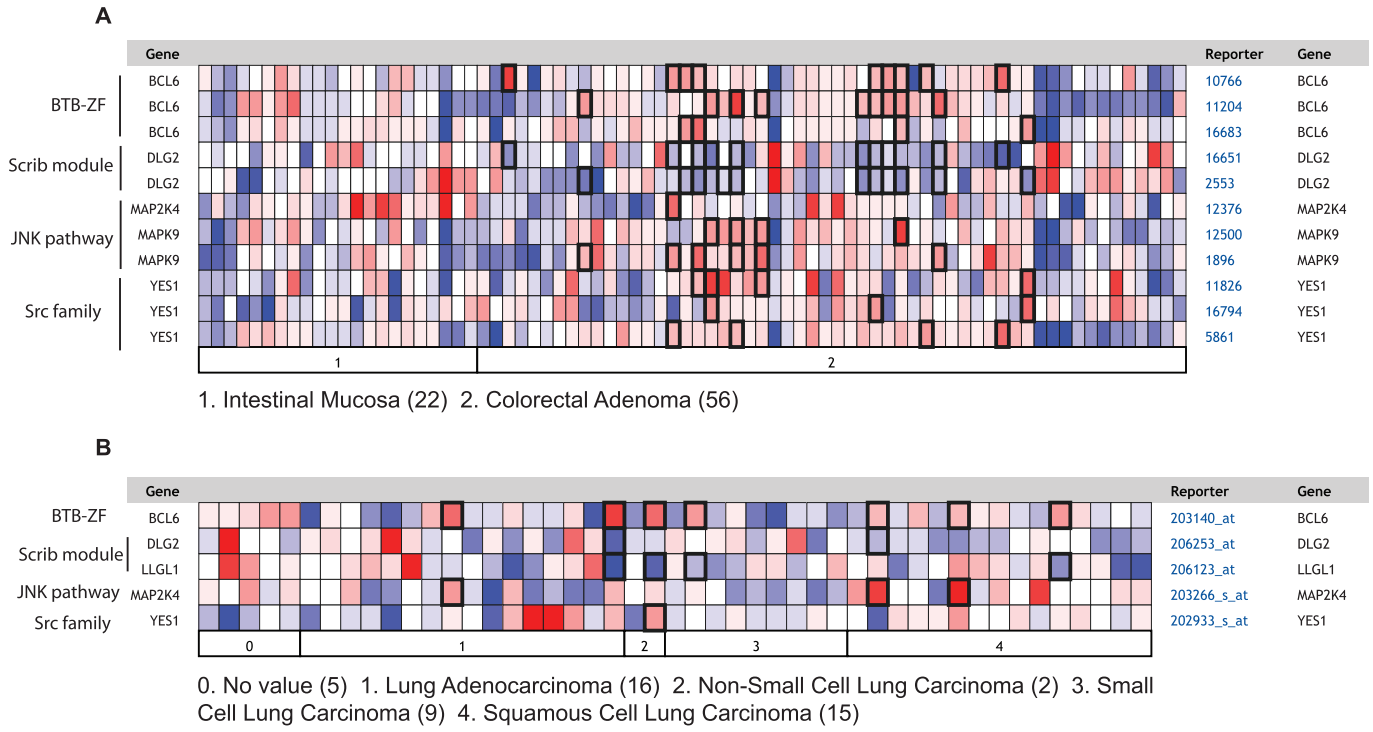


Fig. 10. Heatmaps of expression of *Bcl6* relative to polarity or cytoskeletal regulatory genes in the Gaspar colon and Rohrbeck Lung datasets. (A) Gaspar Colon data set. (B) Rohrbeck Lung data set. Samples are stratified into normal tissue (intestinal mucosa for Gaspar Colon or no value for Rohrbeck Lung) and cancer grades for Rohrbeck Lung. Relative expression levels of the indicated gene probesets are indicated. The Gaspar Colon dataset has 3 probes to *Bcl6* and *Yes1*, and 2 probes to *Dlg2* and *MAPK9*. Red is high expression and blue is low expression. The outlined samples indicate those where *Bcl6* is high and *Dlg2* or *Llgl1* are low or *MAP2K4, MAPK9* or *Yes1* are high.

et al., 2013; C.P., A.B., H.R., unpublished data), *RhoGEF2* or *Src64B* cooperation with *ab* showed similar properties (Fig. 4C). By contrast, *DRac1* Ras^{V12} tumours showed strong cell-autonomous overgrowth and invasive properties, whereas *DRac1 ab* expressing cells did not overgrow relative to wild-type tissue, but instead the surrounding wild-type tissue was induced to overgrow (Fig. 4C).

The phenomenon of non-cell autonomous overgrowth observed in *DRac1 ab* mosaic eye-antennal discs (and to some extent in *ab RhoGEF2* and *ab Src64B* mosaic discs) is similar to the effect that "undead" cells (cells where apoptosis is initiated by activation of initiator caspases, but effector caspase activation is blocked – and thus cell death – by expression of the inhibitor, p35) have upon their surrounding wild-type neighbours (Martin et al., 2009; Morata et al., 2011; Perez-Garijo et al., 2009; Ryoo and Bergmann, 2012). This occurs by the release of Wingless (Wg) and Decapentaplegic (Dpp) and perhaps other morphogens from the undead cells, which promote compensatory proliferation in the surrounding wild-type cells. The similarity of these phenotypes suggests that *DRac1 ab* expressing cells might be in an "undead" state, and release Dpp and Wg, thereby inducing proliferative overgrowth of the surrounding wild-type cells. Alternatively, these cells might be deficient in mitochondrial function, which together with expression of a cell-survival factor, such as Ras^{V12}, results in non-cell autonomous overgrowth without evidence of caspase activation (Ohsawa et al., 2012). In this scenario, the mitochondrial dysfunction results in increased reactive oxygen species (ROS) that activate JNK signalling, which subsequently inactivates Hippo pathway signalling, leading to increased expression of the target genes Wingless and Unpaired (Upd) that activate Wg signalling and Jak/Stat signalling, respectively, in the neighbouring wild-type cells. However, since we observed TUNEL-positive cells in *DRac1 ab, RhoGEF2 ab* and *Src64B ab* expressing clones, it is more likely that the first of these mechanisms is responsible for the non-cell autonomous overgrowth, however this requires further investigation. Interestingly, in undead cells JNK activation is required for Dpp and Wg production and non-cell autonomous overgrowth (Morata et al., 2011; Perez-Garijo et al., 2009). Furthermore, strong activation of JNK signalling together with Ras^{V12} results in non-cell autonomous overgrowth (Uhlirova et al., 2005), although at presumably lower levels of JNK activation, cell autonomous overgrowth occurs (Brumby et al., 2011; Igaki et al., 2006; Uhlirova and Bohmann, 2006). Therefore it is possible that the different effects on non-cell autonomous versus autonomous cell overgrowth in *DRac1 ab* versus *RhoGEF2 ab* or *Src64B ab*-expressing cells might depend on the level of JNK activation. Nonetheless, at early stages, *ab*-driven R*hoGEF2, Src64B* or *DRac1* tumours were similar in inducing non-cell autonomous effects, but at later times the *RhoGEF2 ab* and *Src64B ab*-expressing cells showed more predominant autonomous cell overgrowth, whilst the *DRac1 ab* expressing cells did not, suggesting that there are likely to be molecular differences between *DRac1* and *RhoGEF2* or *Src64B* in their cooperative interactions with *ab* that impact on cell proliferation or survival of the tumour cells.

Our profiling of Ab targets and deregulated genes revealed that *dac, dan, eya* and *ct* eye-antennal differentiation genes were repressed, along with changes in expression of cell growth/proliferation and survival genes that would be expected to promote tumorigenic growth in cooperation with *scrib* loss-of-function (Turkel et al., 2013). $scrib^{-}$ *ab* tumours showed downregulation of Dac, but the antennal cell fate expression domain of Dll was not affected (Turkel et al., 2013). Similarly, *ab* expression with either of the cytoskeletal genes resulted in repression of Dac, however *Src64B ab* tumours additionally repressed Dll, in contrast to *DRac1 ab, RhoGEF2 ab* and $scrib^{-}$ *ab* tumours where Dll was unaffected. This data suggests that *Src64B*

Downloaded from http://bio.biologists.org/ at La Trobe University on December 16, 2020

Biology Open (2015) 4, 1024-1039 doi:10.1242/bio.012815

expression exerts an additional effect on *ab*-expressing cells to inhibit Dll gene expression and differentiation. *Src* upregulation activates the JNK and Stat signalling pathways, affects adherens junction function and represses Hippo signalling (Enomoto and Igaki, 2013; Kohlmaier et al., 2014; Ma et al., 2013; Read et al., 2004; Sotillos et al., 2013; Vidal et al., 2006). Furthermore, recent studies have shown that overexpression of *Src64B* in the *Drosophila* intestinal stem cells can alter differentiation and result in amplification of progenitor cell pools (Cordero et al., 2014; Kohlmaier et al., 2014). *scrib* mutant cells also upregulate JNK, downregulate the E-cadherin/β-catenin adhesion complex and repress Hippo signalling (Brumby and Richardson, 2003; Doggett et al., 2011; Igaki et al., 2006; Leong et al., 2009; Uhlirova and Bohmann, 2006). Furthermore, the Jak/Stat ligand, Upd3, is also upregulated in the *scrib*$^{-}$ cells, where it drives tumour overgrowth, and is also required to activate Jak/Stat signalling in the wild-type neighbouring cells in cell competition (Bunker et al., 2015; Chen et al., 2012; Schroeder et al., 2013). RhoGEF2 and DRac1 also upregulate JNK signalling (Brumby et al., 2011; Khoo et al., 2013), and might also repress Hippo signalling to promote tissue growth, since regulators of actin cytoskeletal tension, such as activated Rok and Myosin II regulatory light chain, induce Yki target gene expression (Fernandez et al., 2011; Halder et al., 2012; Rauskolb et al., 2014; Sansores-Garcia et al., 2011). However, in *Drosophila* it is unknown if RhoGEF2 or DRac1 affect Jak/Stat signalling. Since *scrib* loss-of-function and *Src* activation deregulate similar pathways, the precise mechanism by which *Src64B* cooperates with *ab* to block expression of Dll in the developing eye-antennal disc remains to be determined.

Cooperation of BTB-ZF transcription factors with deregulated cytoskeletal or polarity genes in human cancer

Our finding that there was a significant correlation between increased expression of human BTB-ZF oncogenic genes, *Bcl6* or *ZBTB7A*, and downregulation of the cell polarity genes, *Dlg2* and *Llgl1*, or homologs of *JNKK* (*MAPK2K4, MAPK2K7*), *JNK* (*MAPK8, MAPK9*, *MAPK10*), *RhoGEF2* (*ArhGEF11*, *ArhGEF12*) or *Src* (*Yes1, Src*) cytoskeletal genes in various epithelial cancers, suggests that the concordant expression of these genes might be contributing to human epithelial cancer initiation and progression. Whilst this study only focused on two of the 47 BTB-ZF genes in the human genome, it raises the question of whether other BTB-ZF genes might also show correlations with the expression of cytoskeletal or cell polarity genes in human epithelial cancers. However, tissue and cancer-grade specific effects might be observed, as a recently published study revealed that *ZBTB7A* was commonly deleted in late stage oesophageal, bladder, colorectal, lung, ovarian and uterine cancers (Liu et al., 2014). Moreover, they found that low *ZBTB7A* expression correlates with poor prognosis in colon cancer patients, suggesting that *ZBTB7A* plays a tumour suppressor function in these cancers. Interestingly, this study also found that in colon cancer xenografts, *ZBTB7A* represses the expression of genes in the glycolytic pathway, a metabolic pathway that is required for aggressive tumour growth, and that inhibition of this pathway reduces tumour growth. Pertinent to this finding, we found that blocking glycolytic pathways in *Drosophila* polarity-impaired tumours, impedes tumour growth without substantially affecting normal tissues (Willoughby et al., 2013), suggesting that downregulation of the Scribble polarity module might upregulate glycolytic metabolic pathways and be dependent on them for tumour growth and survival. It is therefore possible that the cooperation between *ab* and *scrib*$^{-}$ or cytoskeletal genes in *Drosophila* may also reflect a need for upregulation of the glycolytic pathway. In human epithelial cancers, the correlations observed between elevated *ZBTB7A* expression and reduced expression of the Scribble polarity module gene (or high expression of cytoskeletal genes) might also indicate a requirement for glycolytic pathway activation for tumorigenesis. Further studies are clearly required to examine the cooperative effects of *Bcl6* or *ZBTB7A* with deregulated cytoskeletal or cell polarity genes in human epithelial cell lines and mouse models in order to discern whether our findings in *Drosophila* are indeed conserved in mammalian systems.

Identifying cooperative interactions in cancer is likely to provide novel therapeutic approaches in combating the tumour. Indeed, recently a small molecule inhibitor targeting Bcl6 has been developed, and combining this with a Stat3 inhibitor resulted in enhanced cell killing in triple negative breast cancer cell lines (Walker et al., 2014). Since in *Drosophila* and human cells, Src upregulates Stat activity (Cordero et al., 2014; Frame, 2004; Kohlmaier et al., 2014; Read et al., 2004; Sotillos et al., 2013), tumours showing high Bcl6 and Src or Yes1 expression would be predicted to be sensitive to this combined therapeutic regime. Interestingly, a predominance of the significant correlations that were observed in the human epithelial cancer datasets with either *Bcl6* or *ZBTB7A* involved upregulation of JNKK and JNK family genes. Since JNK signalling is central to many cooperative interactions examined by us and others (Brumby et al., 2011; Brumby and Richardson, 2003; Enomoto and Igaki, 2013; Igaki et al., 2006; Leong et al., 2009; Turkel et al., 2013; Uhlirova and Bohmann, 2006), inhibiting the JNK pathway in addition to Bcl6 in Bcl6-driven cancers might also be a promising therapeutic approach to combat these cancers. In summary, our functional studies in *Drosophila* and bioinformatics analysis of human cancers has shown that cooperative tumorigenic interactions occur between BTB-ZF genes and cell polarity or cytoskeletal genes, and warrants further investigation to determine whether restoring normal expression of these genes or downstream pathways in human cancer cells can reduce tumorigenesis.

MATERIALS AND METHODS

Drosophila stocks

The following *Drosophila* stocks were used: *ey-FLP1*, *UAS-mCD8-GFP;; Tub-GAL4*, *FRT82B*, *Tub-GAL80* (Lee and Treisman, 2001); *UAS-ab*^{55} *(III)* (Cook et al., 2004); *UAS-RhoGEF2 (II)* (Padash Barmchi et al., 2005); *UAS-Src64B (II)* (R. Cagan, Mount Sinai School of Medicine, New York, USA); *UAS-DRac1 (II)* (Luo et al., 1994); *scrib*^{1} (Bilder and Perrimon, 2000) and *ey-GAL4* (Bloomington Stock Centre). *FRT82B* recombinant stocks were generated for all transgenic lines for mosaic analysis.

Mosaic analysis

Clonal analysis utilised MARCM (mosaic analysis with repressible cell marker) (Lee and Luo, 1999) with *FRT82B* and *ey-FLP1* to induce clones and *mCD8-GFP* expression to mark mutant tissue. All fly crosses were carried out at 25°C and grown on standard fly media.

Immunostaining

Third-instar larval eye-antennal discs were dissected in phosphate-buffered saline (PBS), fixed in 4% paraformaldehyde for 30 min, and washed in PBS +0.1% Triton X-100 (PBT). Samples were blocked in 2% NGS in PBT with 1.5% saponin for 1 h in room temperature and then incubated in primary antibodies over night at 4°C in 2% NGS in PBT. Samples were then washed two times in PBT for 30 min before addition of the secondary antibody. EdU and TUNEL labelling were performed as previously described (Turkel et al., 2013).

Antibodies used were: mouse anti-Elav (DSHB, 1/20), mouse anti-Dll (Duncan et al., 1998, 1/500) and mouse anti-Dac (DSHB, 1/10). Secondary antibodies were: anti-mouse Alexa 568 or 633 (Invitrogen) at 1/400 dilution.

Downloaded from http://bio.biologists.org/ at La Trobe University on December 16, 2020

F-actin was detected with phalloidin–tetramethylrhodamine isothioblueate (TRITC; Sigma, 0.3 µM, 1/1000) and DNA was detected using DAPI staining. Samples were mounted in 80% (v/v) glycerol/PBS.

Imaging

Images of fixed and mounted samples onto the glass slides were captured using BioRad, Olympus Fluoview FV100 and Leica TCS SP5 confocal laser microscopes. Single optical sections were selected in FluoView software before being processed in Adobe Photoshop CS6 and assembled into figures in Adobe Illustrator CS6.

Adult flies were frozen at −20°C before imaging in order to facilitate positioning them under the microscope. Images were captured on Lumenera Infinity 1 camera attached to Olympus SZX7 dissection microscope and processed using Adobe Photoshop CS3.

Quantification of clone volume

Volumetric clone analysis was performed using Volocity 3D Image Analysis Software (Perkin-Elmer). To determine the ratio of clonal tissue volume to total volume of the eye-antennal disc for each genotype and time point, GFP^+ clonal tissue relative to total disc area (as marked by Phallodin to visualize the cells) was measured from confocal Z sections encompassing the entire eye-antennal disc. The data for each genotype was compared using GraphPad Prism 6 using unpaired *t*-tests. Error bars represent s.e.m. and the significance was set at $P<0.05$.

Quantification of EdU and TUNEL staining

For TUNEL and EdU labelling, 6 to 10 discs for each genotype were analysed. TUNEL was quantified using Photoshop 5.1 Extended. EDU was quantified using a program designed by David Tapiador, available at https://github.com/nogates/counting-semaphore.

Analysis of published datasets

Using Oncomine (Research Premium Edition), we identified 18 published gene expression data sets that contain epithelial cancer samples. Data was filtered down to the genes of interest and was downloaded for further analysis. Eleven of the 18 data sets that have at least 30 samples and contain at least three quarters of our query genes were analysed for correlation of expression levels between BCL6/ZBTB7A and each of the genes in our gene panel. These data sets were: Boersma Breast (Boersma et al., 2008), Collisson Pancreas all-adenocarcinoma (Collisson et al., 2011), Gaspar Colon (Gaspar et al., 2008), Grützmann Pancreas (Grützmann et al., 2004), Ma Breast 2 (Ma et al., 2004), Ma Breast 4 (Ma et al., 2009), Rohrbeck Lung (Rohrbeck et al., 2008), Skrzypczak Colorectal 2 (Skrzypczak et al., 2010), Tomlins Prostate (Tomlins et al., 2007), Toruner Head-Neck all-oral squamous carcinoma (Toruner et al., 2004) and Zhai Cervix (Zhai et al., 2007). Where data is available, samples are stratified into normal (no cancer) and cancer for separate analysis to identify cancer-specific gene expression correlations. All analyses were done using the R software package.

Acknowledgements

We thank David Tapiador for developing the program for quantification of EdU labelled tissues. We also acknowledge Bloomington, Vienna RNAi and National Institute of Genetics (Japan) Stock Centers for the provision of fly strains and OzDros for quarantine and handling of flies imported into Australia and Flybase for its wealth of information.

Competing interests

The authors declare no competing or financial interests.

Author contributions

N.T., M.P., H.E.R. and A.M.B. conceived and designed the experiments. N.T., M.P. and C.P. performed the experiments. N.T., M.P., C.P., J.L., A.M.B. and H.E.R. analysed the data. N.T., M.P. and H.E.R. wrote the paper.

Funding

H.E.R. is supported by a Senior Research Fellowship from the National Health and Medical Research Council (NHMRC) Australia, M.P. from funding from the Cancer Council Victoria Australia, and C.P. was supported by an Australian Postgraduate Award. This work was supported by grants from the NHMRC, #400211 to H.E.R. and A.M.B., and #509051 to A.M.B., and Peter Mac Internal funds to H.E.R.

Supplementary material

Supplementary material available online at
http://bio.biologists.org/lookup/suppl/doi:10.1242/bio.012815/-/DC1

References

Aggarwal, A., Hunter, W. J., III, Aggarwal, H., Silva, E. D., Davey, M. S., Murphy, R. F. and Agrawal, D. K. (2010). Expression of leukemia/lymphoma-related factor (LRF/POKEMON) in human breast carcinoma and other cancers. *Exp. Mol. Pathol.* **89**, 140-148.

Aggarwal, H., Aggarwal, A., Hunter, W. J., III, Yohannes, P., Khan, A. U. and Agrawal, D. K. (2011). Expression of leukemia/lymphoma related factor (LRF/Pokemon) in human benign prostate hyperplasia and prostate cancer. *Exp. Mol. Pathol.* **90**, 226-230.

Barrett, K., Leptin, M. and Settleman, J. (1997). The Rho GTPase and a putative RhoGEF mediate a signaling pathway for the cell shape changes in Drosophila gastrulation. *Cell* **91**, 905-915.

Bilder, D. and Perrimon, N. (2000). Localization of apical epithelial determinants by the basolateral PDZ protein Scribble. *Nature* **403**, 676-680.

Boersma, B. J., Reimers, M., Yi, M., Ludwig, J. A., Luke, B. T., Stephens, R. M., Yfantis, H. G., Lee, D. H., Weinstein, J. N. and Ambs, S. (2008). A stromal gene signature associated with inflammatory breast cancer. *Int. J. Cancer* **122**, 1324-1332.

Brumby, A. M. and Richardson, H. E. (2003). scribble mutants cooperate with oncogenic Ras or Notch to cause neoplastic overgrowth in Drosophila. *EMBO J.* **22**, 5769-5779.

Brumby, A. M. and Richardson, H. E. (2005). Using Drosophila melanogaster to map human cancer pathways. *Nat. Rev. Cancer* **5**, 626-639.

Brumby, A. M., Goulding, K. R., Schlosser, T., Loi, S., Galea, R., Khoo, P., Bolden, J. E., Aigaki, T., Humbert, P. O. and Richardson, H. E. (2011). Identification of novel Ras-cooperating Oncogenes in Drosophila melanogaster: a RhoGEF/Rho-family/JNK Pathway is a Central Driver of Tumorigenesis. *Genetics* **188**, 105-125.

Bunker, B. D., Nellimoottil, T. T., Boileau, R. M., Classen, A. K. and Bilder, D. (2015). The transcriptional response to tumorigenic polarity loss in Drosophila. *Elife* **4**, e03189.

Chen, R., Amoui, M., Zhang, Z. and Mardon, G. (1997). Dachshund and eyes absent proteins form a complex and function synergistically to induce ectopic eye development in Drosophila. *Cell* **91**, 893-903.

Chen, C.-L., Schroeder, M. C., Kango-Singh, M., Tao, C. and Halder, G. (2012). Tumor suppression by cell competition through regulation of the Hippo pathway. *Proc. Natl. Acad. Sci. USA* **109**, 484-489.

Cheng, L.Y., Parsons, L. M. and Richardson, H. E. (2013). Modelling cancer in Drosophila: The next generation. In Encyclopedia Life Sciences (eLS). Chichester: John Wiley & Sons Ltd.

Collisson, E. A., Sadanandam, A., Olson, P., Gibb, W. J., Truitt, M., Gu, S., Cooc, J., Weinkle, J., Kim, G. E., Jakkula, L. et al. (2011). Subtypes of pancreatic ductal adenocarcinoma and their differing responses to therapy. *Nat. Med.* **17**, 500-503.

Cook, O., Biehs, B. and Bier, E. (2004). brinker and optomotor-blind act coordinately to initiate development of the L5 wing vein primordium in Drosophila. *Development* **131**, 2113-2124.

Cordero, J. B., Ridgway, R. A., Valeri, N., Nixon, C., Frame, M. C., Muller, W. J., Vidal, M. and Sansom, O. J. (2014). c-Src drives intestinal regeneration and transformation. *EMBO J.* **33**, 1474-1491.

Costoya, J. A. (2007). Functional analysis of the role of POK transcriptional repressors. *Brief Funct. Genomic Proteomic* **6**, 8-18.

Dodson, G. S., Guarnieri, D. J. and Simon, M. A. (1998). Src64 is required for ovarian ring canal morphogenesis during Drosophila oogenesis. *Development* **125**, 2883-2892.

Doggett, K., Grusche, F. A., Richardson, H. E. and Brumby, A. M. (2011). Loss of the Drosophila cell polarity regulator Scribbled promotes epithelial tissue overgrowth and cooperation with oncogenic Ras-Raf through impaired Hippo pathway signaling. *BMC Dev. Biol.* **11**, 57.

Dominguez, M. and Casares, F. (2005). Organ specification-growth control connection: new in-sights from the Drosophila eye-antennal disc. *Dev. Dyn.* **232**, 673-684.

Dow, L. E., Elsum, I. A., King, C. L., Kinross, K. M., Richardson, H. E. and Humbert, P. O. (2008). Loss of human Scribble cooperates with H-Ras to promote cell invasion through deregulation of MAPK signalling. *Oncogene* **27**, 5988-6001.

Duncan, D. M., Burgess, E. A. and Duncan, I. (1998). Control of distal antennal identity and tarsal development in Drosophila by spineless-aristapedia, a homolog of the mammalian dioxin receptor. *Genes Dev.* **12**, 1290-1303.

Elsum, I., Yates, L., Humbert, P. O. and Richardson, H. E. (2012). The Scribble-Dlg-Lgl polarity module in development and cancer: from flies to man. *Essays Biochem.* **53**, 141-168.

Downloaded from http://bio.biologists.org/ at La Trobe University on December 16, 2020

Biology Open (2015) 4, 1024-1039 doi:10.1242/bio.012815

Elsum, I. A., Yates, L. L., Pearson, H. B., Phesse, T. J., Long, F., O'Donoghue, R., Ernst, M., Cullinane, C. and Humbert, P. O. (2013). Scrib heterozygosity predisposes to lung cancer and cooperates with KRas hyperactivation to accelerate lung cancer progression in vivo. *Oncogene* **33**, 5523-5533.

Enomoto, M. and Igaki, T. (2013). Src controls tumorigenesis via JNK-dependent regulation of the Hippo pathway in Drosophila. *EMBO Rep.* **14**, 65-72.

Fernandez, B. G., Gaspar, P., Bras-Pereira, C., Jezowska, B., Rebelo, S. R. and Janody, F. (2011). Actin-Capping Protein and the Hippo pathway regulate F-actin and tissue growth in Drosophila. *Development* **138**, 2337-2346.

Fernández, B. G., Jezowska, B. and Janody, F. (2014). Drosophila actin-Capping Protein limits JNK activation by the Src proto-oncogene. *Oncogene* **33**, 2027-2039.

Frame, M. C. (2004). Newest findings on the oldest oncogene; how activated src does it. *J. Cell Sci.* **117**, 989-998.

Gaspar, C., Cardoso, J., Franken, P., Molenaar, L., Morreau, H., Möslein, G., Sampson, J., Boer, J. M., de Menezes, R. X. and Fodde, R. (2008). Cross-species comparison of human and mouse intestinal polyps reveals conserved mechanisms in adenomatous polyposis coli (APC)-driven tumorigenesis. *Am. J. Pathol.* **172**, 1363-1380.

Godde, N. J., Sheridan, J. M., Smith, L. K., Pearson, H. B., Britt, K. L., Galea, R. C., Yates, L. L., Visvader, J. E. and Humbert, P. O. (2014). Scribble modulates the MAPK/Fra1 pathway to disrupt luminal and ductal integrity and suppress tumour formation in the mammary gland. *PLoS Genet.* **10**, e1004323.

Gonzalez, C. (2013). Drosophila melanogaster: a model and a tool to investigate malignancy and identify new therapeutics. *Nat. Rev. Cancer* **13**, 172-183.

Grieder, N. C., Charlafti, I., Kloter, U., Jackle, H., Schafer, U. and Gehring, W. J. (2007). Misexpression screen in Drosophila melanogaster aiming to reveal novel factors involved in formation of body parts. *Genetics* **175**, 1707-1718.

Grützmann, R., Pilarsky, C., Ammerpohl, O., Luttges, J., Böhme, A., Sipos, B., Foerder, M., Alldinger, I., Jahnke, B., Schackert, H. K. et al. (2004). Gene expression profiling of microdissected pancreatic ductal carcinomas using high-density DNA microarrays. *Neoplasia* **6**, 611-622.

Grzeschik, N. A., Amin, N., Secombe, J., Brumby, A. M. and Richardson, H. E. (2007). Abnormalities in cell proliferation and apico-basal cell polarity are separable in Drosophila lgl mutant clones in the developing eye. *Dev. Biol.* **311**, 106-123.

Grzeschik, N. A., Parsons, L. M., Allott, M. L., Harvey, K. F. and Richardson, H. E. (2010). Lgl, aPKC, and Crumbs regulate the Salvador/Warts/Hippo pathway through two distinct mechanisms. *Curr. Biol.* **20**, 573-581.

Guarnieri, D. J., Dodson, G. S. and Simon, M. A. (1998). SRC64 regulates the localization of a Tec-family kinase required for Drosophila ring canal growth. *Mol. Cell* **1**, 831-840.

Guo, C., Zhu, K., Sun, W., Yang, B., Gu, W., Luo, J., Peng, B. and Zheng, J. (2014). The effect of Pokemon on bladder cancer epithelial-mesenchymal transition. *Biochem. Biophys. Res. Commun.* **443**, 1226-1231.

Häcker, U. and Perrimon, N. (1998). DRhoGEF2 encodes a member of the Dbl family of oncogenes and controls cell shape changes during gastrulation in Drosophila. *Genes Dev.* **12**, 274-284.

Halder, G., Dupont, S. and Piccolo, S. (2012). Transduction of mechanical and cytoskeletal cues by YAP and TAZ. *Nat. Rev. Mol. Cell Biol.* **13**, 591-600.

Hanahan, D. and Weinberg, R. A. (2011). Hallmarks of cancer: the next generation. *Cell* **144**, 646-674.

Harden, N., Loh, H. Y., Chia, W. and Lim, L. (1995). A dominant inhibitory version of the small GTP-binding protein Rac disrupts cytoskeletal structures and inhibits developmental cell shape changes in Drosophila. *Development* **121**, 903-914.

Hattori, Y., Usui, T., Satoh, D., Moriyama, S., Shimono, K., Itoh, T., Shirahige, K. and Uemura, T. (2013). Sensory-neuron subtype-specific transcriptional programs controlling dendrite morphogenesis: genome-wide analysis of Abrupt and Knot/Collier. *Dev. Cell* **27**, 530-544.

Hatzi, K. and Melnick, A. (2014). Breaking bad in the germinal center: how deregulation of BCL6 contributes to lymphomagenesis. *Trends Mol. Med.* **20**, 343-352.

Hu, S., Fambrough, D., Atashi, J. R., Goodman, C. S. and Crews, S. T. (1995). The Drosophila abrupt gene encodes a BTB-zinc finger regulatory protein that controls the specificity of neuromuscular connections. *Genes Dev.* **9**, 2936-2948.

Humbert, P. O., Grzeschik, N. A., Brumby, A. M., Galea, R., Elsum, I. and Richardson, H. E. (2008). Control of tumourigenesis by the Scribble/Dlg/Lgl polarity module. *Oncogene* **27**, 6888-6907.

Igaki, T., Pagliarini, R. A. and Xu, T. (2006). Loss of cell polarity drives tumor growth and invasion through JNK activation in Drosophila. *Curr. Biol.* **16**, 1139-1146.

Jaffe, A. B. and Hall, A. (2005). Rho GTPases: biochemistry and biology. *Annu. Rev. Cell Dev. Biol.* **21**, 247-269.

Jang, A. C.-C., Chang, Y.-C., Bai, J. and Montell, D. (2009). Border-cell migration requires integration of spatial and temporal signals by the BTB protein Abrupt. *Nat. Cell Biol.* **11**, 569-579.

Jeon, B.-N., Yoo, J.-Y., Choi, W.-I., Lee, C.-E., Yoon, H.-G. and Hur, M.-W. (2008). Proto-oncogene FBI-1 (Pokemon/ZBTB7A) represses transcription of the tumor suppressor Rb gene via binding competition with Sp1 and recruitment of co-repressors. *J. Biol. Chem.* **283**, 33199-33210.

Kelly, K. F. and Daniel, J. M. (2006). POZ for effect–POZ-ZF transcription factors in cancer and development. *Trends Cell Biol.* **16**, 578-587.

Kelso, R. J., Hudson, A. M. and Cooley, L. (2002). Drosophila Kelch regulates actin organization via Src64-dependent tyrosine phosphorylation. *J. Cell Biol.* **156**, 703-713.

Khoo, P., Allan, K., Willoughby, L., Brumby, A. M. and Richardson, H. E. (2013). In Drosophila, RhoGEF2 cooperates with activated Ras in tumorigenesis through a pathway involving Rho1-Rok-Myosin-II and JNK signalling. *Dis. Model. Mech.* **6**, 661-678.

Kohlmaier, A., Fassnacht, C., Jin, Y., Reuter, H., Begum, J., Dutta, D. and Edgar, B. A. (2014). Src kinase function controls progenitor cell pools during regeneration and tumor onset in the Drosophila intestine. *Oncogene* **34**, 2371-2384.

Kulshammer, E. and Uhlirova, M. (2013). The actin cross-linker Filamin/Cheerio mediates tumor malignancy downstream of JNK signaling. *J. Cell Sci.* **126**, 927-938.

Lee, T. and Luo, L. (1999). Mosaic analysis with a repressible cell marker for studies of gene function in neuronal morphogenesis. *Neuron* **22**, 451-461.

Lee, J. D. and Treisman, J. E. (2001). The role of Wingless signaling in establishing the anteroposterior and dorsoventral axes of the eye disc. *Development* **128**, 1519-1529.

Leong, G. R., Goulding, K. R., Amin, N., Richardson, H. E. and Brumby, A. M. (2009). Scribble mutants promote aPKC and JNK-dependent epithelial neoplasia independently of Crumbs. *BMC Biol.* **7**, 62.

Liu, K., Liu, F., Zhang, N., Liu, S. and Jiang, Y. (2012). Pokemon silencing leads to Bim-mediated anoikis of human hepatoma cell QGY7703. *Int. J. Mol. Sci.* **13**, 5818-5831.

Liu, X.-S., Haines, J. E., Mehanna, E. K., Genet, M. D., Ben-Sahra, I., Asara, J. M., Manning, B. D. and Yuan, Z.-M. (2014). ZBTB7A acts as a tumor suppressor through the transcriptional repression of glycolysis. *Genes Dev.* **28**, 1917-1928.

Luo, L., Liao, Y. J., Jan, L. Y. and Jan, Y. N. (1994). Distinct morphogenetic functions of similar small GTPases: Drosophila Drac1 is involved in axonal outgrowth and myoblast fusion. *Genes Dev.* **8**, 1787-1802.

Ma, X.-J., Wang, Z., Ryan, P. D., Isakoff, S. J., Barmettler, A., Fuller, A., Muir, B., Mohapatra, G., Salunga, R., Tuggle, J. T. et al. (2004). A two-gene expression ratio predicts clinical outcome in breast cancer patients treated with tamoxifen. *Cancer Cell* **5**, 607-616.

Ma, X.-J., Dahiya, S., Richardson, E., Erlander, M. and Sgroi, D. C. (2009). Gene expression profiling of the tumor microenvironment during breast cancer progression. *Breast Cancer Res.* **11**, R7.

Ma, X., Shao, Y., Zheng, H., Li, M., Li, W. and Xue, L. (2013). Src42A modulates tumor invasion and cell death via Ben/dUev1a-mediated JNK activation in Drosophila. *Cell Death Dis.* **4**, e864.

Maeda, T., Hobbs, R. M. and Pandolfi, P. P. (2005). The transcription factor Pokemon: a new key player in cancer pathogenesis. *Cancer Res.* **65**, 8575-8578.

Martin, F. A., Perez-Garijo, A. and Morata, G. (2009). Apoptosis in Drosophila: compensatory proliferation and undead cells. *Int. J. Dev. Biol.* **53**, 1341-1347.

Morata, G., Shlevkov, E. and Pérez-Garijo, A. (2011). Mitogenic signaling from apoptotic cells in Drosophila. *Dev. Growth Differ.* **53**, 168-176.

Mulinari, S., Barmchi, M. P. and Häcker, U. (2008). DRhoGEF2 and diaphanous regulate contractile force during segmental groove morphogenesis in the Drosophila embryo. *Mol. Biol. Cell* **19**, 1883-1892.

Nikolaidou, K. K. and Barrett, K. (2004). A Rho GTPase signaling pathway is used reiteratively in epithelial folding and potentially selects the outcome of Rho activation. *Curr. Biol.* **14**, 1822-1826.

Ohsawa, S., Sato, Y., Enomoto, M., Nakamura, M., Betsumiya, A. and Igaki, T. (2012). Mitochondrial defect drives non-autonomous tumour progression through Hippo signalling in Drosophila. *Nature* **490**, 547-551.

O'Reilly, A. M., Ballew, A. C., Miyazawa, B., Stocker, H., Hafen, E. and Simon, M. A. (2006). Csk differentially regulates Src64 during distinct morphological events in Drosophila germ cells. *Development* **133**, 2627-2638.

Padash Barmchi, M., Rogers, S. and Häcker, U. (2005). DRhoGEF2 regulates actin organization and contractility in the Drosophila blastoderm embryo. *J. Cell Biol.* **168**, 575-585.

Pearson, H. B., Perez-Mancera, P. A., Dow, L. E., Ryan, A., Tennstedt, P., Bogani, D., Elsum, I., Greenfield, A., Tuveson, D. A., Simon, R. et al. (2011). SCRIB expression is deregulated in human prostate cancer, and its deficiency in mice promotes prostate neoplasia. *J. Clin. Invest.* **121**, 4257-4267.

Pedraza, L. G., Stewart, R. A., Li, D.-M. and Xu, T. (2004). Drosophila Src-family kinases function with Csk to regulate cell proliferation and apoptosis. *Oncogene* **23**, 4754-4762.

Perez-Garijo, A., Shlevkov, E. and Morata, G. (2009). The role of Dpp and Wg in compensatory proliferation and in the formation of hyperplastic overgrowths caused by apoptotic cells in the Drosophila wing disc. *Development* **136**, 1169-1177.

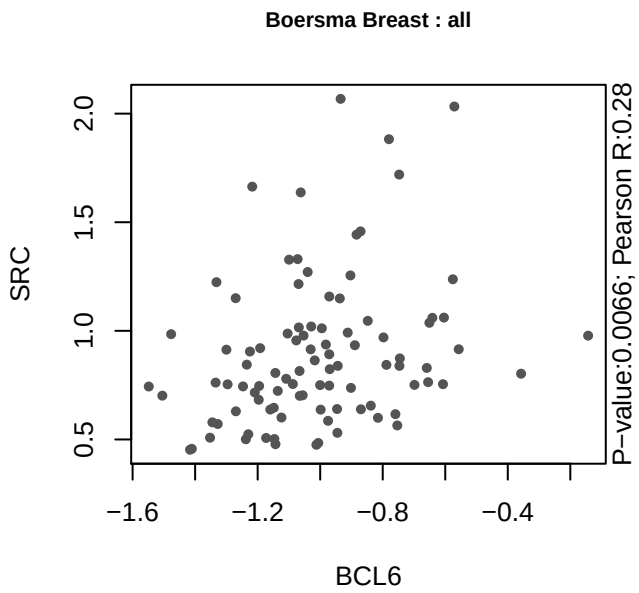
Pirraglia, C. and Myat, M. M. (2010). Genetic regulation of salivary gland development in Drosophila melanogaster. *Front. Oral Biol.* **14**, 32-47.

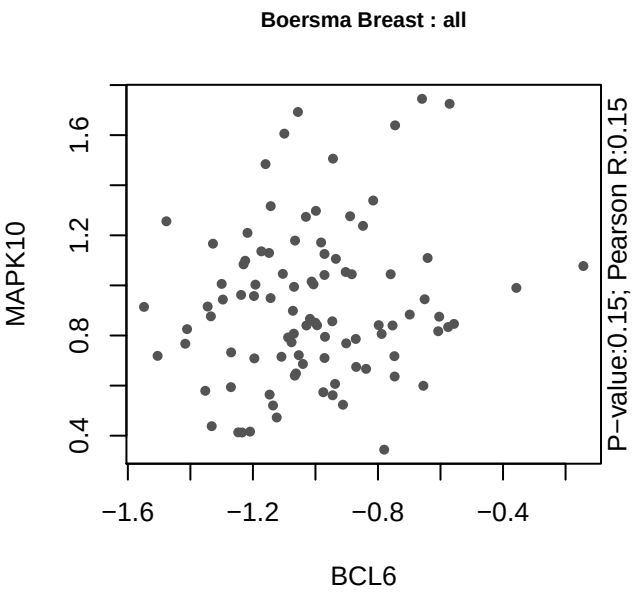
Pirraglia, C., Jattani, R. and Myat, M. M. (2006). Rac function in epithelial tube morphogenesis. *Dev. Biol.* **290**, 435-446.

Downloaded from http://bio.biologists.org/ at La Trobe University on December 16, 2020

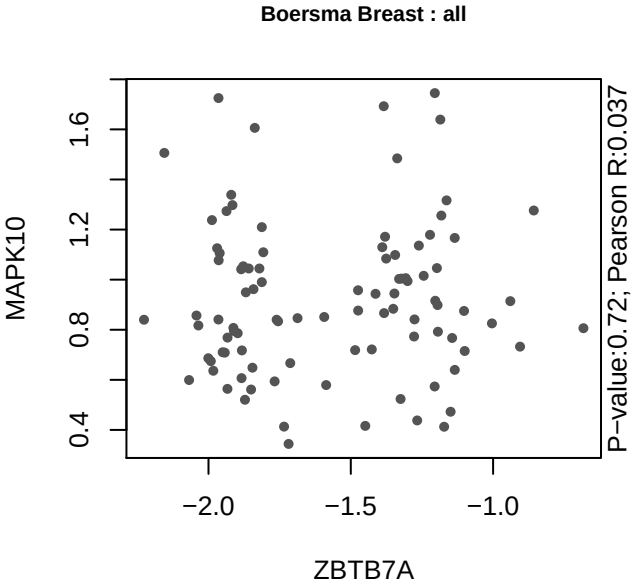
Qu, H., Qu, D., Chen, F., Zhang, Z., Liu, B. and Liu, H. (2010). ZBTB7 overexpression contributes to malignancy in breast cancer. *Cancer Invest.* **28**, 672-678.
Rauskolb, C., Sun, S., Sun, G., Pan, Y. and Irvine, K. D. (2014). Cytoskeletal tension inhibits Hippo signaling through an Ajuba-Warts complex. *Cell* **158**, 143-156.
Read, R. D., Bach, E. A. and Cagan, R. L. (2004). Drosophila C-terminal Src kinase negatively regulates organ growth and cell proliferation through inhibition of the Src, Jun N-terminal kinase, and STAT pathways. *Mol. Cell. Biol.* **24**, 6676-6689.
Rogers, S. L., Wiedemann, U., Häcker, U., Turck, C. and Vale, R. D. (2004). Drosophila RhoGEF2 associates with microtubule plus ends in an EB1-dependent manner. *Curr. Biol.* **14**, 1827-1833.
Rohrbeck, A., Neukirchen, J., Rosskopf, M., Pardillos, G. G., Geddert, H., Schwalen, A., Gabbert, H. E., von Haeseler, A., Pitschke, G., Schott, M. et al. (2008). Gene expression profiling for molecular distinction and characterization of laser captured primary lung cancers. *J. Transl. Med.* **6**, 69.
Roulier, E. M., Panzer, S. and Beckendorf, S. K. (1998). The Tec29 tyrosine kinase is required during Drosophila embryogenesis and interacts with Src64 in ring canal development. *Mol. Cell* **1**, 819-829.
Rudrapatna, V. A., Cagan, R. L. and Das, T. K. (2012). Drosophila cancer models. *Dev. Dyn.* **241**, 107-118.
Ryoo, H. D. and Bergmann, A. (2012). The role of apoptosis-induced proliferation for regeneration and cancer. *Cold Spring Harb. Perspect. Biol.* **4**, a008797.
Sansores-Garcia, L., Bossuyt, W., Wada, K.-I., Yonemura, S., Tao, C., Sasaki, H. and Halder, G. (2011). Modulating F-actin organization induces organ growth by affecting the Hippo pathway. *EMBO J.* **30**, 2325-2335.
Schmidt, A. and Hall, A. (2002). Guanine nucleotide exchange factors for Rho GTPases: turning on the switch. *Genes Dev.* **16**, 1587-1609.
Schroeder, M. C., Chen, C.-L., Gajewski, K. and Halder, G. (2013). A non-cell-autonomous tumor suppressor role for Stat in eliminating oncogenic scribble cells. *Oncogene* **32**, 4471-4479.
Sena, P., Mariani, F., Benincasa, M., De Leon, M. P., Di Gregorio, C., Mancini, S., Cavani, F., Smargiassi, A., Palumbo, C. and Roncucci, L. (2014). Morphological and quantitative analysis of BCL6 expression in human colorectal carcinogenesis. *Oncol. Rep.* **31**, 103-110.
Settleman, J. (1999). Rho GTPases in development. *Prog. Mol. Subcell. Biol.* **22**, 201-229.
Shen, W. and Mardon, G. (1997). Ectopic eye development in Drosophila induced by directed dachshund expression. *Development* **124**, 45-52.
Skrzypczak, M., Goryca, K., Rubel, T., Paziewska, A., Mikula, M., Jarosz, D., Pachlewski, J., Oledzki, J. and Ostrowski, J. (2010). Modeling oncogenic signaling in colon tumors by multidirectional analyses of microarray data directed for maximization of analytical reliability. *PLoS ONE* **5**, e13091.
Sotillos, S., Krahn, M., Espinosa-Vazquez, J. M. and Hombria, J. C.-G. (2013). Src kinases mediate the interaction of the apical determinant Bazooka/PAR3 with STAT92E and increase signalling efficiency in Drosophila ectodermal cells. *Development* **140**, 1507-1516.
Stefanatos, R. K. A. and Vidal, M. (2011). Tumor invasion and metastasis in Drosophila: a bold past, a bright future. *J. Genet. Genomics* **38**, 431-438.
Strong, T. C. and Thomas, J. H. (2011). Maternal and zygotic requirements for src64 during Drosophila cellularization. *Genesis* **49**, 912-918.
Szczepanowska, J. (2009). Involvement of Rac/Cdc42/PAK pathway in cytoskeletal rearrangements. *Acta Biochim. Pol.* **56**, 225-234.
Takahashi, F., Endo, S., Kojima, T. and Saigo, K. (1996). Regulation of cell-cell contacts in developing Drosophila eyes by Dsrc41, a new, close relative of vertebrate c-src. *Genes Dev.* **10**, 1645-1656.
Thomas, S. M. and Brugge, J. S. (1997). Cellular functions regulated by Src family kinases. *Annu. Rev. Cell Dev. Biol.* **13**, 513-609.
Tomlins, S. A., Mehra, R., Rhodes, D. R., Cao, X., Wang, L., Dhanasekaran, S. M., Kalyana-Sundaram, S., Wei, J. T., Rubin, M. A., Pienta, K. J. et al. (2007). Integrative molecular concept modeling of prostate cancer progression. *Nat. Genet.* **39**, 41-51.
Toruner, G. A., Ulger, C., Alkan, M., Galante, A. T., Rinaggio, J., Wilk, R., Tian, B., Soteropoulos, P., Hameed, M. R., Schwalb, M. N. et al. (2004). Association between gene expression profile and tumor invasion in oral squamous cell carcinoma. *Cancer Genet. Cytogenet.* **154**, 27-35.
Turkel, N., Sahota, V. K., Bolden, J. E., Goulding, K. R., Doggett, K., Willoughby, L. F., Blanco, E., Martin-Blanco, E., Corominas, M., Ellul, J. et al. (2013). The BTB-zinc finger transcription factor abrupt acts as an epithelial oncogene in Drosophila melanogaster through maintaining a progenitor-like cell state. *PLoS Genet.* **9**, e1003627.
Uhlirova, M. and Bohmann, D. (2006). JNK- and Fos-regulated Mmp1 expression cooperates with Ras to induce invasive tumors in Drosophila. *EMBO J.* **25**, 5294-5304.
Uhlirova, M., Jasper, H. and Bohmann, D. (2005). Non-cell-autonomous induction of tissue overgrowth by JNK/Ras cooperation in a Drosophila tumor model. *Proc. Natl. Acad. Sci. USA* **102**, 13123-13128.
Van Aelst, L. and D'Souza-Schorey, C. (1997). Rho GTPases and signaling networks. *Genes Dev.* **11**, 2295-2322.
Vidal, M., Larson, D. E. and Cagan, R. L. (2006). Csk-deficient boundary cells are eliminated from normal Drosophila epithelia by exclusion, migration, and apoptosis. *Dev. Cell* **10**, 33-44.
Vidal, M., Warner, S., Read, R. and Cagan, R. L. (2007). Differing Src signaling levels have distinct outcomes in Drosophila. *Cancer Res.* **67**, 10278-10285.
Vidal, M., Salavaggione, L., Ylagan, L., Wilkins, M., Watson, M., Weilbaecher, K. and Cagan, R. (2010). A role for the epithelial microenvironment at tumor boundaries: evidence from Drosophila and human squamous cell carcinomas. *Am. J. Pathol.* **176**, 3007-3014.
Walker, S. R., Liu, S., Xiang, M., Nicolais, M., Hatzi, K., Giannopoulou, E., Elemento, O., Cerchietti, L., Melnick, A. and Frank, D. A. (2014). The transcriptional modulator BCL6 as a molecular target for breast cancer therapy. *Oncogene* **34**, 1073-1082.
Willoughby, L. F., Schlosser, T., Manning, S. A., Parisot, J. P., Street, I. P., Richardson, H. E., Humbert, P. O. and Brumby, A. M. (2013). An in vivo large-scale chemical screening platform using Drosophila for anti-cancer drug discovery. *Dis. Model. Mech.* **6**, 521-529.
Worsham, M. J., Lu, M., Chen, K. M., Stephen, J. K., Havard, S. and Schweitzer, V. P. (2012). Malignant and nonmalignant gene signatures in squamous head and neck cancer. *J. Oncol.* **2012**, 752860.
Wu, Q., Liu, X., Yan, H., He, Y.-H., Ye, S., Cheng, X.-W., Zhu, G.-L., Wu, W.-Y., Wang, X.-N., Kong, X.-J. et al. (2014). B-cell lymphoma 6 protein stimulates oncogenicity of human breast cancer cells. *BMC Cancer* **14**, 418.
Zhai, Y., Kuick, R., Nan, B., Ota, I., Weiss, S. J., Trimble, C. L., Fearon, E. R. and Cho, K. R. (2007). Gene expression analysis of preinvasive and invasive cervical squamous cell carcinomas identifies HOXC10 as a key mediator of invasion. *Cancer Res.* **67**, 10163-10172.
Zhang, Y.-Q., Xiao, C.-X., Lin, B.-Y., Shi, Y., Liu, Y.-P., Liu, J.-J., Guleng, B. and Ren, J.-L. (2013). Silencing of Pokemon enhances caspase-dependent apoptosis via fas- and mitochondria-mediated pathways in hepatocellular carcinoma cells. *PLoS ONE* **8**, e68981.
Zhao, Z.-H., Wang, S.-F., Yu, L., Wang, J., Chang, H., Yan, W.-L., Zhang, J. and Fu, K. (2008). Overexpression of Pokemon in non-small cell lung cancer and foreshowing tumor biological behavior as well as clinical results. *Lung Cancer* **62**, 113-119.
Zhao, G.-T., Yang, L.-J., Li, X.-X., Cui, H.-L. and Guo, R. (2013). Expression of the proto-oncogene Pokemon in colorectal cancer–inhibitory effects of an siRNA. *Asian Pac. J. Cancer Prev.* **14**, 4999-5005.

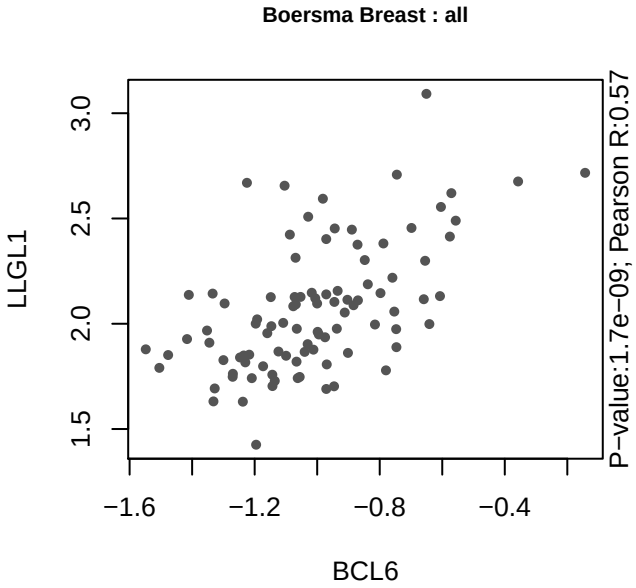
Downloaded from http://bio.biologists.org/ at La Trobe University on December 16, 2020

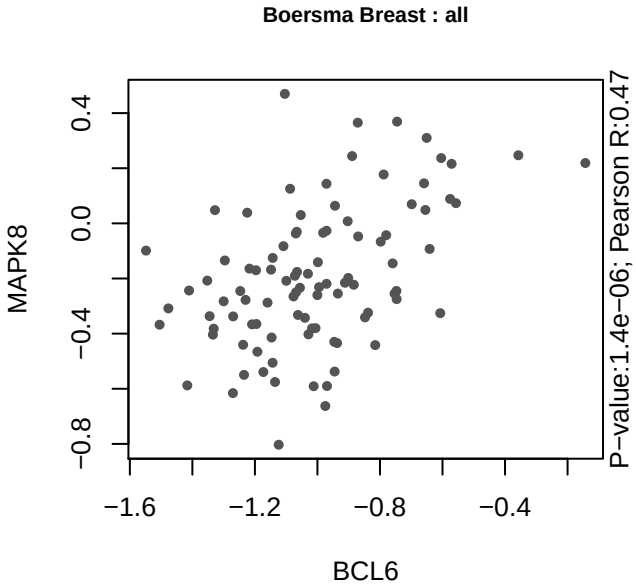

Boersma Breast : all
SRC
BCL6
P−value:0.0066; Pearson R:0.28
0.5
1.0
1.5
2.0
−1.6
−1.2
−0.8
−0.4

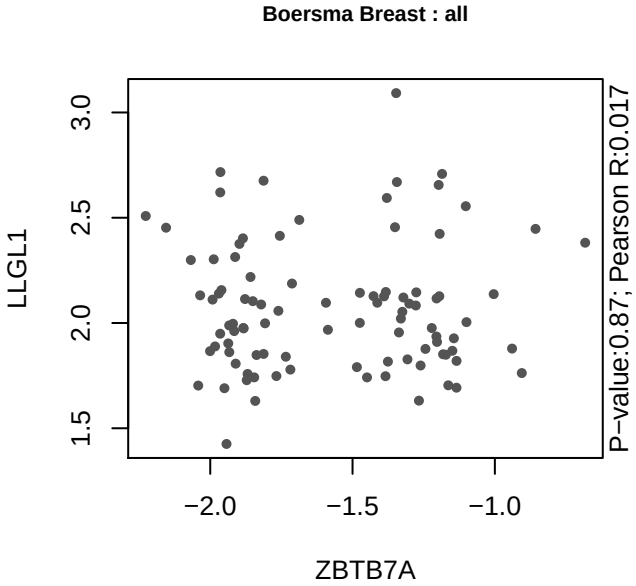

Boersma Breast : all
MAPK10
BCL6
P−value:0.15; Pearson R:0.15
0.4
0.8
1.2
1.6
−1.6
−1.2
−0.8
−0.4

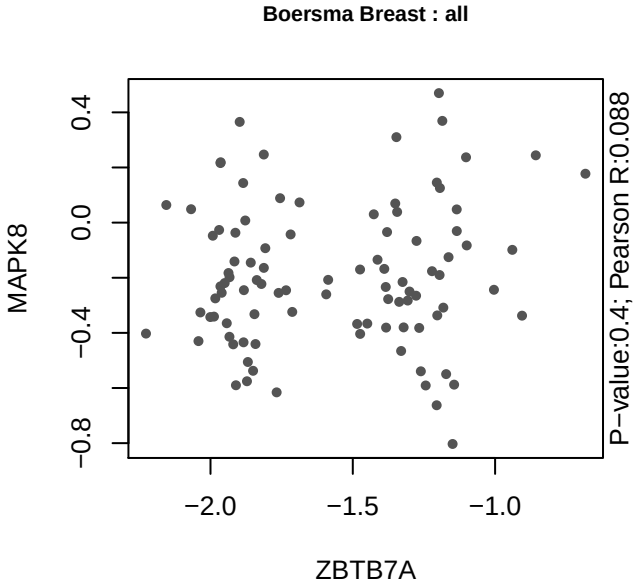

Boersma Breast : all
SRC
ZBTB7A
P−value:0.0033; Pearson R:−0.3
0.5
1.0
1.5
2.0
−2.0
−1.5
−1.0

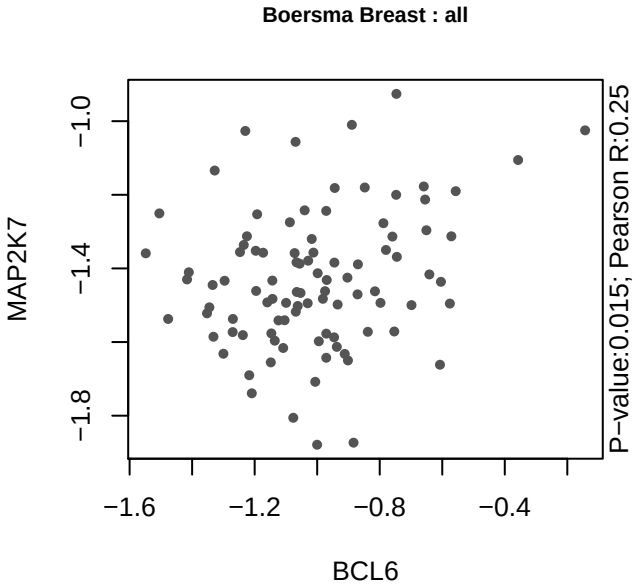

Boersma Breast : all
MAPK10
ZBTB7A
P−value:0.72; Pearson R:0.037
0.4
0.8
1.2
1.6
−2.0
−1.5
−1.0

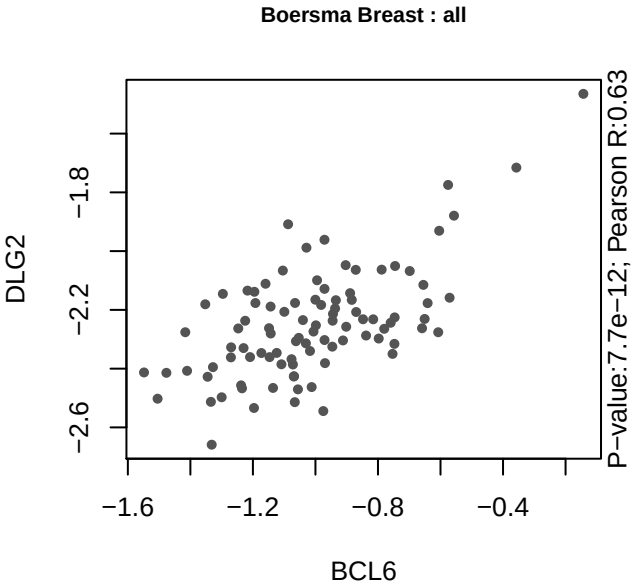

Boersma Breast : all
LLGL1
BCL6
P−value:1.7e−09; Pearson R:0.57

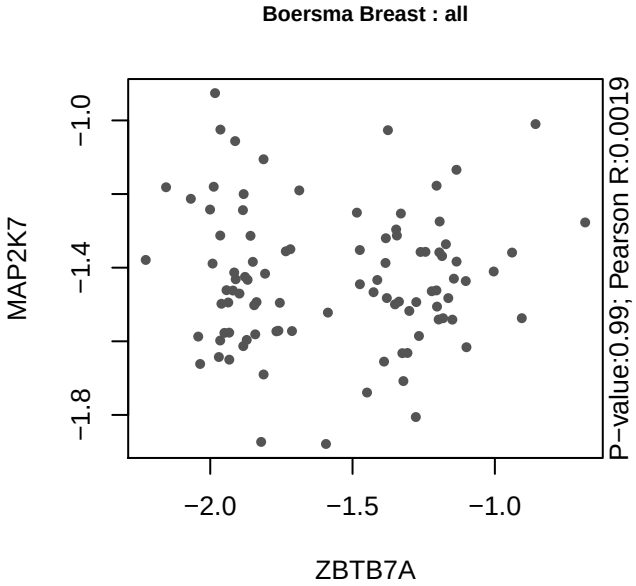

Boersma Breast : all
MAPK8
BCL6
P−value:1.4e−06; Pearson R:0.47

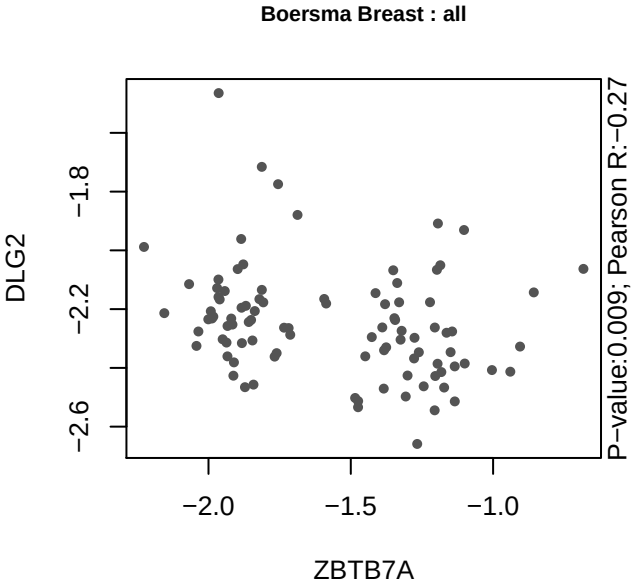

Boersma Breast : all
LLGL1
ZBTB7A
P−value:0.87; Pearson R:0.017

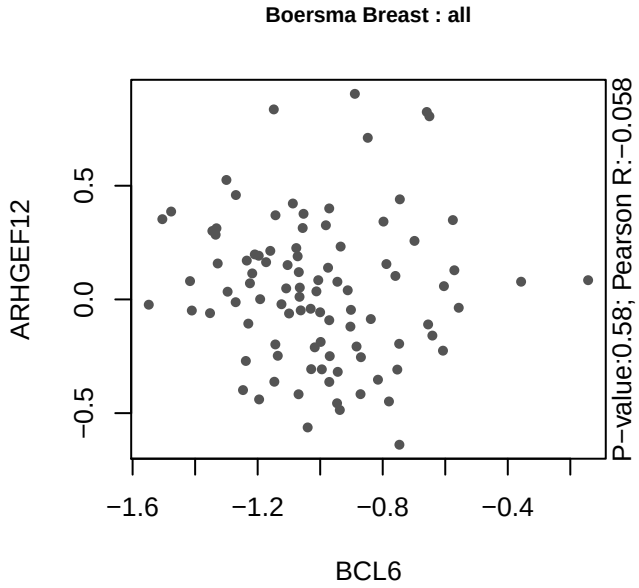

Boersma Breast : all
MAPK8
ZBTB7A
P−value:0.4; Pearson R:0.088

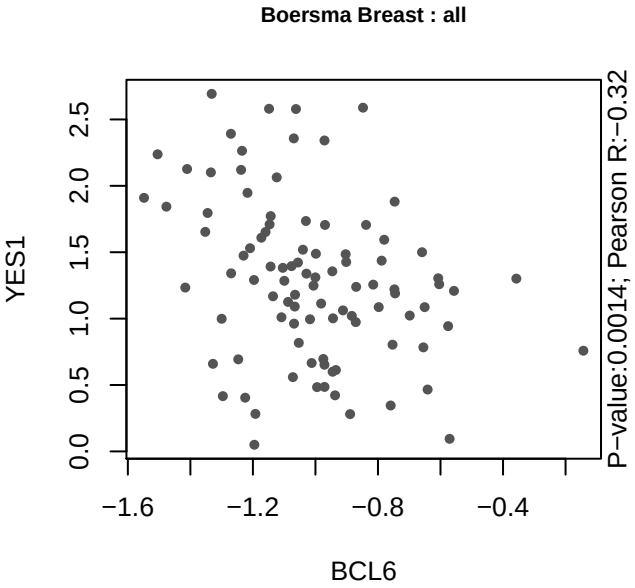

Boersma Breast : all
MAP2K7
BCL6
P−value:0.015; Pearson R:0.25


Boersma Breast : all
DLG2
BCL6
P−value:7.7e−12; Pearson R:0.63

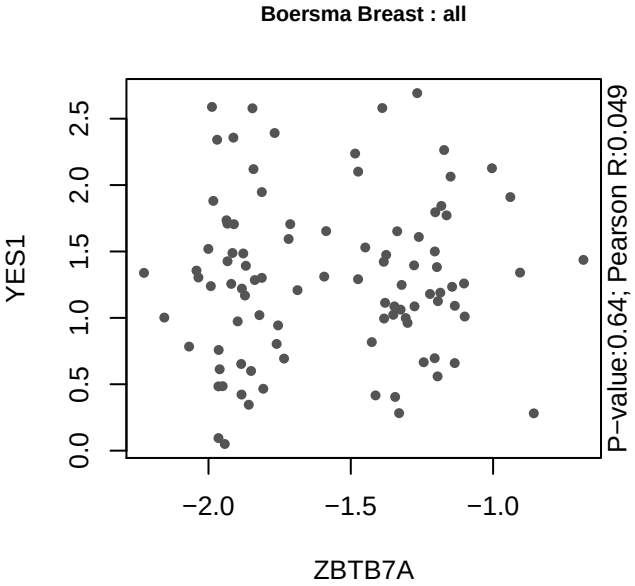

Boersma Breast : all
MAP2K7
ZBTB7A
P−value:0.99; Pearson R:0.0019

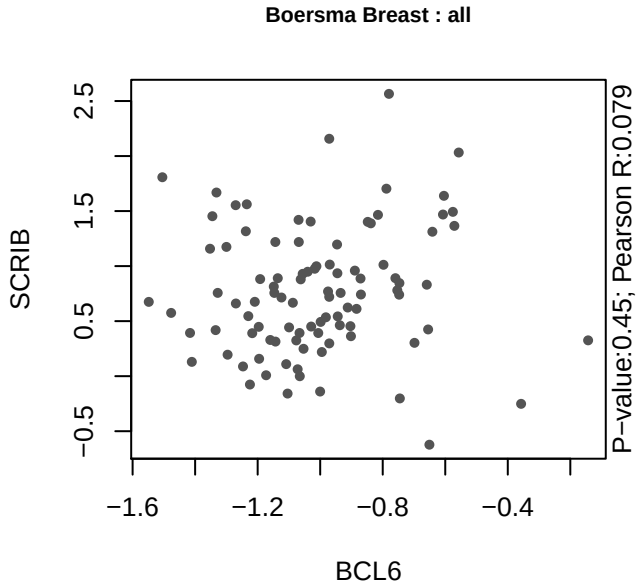

Boersma Breast : all
DLG2
ZBTB7A
P−value:0.009; Pearson R:−0.27

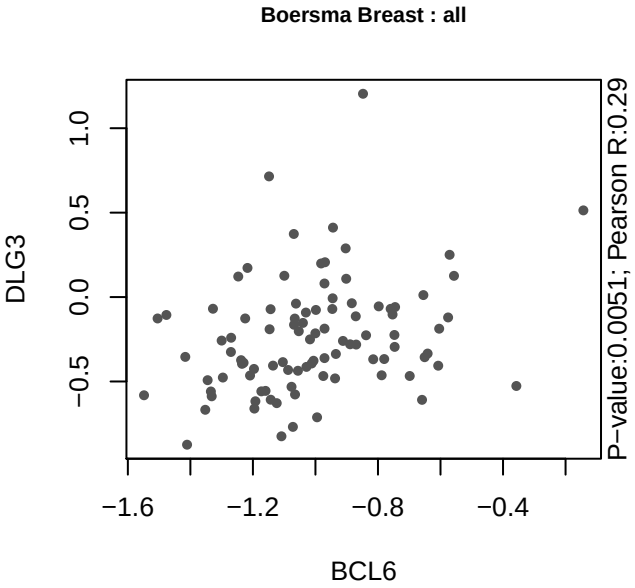

Boersma Breast : all
ARHGEF12
BCL6
P−value:0.58; Pearson R:−0.058


Boersma Breast : all
YES1
BCL6
P−value:0.0014; Pearson R:−0.32

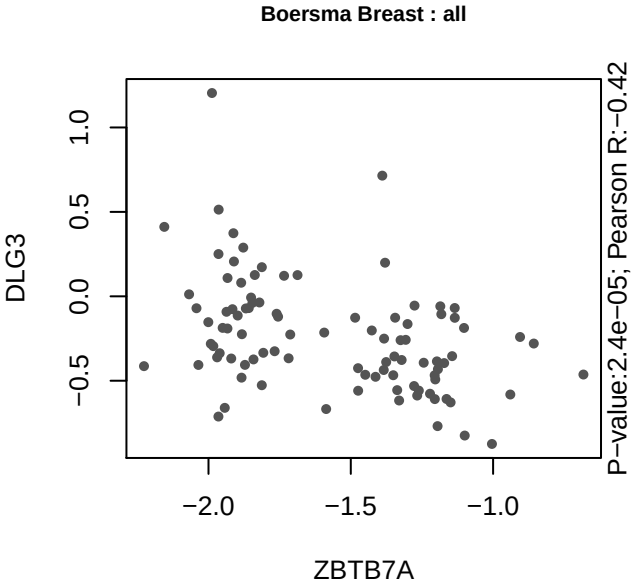

Boersma Breast : all
ARHGEF12
ZBTB7A
P−value:4.9e−10; Pearson R:0.58

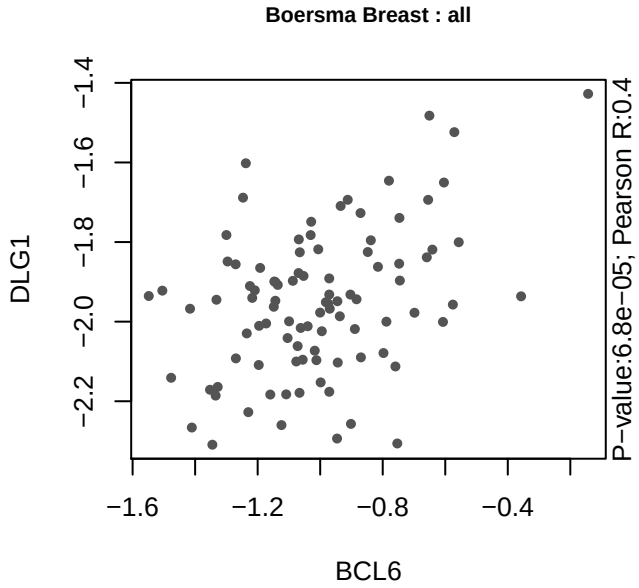

Boersma Breast : all
YES1
ZBTB7A
P−value:0.64; Pearson R:0.049

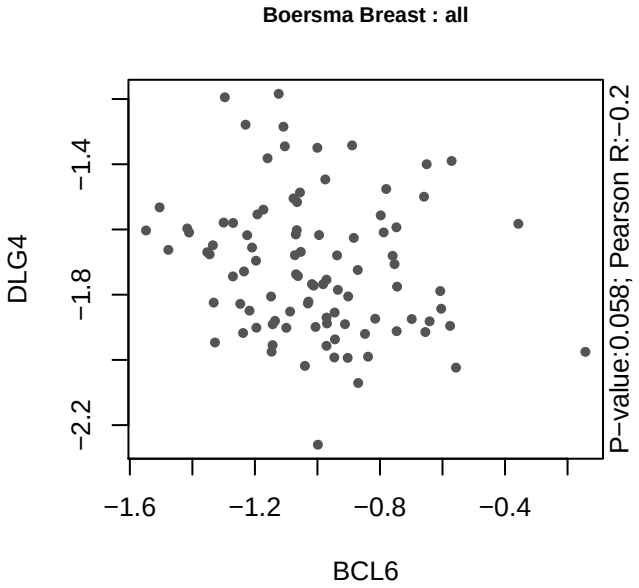

Boersma Breast : all
SCRIB
BCL6
P−value:0.45; Pearson R:0.079

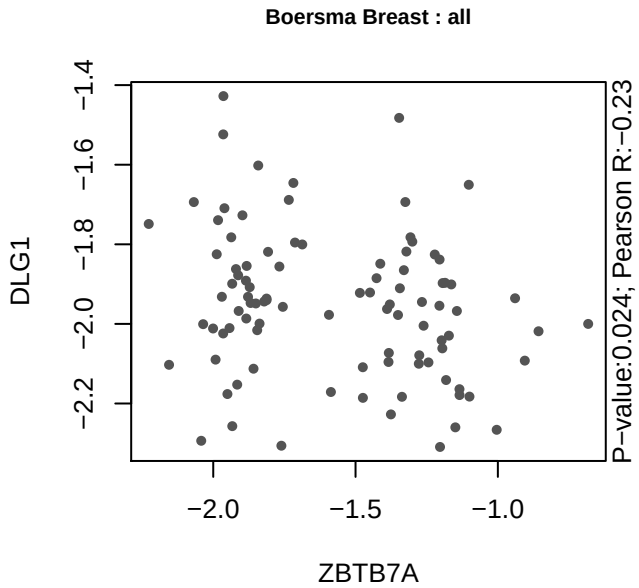

Boersma Breast : all
DLG3
BCL6
P−value:0.0051; Pearson R:0.29

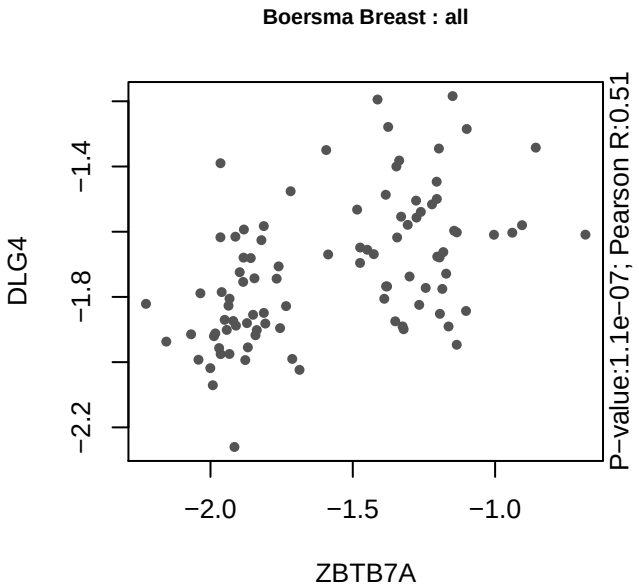

Boersma Breast : all
SCRIB
ZBTB7A
P−value:0.14; Pearson R:−0.15

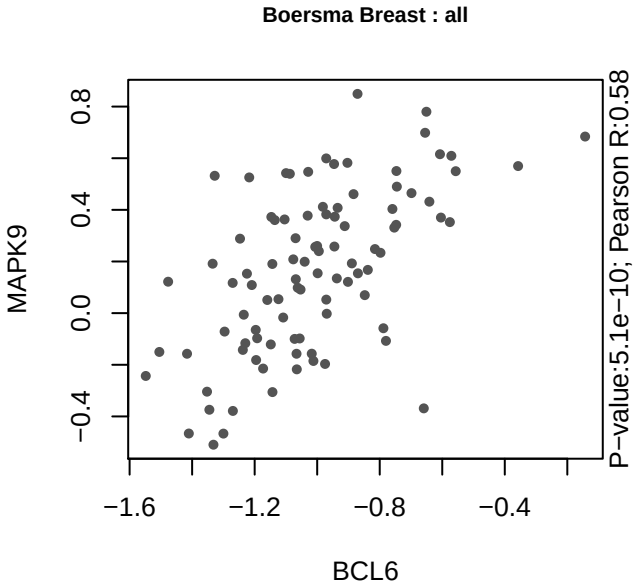

Boersma Breast : all
DLG3
ZBTB7A
P−value:2.4e−05; Pearson R:−0.42

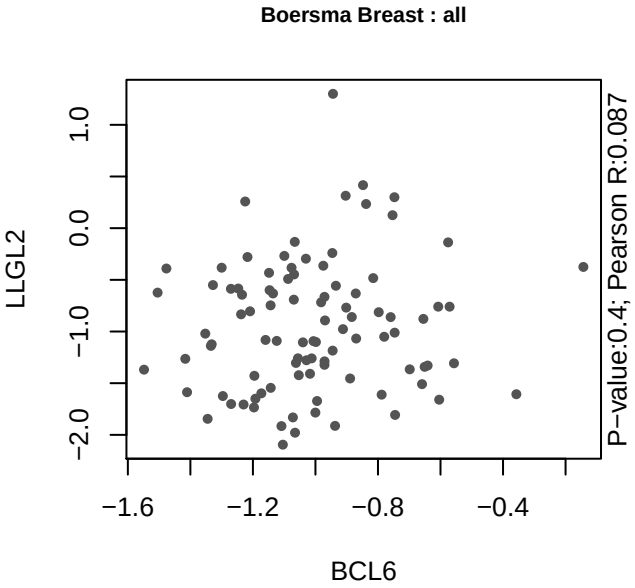

Boersma Breast : all
DLG1
BCL6
P−value:6.8e−05; Pearson R:0.4
−1.4
−1.6
−1.8
−2.0
−2.2
−1.6
−1.2
−0.8
−0.4

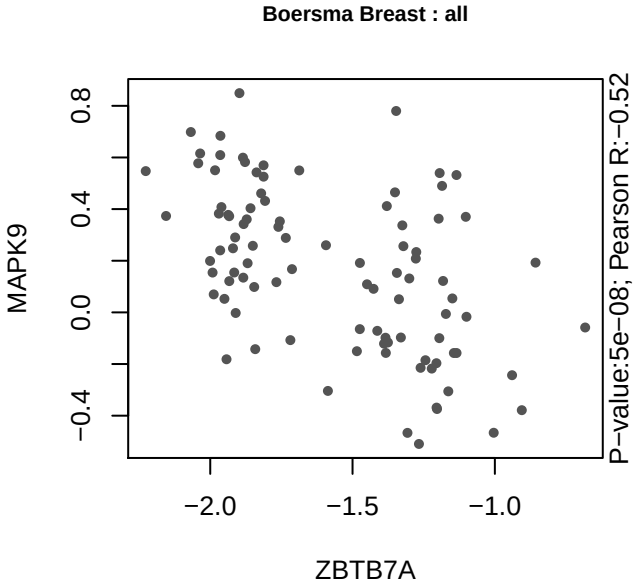

Boersma Breast : all
DLG4
BCL6
P−value:0.058; Pearson R:−0.2
−1.4
−1.8
−2.2
−1.6
−1.2
−0.8
−0.4

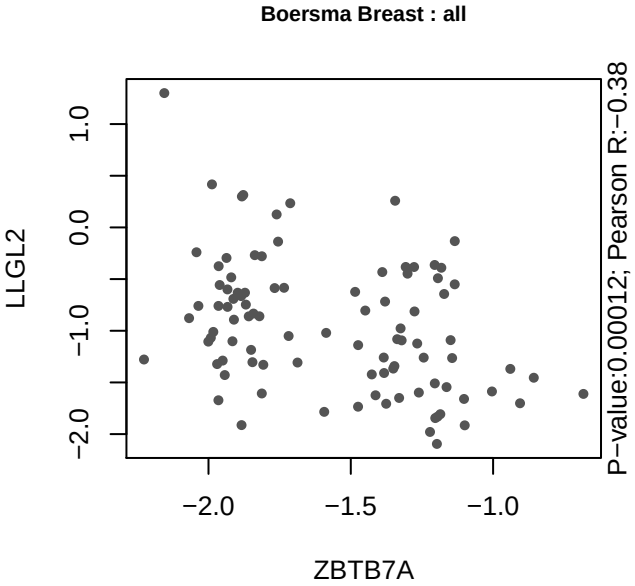

Boersma Breast : all
DLG1
ZBTB7A
P−value:0.024; Pearson R:−0.23
−1.4
−1.6
−1.8
−2.0
−2.2
−2.0
−1.5
−1.0

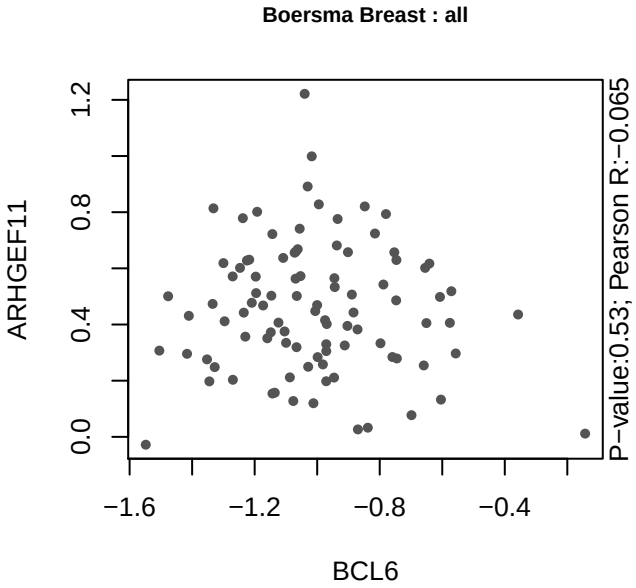

Boersma Breast : all
DLG4
ZBTB7A
P−value:1.1e−07; Pearson R:0.51
−1.4
−1.8
−2.2
−2.0
−1.5
−1.0

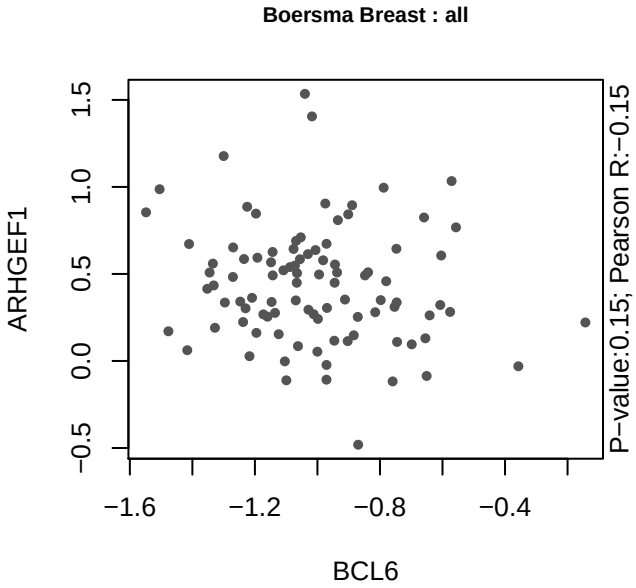

Boersma Breast : all
MAPK9
BCL6
P−value:5.1e−10; Pearson R:0.58

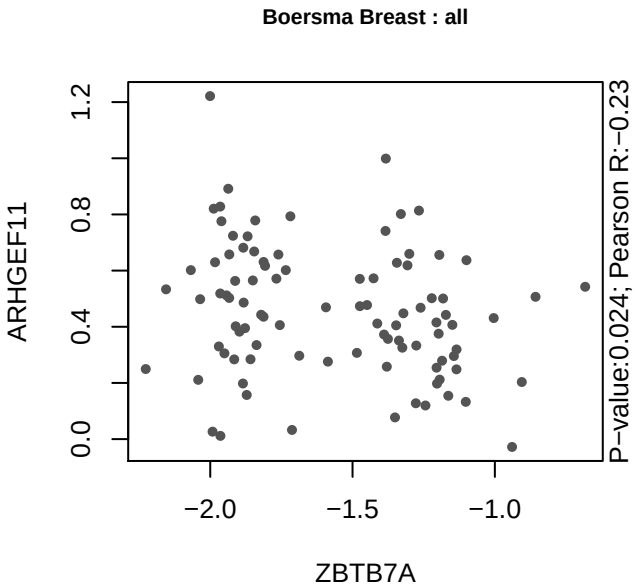

Boersma Breast : all
LLGL2
BCL6
P−value:0.4; Pearson R:0.087

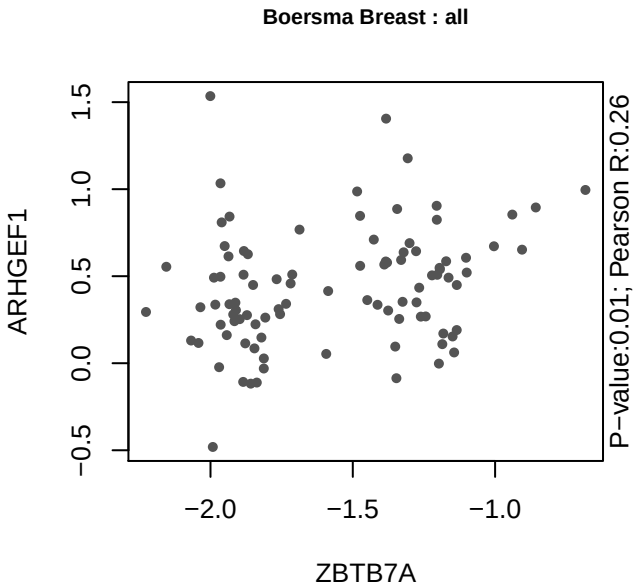

Boersma Breast : all
MAPK9
ZBTB7A
P−value:5e−08; Pearson R:−0.52

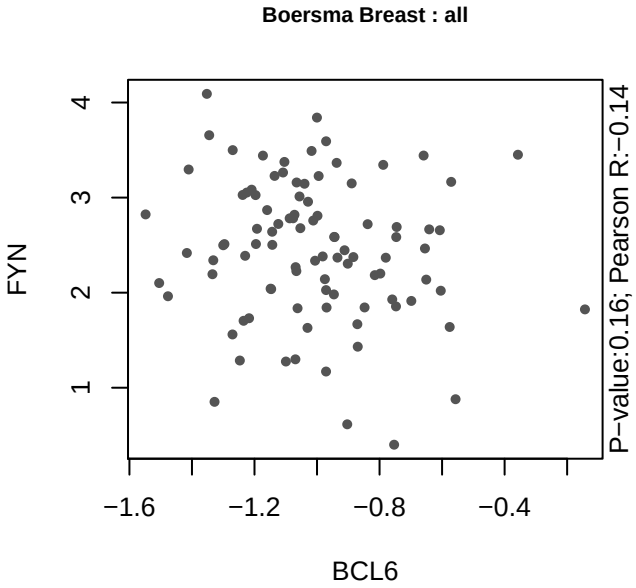

Boersma Breast : all
LLGL2
ZBTB7A
P−value:0.00012; Pearson R:−0.38

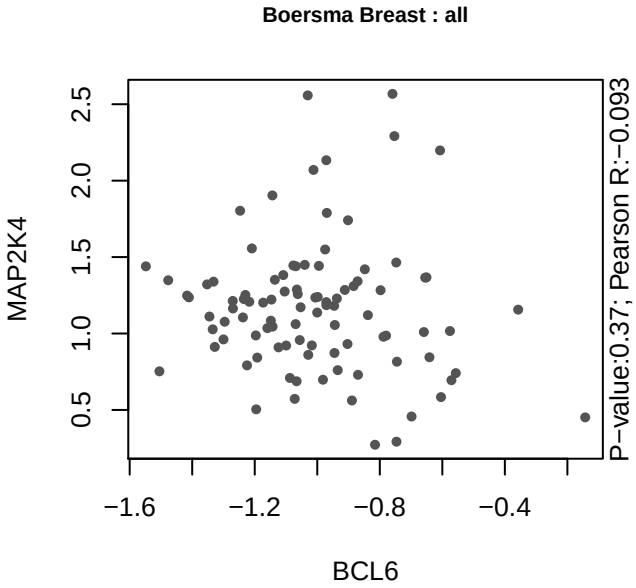

Boersma Breast : all
ARHGEF11
BCL6
P−value:0.53; Pearson R:−0.065
0.0
0.4
0.8
1.2
−1.6
−1.2
−0.8
−0.4

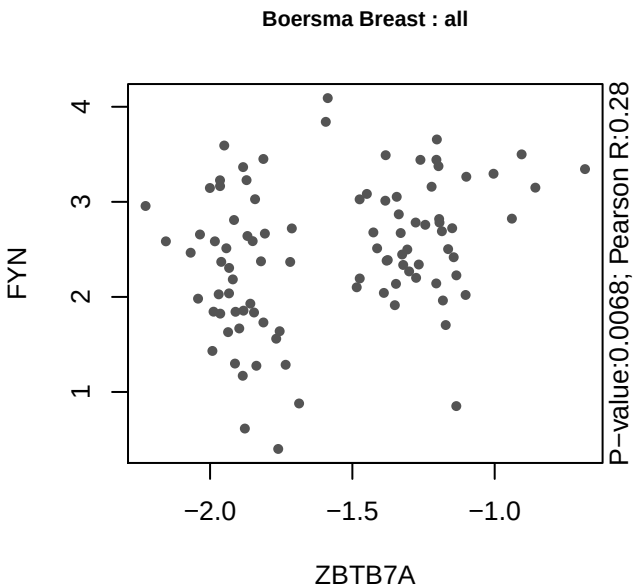

Boersma Breast : all
ARHGEF1
BCL6
P−value:0.15; Pearson R:−0.15
−0.5
0.0
0.5
1.0
1.5
−1.6
−1.2
−0.8
−0.4

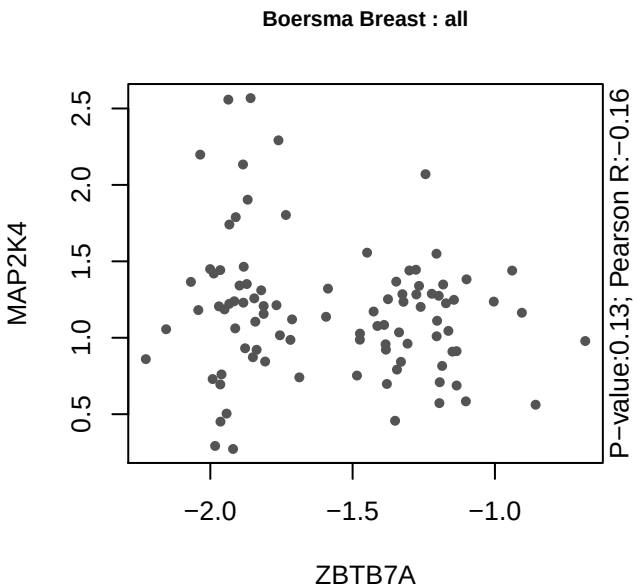

Boersma Breast : all
ARHGEF11
ZBTB7A
P−value:0.024; Pearson R:−0.23
0.0
0.4
0.8
1.2
−2.0
−1.5
−1.0

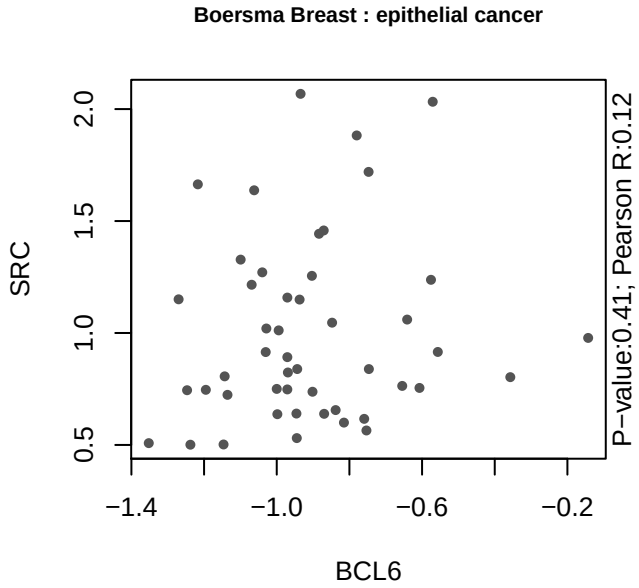

Boersma Breast : all
ARHGEF1
ZBTB7A
P−value:0.01; Pearson R:0.26
−0.5
0.0
0.5
1.0
1.5
−2.0
−1.5
−1.0

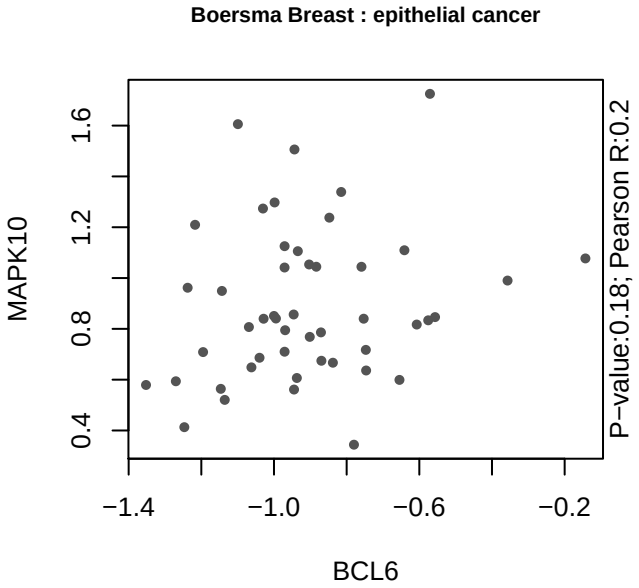

Boersma Breast : all
FYN
BCL6
P−value:0.16; Pearson R:−0.14
1
2
3
4
−1.6
−1.2
−0.8
−0.4

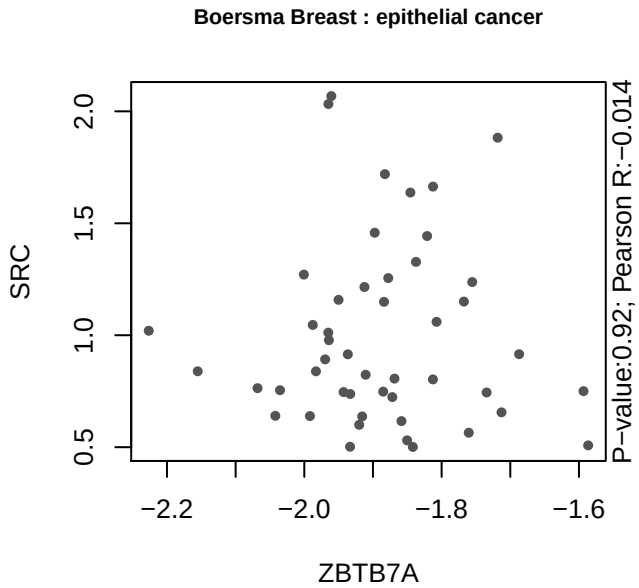

Boersma Breast : all
MAP2K4
BCL6
P−value:0.37; Pearson R:−0.093
0.5
1.0
1.5
2.0
2.5
−1.6
−1.2
−0.8
−0.4

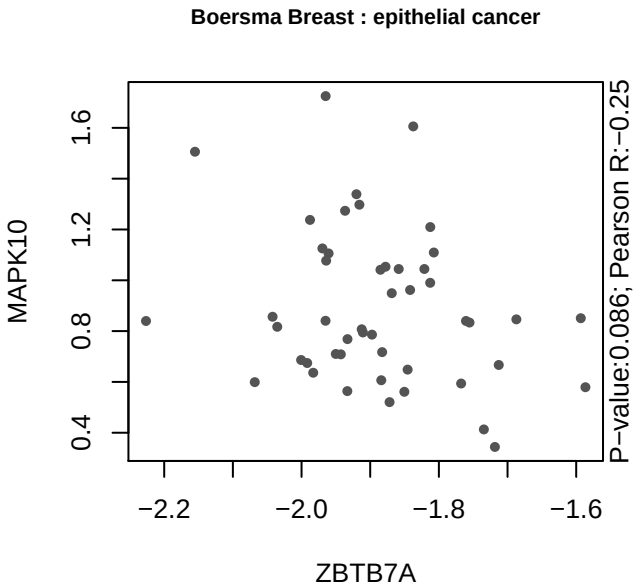

Boersma Breast : all
FYN
ZBTB7A
P−value:0.0068; Pearson R:0.28
1
2
3
4
−2.0
−1.5
−1.0

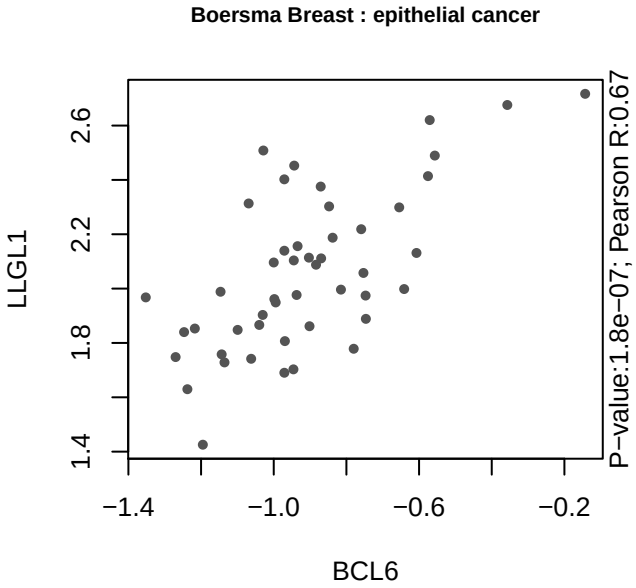

Boersma Breast : all
MAP2K4
ZBTB7A
P−value:0.13; Pearson R:−0.16
0.5
1.0
1.5
2.0
2.5
−2.0
−1.5
−1.0

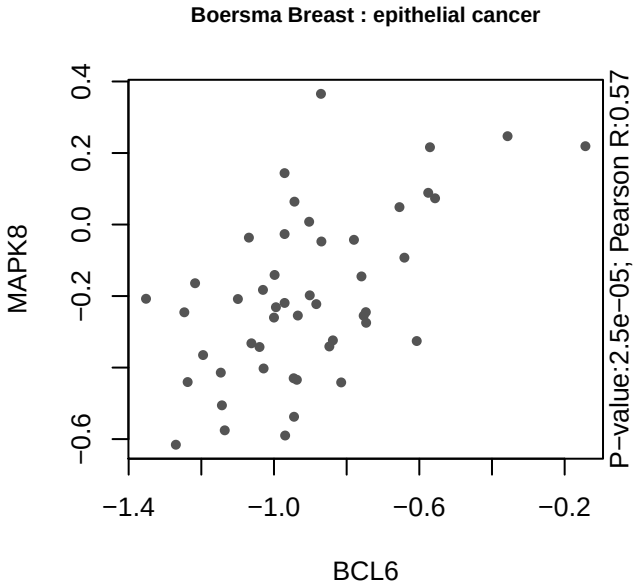

Boersma Breast : epithelial cancer
SRC
BCL6
P−value:0.41; Pearson R:0.12
0.5
1.0
1.5
2.0
−1.4
−1.0
−0.6
−0.2

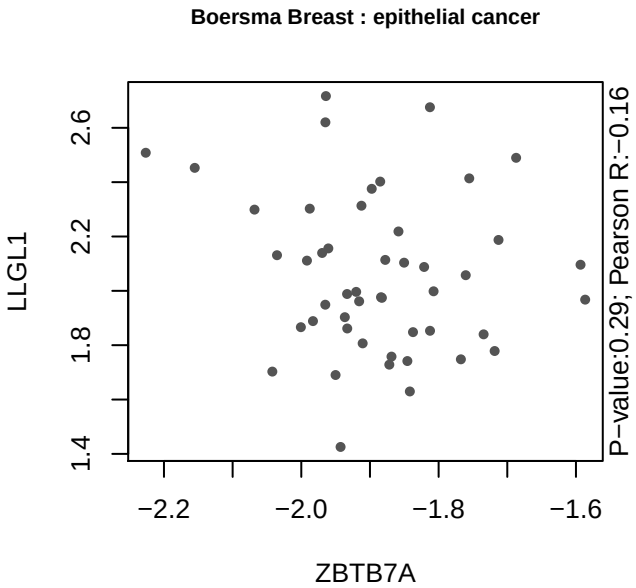

Boersma Breast : epithelial cancer
MAPK10
BCL6
P−value:0.18; Pearson R:0.2
0.4
0.8
1.2
1.6
−1.4
−1.0
−0.6
−0.2

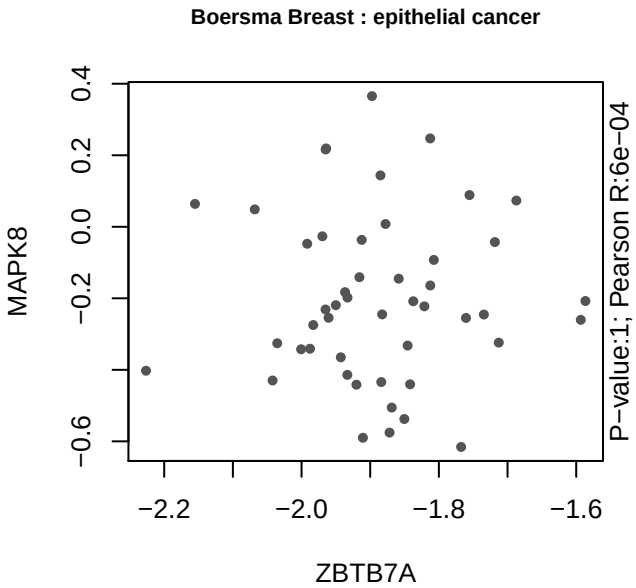

Boersma Breast : epithelial cancer
SRC
ZBTB7A
P−value:0.92; Pearson R:−0.014
0.5
1.0
1.5
2.0
−2.2
−2.0
−1.8
−1.6

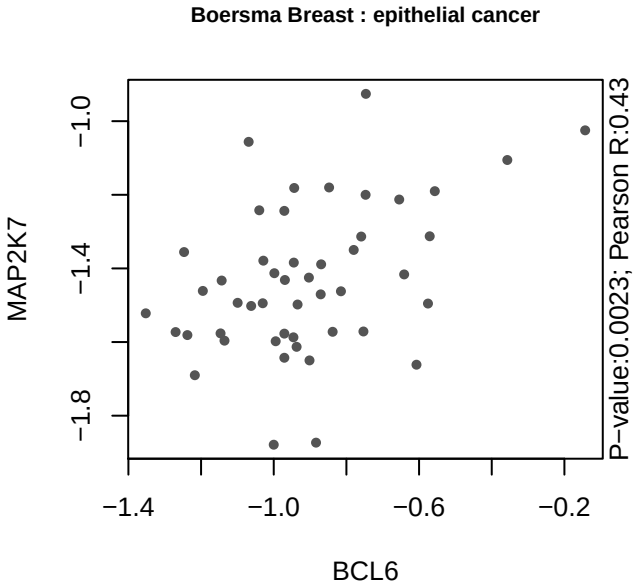

Boersma Breast : epithelial cancer
MAPK10
ZBTB7A
P−value:0.086; Pearson R:−0.25
0.4
0.8
1.2
1.6
−2.2
−2.0
−1.8
−1.6

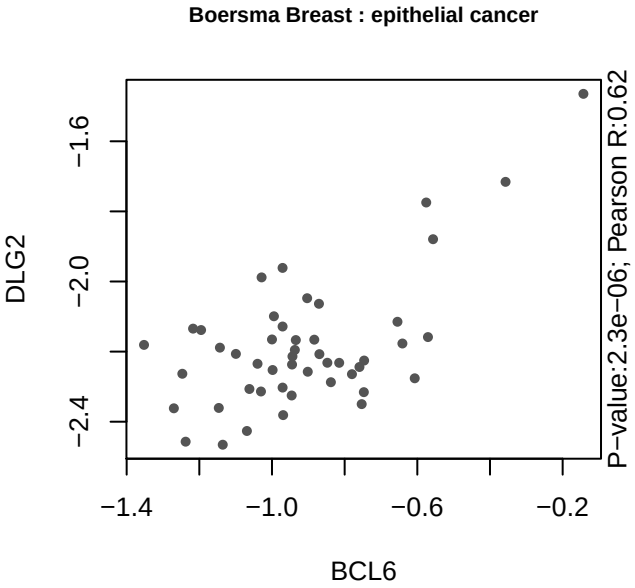

Boersma Breast : epithelial cancer
LLGL1
BCL6
P−value:1.8e−07; Pearson R:0.67
1.4
1.8
2.2
2.6
−1.4
−1.0
−0.6
−0.2

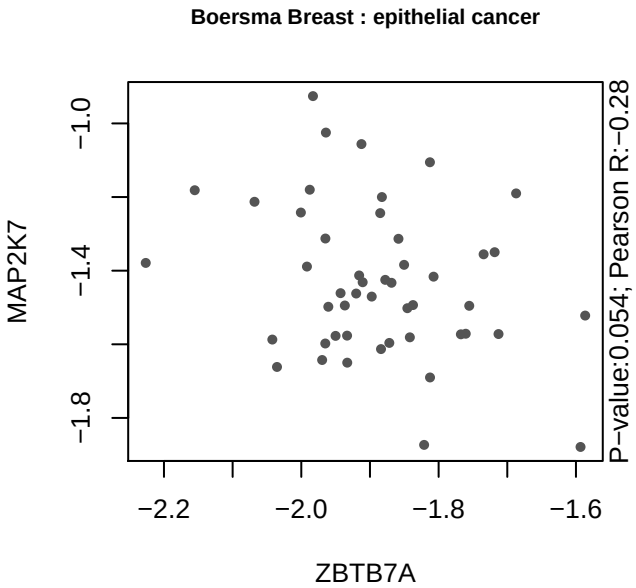

Boersma Breast : epithelial cancer
MAPK8
BCL6
P−value:2.5e−05; Pearson R:0.57
−0.6
−0.2
0.0
0.2
0.4
−1.4
−1.0
−0.6
−0.2

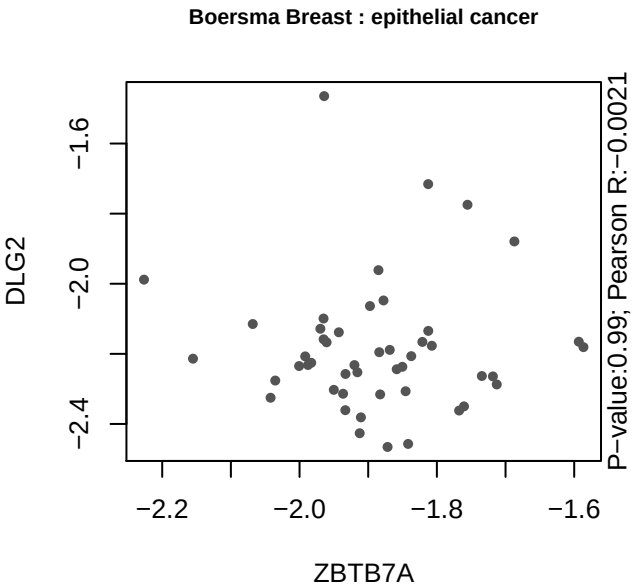

Boersma Breast : epithelial cancer
LLGL1
ZBTB7A
P−value:0.29; Pearson R:−0.16
1.4
1.8
2.2
2.6
−2.2
−2.0
−1.8
−1.6

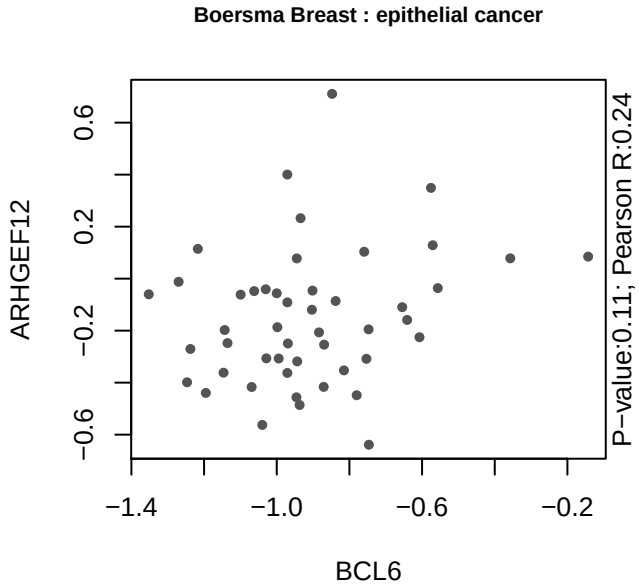

Boersma Breast : epithelial cancer
MAPK8
ZBTB7A
P−value:1; Pearson R:6e−04
−0.6
−0.2
0.0
0.2
0.4
−2.2
−2.0
−1.8
−1.6

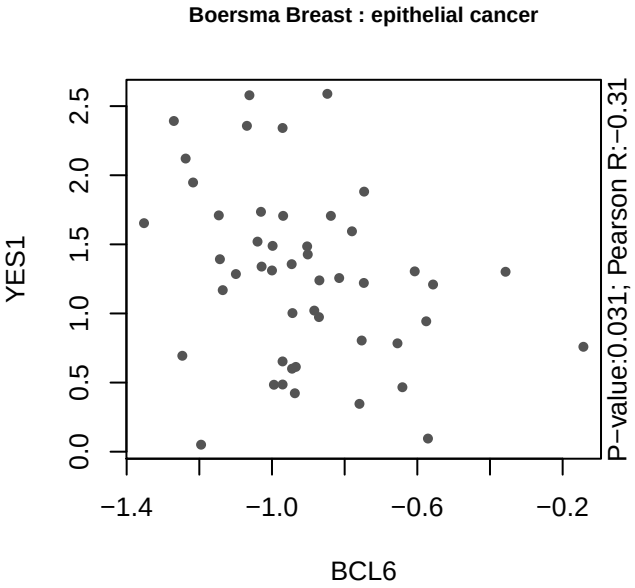

Boersma Breast : epithelial cancer
MAP2K7
BCL6
P−value:0.0023; Pearson R:0.43
−1.0
−1.4
−1.8
−1.4
−1.0
−0.6
−0.2

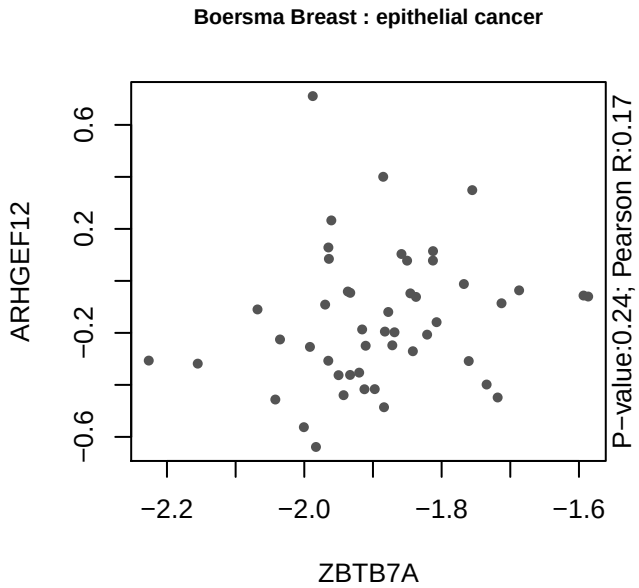

Boersma Breast : epithelial cancer
DLG2
BCL6
P−value:2.3e−06; Pearson R:0.62
−1.6
−2.0
−2.4
−1.4
−1.0
−0.6
−0.2

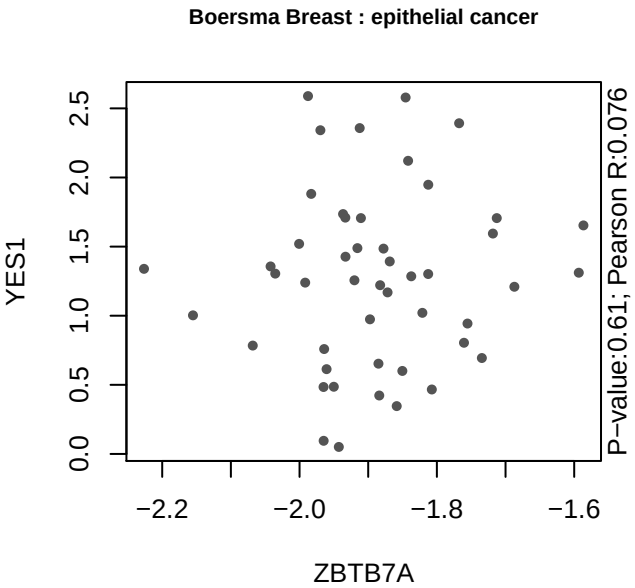

Boersma Breast : epithelial cancer
MAP2K7
ZBTB7A
P−value:0.054; Pearson R:−0.28
−1.0
−1.4
−1.8
−2.2
−2.0
−1.8
−1.6

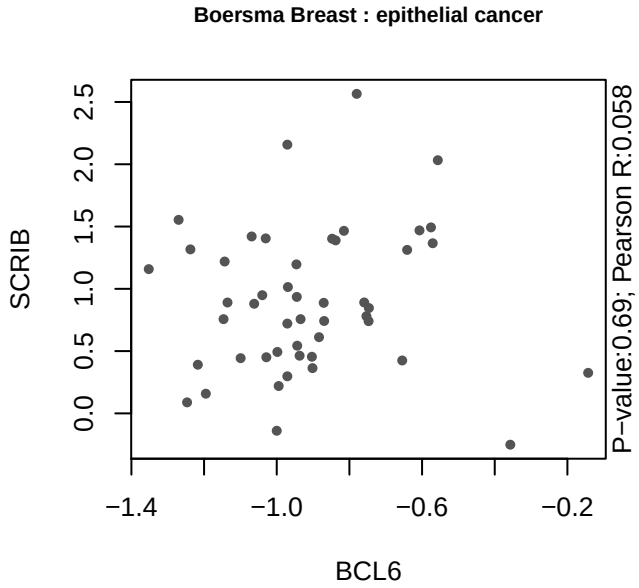

Boersma Breast : epithelial cancer
DLG2
ZBTB7A
P−value:0.99; Pearson R:−0.0021
−1.6
−2.0
−2.4
−2.2
−2.0
−1.8
−1.6

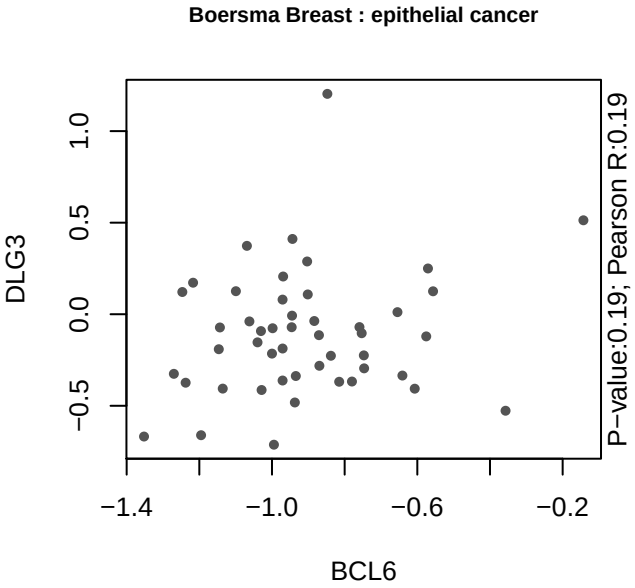

Boersma Breast : epithelial cancer
ARHGEF12
BCL6
P−value:0.11; Pearson R:0.24
0.6
0.2
−0.2
−0.6
−1.4
−1.0
−0.6
−0.2

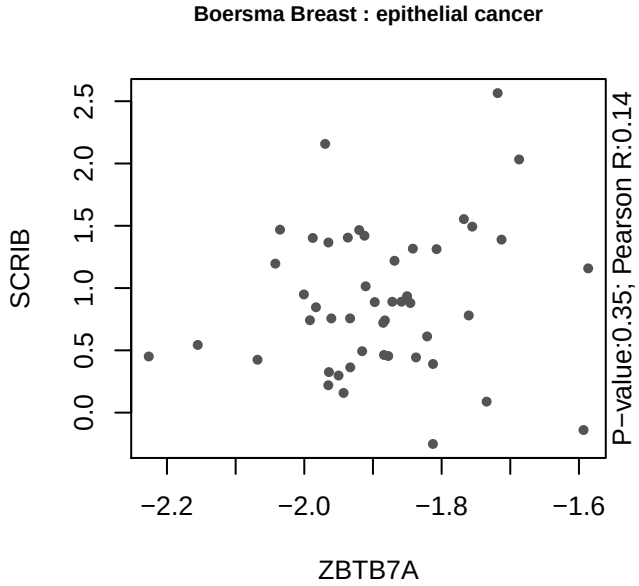

Boersma Breast : epithelial cancer
YES1
BCL6
P−value:0.031; Pearson R:−0.31
2.5
2.0
1.5
1.0
0.5
0.0
−1.4
−1.0
−0.6
−0.2

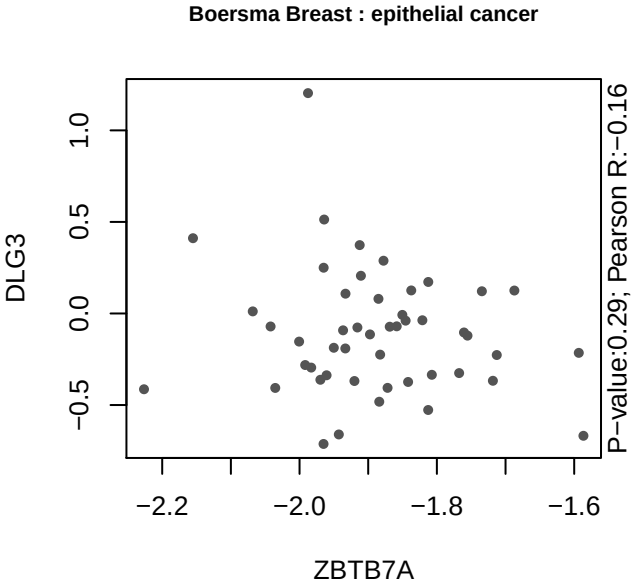

Boersma Breast : epithelial cancer
ARHGEF12
ZBTB7A
P−value:0.24; Pearson R:0.17
0.6
0.2
−0.2
−0.6
−2.2
−2.0
−1.8
−1.6

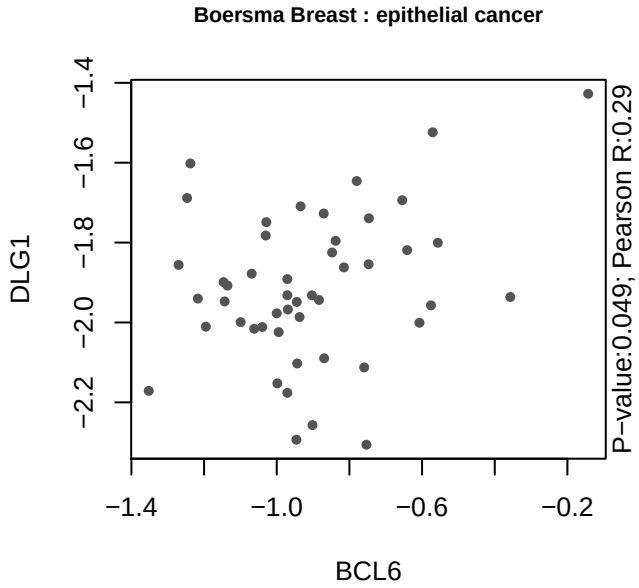

Boersma Breast : epithelial cancer
YES1
ZBTB7A
P−value:0.61; Pearson R:0.076
2.5
2.0
1.5
1.0
0.5
0.0
−2.2
−2.0
−1.8
−1.6

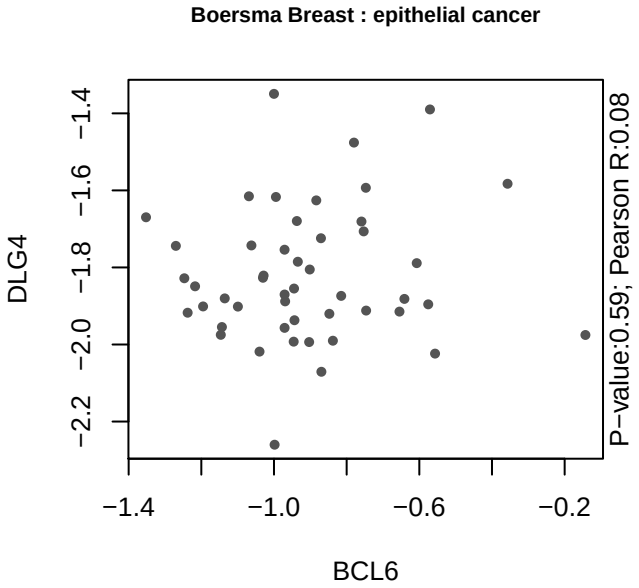

Boersma Breast : epithelial cancer
SCRIB
BCL6
P−value:0.69; Pearson R:0.058

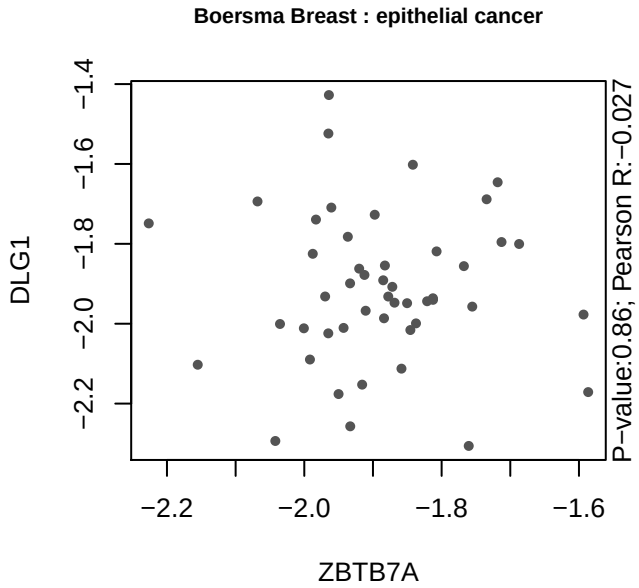

Boersma Breast : epithelial cancer
DLG3
BCL6
P−value:0.19; Pearson R:0.19

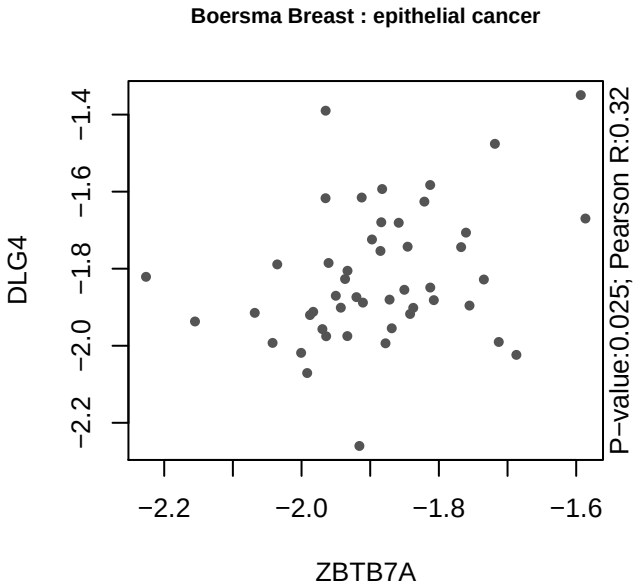

Boersma Breast : epithelial cancer
SCRIB
ZBTB7A
P−value:0.35; Pearson R:0.14

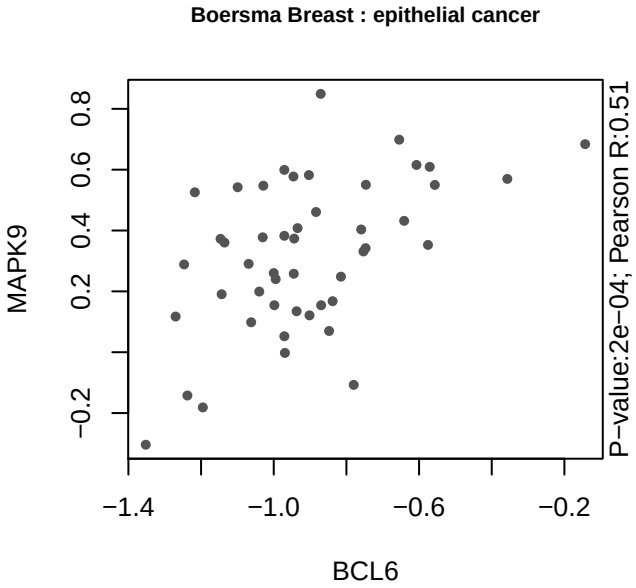

Boersma Breast : epithelial cancer
DLG3
ZBTB7A
P−value:0.29; Pearson R:−0.16

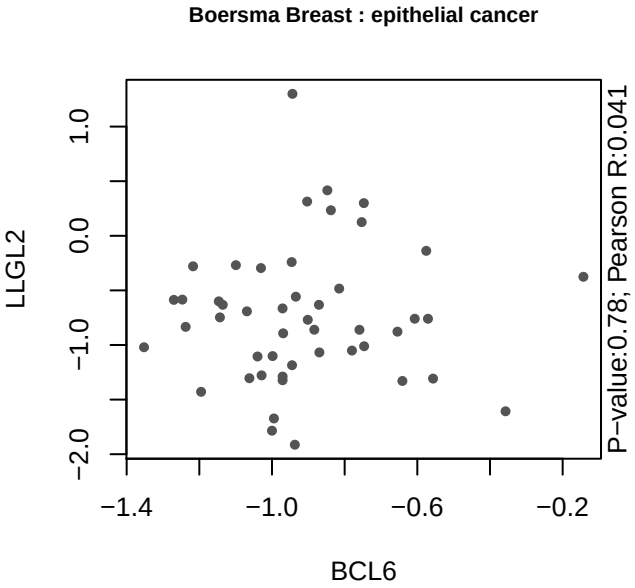

Boersma Breast : epithelial cancer
DLG1
BCL6
P−value:0.049; Pearson R:0.29
−1.4
−1.6
−1.8
−2.0
−2.2
−1.4
−1.0
−0.6
−0.2

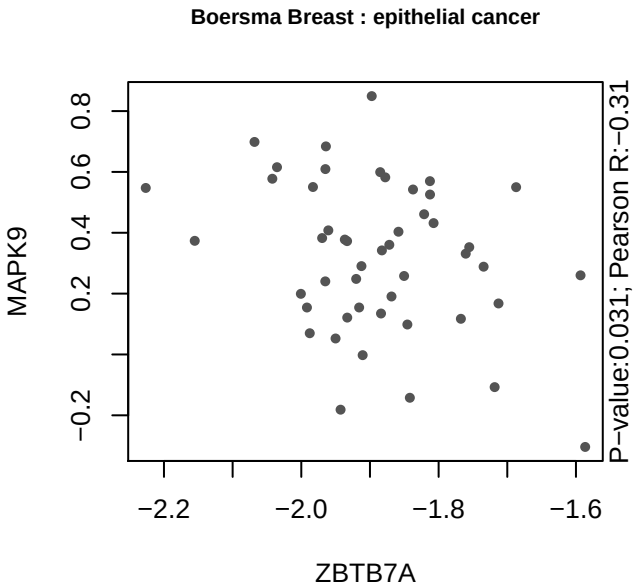

Boersma Breast : epithelial cancer
DLG4
BCL6
P−value:0.59; Pearson R:0.08
−1.4
−1.6
−1.8
−2.0
−2.2
−1.4
−1.0
−0.6
−0.2

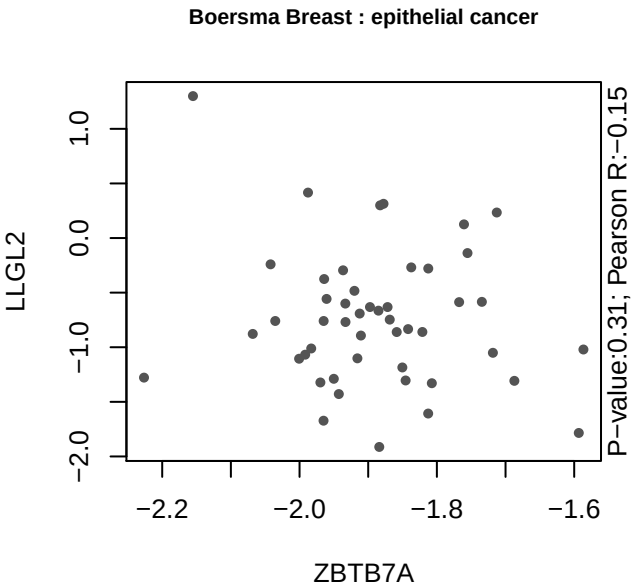

Boersma Breast : epithelial cancer
DLG1
ZBTB7A
P−value:0.86; Pearson R:−0.027
−1.4
−1.6
−1.8
−2.0
−2.2
−2.2
−2.0
−1.8
−1.6

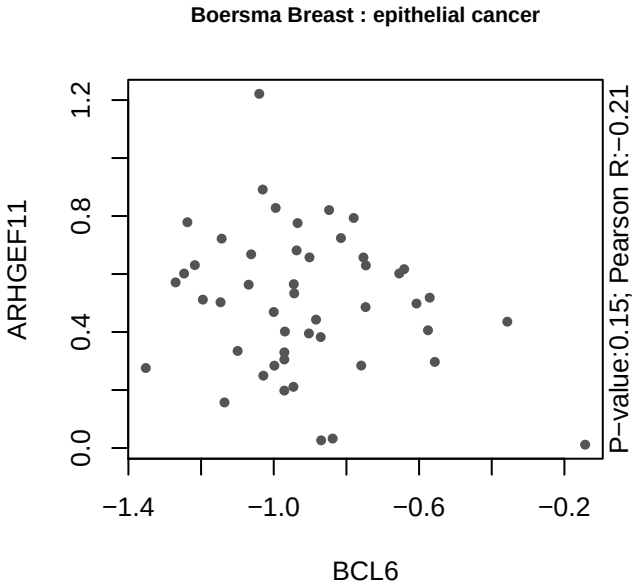

Boersma Breast : epithelial cancer
DLG4
ZBTB7A
P−value:0.025; Pearson R:0.32
−1.4
−1.6
−1.8
−2.0
−2.2
−2.2
−2.0
−1.8
−1.6

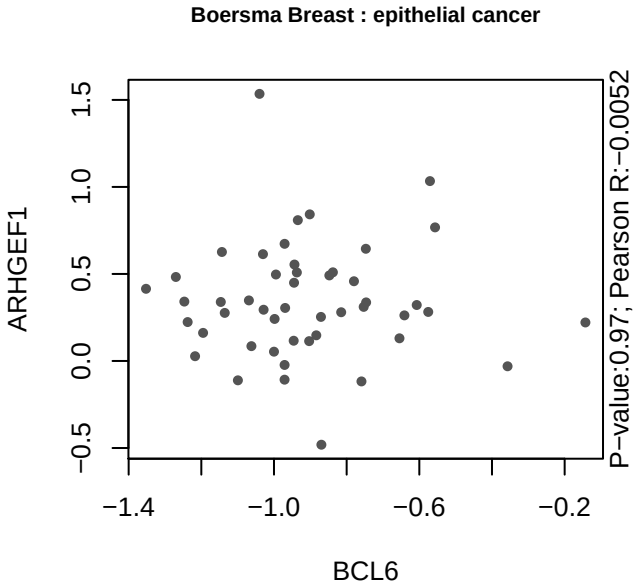

Boersma Breast : epithelial cancer
MAPK9
BCL6
P−value:2e−04; Pearson R:0.51
−0.2
0.2
0.4
0.6
0.8
−1.4
−1.0
−0.6
−0.2

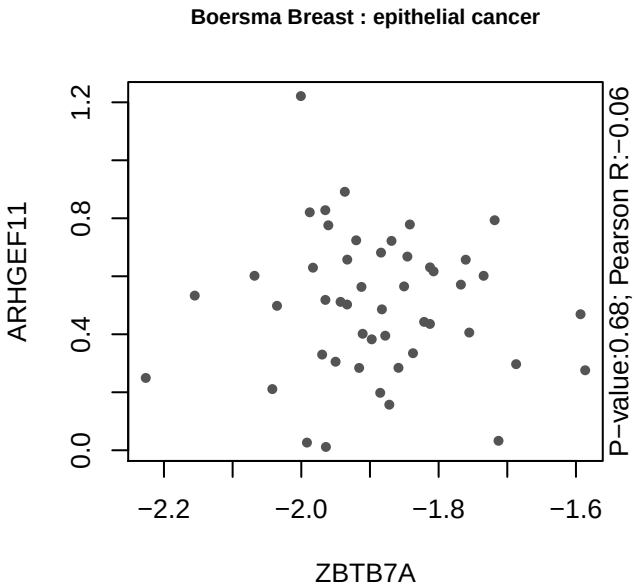

Boersma Breast : epithelial cancer
LLGL2
BCL6
P−value:0.78; Pearson R:0.041
−2.0
−1.0
0.0
1.0
−1.4
−1.0
−0.6
−0.2

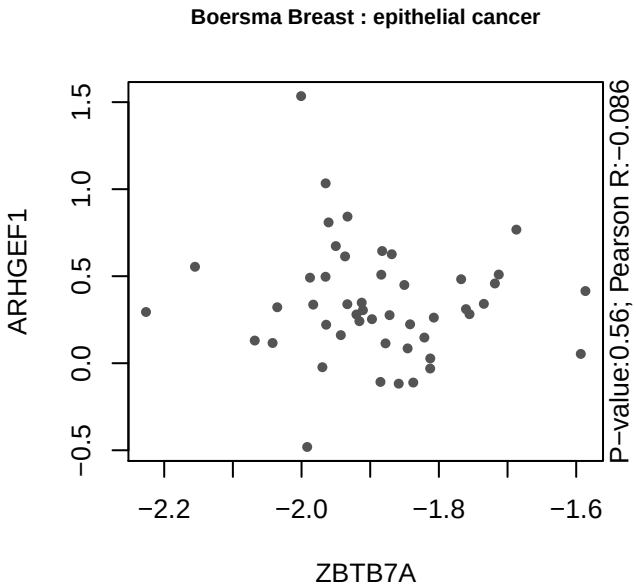

Boersma Breast : epithelial cancer
MAPK9
ZBTB7A
P−value:0.031; Pearson R:−0.31
−0.2
0.2
0.4
0.6
0.8
−2.2
−2.0
−1.8
−1.6

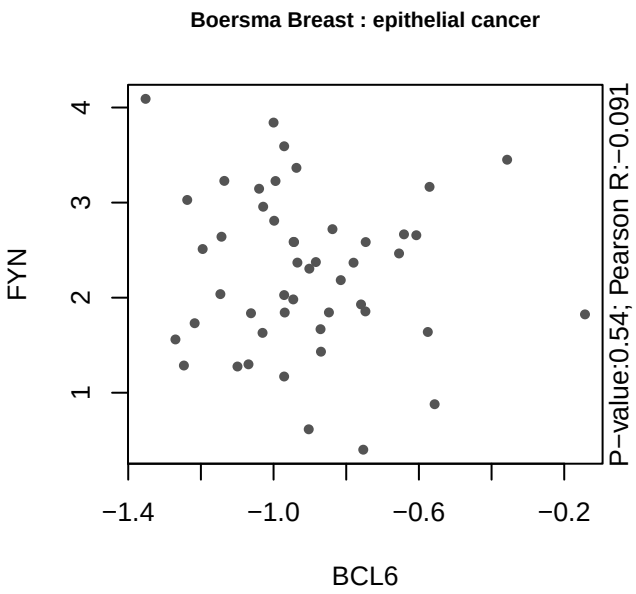

Boersma Breast : epithelial cancer
LLGL2
ZBTB7A
P−value:0.31; Pearson R:−0.15
−2.0
−1.0
0.0
1.0
−2.2
−2.0
−1.8
−1.6

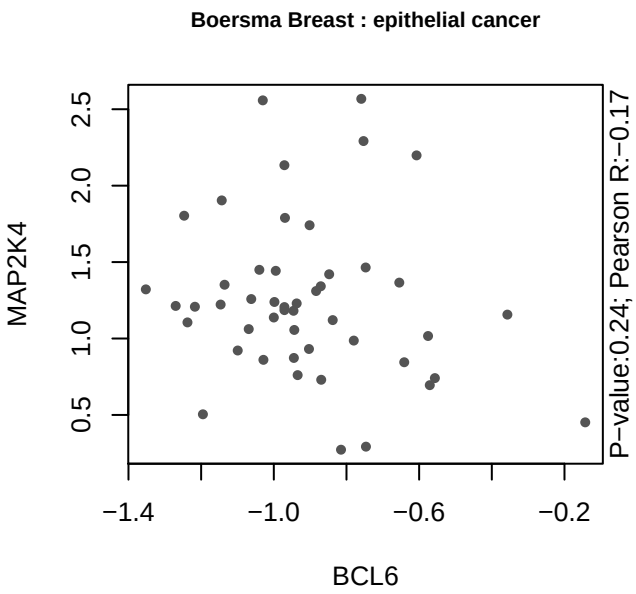

Boersma Breast : epithelial cancer
ARHGEF11
BCL6
P−value:0.15; Pearson R:−0.21
0.0
0.4
0.8
1.2
−1.4
−1.0
−0.6
−0.2

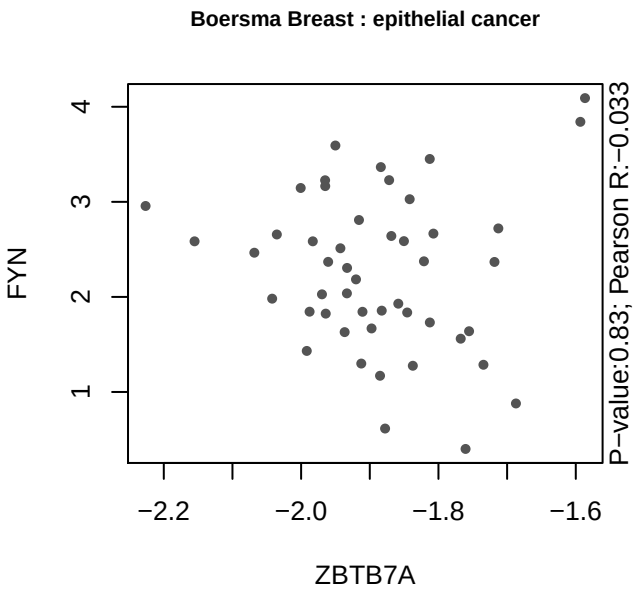

Boersma Breast : epithelial cancer
ARHGEF1
BCL6
P−value:0.97; Pearson R:−0.0052
−0.5
0.0
0.5
1.0
1.5
−1.4
−1.0
−0.6
−0.2

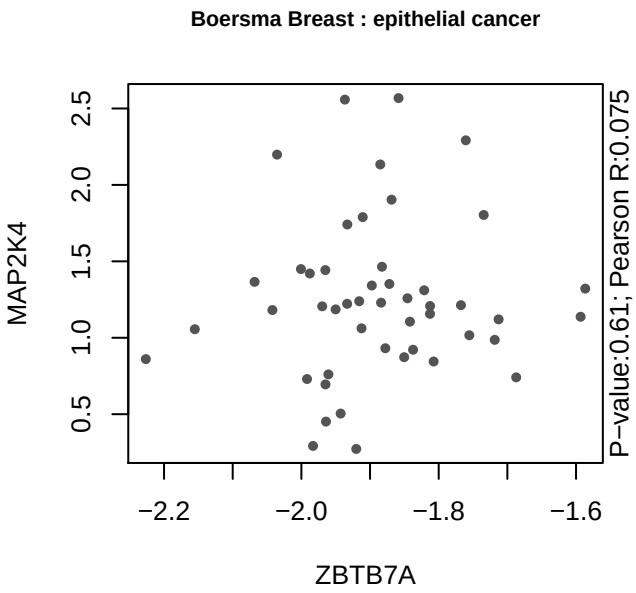

Boersma Breast : epithelial cancer
ARHGEF11
ZBTB7A
P−value:0.68; Pearson R:−0.06
0.0
0.4
0.8
1.2
−2.2
−2.0
−1.8
−1.6

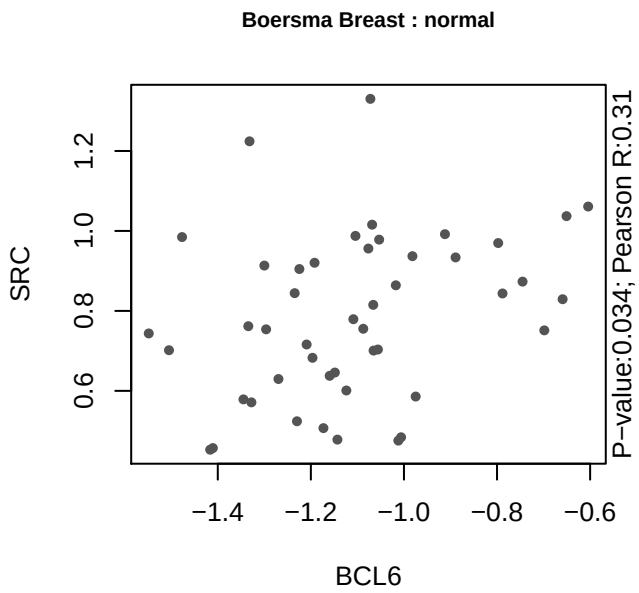

Boersma Breast : epithelial cancer
ARHGEF1
ZBTB7A
P−value:0.56; Pearson R:−0.086
−0.5
0.0
0.5
1.0
1.5
−2.2
−2.0
−1.8
−1.6

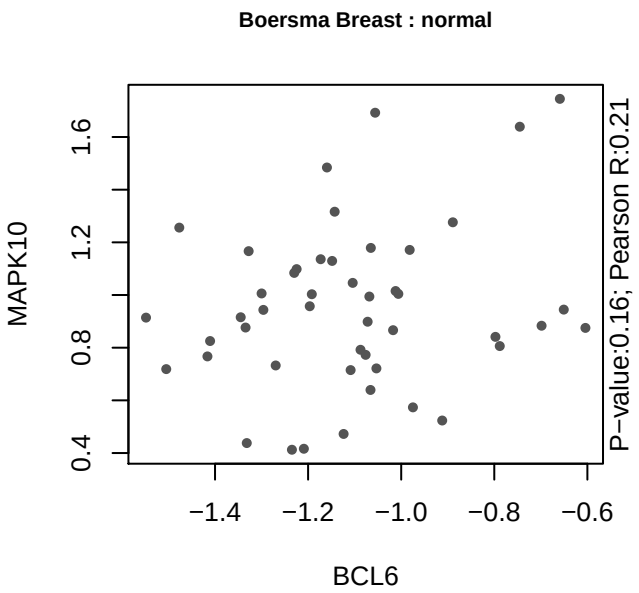

Boersma Breast : epithelial cancer
FYN
BCL6
P−value:0.54; Pearson R:−0.091
1
2
3
4
−1.4
−1.0
−0.6
−0.2

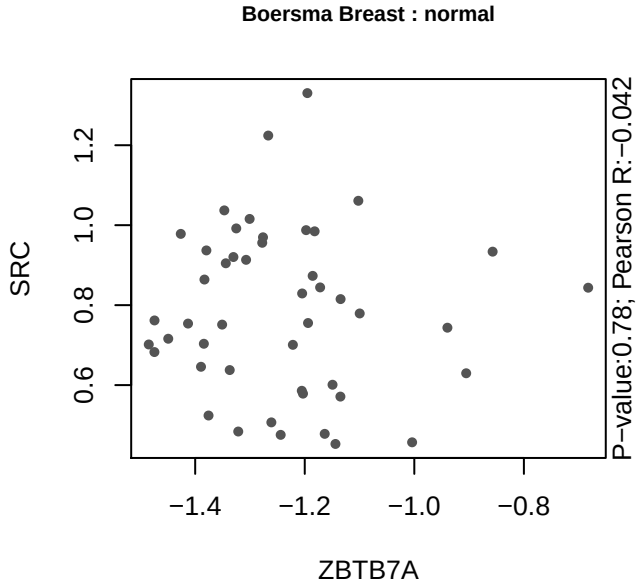

Boersma Breast : epithelial cancer
MAP2K4
BCL6
P−value:0.24; Pearson R:−0.17
0.5
1.0
1.5
2.0
2.5
−1.4
−1.0
−0.6
−0.2

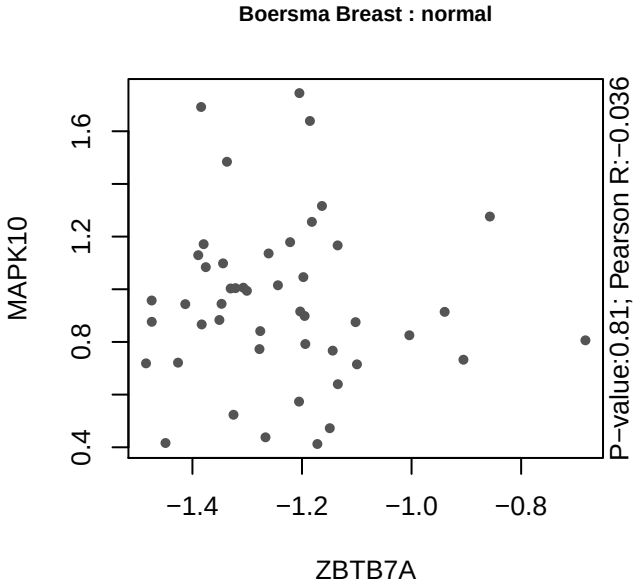

Boersma Breast : epithelial cancer
FYN
ZBTB7A
P−value:0.83; Pearson R:−0.033
1
2
3
4
−2.2
−2.0
−1.8
−1.6

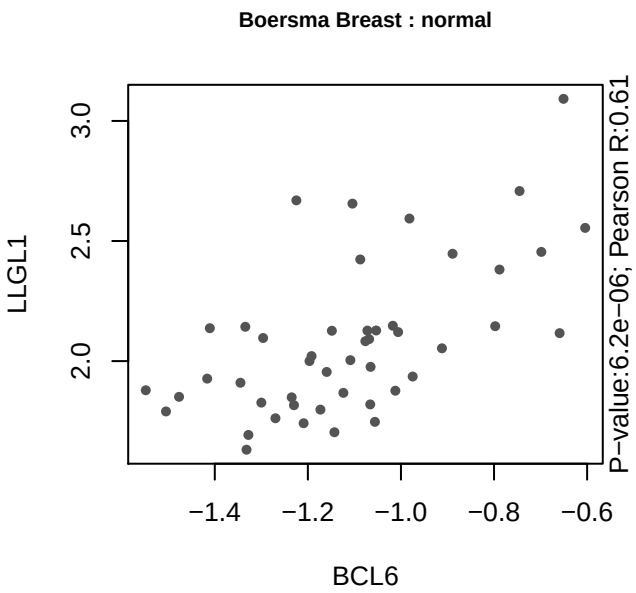

Boersma Breast : epithelial cancer
MAP2K4
ZBTB7A
P−value:0.61; Pearson R:0.075
0.5
1.0
1.5
2.0
2.5
−2.2
−2.0
−1.8
−1.6

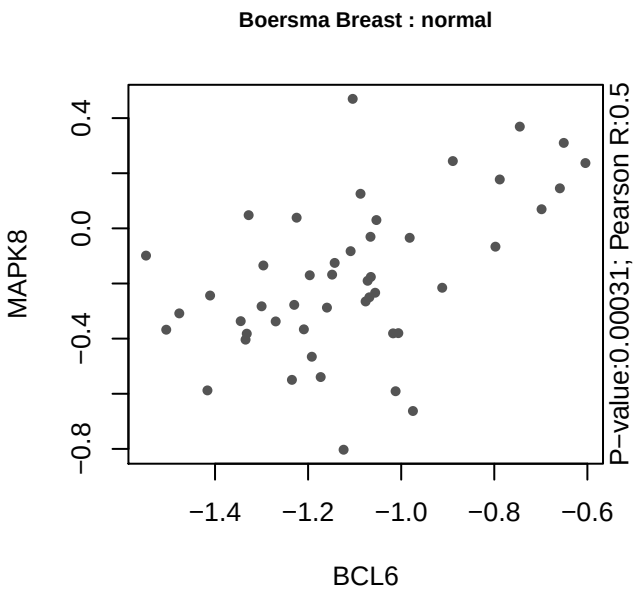

Boersma Breast : normal
SRC
BCL6
P−value:0.034; Pearson R:0.31
0.6
0.8
1.0
1.2
−1.4
−1.2
−1.0
−0.8
−0.6

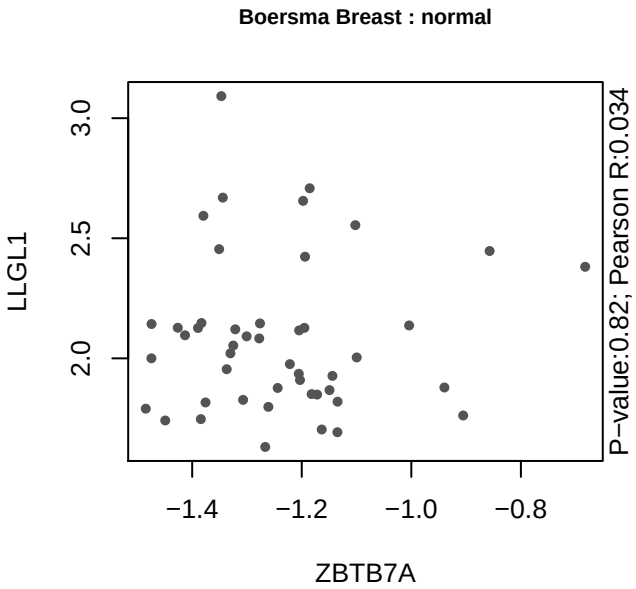

Boersma Breast : normal
MAPK10
BCL6
P−value:0.16; Pearson R:0.21
0.4
0.8
1.2
1.6
−1.4
−1.2
−1.0
−0.8
−0.6

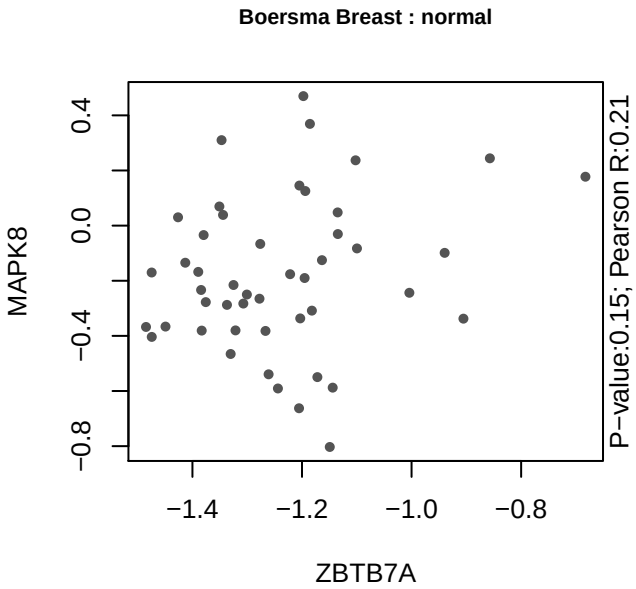

Boersma Breast : normal
SRC
ZBTB7A
P−value:0.78; Pearson R:−0.042
0.6
0.8
1.0
1.2
−1.4
−1.2
−1.0
−0.8

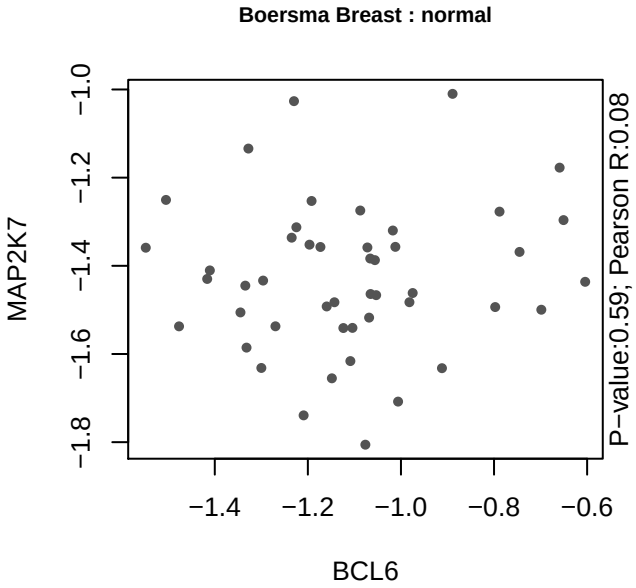

Boersma Breast : normal
MAPK10
ZBTB7A
P−value:0.81; Pearson R:−0.036
0.4
0.8
1.2
1.6
−1.4
−1.2
−1.0
−0.8

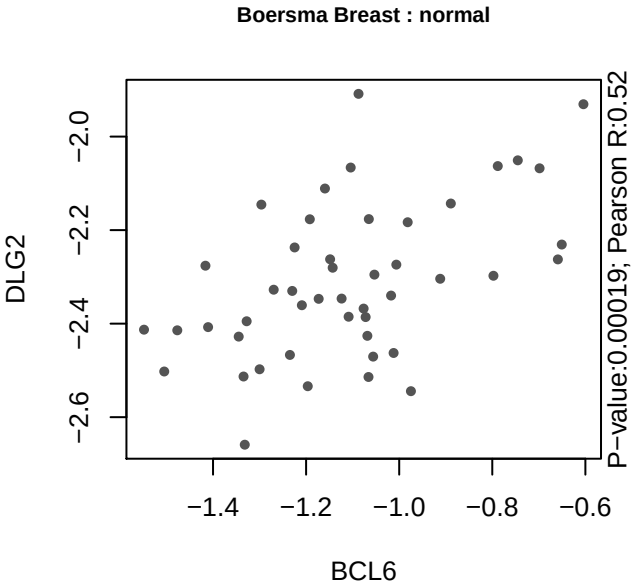

Boersma Breast : normal
LLGL1
BCL6
P−value:6.2e−06; Pearson R:0.61

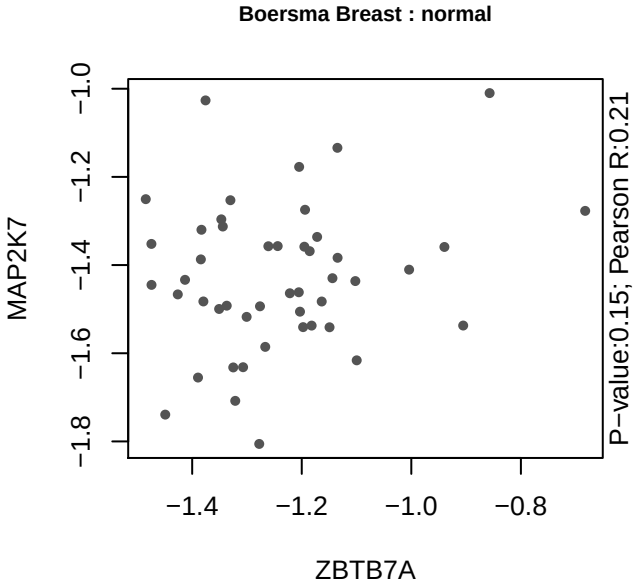

Boersma Breast : normal
MAPK8
BCL6
P−value:0.00031; Pearson R:0.5

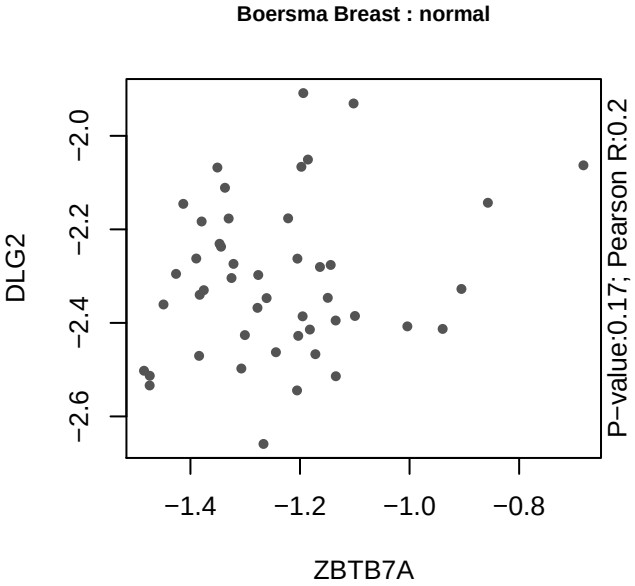

Boersma Breast : normal
LLGL1
ZBTB7A
P−value:0.82; Pearson R:0.034

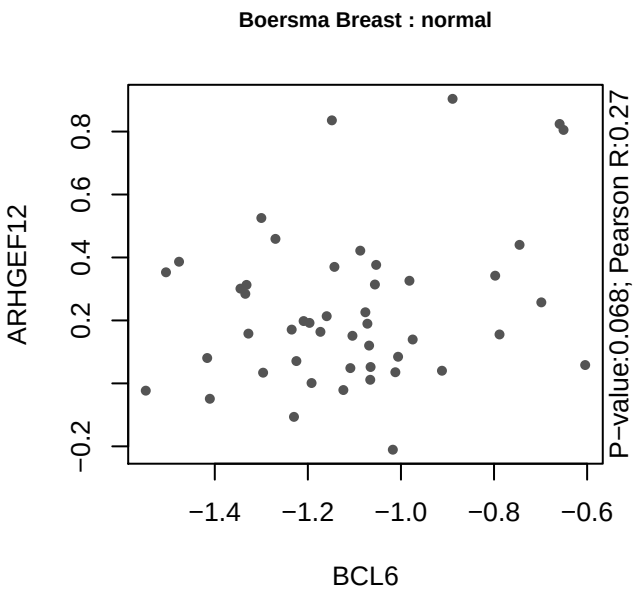

Boersma Breast : normal
MAPK8
ZBTB7A
P−value:0.15; Pearson R:0.21

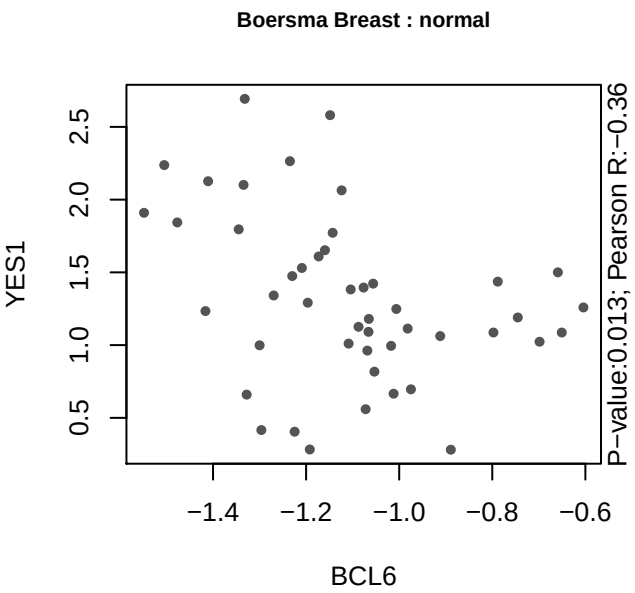

Boersma Breast : normal
MAP2K7
BCL6
P−value:0.59; Pearson R:0.08

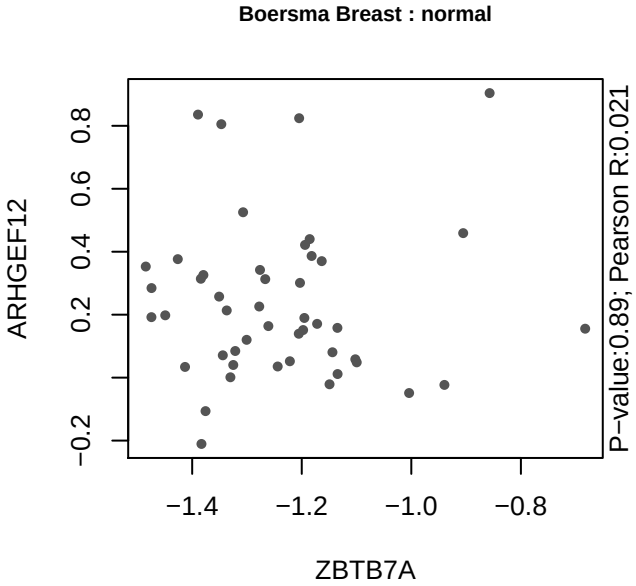

Boersma Breast : normal
DLG2
BCL6
P−value:0.00019; Pearson R:0.52

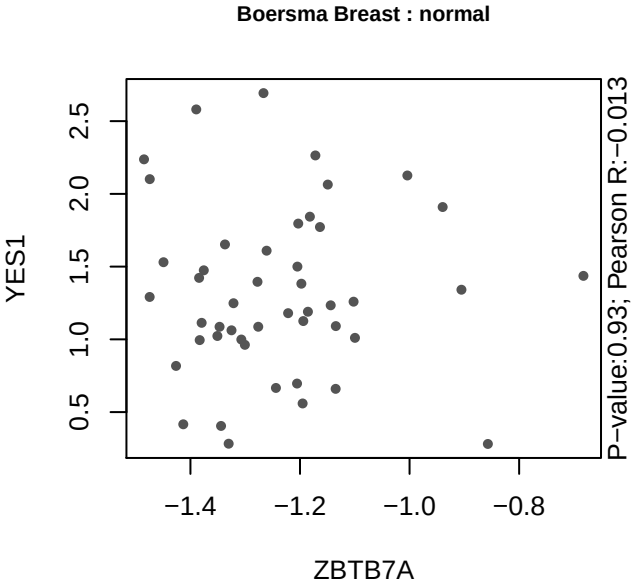

Boersma Breast : normal
MAP2K7
ZBTB7A
P−value:0.15; Pearson R:0.21

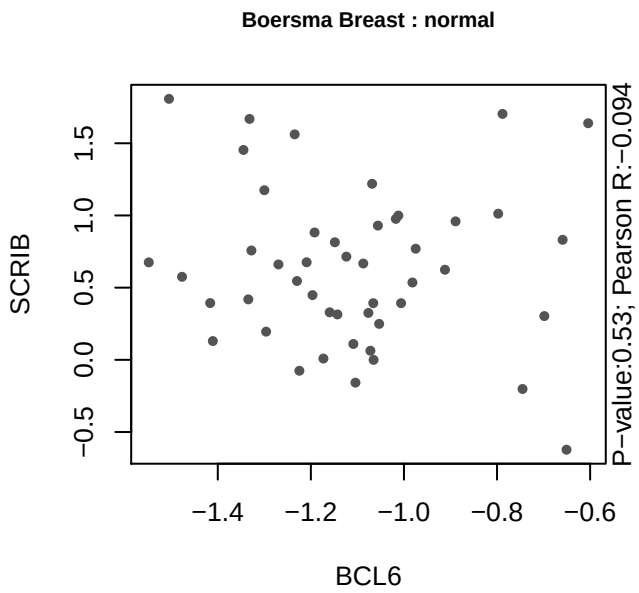

Boersma Breast : normal
DLG2
ZBTB7A
P−value:0.17; Pearson R:0.2

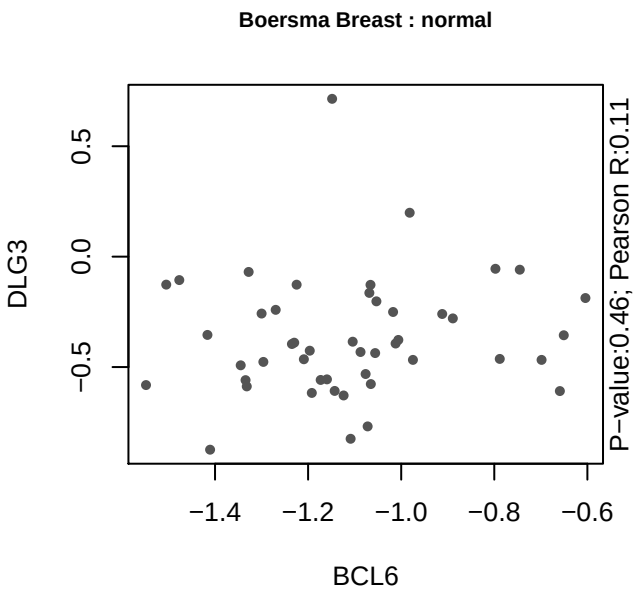

Boersma Breast : normal
ARHGEF12
BCL6
P−value:0.068; Pearson R:0.27

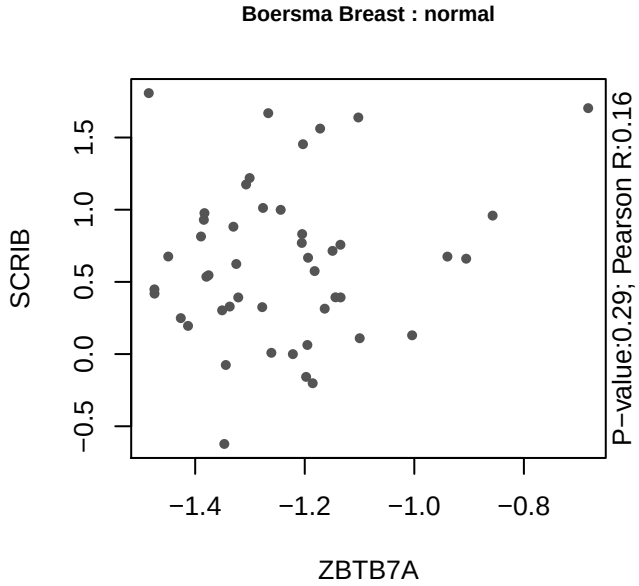

Boersma Breast : normal
YES1
BCL6
P−value:0.013; Pearson R:−0.36

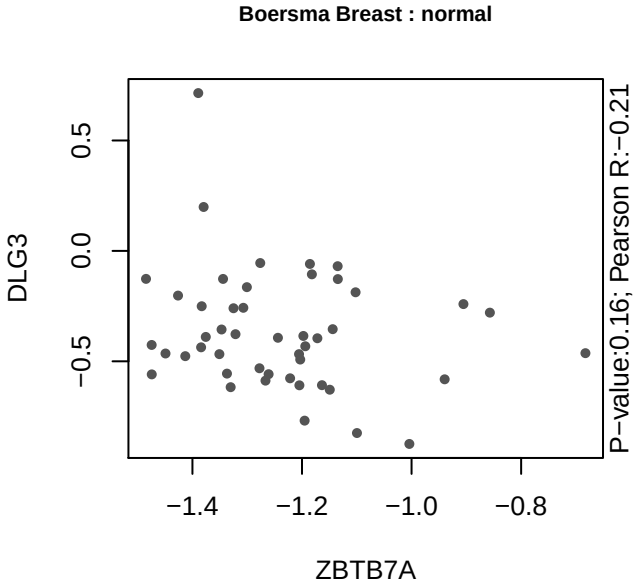

Boersma Breast : normal
ARHGEF12
ZBTB7A
P−value:0.89; Pearson R:0.021

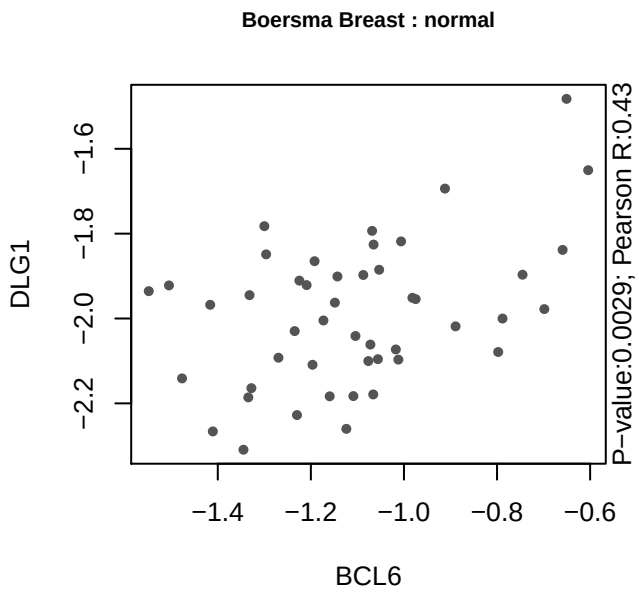

Boersma Breast : normal
YES1
ZBTB7A
P−value:0.93; Pearson R:−0.013

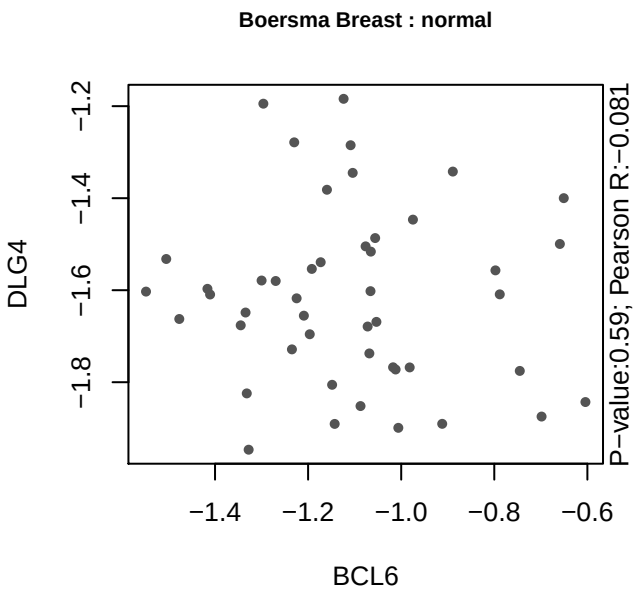

Boersma Breast : normal
SCRIB
BCL6
P−value:0.53; Pearson R:−0.094

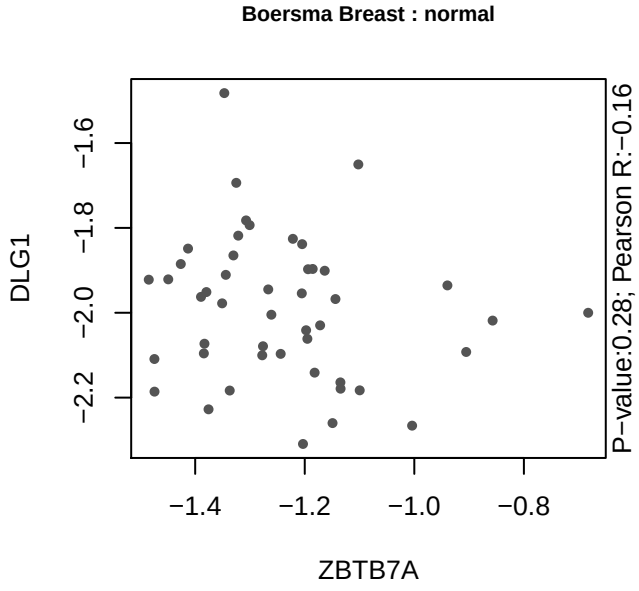

Boersma Breast : normal
DLG3
BCL6
P−value:0.46; Pearson R:0.11

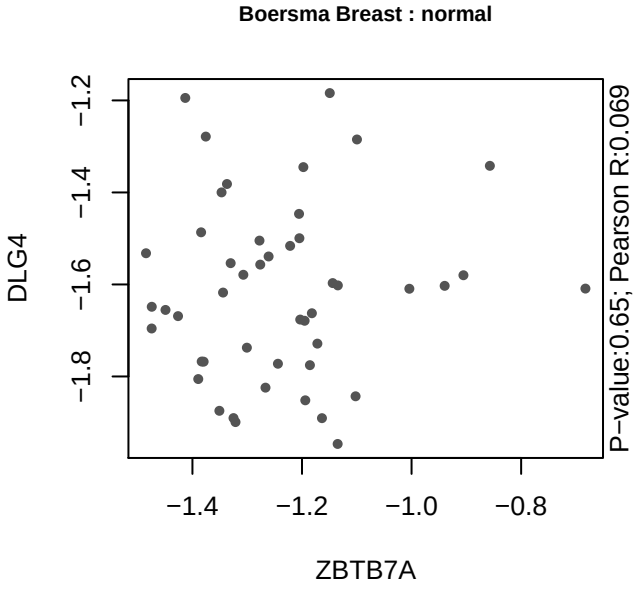

Boersma Breast : normal
SCRIB
ZBTB7A
P−value:0.29; Pearson R:0.16

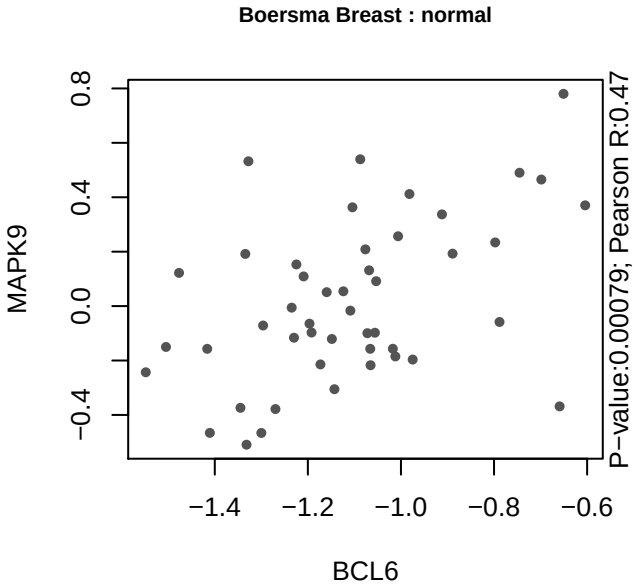

Boersma Breast : normal
DLG3
ZBTB7A
P−value:0.16; Pearson R:−0.21

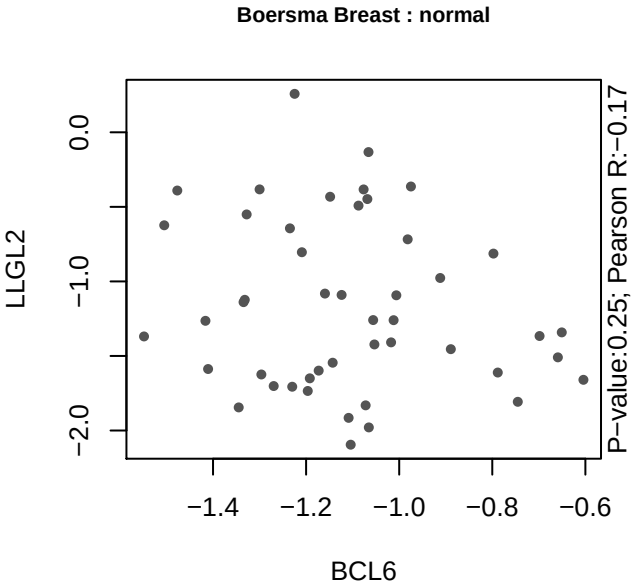

Boersma Breast : normal
DLG1
BCL6
P−value:0.0029; Pearson R:0.43
−2.2
−2.0
−1.8
−1.6
−1.4
−1.2
−1.0
−0.8
−0.6

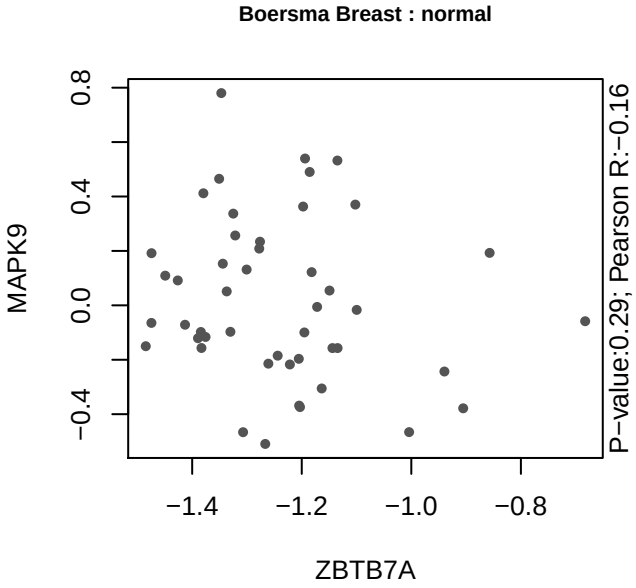

Boersma Breast : normal
DLG4
BCL6
P−value:0.59; Pearson R:−0.081
−1.8
−1.6
−1.4
−1.2
−1.4
−1.2
−1.0
−0.8
−0.6

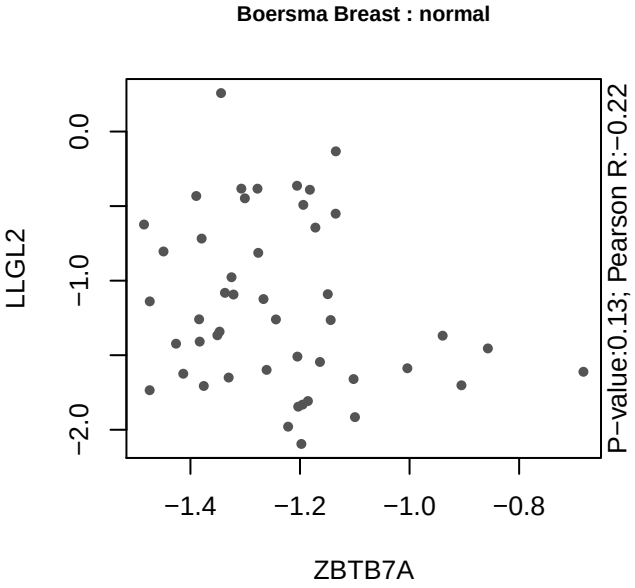

Boersma Breast : normal
DLG1
ZBTB7A
P−value:0.28; Pearson R:−0.16
−2.2
−2.0
−1.8
−1.6
−1.4
−1.2
−1.0
−0.8

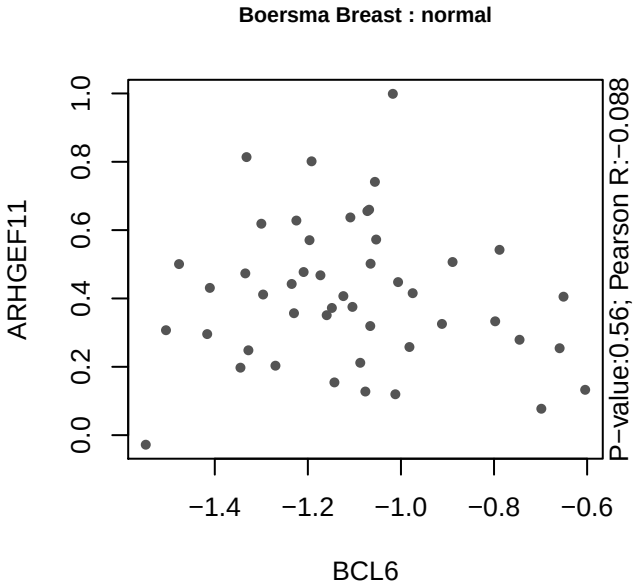

Boersma Breast : normal
DLG4
ZBTB7A
P−value:0.65; Pearson R:0.069
−1.8
−1.6
−1.4
−1.2
−1.4
−1.2
−1.0
−0.8

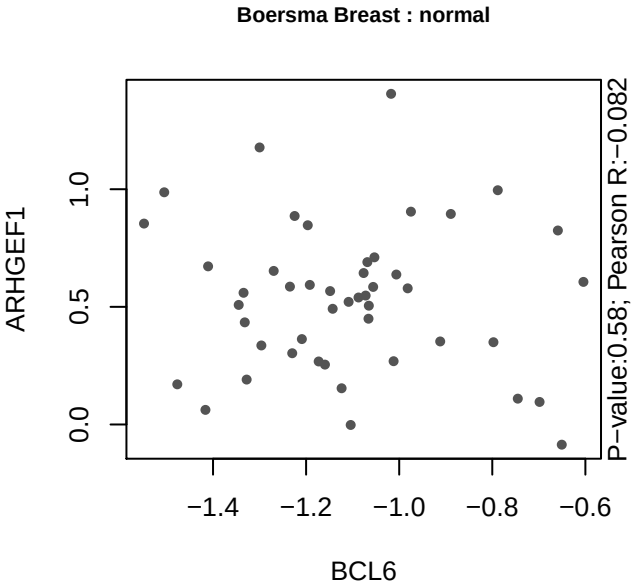

Boersma Breast : normal
MAPK9
BCL6
P−value:0.00079; Pearson R:0.47
0.8
0.4
0.0
−0.4
−1.4
−1.2
−1.0
−0.8
−0.6

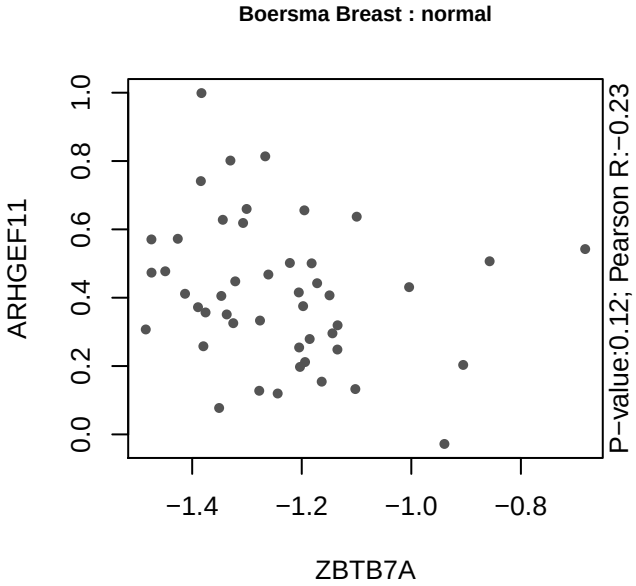

Boersma Breast : normal
LLGL2
BCL6
P−value:0.25; Pearson R:−0.17
0.0
−1.0
−2.0
−1.4
−1.2
−1.0
−0.8
−0.6

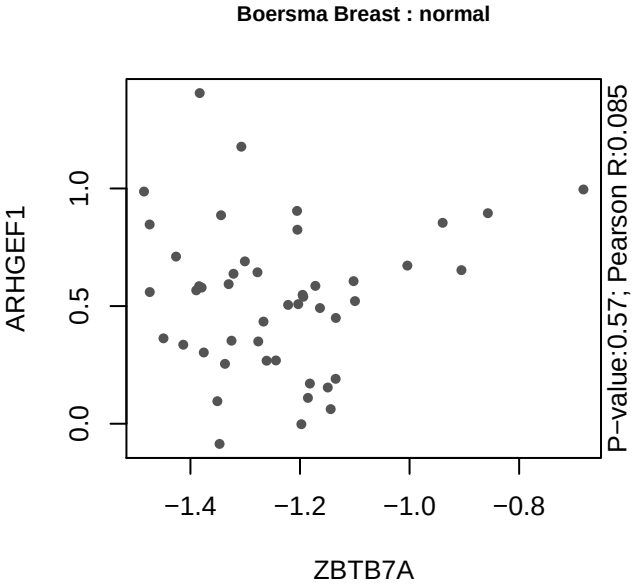

Boersma Breast : normal
MAPK9
ZBTB7A
P−value:0.29; Pearson R:−0.16
0.8
0.4
0.0
−0.4
−1.4
−1.2
−1.0
−0.8

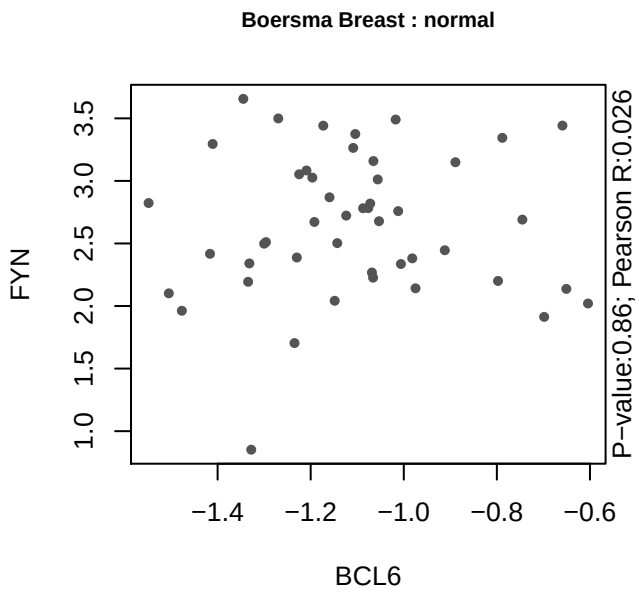

Boersma Breast : normal
LLGL2
ZBTB7A
P−value:0.13; Pearson R:−0.22
0.0
−1.0
−2.0
−1.4
−1.2
−1.0
−0.8

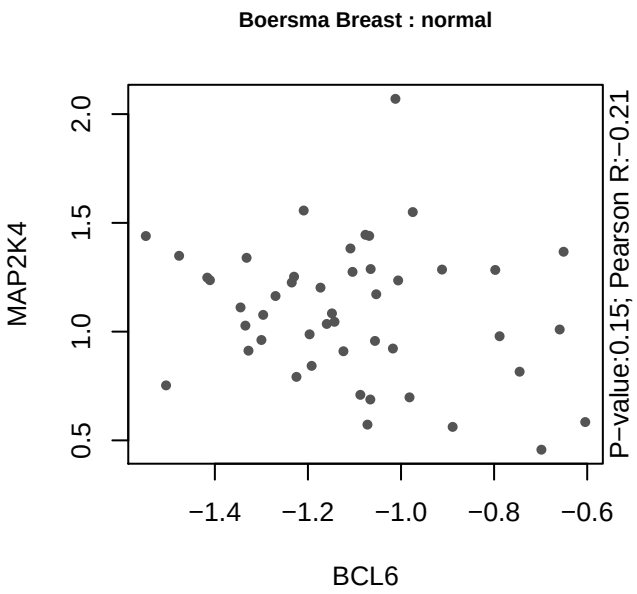

Boersma Breast : normal
ARHGEF11
BCL6
P−value:0.56; Pearson R:−0.088

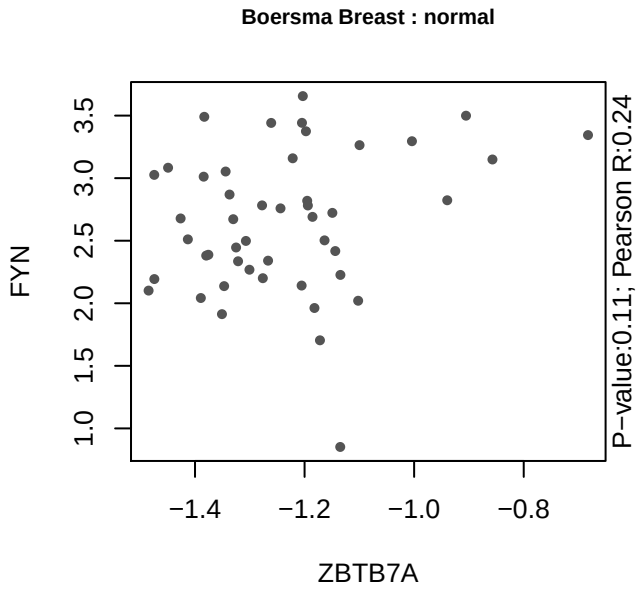

Boersma Breast : normal
ARHGEF1
BCL6
P−value:0.58; Pearson R:−0.082

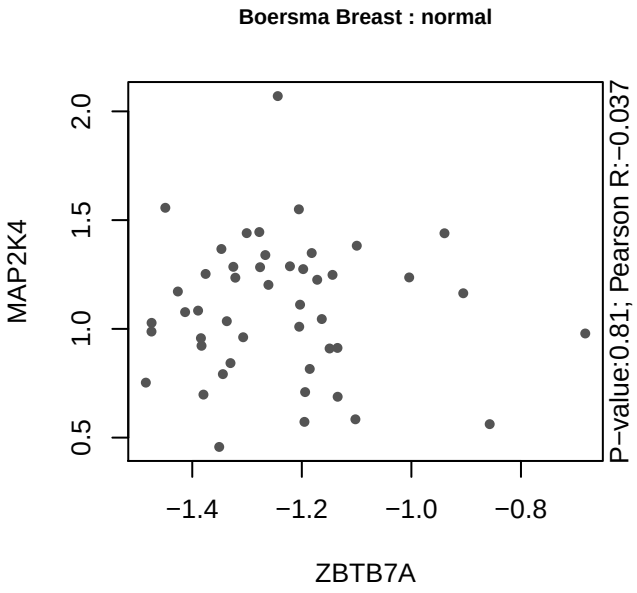

Boersma Breast : normal
ARHGEF11
ZBTB7A
P−value:0.12; Pearson R:−0.23

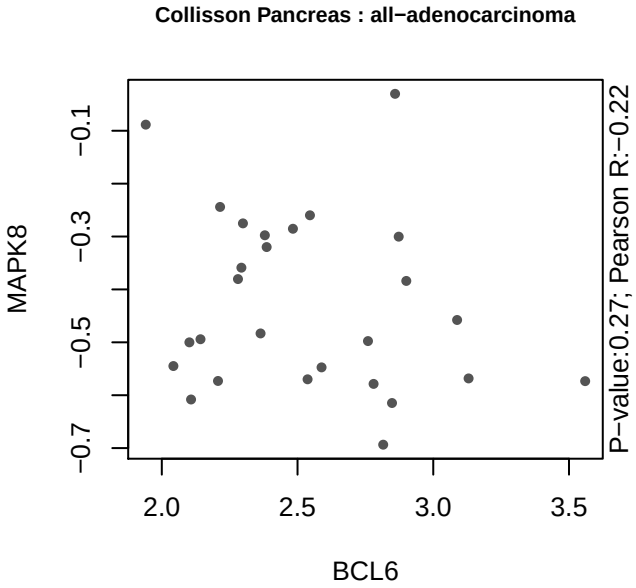

Boersma Breast : normal
ARHGEF1
ZBTB7A
P−value:0.57; Pearson R:0.085

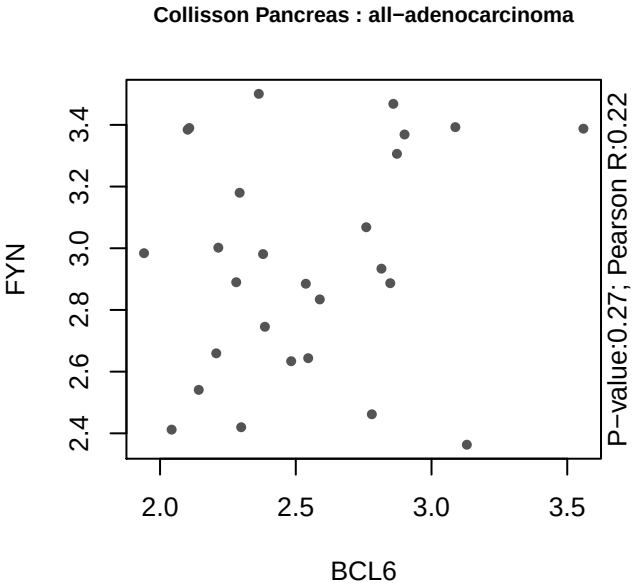

Boersma Breast : normal
FYN
BCL6
P−value:0.86; Pearson R:0.026

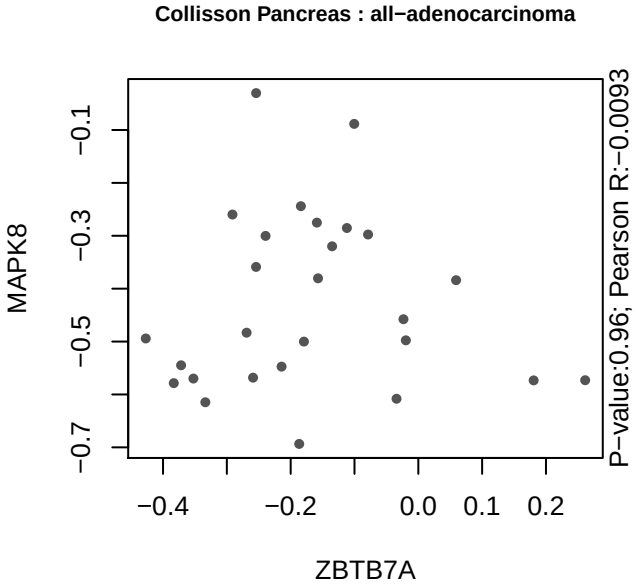

Boersma Breast : normal
MAP2K4
BCL6
P−value:0.15; Pearson R:−0.21

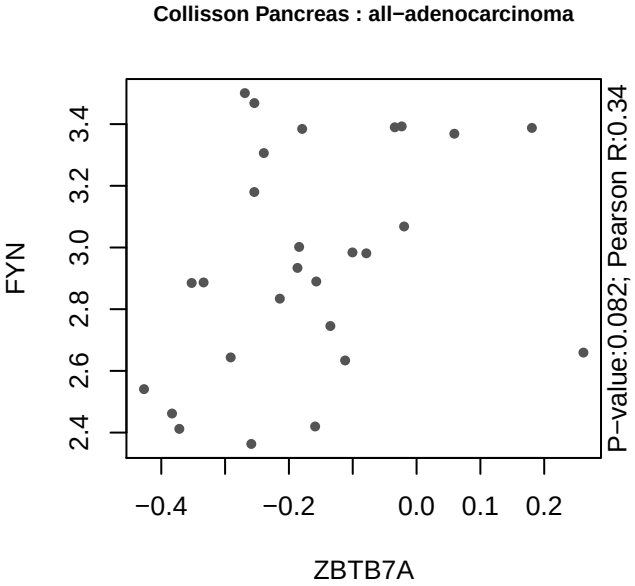

Boersma Breast : normal
FYN
ZBTB7A
P−value:0.11; Pearson R:0.24

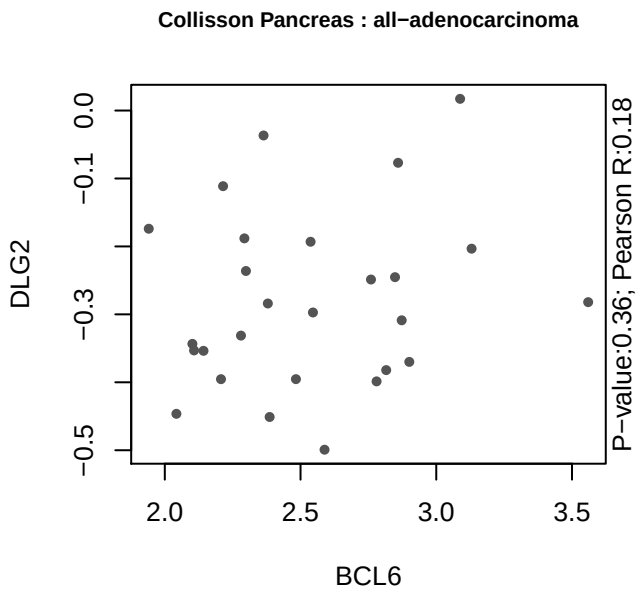

Boersma Breast : normal
MAP2K4
ZBTB7A
P−value:0.81; Pearson R:−0.037

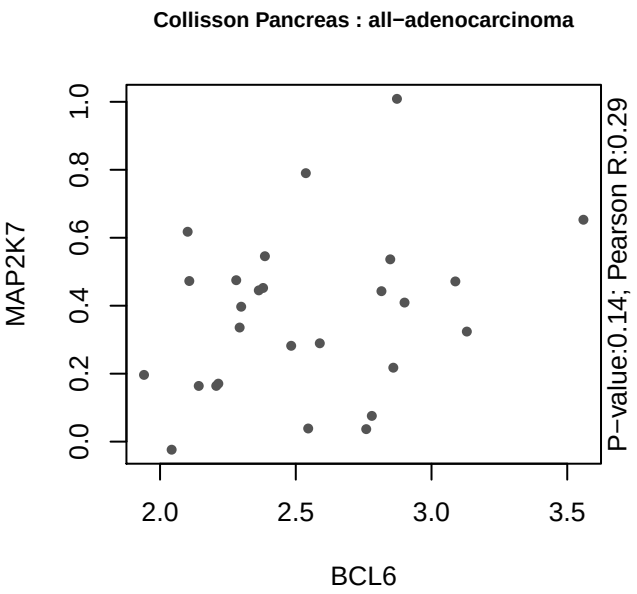

Collisson Pancreas : all−adenocarcinoma
MAPK8
BCL6
P−value:0.27; Pearson R:−0.22

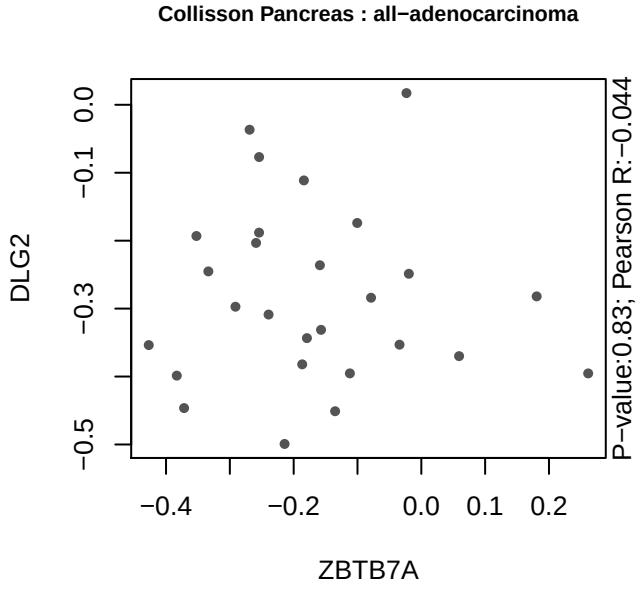

Collisson Pancreas : all−adenocarcinoma
FYN
BCL6
P−value:0.27; Pearson R:0.22

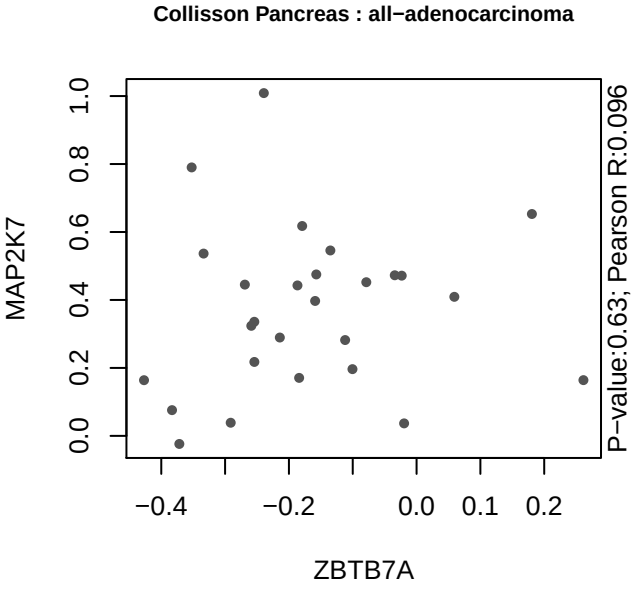

Collisson Pancreas : all−adenocarcinoma
MAPK8
ZBTB7A
P−value:0.96; Pearson R:−0.0093

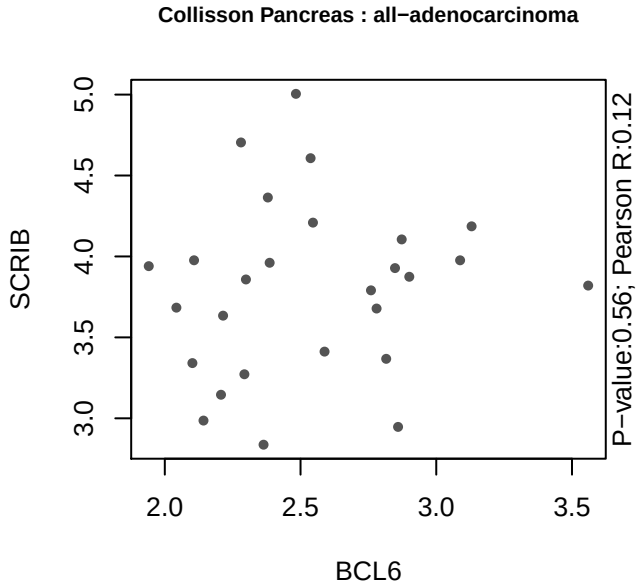

Collisson Pancreas : all−adenocarcinoma
FYN
ZBTB7A
P−value:0.082; Pearson R:0.34

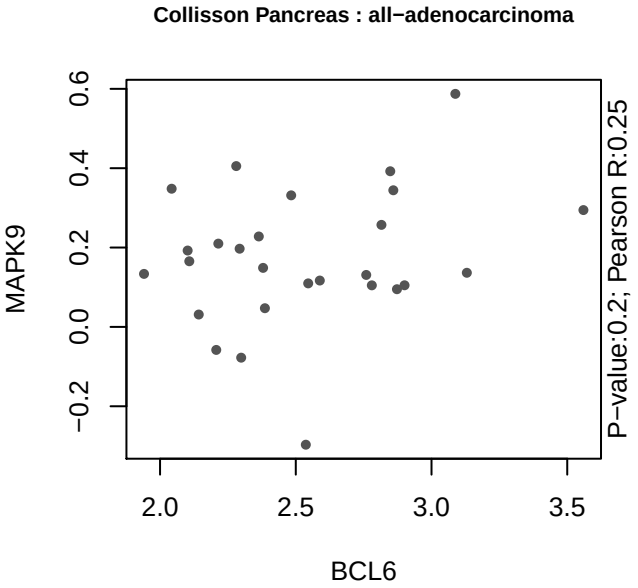

Collisson Pancreas : all−adenocarcinoma
DLG2
BCL6
P−value:0.36; Pearson R:0.18
−0.5
−0.3
−0.1
0.0
2.0
2.5
3.0
3.5

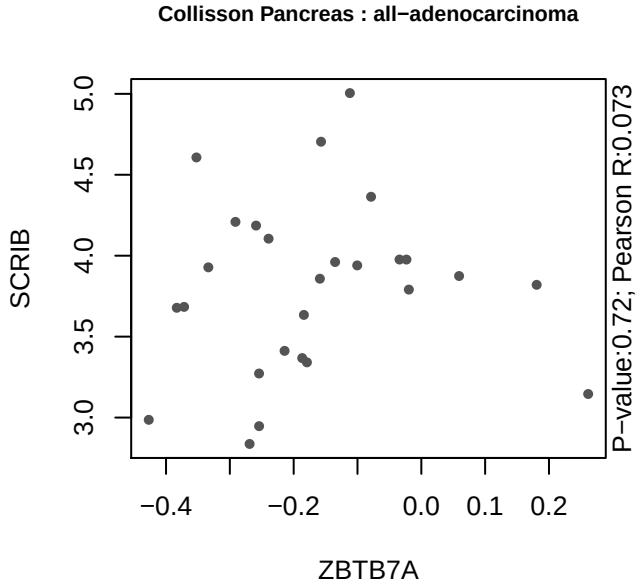

Collisson Pancreas : all−adenocarcinoma
MAP2K7
BCL6
P−value:0.14; Pearson R:0.29
0.0
0.2
0.4
0.6
0.8
1.0
2.0
2.5
3.0
3.5

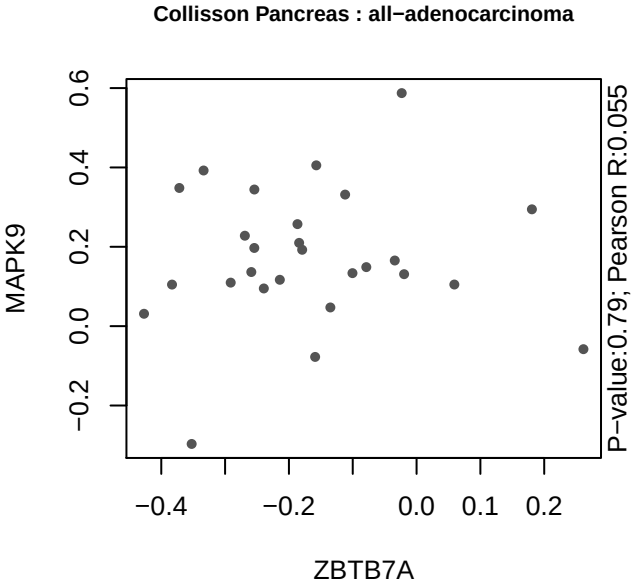

Collisson Pancreas : all−adenocarcinoma
DLG2
ZBTB7A
P−value:0.83; Pearson R:−0.044
−0.5
−0.3
−0.1
0.0
−0.4
−0.2
0.0
0.1
0.2

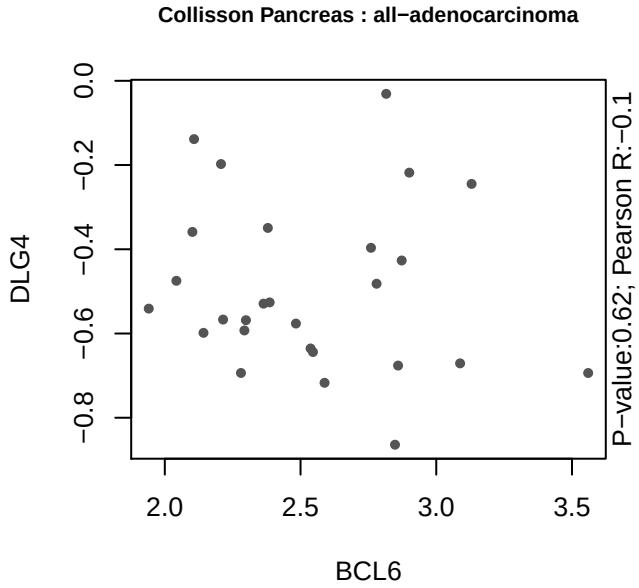

Collisson Pancreas : all−adenocarcinoma
MAP2K7
ZBTB7A
P−value:0.63; Pearson R:0.096
0.0
0.2
0.4
0.6
0.8
1.0
−0.4
−0.2
0.0
0.1
0.2

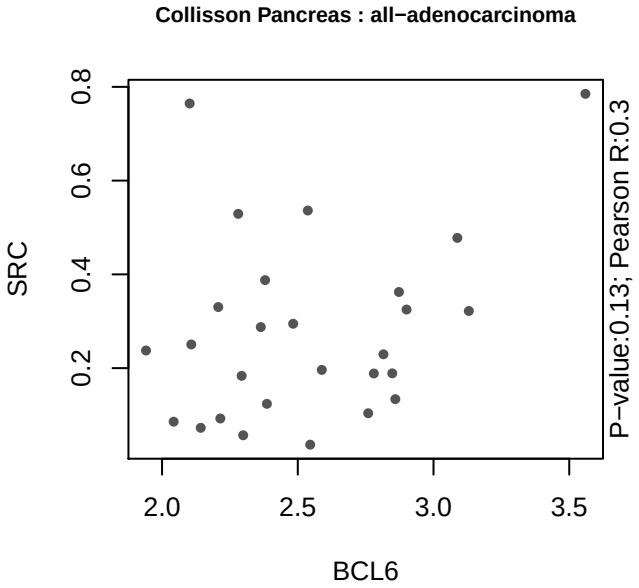

Collisson Pancreas : all−adenocarcinoma
SCRIB
BCL6
P−value:0.56; Pearson R:0.12
3.0
3.5
4.0
4.5
5.0
2.0
2.5
3.0
3.5

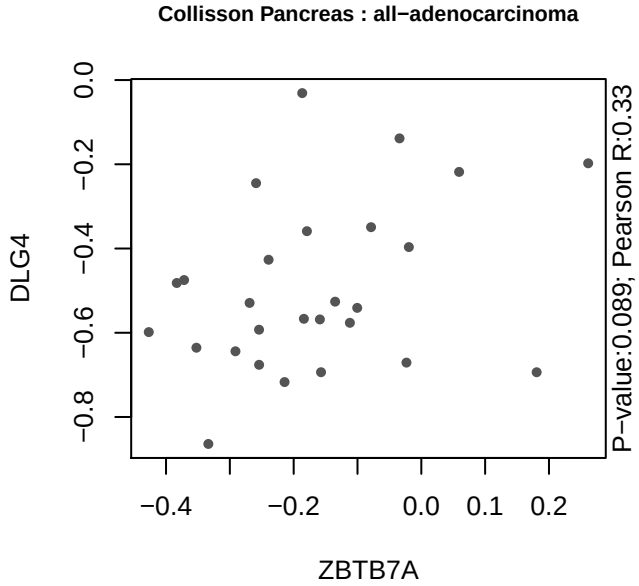

Collisson Pancreas : all−adenocarcinoma
MAPK9
BCL6
P−value:0.2; Pearson R:0.25
−0.2
0.0
0.2
0.4
0.6
2.0
2.5
3.0
3.5

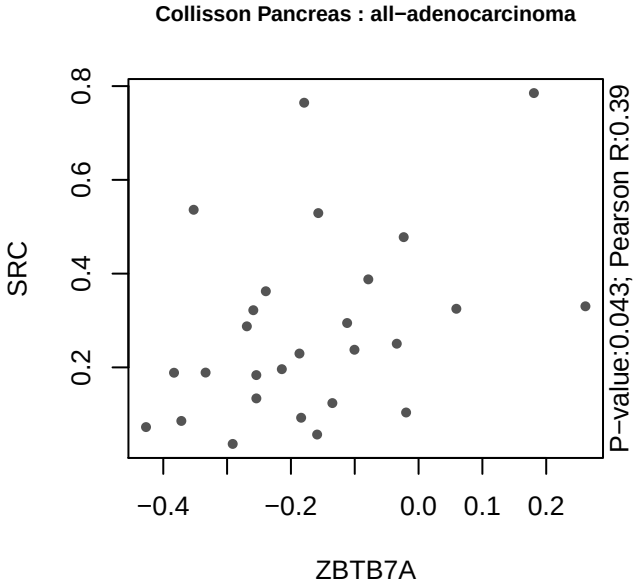

Collisson Pancreas : all−adenocarcinoma
SCRIB
ZBTB7A
P−value:0.72; Pearson R:0.073
3.0
3.5
4.0
4.5
5.0
−0.4
−0.2
0.0
0.1
0.2

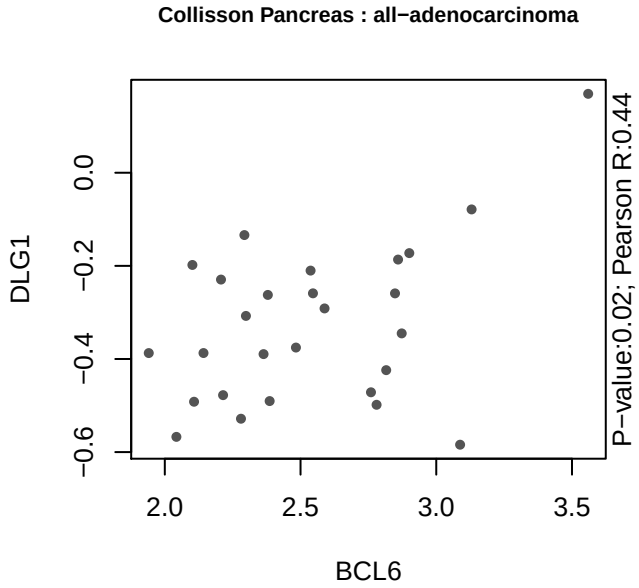

Collisson Pancreas : all−adenocarcinoma
MAPK9
ZBTB7A
P−value:0.79; Pearson R:0.055
−0.2
0.0
0.2
0.4
0.6
−0.4
−0.2
0.0
0.1
0.2

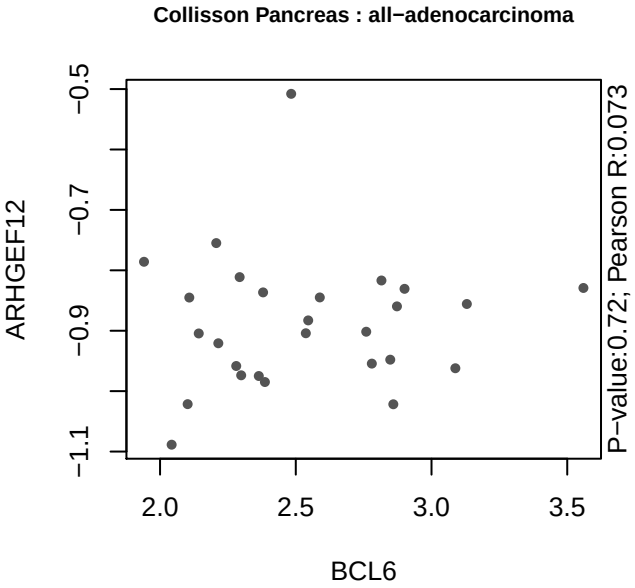

Collisson Pancreas : all−adenocarcinoma
DLG4
BCL6
P−value:0.62; Pearson R:−0.1
0.0
−0.2
−0.4
−0.6
−0.8
2.0
2.5
3.0
3.5

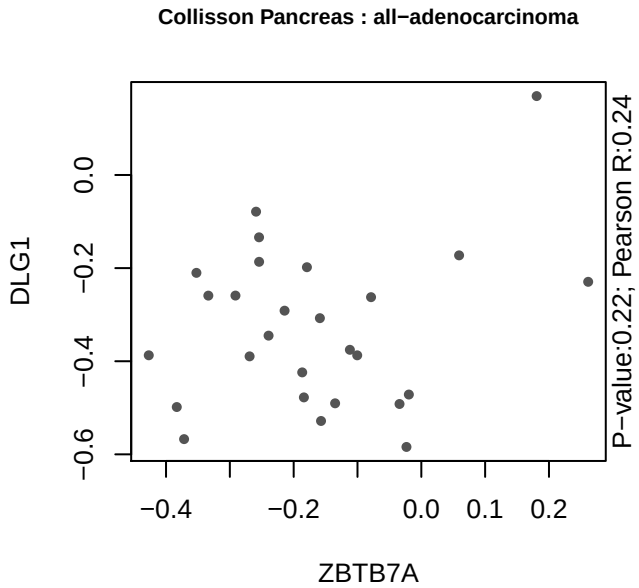

Collisson Pancreas : all−adenocarcinoma
SRC
BCL6
P−value:0.13; Pearson R:0.3
0.8
0.6
0.4
0.2
2.0
2.5
3.0
3.5

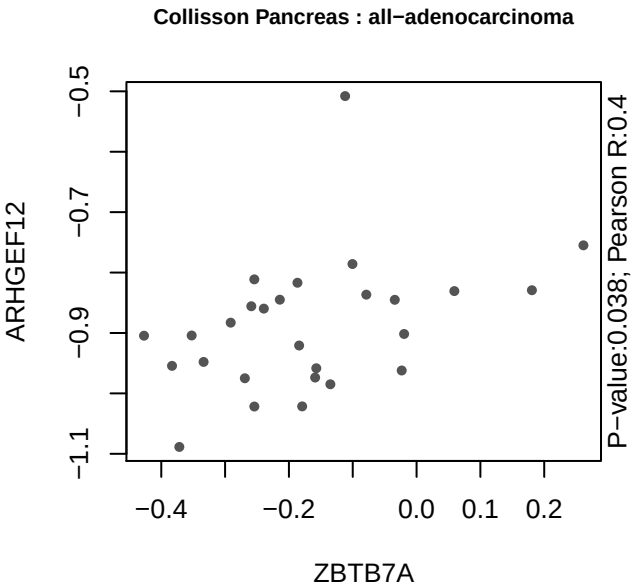

Collisson Pancreas : all−adenocarcinoma
DLG4
ZBTB7A
P−value:0.089; Pearson R:0.33
0.0
−0.2
−0.4
−0.6
−0.8
−0.4
−0.2
0.0
0.1
0.2

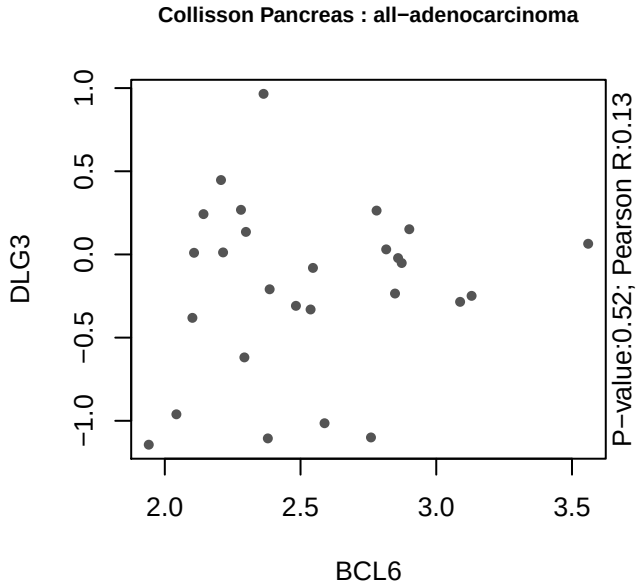

Collisson Pancreas : all−adenocarcinoma
SRC
ZBTB7A
P−value:0.043; Pearson R:0.39
0.8
0.6
0.4
0.2
−0.4
−0.2
0.0
0.1
0.2

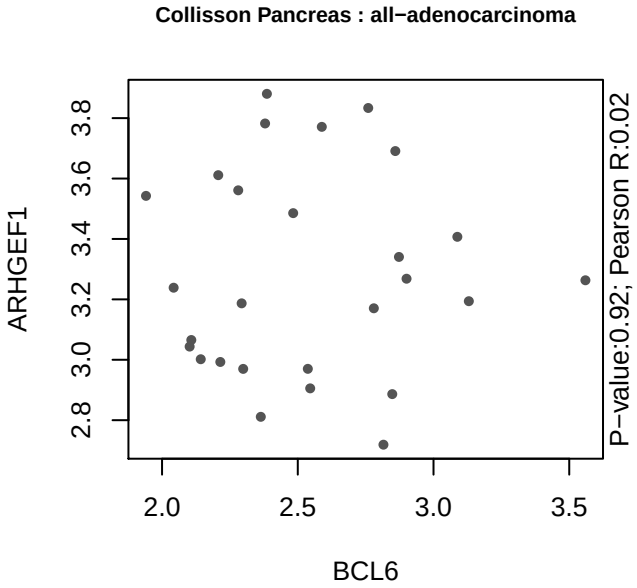

Collisson Pancreas : all−adenocarcinoma
DLG1
BCL6
P−value:0.02; Pearson R:0.44
−0.6
−0.4
−0.2
0.0
2.0
2.5
3.0
3.5

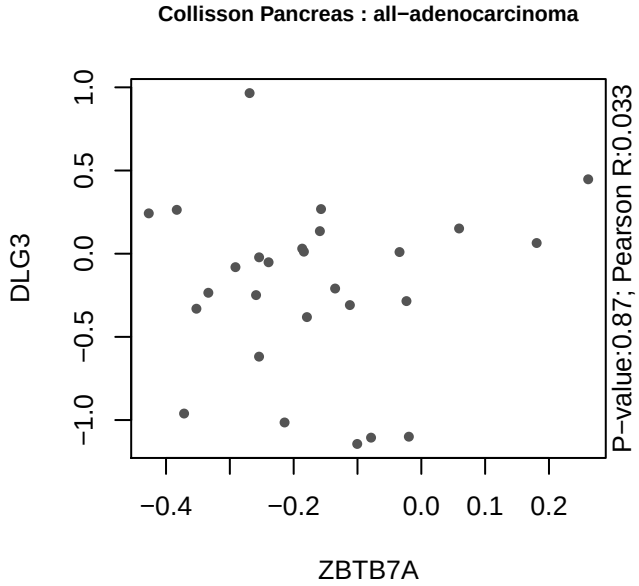

Collisson Pancreas : all−adenocarcinoma
ARHGEF12
BCL6
P−value:0.72; Pearson R:0.073
−1.1
−0.9
−0.7
−0.5
2.0
2.5
3.0
3.5

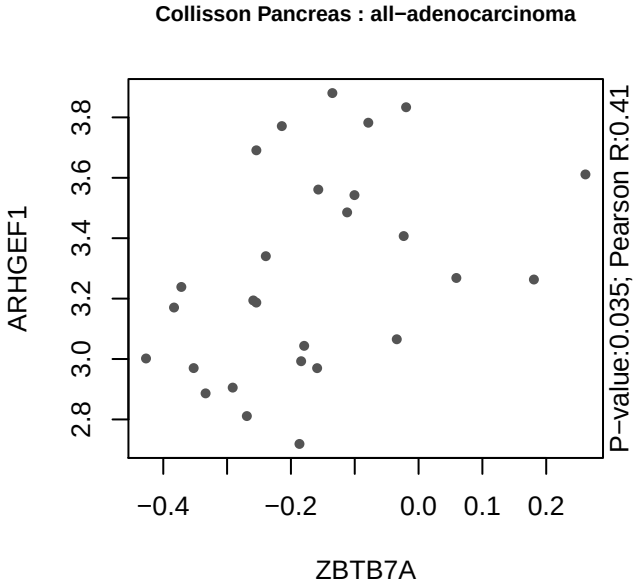

Collisson Pancreas : all−adenocarcinoma
DLG1
ZBTB7A
P−value:0.22; Pearson R:0.24
−0.6
−0.4
−0.2
0.0
−0.4
−0.2
0.0
0.1
0.2

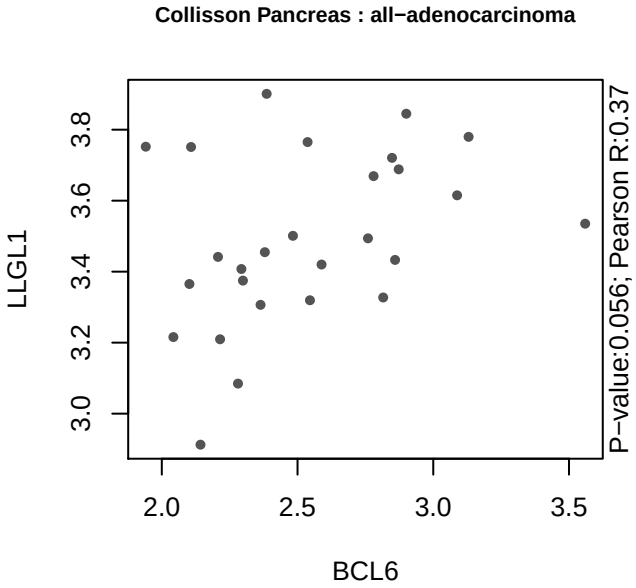

Collisson Pancreas : all−adenocarcinoma
ARHGEF12
ZBTB7A
P−value:0.038; Pearson R:0.4
−1.1
−0.9
−0.7
−0.5
−0.4
−0.2
0.0
0.1
0.2

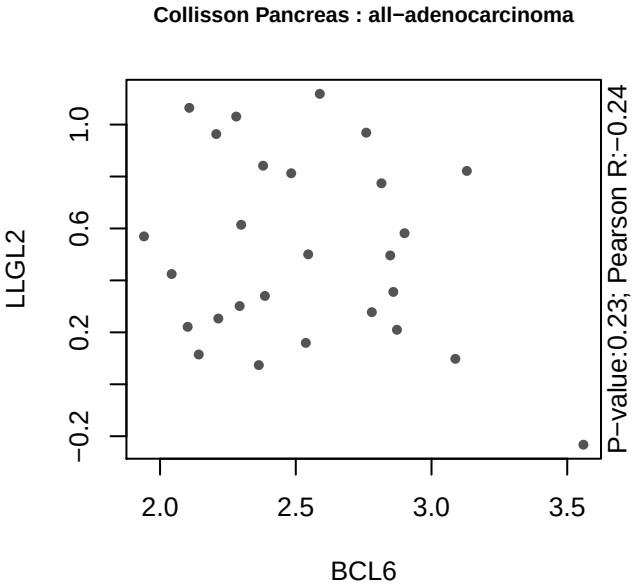

Collisson Pancreas : all−adenocarcinoma
DLG3
BCL6
P−value:0.52; Pearson R:0.13

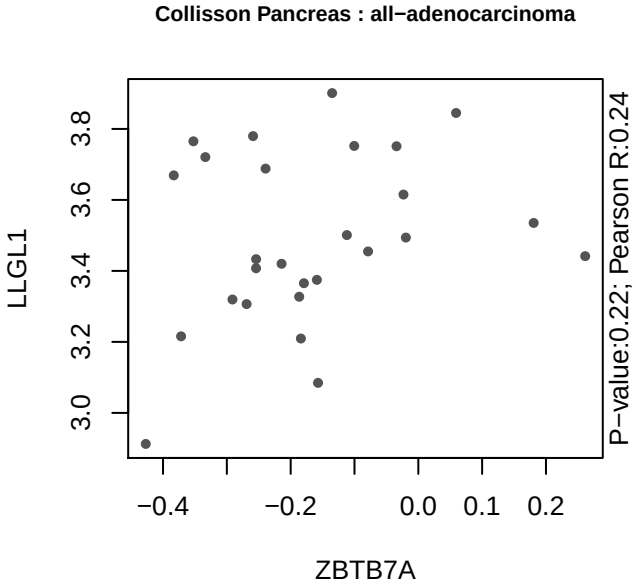

Collisson Pancreas : all−adenocarcinoma
ARHGEF1
BCL6
P−value:0.92; Pearson R:0.02

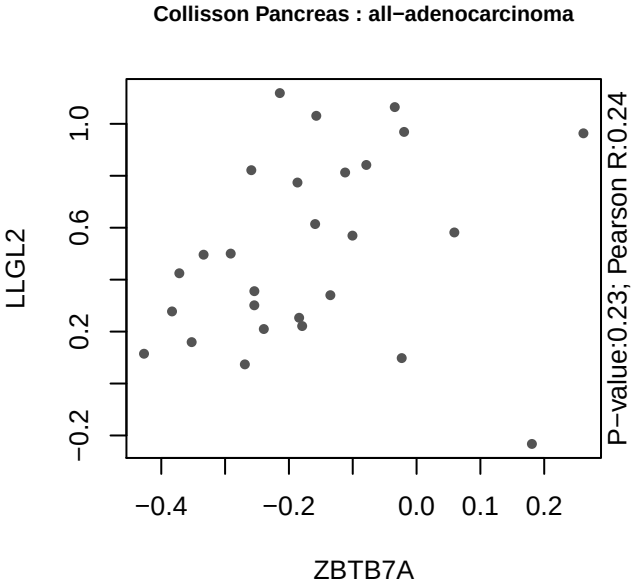

Collisson Pancreas : all−adenocarcinoma
DLG3
ZBTB7A
P−value:0.87; Pearson R:0.033

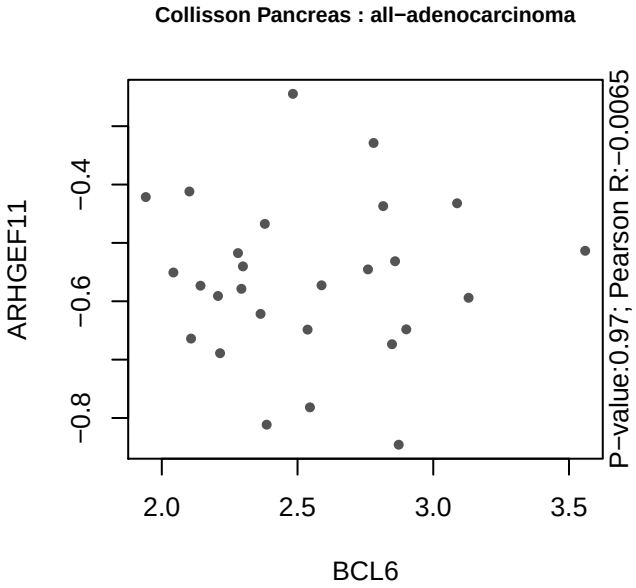

Collisson Pancreas : all−adenocarcinoma
ARHGEF1
ZBTB7A
P−value:0.035; Pearson R:0.41

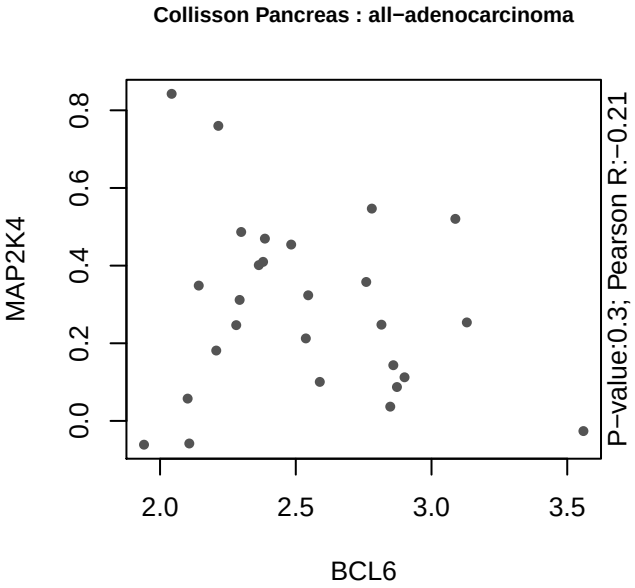

Collisson Pancreas : all−adenocarcinoma
LLGL1
BCL6
P−value:0.056; Pearson R:0.37

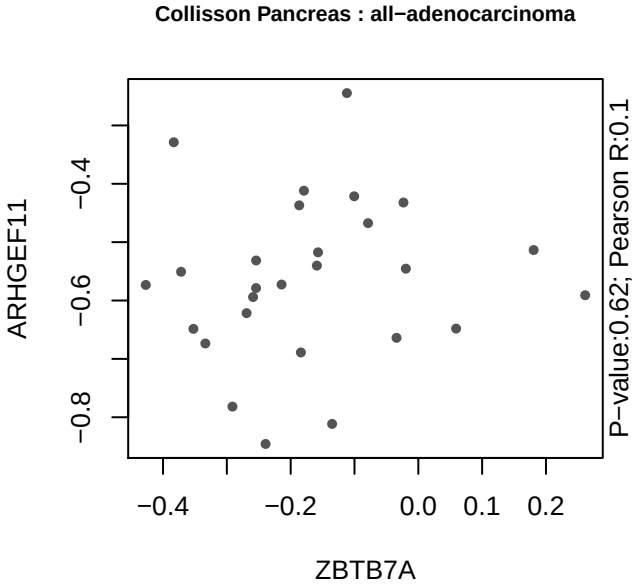

Collisson Pancreas : all−adenocarcinoma
LLGL2
BCL6
P−value:0.23; Pearson R:−0.24

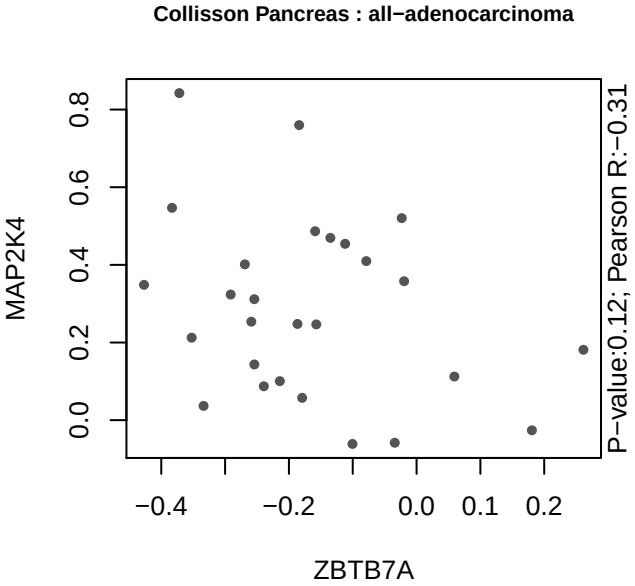

Collisson Pancreas : all−adenocarcinoma
LLGL1
ZBTB7A
P−value:0.22; Pearson R:0.24

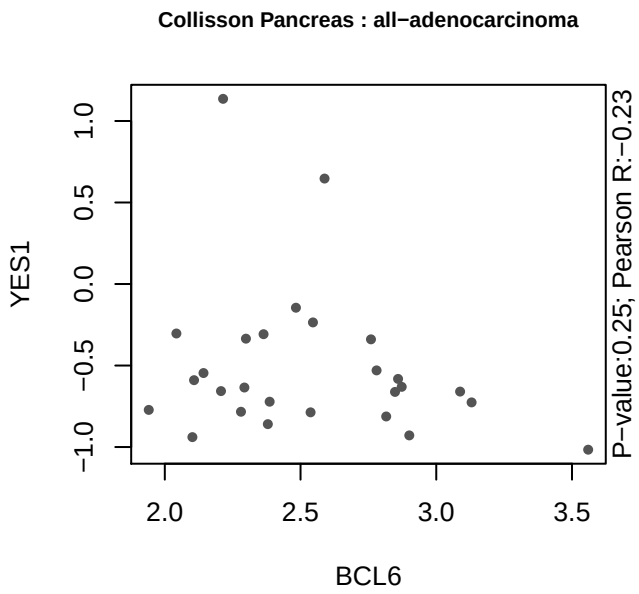

Collisson Pancreas : all−adenocarcinoma
LLGL2
ZBTB7A
P−value:0.23; Pearson R:0.24

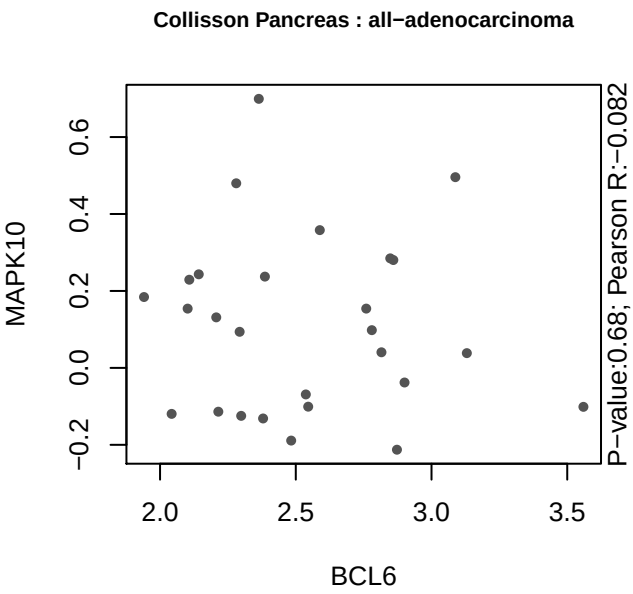

Collisson Pancreas : all−adenocarcinoma
ARHGEF11
−0.4
−0.6
−0.8
2.0
2.5
3.0
3.5
BCL6
P−value:0.97; Pearson R:−0.0065

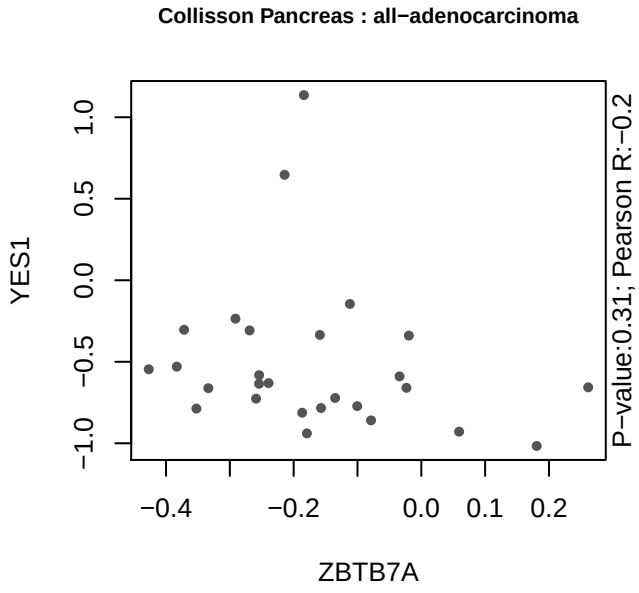

Collisson Pancreas : all−adenocarcinoma
MAP2K4
0.0
0.2
0.4
0.6
0.8
2.0
2.5
3.0
3.5
BCL6
P−value:0.3; Pearson R:−0.21

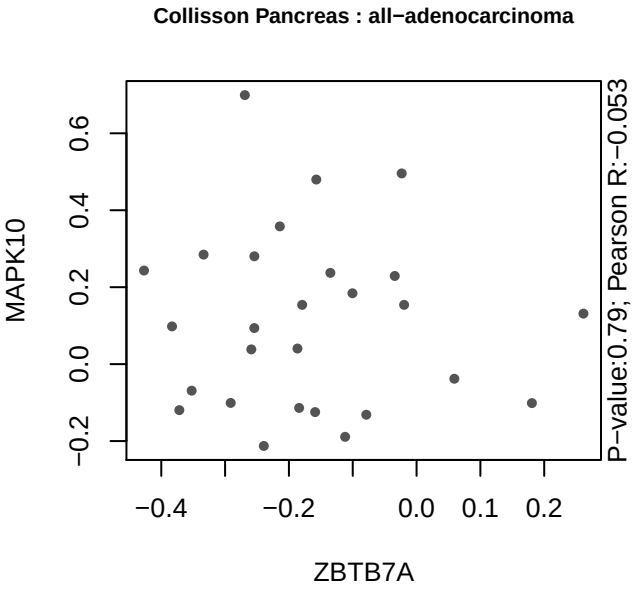

Collisson Pancreas : all−adenocarcinoma
ARHGEF11
−0.4
−0.6
−0.8
−0.4
−0.2
0.0
0.1
0.2
ZBTB7A
P−value:0.62; Pearson R:0.1

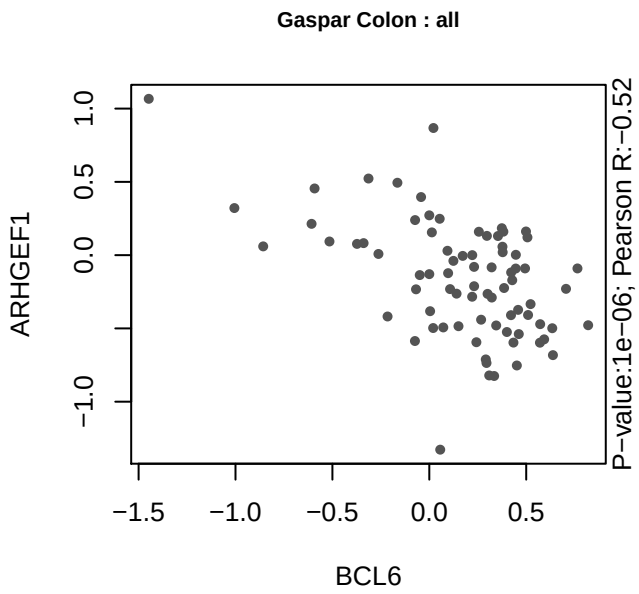

Collisson Pancreas : all−adenocarcinoma
MAP2K4
0.0
0.2
0.4
0.6
0.8
−0.4
−0.2
0.0
0.1
0.2
ZBTB7A
P−value:0.12; Pearson R:−0.31

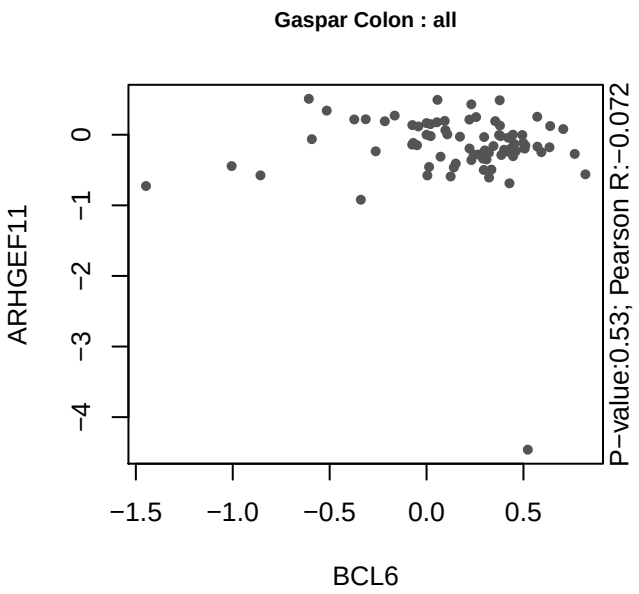

Collisson Pancreas : all−adenocarcinoma
YES1
BCL6
P−value:0.25; Pearson R:−0.23

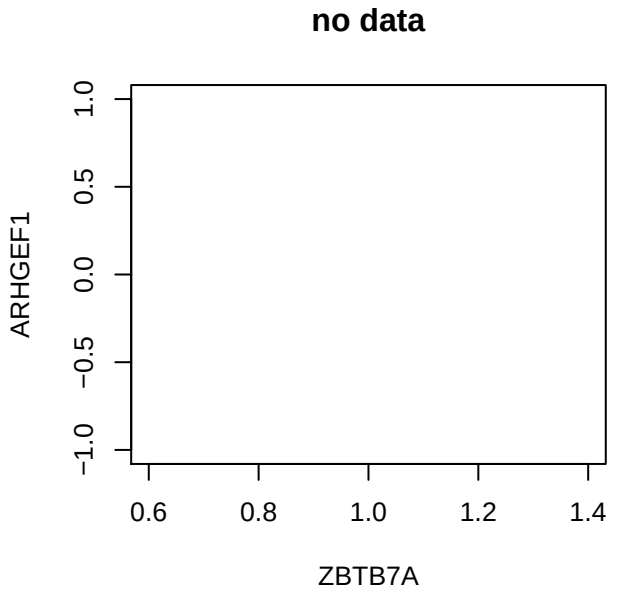

Collisson Pancreas : all−adenocarcinoma
MAPK10
BCL6
P−value:0.68; Pearson R:−0.082

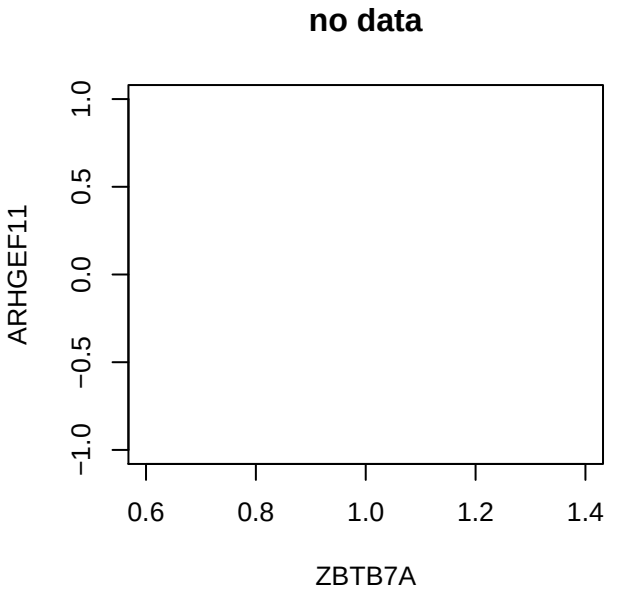

Collisson Pancreas : all−adenocarcinoma
YES1
ZBTB7A
P−value:0.31; Pearson R:−0.2

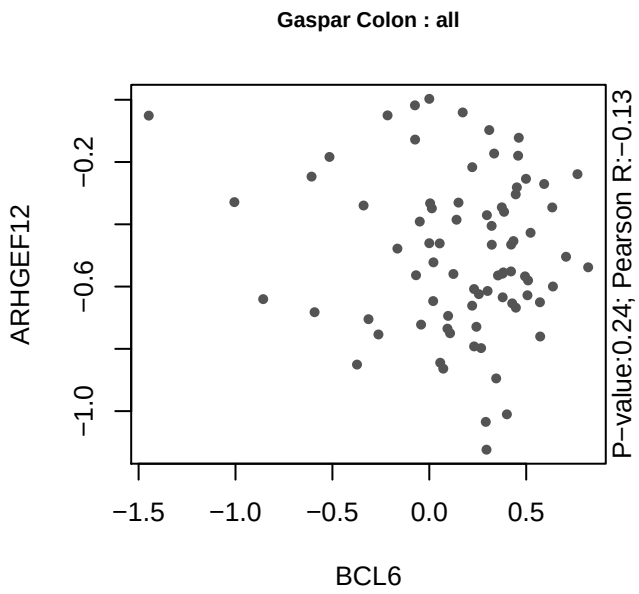

Collisson Pancreas : all−adenocarcinoma
MAPK10
ZBTB7A
P−value:0.79; Pearson R:−0.053

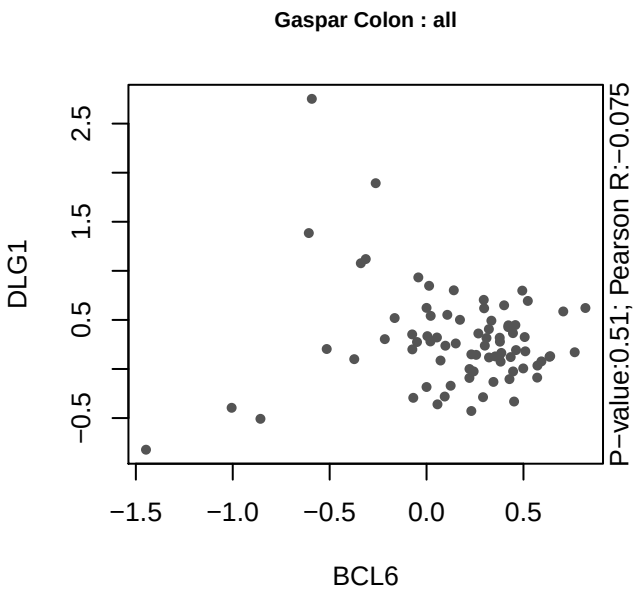

Gaspar Colon : all
ARHGEF1
BCL6
P−value:1e−06; Pearson R:−0.52
1.0
0.5
0.0
−1.0
−1.5
−1.0
−0.5
0.0
0.5

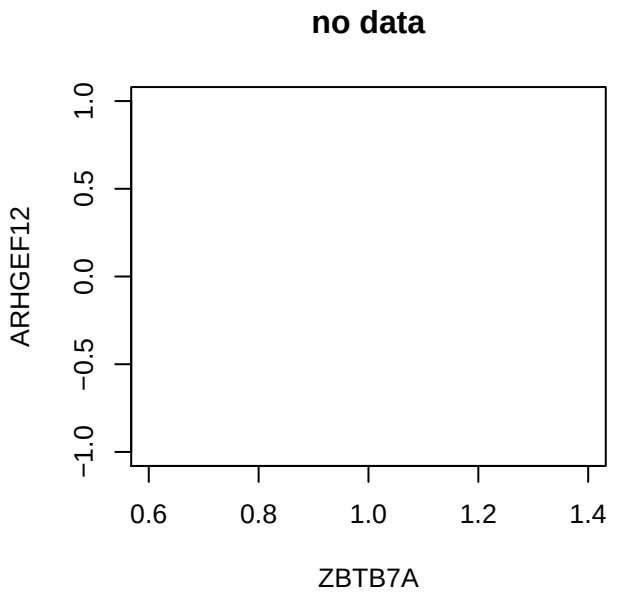

Gaspar Colon : all
ARHGEF11
BCL6
P−value:0.53; Pearson R:−0.072
0
−1
−2
−3
−4
−1.5
−1.0
−0.5
0.0
0.5

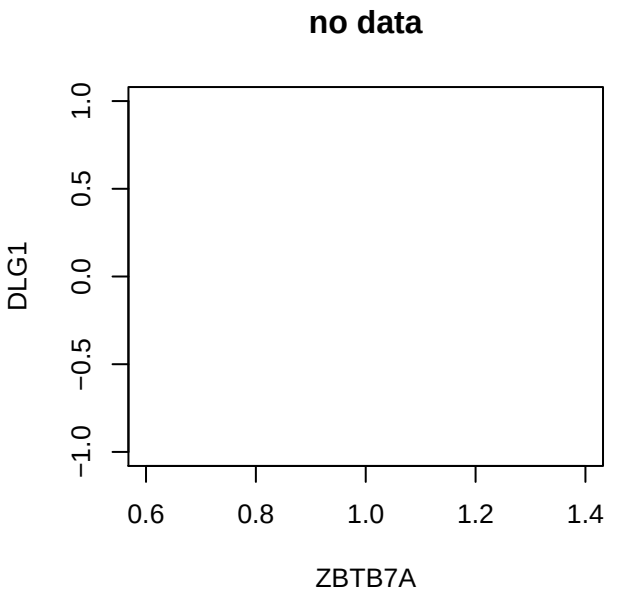

no data
ARHGEF1
ZBTB7A
1.0
0.5
0.0
−0.5
−1.0
0.6
0.8
1.0
1.2
1.4

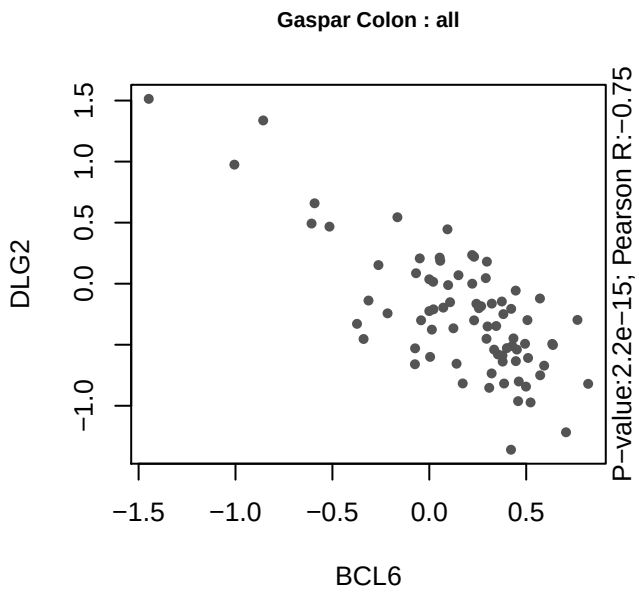

no data
ARHGEF11
ZBTB7A
1.0
0.5
0.0
−0.5
−1.0
0.6
0.8
1.0
1.2
1.4

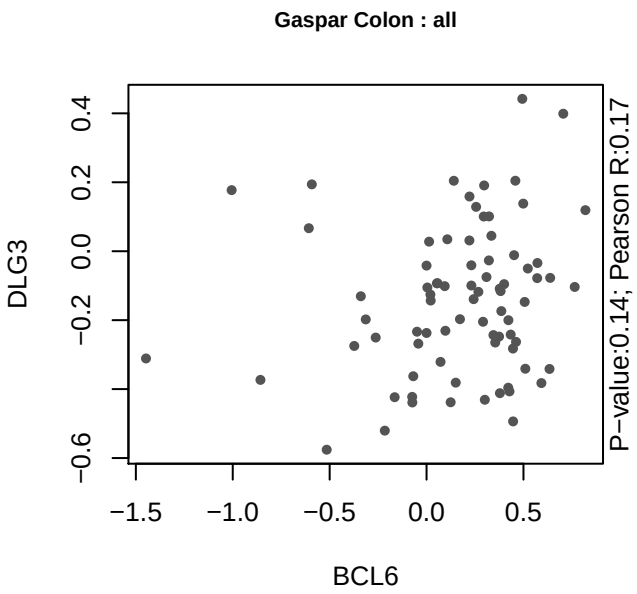

Gaspar Colon : all
ARHGEF12
BCL6
P−value:0.24; Pearson R:−0.13
−1.0
−0.6
−0.2
−1.5
−1.0
−0.5
0.0
0.5

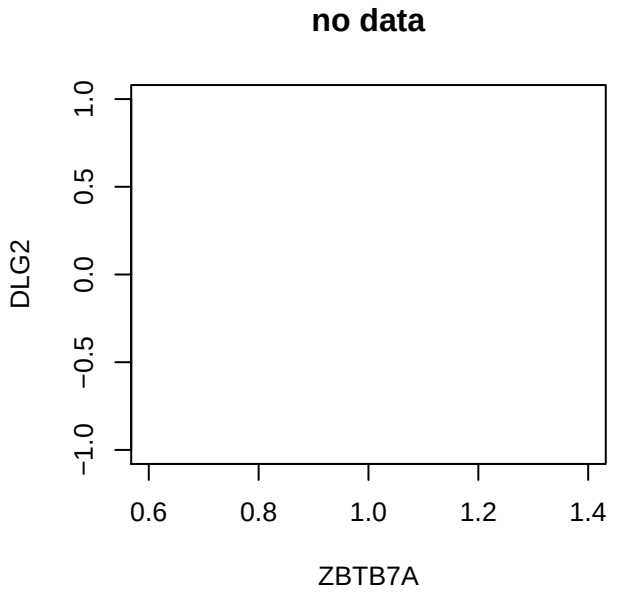

Gaspar Colon : all
DLG1
BCL6
P−value:0.51; Pearson R:−0.075
−0.5
0.5
1.5
2.5
−1.5
−1.0
−0.5
0.0
0.5

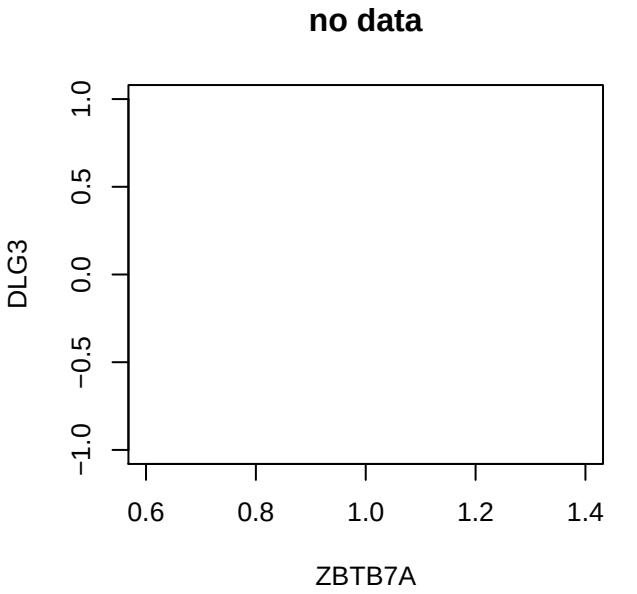

no data
ARHGEF12
ZBTB7A
−1.0
−0.5
0.0
0.5
1.0
0.6
0.8
1.0
1.2
1.4

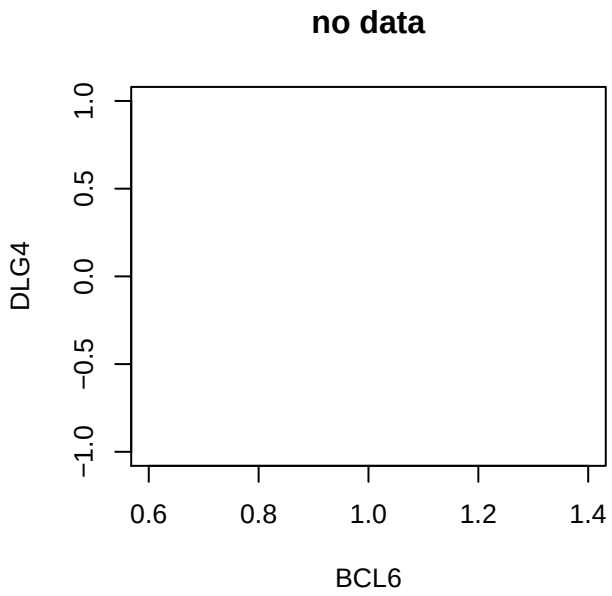

no data
DLG1
ZBTB7A
−1.0
−0.5
0.0
0.5
1.0
0.6
0.8
1.0
1.2
1.4

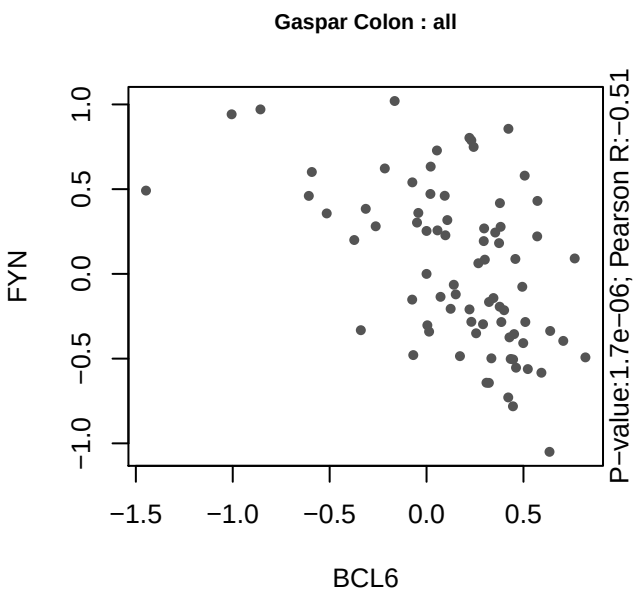

Gaspar Colon : all
DLG2
BCL6
P−value:2.2e−15; Pearson R:−0.75

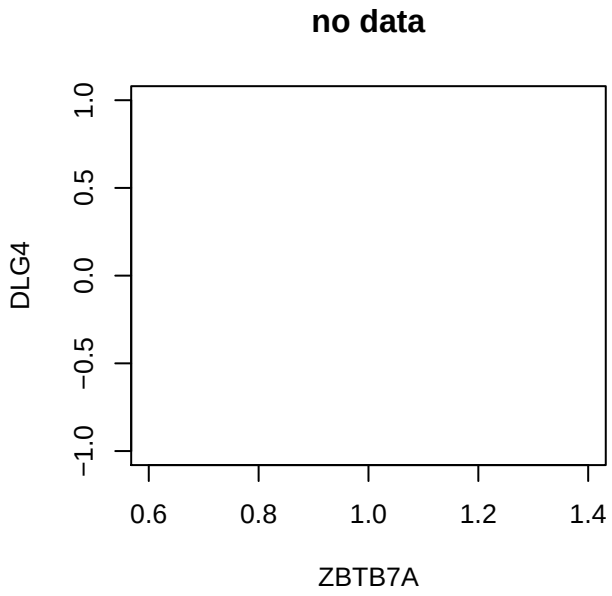

Gaspar Colon : all
DLG3
BCL6
P−value:0.14; Pearson R:0.17

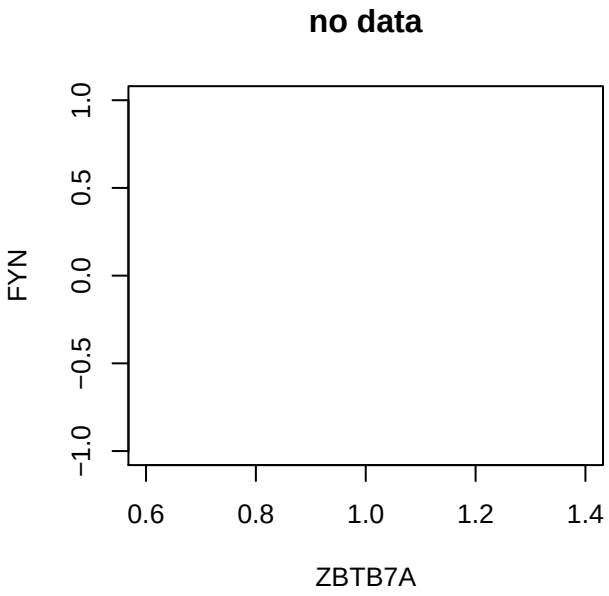

no data
DLG2
ZBTB7A

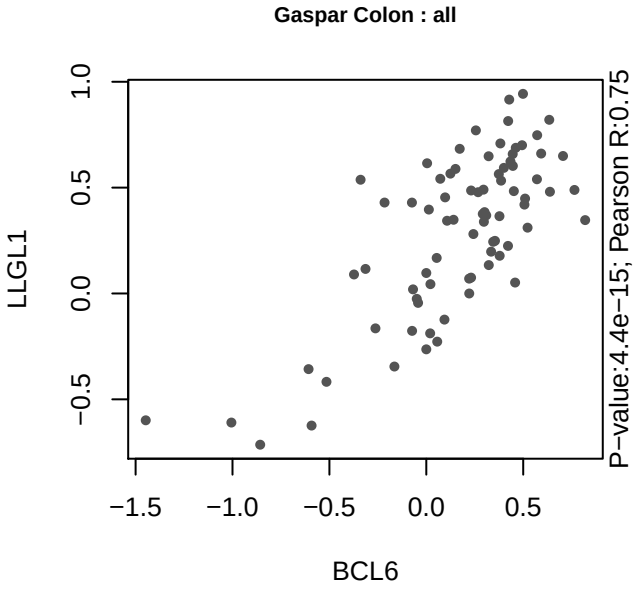

no data
DLG3
ZBTB7A

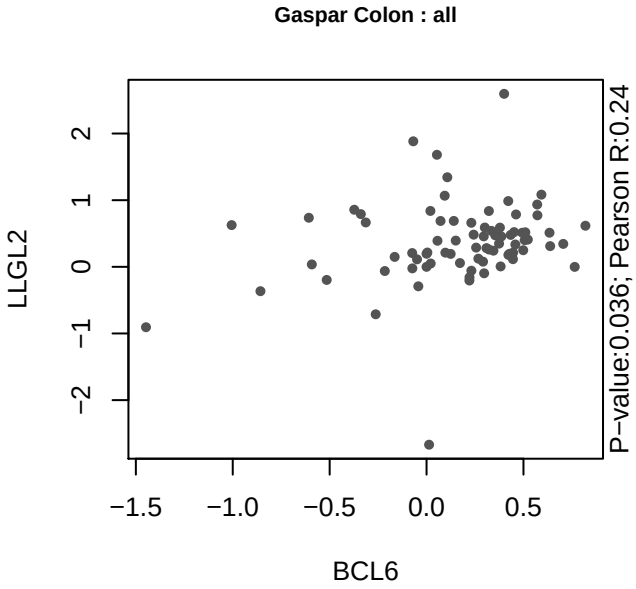

no data
DLG4
BCL6
1.0
0.5
0.0
−0.5
−1.0
0.6
0.8
1.0
1.2
1.4

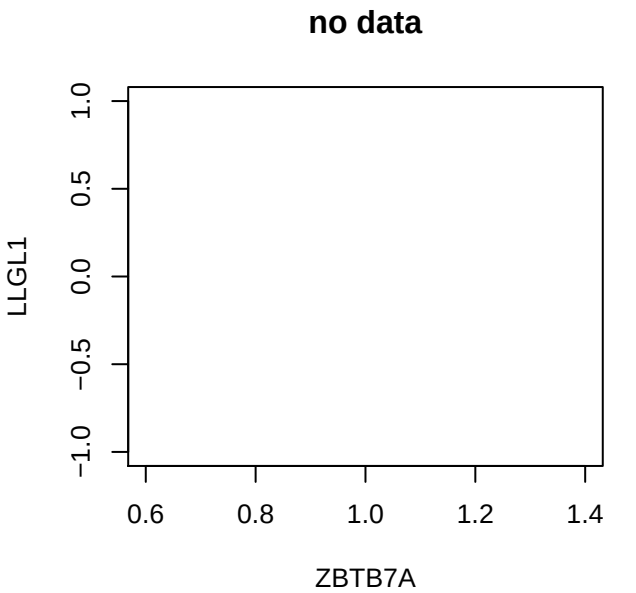

Gaspar Colon : all
FYN
BCL6
P−value:1.7e−06; Pearson R:−0.51
1.0
0.5
0.0
−0.5
−1.0
−1.5
−1.0
−0.5
0.0
0.5

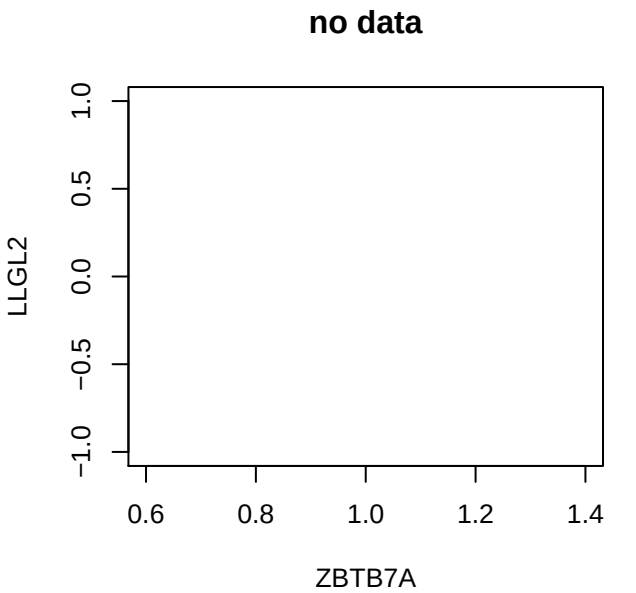

no data
DLG4
ZBTB7A
1.0
0.5
0.0
−0.5
−1.0
0.6
0.8
1.0
1.2
1.4

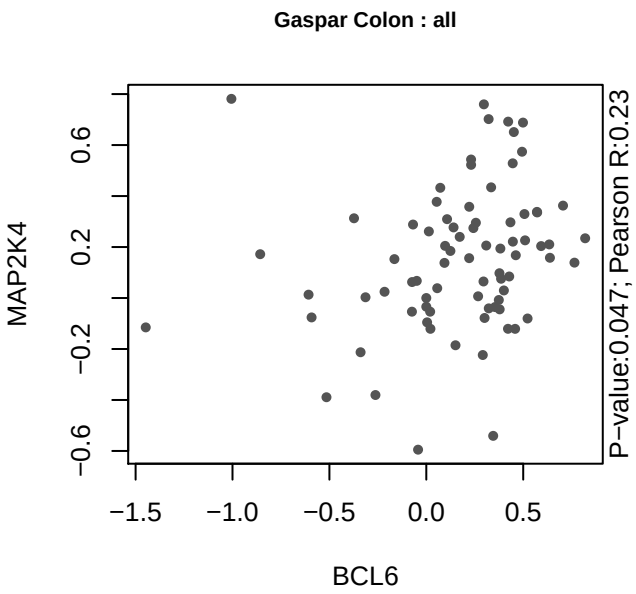

no data
FYN
ZBTB7A
1.0
0.5
0.0
−0.5
−1.0
0.6
0.8
1.0
1.2
1.4

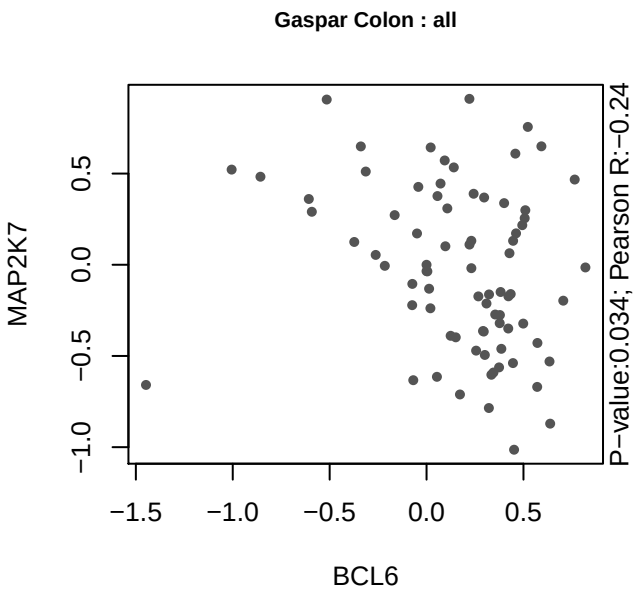

Gaspar Colon : all
LLGL1
BCL6
P−value:4.4e−15; Pearson R:0.75
1.0
0.5
0.0
−0.5
−1.5
−1.0
−0.5
0.0
0.5

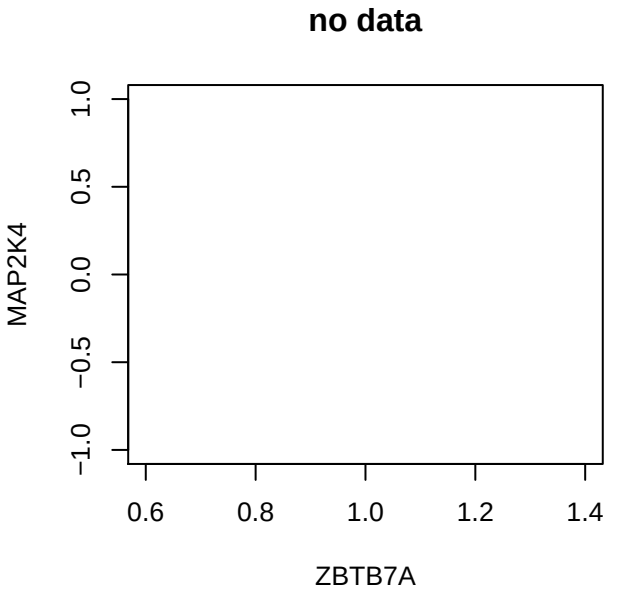

Gaspar Colon : all
LLGL2
BCL6
P−value:0.036; Pearson R:0.24
2
1
0
−1
−2
−1.5
−1.0
−0.5
0.0
0.5

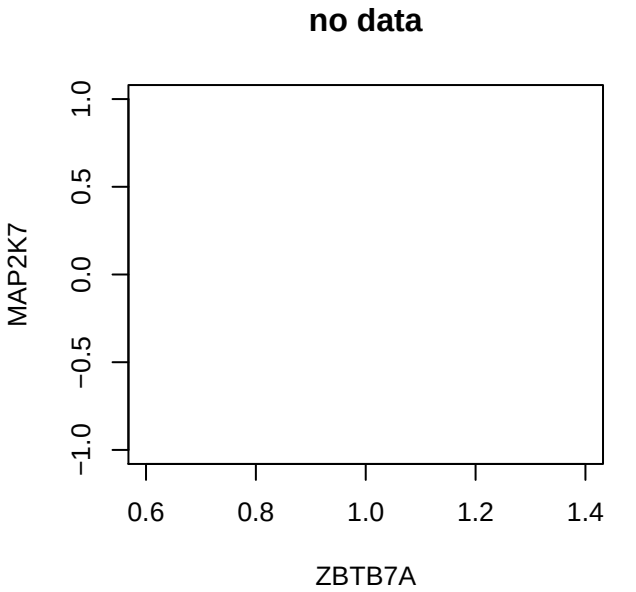

no data
LLGL1
ZBTB7A
1.0
0.5
0.0
−0.5
−1.0
0.6
0.8
1.0
1.2
1.4

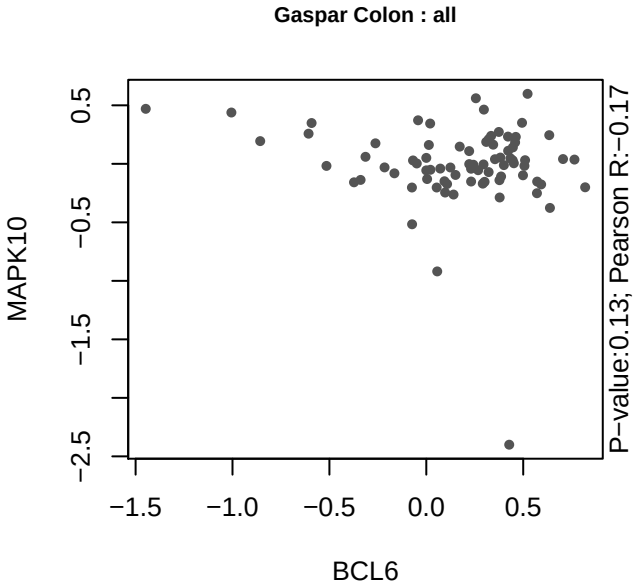

no data
LLGL2
ZBTB7A
1.0
0.5
0.0
−0.5
−1.0
0.6
0.8
1.0
1.2
1.4

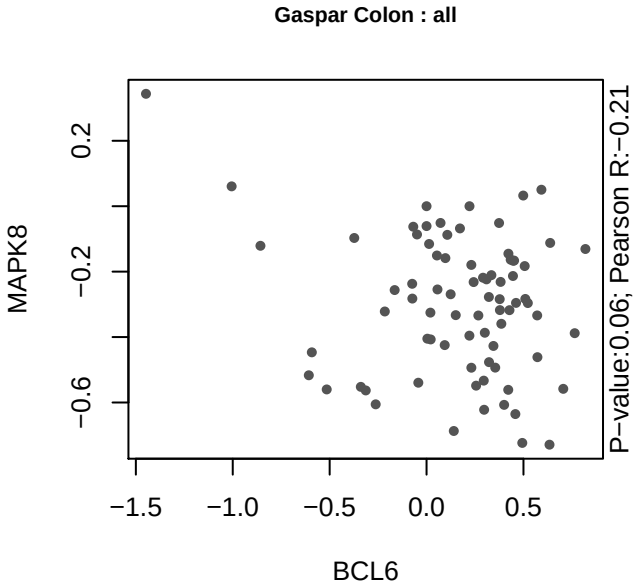

Gaspar Colon : all
MAP2K4
BCL6
P−value:0.047; Pearson R:0.23

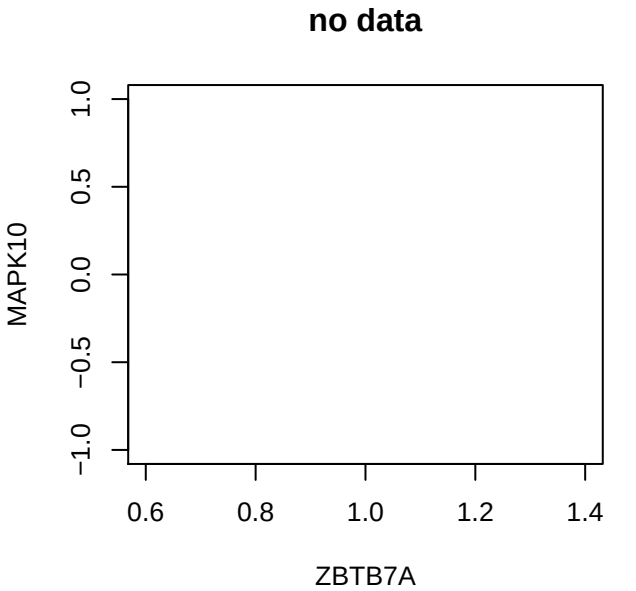

Gaspar Colon : all
MAP2K7
BCL6
P−value:0.034; Pearson R:−0.24

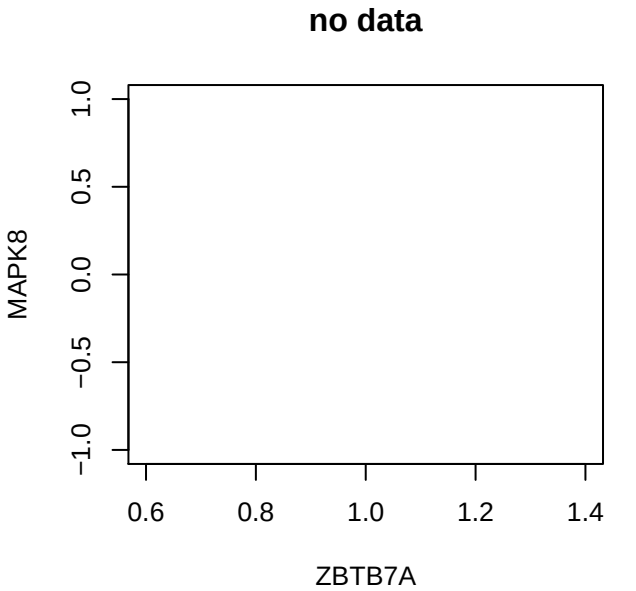

no data
MAP2K4
ZBTB7A

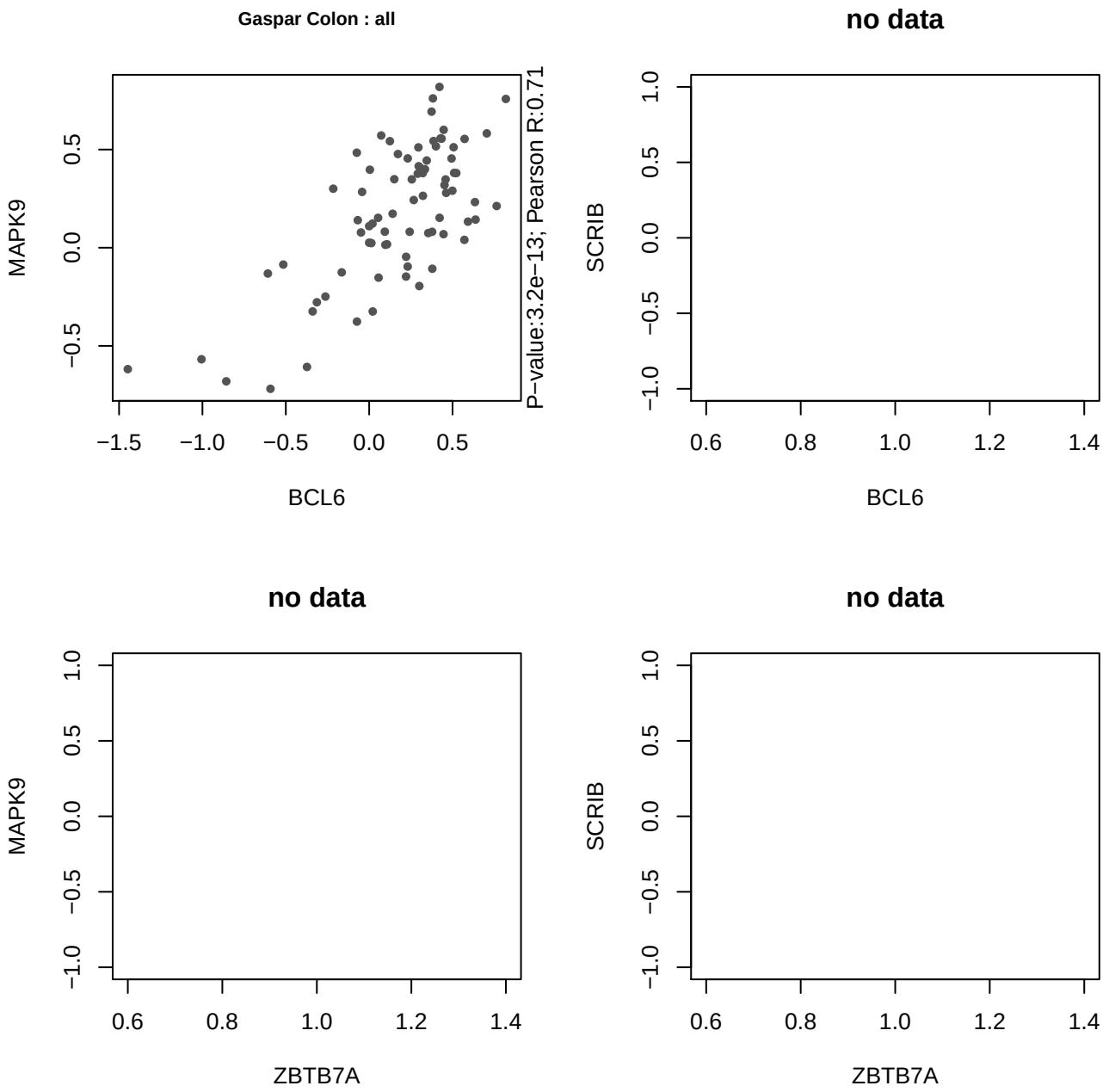

no data
MAP2K7
ZBTB7A

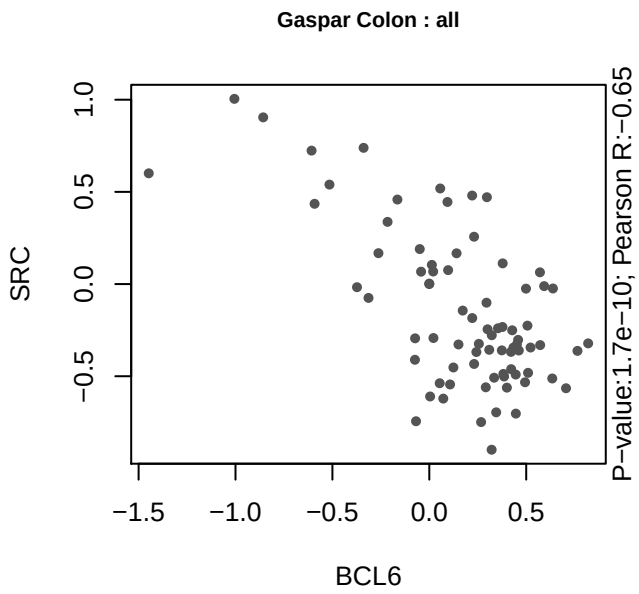

Gaspar Colon : all
MAPK10
BCL6
P−value:0.13; Pearson R:−0.17
0.5
−0.5
−1.5
−2.5
−1.5
−1.0
−0.5
0.0
0.5

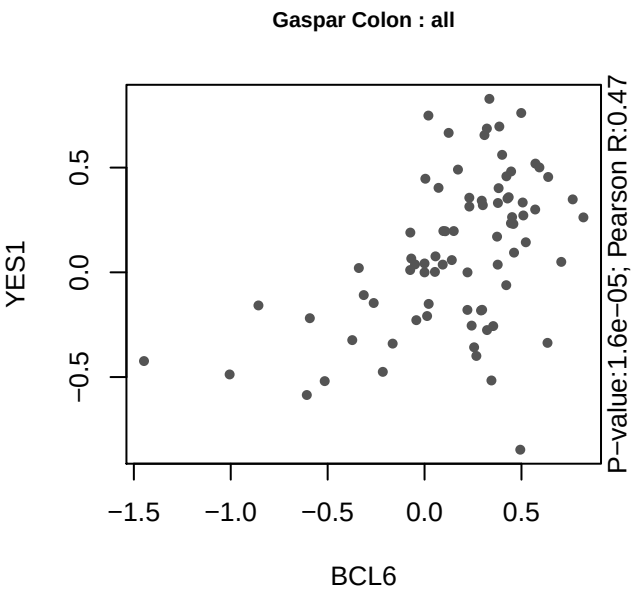

Gaspar Colon : all
MAPK8
BCL6
P−value:0.06; Pearson R:−0.21
0.2
−0.2
−0.6
−1.5
−1.0
−0.5
0.0
0.5

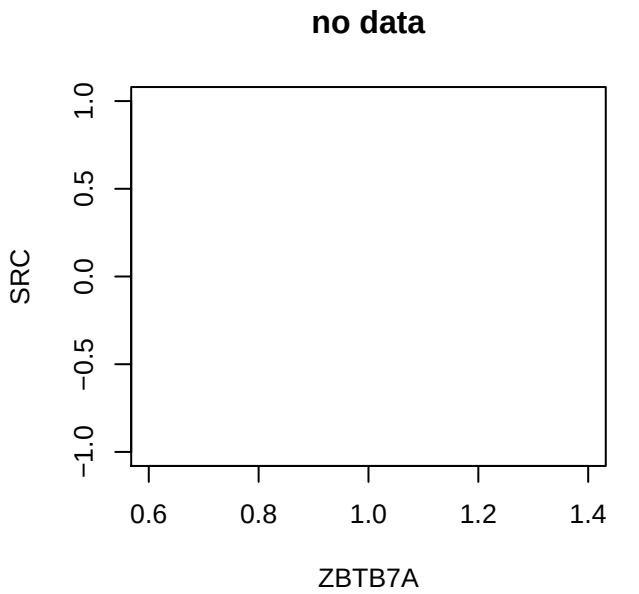

no data
MAPK10
ZBTB7A
1.0
0.5
0.0
−0.5
−1.0
0.6
0.8
1.0
1.2
1.4

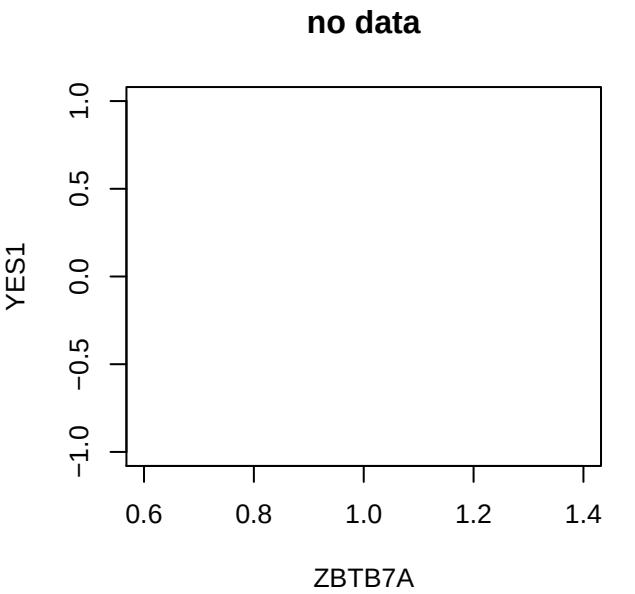

no data
MAPK8
ZBTB7A
1.0
0.5
0.0
−0.5
−1.0
0.6
0.8
1.0
1.2
1.4

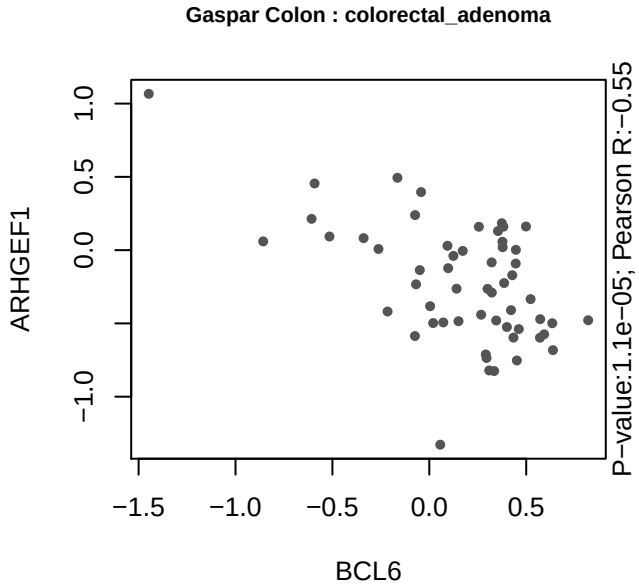

Gaspar Colon : all
P−value:3.2e−13; Pearson R:0.71
MAPK9
BCL6
no data
SCRIB
BCL6
no data
MAPK9
ZBTB7A
no data
SCRIB
ZBTB7A

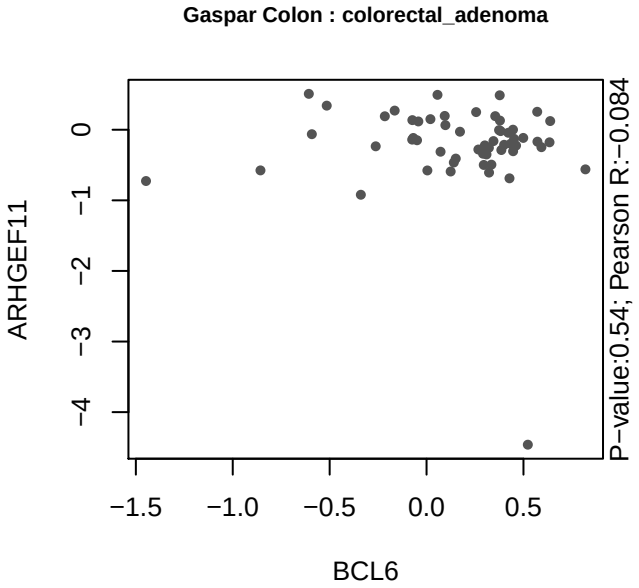

Gaspar Colon : all
SRC
BCL6
P−value:1.7e−10; Pearson R:−0.65
1.0
0.5
0.0
−0.5
−1.5
−1.0
−0.5
0.0
0.5

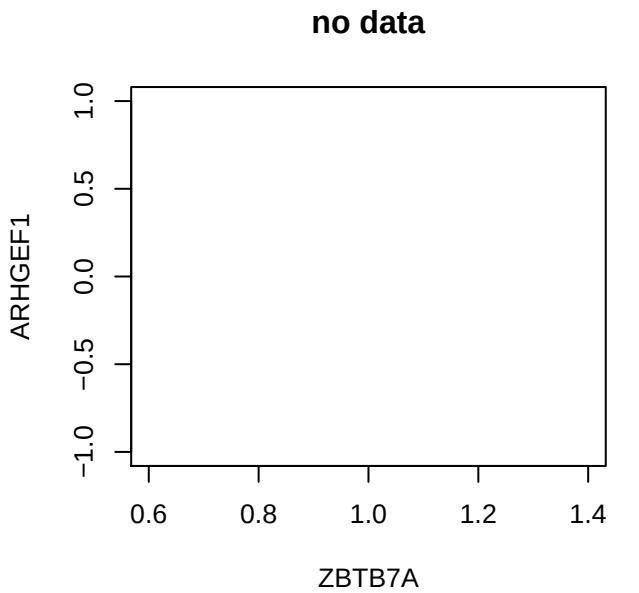

Gaspar Colon : all
YES1
BCL6
P−value:1.6e−05; Pearson R:0.47
0.5
0.0
−0.5
−1.5
−1.0
−0.5
0.0
0.5

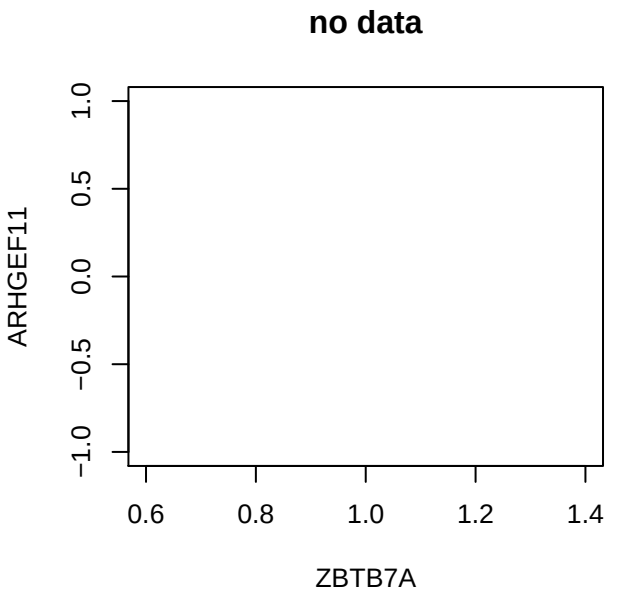

no data
SRC
ZBTB7A
1.0
0.5
0.0
−0.5
−1.0
0.6
0.8
1.0
1.2
1.4

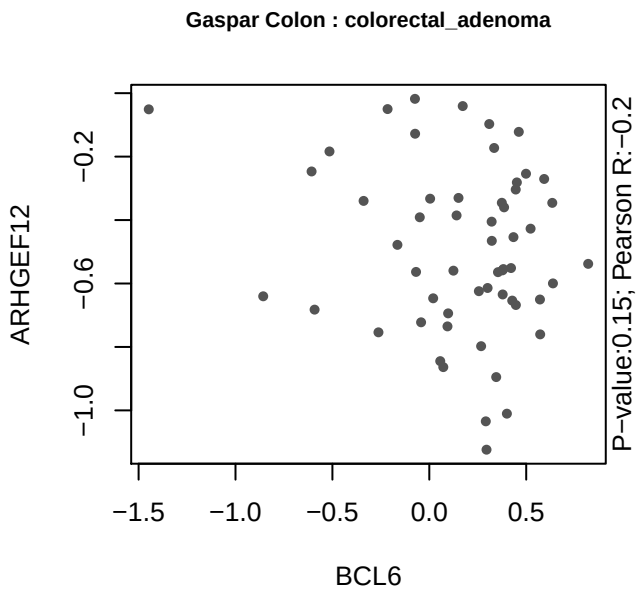

no data
YES1
ZBTB7A
1.0
0.5
0.0
−0.5
−1.0
0.6
0.8
1.0
1.2
1.4

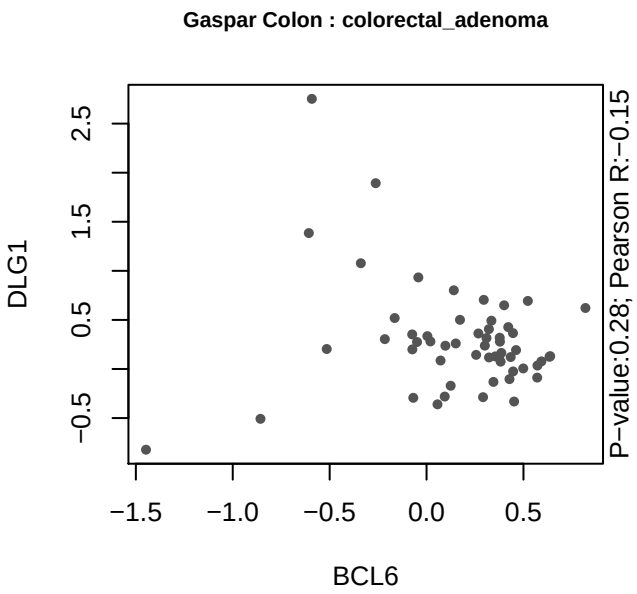

Gaspar Colon : colorectal_adenoma
ARHGEF1
BCL6
P−value:1.1e−05; Pearson R:−0.55
1.0
0.5
0.0
−1.0
−1.5
−1.0
−0.5
0.0
0.5

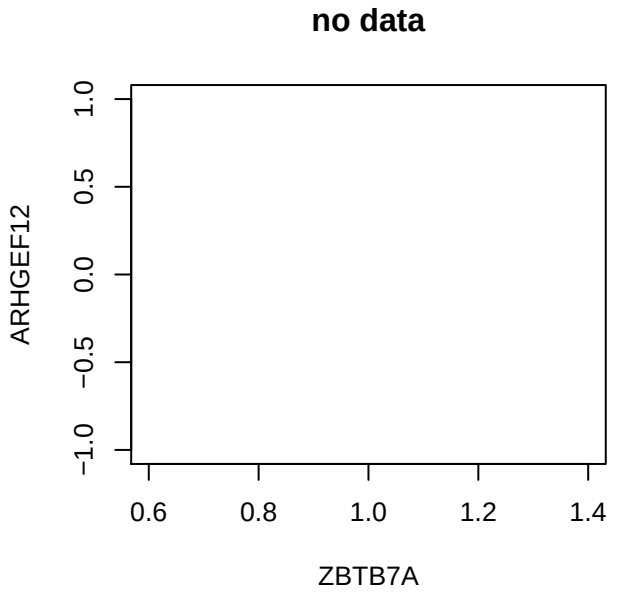

Gaspar Colon : colorectal_adenoma
ARHGEF11
BCL6
P−value:0.54; Pearson R:−0.084
0
−1
−2
−3
−4
−1.5
−1.0
−0.5
0.0
0.5

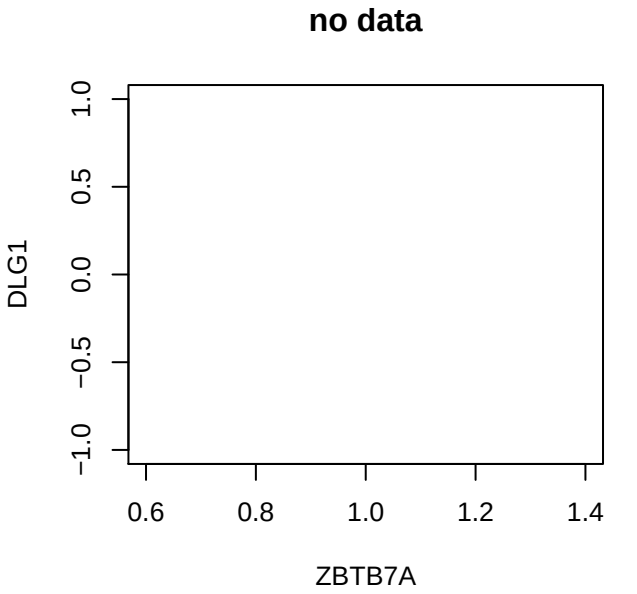

no data
ARHGEF1
ZBTB7A
1.0
0.5
0.0
−0.5
−1.0
0.6
0.8
1.0
1.2
1.4

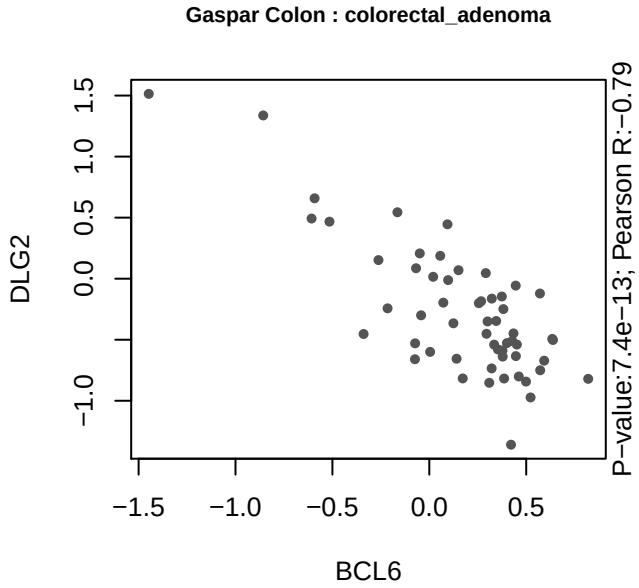

no data
ARHGEF11
ZBTB7A
1.0
0.5
0.0
−0.5
−1.0
0.6
0.8
1.0
1.2
1.4

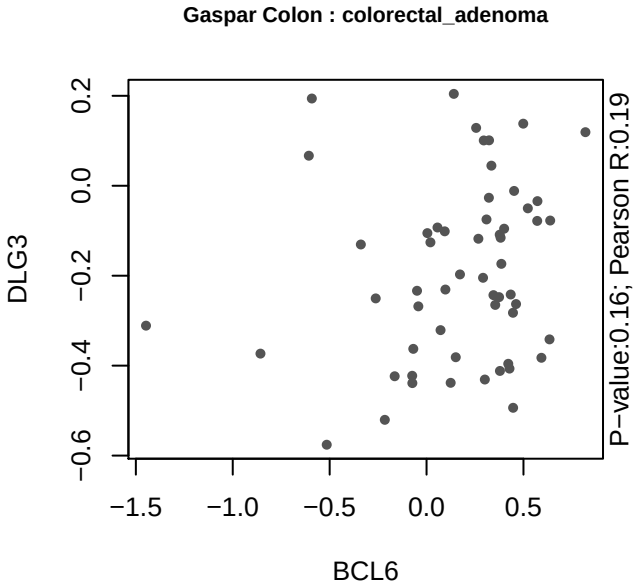

Gaspar Colon : colorectal_adenoma
ARHGEF12
BCL6
P−value:0.15; Pearson R:−0.2

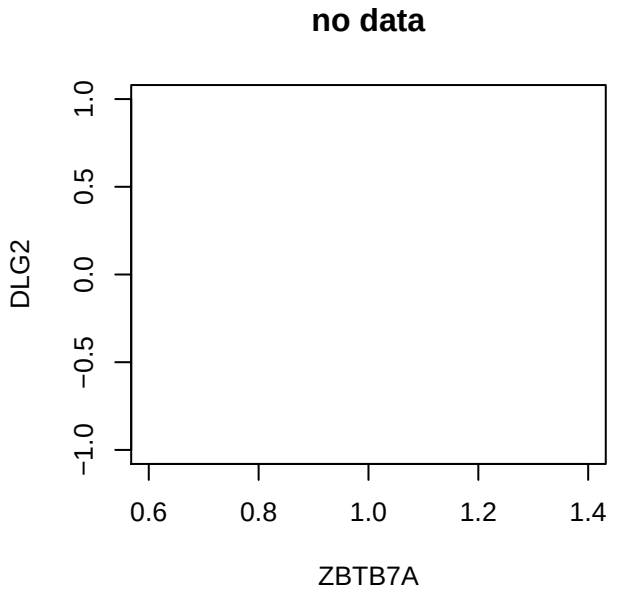

Gaspar Colon : colorectal_adenoma
DLG1
BCL6
P−value:0.28; Pearson R:−0.15

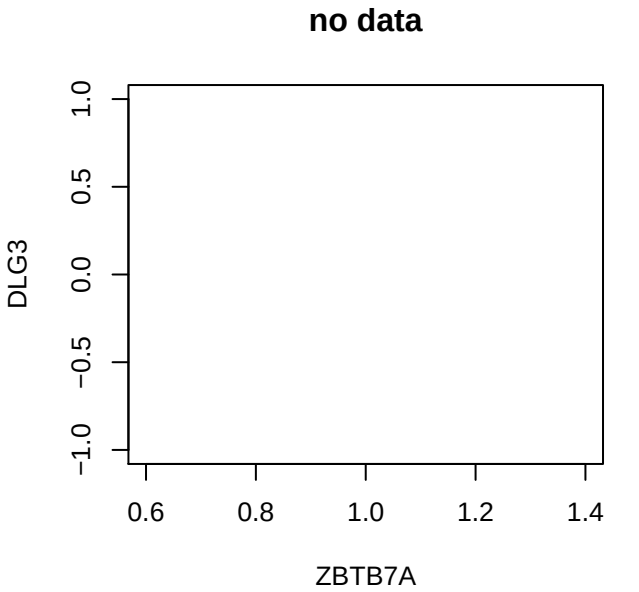

no data
ARHGEF12
ZBTB7A

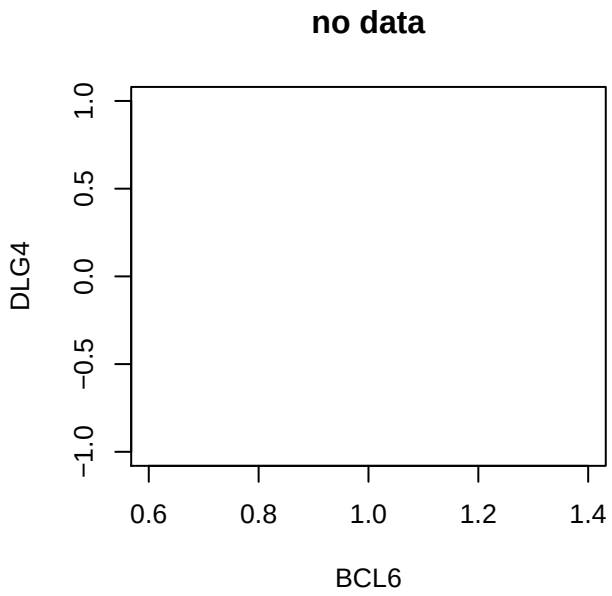

no data
DLG1
ZBTB7A

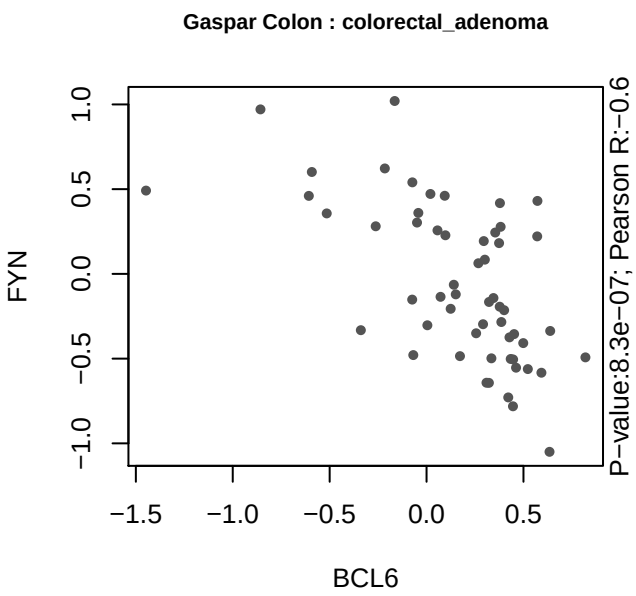

Gaspar Colon : colorectal_adenoma
DLG2
BCL6
P−value:7.4e−13; Pearson R:−0.79
−1.5
−1.0
−0.5
0.0
0.5
1.0
1.5

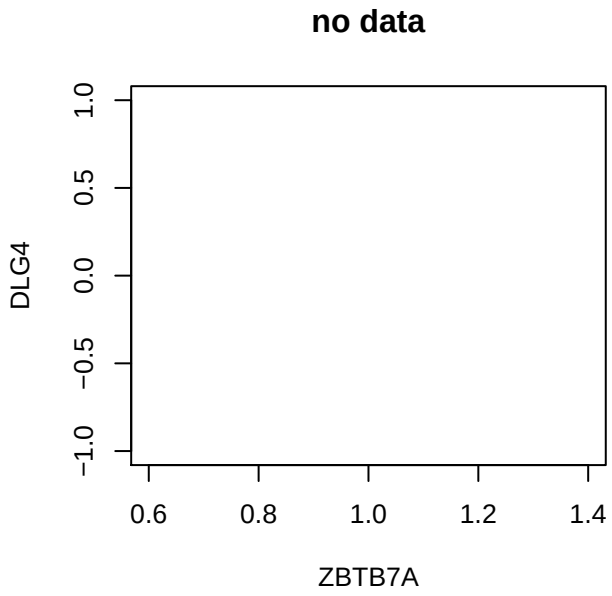

Gaspar Colon : colorectal_adenoma
DLG3
BCL6
P−value:0.16; Pearson R:0.19
−0.6
−0.4
−0.2
0.0
0.2

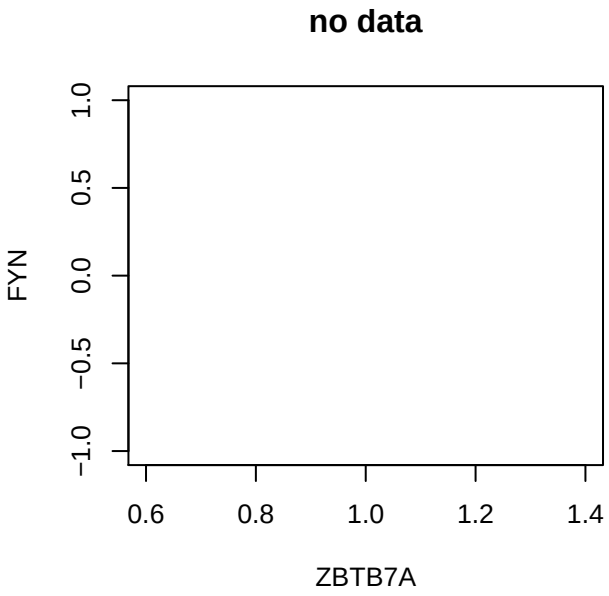

no data
DLG2
ZBTB7A
0.6
0.8
1.0
1.2
1.4

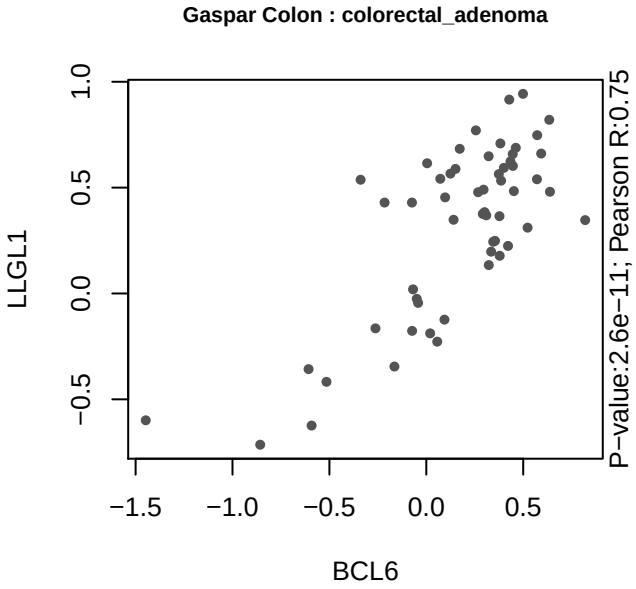

no data
DLG3
ZBTB7A
0.6
0.8
1.0
1.2
1.4

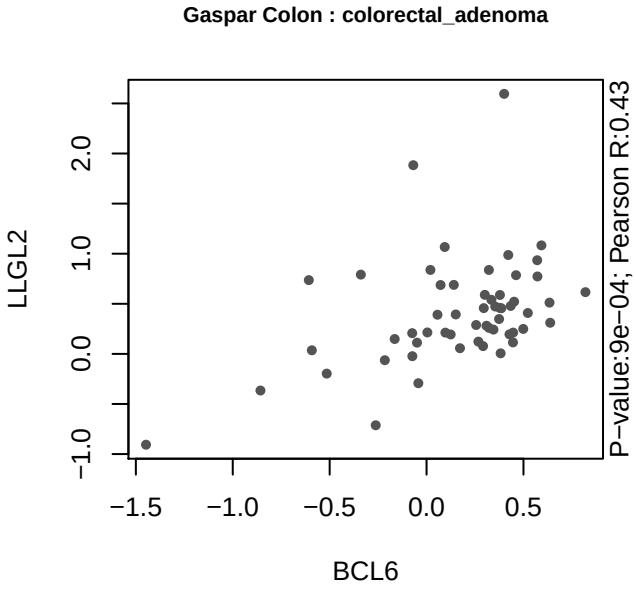

no data
DLG4
BCL6
1.0
0.5
0.0
−0.5
−1.0
0.6
0.8
1.0
1.2
1.4

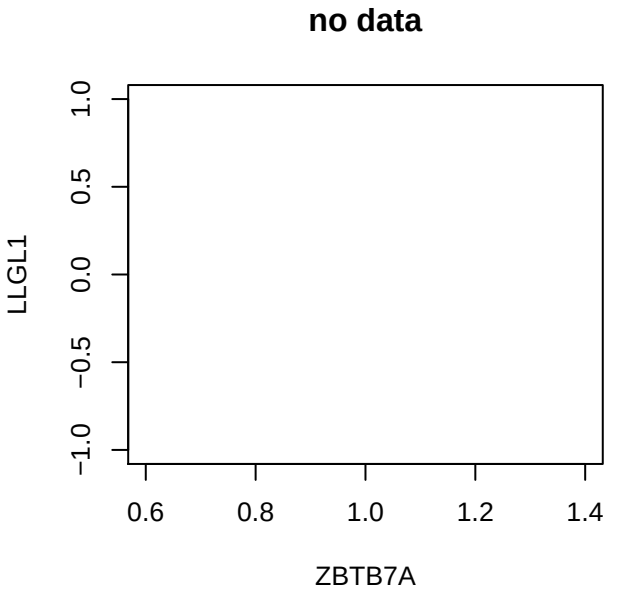

Gaspar Colon : colorectal_adenoma
FYN
BCL6
P−value:8.3e−07; Pearson R:−0.6
1.0
0.5
0.0
−0.5
−1.0
−1.5
−1.0
−0.5
0.0
0.5

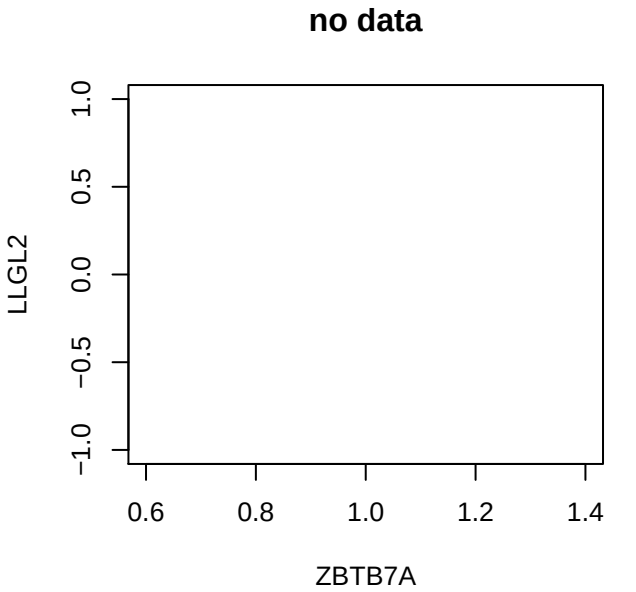

no data
DLG4
ZBTB7A
1.0
0.5
0.0
−0.5
−1.0
0.6
0.8
1.0
1.2
1.4

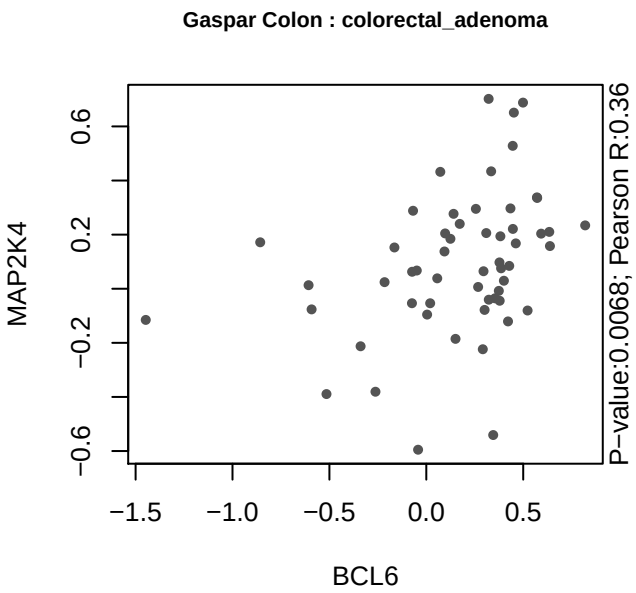

no data
FYN
ZBTB7A
1.0
0.5
0.0
−0.5
−1.0
0.6
0.8
1.0
1.2
1.4

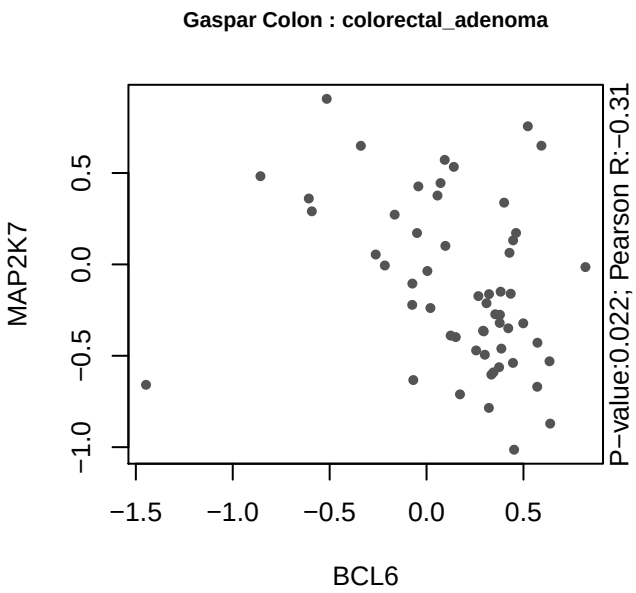

Gaspar Colon : colorectal_adenoma
LLGL1
BCL6
P−value:2.6e−11; Pearson R:0.75

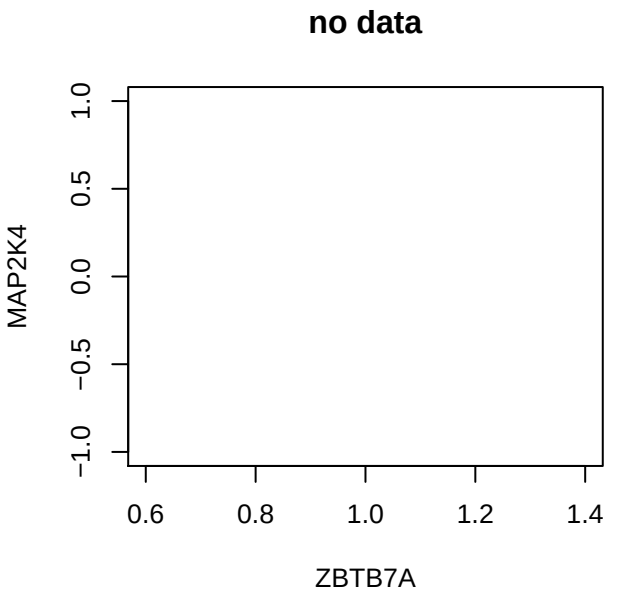

Gaspar Colon : colorectal_adenoma
LLGL2
BCL6
P−value:9e−04; Pearson R:0.43

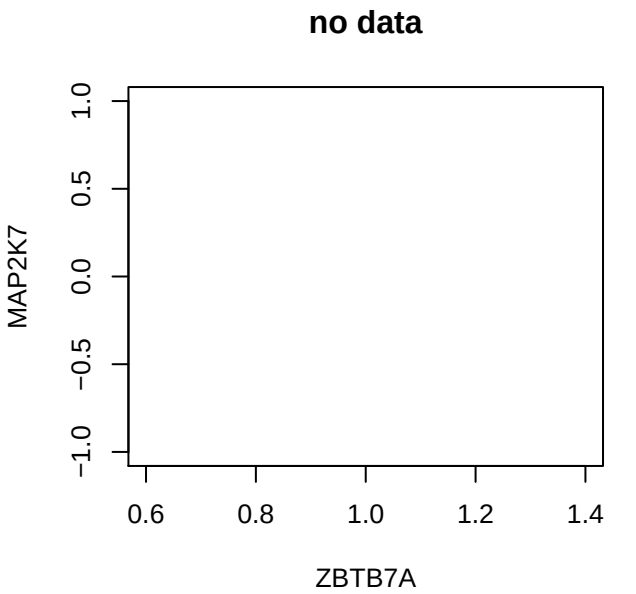

no data
LLGL1
ZBTB7A

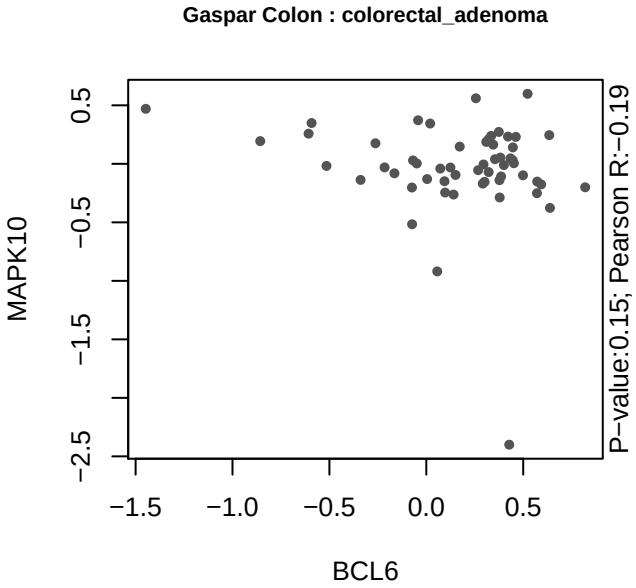

no data
LLGL2
ZBTB7A

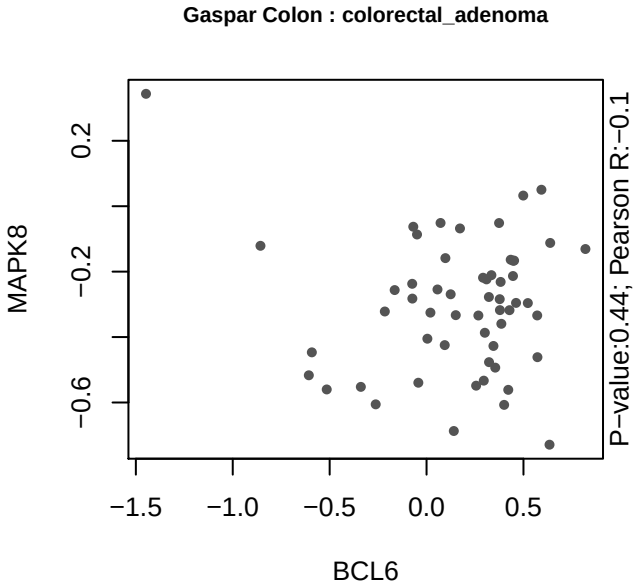

Gaspar Colon : colorectal_adenoma
MAP2K4
BCL6
P−value:0.0068; Pearson R:0.36
−1.5
−1.0
−0.5
0.0
0.5
−0.6
−0.2
0.2
0.6

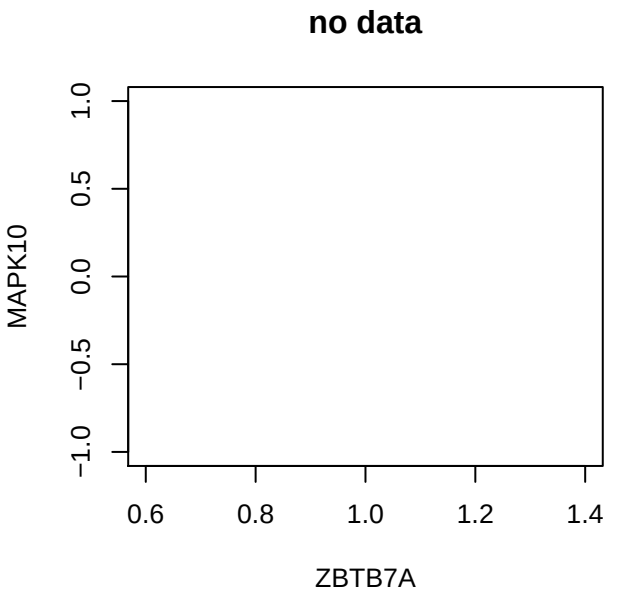

Gaspar Colon : colorectal_adenoma
MAP2K7
BCL6
P−value:0.022; Pearson R:−0.31
−1.5
−1.0
−0.5
0.0
0.5
−1.0
−0.5
0.0
0.5

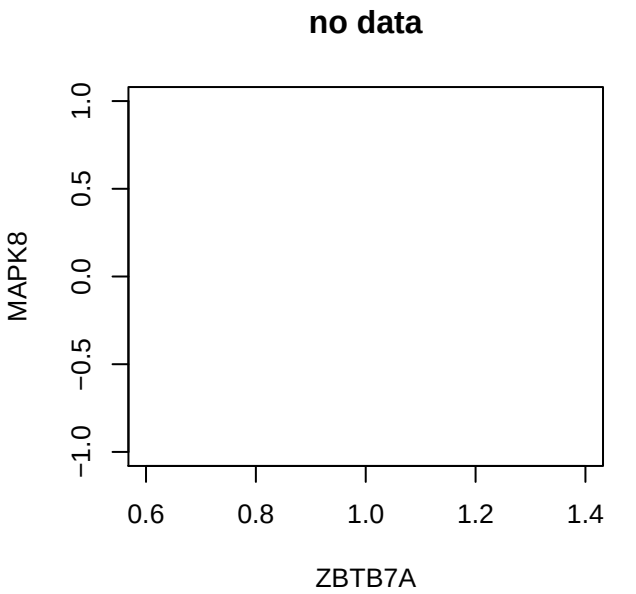

no data
MAP2K4
ZBTB7A
0.6
0.8
1.0
1.2
1.4
−1.0
−0.5
0.0
0.5
1.0

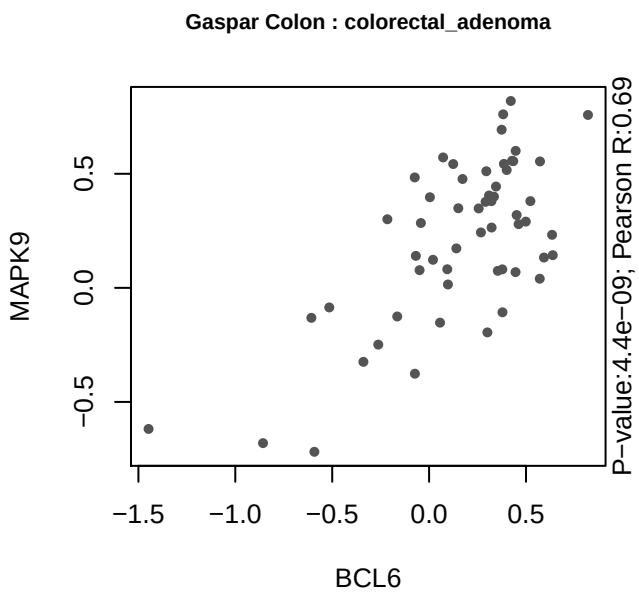

no data
MAP2K7
ZBTB7A
0.6
0.8
1.0
1.2
1.4
−1.0
−0.5
0.0
0.5
1.0

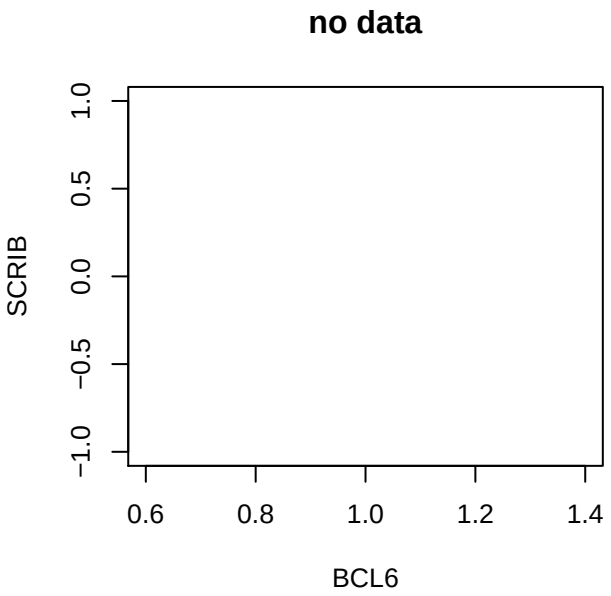

Gaspar Colon : colorectal_adenoma
MAPK10
BCL6
P−value:0.15; Pearson R:−0.19
0.5
−0.5
−1.5
−2.5
−1.5
−1.0
−0.5
0.0
0.5

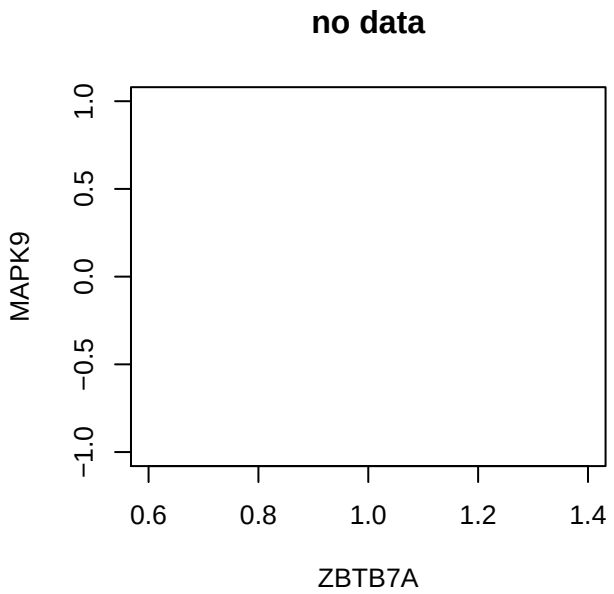

Gaspar Colon : colorectal_adenoma
MAPK8
BCL6
P−value:0.44; Pearson R:−0.1
0.2
−0.2
−0.6
−1.5
−1.0
−0.5
0.0
0.5

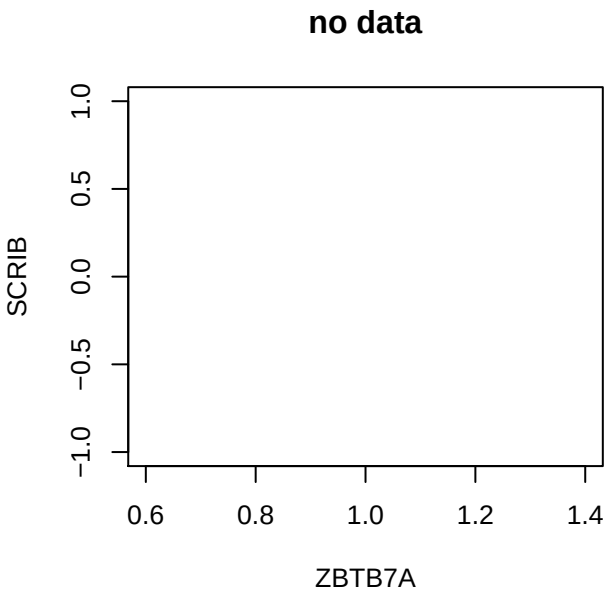

no data
MAPK10
ZBTB7A
1.0
0.5
0.0
−0.5
−1.0
0.6
0.8
1.0
1.2
1.4

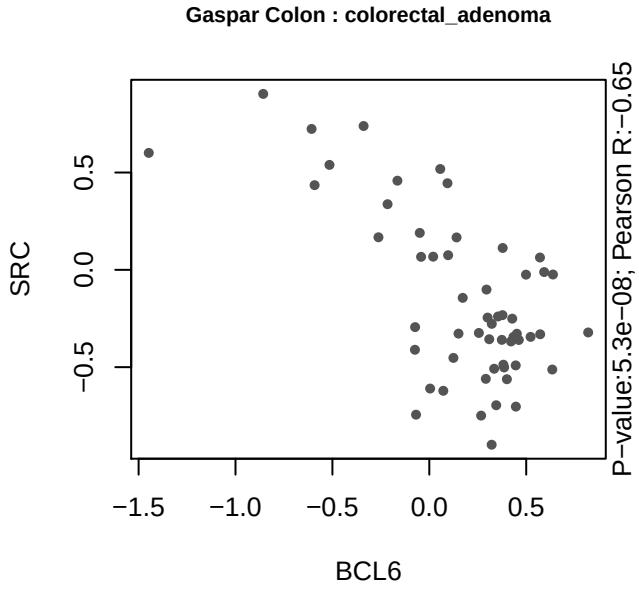

no data
MAPK8
ZBTB7A
1.0
0.5
0.0
−0.5
−1.0
0.6
0.8
1.0
1.2
1.4

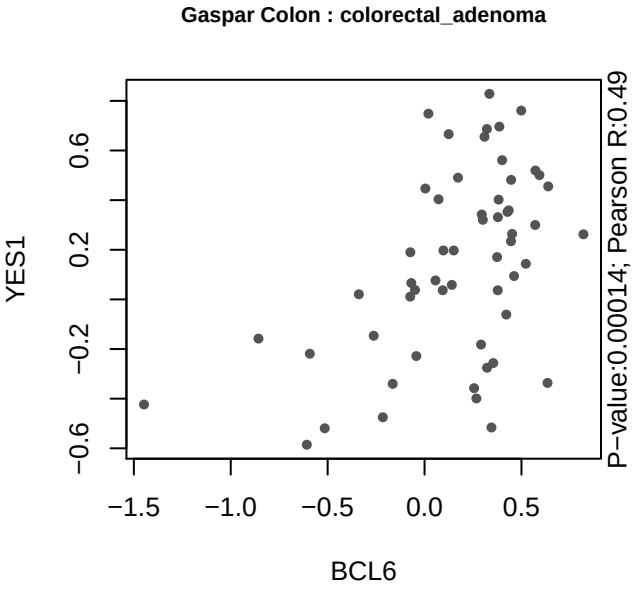

Gaspar Colon : colorectal_adenoma
MAPK9
BCL6
P−value:4.4e−09; Pearson R:0.69
−1.5
−1.0
−0.5
0.0
0.5
−0.5
0.0
0.5

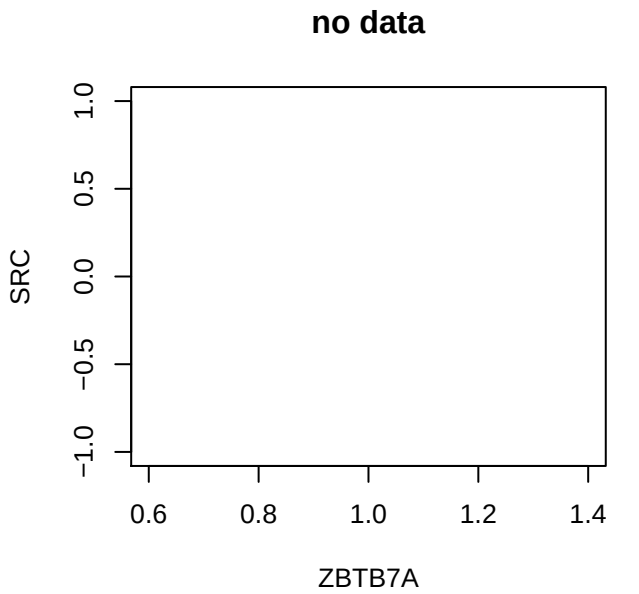

no data
SCRIB
BCL6
−1.0
−0.5
0.0
0.5
1.0
0.6
0.8
1.0
1.2
1.4

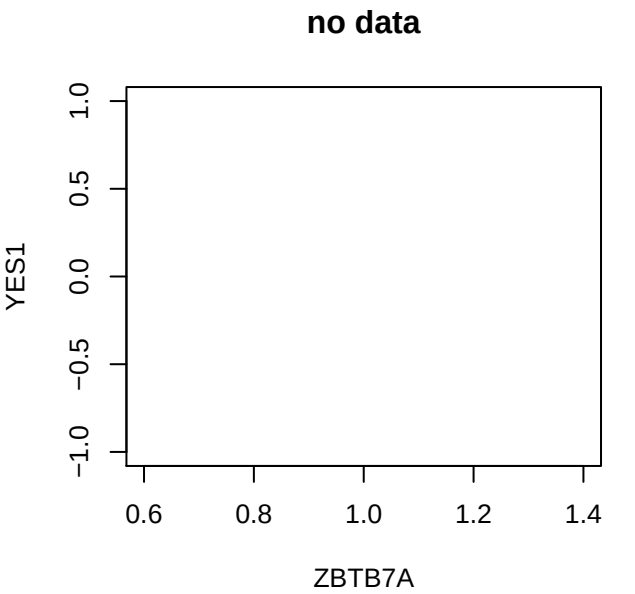

no data
MAPK9
ZBTB7A
−1.0
−0.5
0.0
0.5
1.0
0.6
0.8
1.0
1.2
1.4

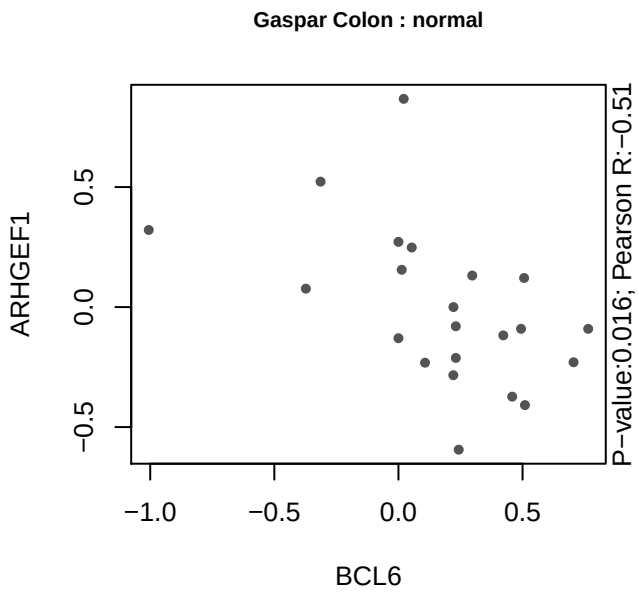

no data
SCRIB
ZBTB7A
−1.0
−0.5
0.0
0.5
1.0
0.6
0.8
1.0
1.2
1.4

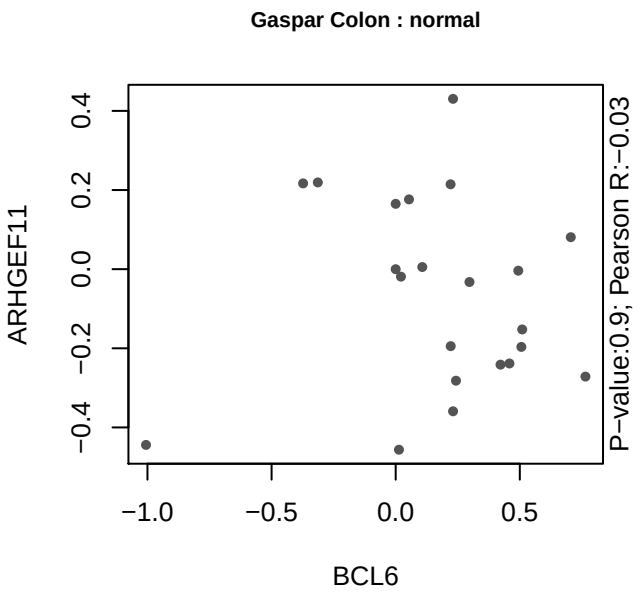

Gaspar Colon : colorectal_adenoma
SRC
BCL6
P−value:5.3e−08; Pearson R:−0.65
−1.5
−1.0
−0.5
0.0
0.5
−0.5
0.0
0.5

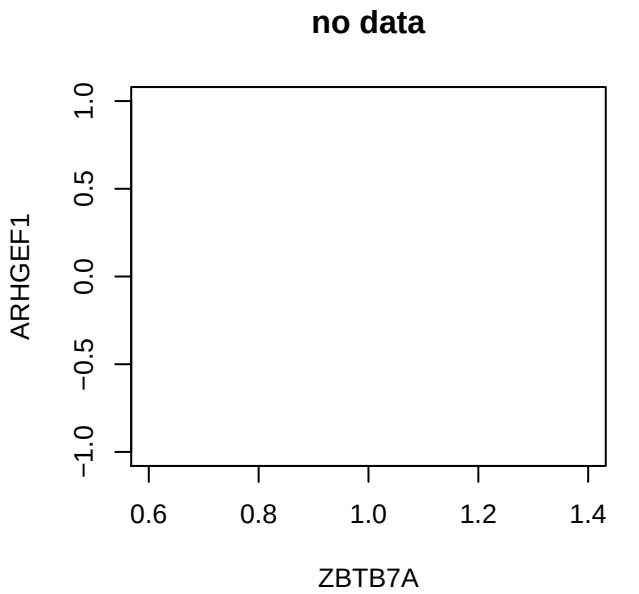

Gaspar Colon : colorectal_adenoma
YES1
BCL6
P−value:0.00014; Pearson R:0.49
−1.5
−1.0
−0.5
0.0
0.5
−0.6
−0.2
0.2
0.6

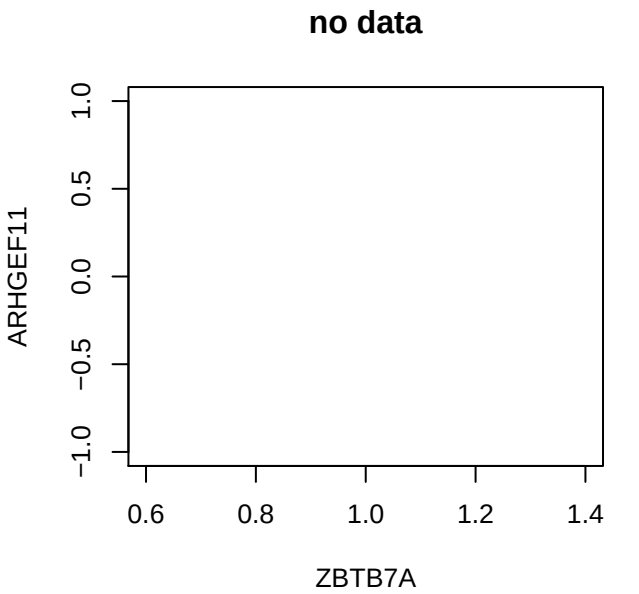

no data
SRC
ZBTB7A
0.6
0.8
1.0
1.2
1.4
−1.0
−0.5
0.0
0.5
1.0

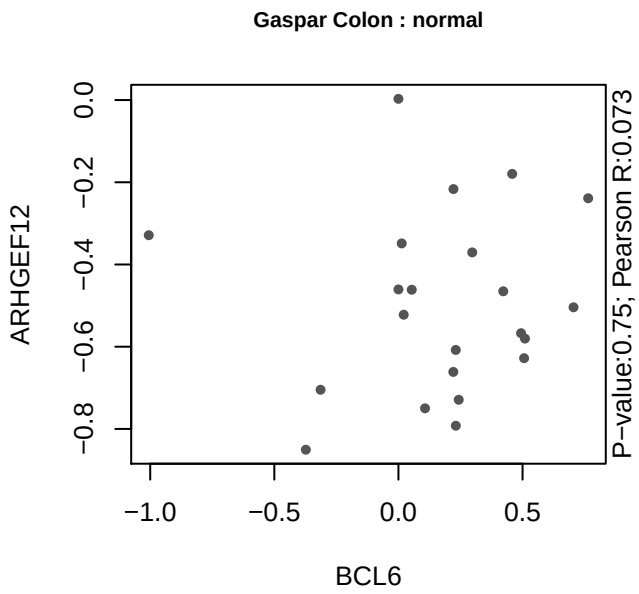

no data
YES1
ZBTB7A
0.6
0.8
1.0
1.2
1.4
−1.0
−0.5
0.0
0.5
1.0

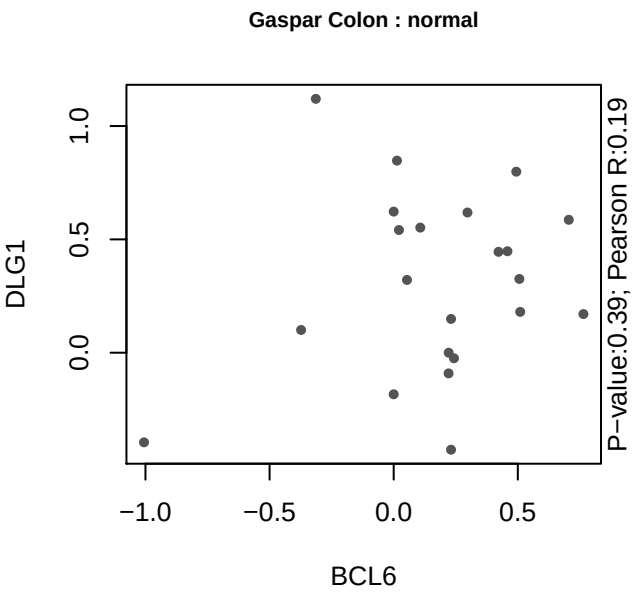

Gaspar Colon : normal
ARHGEF1
BCL6
P−value:0.016; Pearson R:−0.51
−1.0
−0.5
0.0
0.5
−0.5
0.0
0.5

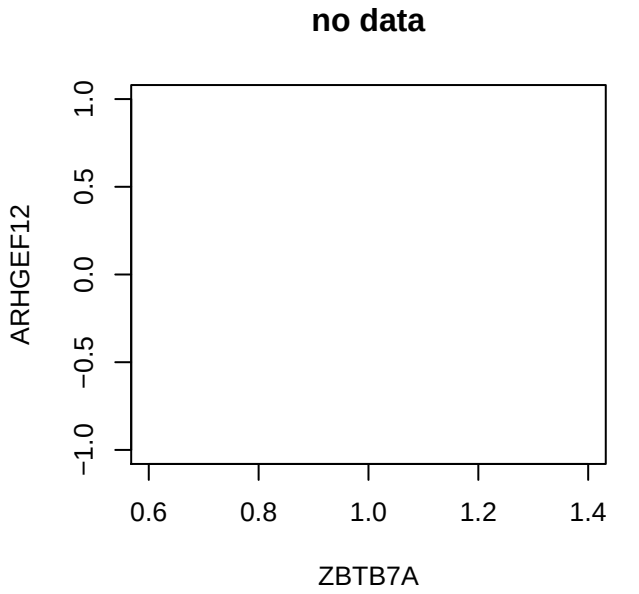

Gaspar Colon : normal
ARHGEF11
BCL6
P−value:0.9; Pearson R:−0.03
−1.0
−0.5
0.0
0.5
−0.4
−0.2
0.0
0.2
0.4

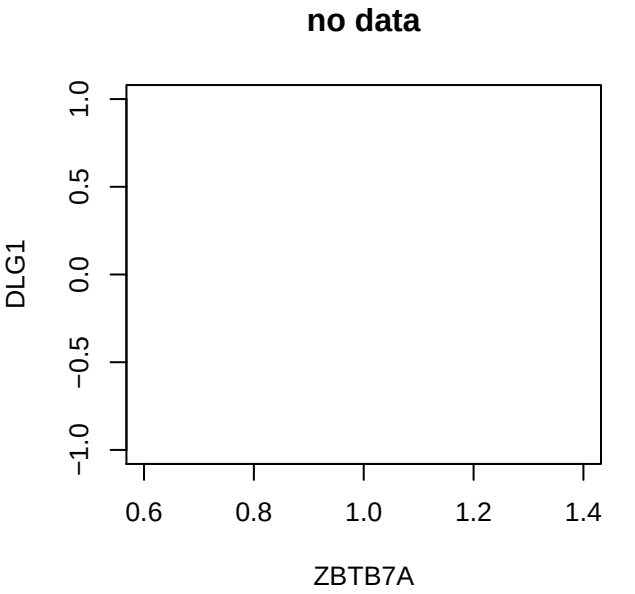

no data
ARHGEF1
ZBTB7A
0.6
0.8
1.0
1.2
1.4
−1.0
−0.5
0.0
0.5
1.0

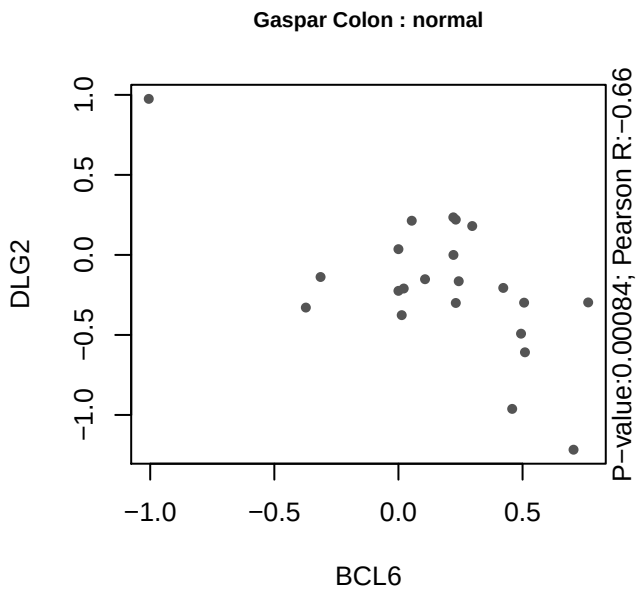

no data
ARHGEF11
ZBTB7A
0.6
0.8
1.0
1.2
1.4
−1.0
−0.5
0.0
0.5
1.0

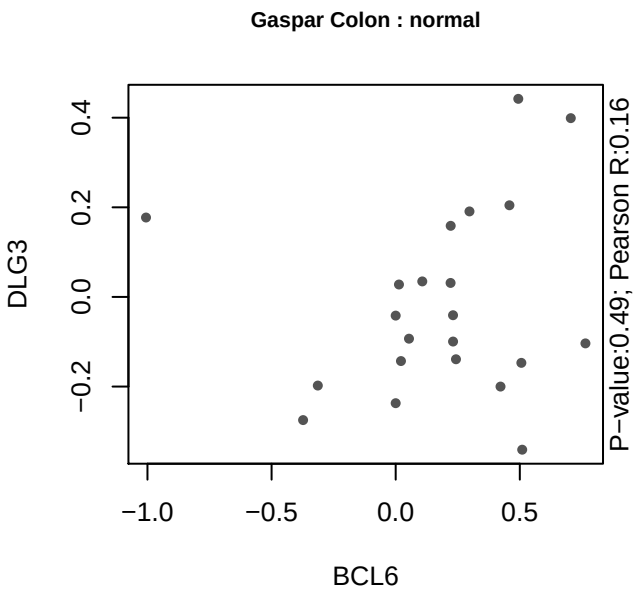

Gaspar Colon : normal
ARHGEF12
BCL6
P−value:0.75; Pearson R:0.073
0.0
−0.2
−0.4
−0.6
−0.8
−1.0
−0.5
0.0
0.5

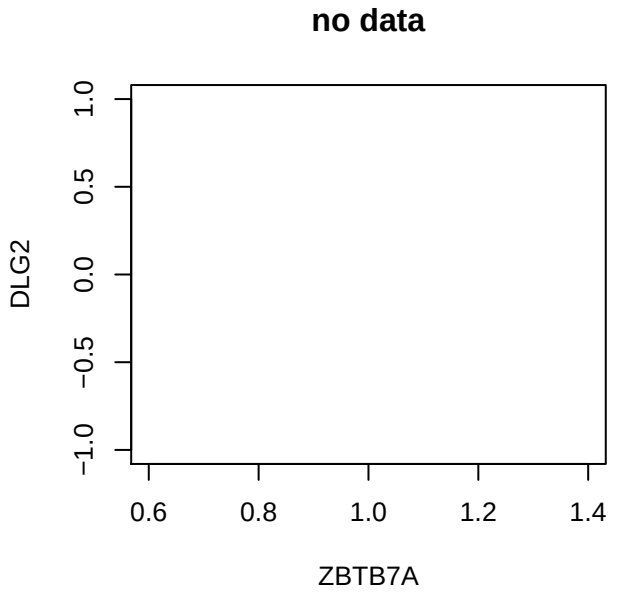

Gaspar Colon : normal
DLG1
BCL6
P−value:0.39; Pearson R:0.19
1.0
0.5
0.0
−1.0
−0.5
0.0
0.5

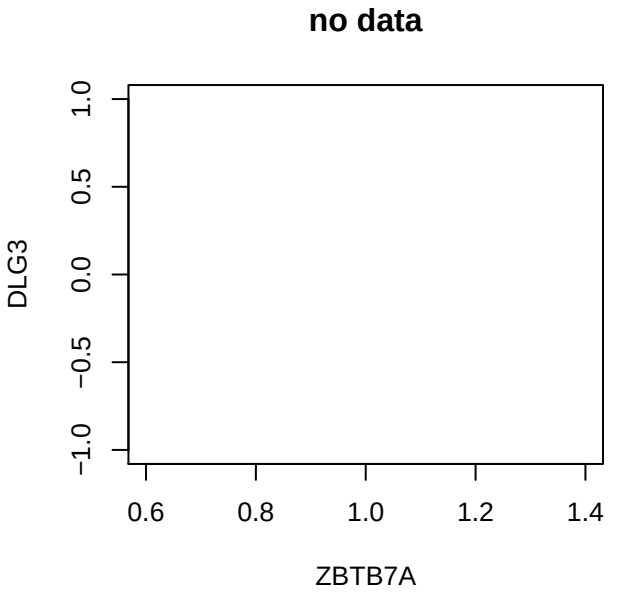

no data
ARHGEF12
ZBTB7A
1.0
0.5
0.0
−0.5
−1.0
0.6
0.8
1.0
1.2
1.4

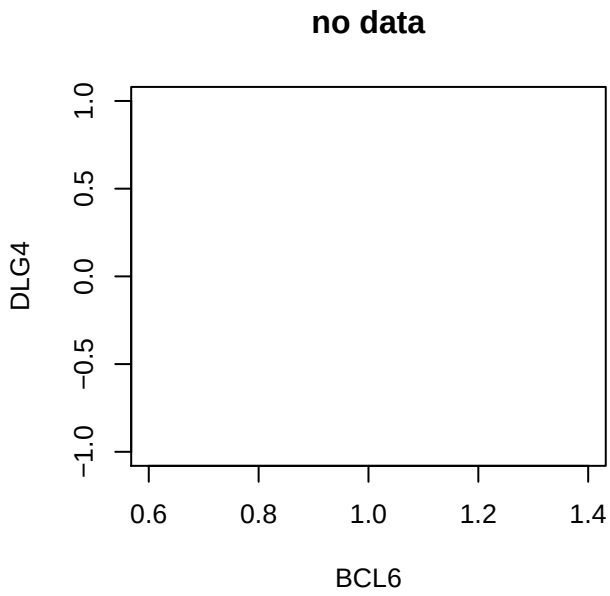

no data
DLG1
ZBTB7A
1.0
0.5
0.0
−0.5
−1.0
0.6
0.8
1.0
1.2
1.4

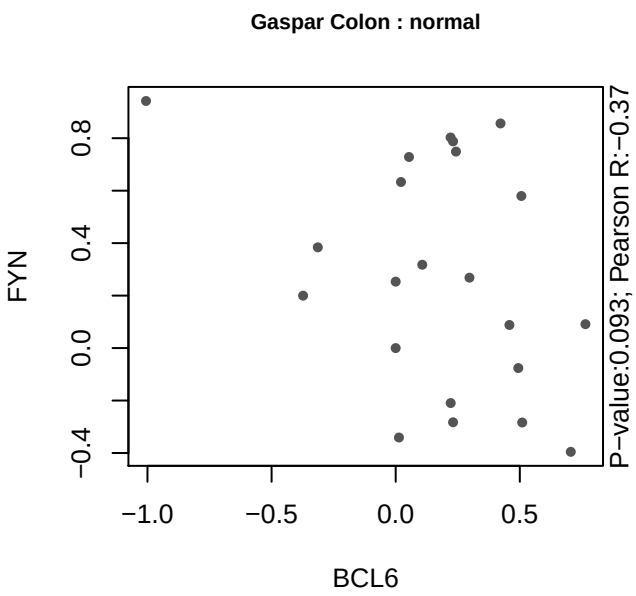

Gaspar Colon : normal
DLG2
BCL6
P−value:0.00084; Pearson R:−0.66
−1.0
−0.5
0.0
0.5
1.0

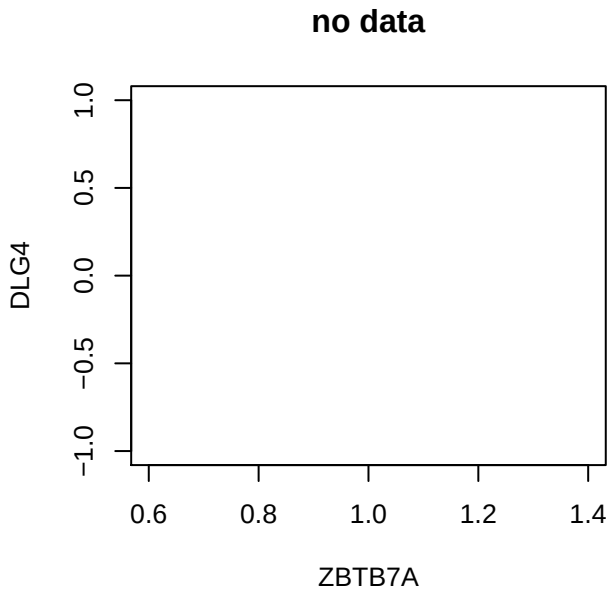

Gaspar Colon : normal
DLG3
BCL6
P−value:0.49; Pearson R:0.16
−0.2
0.0
0.2
0.4

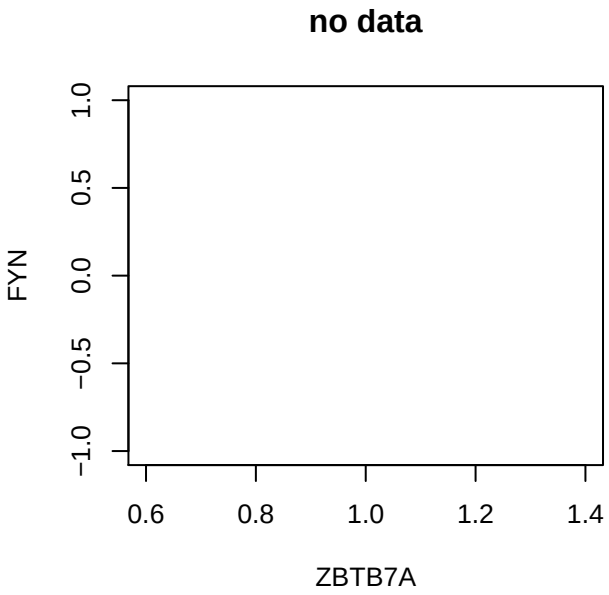

no data
DLG2
ZBTB7A
0.6
0.8
1.0
1.2
1.4

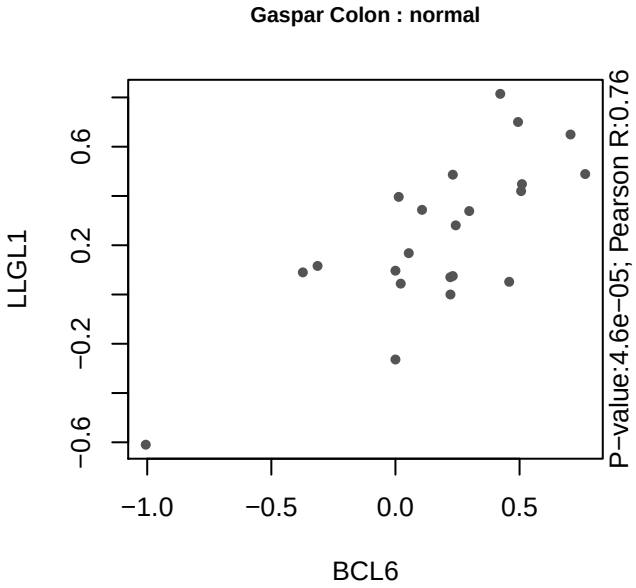

no data
DLG3
ZBTB7A
0.6
0.8
1.0
1.2
1.4

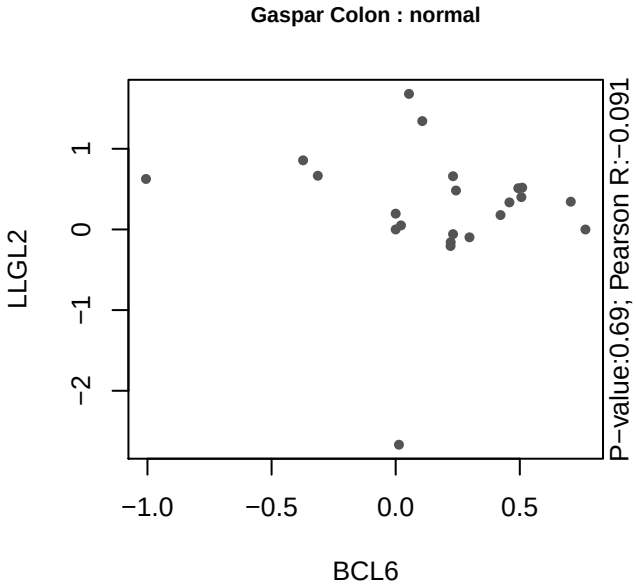

no data
DLG4
BCL6
1.0
0.5
0.0
−0.5
−1.0
0.6
0.8
1.0
1.2
1.4

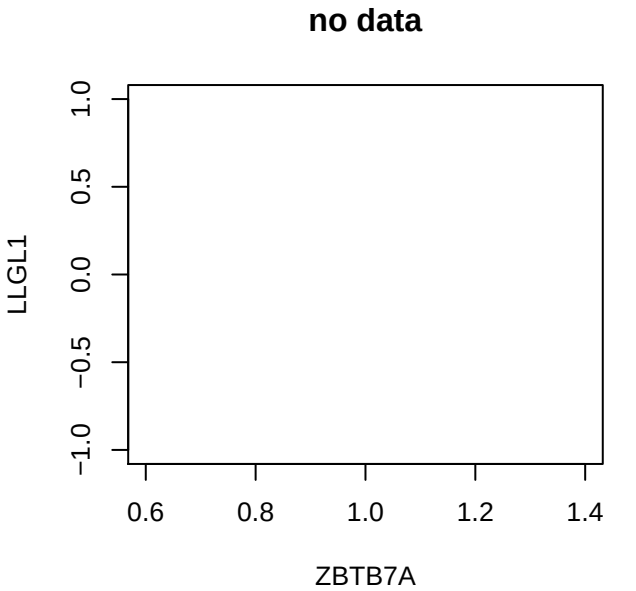

Gaspar Colon : normal
FYN
BCL6
P−value:0.093; Pearson R:−0.37
0.8
0.4
0.0
−0.4
−1.0
−0.5
0.0
0.5

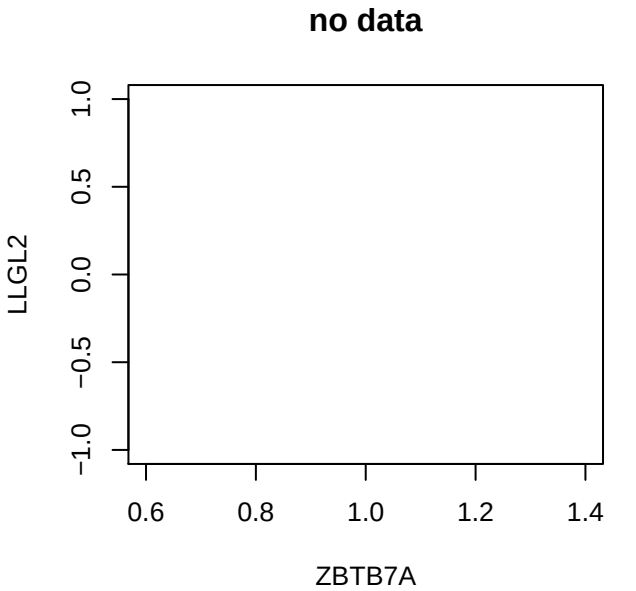

no data
DLG4
ZBTB7A
1.0
0.5
0.0
−0.5
−1.0
0.6
0.8
1.0
1.2
1.4

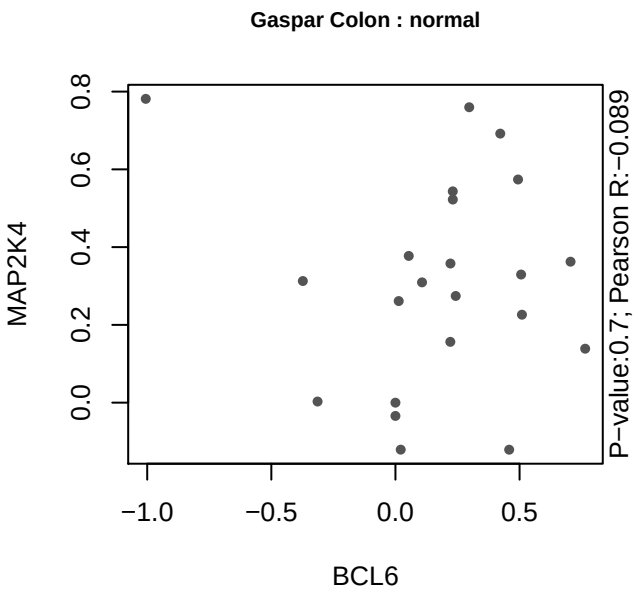

no data
FYN
ZBTB7A
1.0
0.5
0.0
−0.5
−1.0
0.6
0.8
1.0
1.2
1.4

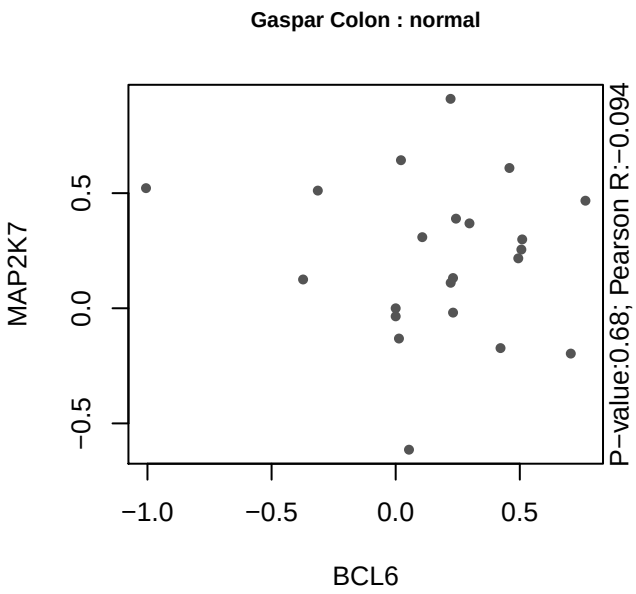

Gaspar Colon : normal
LLGL1
BCL6
P−value:4.6e−05; Pearson R:0.76
−1.0
−0.5
0.0
0.5
−0.6
−0.2
0.2
0.6

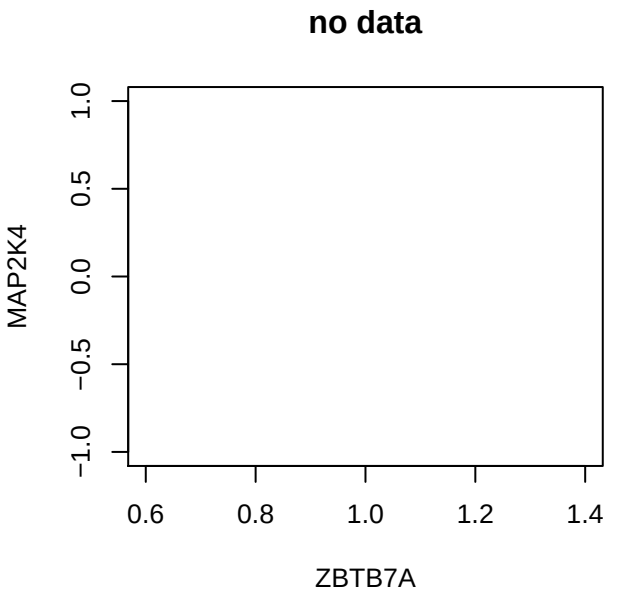

Gaspar Colon : normal
LLGL2
BCL6
P−value:0.69; Pearson R:−0.091
−1.0
−0.5
0.0
0.5
−2
−1
0
1

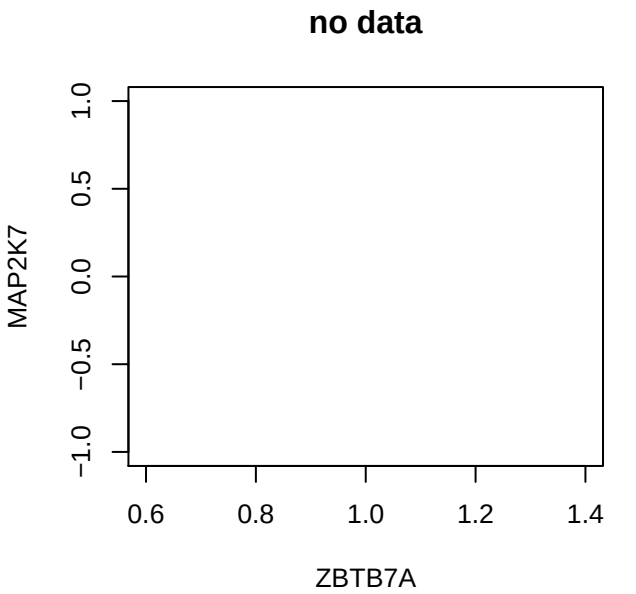

no data
LLGL1
ZBTB7A
0.6
0.8
1.0
1.2
1.4
−1.0
−0.5
0.0
0.5
1.0

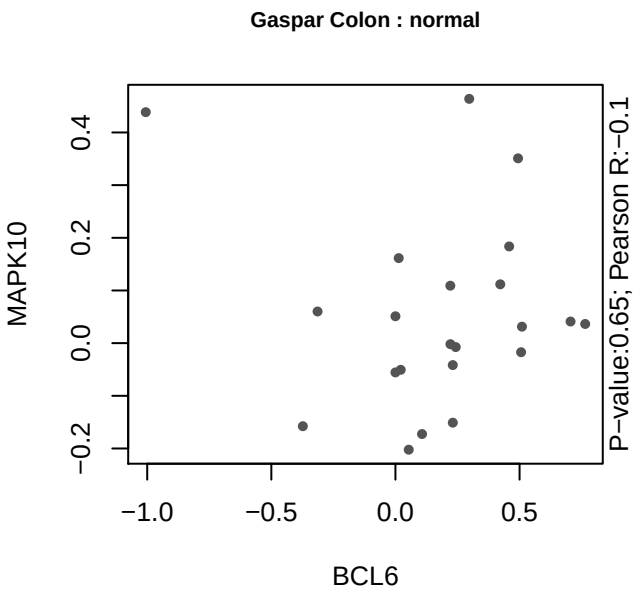

no data
LLGL2
ZBTB7A
0.6
0.8
1.0
1.2
1.4
−1.0
−0.5
0.0
0.5
1.0

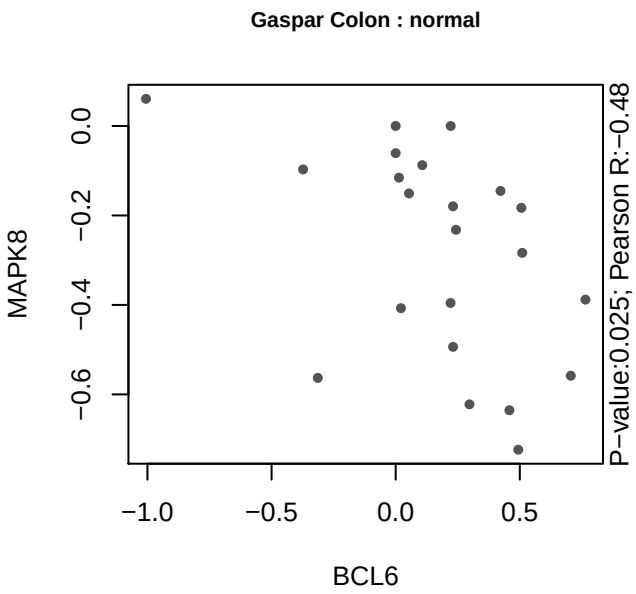

Gaspar Colon : normal
MAP2K4
BCL6
P−value:0.7; Pearson R:−0.089
0.0
0.2
0.4
0.6
0.8
−1.0
−0.5
0.0
0.5

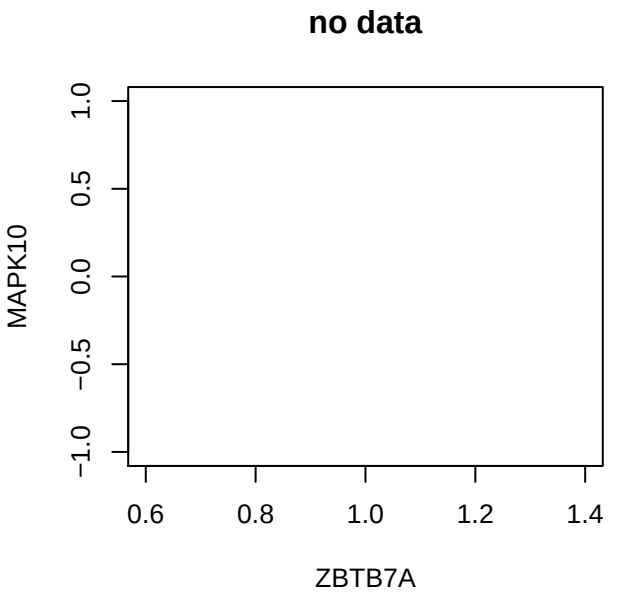

Gaspar Colon : normal
MAP2K7
BCL6
P−value:0.68; Pearson R:−0.094
−0.5
0.0
0.5
−1.0
−0.5
0.0
0.5

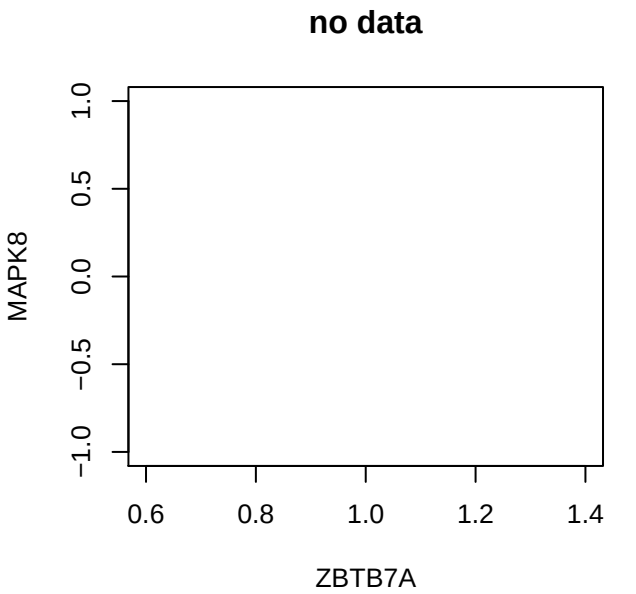

no data
MAP2K4
ZBTB7A
−1.0
−0.5
0.0
0.5
1.0
0.6
0.8
1.0
1.2
1.4

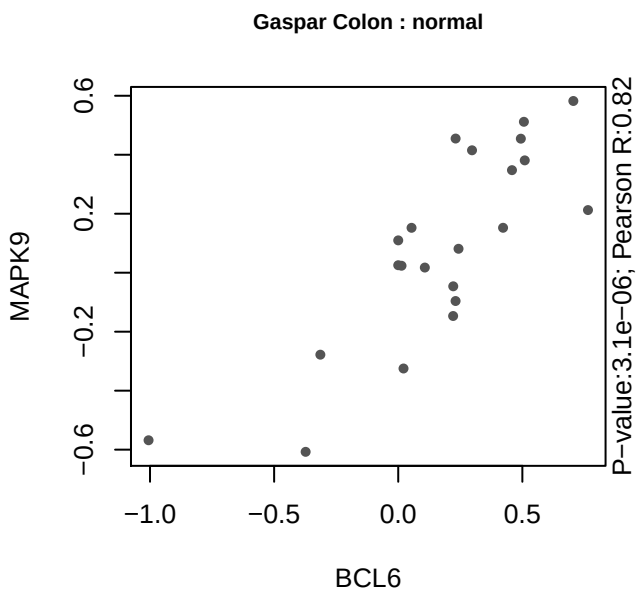

no data
MAP2K7
ZBTB7A
−1.0
−0.5
0.0
0.5
1.0
0.6
0.8
1.0
1.2
1.4

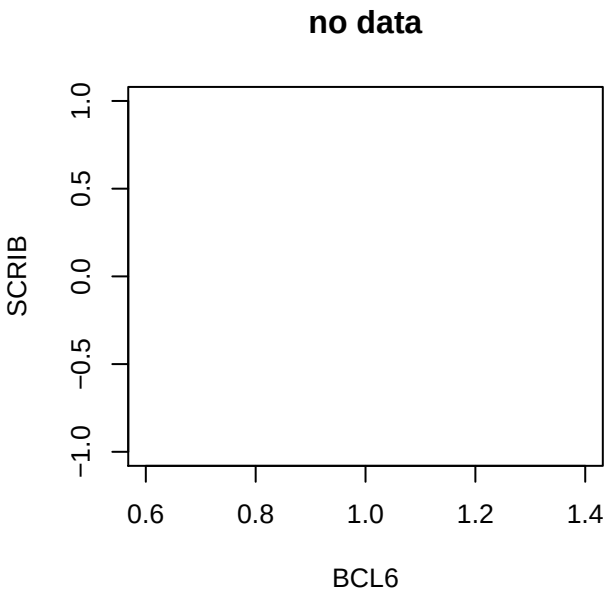

Gaspar Colon : normal
MAPK10
BCL6
P−value:0.65; Pearson R:−0.1
−1.0
−0.5
0.0
0.5
−0.2
0.0
0.2
0.4

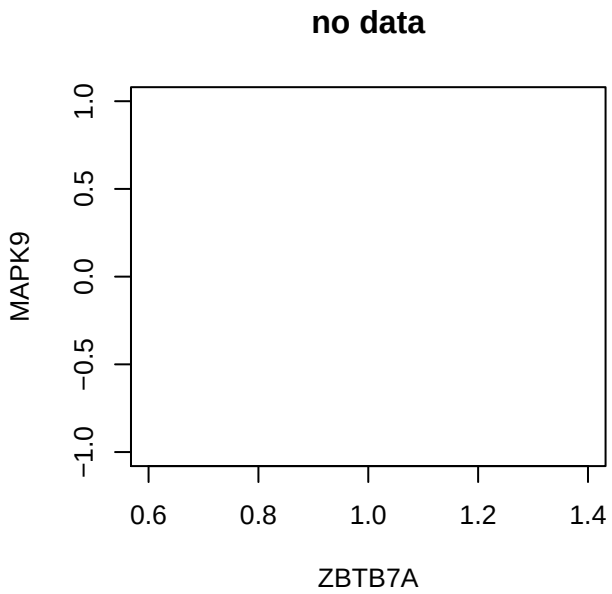

Gaspar Colon : normal
MAPK8
BCL6
P−value:0.025; Pearson R:−0.48
−1.0
−0.5
0.0
0.5
−0.6
−0.4
−0.2
0.0

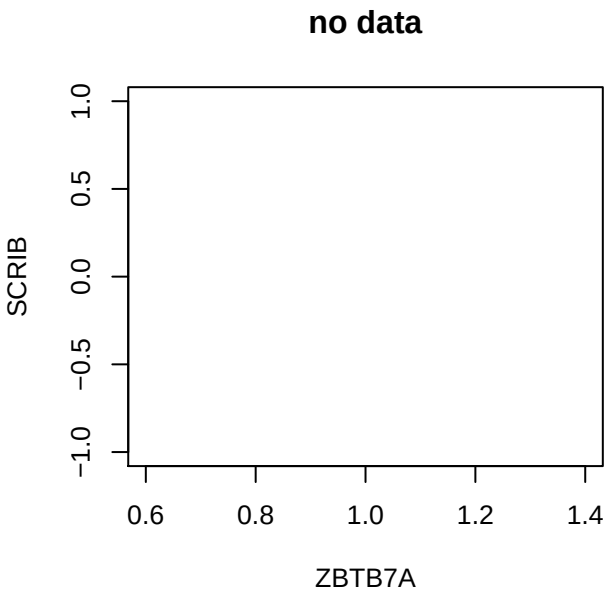

no data
MAPK10
ZBTB7A
0.6
0.8
1.0
1.2
1.4
−1.0
−0.5
0.0
0.5
1.0

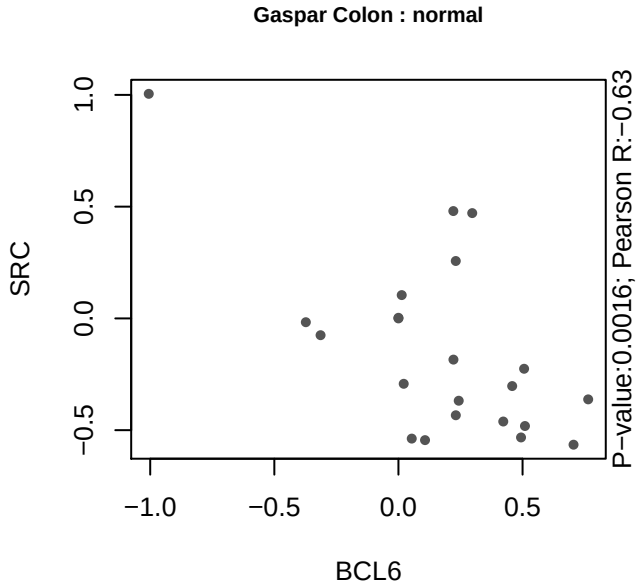

no data
MAPK8
ZBTB7A
0.6
0.8
1.0
1.2
1.4
−1.0
−0.5
0.0
0.5
1.0

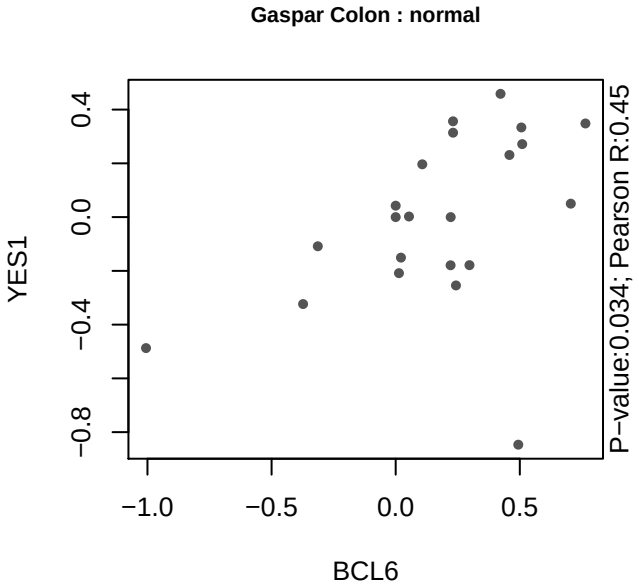

Gaspar Colon : normal
MAPK9
BCL6
P−value:3.1e−06; Pearson R:0.82
0.6
0.2
−0.2
−0.6
−1.0
−0.5
0.0
0.5

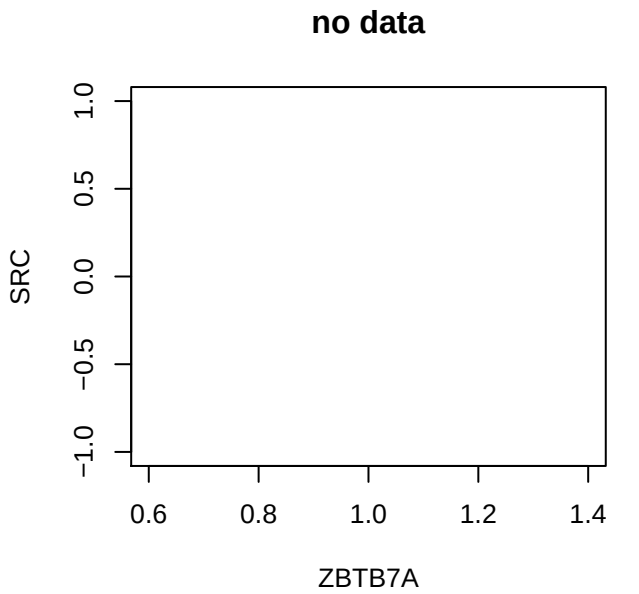

no data
SCRIB
BCL6
1.0
0.5
0.0
−0.5
−1.0
0.6
0.8
1.0
1.2
1.4

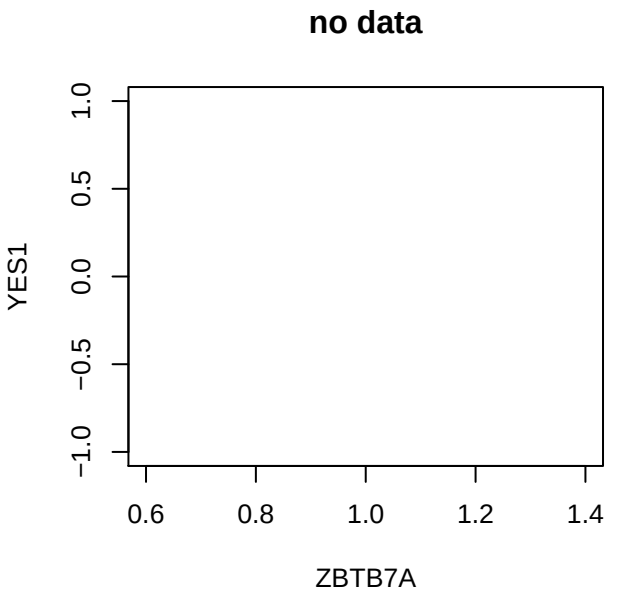

no data
MAPK9
ZBTB7A
1.0
0.5
0.0
−0.5
−1.0
0.6
0.8
1.0
1.2
1.4

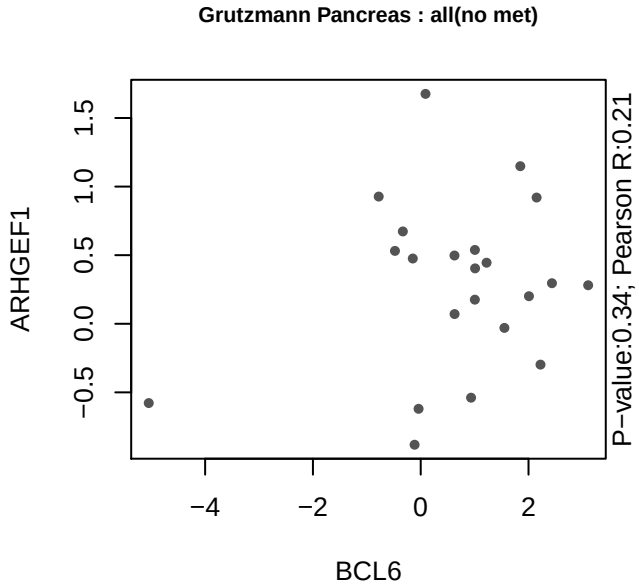

no data
SCRIB
ZBTB7A
1.0
0.5
0.0
−0.5
−1.0
0.6
0.8
1.0
1.2
1.4

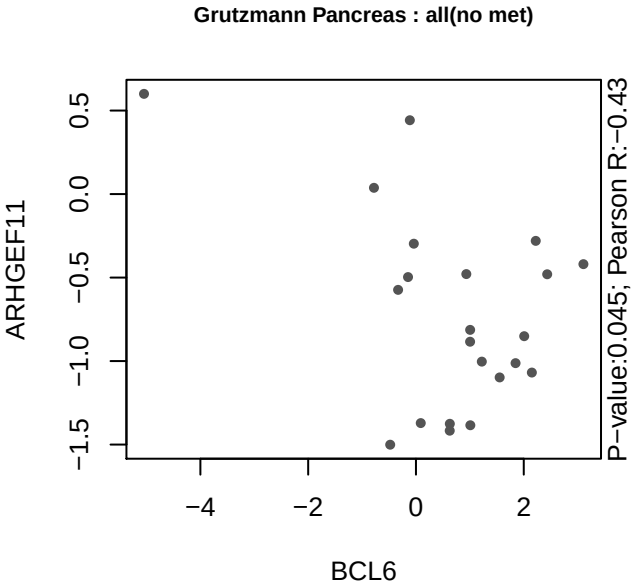

Gaspar Colon : normal
SRC
BCL6
P−value:0.0016; Pearson R:−0.63
1.0
0.5
0.0
−0.5
−1.0
−0.5
0.0
0.5

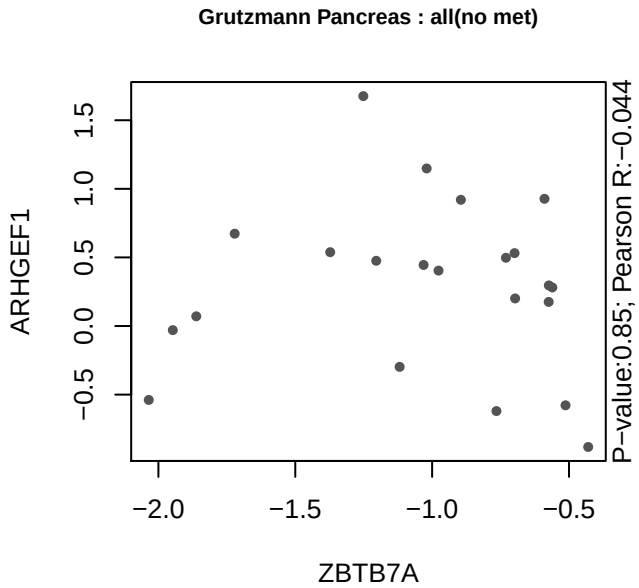

Gaspar Colon : normal
YES1
BCL6
P−value:0.034; Pearson R:0.45
0.4
0.0
−0.4
−0.8
−1.0
−0.5
0.0
0.5

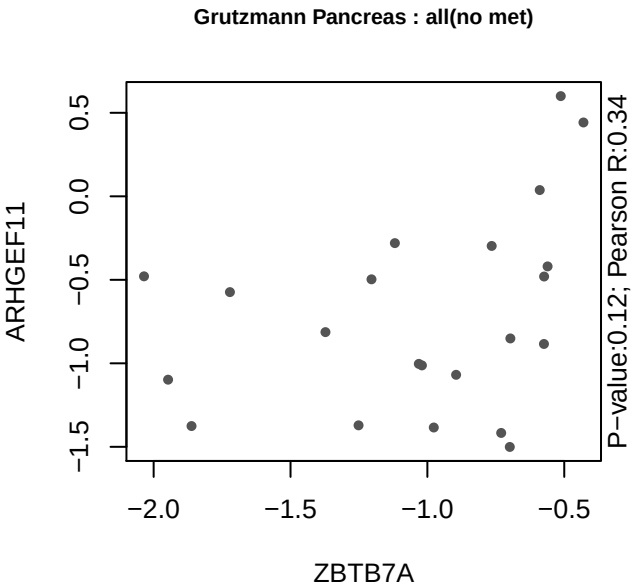

no data
SRC
ZBTB7A
1.0
0.5
0.0
−0.5
−1.0
0.6
0.8
1.0
1.2
1.4

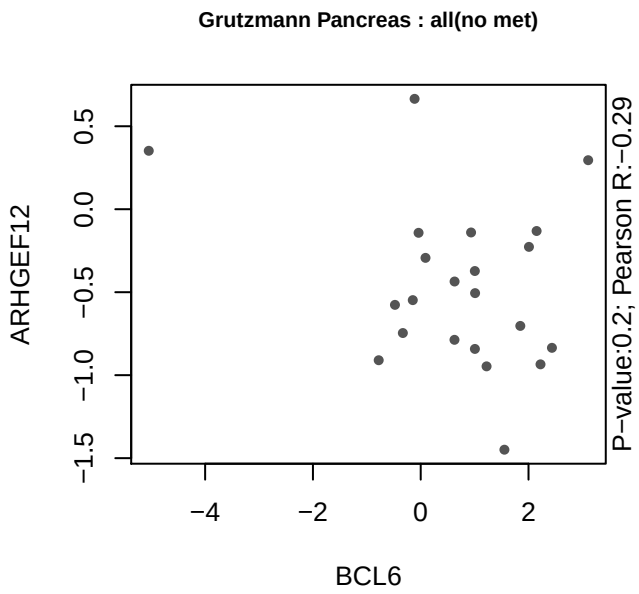

no data
YES1
ZBTB7A
1.0
0.5
0.0
−0.5
−1.0
0.6
0.8
1.0
1.2
1.4

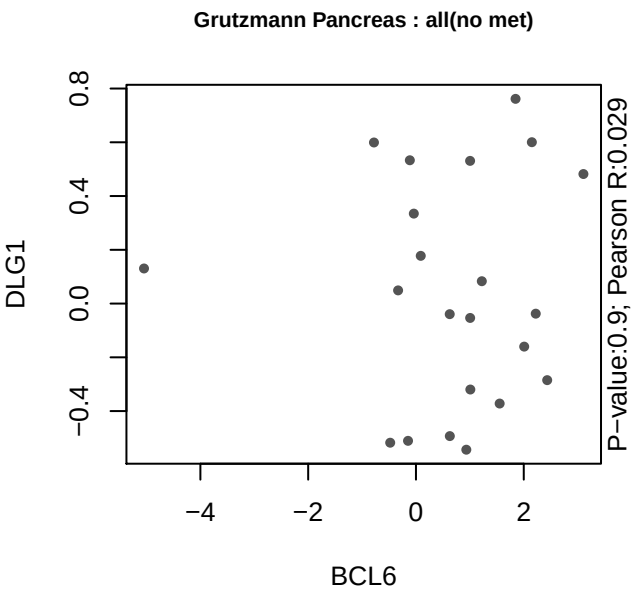

Grutzmann Pancreas : all(no met)
ARHGEF1
BCL6
P−value:0.34; Pearson R:0.21

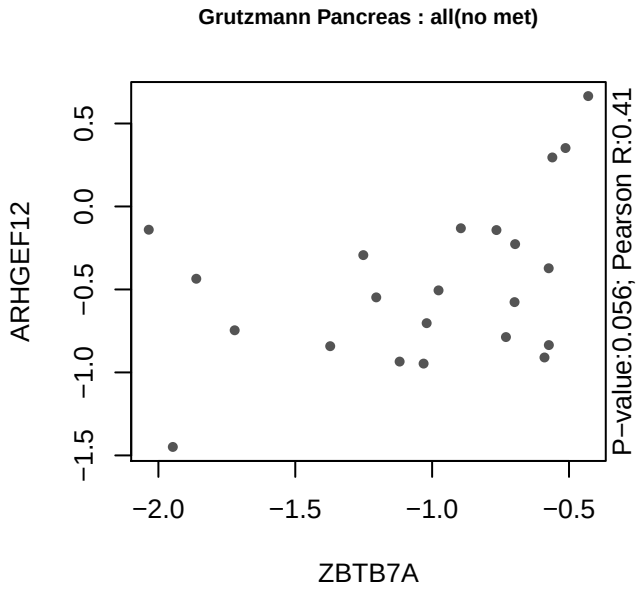

Grutzmann Pancreas : all(no met)
ARHGEF11
BCL6
P−value:0.045; Pearson R:−0.43

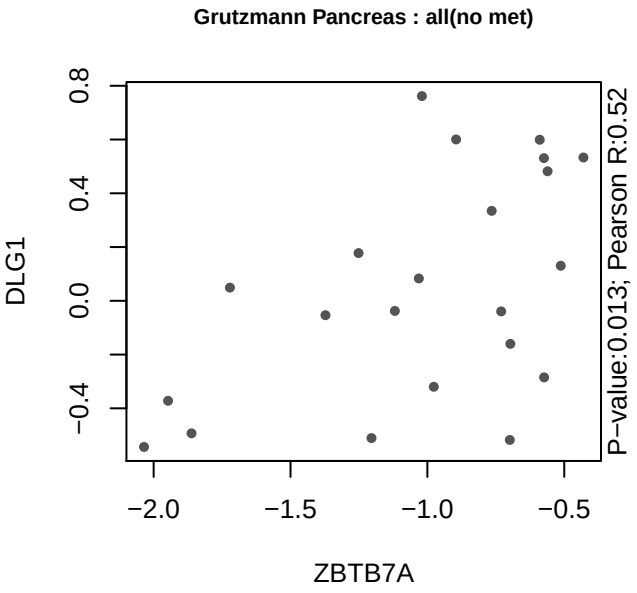

Grutzmann Pancreas : all(no met)
ARHGEF1
ZBTB7A
P−value:0.85; Pearson R:−0.044

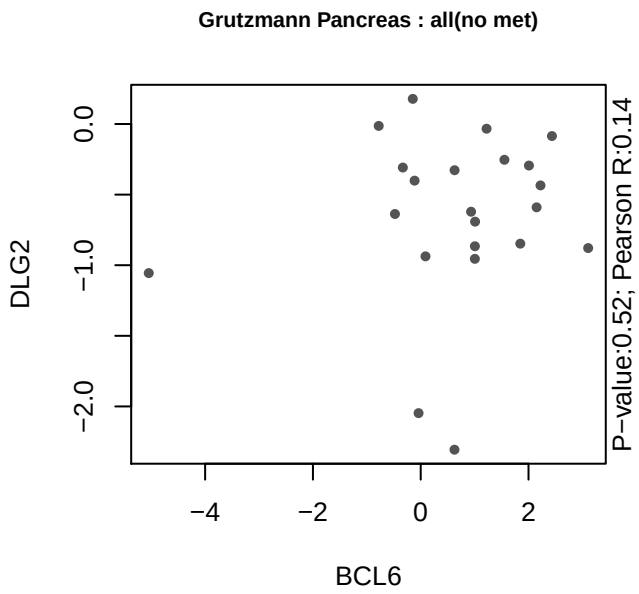

Grutzmann Pancreas : all(no met)
ARHGEF11
ZBTB7A
P−value:0.12; Pearson R:0.34

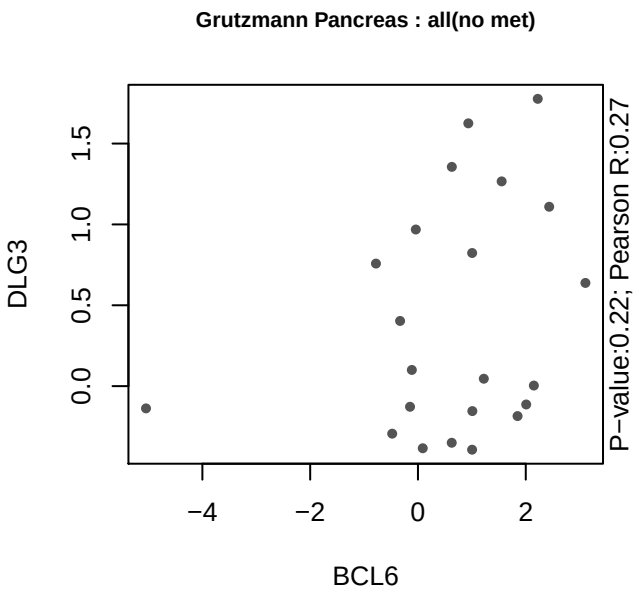

Grutzmann Pancreas : all(no met)
ARHGEF12
BCL6
P−value:0.2; Pearson R:−0.29

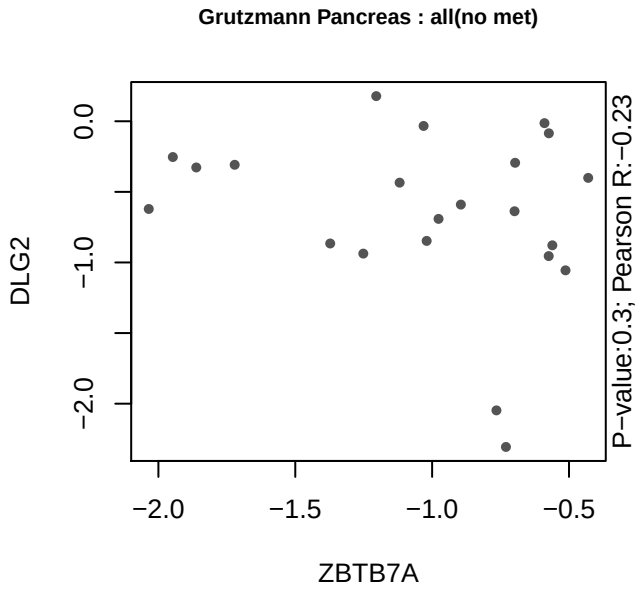

Grutzmann Pancreas : all(no met)
DLG1
BCL6
P−value:0.9; Pearson R:0.029

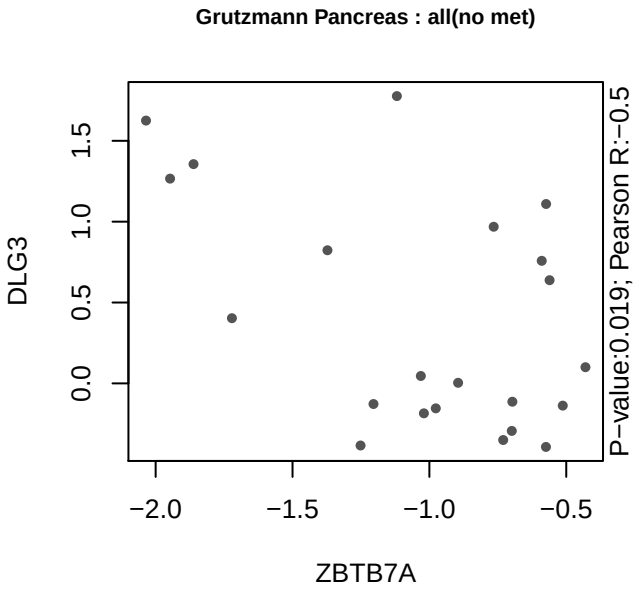

Grutzmann Pancreas : all(no met)
ARHGEF12
ZBTB7A
P−value:0.056; Pearson R:0.41

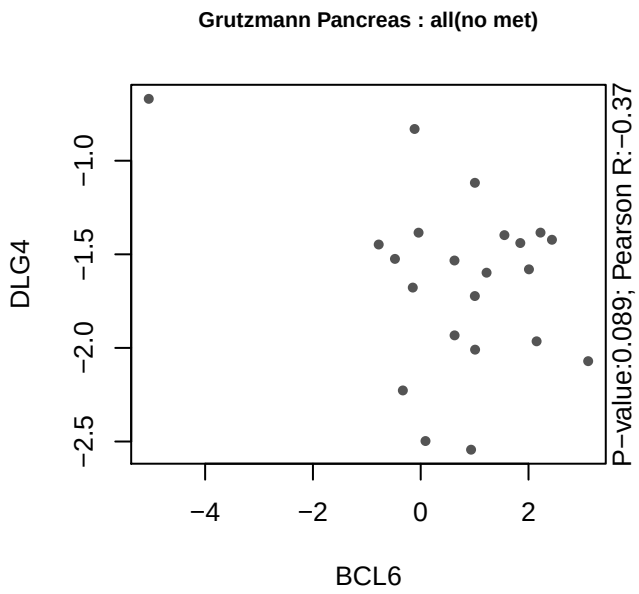

Grutzmann Pancreas : all(no met)
DLG1
ZBTB7A
P−value:0.013; Pearson R:0.52

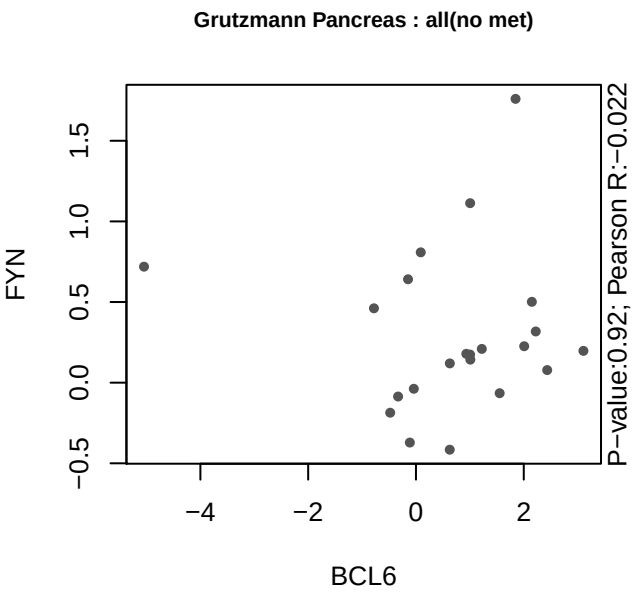

Grutzmann Pancreas : all(no met)
DLG2
BCL6
P−value:0.52; Pearson R:0.14

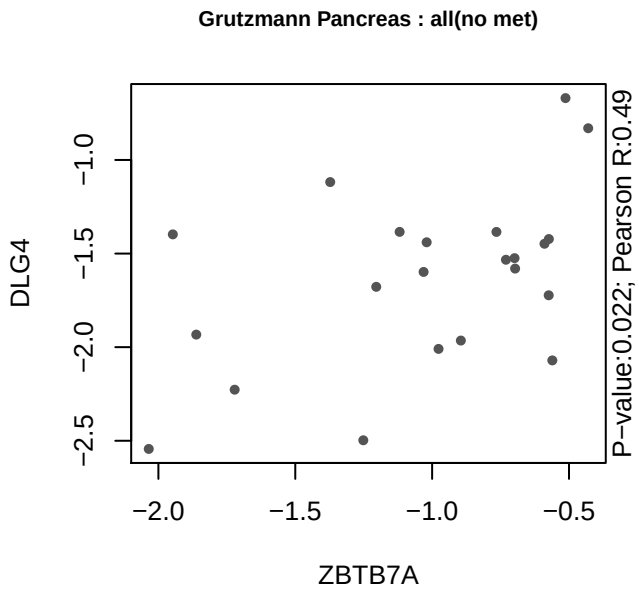

Grutzmann Pancreas : all(no met)
DLG3
BCL6
P−value:0.22; Pearson R:0.27

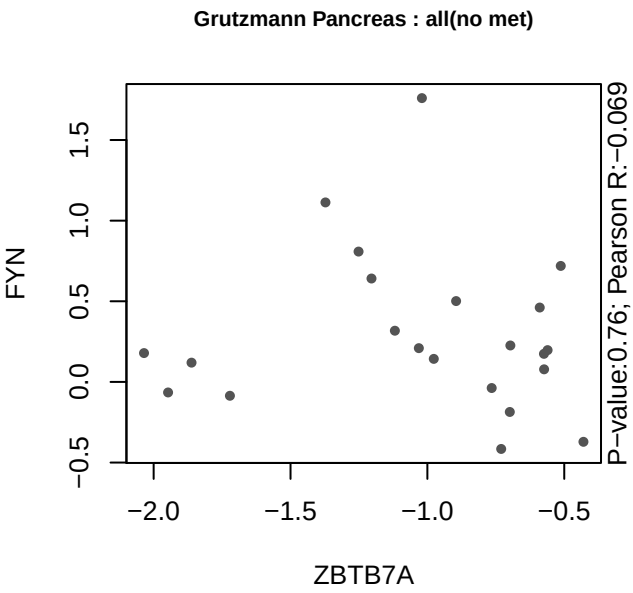

Grutzmann Pancreas : all(no met)
DLG2
ZBTB7A
P−value:0.3; Pearson R:−0.23

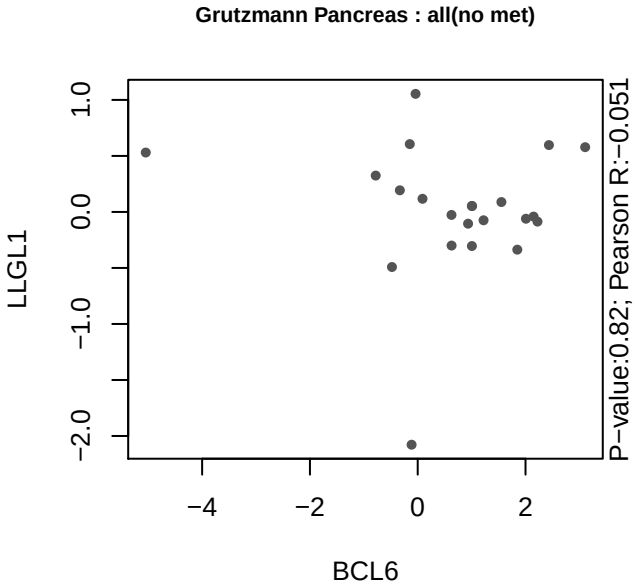

Grutzmann Pancreas : all(no met)
DLG3
ZBTB7A
P−value:0.019; Pearson R:−0.5

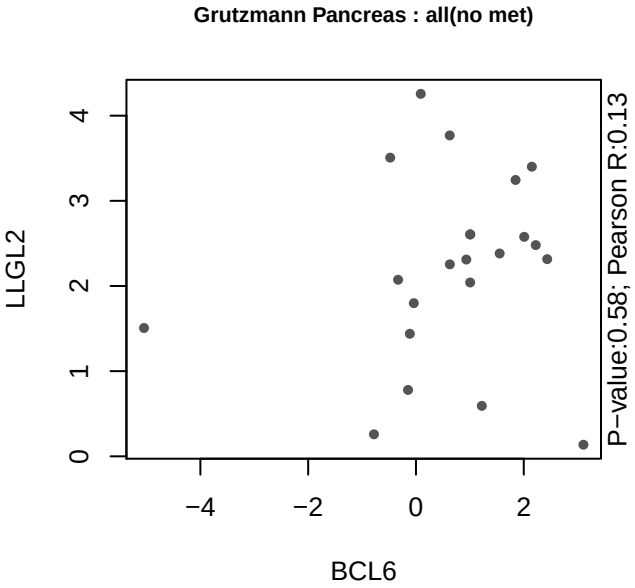

Grutzmann Pancreas : all(no met)
DLG4
BCL6
P−value:0.089; Pearson R:−0.37

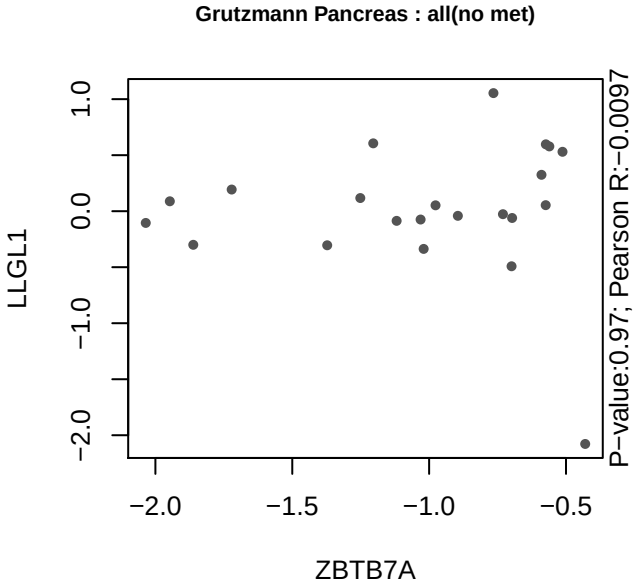

Grutzmann Pancreas : all(no met)
FYN
BCL6
P−value:0.92; Pearson R:−0.022

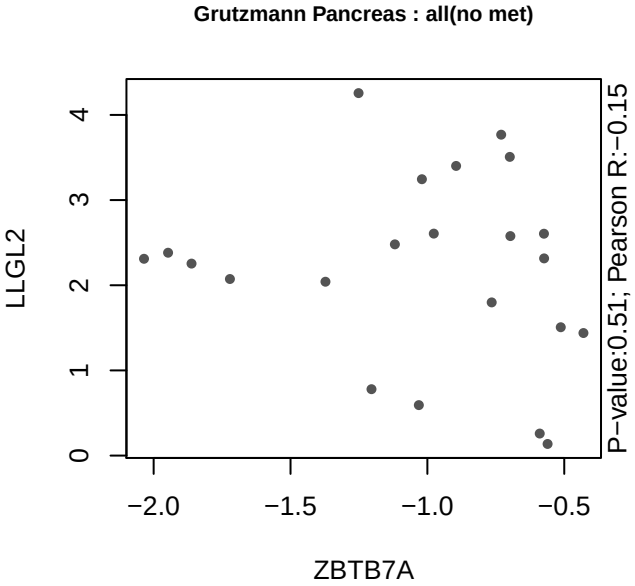

Grutzmann Pancreas : all(no met)
DLG4
ZBTB7A
P−value:0.022; Pearson R:0.49

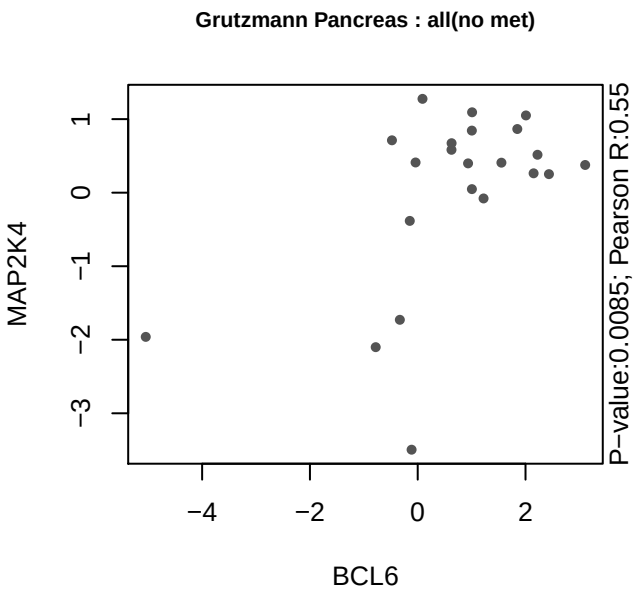

Grutzmann Pancreas : all(no met)
FYN
ZBTB7A
P−value:0.76; Pearson R:−0.069

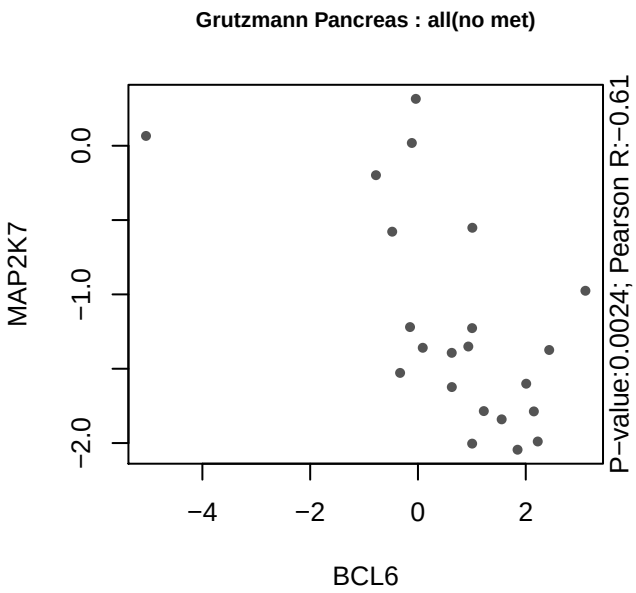

Grutzmann Pancreas : all(no met)
LLGL1
BCL6
P−value:0.82; Pearson R:−0.051

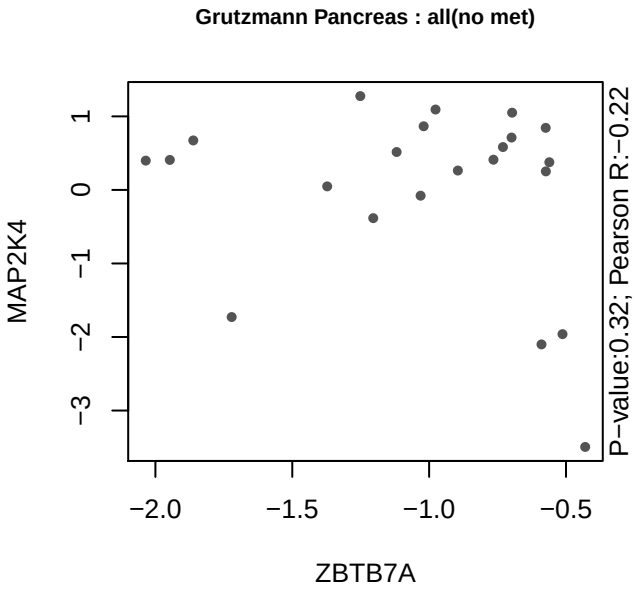

Grutzmann Pancreas : all(no met)
LLGL2
BCL6
P−value:0.58; Pearson R:0.13

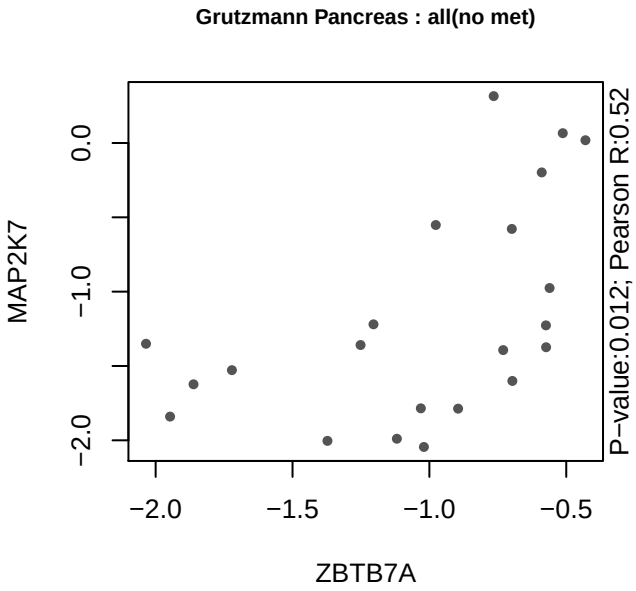

Grutzmann Pancreas : all(no met)
LLGL1
ZBTB7A
P−value:0.97; Pearson R:−0.0097

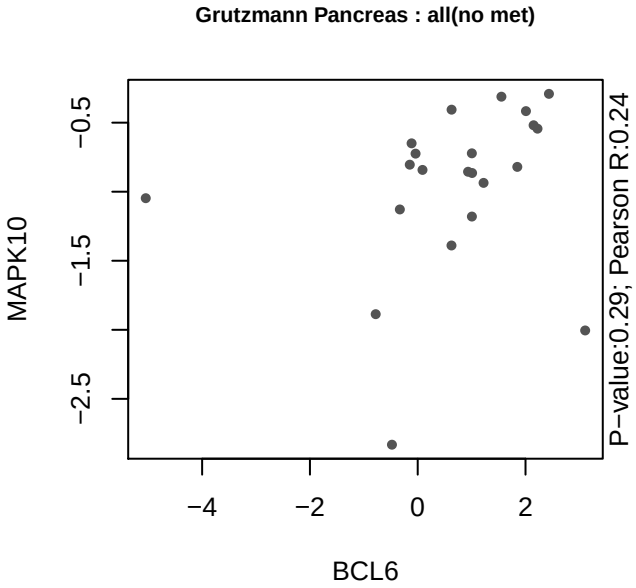

Grutzmann Pancreas : all(no met)
LLGL2
ZBTB7A
P−value:0.51; Pearson R:−0.15

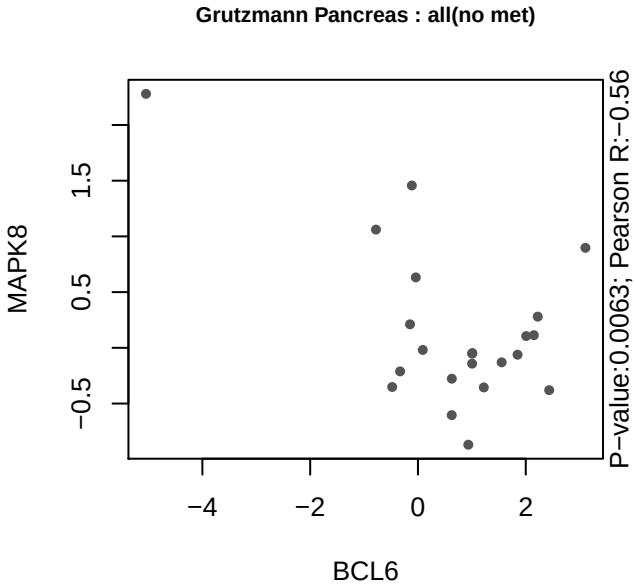

Grutzmann Pancreas : all(no met)
MAP2K4
BCL6
P−value:0.0085; Pearson R:0.55

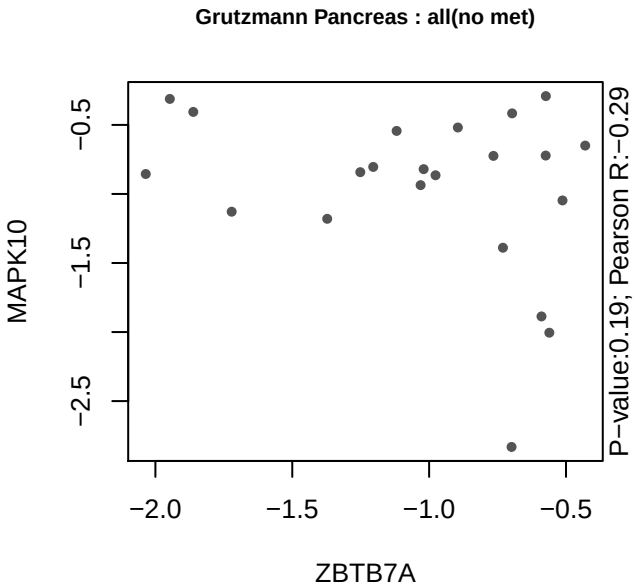

Grutzmann Pancreas : all(no met)
MAP2K7
BCL6
P−value:0.0024; Pearson R:−0.61

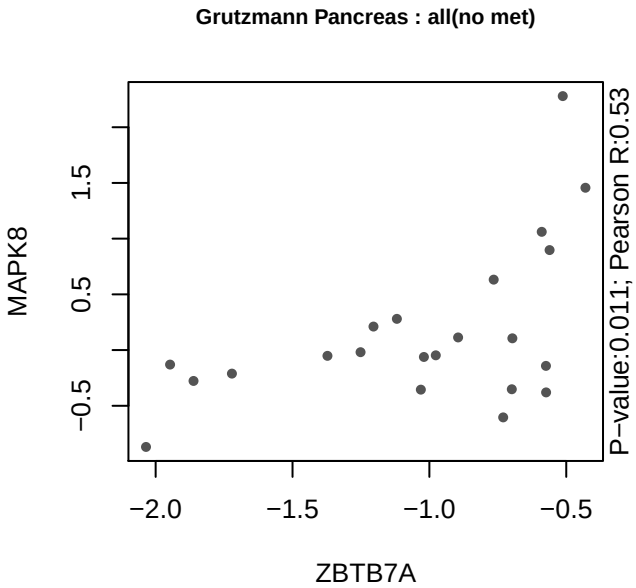

Grutzmann Pancreas : all(no met)
MAP2K4
ZBTB7A
P−value:0.32; Pearson R:−0.22

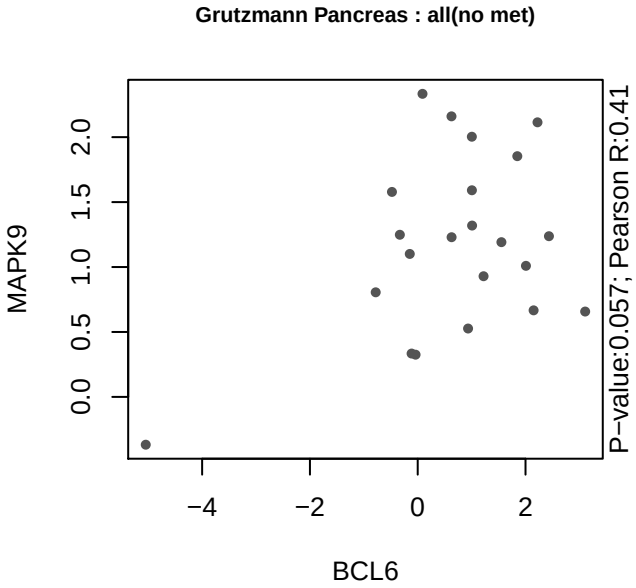

Grutzmann Pancreas : all(no met)
MAP2K7
ZBTB7A
P−value:0.012; Pearson R:0.52

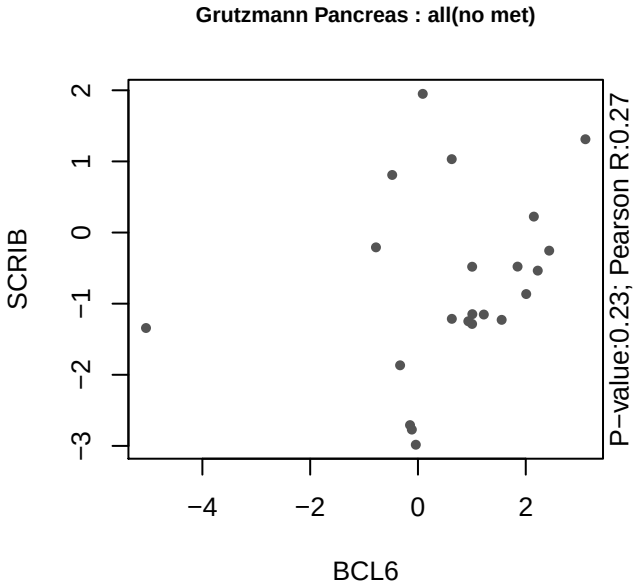

Grutzmann Pancreas : all(no met)
MAPK10
BCL6
P−value:0.29; Pearson R:0.24
−0.5
−1.5
−2.5
−4
−2
0
2

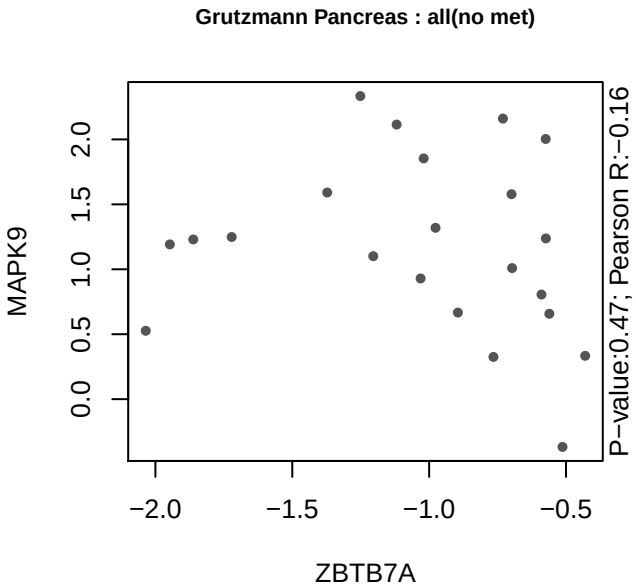

Grutzmann Pancreas : all(no met)
MAPK8
BCL6
P−value:0.0063; Pearson R:−0.56
1.5
0.5
−0.5
−4
−2
0
2

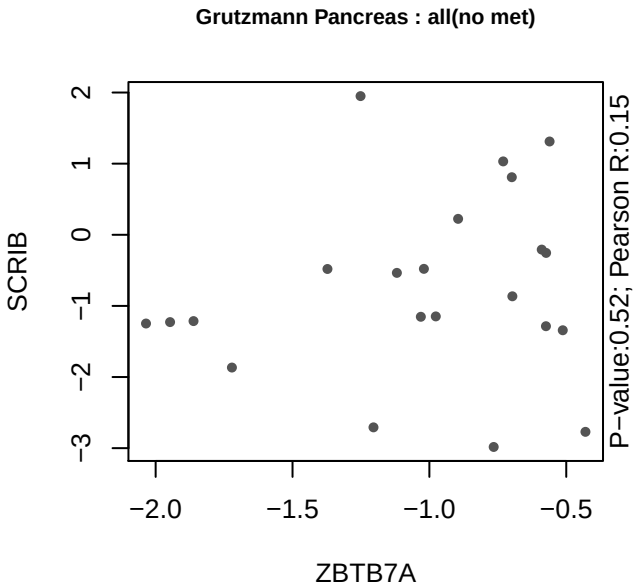

Grutzmann Pancreas : all(no met)
MAPK10
ZBTB7A
P−value:0.19; Pearson R:−0.29
−0.5
−1.5
−2.5
−2.0
−1.5
−1.0
−0.5

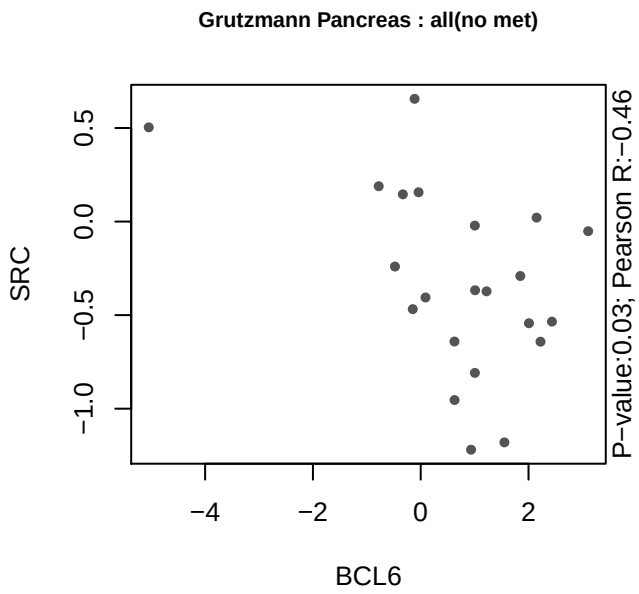

Grutzmann Pancreas : all(no met)
MAPK8
ZBTB7A
P−value:0.011; Pearson R:0.53
1.5
0.5
−0.5
−2.0
−1.5
−1.0
−0.5

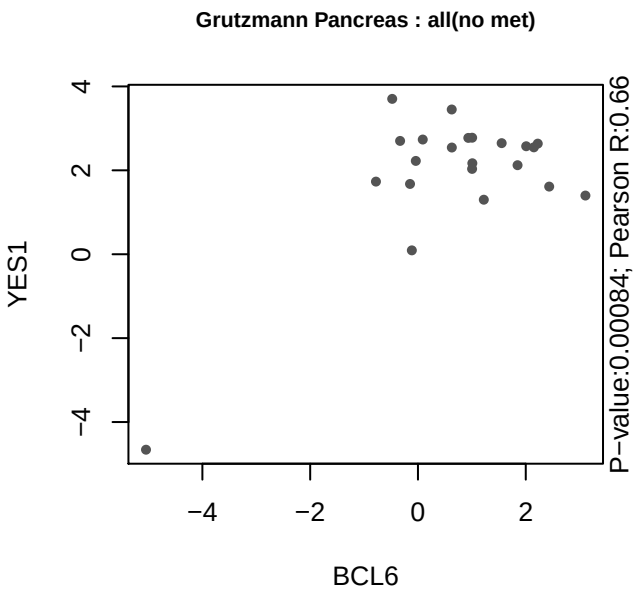

Grutzmann Pancreas : all(no met)
MAPK9
BCL6
P−value:0.057; Pearson R:0.41

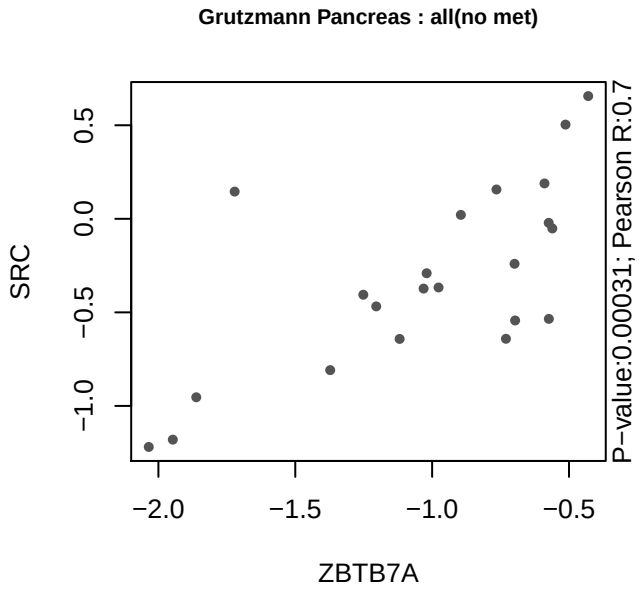

Grutzmann Pancreas : all(no met)
SCRIB
BCL6
P−value:0.23; Pearson R:0.27

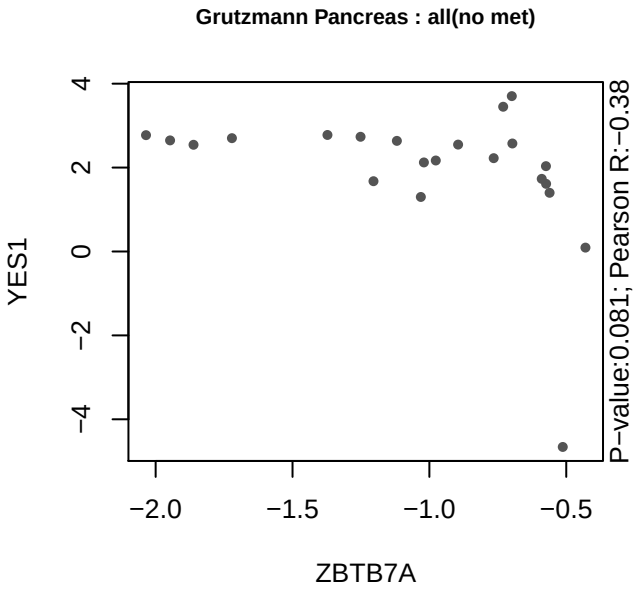

Grutzmann Pancreas : all(no met)
MAPK9
ZBTB7A
P−value:0.47; Pearson R:−0.16

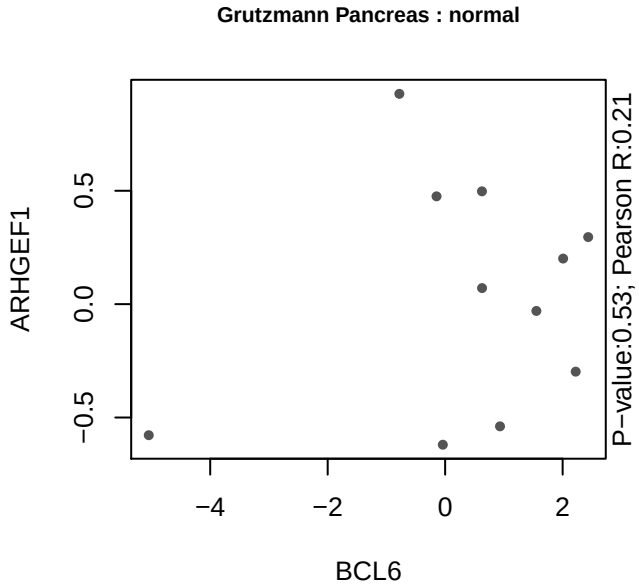

Grutzmann Pancreas : all(no met)
SCRIB
ZBTB7A
P−value:0.52; Pearson R:0.15

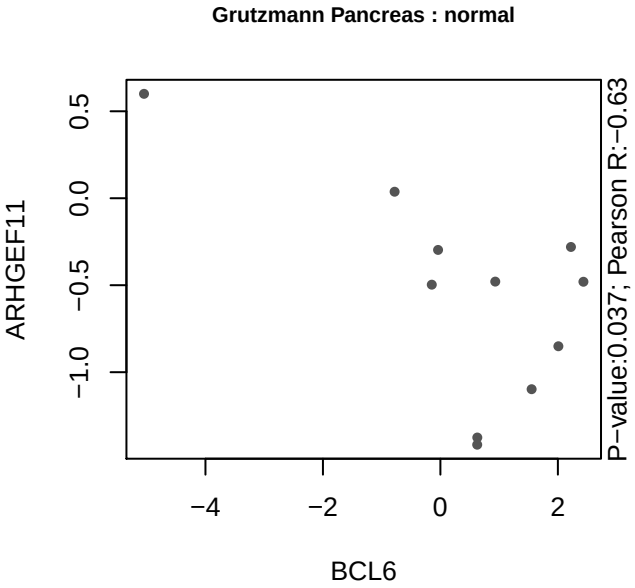

Grutzmann Pancreas : all(no met)
SRC
BCL6
P−value:0.03; Pearson R:−0.46

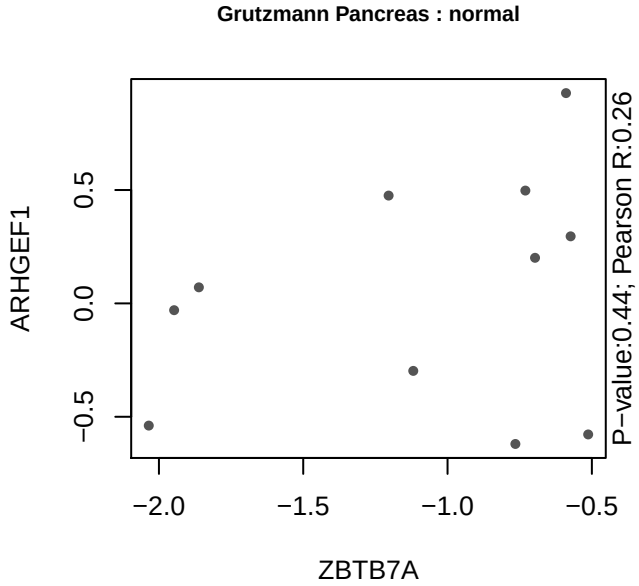

Grutzmann Pancreas : all(no met)
YES1
BCL6
P−value:0.00084; Pearson R:0.66

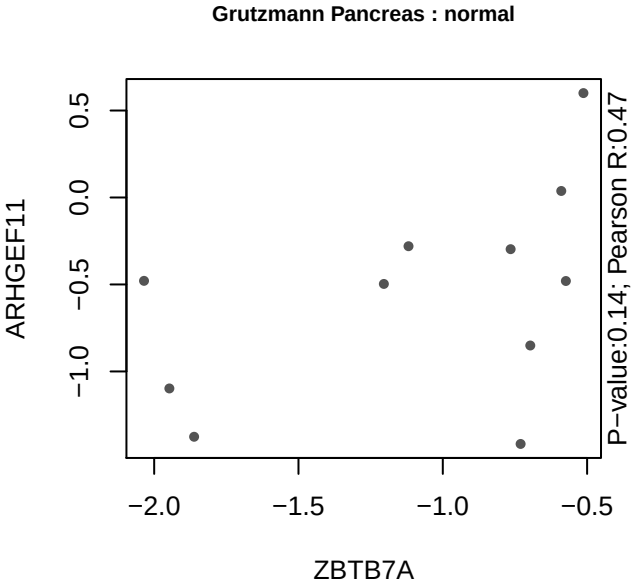

Grutzmann Pancreas : all(no met)
SRC
ZBTB7A
P−value:0.00031; Pearson R:0.7

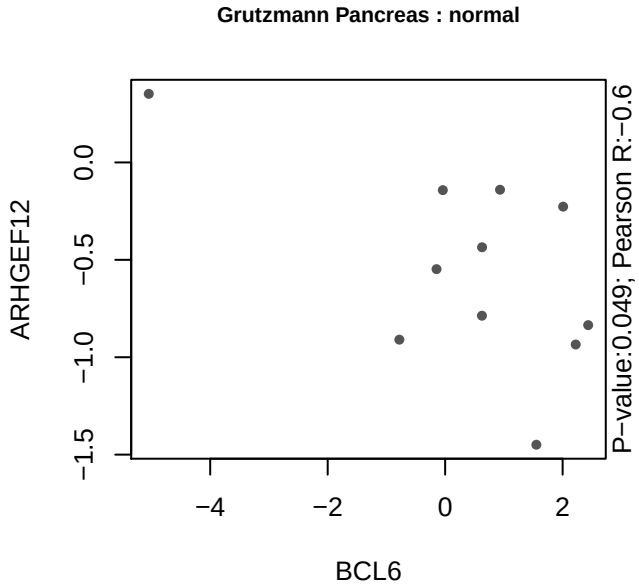

Grutzmann Pancreas : all(no met)
YES1
ZBTB7A
P−value:0.081; Pearson R:−0.38

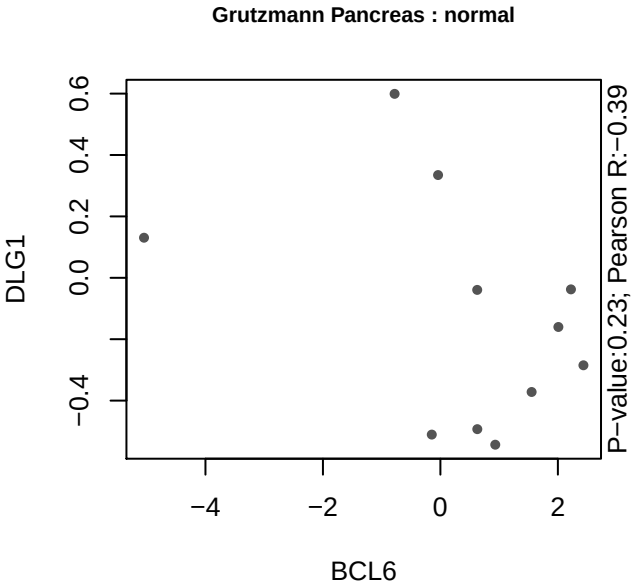

Grutzmann Pancreas : normal
ARHGEF1
BCL6
P−value:0.53; Pearson R:0.21

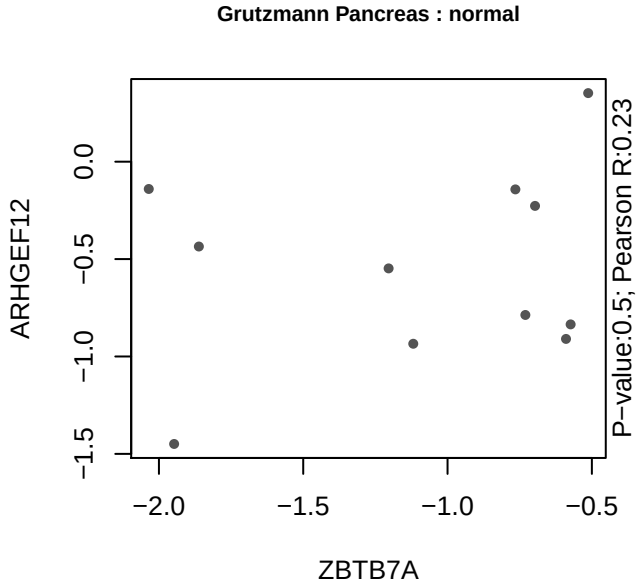

Grutzmann Pancreas : normal
ARHGEF11
BCL6
P−value:0.037; Pearson R:−0.63

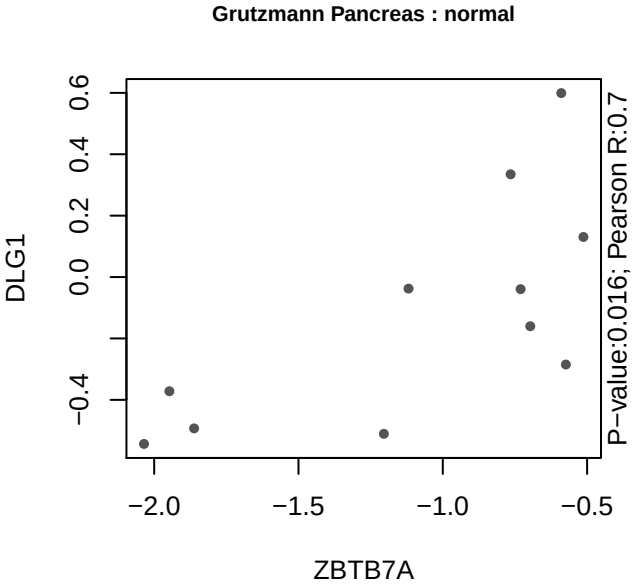

Grutzmann Pancreas : normal
ARHGEF1
ZBTB7A
P−value:0.44; Pearson R:0.26

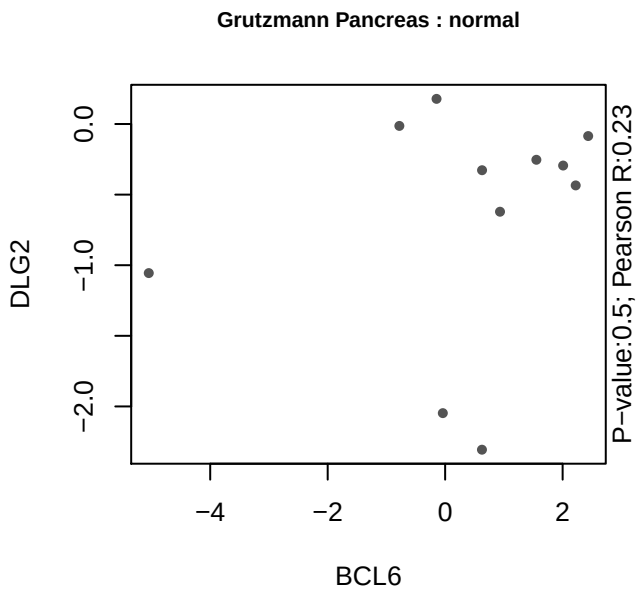

Grutzmann Pancreas : normal
ARHGEF11
ZBTB7A
P−value:0.14; Pearson R:0.47

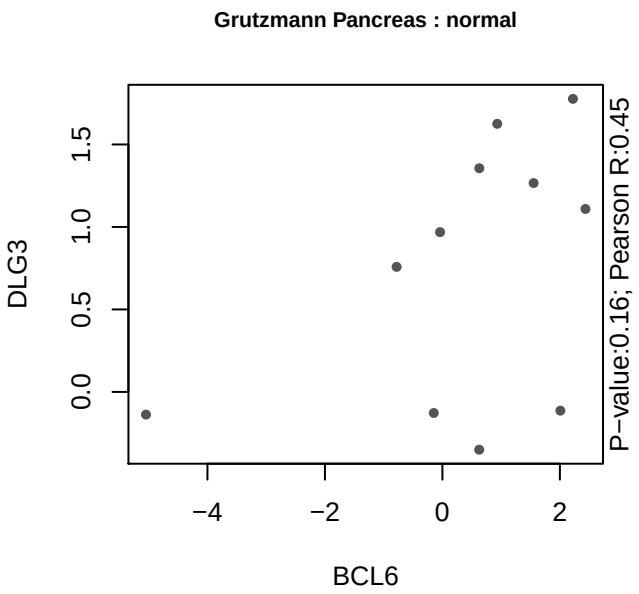

Grutzmann Pancreas : normal
ARHGEF12
BCL6
P−value:0.049; Pearson R:−0.6

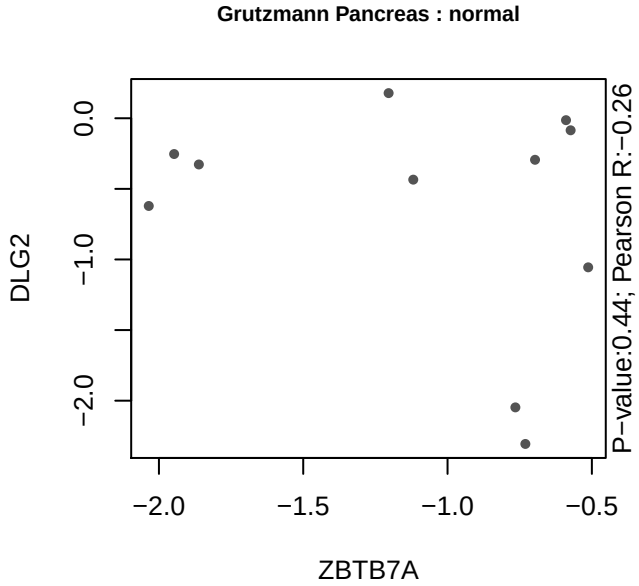

Grutzmann Pancreas : normal
DLG1
BCL6
P−value:0.23; Pearson R:−0.39

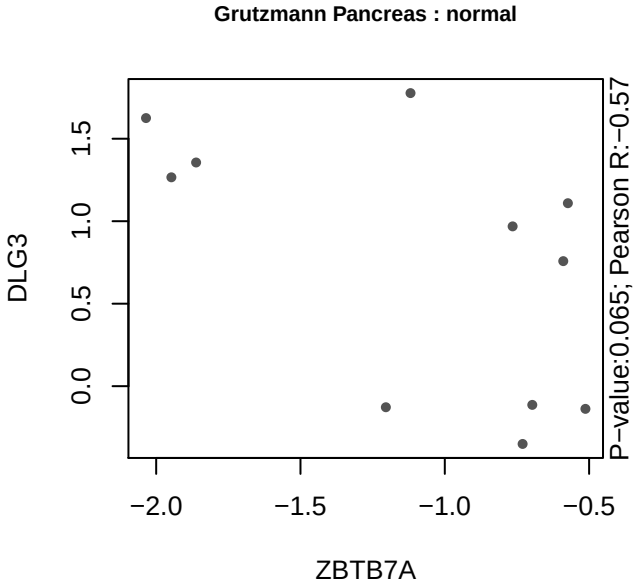

Grutzmann Pancreas : normal
ARHGEF12
ZBTB7A
P−value:0.5; Pearson R:0.23

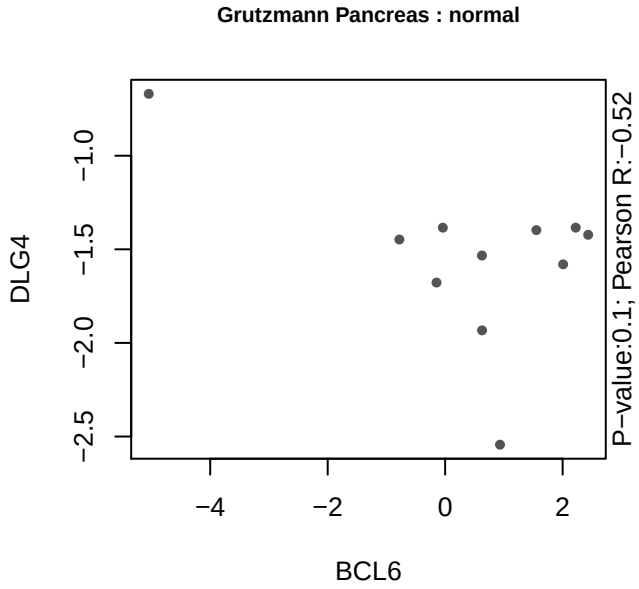

Grutzmann Pancreas : normal
DLG1
ZBTB7A
P−value:0.016; Pearson R:0.7

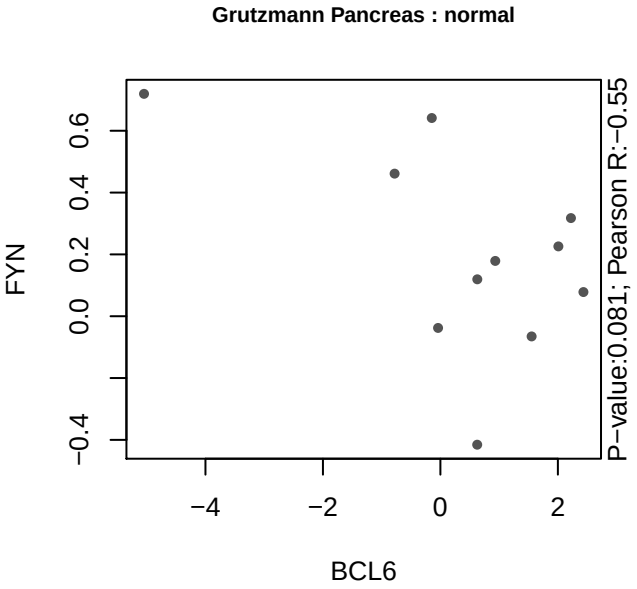

Grutzmann Pancreas : normal
DLG2
BCL6
P−value:0.5; Pearson R:0.23

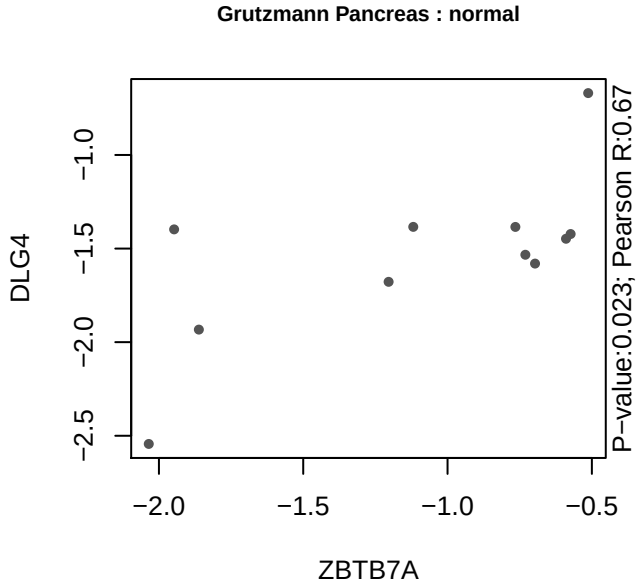

Grutzmann Pancreas : normal
DLG3
BCL6
P−value:0.16; Pearson R:0.45

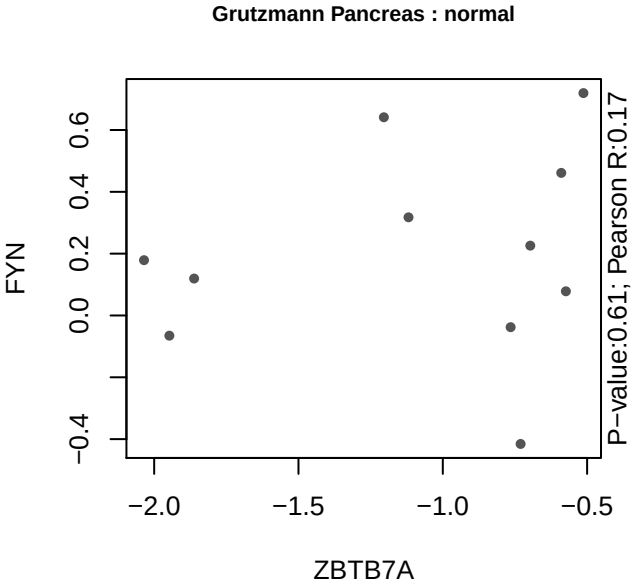

Grutzmann Pancreas : normal
DLG2
ZBTB7A
P−value:0.44; Pearson R:−0.26

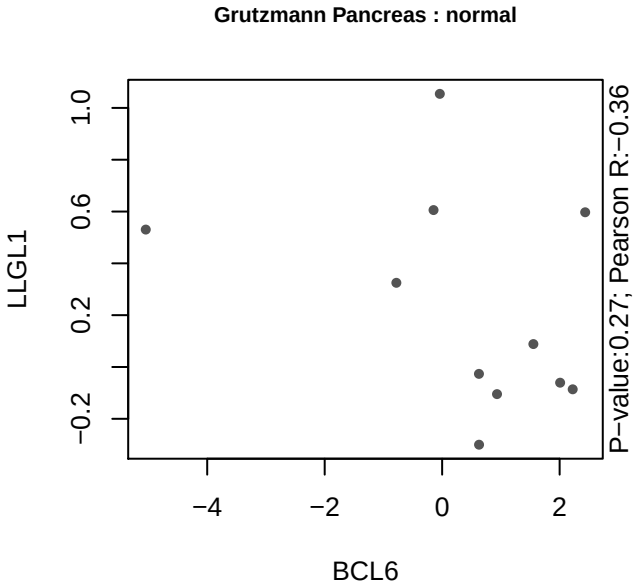

Grutzmann Pancreas : normal
DLG3
ZBTB7A
P−value:0.065; Pearson R:−0.57

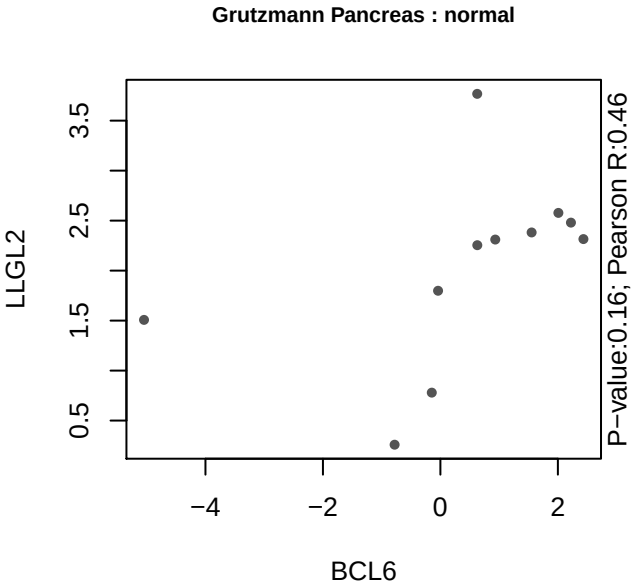

Grutzmann Pancreas : normal
DLG4
BCL6
P−value:0.1; Pearson R:−0.52

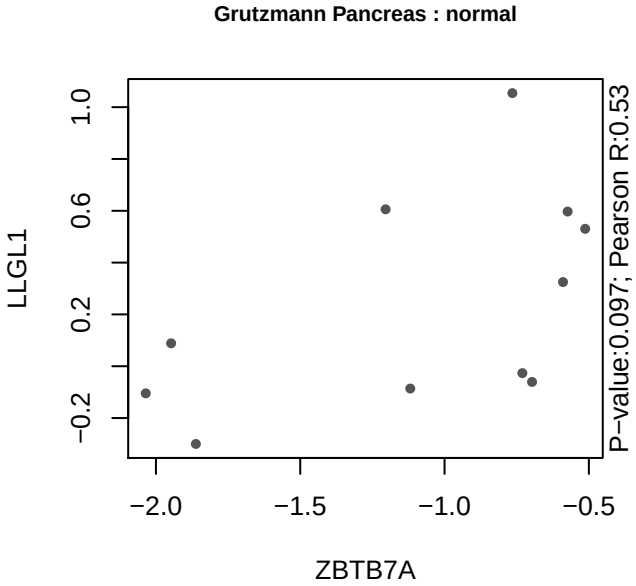

Grutzmann Pancreas : normal
FYN
BCL6
P−value:0.081; Pearson R:−0.55

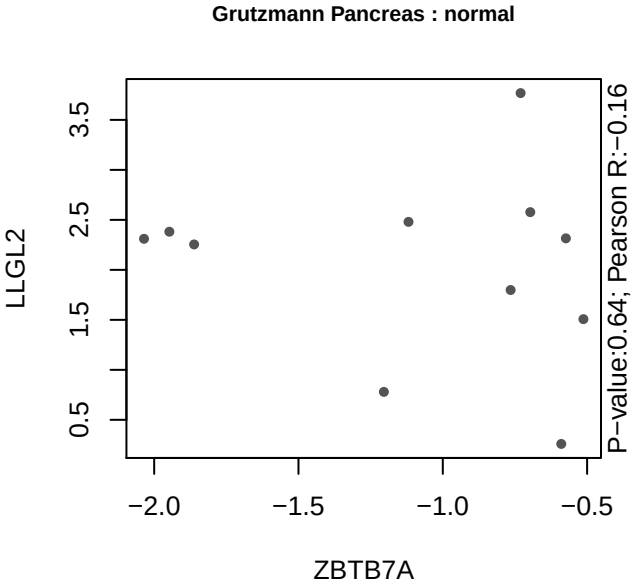

Grutzmann Pancreas : normal
DLG4
ZBTB7A
P−value:0.023; Pearson R:0.67

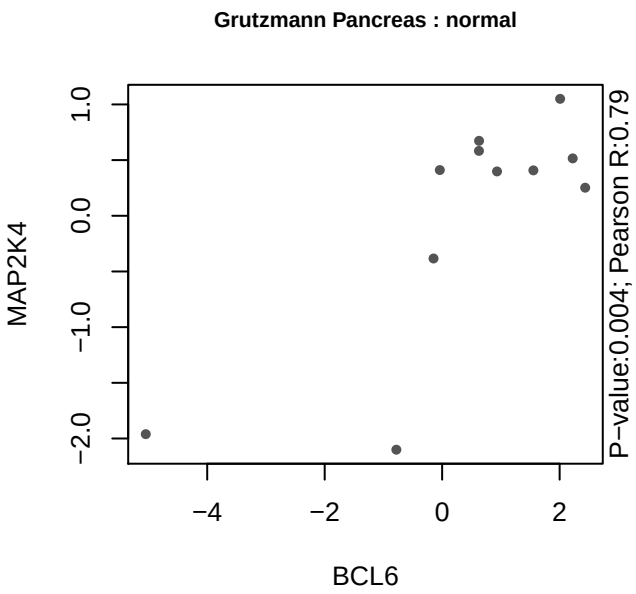

Grutzmann Pancreas : normal
FYN
ZBTB7A
P−value:0.61; Pearson R:0.17

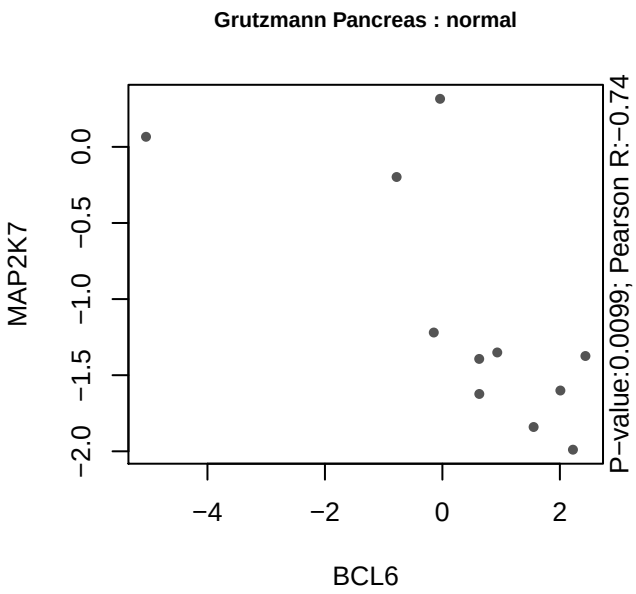

Grutzmann Pancreas : normal
LLGL1
BCL6
P−value:0.27; Pearson R:−0.36

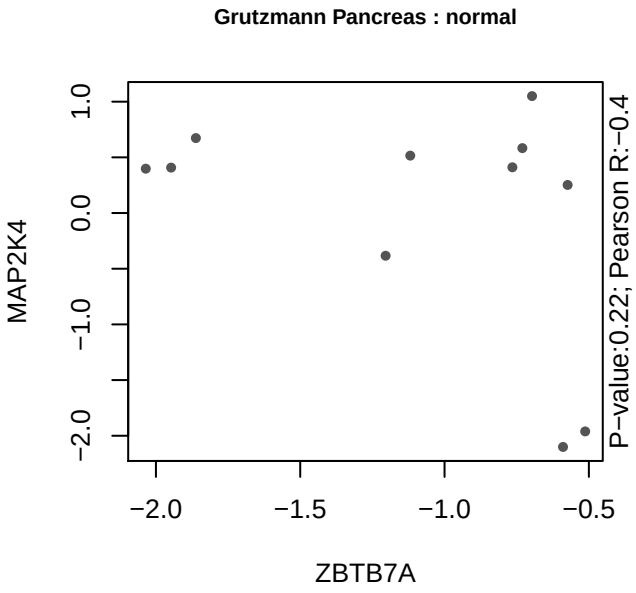

Grutzmann Pancreas : normal
LLGL2
BCL6
P−value:0.16; Pearson R:0.46

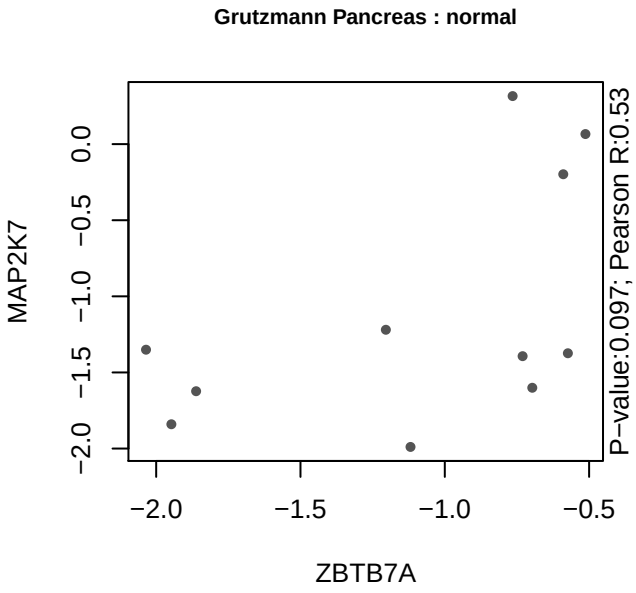

Grutzmann Pancreas : normal
LLGL1
ZBTB7A
P−value:0.097; Pearson R:0.53

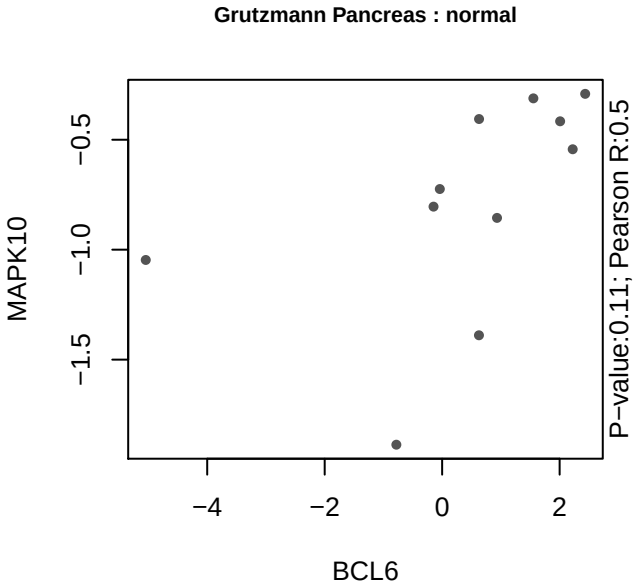

Grutzmann Pancreas : normal
LLGL2
ZBTB7A
P−value:0.64; Pearson R:−0.16

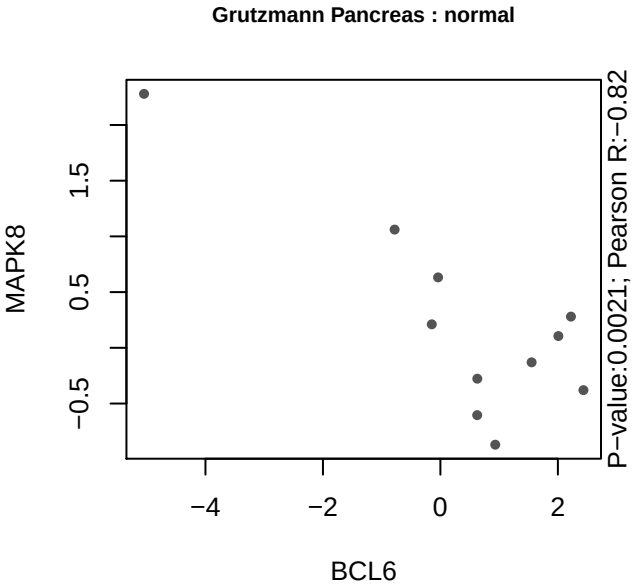

Grutzmann Pancreas : normal
MAP2K4
BCL6
P−value:0.004; Pearson R:0.79

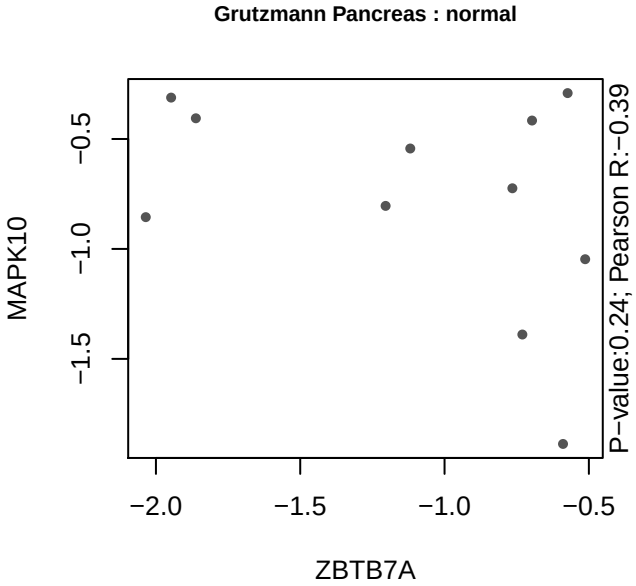

Grutzmann Pancreas : normal
MAP2K7
BCL6
P−value:0.0099; Pearson R:−0.74

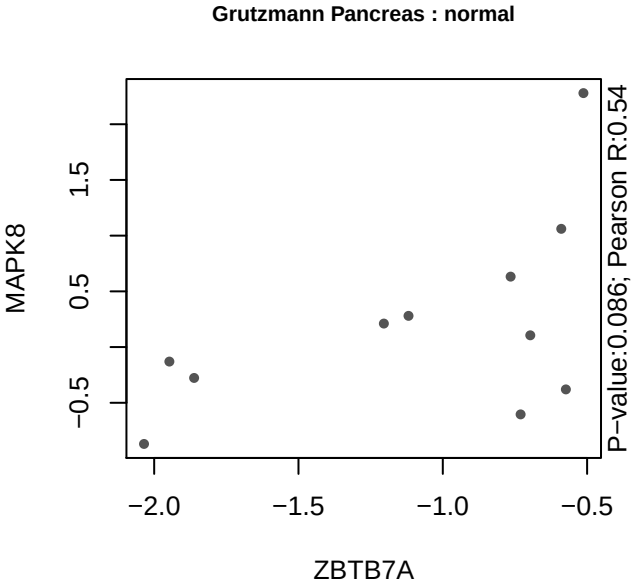

Grutzmann Pancreas : normal
MAP2K4
ZBTB7A
P−value:0.22; Pearson R:−0.4

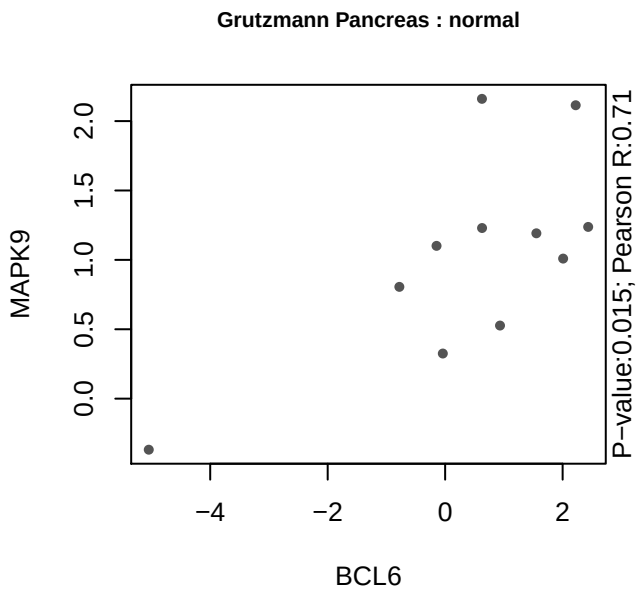

Grutzmann Pancreas : normal
MAP2K7
ZBTB7A
P−value:0.097; Pearson R:0.53

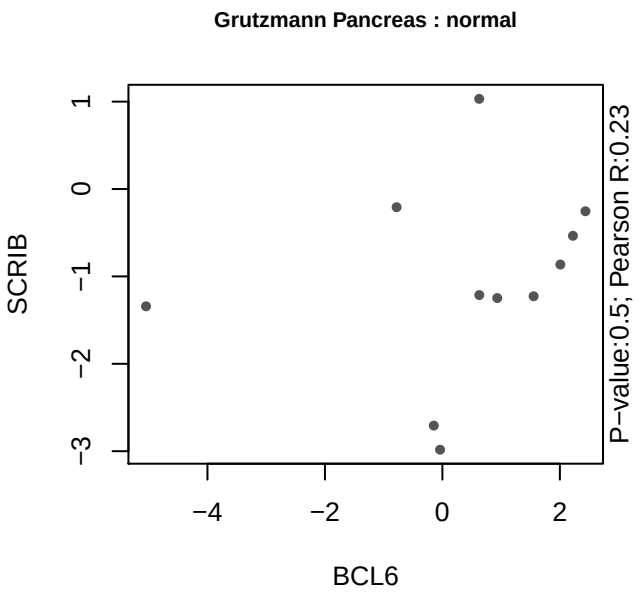

Grutzmann Pancreas : normal
MAPK10
BCL6
P−value:0.11; Pearson R:0.5

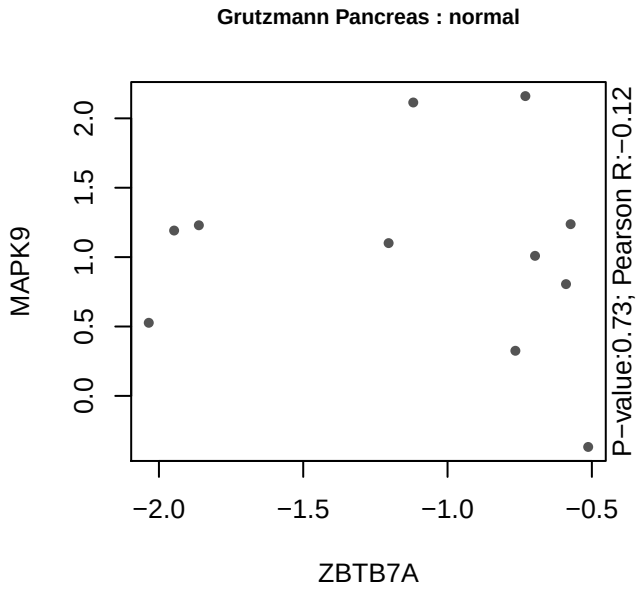

Grutzmann Pancreas : normal
MAPK8
BCL6
P−value:0.0021; Pearson R:−0.82

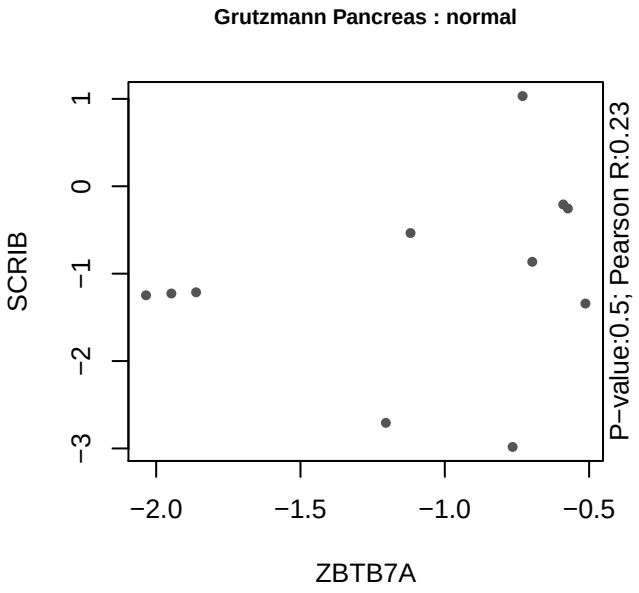

Grutzmann Pancreas : normal
MAPK10
ZBTB7A
P−value:0.24; Pearson R:−0.39

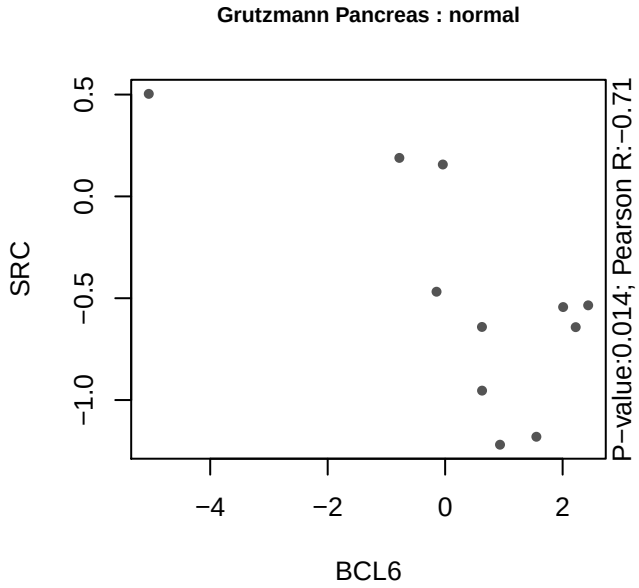

Grutzmann Pancreas : normal
MAPK8
ZBTB7A
P−value:0.086; Pearson R:0.54

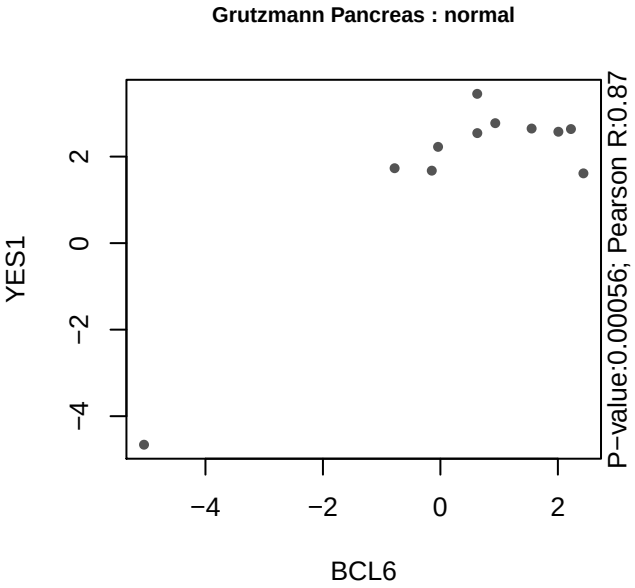

Grutzmann Pancreas : normal
MAPK9
BCL6
P−value:0.015; Pearson R:0.71

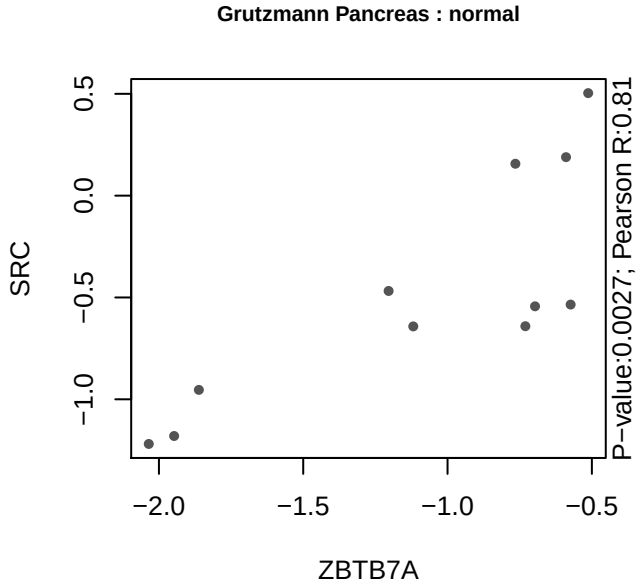

Grutzmann Pancreas : normal
SCRIB
BCL6
P−value:0.5; Pearson R:0.23

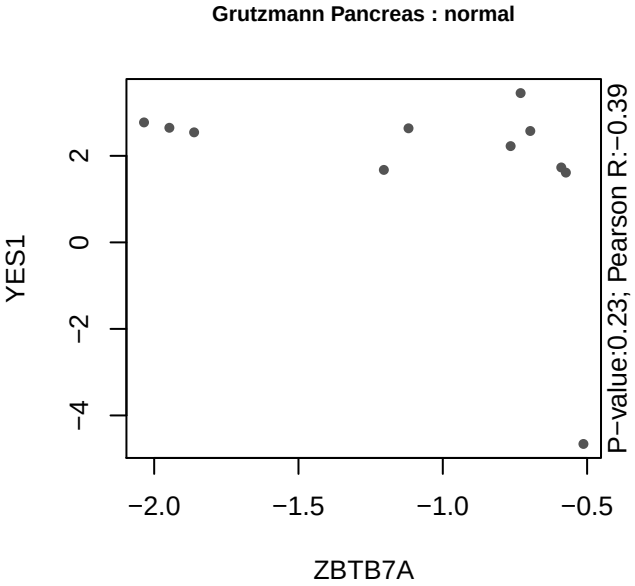

Grutzmann Pancreas : normal
MAPK9
ZBTB7A
P−value:0.73; Pearson R:−0.12

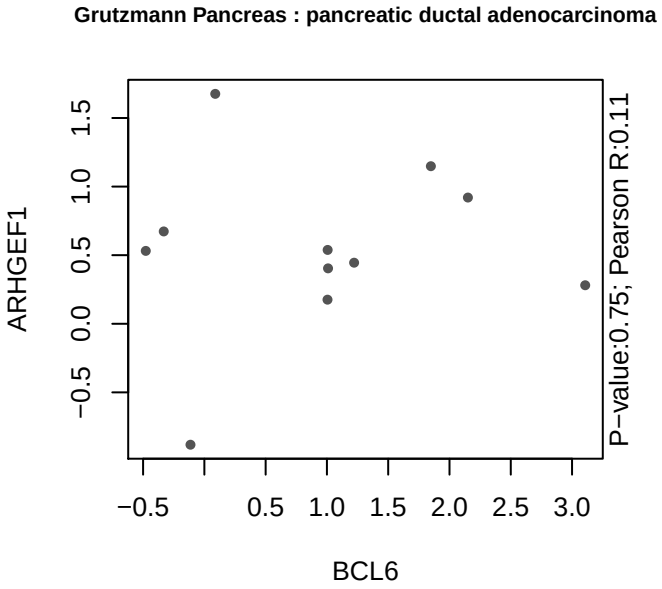

Grutzmann Pancreas : normal
SCRIB
ZBTB7A
P−value:0.5; Pearson R:0.23

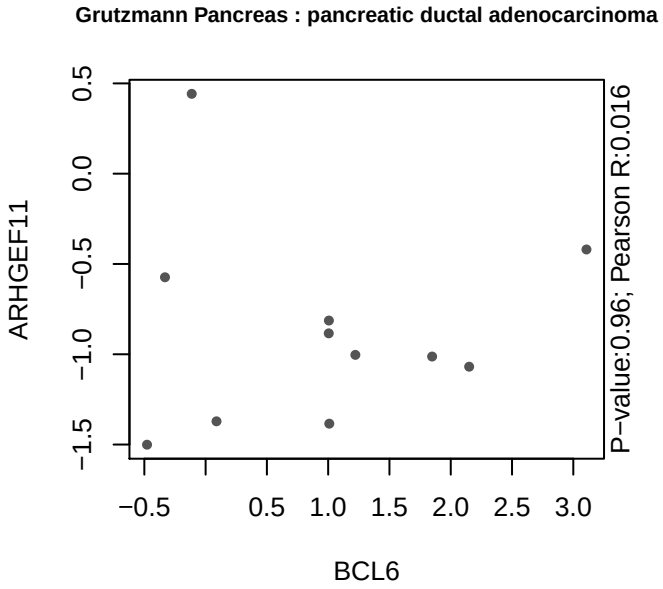

Grutzmann Pancreas : normal
SRC
BCL6
P−value:0.014; Pearson R:−0.71

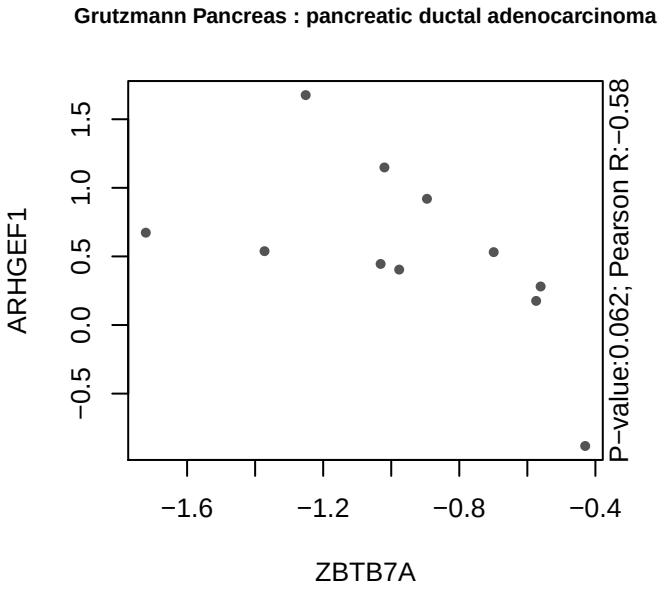

Grutzmann Pancreas : normal
YES1
BCL6
P−value:0.00056; Pearson R:0.87

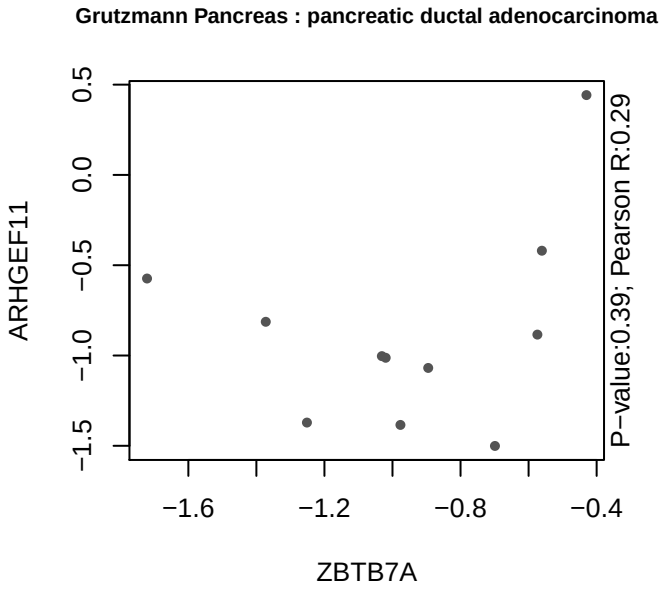

Grutzmann Pancreas : normal
SRC
ZBTB7A
P−value:0.0027; Pearson R:0.81

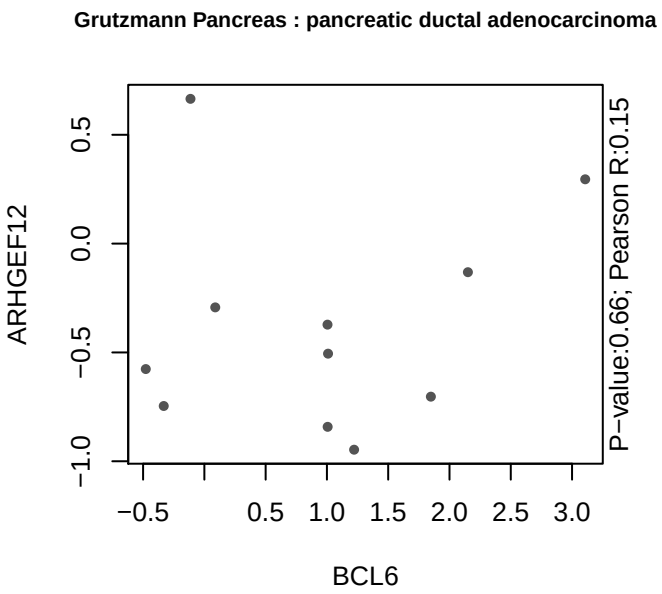

Grutzmann Pancreas : normal
YES1
ZBTB7A
P−value:0.23; Pearson R:−0.39

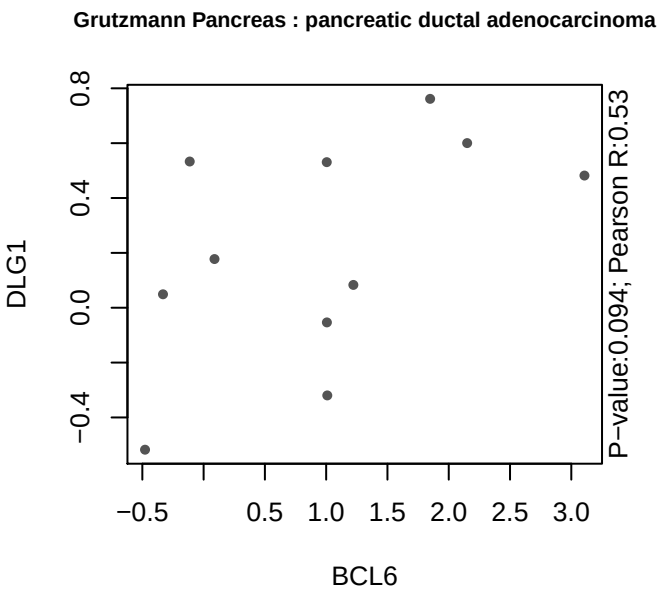

Grutzmann Pancreas : pancreatic ductal adenocarcinoma
ARHGEF1
BCL6
P−value:0.75; Pearson R:0.11

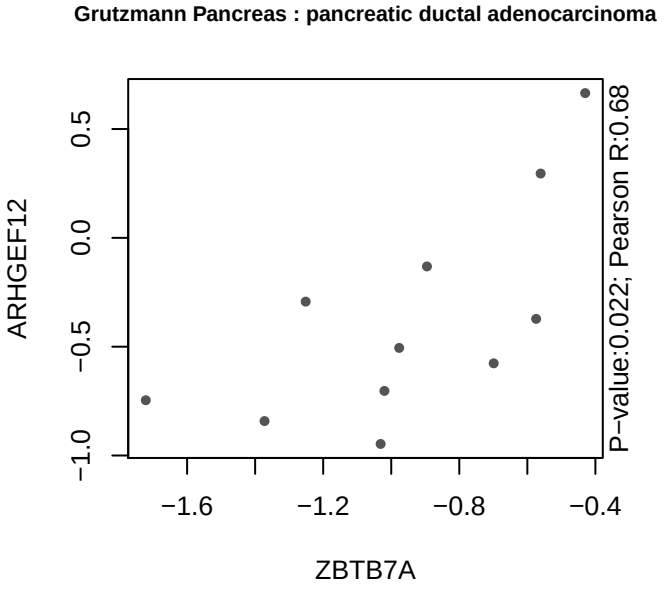

Grutzmann Pancreas : pancreatic ductal adenocarcinoma
ARHGEF11
BCL6
P−value:0.96; Pearson R:0.016

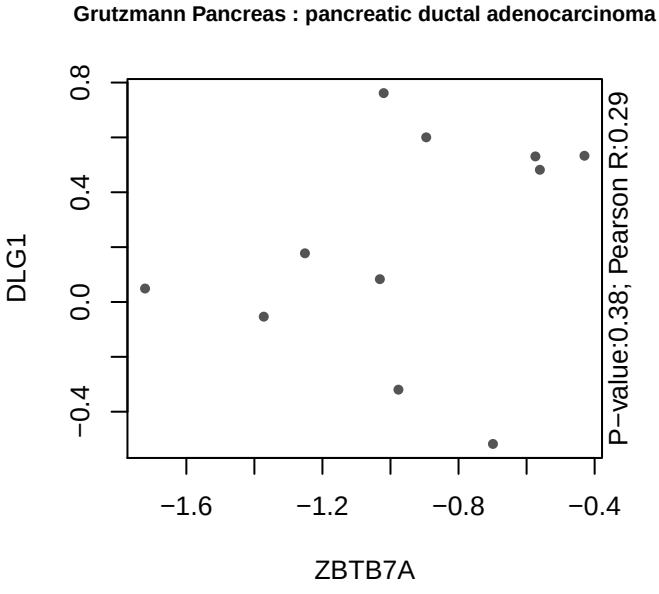

Grutzmann Pancreas : pancreatic ductal adenocarcinoma
ARHGEF1
ZBTB7A
P−value:0.062; Pearson R:−0.58

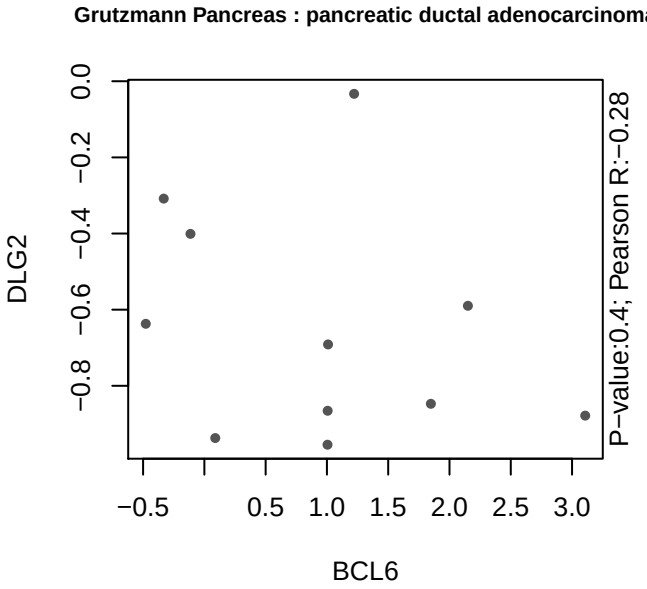

Grutzmann Pancreas : pancreatic ductal adenocarcinoma
ARHGEF11
ZBTB7A
P−value:0.39; Pearson R:0.29

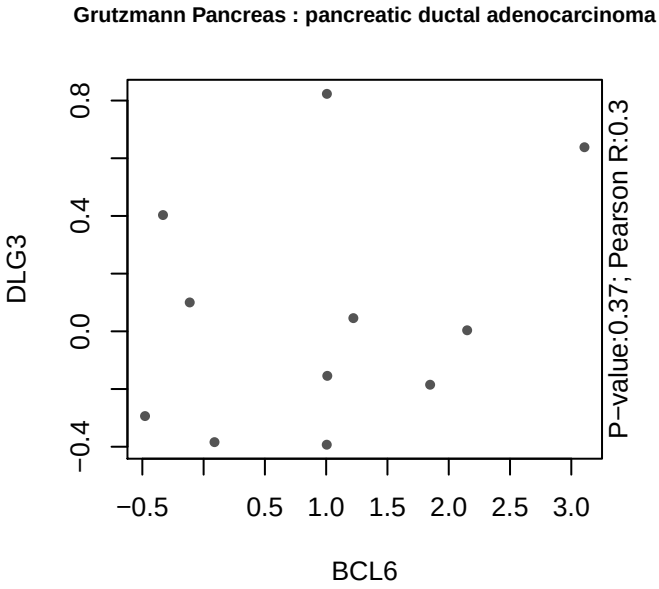

Grutzmann Pancreas : pancreatic ductal adenocarcinoma
ARHGEF12
BCL6
P−value:0.66; Pearson R:0.15
−1.0
−0.5
0.0
0.5
−0.5
0.5
1.0
1.5
2.0
2.5
3.0

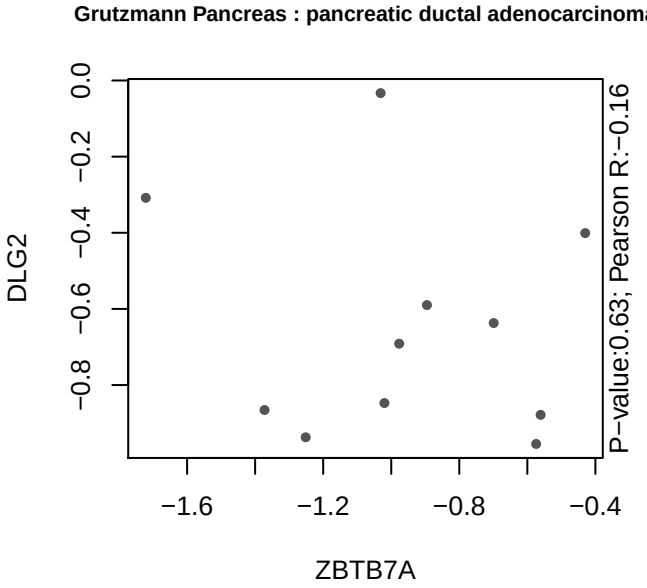

Grutzmann Pancreas : pancreatic ductal adenocarcinoma
DLG1
BCL6
P−value:0.094; Pearson R:0.53
−0.4
0.0
0.4
0.8
−0.5
0.5
1.0
1.5
2.0
2.5
3.0

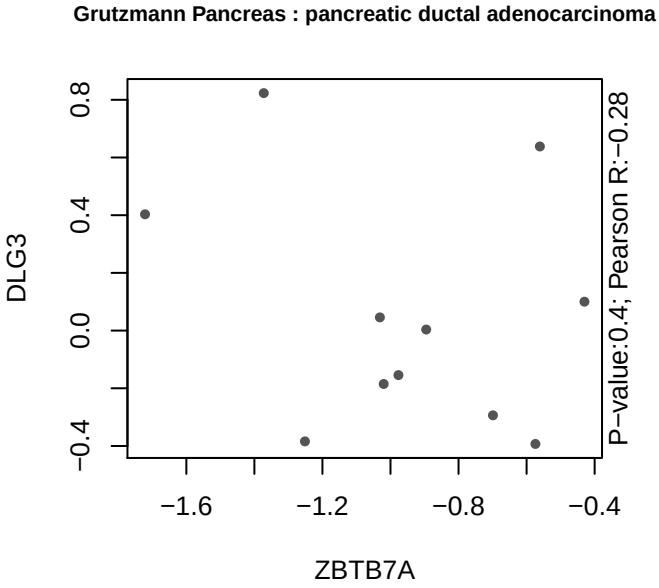

Grutzmann Pancreas : pancreatic ductal adenocarcinoma
ARHGEF12
ZBTB7A
P−value:0.022; Pearson R:0.68
−1.0
−0.5
0.0
0.5
−1.6
−1.2
−0.8
−0.4

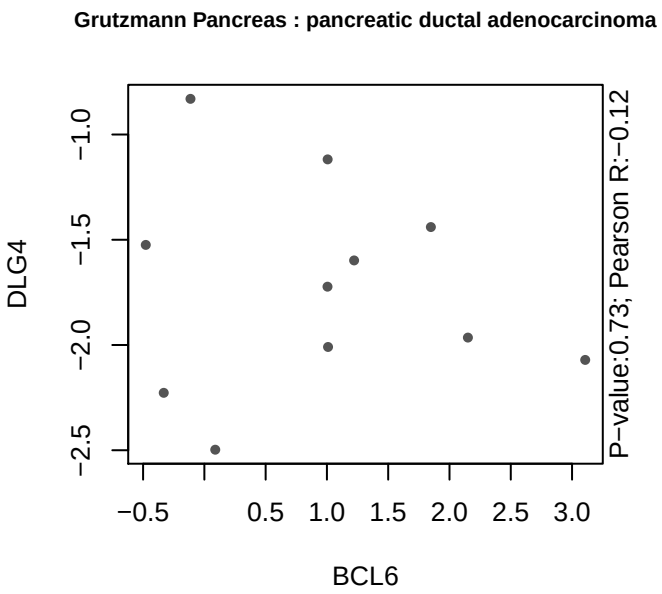

Grutzmann Pancreas : pancreatic ductal adenocarcinoma
DLG1
ZBTB7A
P−value:0.38; Pearson R:0.29
−0.4
0.0
0.4
0.8
−1.6
−1.2
−0.8
−0.4

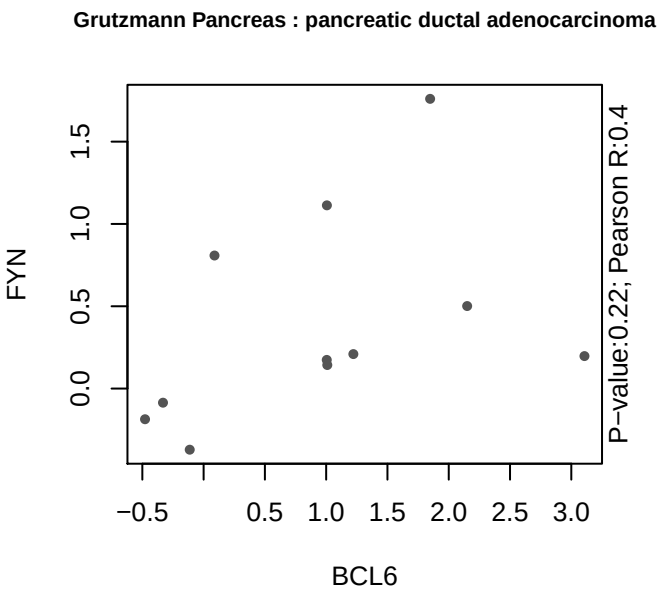

Grutzmann Pancreas : pancreatic ductal adenocarcinoma
DLG2
BCL6
P−value:0.4; Pearson R:−0.28
0.0
−0.2
−0.4
−0.6
−0.8
−0.5
0.5
1.0
1.5
2.0
2.5
3.0

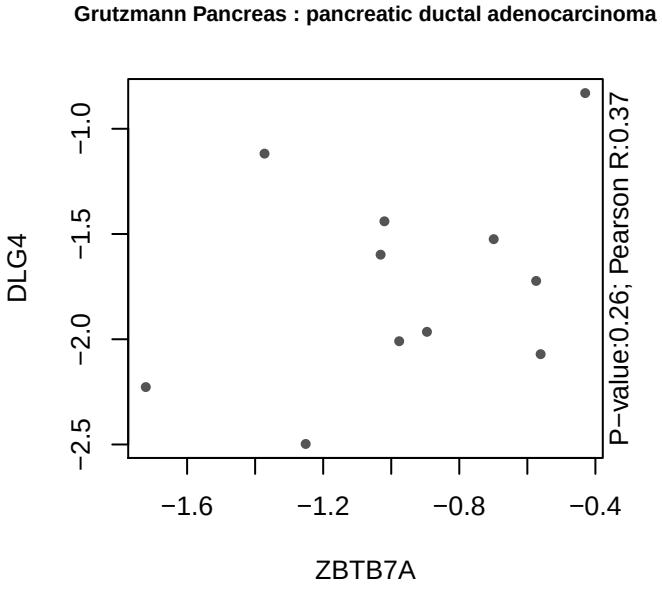

Grutzmann Pancreas : pancreatic ductal adenocarcinoma
DLG3
BCL6
P−value:0.37; Pearson R:0.3
0.8
0.4
0.0
−0.4
−0.5
0.5
1.0
1.5
2.0
2.5
3.0

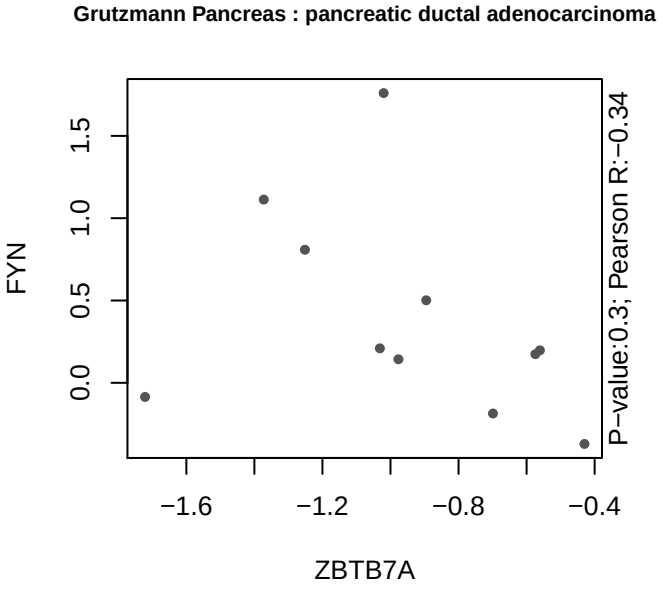

Grutzmann Pancreas : pancreatic ductal adenocarcinoma
DLG2
ZBTB7A
P−value:0.63; Pearson R:−0.16
0.0
−0.2
−0.4
−0.6
−0.8
−1.6
−1.2
−0.8
−0.4

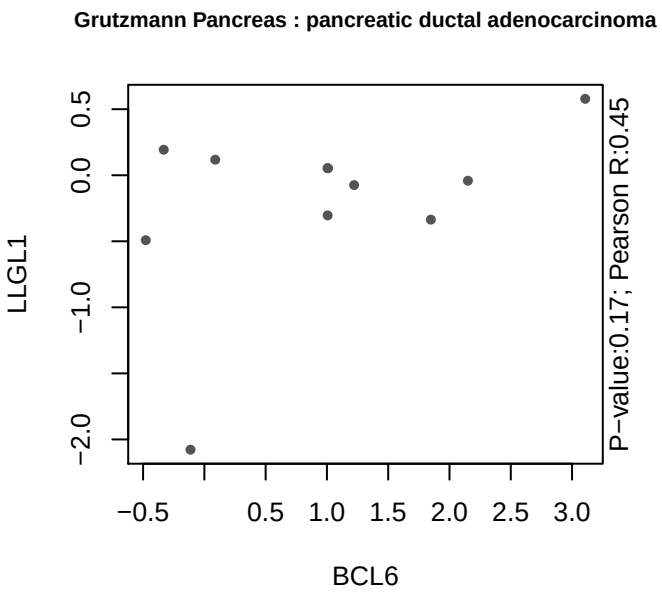

Grutzmann Pancreas : pancreatic ductal adenocarcinoma
DLG3
ZBTB7A
P−value:0.4; Pearson R:−0.28
0.8
0.4
0.0
−0.4
−1.6
−1.2
−0.8
−0.4

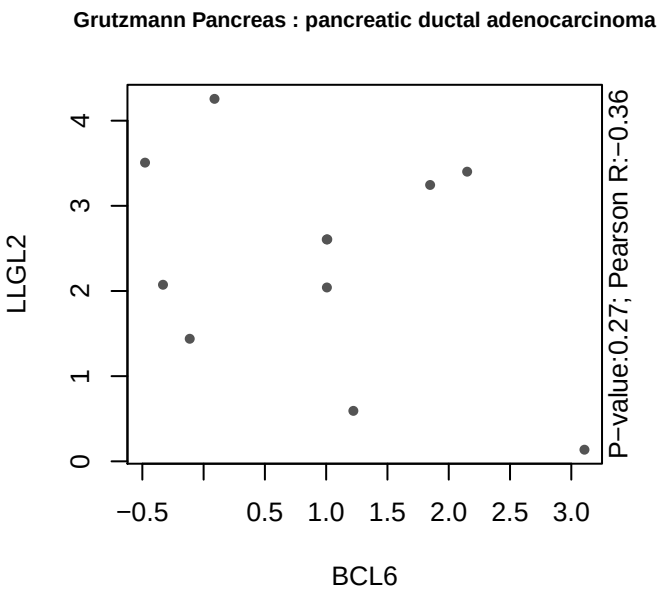

Grutzmann Pancreas : pancreatic ductal adenocarcinoma
DLG4
BCL6
P−value:0.73; Pearson R:−0.12
−1.0
−1.5
−2.0
−2.5
−0.5
0.5
1.0
1.5
2.0
2.5
3.0

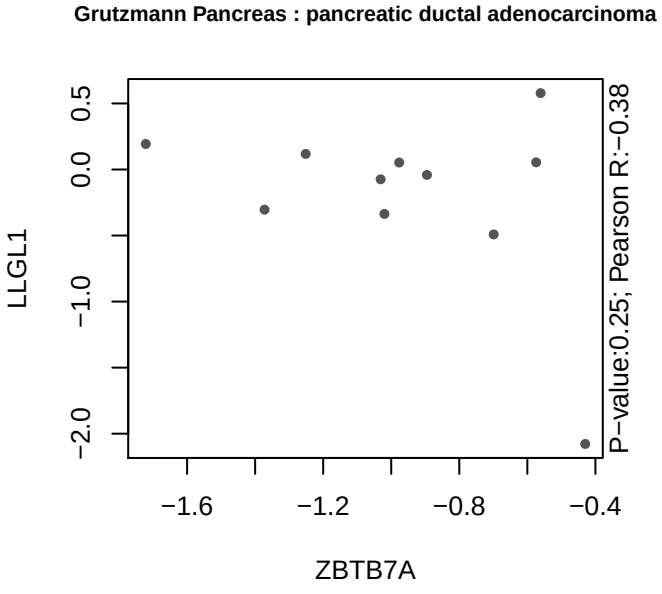

Grutzmann Pancreas : pancreatic ductal adenocarcinoma
FYN
BCL6
P−value:0.22; Pearson R:0.4
0.0
0.5
1.0
1.5
−0.5
0.5
1.0
1.5
2.0
2.5
3.0

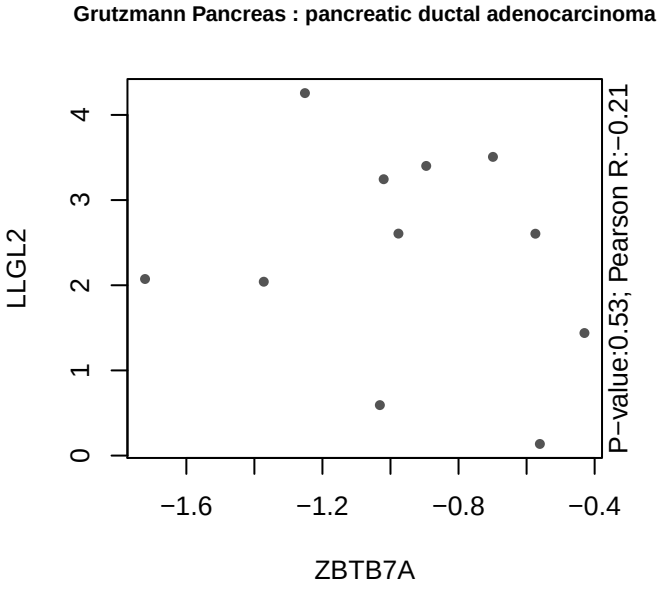

Grutzmann Pancreas : pancreatic ductal adenocarcinoma
DLG4
ZBTB7A
P−value:0.26; Pearson R:0.37
−1.0
−1.5
−2.0
−2.5
−1.6
−1.2
−0.8
−0.4

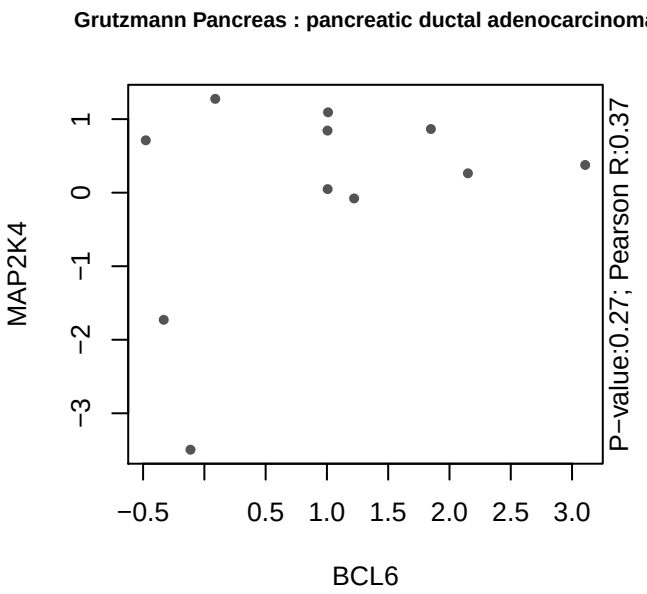

Grutzmann Pancreas : pancreatic ductal adenocarcinoma
FYN
ZBTB7A
P−value:0.3; Pearson R:−0.34
0.0
0.5
1.0
1.5
−1.6
−1.2
−0.8
−0.4

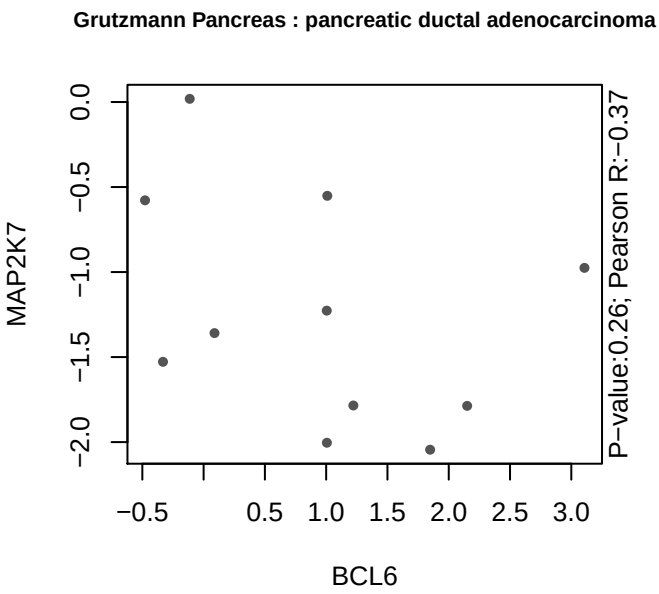

Grutzmann Pancreas : pancreatic ductal adenocarcinoma
LLGL1
BCL6
P−value:0.17; Pearson R:0.45
−2.0
−1.0
0.0
0.5
−0.5
0.5
1.0
1.5
2.0
2.5
3.0

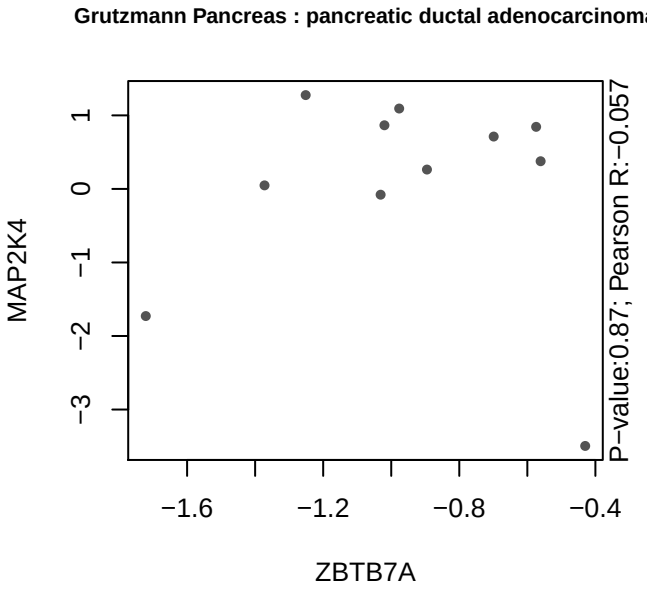

Grutzmann Pancreas : pancreatic ductal adenocarcinoma
LLGL2
BCL6
P−value:0.27; Pearson R:−0.36
0
1
2
3
4
−0.5
0.5
1.0
1.5
2.0
2.5
3.0

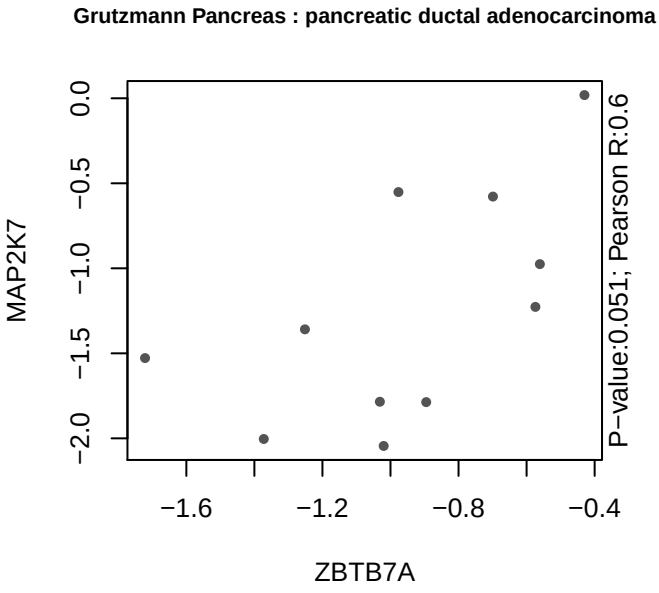

Grutzmann Pancreas : pancreatic ductal adenocarcinoma
LLGL1
ZBTB7A
P−value:0.25; Pearson R:−0.38
−2.0
−1.0
0.0
0.5
−1.6
−1.2
−0.8
−0.4

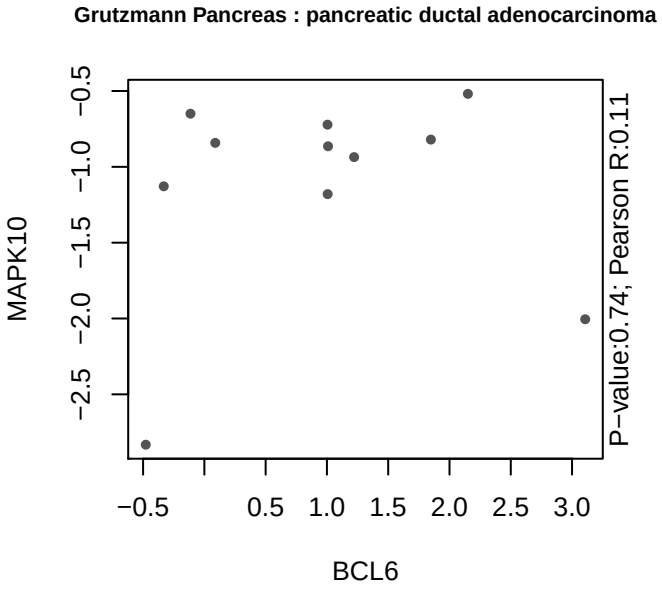

Grutzmann Pancreas : pancreatic ductal adenocarcinoma
LLGL2
ZBTB7A
P−value:0.53; Pearson R:−0.21
0
1
2
3
4
−1.6
−1.2
−0.8
−0.4

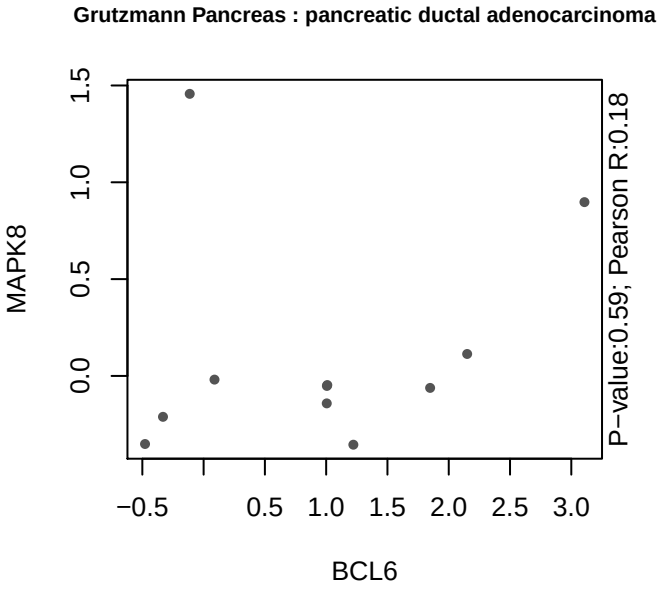

Grutzmann Pancreas : pancreatic ductal adenocarcinoma
MAP2K4
BCL6
P−value:0.27; Pearson R:0.37

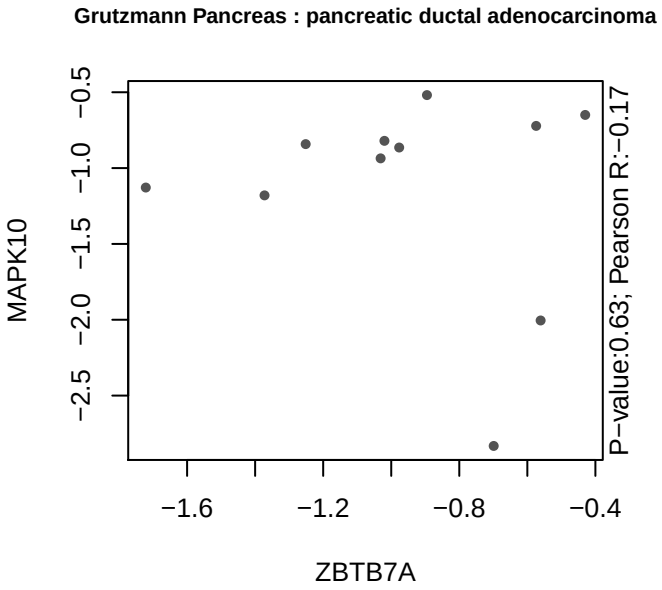

Grutzmann Pancreas : pancreatic ductal adenocarcinoma
MAP2K7
BCL6
P−value:0.26; Pearson R:−0.37

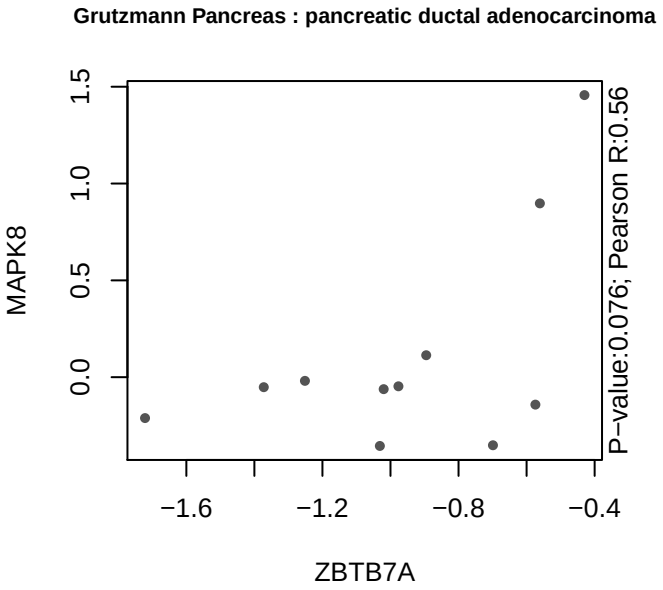

Grutzmann Pancreas : pancreatic ductal adenocarcinoma
MAP2K4
ZBTB7A
P−value:0.87; Pearson R:−0.057

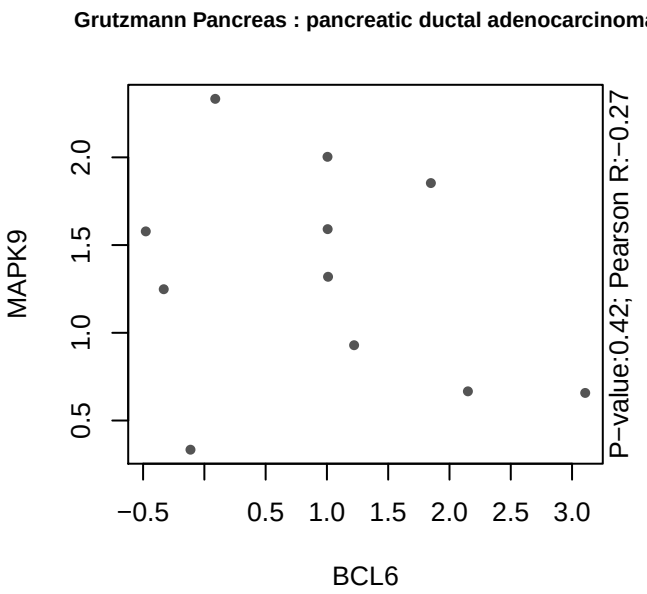

Grutzmann Pancreas : pancreatic ductal adenocarcinoma
MAP2K7
ZBTB7A
P−value:0.051; Pearson R:0.6

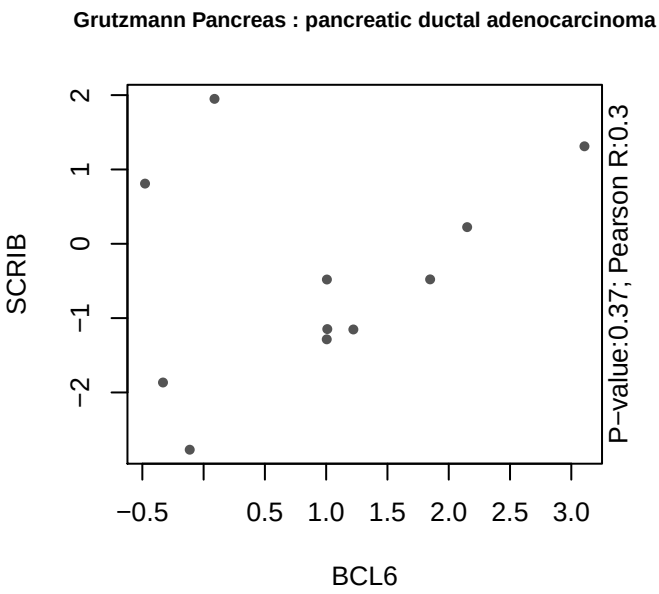

Grutzmann Pancreas : pancreatic ductal adenocarcinoma
MAPK10
BCL6
P−value:0.74; Pearson R:0.11

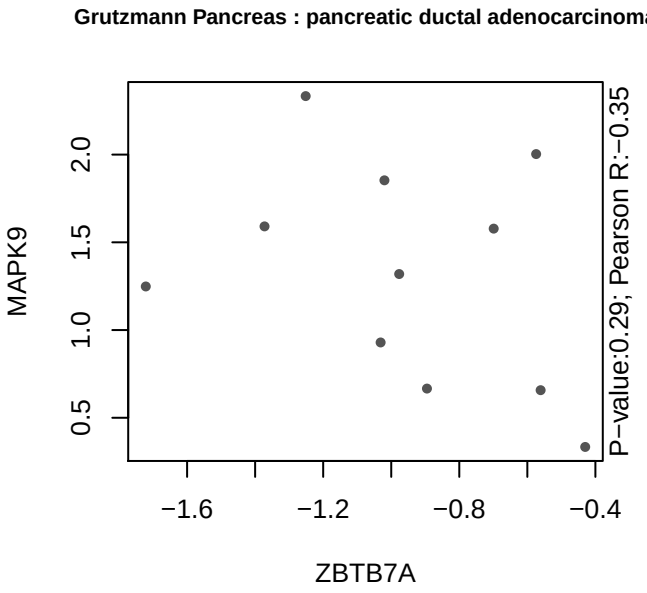

Grutzmann Pancreas : pancreatic ductal adenocarcinoma
MAPK8
BCL6
P−value:0.59; Pearson R:0.18

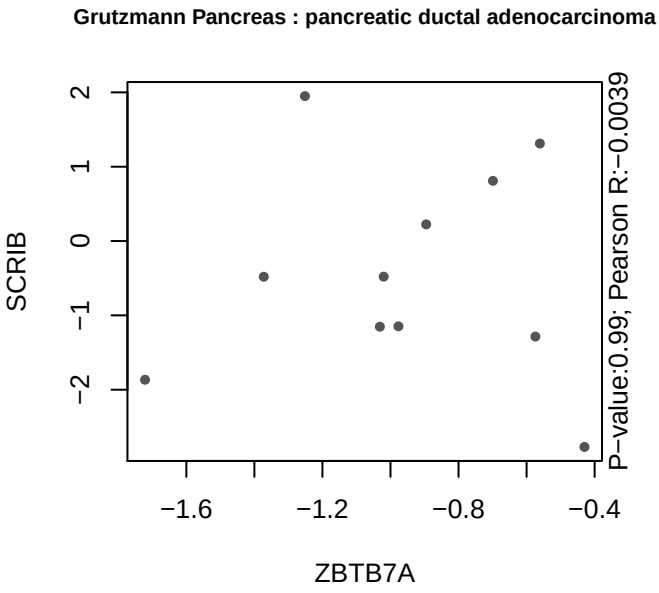

Grutzmann Pancreas : pancreatic ductal adenocarcinoma
MAPK10
ZBTB7A
P−value:0.63; Pearson R:−0.17

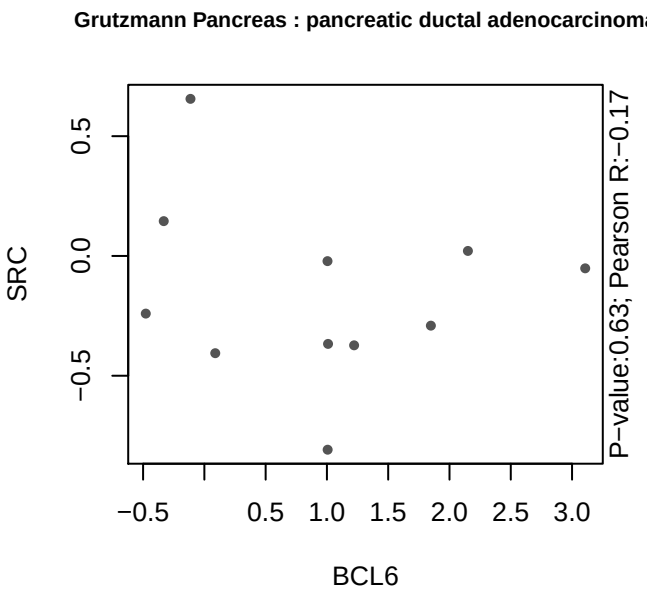

Grutzmann Pancreas : pancreatic ductal adenocarcinoma
MAPK8
ZBTB7A
P−value:0.076; Pearson R:0.56

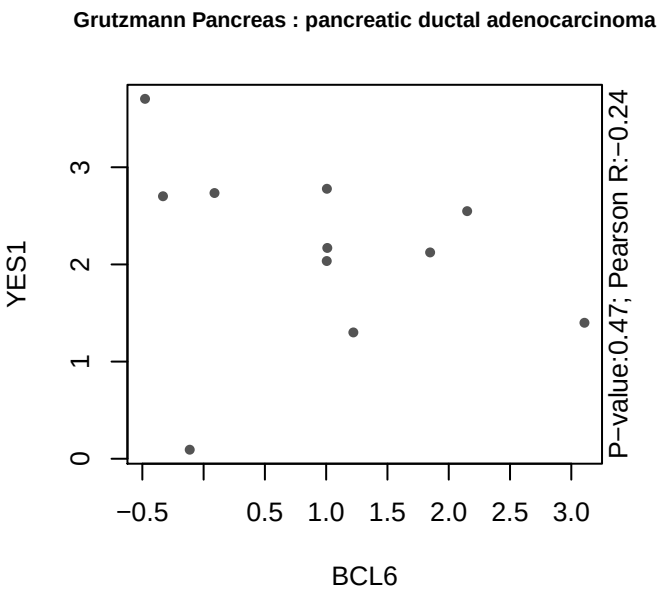

Grutzmann Pancreas : pancreatic ductal adenocarcinoma
MAPK9
BCL6
P−value:0.42; Pearson R:−0.27

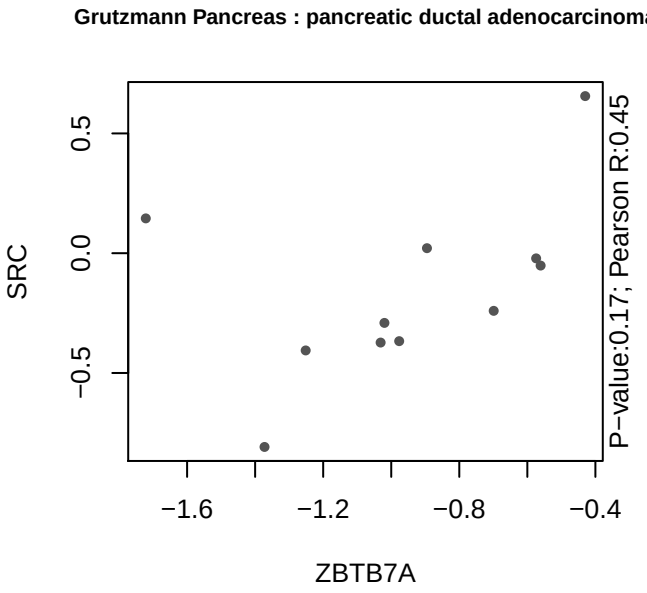

Grutzmann Pancreas : pancreatic ductal adenocarcinoma
SCRIB
BCL6
P−value:0.37; Pearson R:0.3

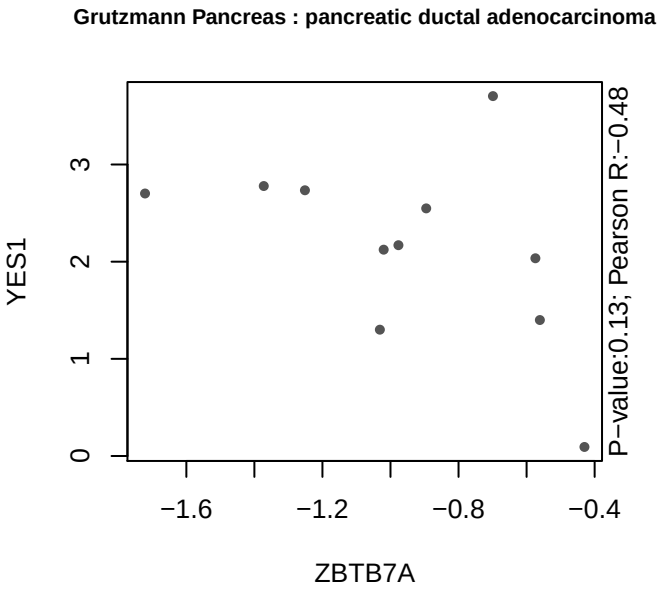

Grutzmann Pancreas : pancreatic ductal adenocarcinoma
MAPK9
ZBTB7A
P−value:0.29; Pearson R:−0.35

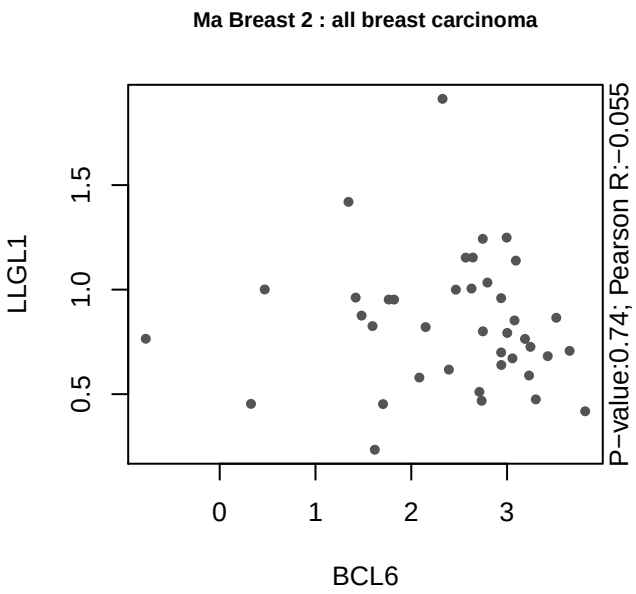

Grutzmann Pancreas : pancreatic ductal adenocarcinoma
SCRIB
ZBTB7A
P−value:0.99; Pearson R:−0.0039

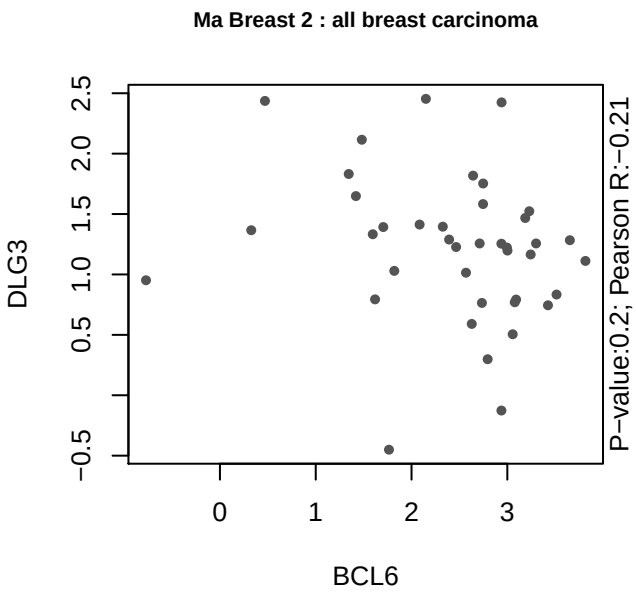

Grutzmann Pancreas : pancreatic ductal adenocarcinoma
SRC
BCL6
P−value:0.63; Pearson R:−0.17

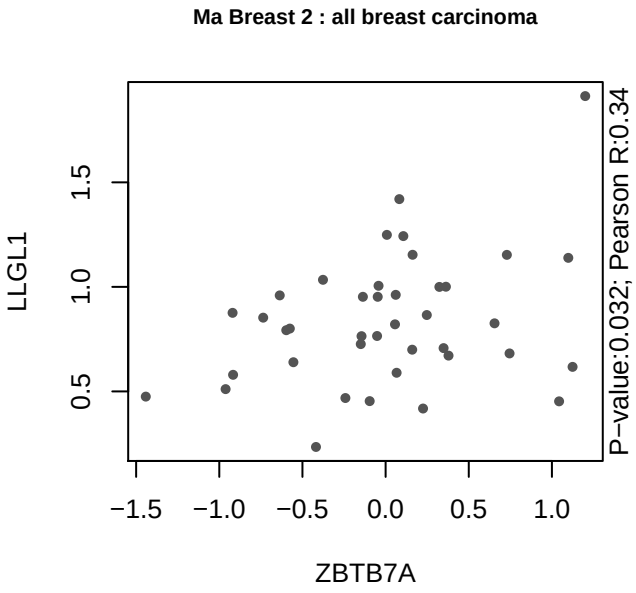

Grutzmann Pancreas : pancreatic ductal adenocarcinoma
YES1
BCL6
P−value:0.47; Pearson R:−0.24

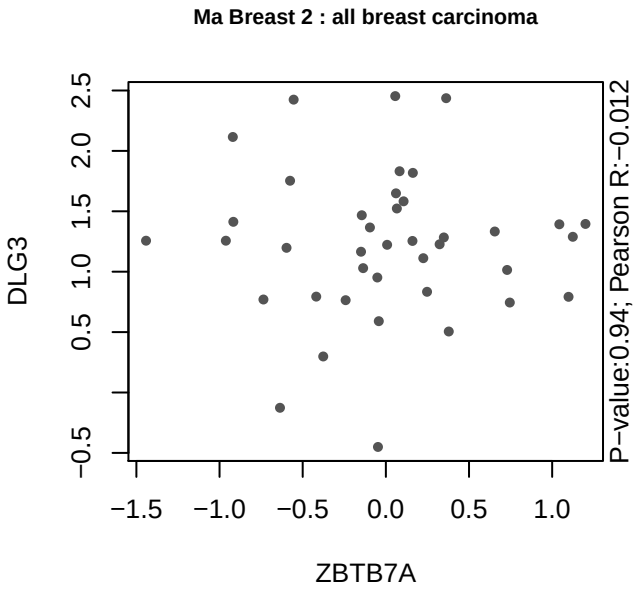

Grutzmann Pancreas : pancreatic ductal adenocarcinoma
SRC
ZBTB7A
P−value:0.17; Pearson R:0.45

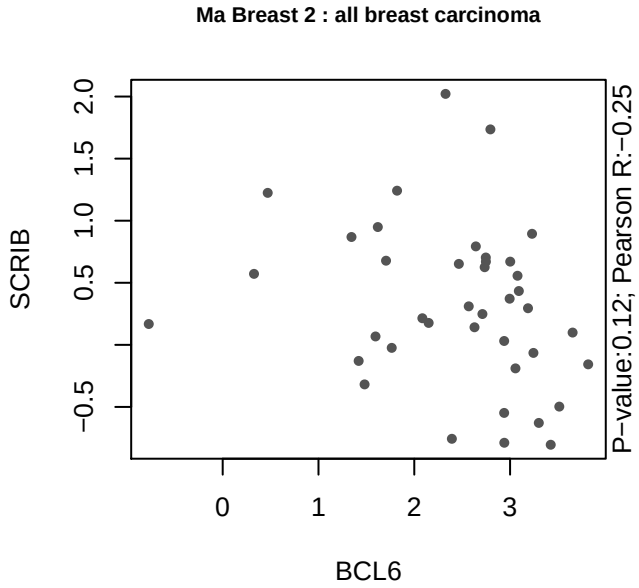

Grutzmann Pancreas : pancreatic ductal adenocarcinoma
YES1
ZBTB7A
P−value:0.13; Pearson R:−0.48

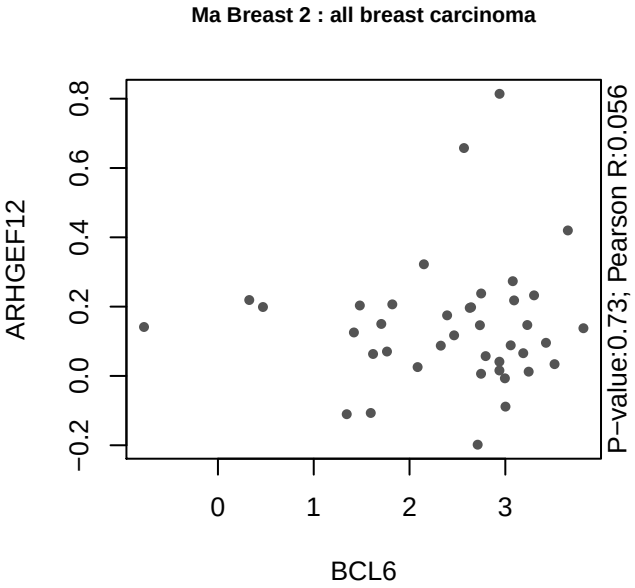

Ma Breast 2 : all breast carcinoma
LLGL1
BCL6
P−value:0.74; Pearson R:−0.055

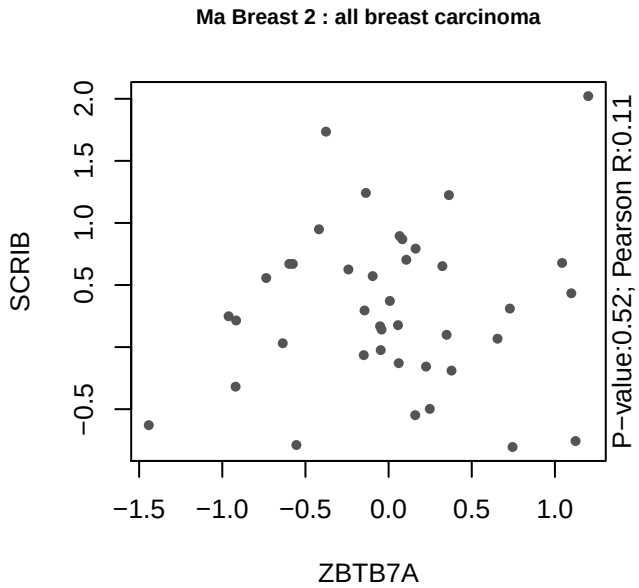

Ma Breast 2 : all breast carcinoma
DLG3
BCL6
P−value:0.2; Pearson R:−0.21

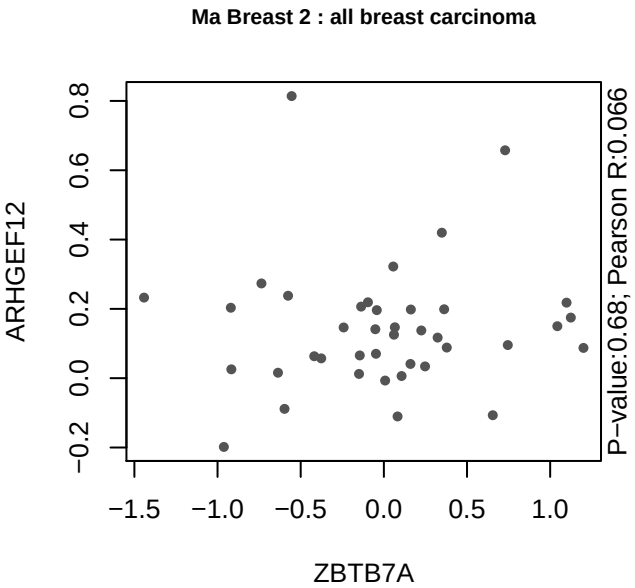

Ma Breast 2 : all breast carcinoma
LLGL1
ZBTB7A
P−value:0.032; Pearson R:0.34

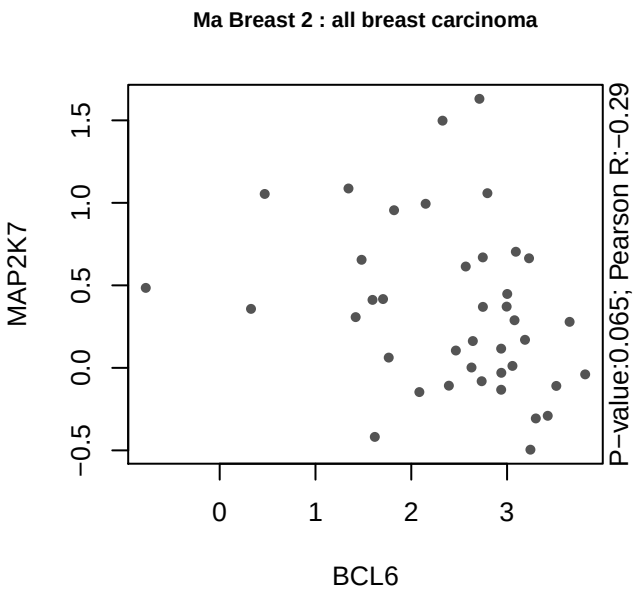

Ma Breast 2 : all breast carcinoma
DLG3
ZBTB7A
P−value:0.94; Pearson R:−0.012

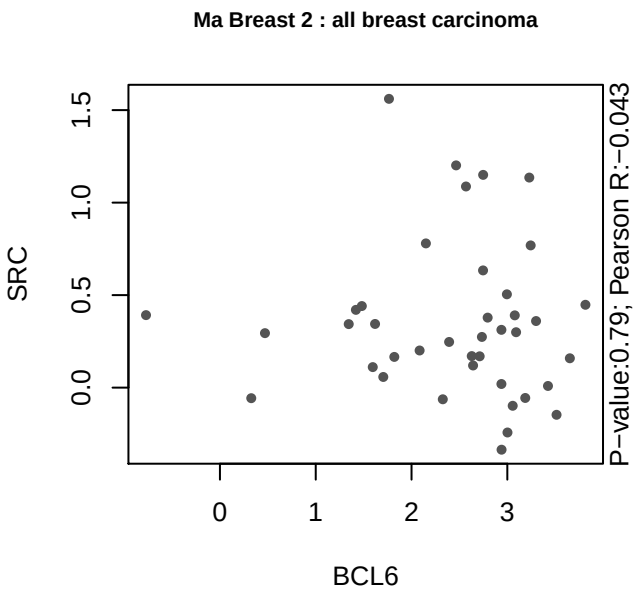

Ma Breast 2 : all breast carcinoma
SCRIB
BCL6
P−value:0.12; Pearson R:−0.25

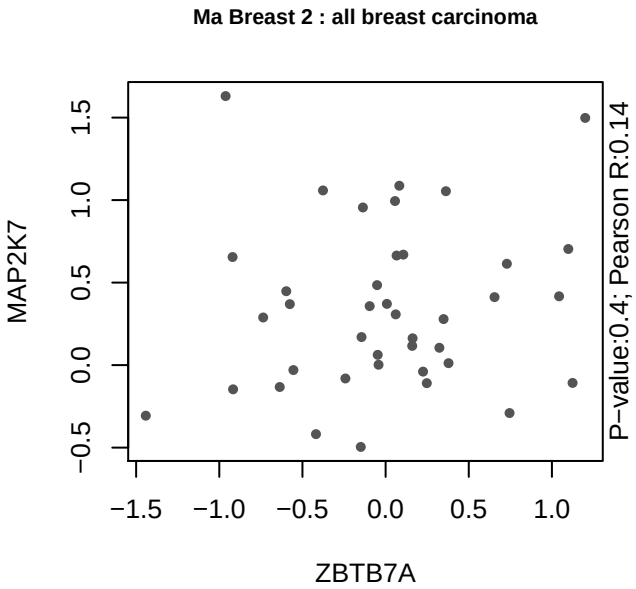

Ma Breast 2 : all breast carcinoma
ARHGEF12
BCL6
P−value:0.73; Pearson R:0.056

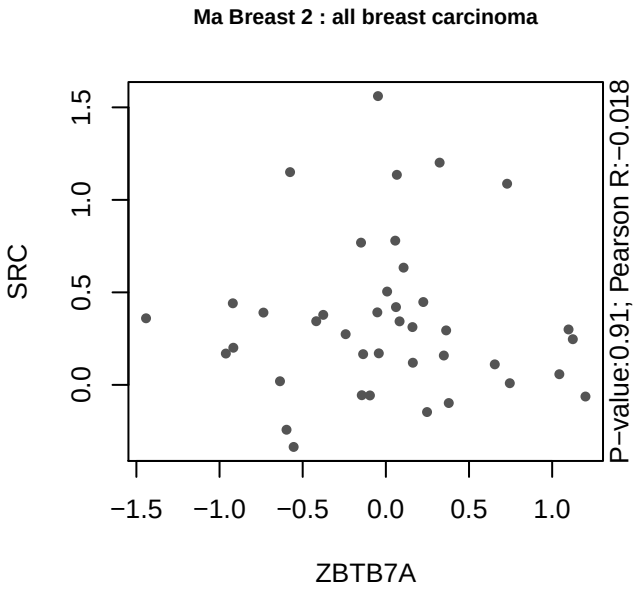

Ma Breast 2 : all breast carcinoma
SCRIB
ZBTB7A
P−value:0.52; Pearson R:0.11

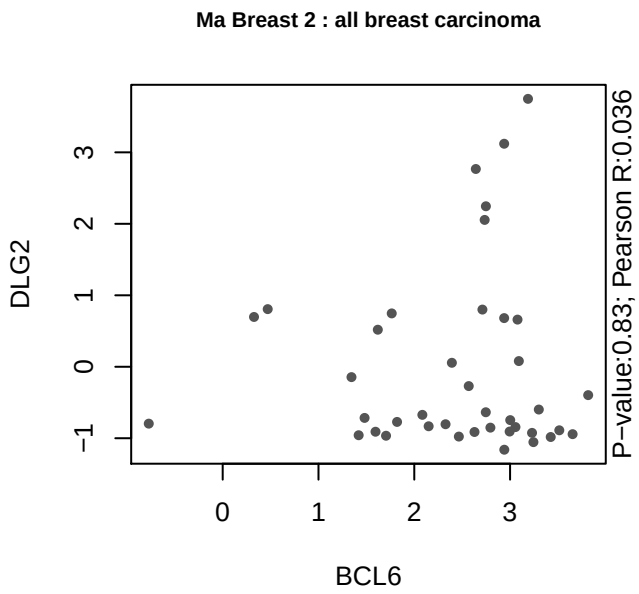

Ma Breast 2 : all breast carcinoma
ARHGEF12
ZBTB7A
P−value:0.68; Pearson R:0.066

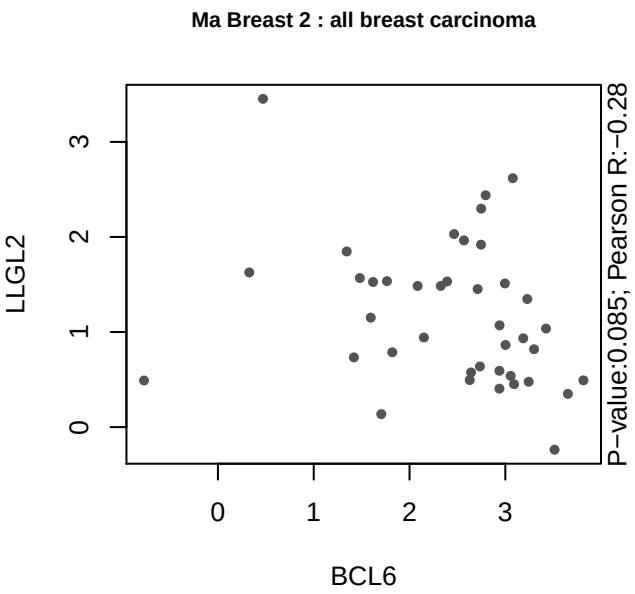

Ma Breast 2 : all breast carcinoma
MAP2K7
BCL6
P−value:0.065; Pearson R:−0.29

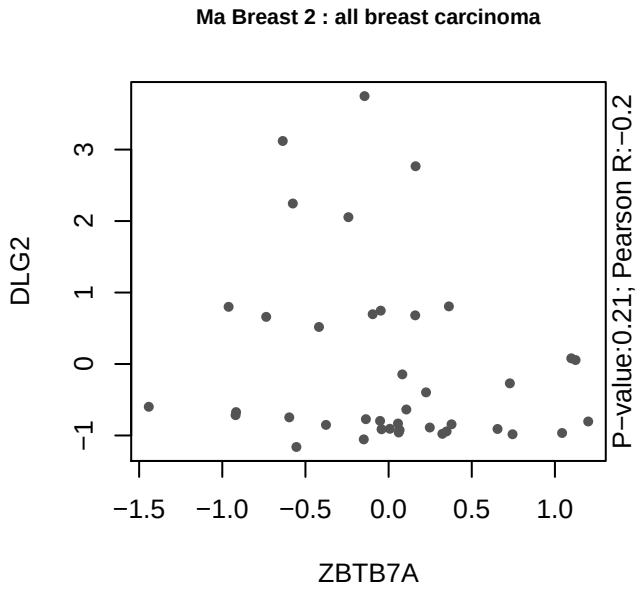

Ma Breast 2 : all breast carcinoma
SRC
BCL6
P−value:0.79; Pearson R:−0.043

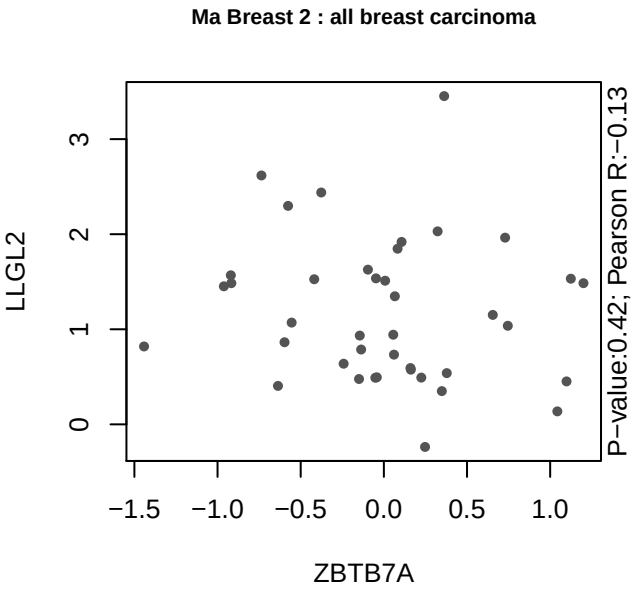

Ma Breast 2 : all breast carcinoma
MAP2K7
ZBTB7A
P−value:0.4; Pearson R:0.14

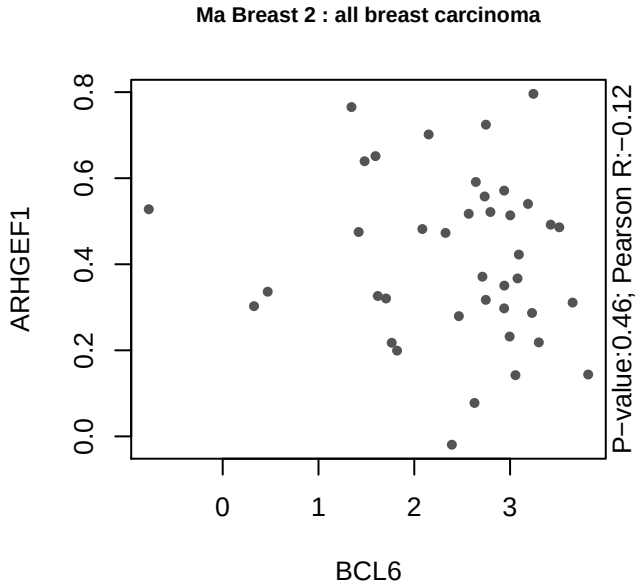

Ma Breast 2 : all breast carcinoma
SRC
ZBTB7A
P−value:0.91; Pearson R:−0.018

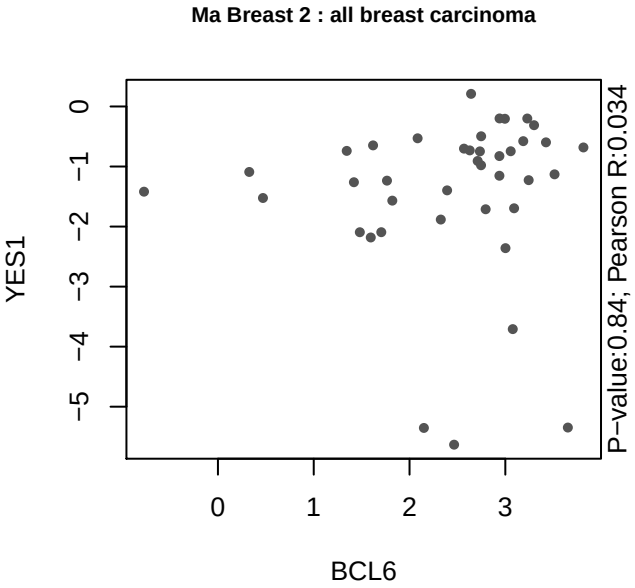

Ma Breast 2 : all breast carcinoma
DLG2
BCL6
P−value:0.83; Pearson R:0.036

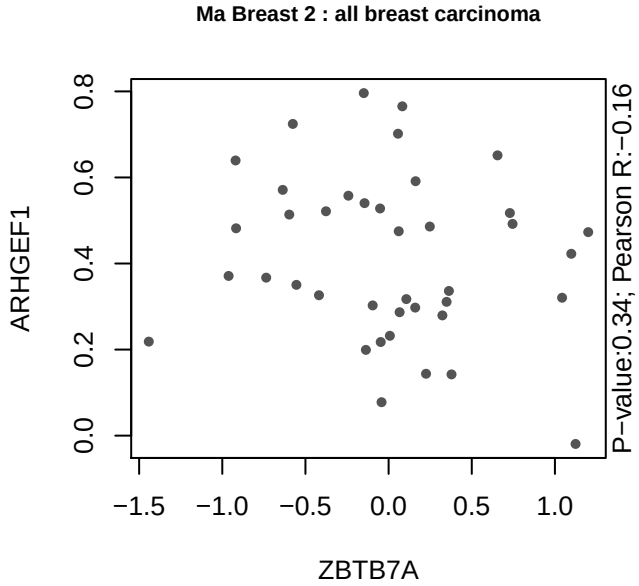

Ma Breast 2 : all breast carcinoma
LLGL2
BCL6
P−value:0.085; Pearson R:−0.28

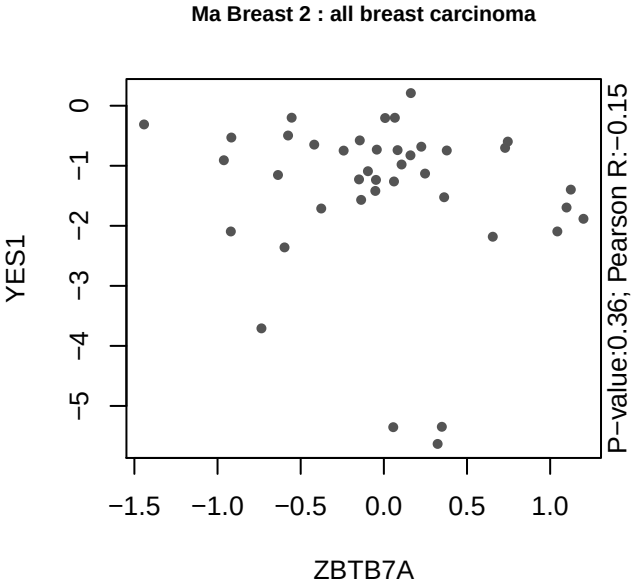

Ma Breast 2 : all breast carcinoma
DLG2
ZBTB7A
P−value:0.21; Pearson R:−0.2

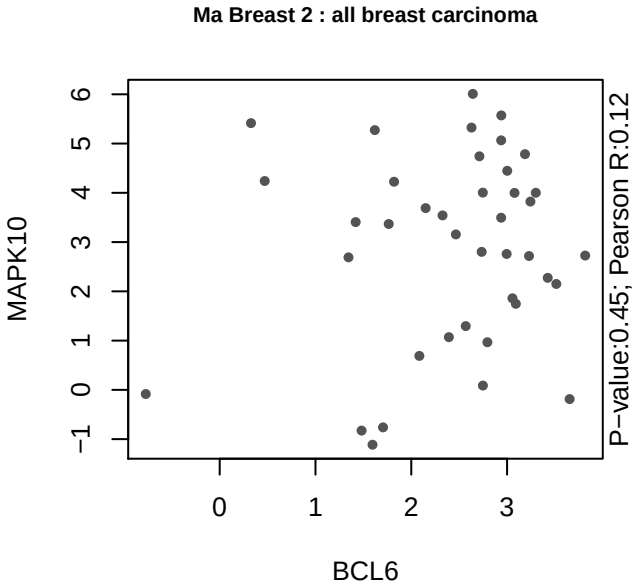

Ma Breast 2 : all breast carcinoma
LLGL2
ZBTB7A
P−value:0.42; Pearson R:−0.13

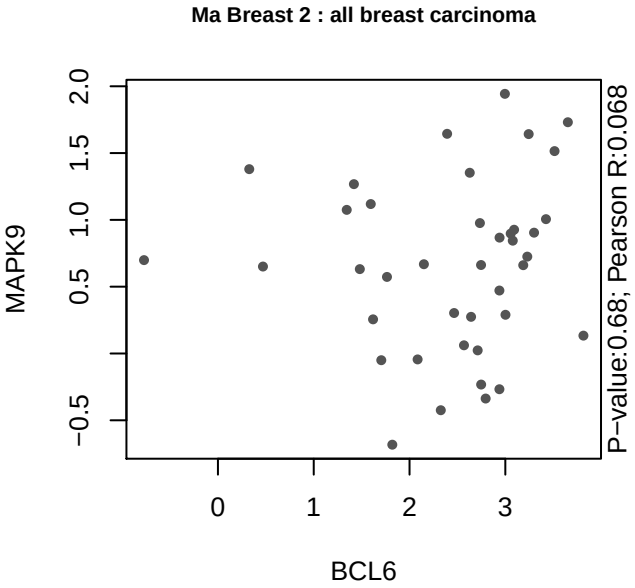

Ma Breast 2 : all breast carcinoma
ARHGEF1
BCL6
P−value:0.46; Pearson R:−0.12

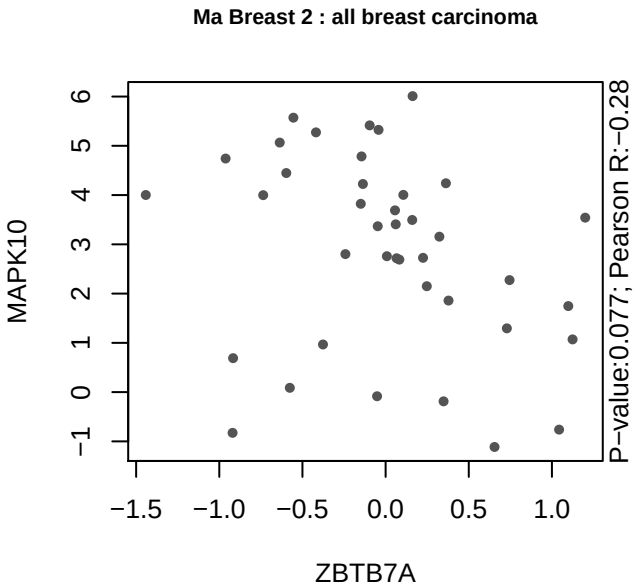

Ma Breast 2 : all breast carcinoma
YES1
BCL6
P−value:0.84; Pearson R:0.034

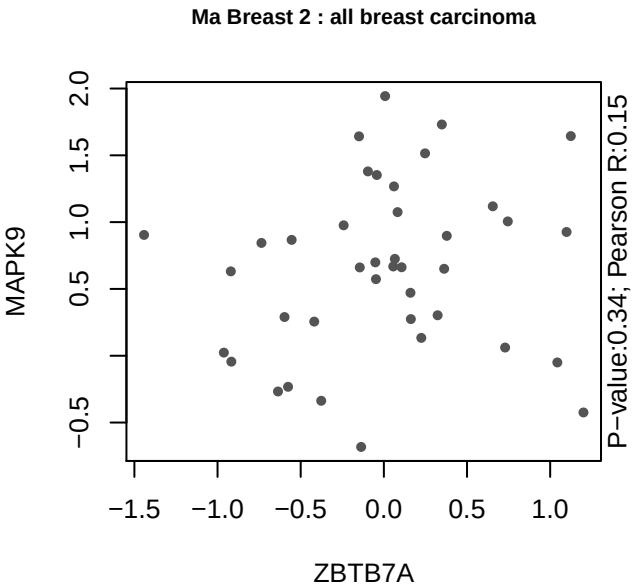

Ma Breast 2 : all breast carcinoma
ARHGEF1
ZBTB7A
P−value:0.34; Pearson R:−0.16

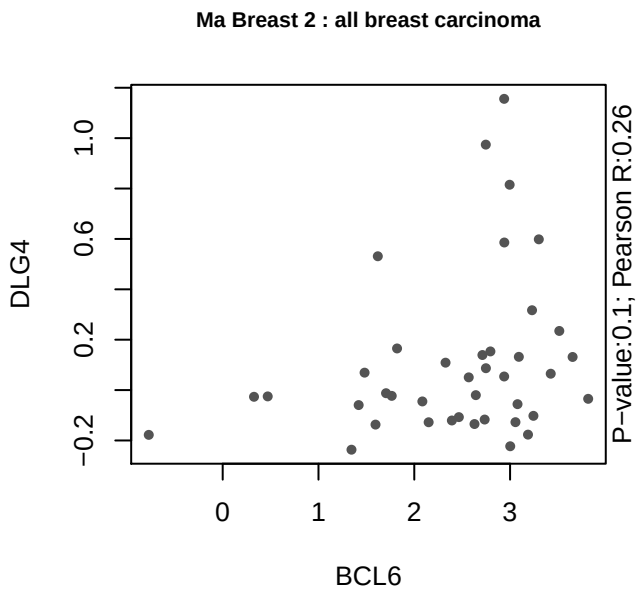

Ma Breast 2 : all breast carcinoma
YES1
ZBTB7A
P−value:0.36; Pearson R:−0.15

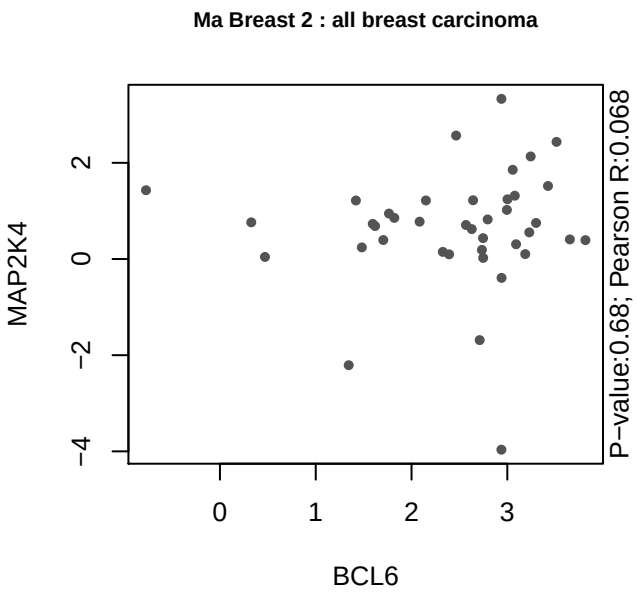

Ma Breast 2 : all breast carcinoma
MAPK10
BCL6
P−value:0.45; Pearson R:0.12

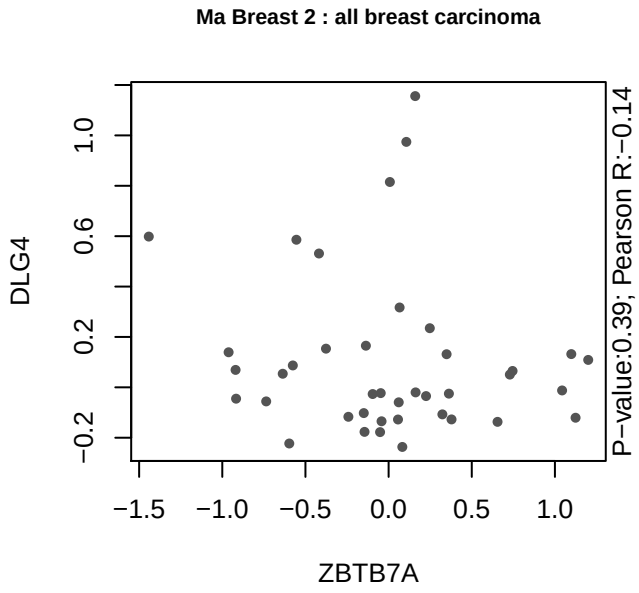

Ma Breast 2 : all breast carcinoma
MAPK9
BCL6
P−value:0.68; Pearson R:0.068

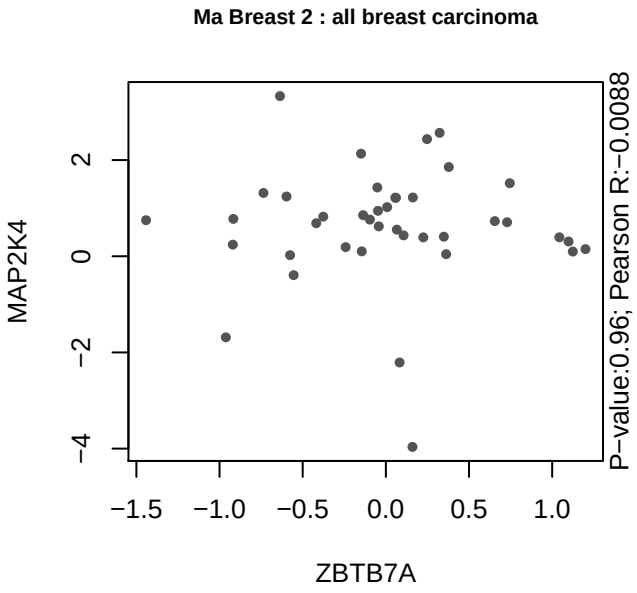

Ma Breast 2 : all breast carcinoma
MAPK10
ZBTB7A
P−value:0.077; Pearson R:−0.28

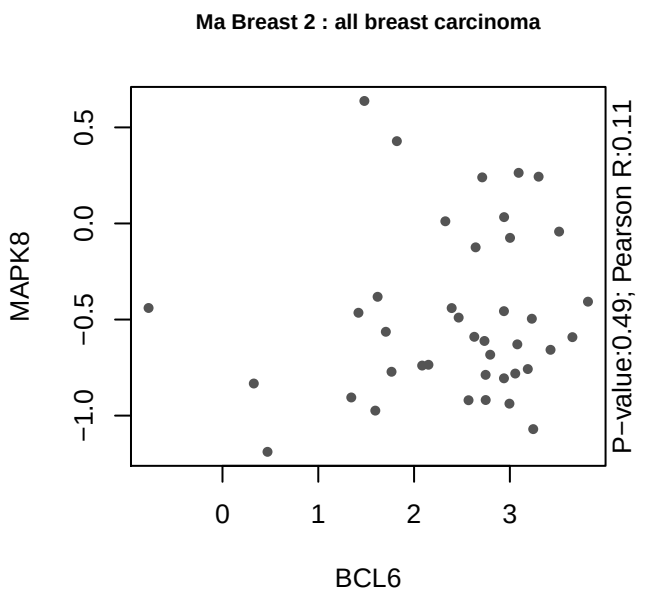

Ma Breast 2 : all breast carcinoma
MAPK9
ZBTB7A
P−value:0.34; Pearson R:0.15

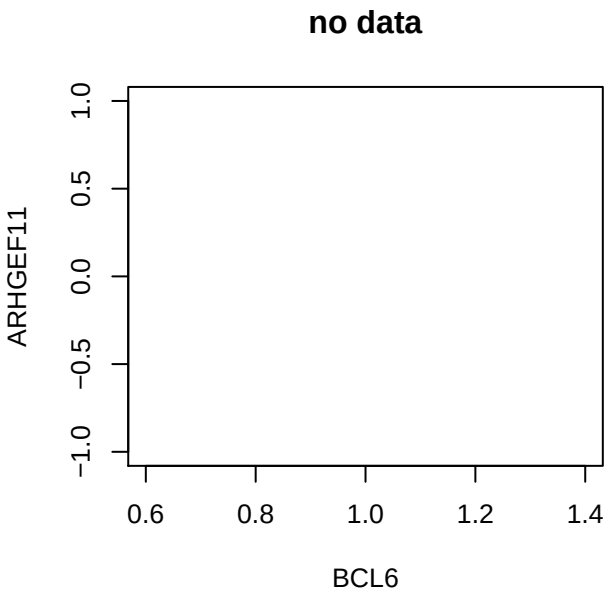

Ma Breast 2 : all breast carcinoma
DLG4
BCL6
P−value:0.1; Pearson R:0.26

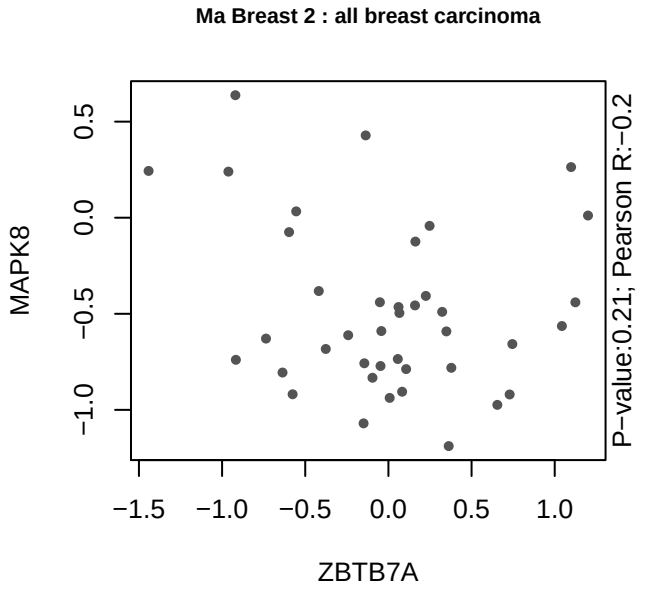

Ma Breast 2 : all breast carcinoma
MAP2K4
BCL6
P−value:0.68; Pearson R:0.068

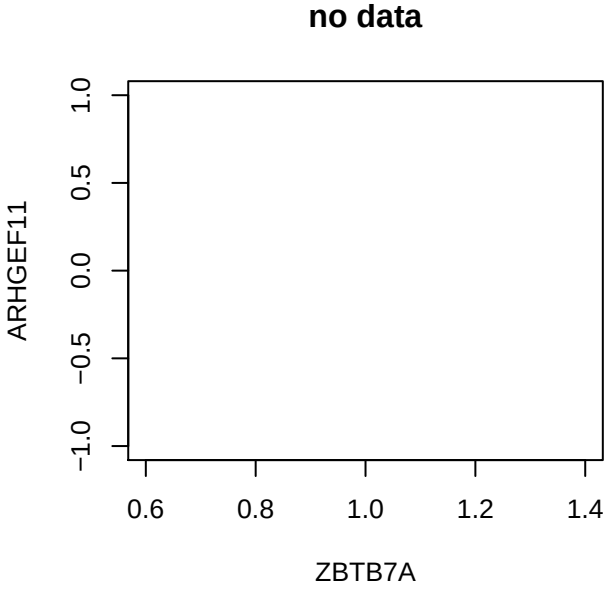

Ma Breast 2 : all breast carcinoma
DLG4
ZBTB7A
P−value:0.39; Pearson R:−0.14

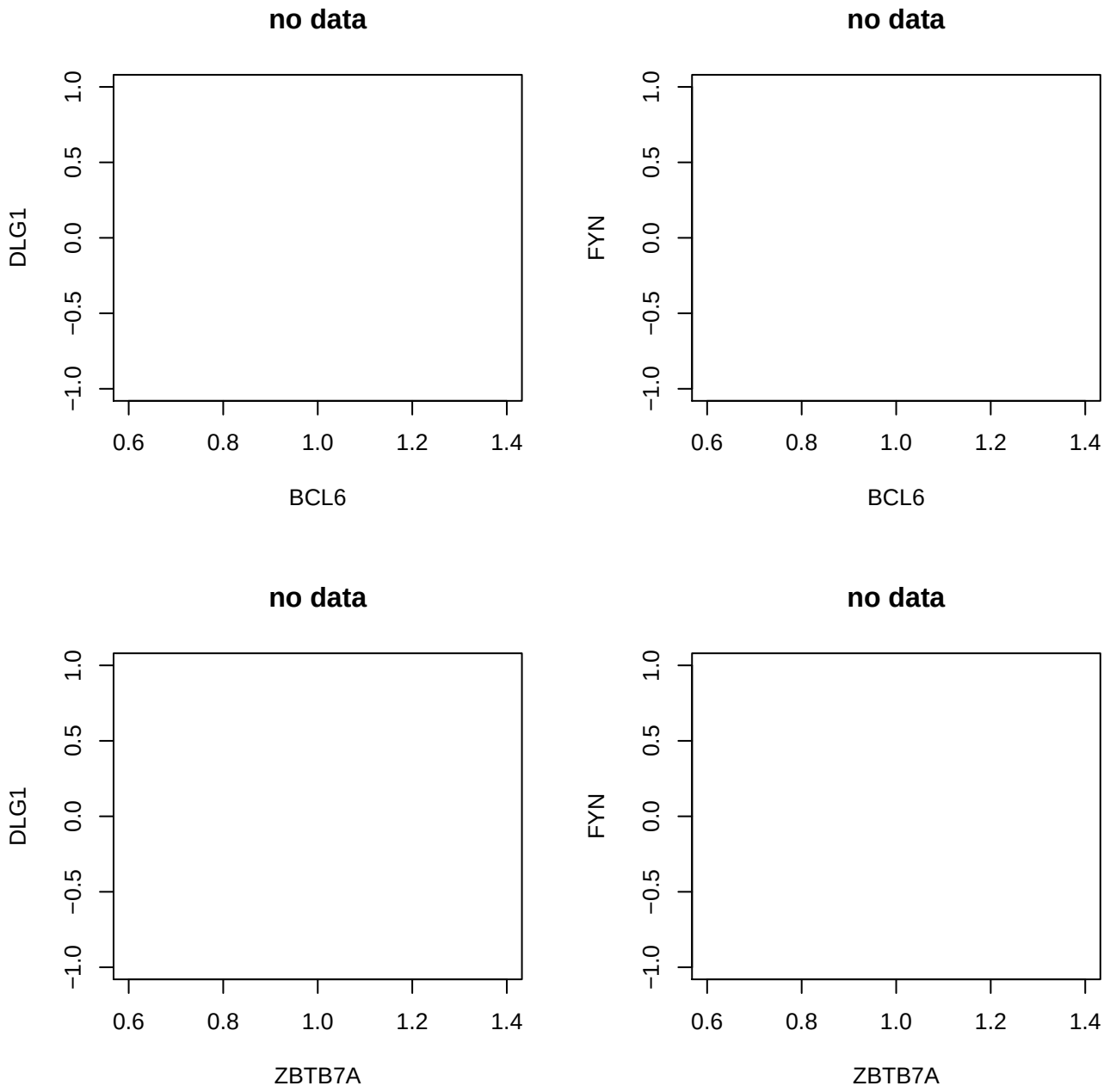

Ma Breast 2 : all breast carcinoma
MAP2K4
ZBTB7A
P−value:0.96; Pearson R:−0.0088

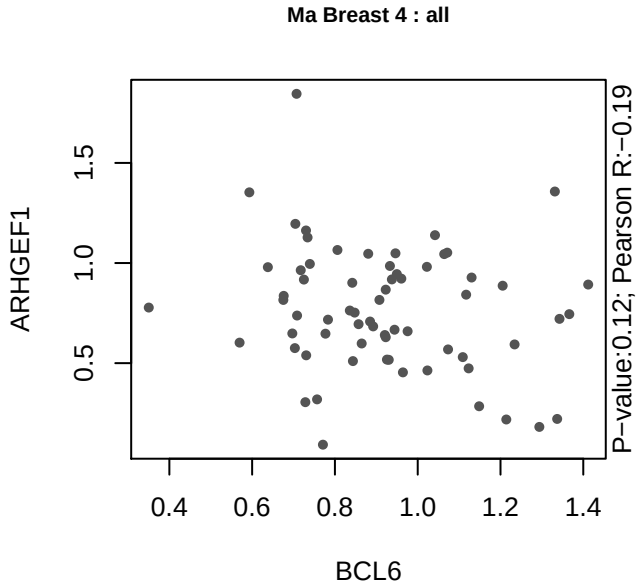

Ma Breast 2 : all breast carcinoma
MAPK8
BCL6
P−value:0.49; Pearson R:0.11

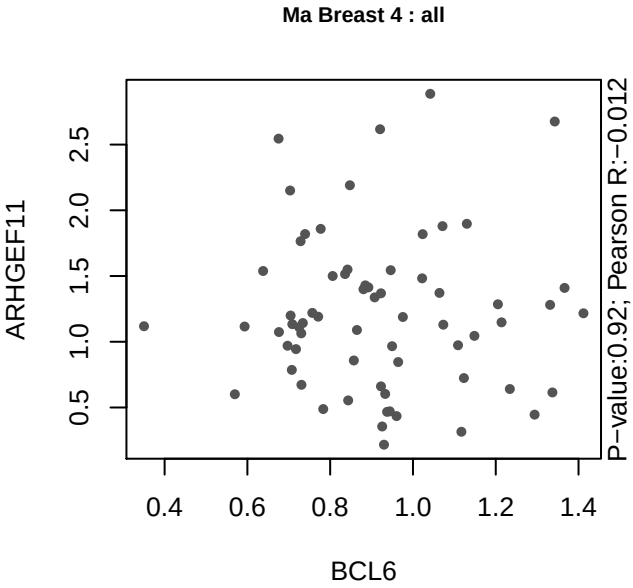

no data
ARHGEF11
BCL6

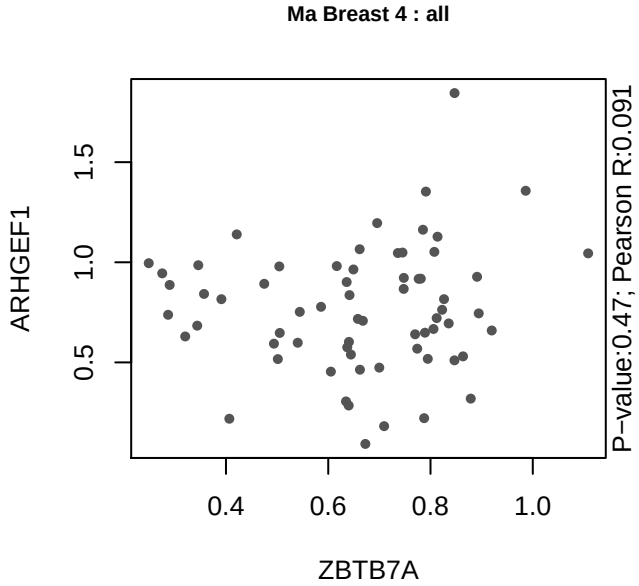

Ma Breast 2 : all breast carcinoma
MAPK8
ZBTB7A
P−value:0.21; Pearson R:−0.2

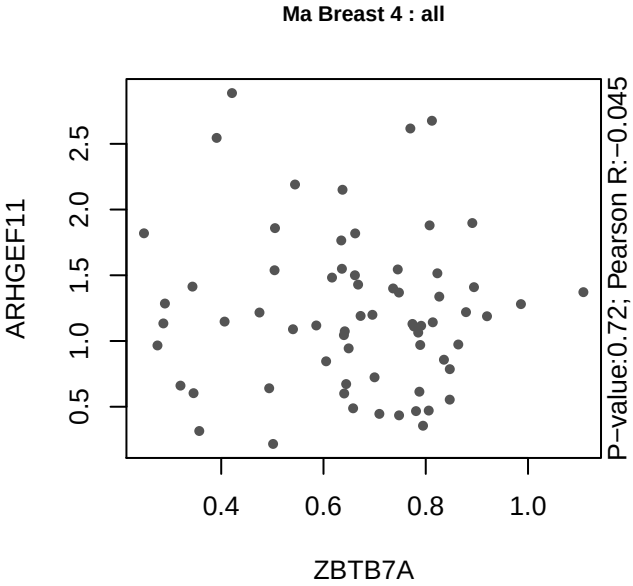

no data
ARHGEF11
ZBTB7A

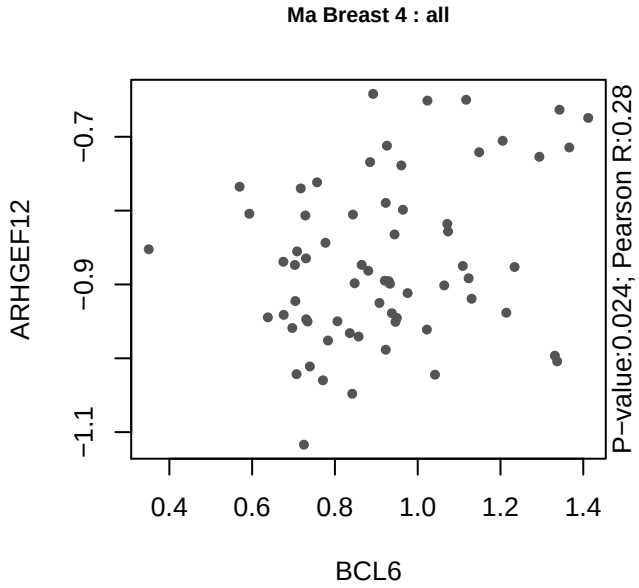

no data
DLG1
BCL6
no data
FYN
BCL6
no data
DLG1
ZBTB7A
no data
FYN
ZBTB7A
1.0
0.5
0.0
−0.5
−1.0
0.6
0.8
1.0
1.2
1.4

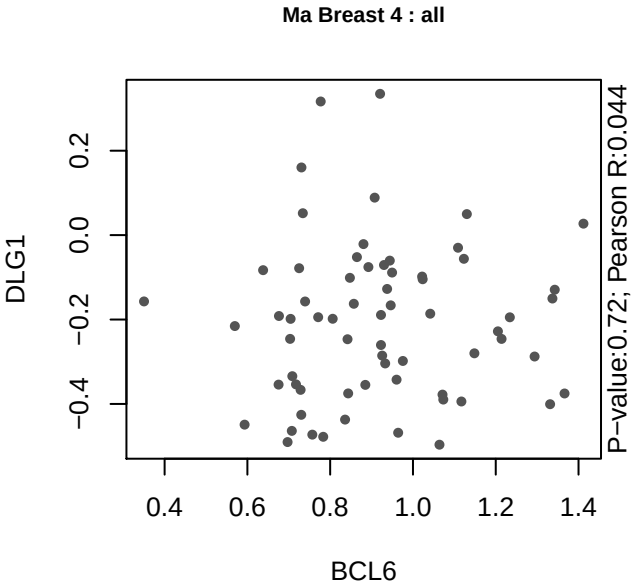

Ma Breast 4 : all
ARHGEF1
BCL6
P−value:0.12; Pearson R:−0.19

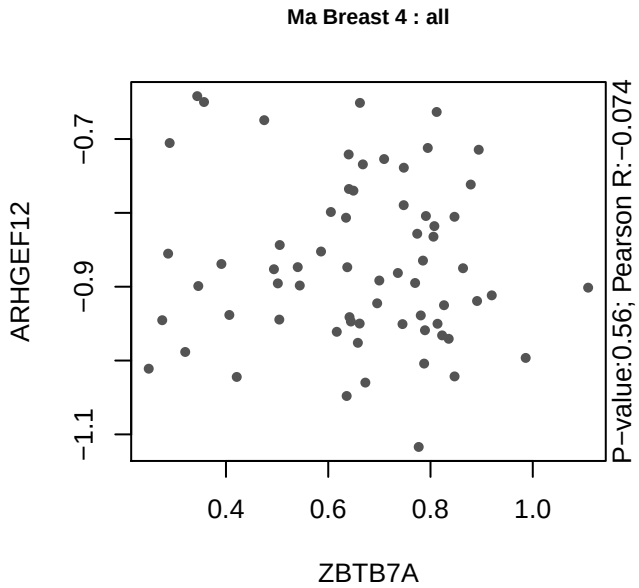

Ma Breast 4 : all
ARHGEF11
BCL6
P−value:0.92; Pearson R:−0.012

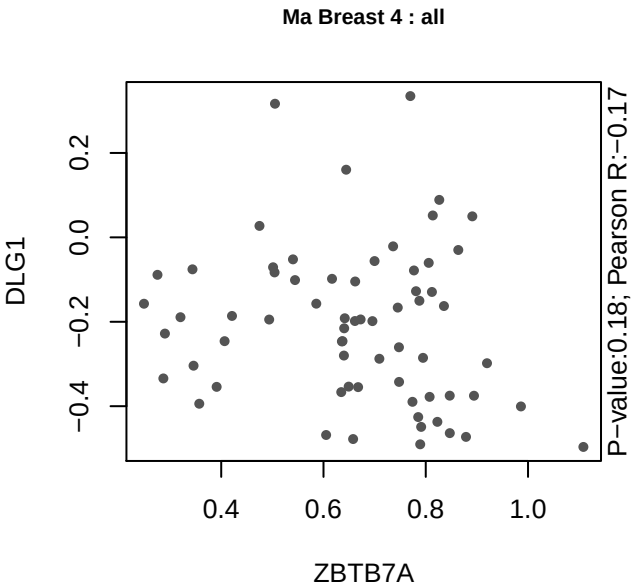

Ma Breast 4 : all
ARHGEF1
ZBTB7A
P−value:0.47; Pearson R:0.091

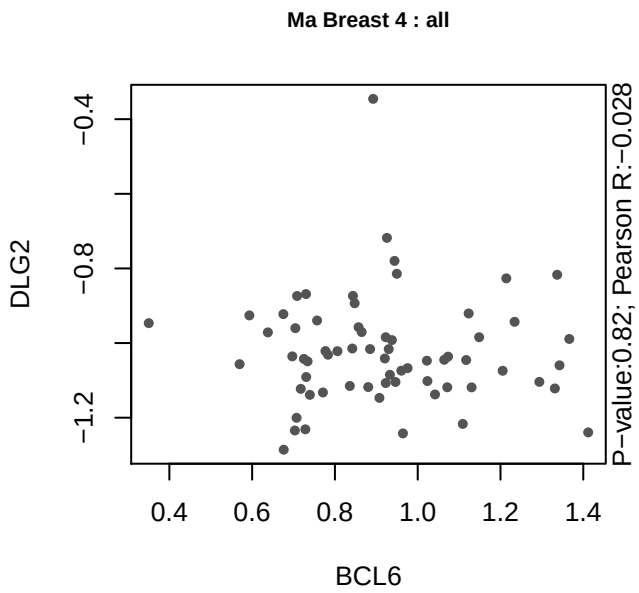

Ma Breast 4 : all
ARHGEF11
ZBTB7A
P−value:0.72; Pearson R:−0.045

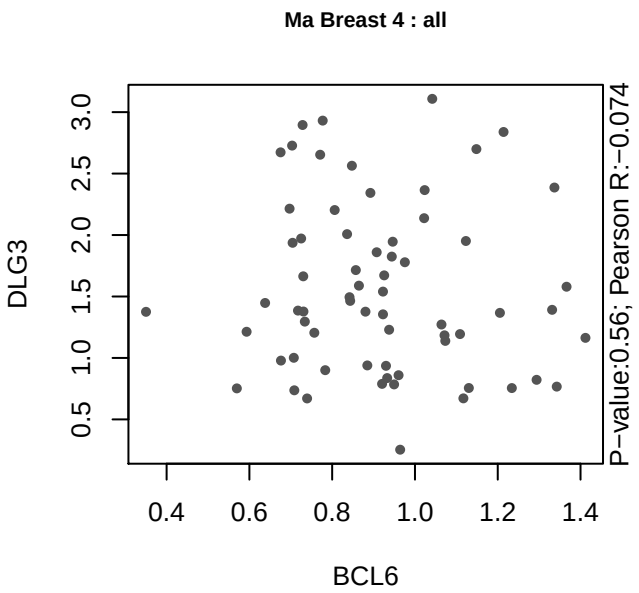

Ma Breast 4 : all
ARHGEF12
BCL6
P−value:0.024; Pearson R:0.28

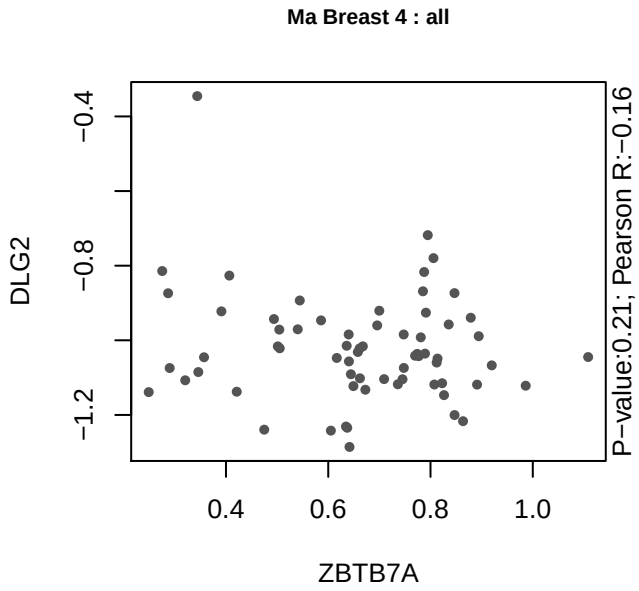

Ma Breast 4 : all
DLG1
BCL6
P−value:0.72; Pearson R:0.044

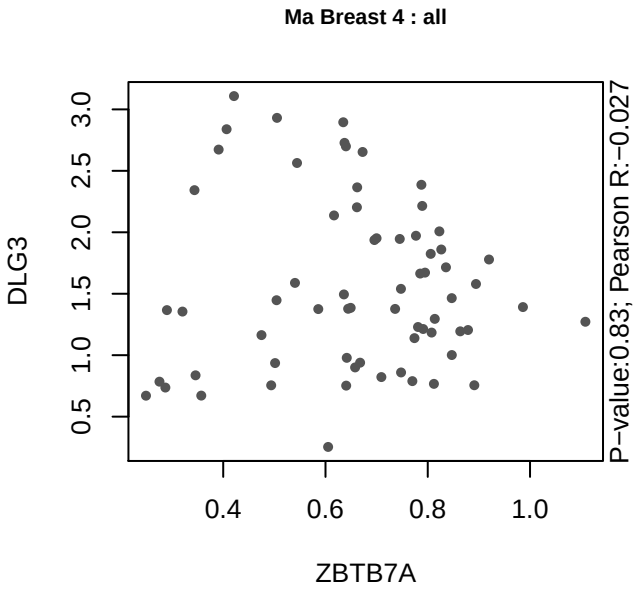

Ma Breast 4 : all
ARHGEF12
ZBTB7A
P−value:0.56; Pearson R:−0.074

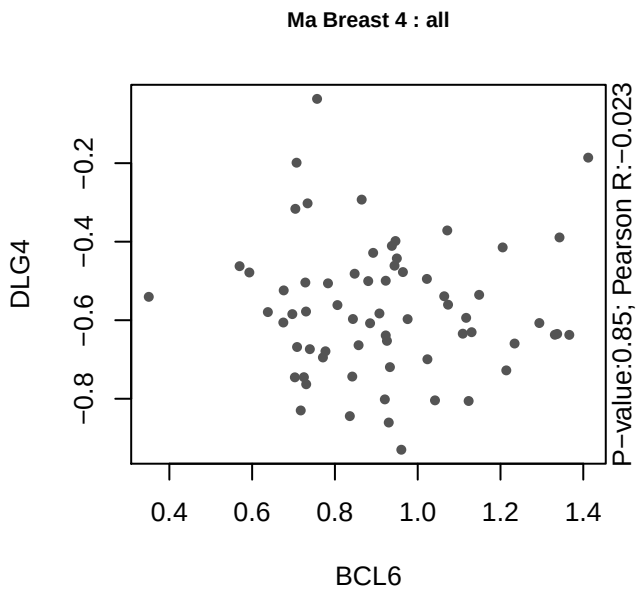

Ma Breast 4 : all
DLG1
ZBTB7A
P−value:0.18; Pearson R:−0.17

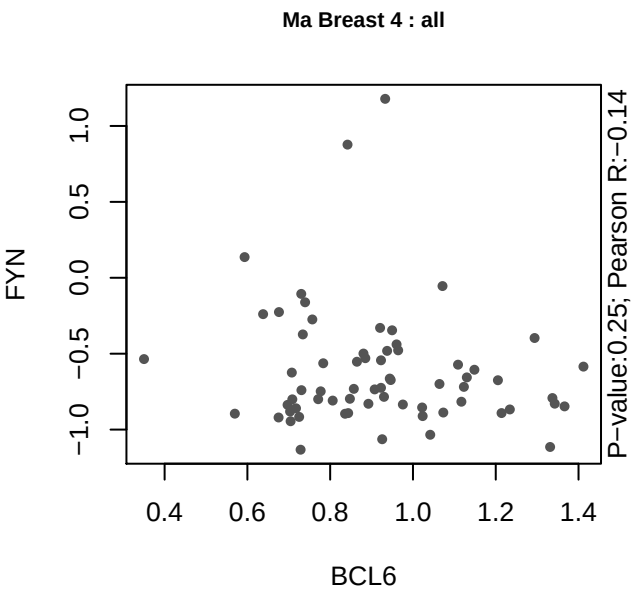

Ma Breast 4 : all
DLG2
BCL6
P−value:0.82; Pearson R:−0.028

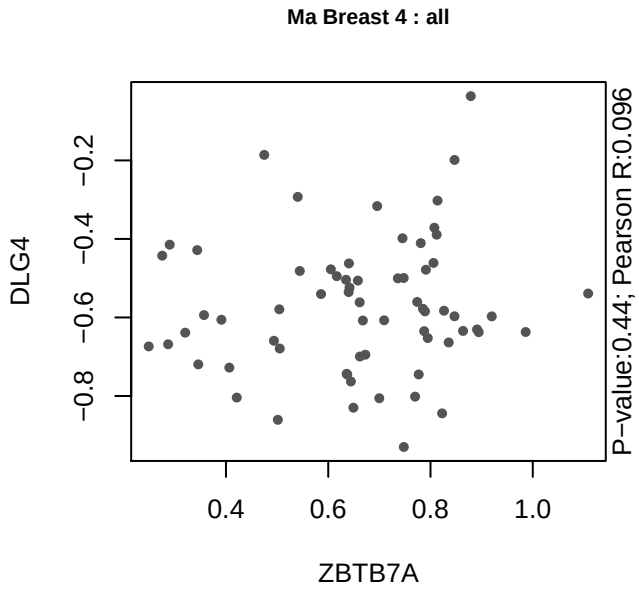

Ma Breast 4 : all
DLG3
BCL6
P−value:0.56; Pearson R:−0.074

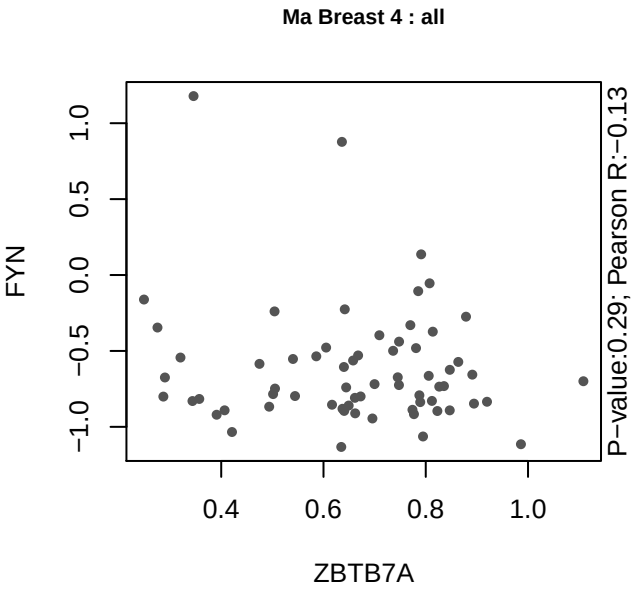

Ma Breast 4 : all
DLG2
ZBTB7A
P−value:0.21; Pearson R:−0.16

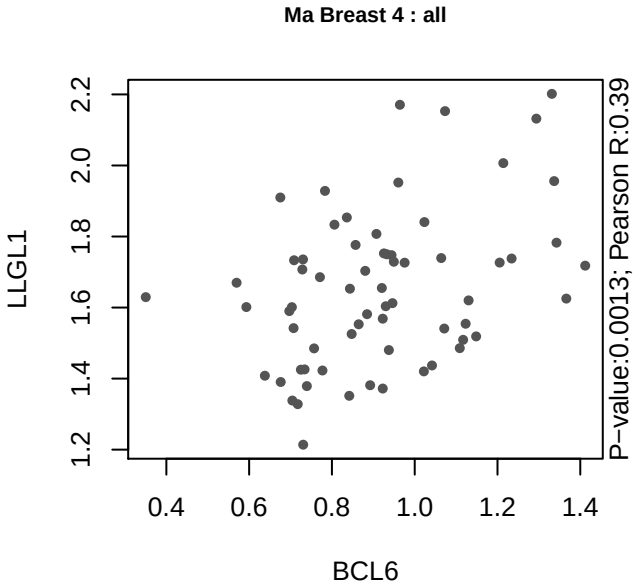

Ma Breast 4 : all
DLG3
ZBTB7A
P−value:0.83; Pearson R:−0.027

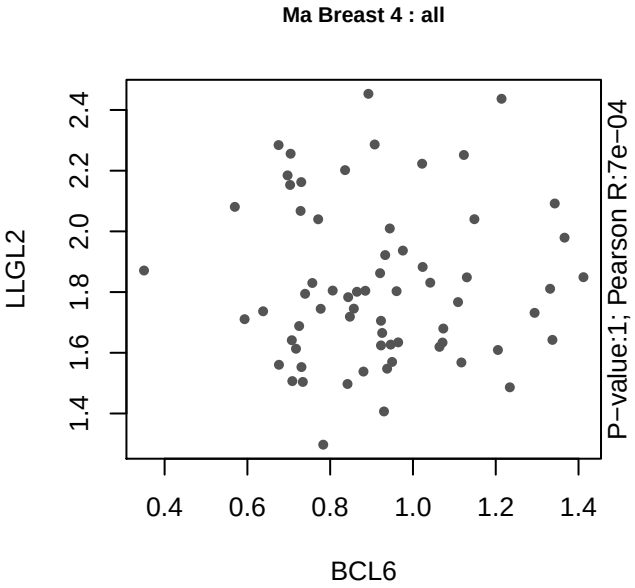

Ma Breast 4 : all
DLG4
BCL6
P−value:0.85; Pearson R:−0.023

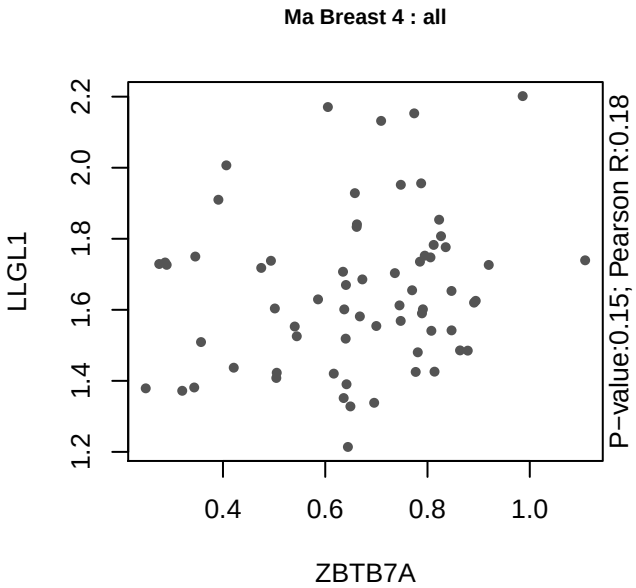

Ma Breast 4 : all
FYN
BCL6
P−value:0.25; Pearson R:−0.14

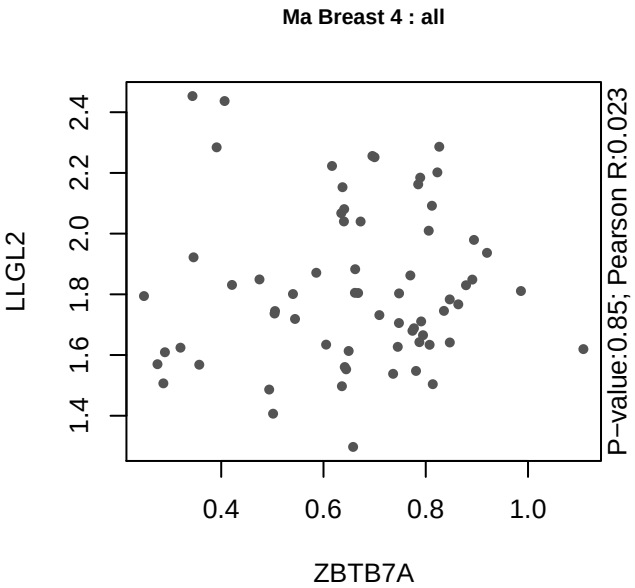

Ma Breast 4 : all
DLG4
ZBTB7A
P−value:0.44; Pearson R:0.096

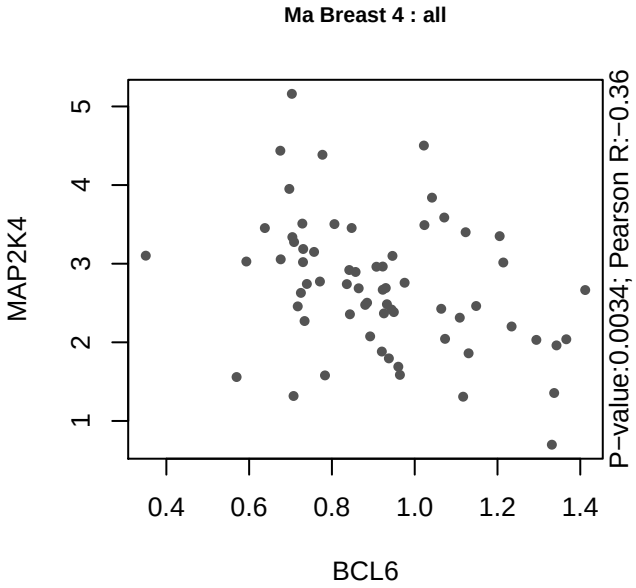

Ma Breast 4 : all
FYN
ZBTB7A
P−value:0.29; Pearson R:−0.13

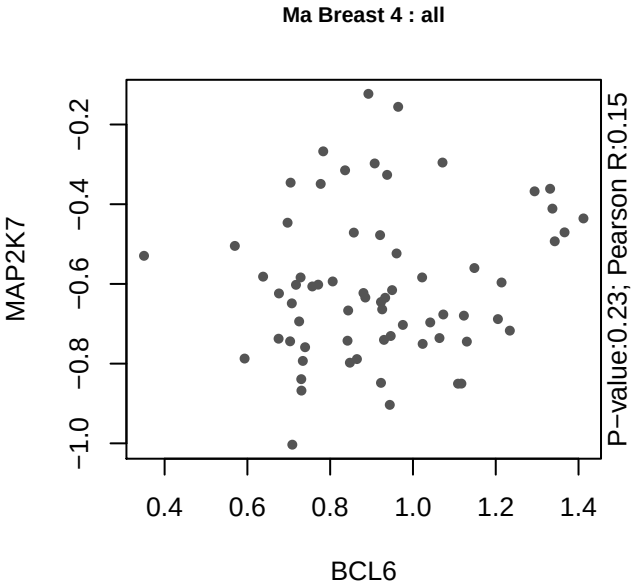

Ma Breast 4 : all
LLGL1
BCL6
P−value:0.0013; Pearson R:0.39

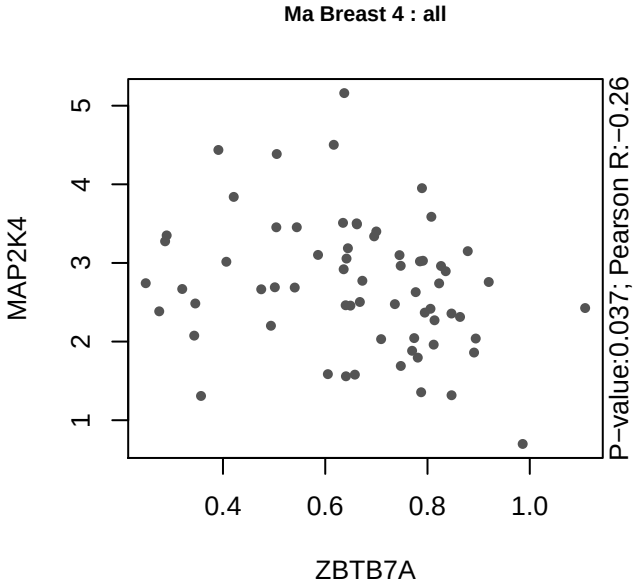

Ma Breast 4 : all
LLGL2
BCL6
P−value:1; Pearson R:7e−04

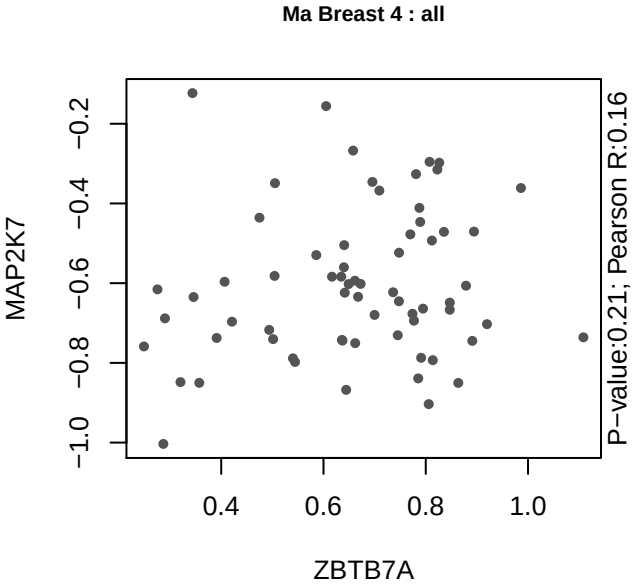

Ma Breast 4 : all
LLGL1
ZBTB7A
P−value:0.15; Pearson R:0.18

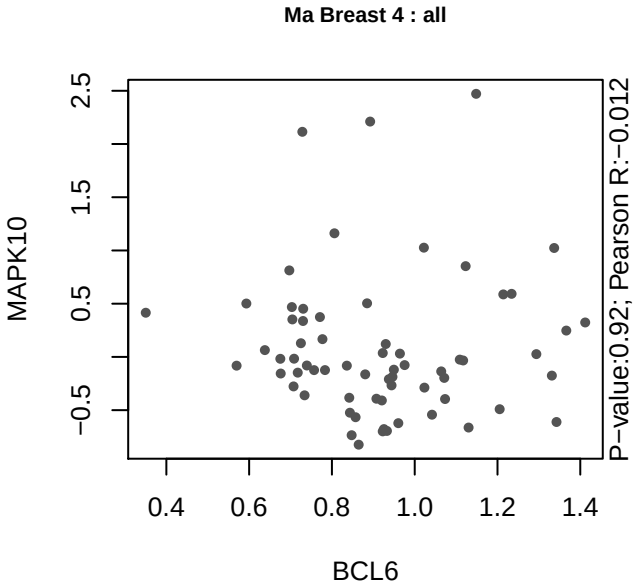

Ma Breast 4 : all
LLGL2
ZBTB7A
P−value:0.85; Pearson R:0.023

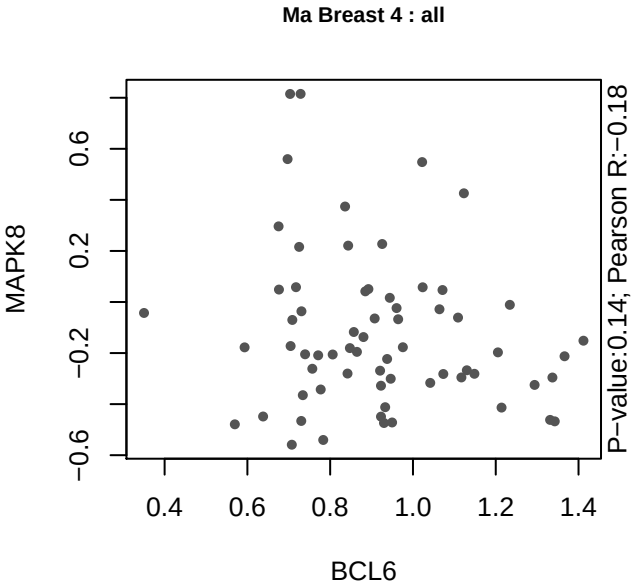

Ma Breast 4 : all
MAP2K4
BCL6
P−value:0.0034; Pearson R:−0.36

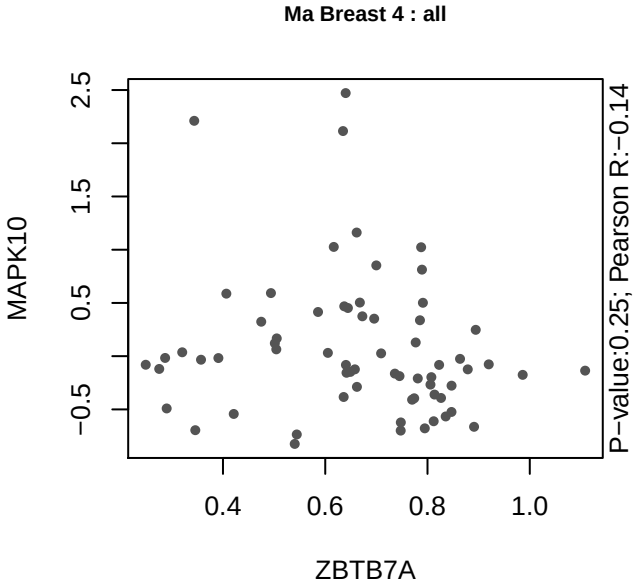

Ma Breast 4 : all
MAP2K7
BCL6
P−value:0.23; Pearson R:0.15

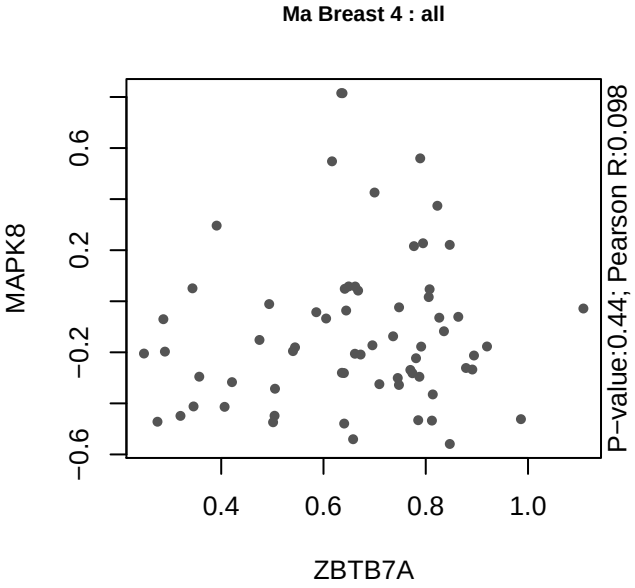

Ma Breast 4 : all
MAP2K4
ZBTB7A
P−value:0.037; Pearson R:−0.26

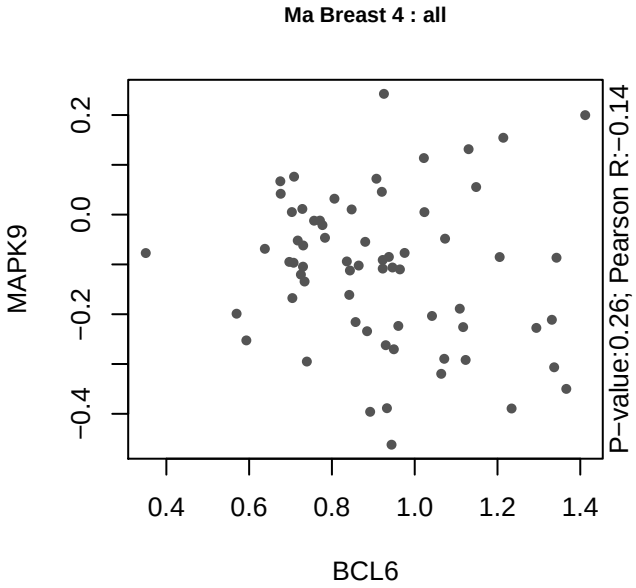

Ma Breast 4 : all
MAP2K7
ZBTB7A
P−value:0.21; Pearson R:0.16

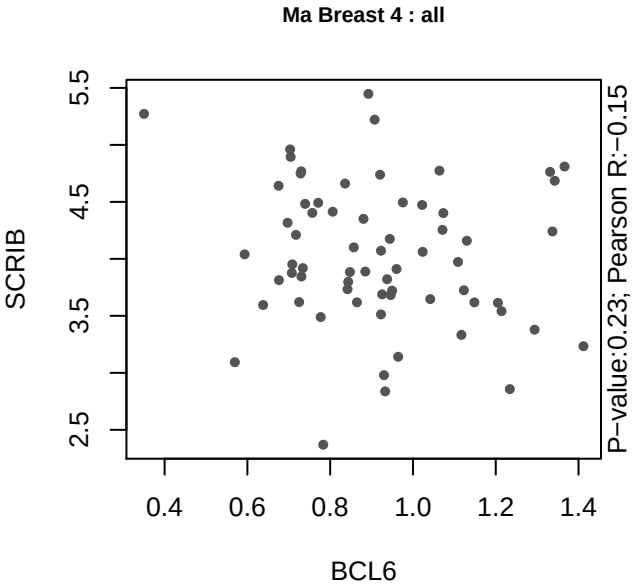

Ma Breast 4 : all
MAPK10
BCL6
P−value:0.92; Pearson R:−0.012
−0.5
0.5
1.5
2.5
0.4
0.6
0.8
1.0
1.2
1.4

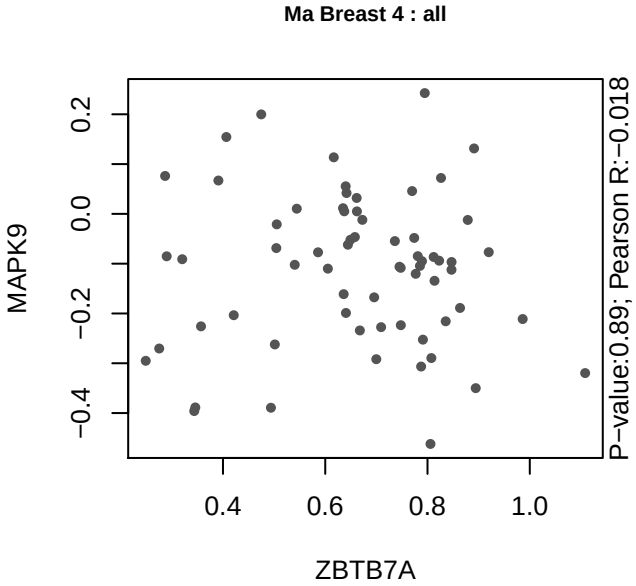

Ma Breast 4 : all
MAPK8
BCL6
P−value:0.14; Pearson R:−0.18
−0.6
−0.2
0.2
0.6
0.4
0.6
0.8
1.0
1.2
1.4

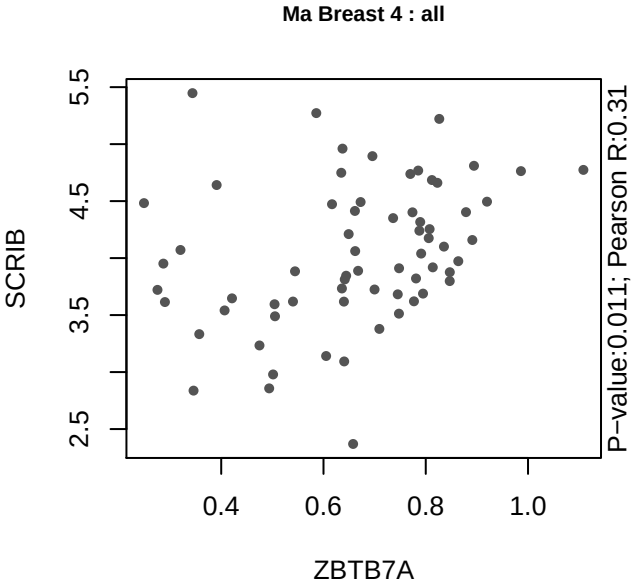

Ma Breast 4 : all
MAPK10
ZBTB7A
P−value:0.25; Pearson R:−0.14
−0.5
0.5
1.5
2.5
0.4
0.6
0.8
1.0

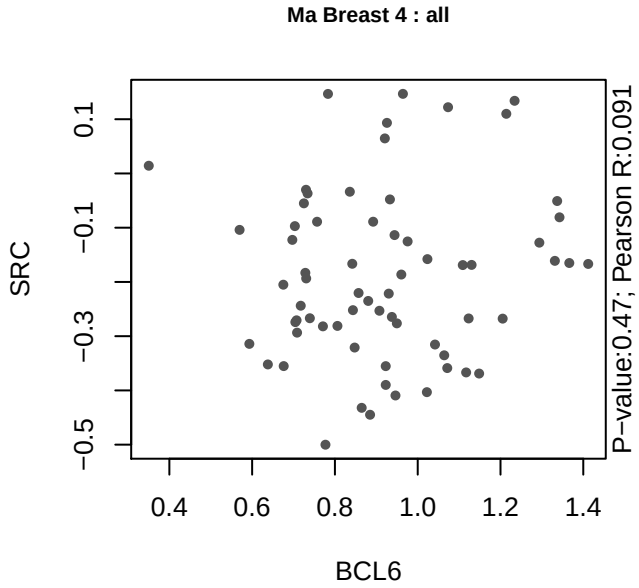

Ma Breast 4 : all
MAPK8
ZBTB7A
P−value:0.44; Pearson R:0.098
−0.6
−0.2
0.2
0.6
0.4
0.6
0.8
1.0

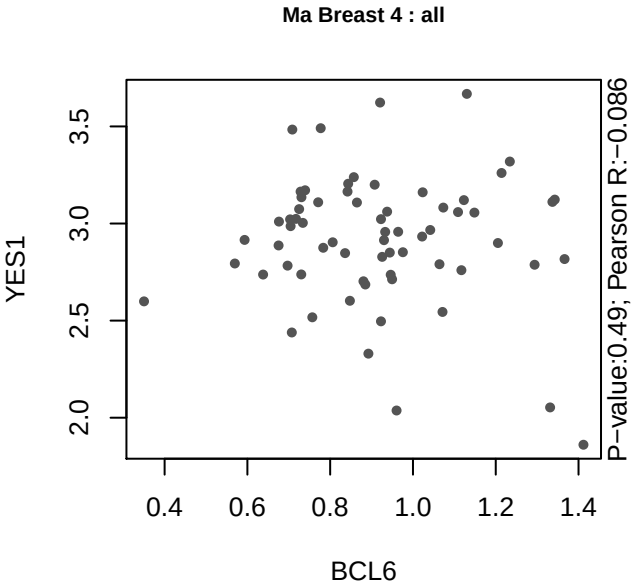

Ma Breast 4 : all
MAPK9
BCL6
P−value:0.26; Pearson R:−0.14

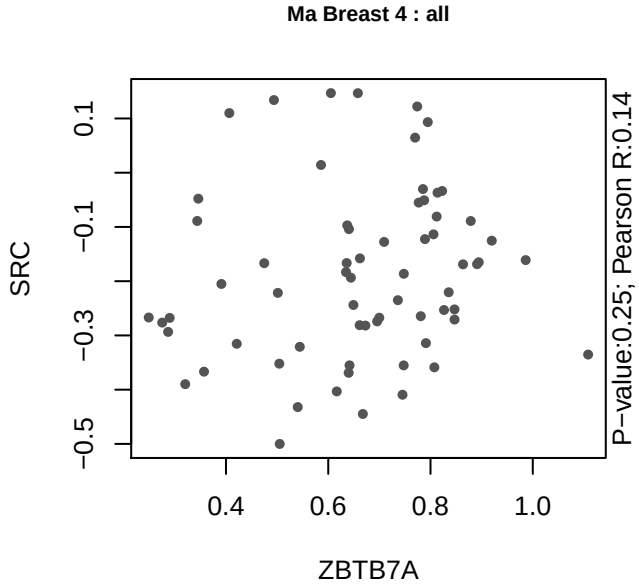

Ma Breast 4 : all
SCRIB
BCL6
P−value:0.23; Pearson R:−0.15

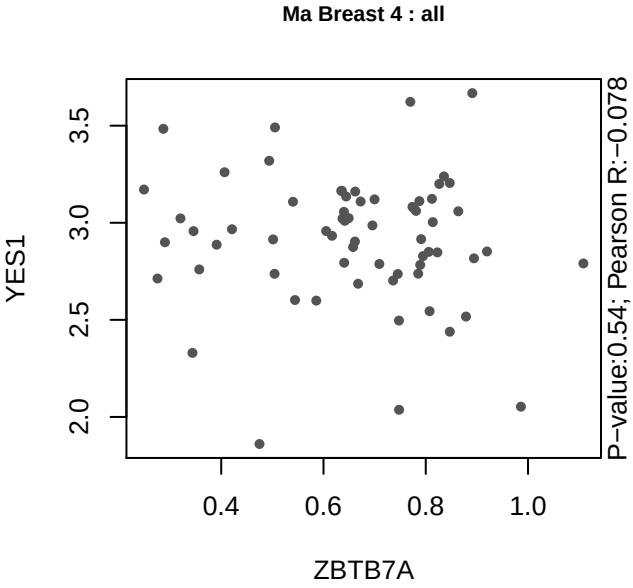

Ma Breast 4 : all
MAPK9
ZBTB7A
P−value:0.89; Pearson R:−0.018

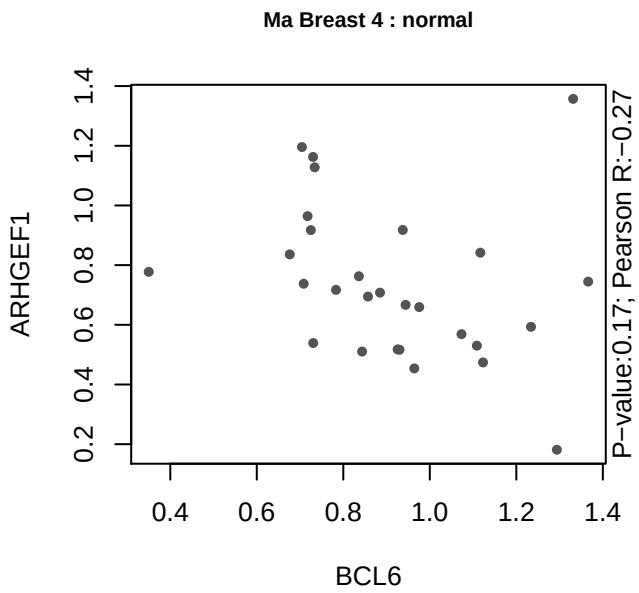

Ma Breast 4 : all
SCRIB
ZBTB7A
P−value:0.011; Pearson R:0.31

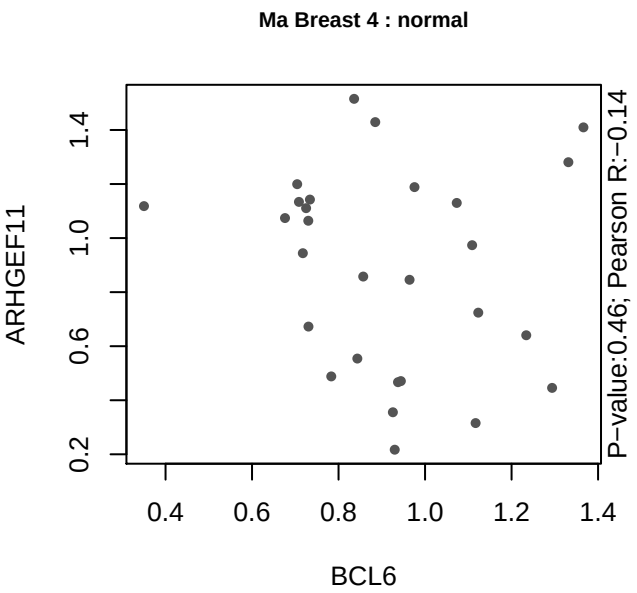

Ma Breast 4 : all
SRC
BCL6
P−value:0.47; Pearson R:0.091
−0.5
−0.3
−0.1
0.1
0.4
0.6
0.8
1.0
1.2
1.4

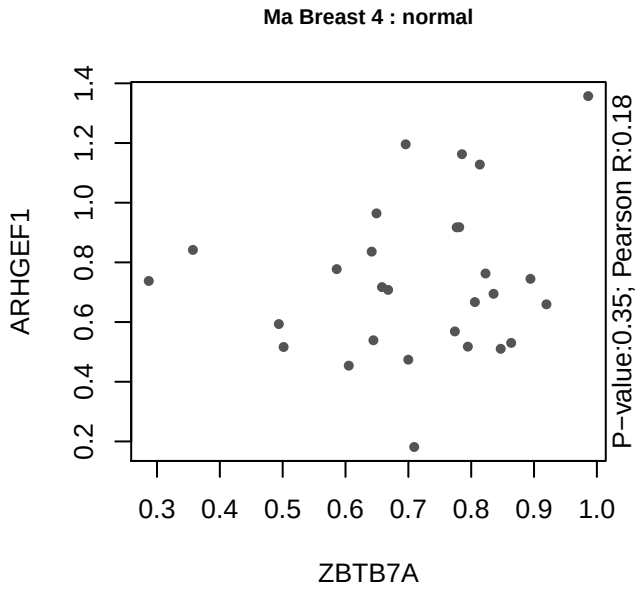

Ma Breast 4 : all
YES1
BCL6
P−value:0.49; Pearson R:−0.086
2.0
2.5
3.0
3.5
0.4
0.6
0.8
1.0
1.2
1.4

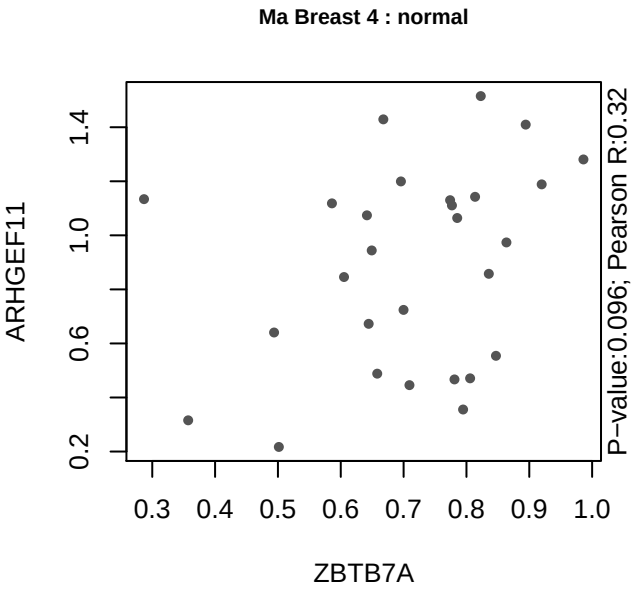

Ma Breast 4 : all
SRC
ZBTB7A
P−value:0.25; Pearson R:0.14
−0.5
−0.3
−0.1
0.1
0.4
0.6
0.8
1.0

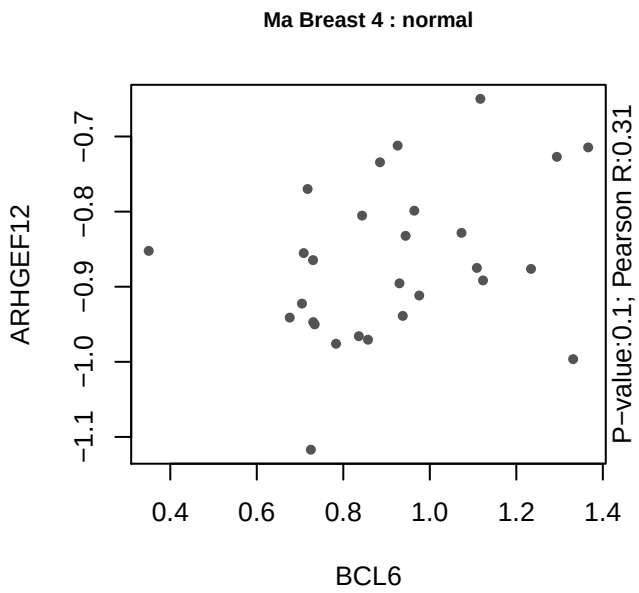

Ma Breast 4 : all
YES1
ZBTB7A
P−value:0.54; Pearson R:−0.078
2.0
2.5
3.0
3.5
0.4
0.6
0.8
1.0

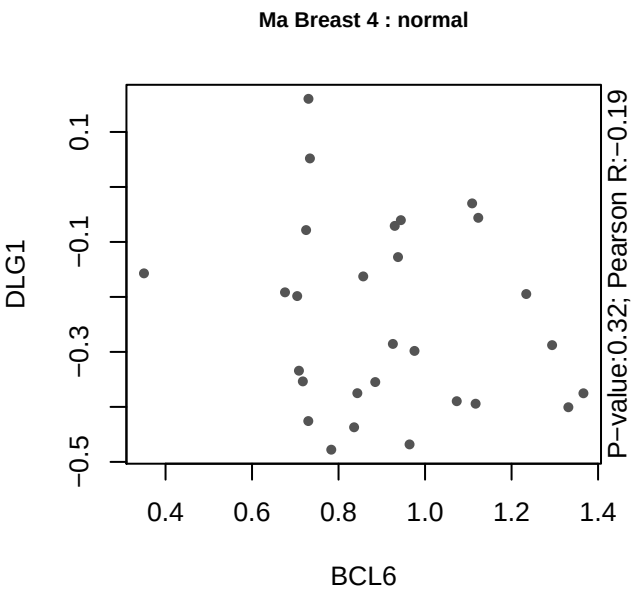

Ma Breast 4 : normal
ARHGEF1
BCL6
P−value:0.17; Pearson R:−0.27

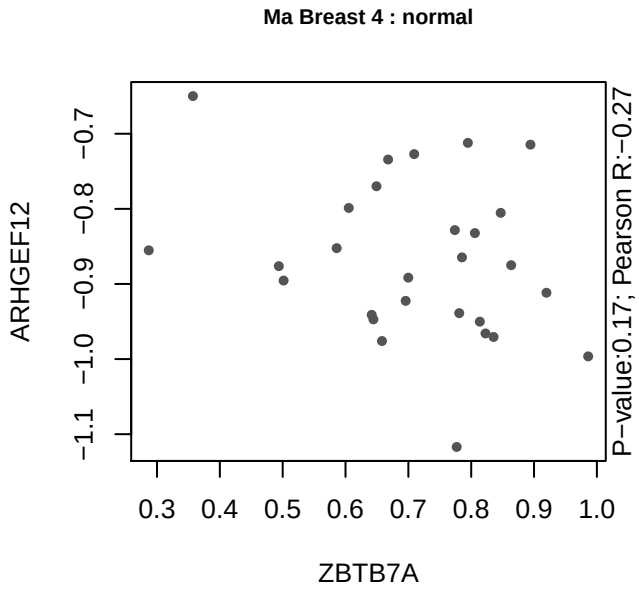

Ma Breast 4 : normal
ARHGEF11
BCL6
P−value:0.46; Pearson R:−0.14

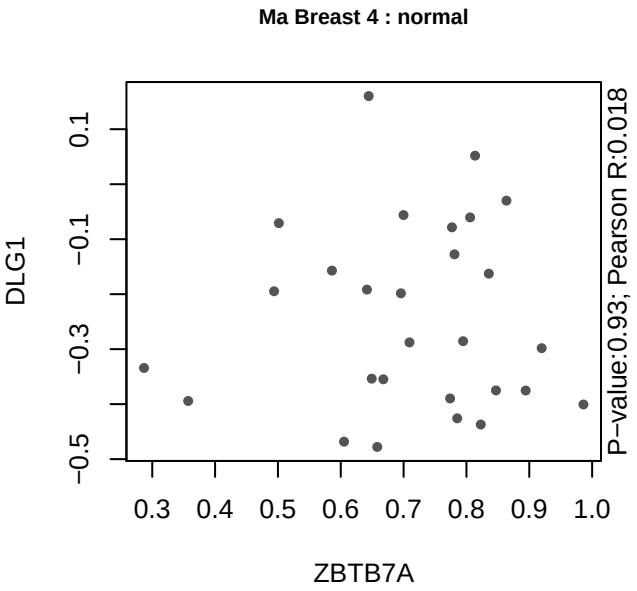

Ma Breast 4 : normal
ARHGEF1
ZBTB7A
P−value:0.35; Pearson R:0.18

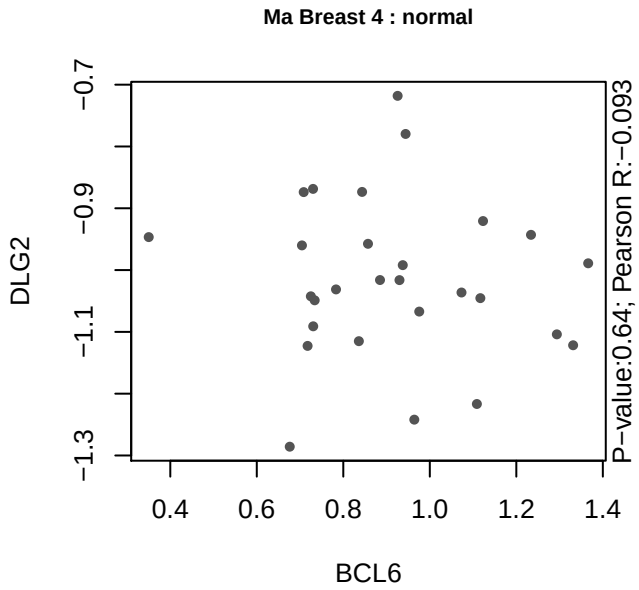

Ma Breast 4 : normal
ARHGEF11
ZBTB7A
P−value:0.096; Pearson R:0.32

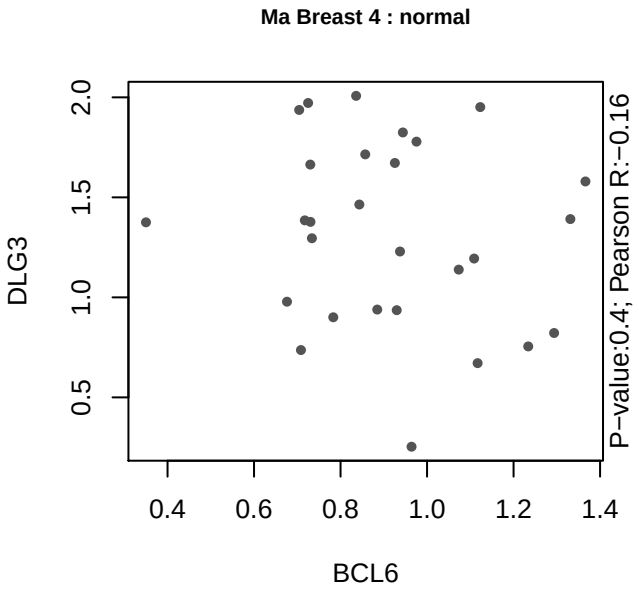

Ma Breast 4 : normal
ARHGEF12
BCL6
P−value:0.1; Pearson R:0.31

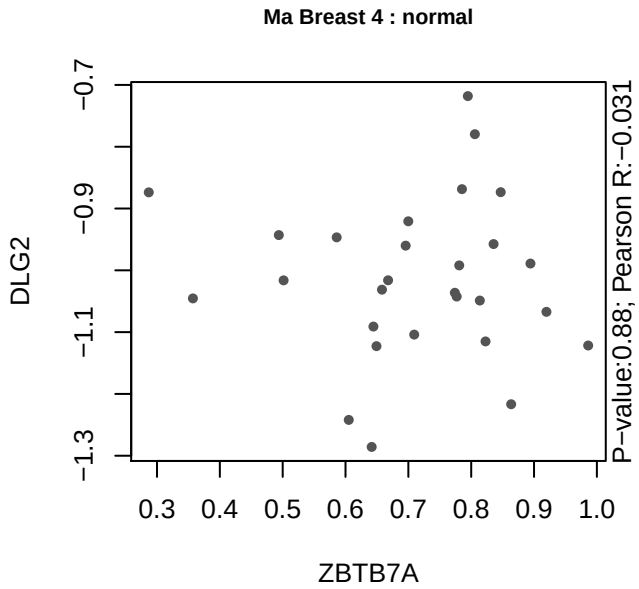

Ma Breast 4 : normal
DLG1
BCL6
P−value:0.32; Pearson R:−0.19

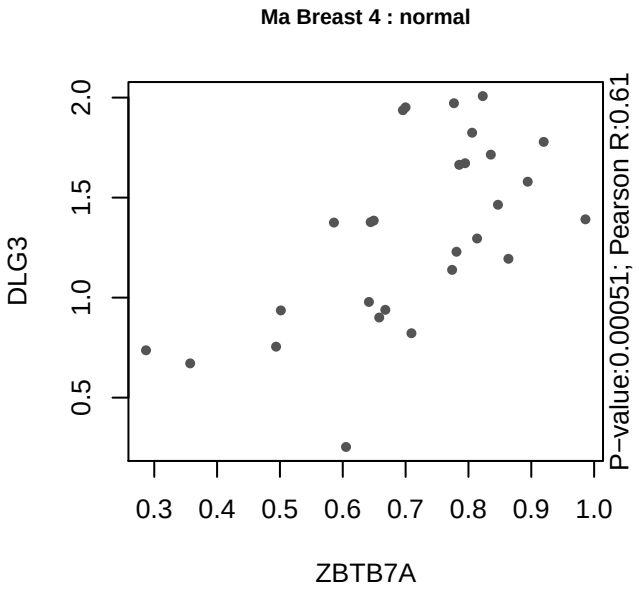

Ma Breast 4 : normal
ARHGEF12
ZBTB7A
P−value:0.17; Pearson R:−0.27

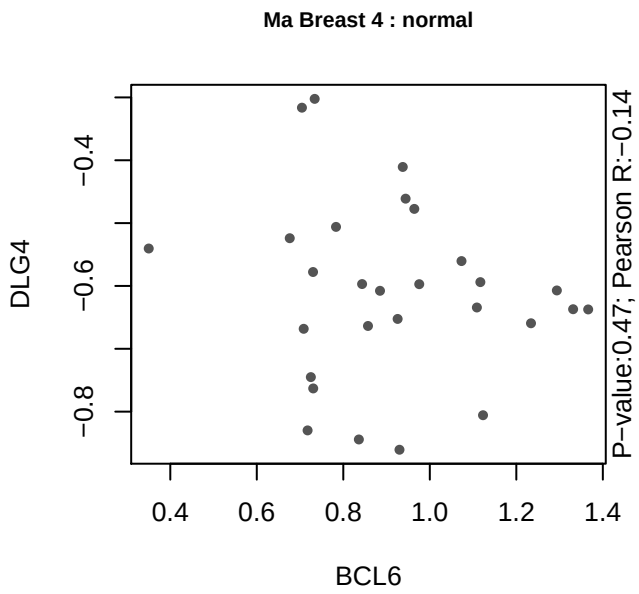

Ma Breast 4 : normal
DLG1
ZBTB7A
P−value:0.93; Pearson R:0.018

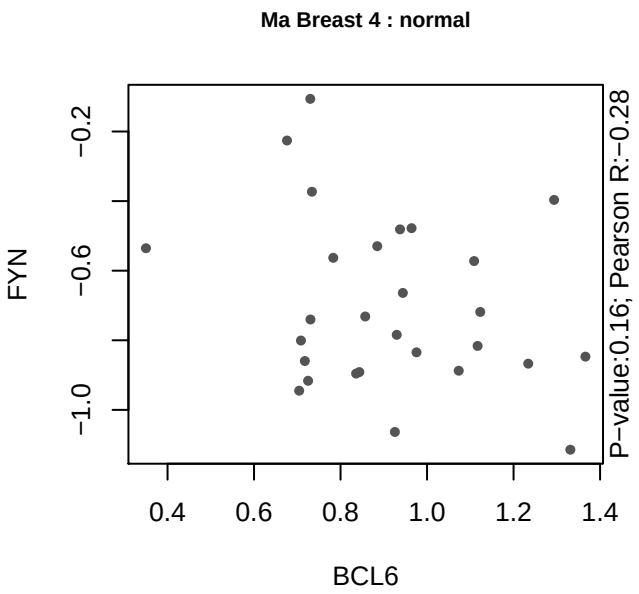

Ma Breast 4 : normal
DLG2
BCL6
P−value:0.64; Pearson R:−0.093

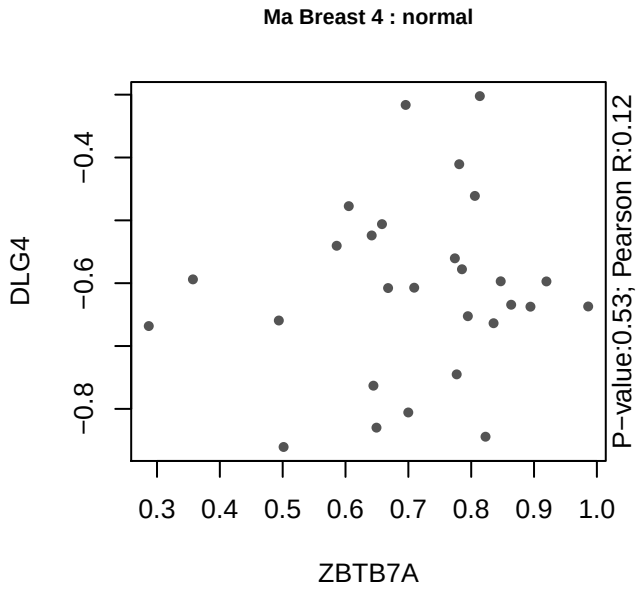

Ma Breast 4 : normal
DLG3
BCL6
P−value:0.4; Pearson R:−0.16

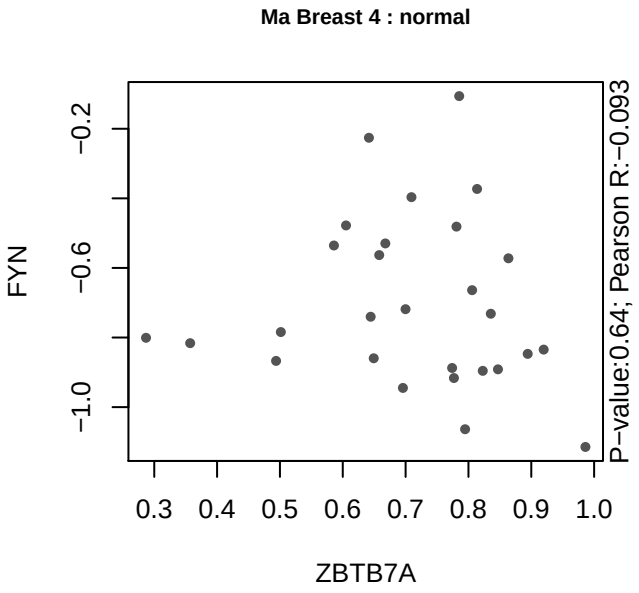

Ma Breast 4 : normal
DLG2
ZBTB7A
P−value:0.88; Pearson R:−0.031

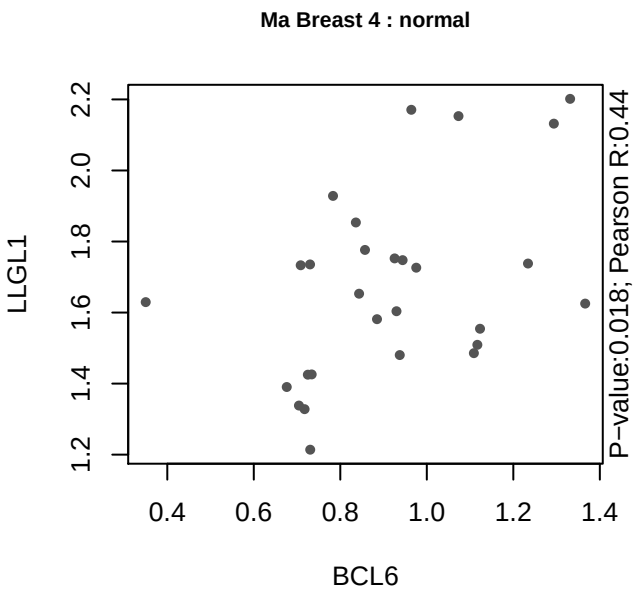

Ma Breast 4 : normal
DLG3
ZBTB7A
P−value:0.00051; Pearson R:0.61

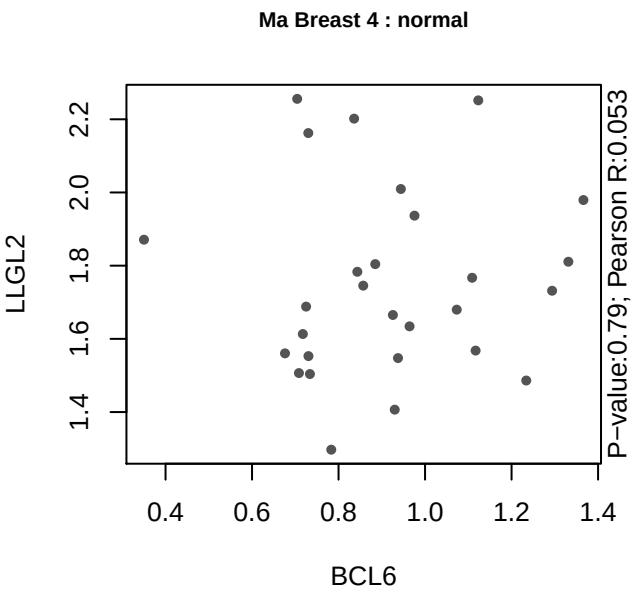

Ma Breast 4 : normal
DLG4
BCL6
P−value:0.47; Pearson R:−0.14

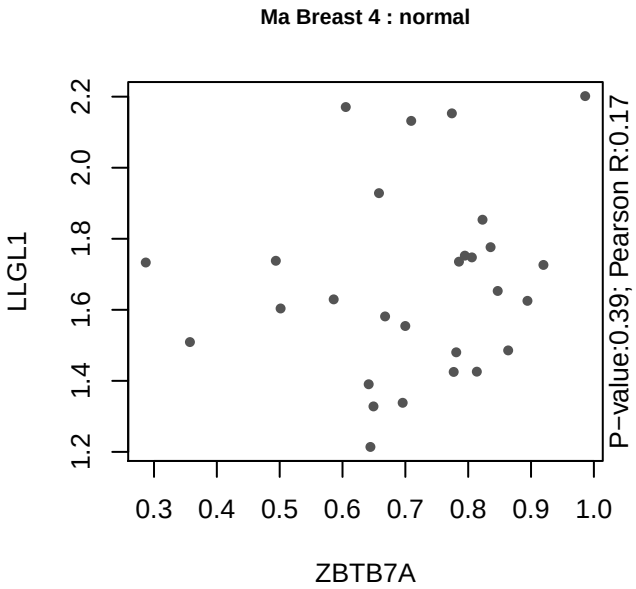

Ma Breast 4 : normal
FYN
BCL6
P−value:0.16; Pearson R:−0.28

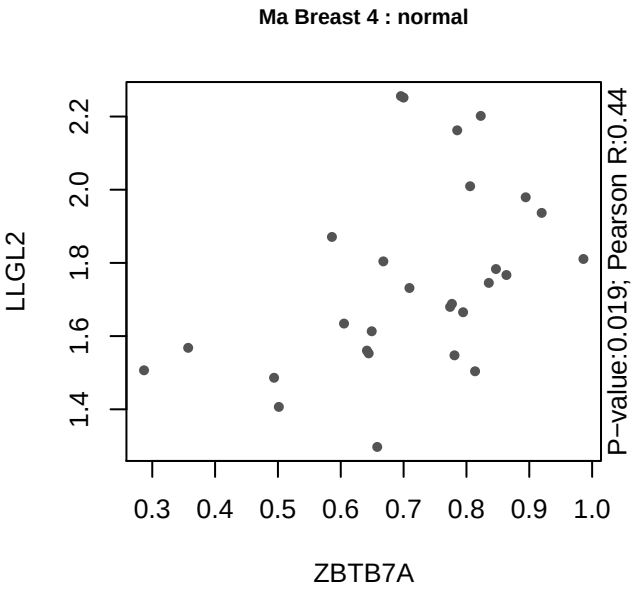

Ma Breast 4 : normal
DLG4
ZBTB7A
P−value:0.53; Pearson R:0.12

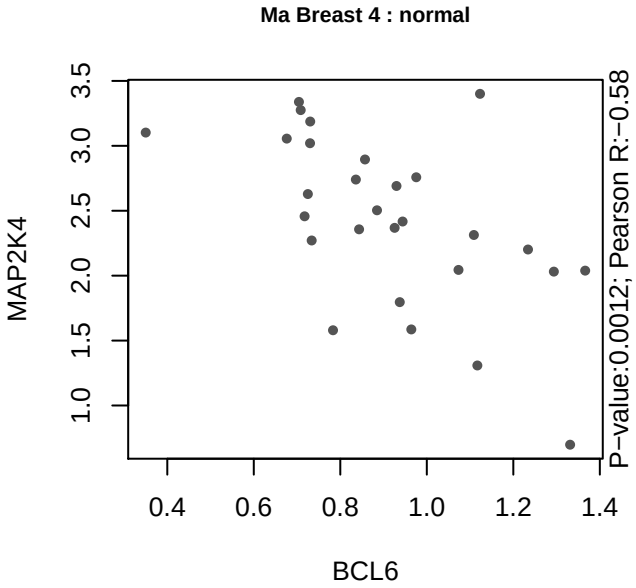

Ma Breast 4 : normal
FYN
ZBTB7A
P−value:0.64; Pearson R:−0.093

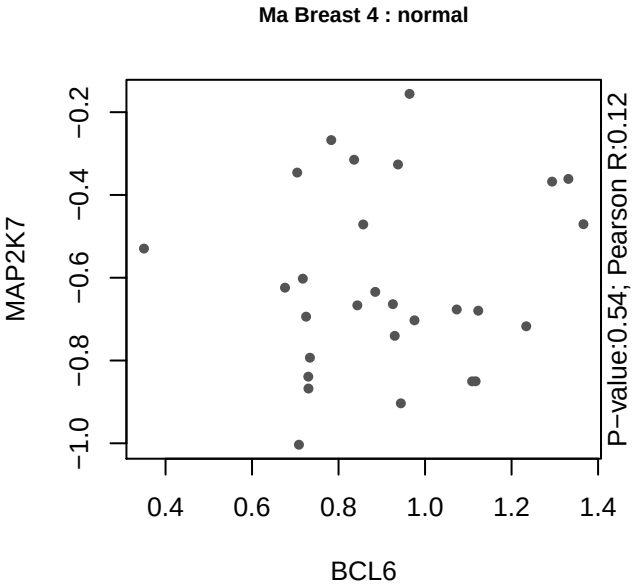

Ma Breast 4 : normal
LLGL1
BCL6
P−value:0.018; Pearson R:0.44

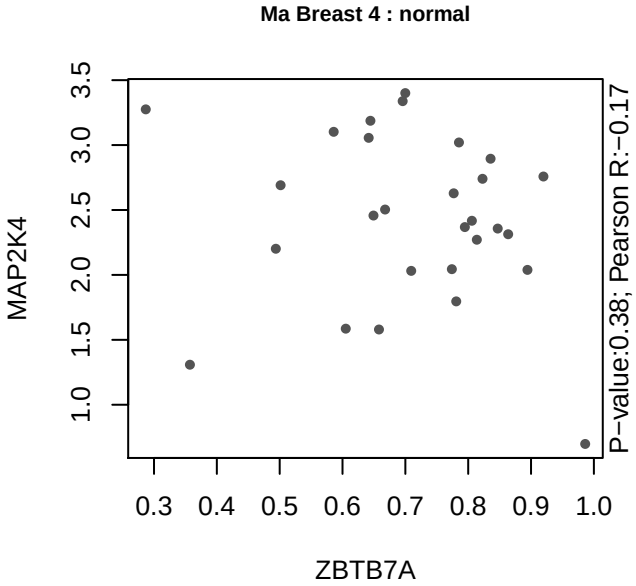

Ma Breast 4 : normal
LLGL2
BCL6
P−value:0.79; Pearson R:0.053

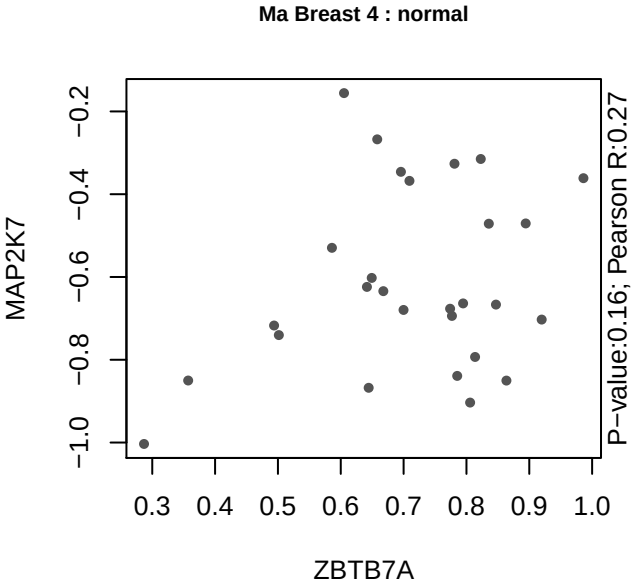

Ma Breast 4 : normal
LLGL1
ZBTB7A
P−value:0.39; Pearson R:0.17

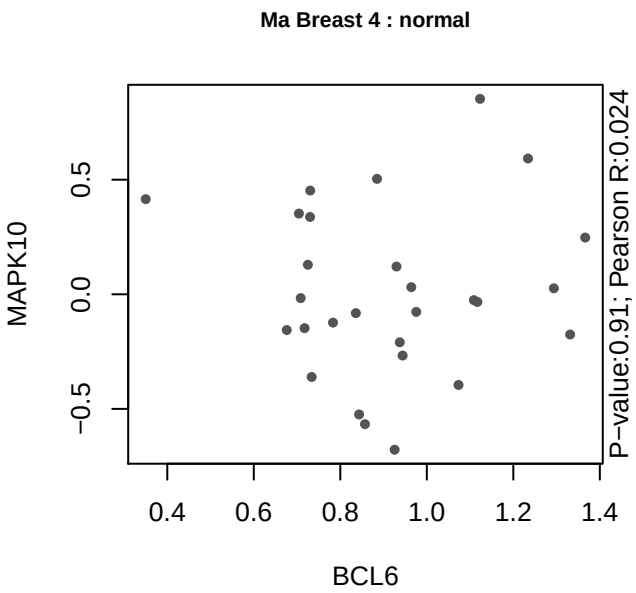

Ma Breast 4 : normal
LLGL2
ZBTB7A
P−value:0.019; Pearson R:0.44

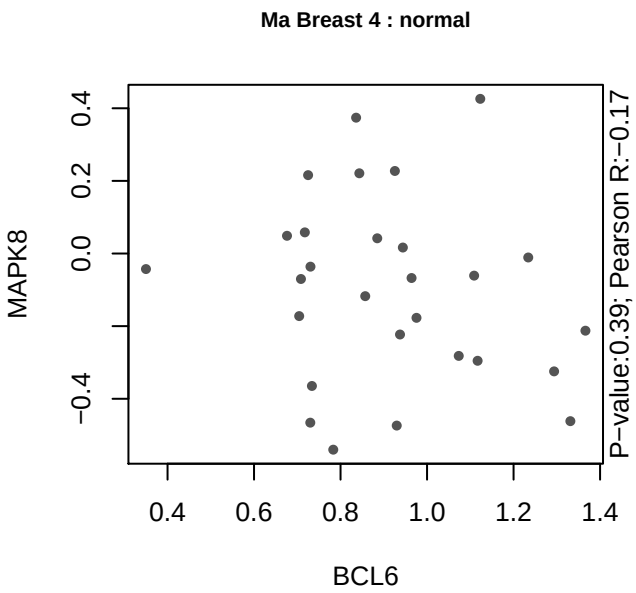

Ma Breast 4 : normal
MAP2K4
BCL6
P−value:0.0012; Pearson R:−0.58

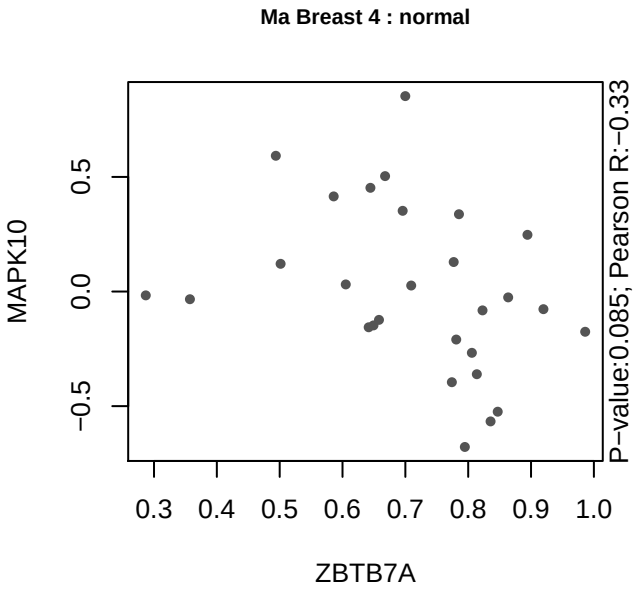

Ma Breast 4 : normal
MAP2K7
BCL6
P−value:0.54; Pearson R:0.12

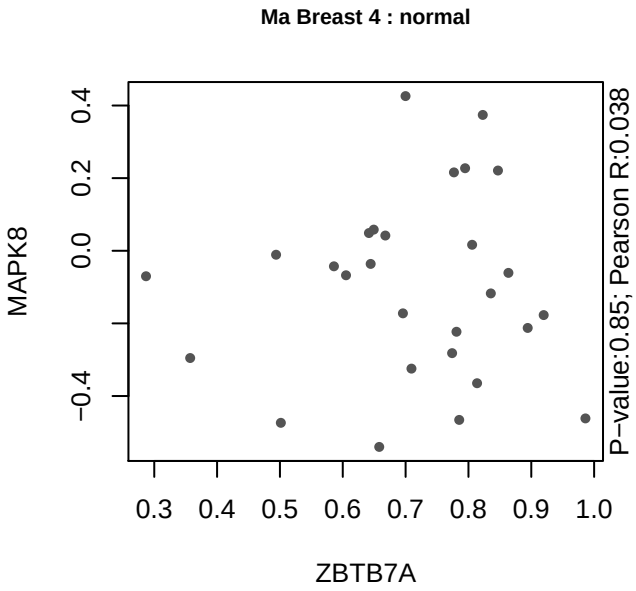

Ma Breast 4 : normal
MAP2K4
ZBTB7A
P−value:0.38; Pearson R:−0.17

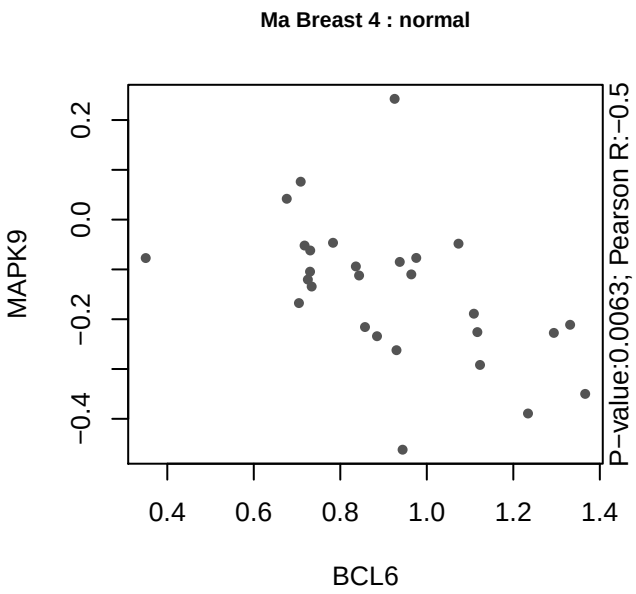

Ma Breast 4 : normal
MAP2K7
ZBTB7A
P−value:0.16; Pearson R:0.27

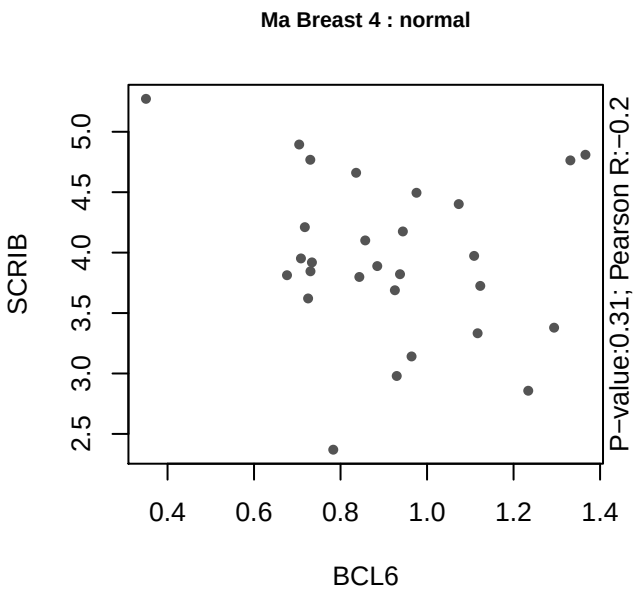

Ma Breast 4 : normal
MAPK10
BCL6
P−value:0.91; Pearson R:0.024
−0.5
0.0
0.5
0.4
0.6
0.8
1.0
1.2
1.4

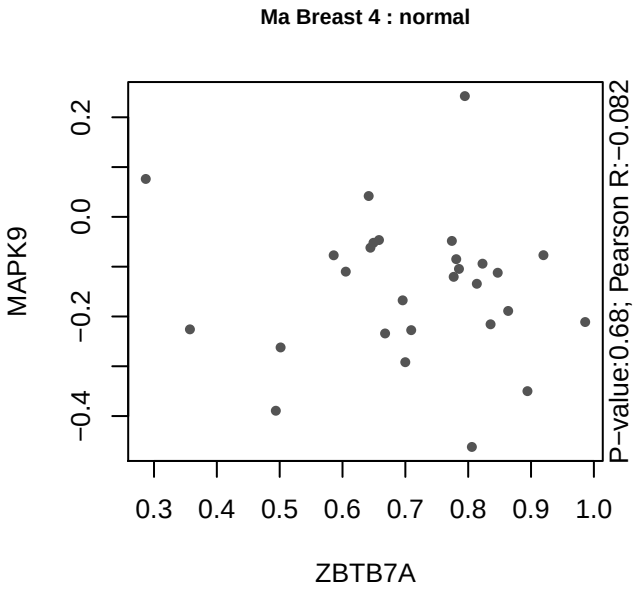

Ma Breast 4 : normal
MAPK8
BCL6
P−value:0.39; Pearson R:−0.17
−0.4
0.0
0.2
0.4
0.4
0.6
0.8
1.0
1.2
1.4

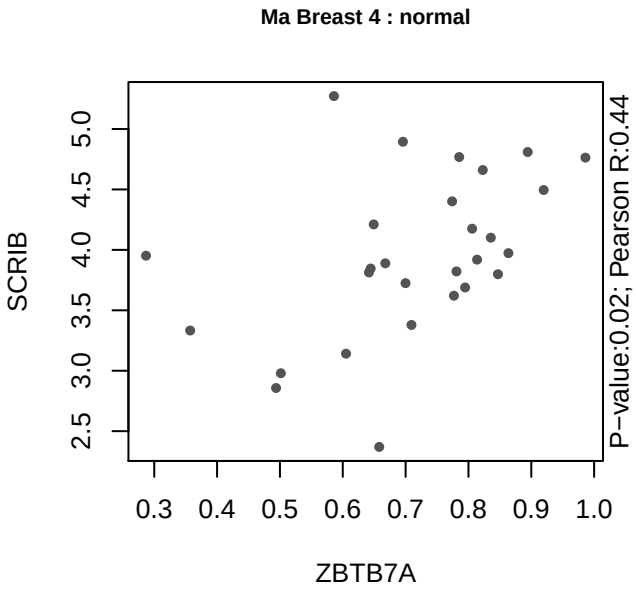

Ma Breast 4 : normal
MAPK10
ZBTB7A
P−value:0.085; Pearson R:−0.33
−0.5
0.0
0.5
0.3
0.4
0.5
0.6
0.7
0.8
0.9
1.0

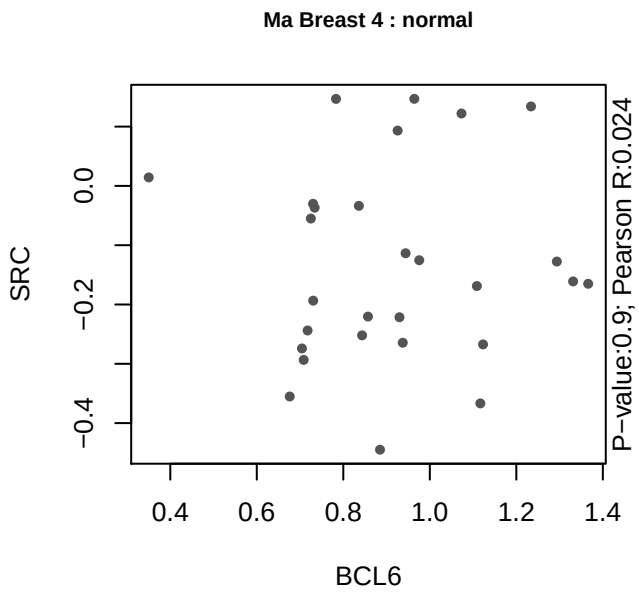

Ma Breast 4 : normal
MAPK8
ZBTB7A
P−value:0.85; Pearson R:0.038
−0.4
0.0
0.2
0.4
0.3
0.4
0.5
0.6
0.7
0.8
0.9
1.0

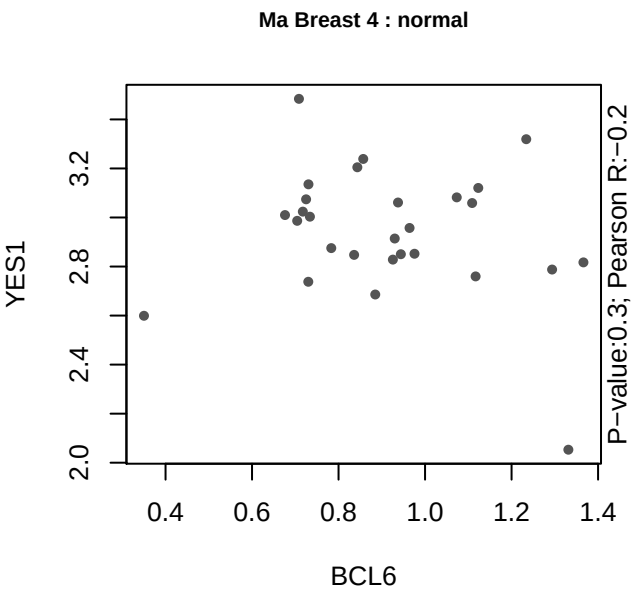

Ma Breast 4 : normal
MAPK9
BCL6
P−value:0.0063; Pearson R:−0.5

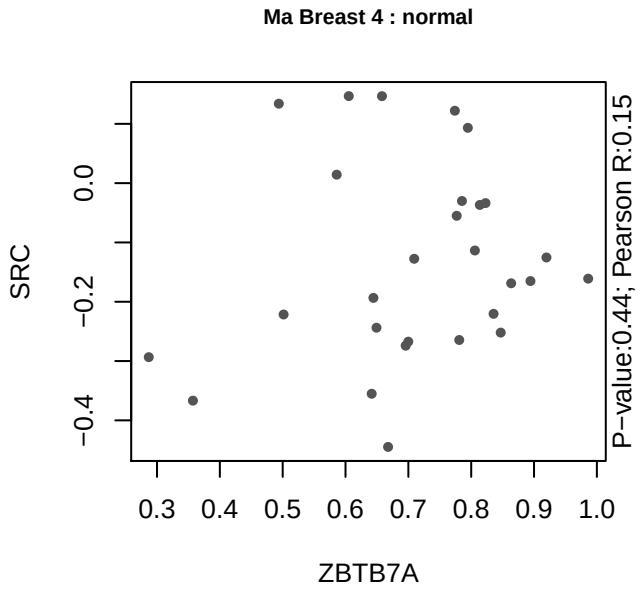

Ma Breast 4 : normal
SCRIB
BCL6
P−value:0.31; Pearson R:−0.2

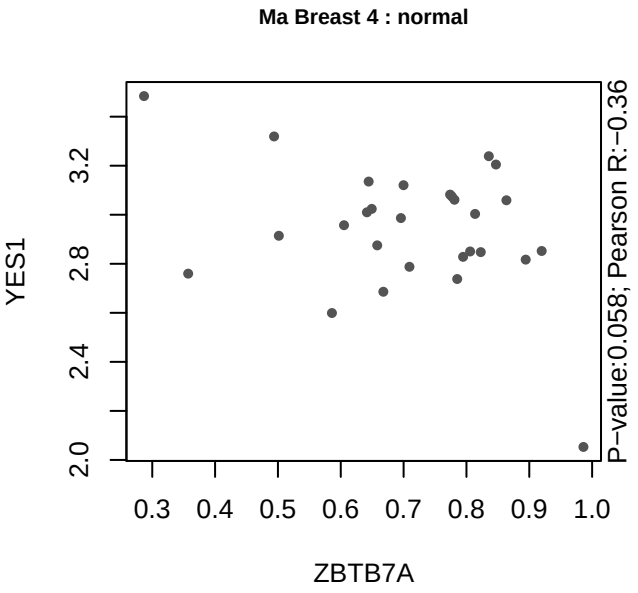

Ma Breast 4 : normal
MAPK9
ZBTB7A
P−value:0.68; Pearson R:−0.082

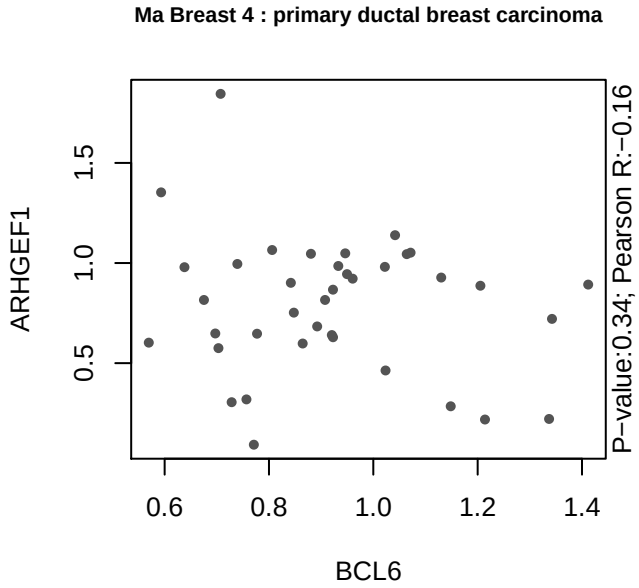

Ma Breast 4 : normal
SCRIB
ZBTB7A
P−value:0.02; Pearson R:0.44

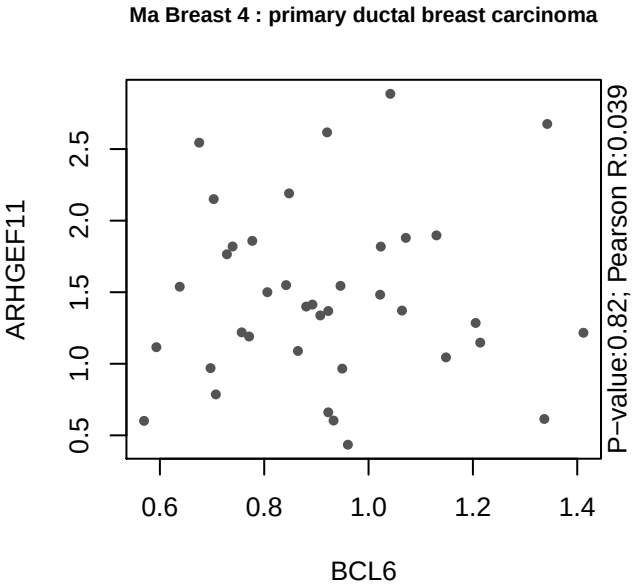

Ma Breast 4 : normal
SRC
BCL6
P−value:0.9; Pearson R:0.024
−0.4
−0.2
0.0
0.4
0.6
0.8
1.0
1.2
1.4

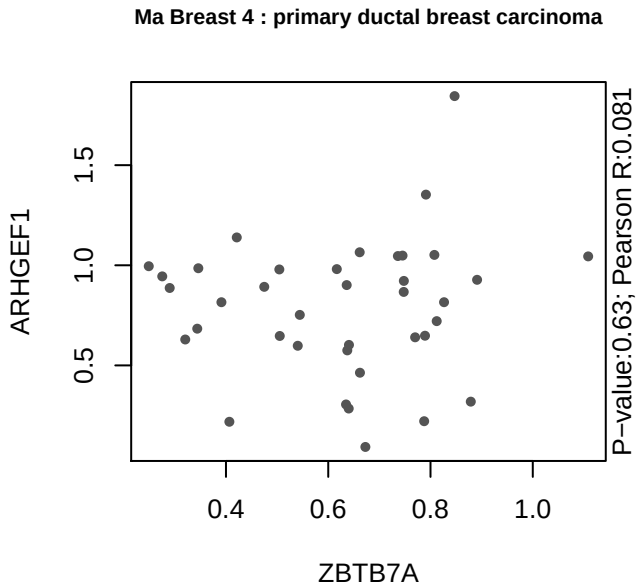

Ma Breast 4 : normal
YES1
BCL6
P−value:0.3; Pearson R:−0.2
2.0
2.4
2.8
3.2
0.4
0.6
0.8
1.0
1.2
1.4

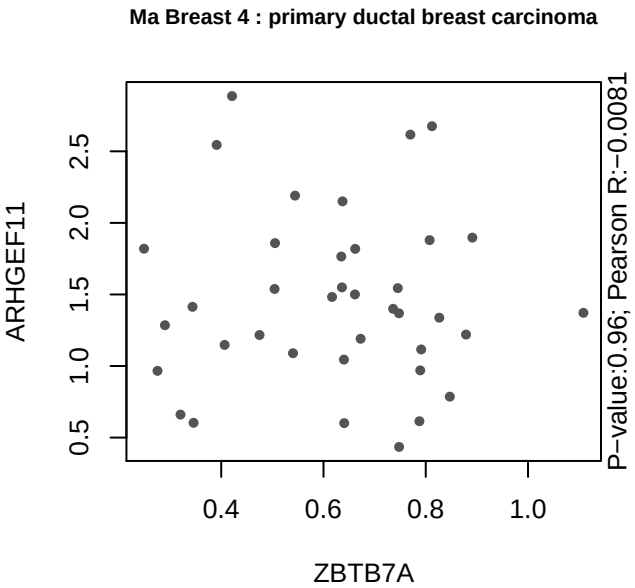

Ma Breast 4 : normal
SRC
ZBTB7A
P−value:0.44; Pearson R:0.15
−0.4
−0.2
0.0
0.3
0.4
0.5
0.6
0.7
0.8
0.9
1.0

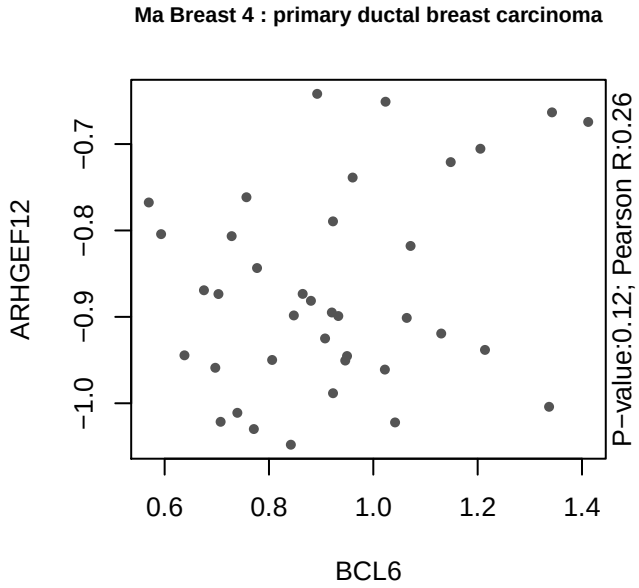

Ma Breast 4 : normal
YES1
ZBTB7A
P−value:0.058; Pearson R:−0.36
2.0
2.4
2.8
3.2
0.3
0.4
0.5
0.6
0.7
0.8
0.9
1.0

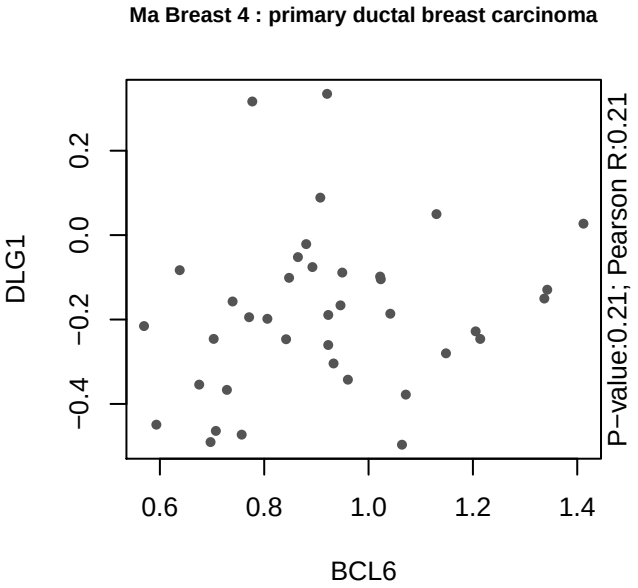

Ma Breast 4 : primary ductal breast carcinoma
ARHGEF1
BCL6
P−value:0.34; Pearson R:−0.16

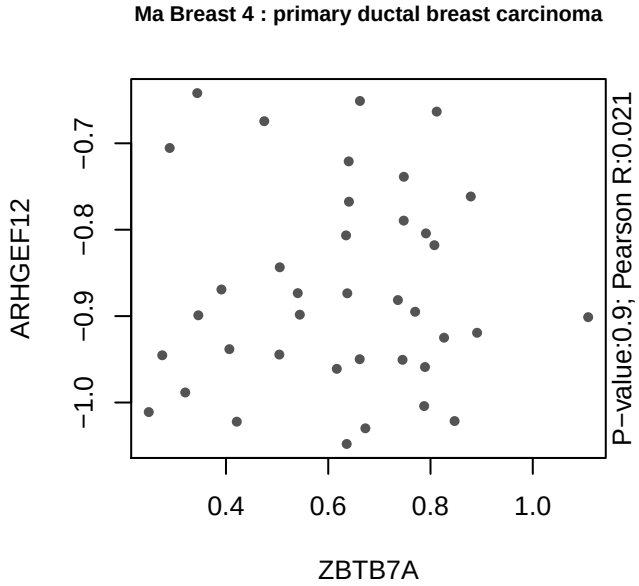

Ma Breast 4 : primary ductal breast carcinoma
ARHGEF11
BCL6
P−value:0.82; Pearson R:0.039

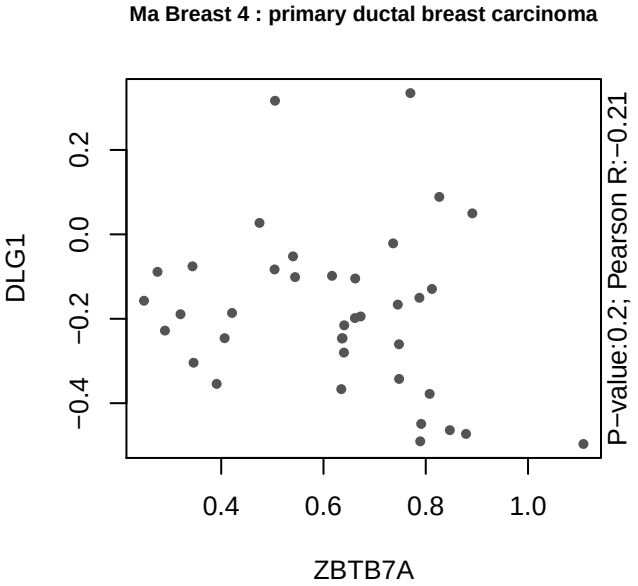

Ma Breast 4 : primary ductal breast carcinoma
ARHGEF1
ZBTB7A
P−value:0.63; Pearson R:0.081

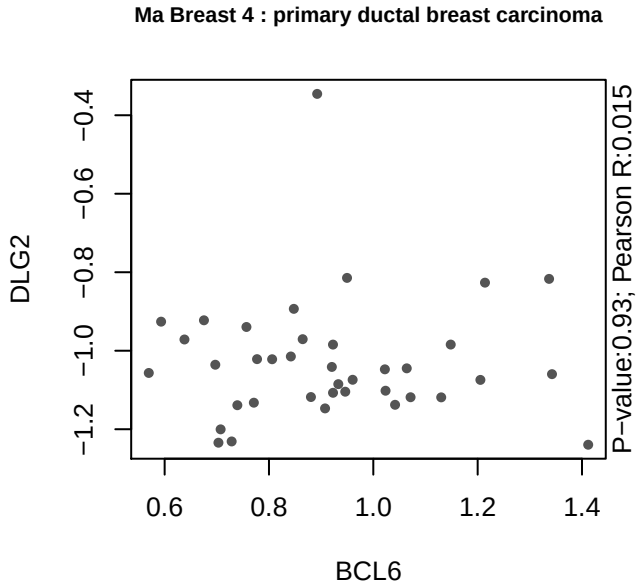

Ma Breast 4 : primary ductal breast carcinoma
ARHGEF11
ZBTB7A
P−value:0.96; Pearson R:−0.0081

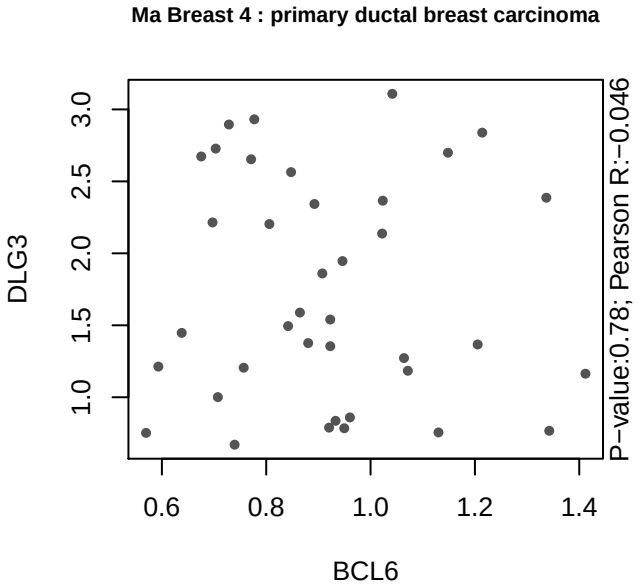

Ma Breast 4 : primary ductal breast carcinoma
ARHGEF12
−1.0
−0.9
−0.8
−0.7
0.6
0.8
1.0
1.2
1.4
BCL6
P−value:0.12; Pearson R:0.26

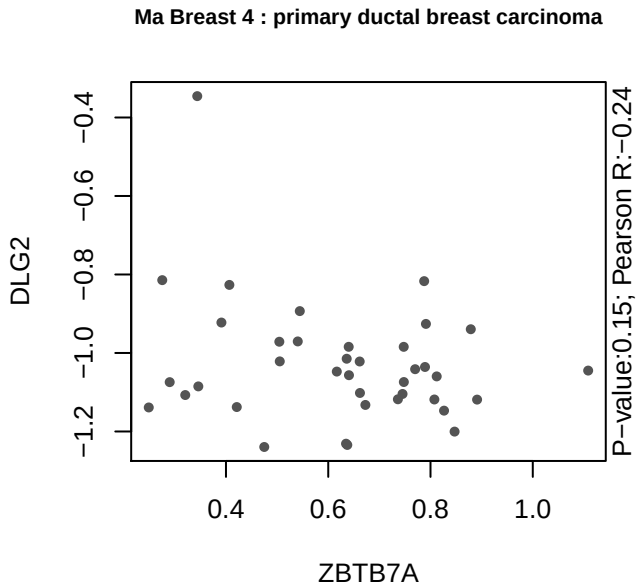

Ma Breast 4 : primary ductal breast carcinoma
DLG1
−0.4
−0.2
0.0
0.2
0.6
0.8
1.0
1.2
1.4
BCL6
P−value:0.21; Pearson R:0.21

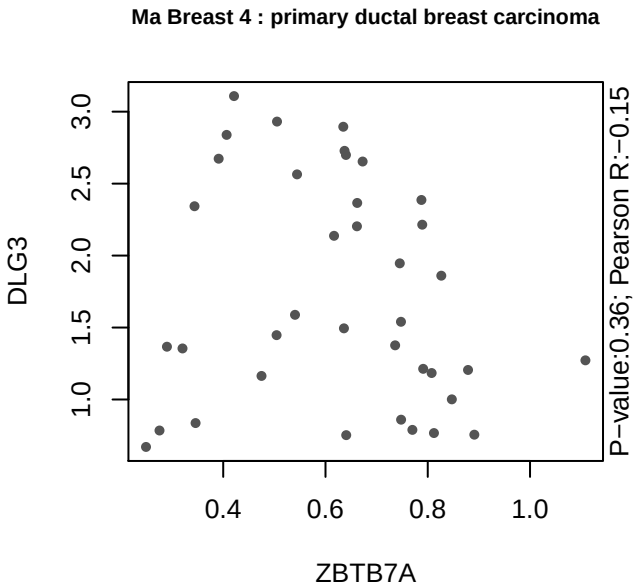

Ma Breast 4 : primary ductal breast carcinoma
ARHGEF12
−1.0
−0.9
−0.8
−0.7
0.4
0.6
0.8
1.0
ZBTB7A
P−value:0.9; Pearson R:0.021

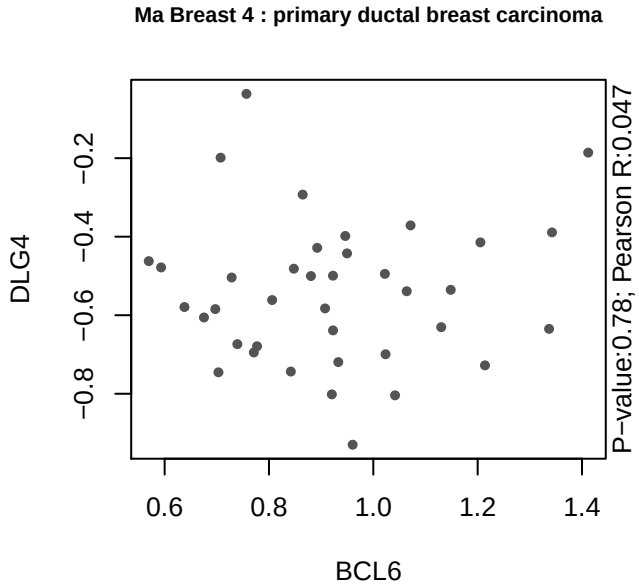

Ma Breast 4 : primary ductal breast carcinoma
DLG1
−0.4
−0.2
0.0
0.2
0.4
0.6
0.8
1.0
ZBTB7A
P−value:0.2; Pearson R:−0.21

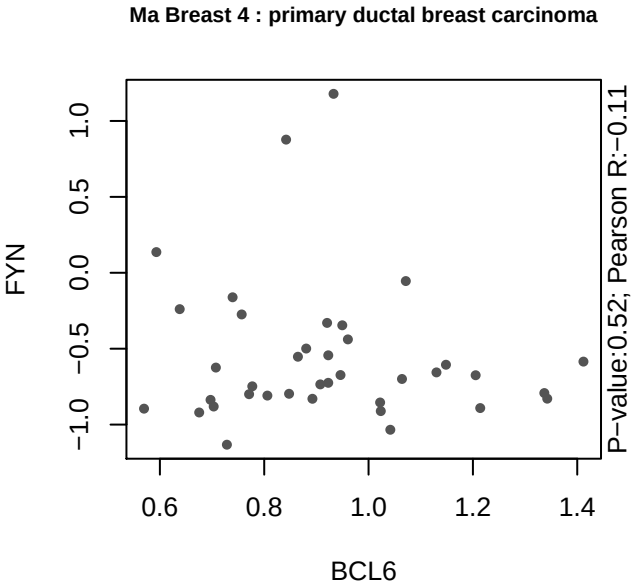

Ma Breast 4 : primary ductal breast carcinoma
DLG2
BCL6
P−value:0.93; Pearson R:0.015

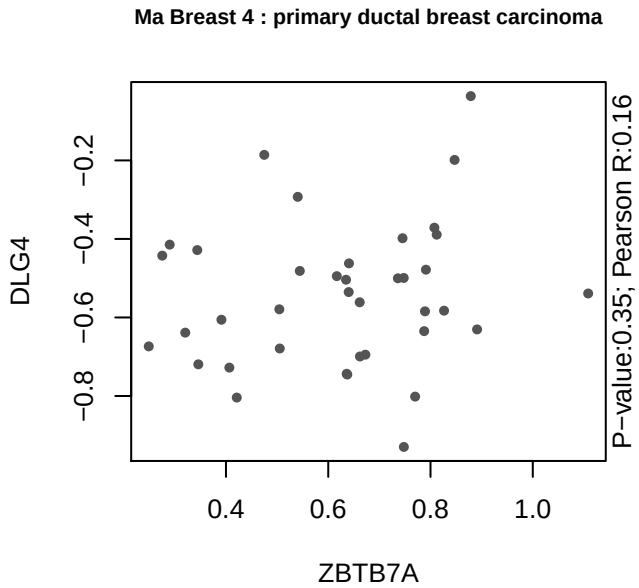

Ma Breast 4 : primary ductal breast carcinoma
DLG3
BCL6
P−value:0.78; Pearson R:−0.046

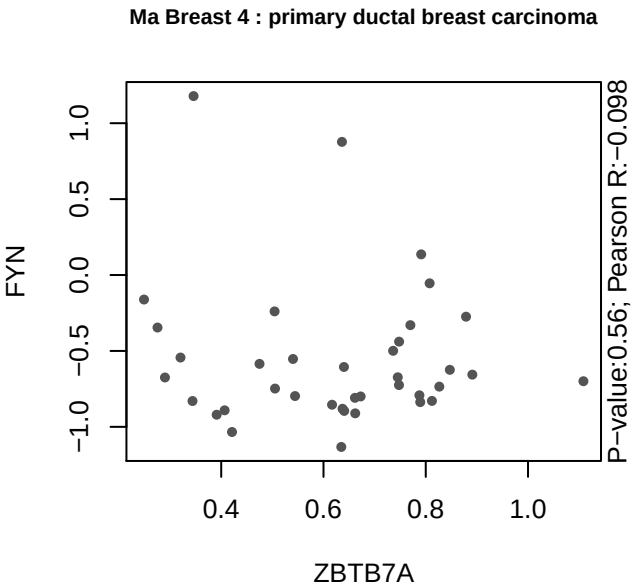

Ma Breast 4 : primary ductal breast carcinoma
DLG2
ZBTB7A
P−value:0.15; Pearson R:−0.24

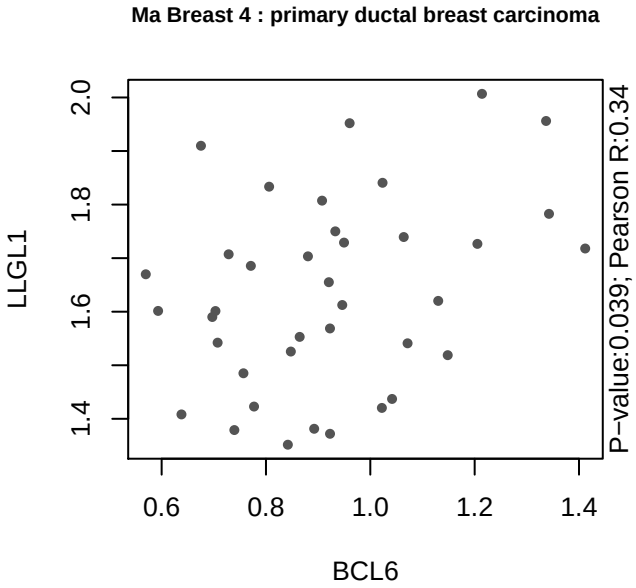

Ma Breast 4 : primary ductal breast carcinoma
DLG3
ZBTB7A
P−value:0.36; Pearson R:−0.15

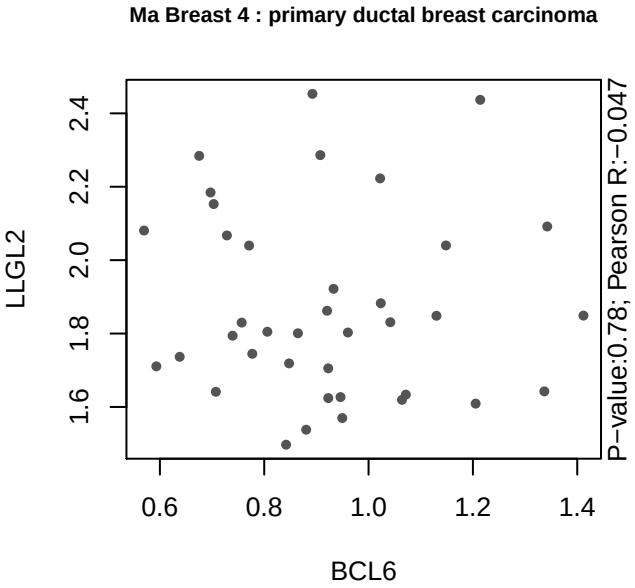

Ma Breast 4 : primary ductal breast carcinoma
DLG4
−0.8
−0.6
−0.4
−0.2
0.6
0.8
1.0
1.2
1.4
BCL6
P−value:0.78; Pearson R:0.047

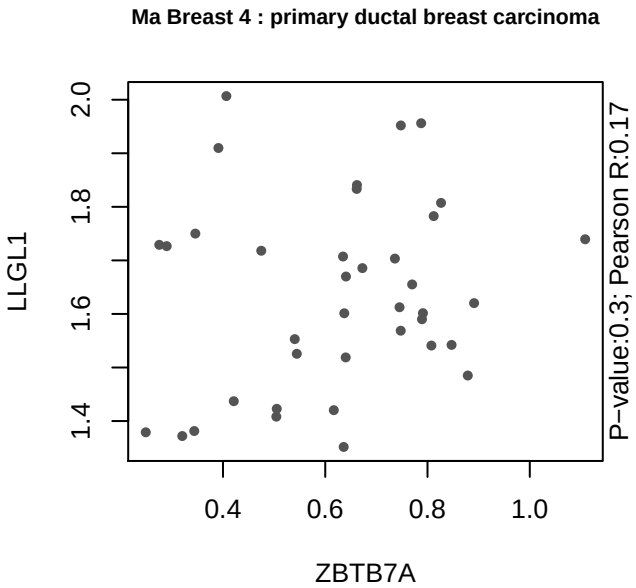

Ma Breast 4 : primary ductal breast carcinoma
FYN
−1.0
−0.5
0.0
0.5
1.0
0.6
0.8
1.0
1.2
1.4
BCL6
P−value:0.52; Pearson R:−0.11

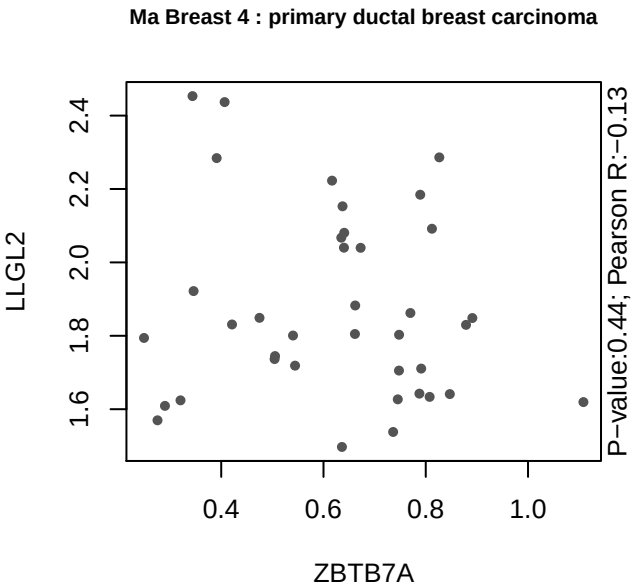

Ma Breast 4 : primary ductal breast carcinoma
DLG4
−0.8
−0.6
−0.4
−0.2
0.4
0.6
0.8
1.0
ZBTB7A
P−value:0.35; Pearson R:0.16

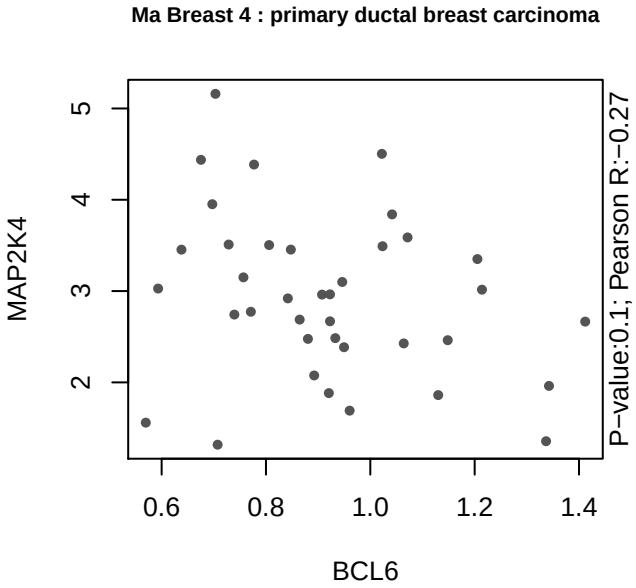

Ma Breast 4 : primary ductal breast carcinoma
FYN
−1.0
−0.5
0.0
0.5
1.0
0.4
0.6
0.8
1.0
ZBTB7A
P−value:0.56; Pearson R:−0.098

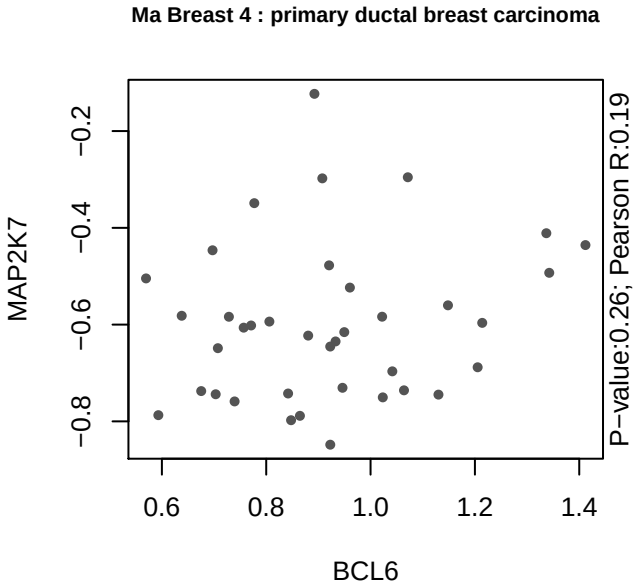

Ma Breast 4 : primary ductal breast carcinoma
LLGL1
BCL6
P−value:0.039; Pearson R:0.34
1.4
1.6
1.8
2.0
0.6
0.8
1.0
1.2
1.4

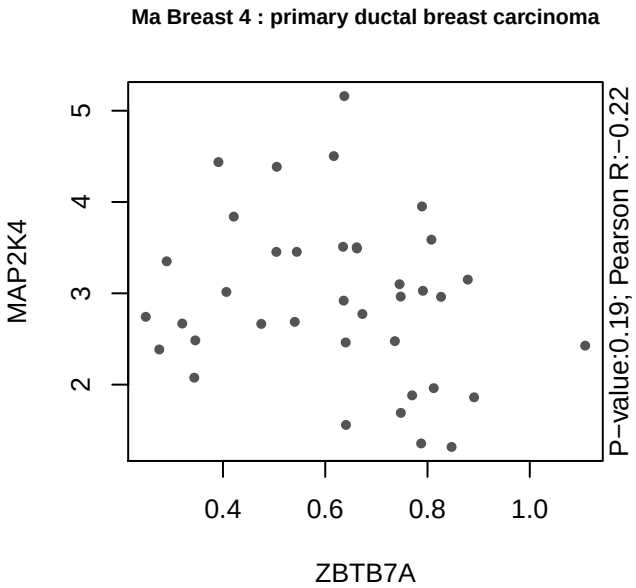

Ma Breast 4 : primary ductal breast carcinoma
LLGL2
BCL6
P−value:0.78; Pearson R:−0.047
1.6
1.8
2.0
2.2
2.4
0.6
0.8
1.0
1.2
1.4

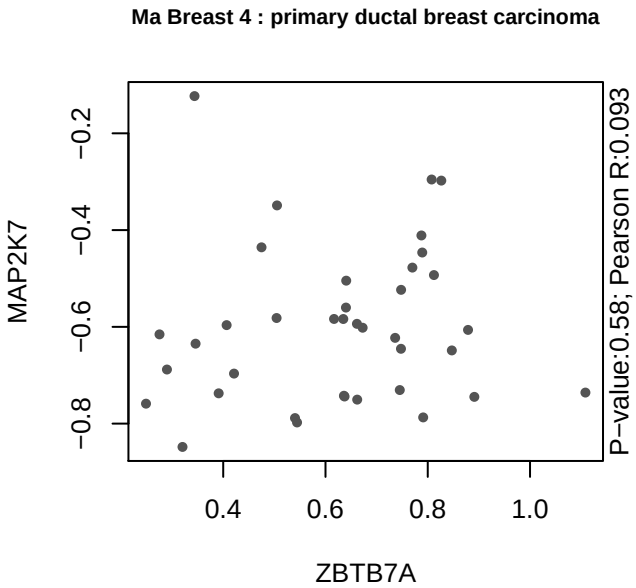

Ma Breast 4 : primary ductal breast carcinoma
LLGL1
ZBTB7A
P−value:0.3; Pearson R:0.17
1.4
1.6
1.8
2.0
0.4
0.6
0.8
1.0

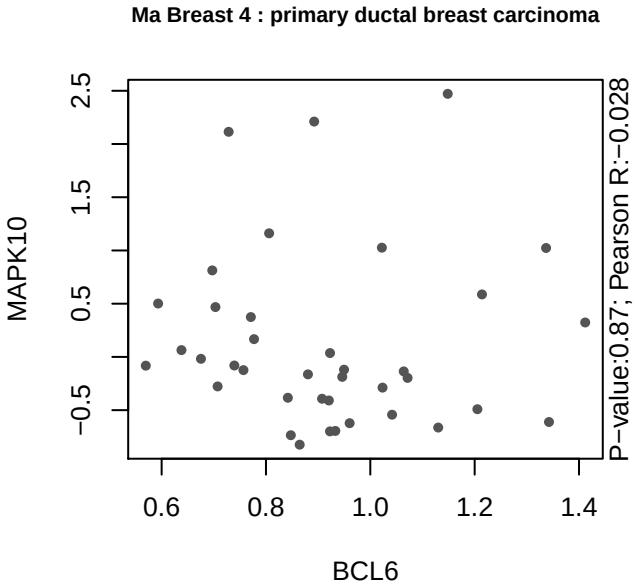

Ma Breast 4 : primary ductal breast carcinoma
LLGL2
ZBTB7A
P−value:0.44; Pearson R:−0.13
1.6
1.8
2.0
2.2
2.4
0.4
0.6
0.8
1.0

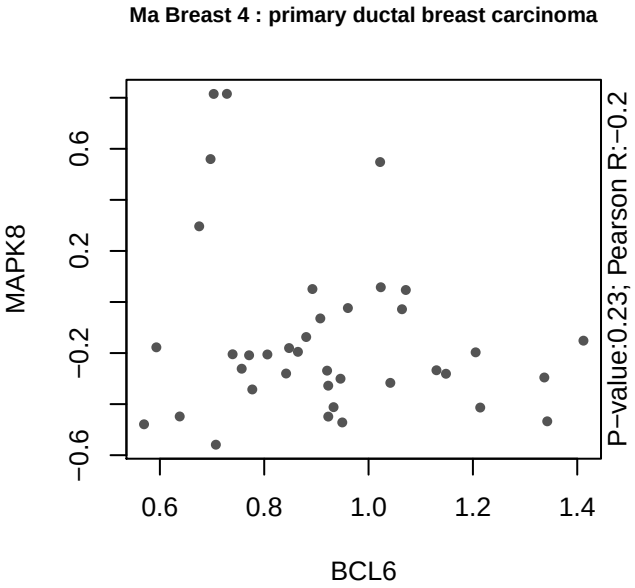

Ma Breast 4 : primary ductal breast carcinoma
MAP2K4
BCL6
P−value:0.1; Pearson R:−0.27

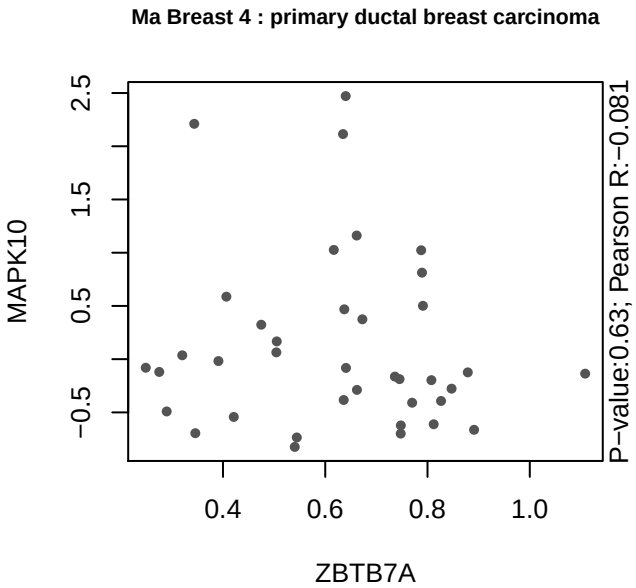

Ma Breast 4 : primary ductal breast carcinoma
MAP2K7
BCL6
P−value:0.26; Pearson R:0.19

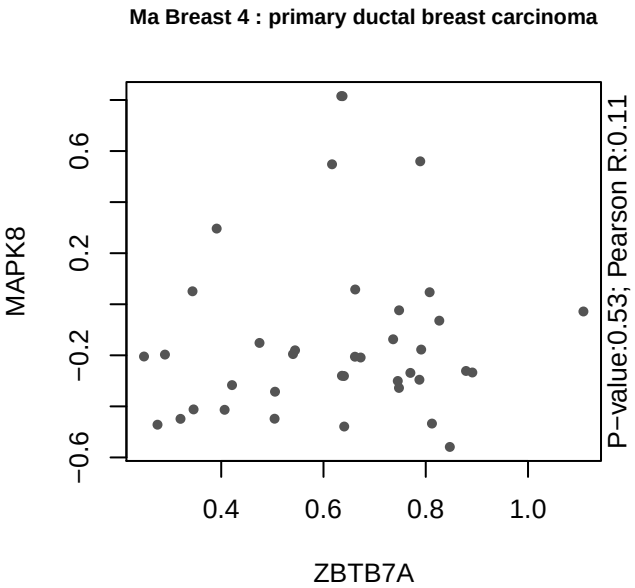

Ma Breast 4 : primary ductal breast carcinoma
MAP2K4
ZBTB7A
P−value:0.19; Pearson R:−0.22

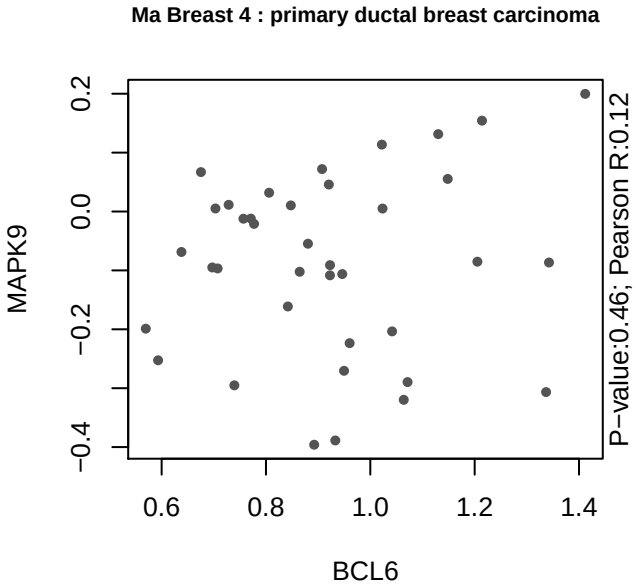

Ma Breast 4 : primary ductal breast carcinoma
MAP2K7
ZBTB7A
P−value:0.58; Pearson R:0.093

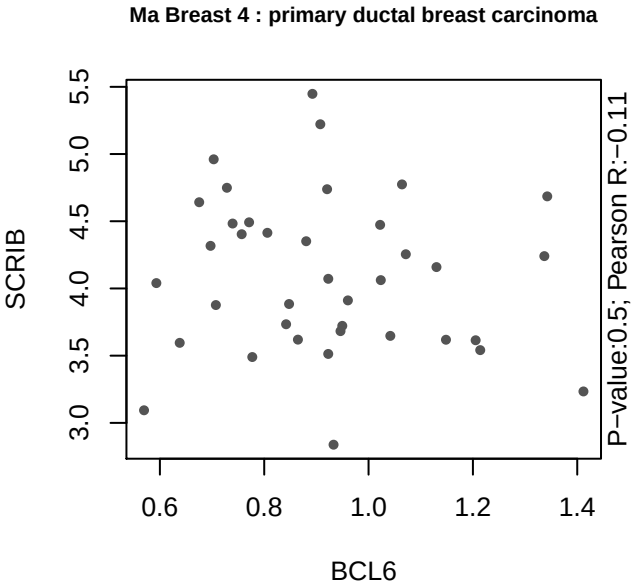

Ma Breast 4 : primary ductal breast carcinoma
MAPK10
BCL6
P−value:0.87; Pearson R:−0.028

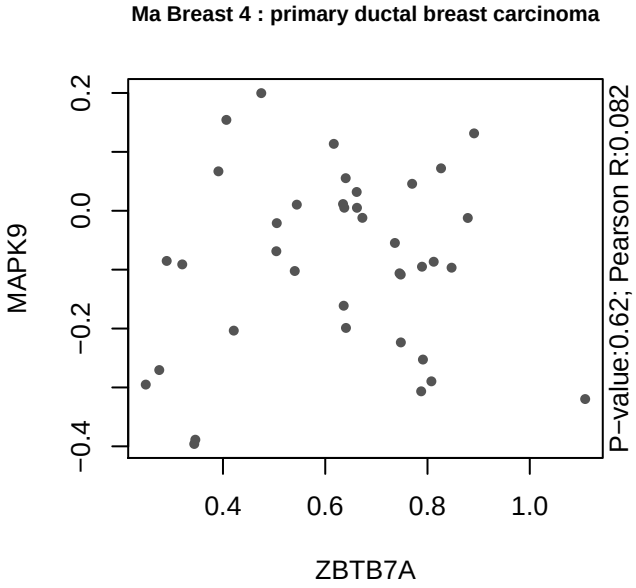

Ma Breast 4 : primary ductal breast carcinoma
MAPK8
BCL6
P−value:0.23; Pearson R:−0.2

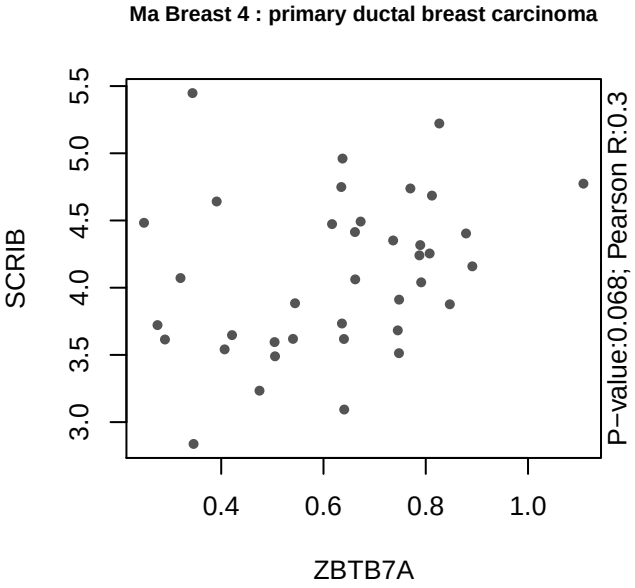

Ma Breast 4 : primary ductal breast carcinoma
MAPK10
ZBTB7A
P−value:0.63; Pearson R:−0.081

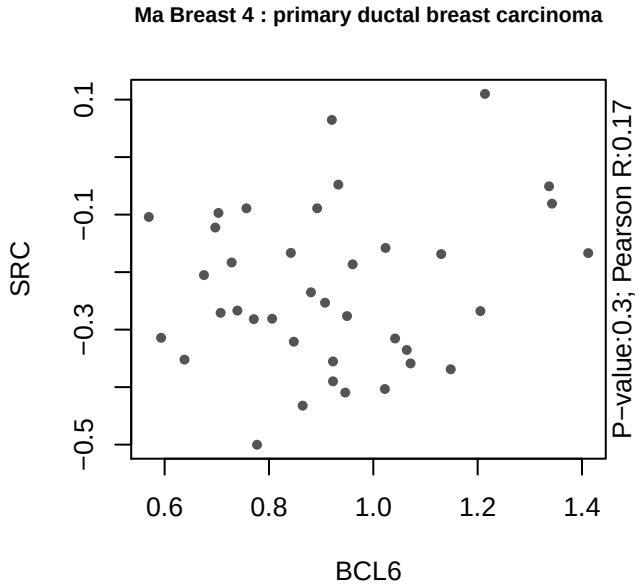

Ma Breast 4 : primary ductal breast carcinoma
MAPK8
ZBTB7A
P−value:0.53; Pearson R:0.11

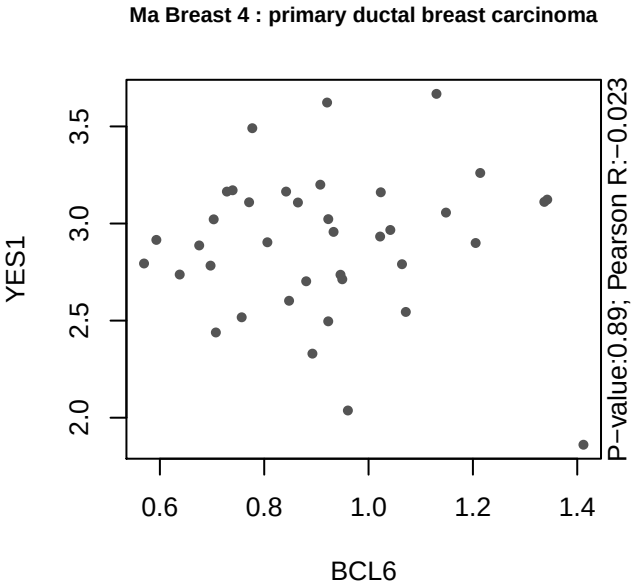

Ma Breast 4 : primary ductal breast carcinoma
MAPK9
BCL6
P−value:0.46; Pearson R:0.12
0.2
0.0
−0.2
−0.4
0.6
0.8
1.0
1.2
1.4

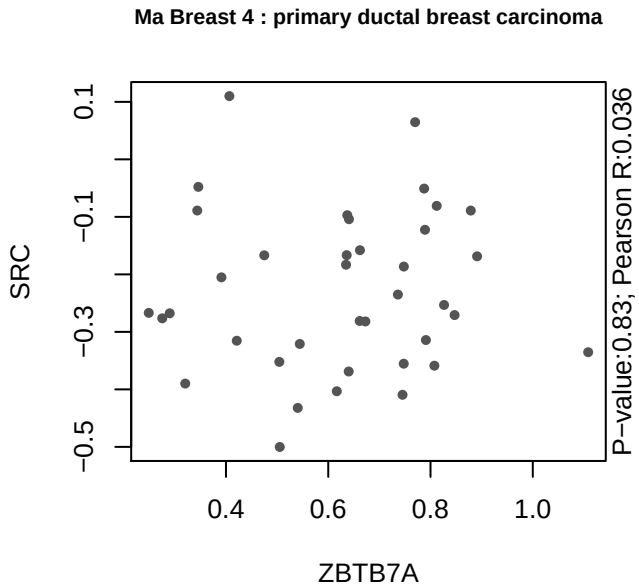

Ma Breast 4 : primary ductal breast carcinoma
SCRIB
BCL6
P−value:0.5; Pearson R:−0.11
5.5
5.0
4.5
4.0
3.5
3.0
0.6
0.8
1.0
1.2
1.4

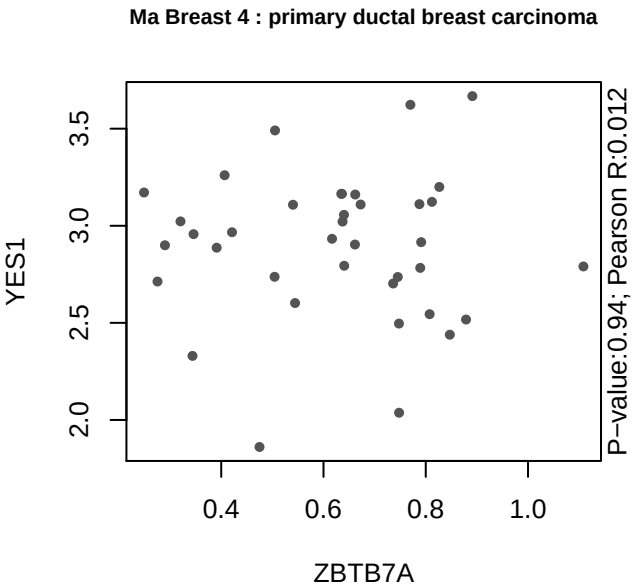

Ma Breast 4 : primary ductal breast carcinoma
MAPK9
ZBTB7A
P−value:0.62; Pearson R:0.082
0.2
0.0
−0.2
−0.4
0.4
0.6
0.8
1.0

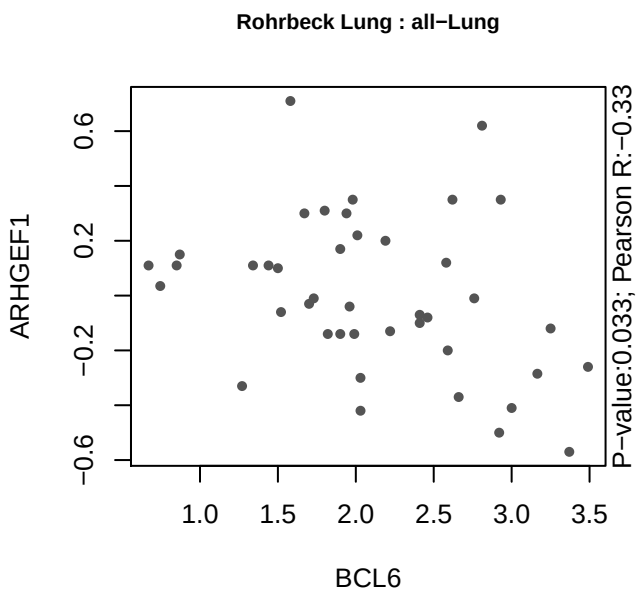

Ma Breast 4 : primary ductal breast carcinoma
SCRIB
ZBTB7A
P−value:0.068; Pearson R:0.3
5.5
5.0
4.5
4.0
3.5
3.0
0.4
0.6
0.8
1.0

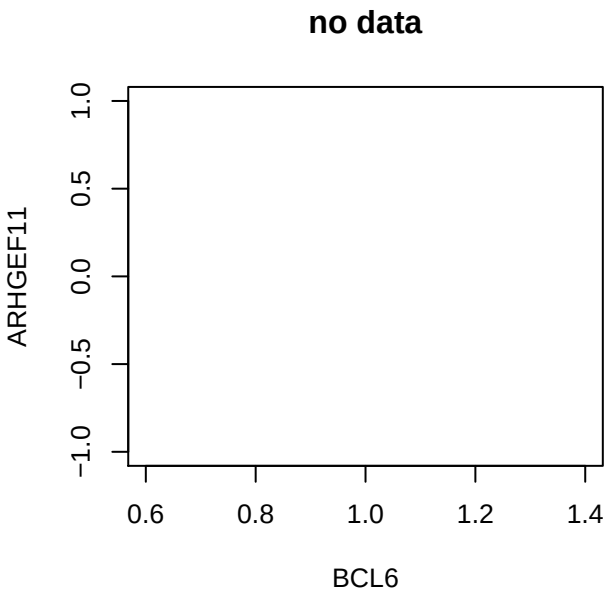

Ma Breast 4 : primary ductal breast carcinoma
SRC
BCL6
P−value:0.3; Pearson R:0.17
0.1
−0.1
−0.3
−0.5
0.6
0.8
1.0
1.2
1.4

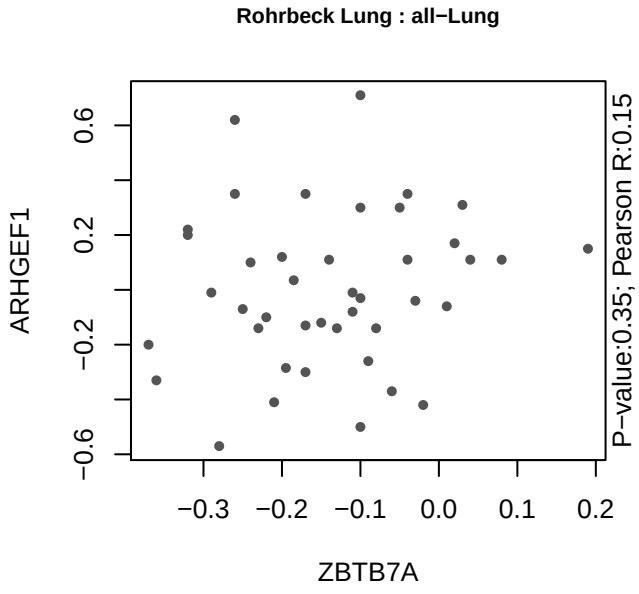

Ma Breast 4 : primary ductal breast carcinoma
YES1
BCL6
P−value:0.89; Pearson R:−0.023
3.5
3.0
2.5
2.0
0.6
0.8
1.0
1.2
1.4

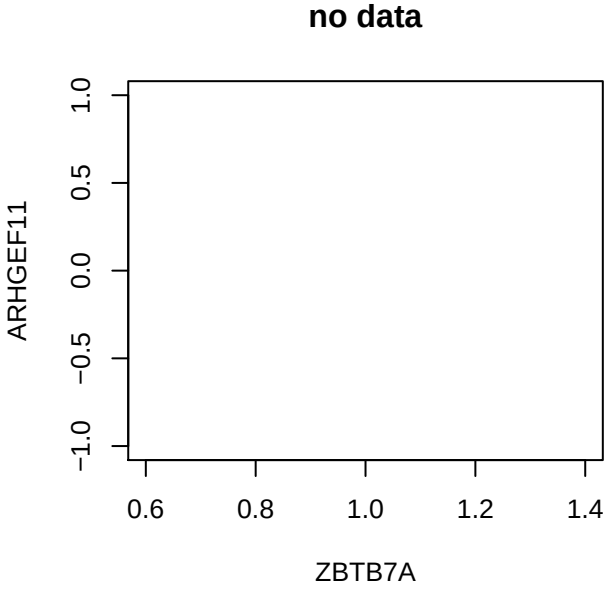

Ma Breast 4 : primary ductal breast carcinoma
SRC
ZBTB7A
P−value:0.83; Pearson R:0.036
0.1
−0.1
−0.3
−0.5
0.4
0.6
0.8
1.0

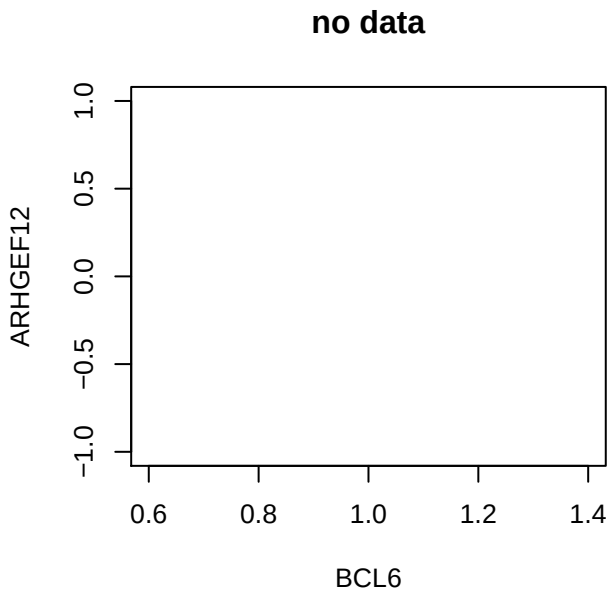

Ma Breast 4 : primary ductal breast carcinoma
YES1
ZBTB7A
P−value:0.94; Pearson R:0.012
3.5
3.0
2.5
2.0
0.4
0.6
0.8
1.0

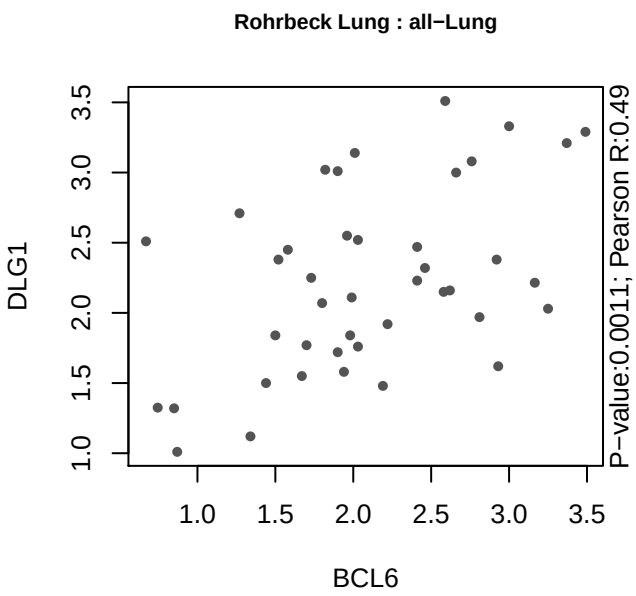

Rohrbeck Lung : all−Lung
ARHGEF1
BCL6
P−value:0.033; Pearson R:−0.33
−0.6
−0.2
0.2
0.6
1.0
1.5
2.0
2.5
3.0
3.5

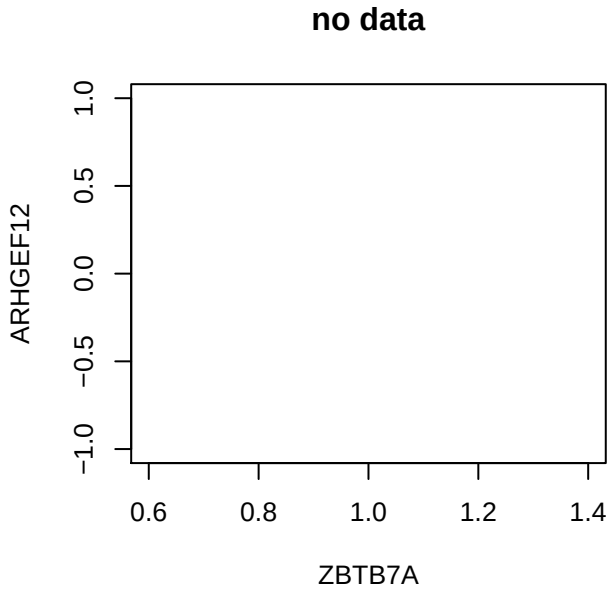

no data
ARHGEF11
BCL6
−1.0
−0.5
0.0
0.5
1.0
0.6
0.8
1.0
1.2
1.4

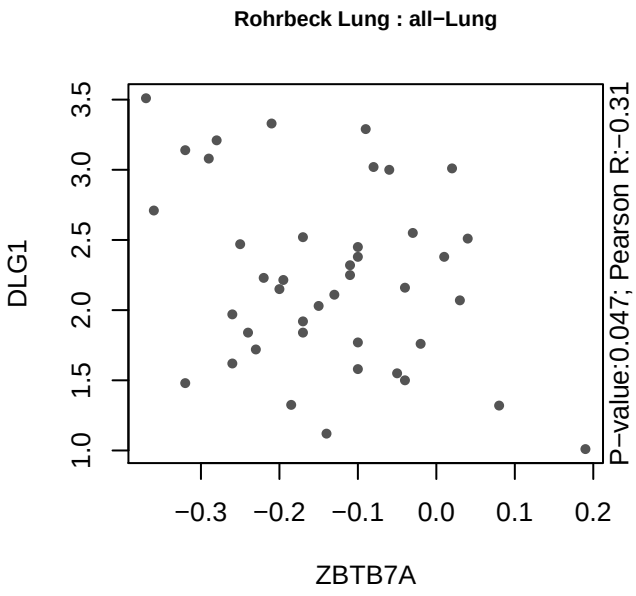

Rohrbeck Lung : all−Lung
ARHGEF1
ZBTB7A
P−value:0.35; Pearson R:0.15
−0.6
−0.2
0.2
0.6
−0.3
−0.2
−0.1
0.0
0.1
0.2

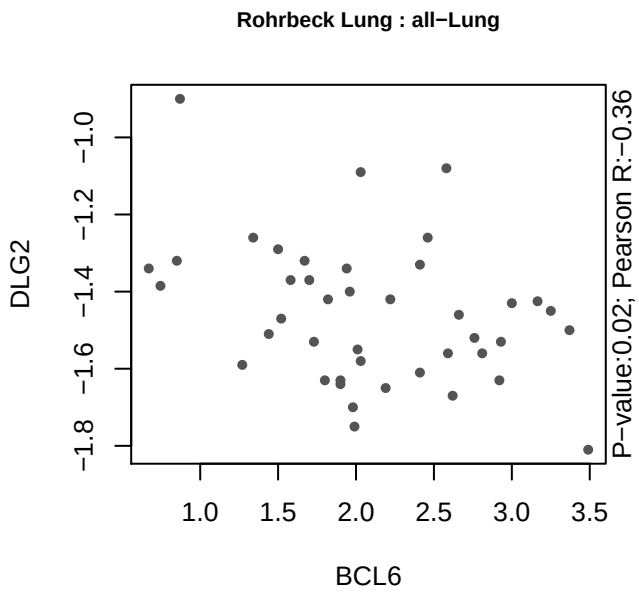

no data
ARHGEF11
ZBTB7A
−1.0
−0.5
0.0
0.5
1.0
0.6
0.8
1.0
1.2
1.4

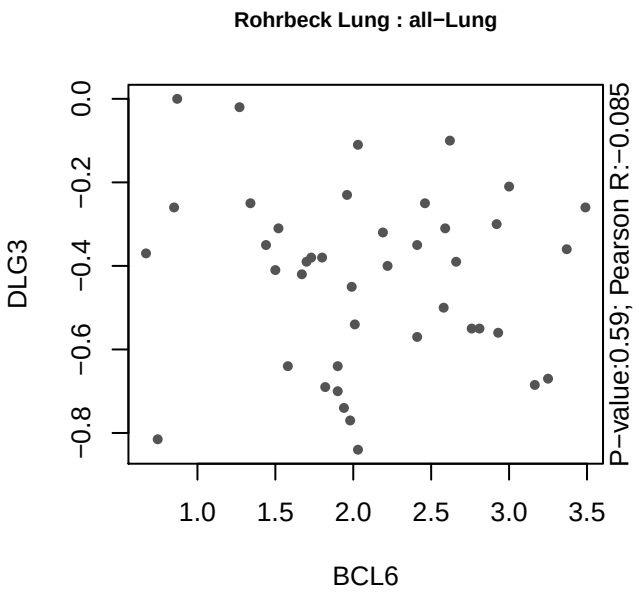

no data
ARHGEF12
BCL6
−1.0
−0.5
0.0
0.5
1.0
0.6
0.8
1.0
1.2
1.4

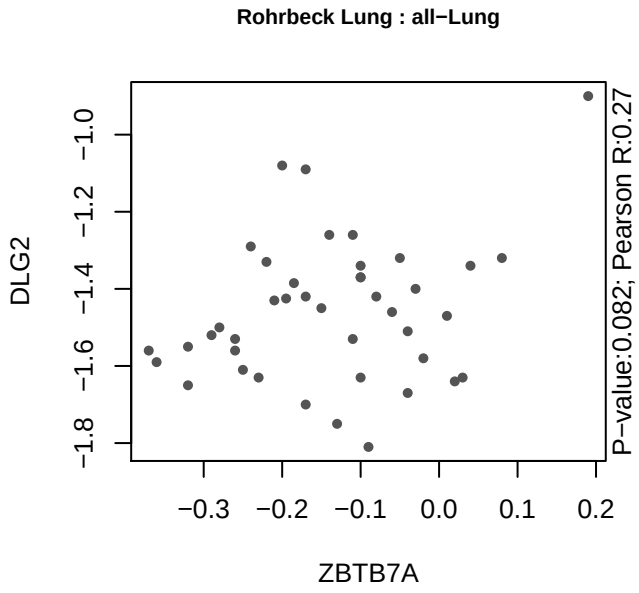

Rohrbeck Lung : all−Lung
DLG1
BCL6
P−value:0.0011; Pearson R:0.49
1.0
1.5
2.0
2.5
3.0
3.5

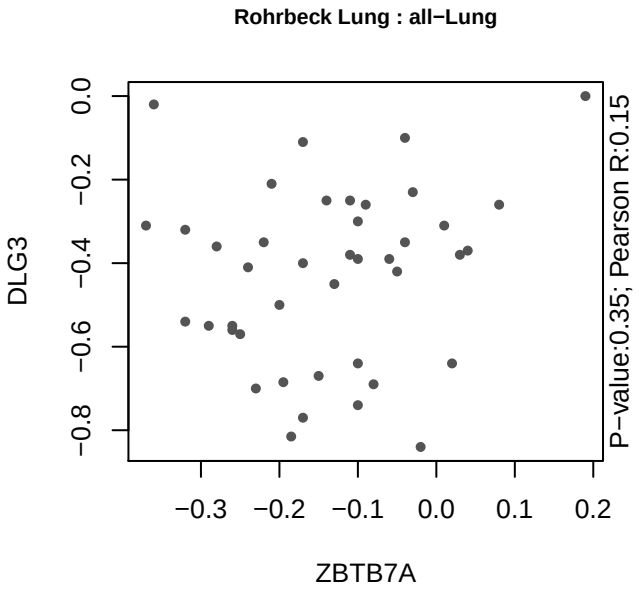

no data
ARHGEF12
ZBTB7A
−1.0
−0.5
0.0
0.5
1.0
0.6
0.8
1.0
1.2
1.4

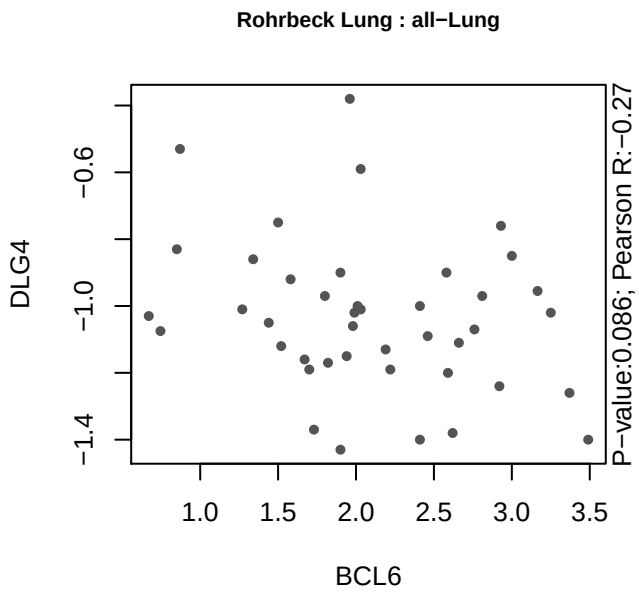

Rohrbeck Lung : all−Lung
DLG1
ZBTB7A
P−value:0.047; Pearson R:−0.31
1.0
1.5
2.0
2.5
3.0
3.5
−0.3
−0.2
−0.1
0.0
0.1
0.2

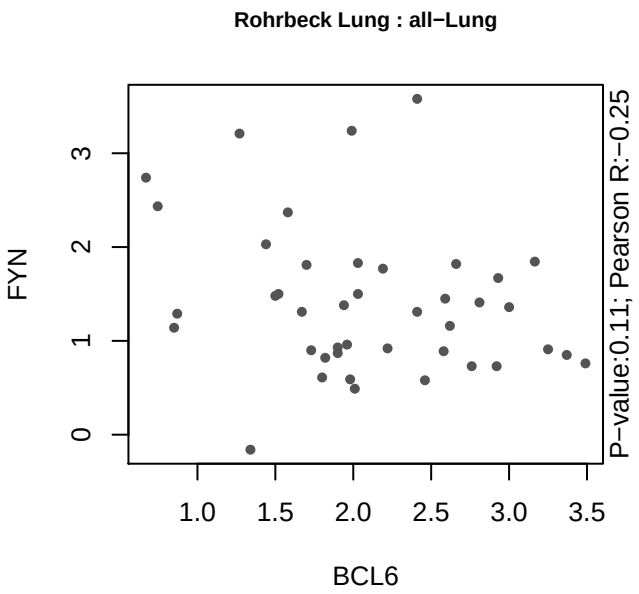

Rohrbeck Lung : all−Lung
DLG2
BCL6
P−value:0.02; Pearson R:−0.36

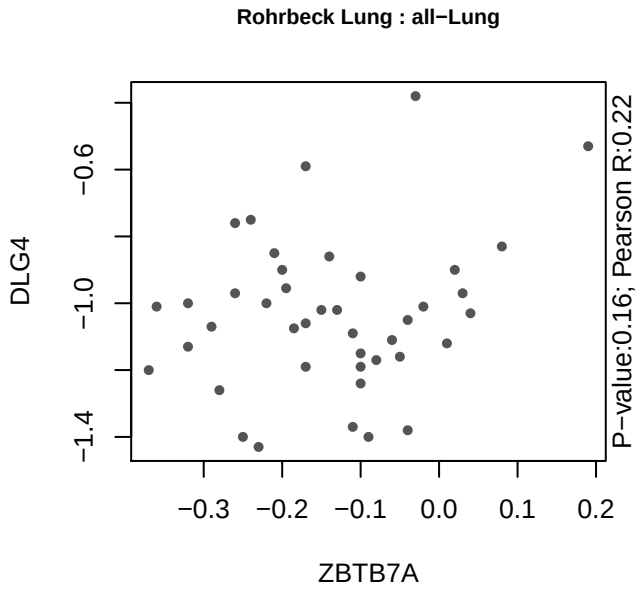

Rohrbeck Lung : all−Lung
DLG3
BCL6
P−value:0.59; Pearson R:−0.085

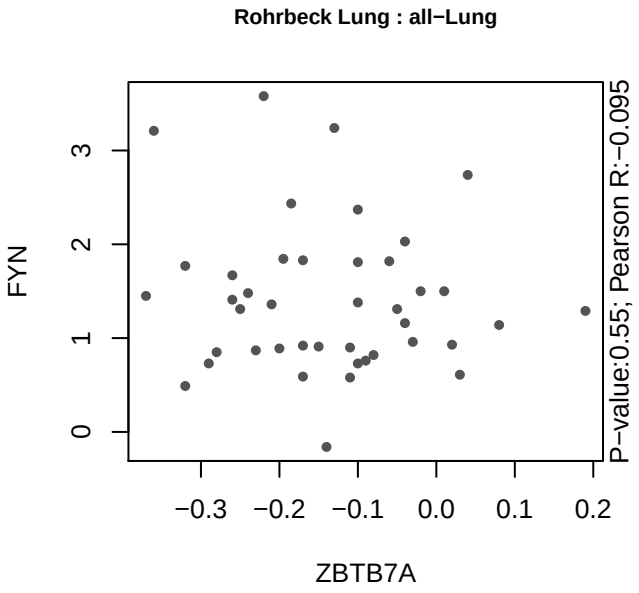

Rohrbeck Lung : all−Lung
DLG2
ZBTB7A
P−value:0.082; Pearson R:0.27

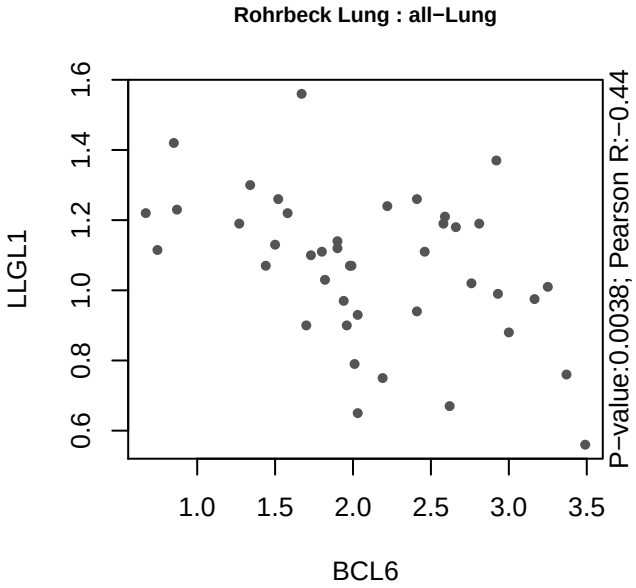

Rohrbeck Lung : all−Lung
DLG3
ZBTB7A
P−value:0.35; Pearson R:0.15

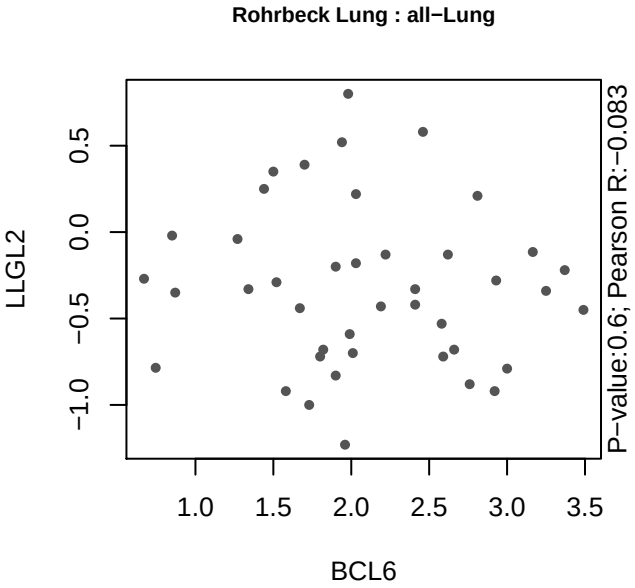

Rohrbeck Lung : all−Lung
DLG4
BCL6
P−value:0.086; Pearson R:−0.27

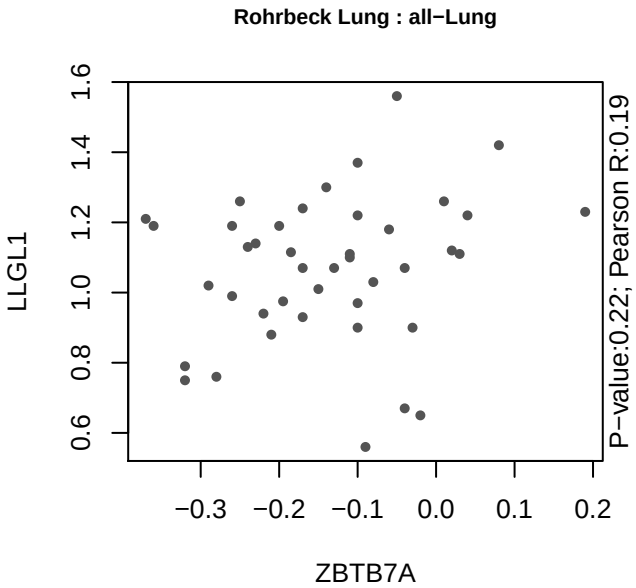

Rohrbeck Lung : all−Lung
FYN
BCL6
P−value:0.11; Pearson R:−0.25

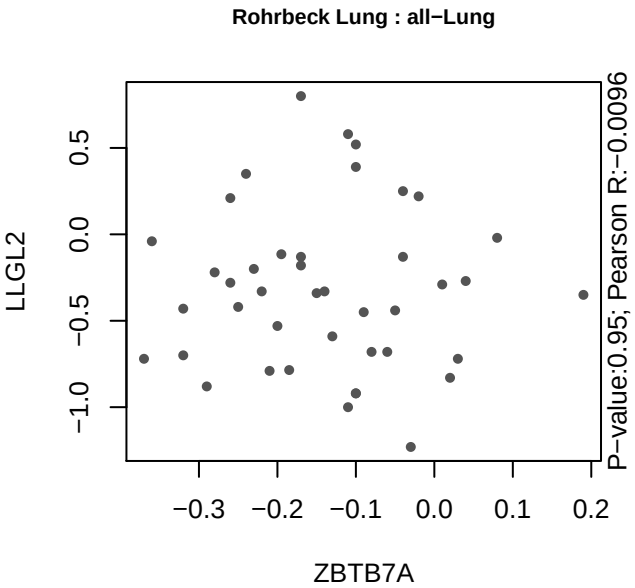

Rohrbeck Lung : all−Lung
DLG4
ZBTB7A
P−value:0.16; Pearson R:0.22

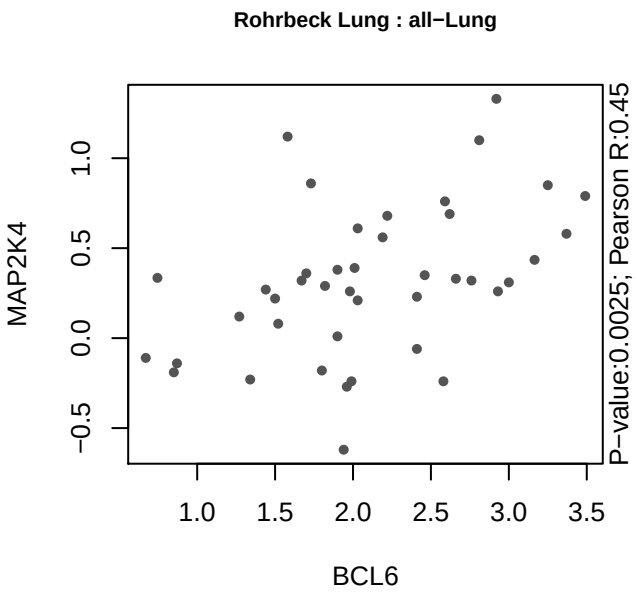

Rohrbeck Lung : all−Lung
FYN
ZBTB7A
P−value:0.55; Pearson R:−0.095

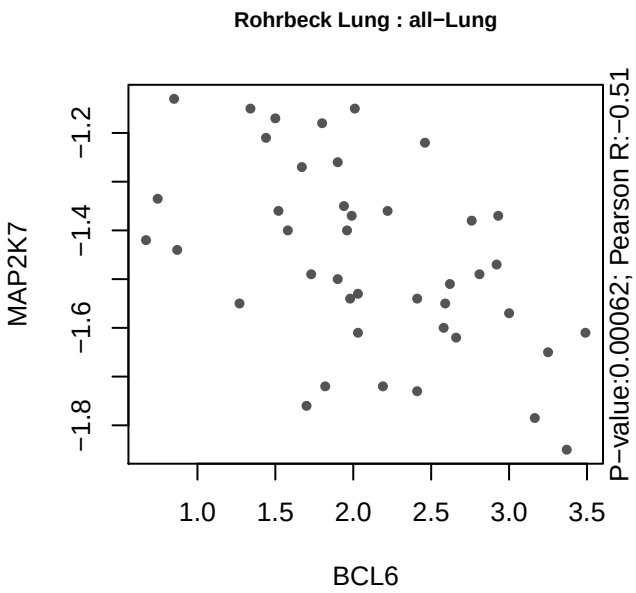

Rohrbeck Lung : all−Lung
LLGL1
BCL6
P−value:0.0038; Pearson R:−0.44

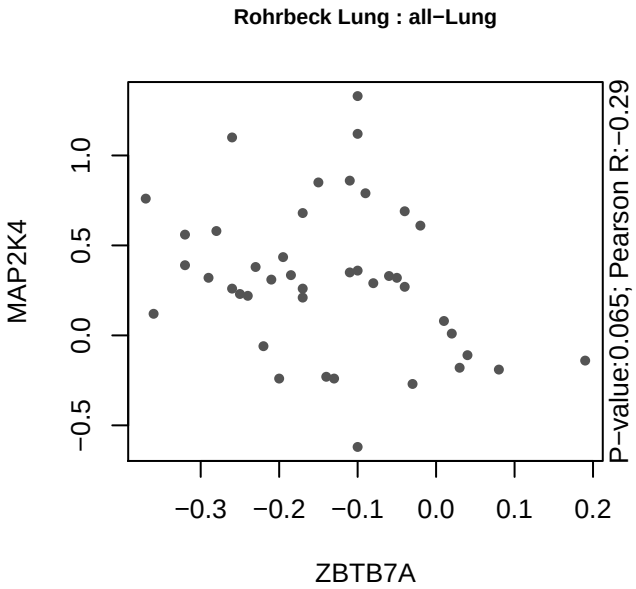

Rohrbeck Lung : all−Lung
LLGL2
BCL6
P−value:0.6; Pearson R:−0.083

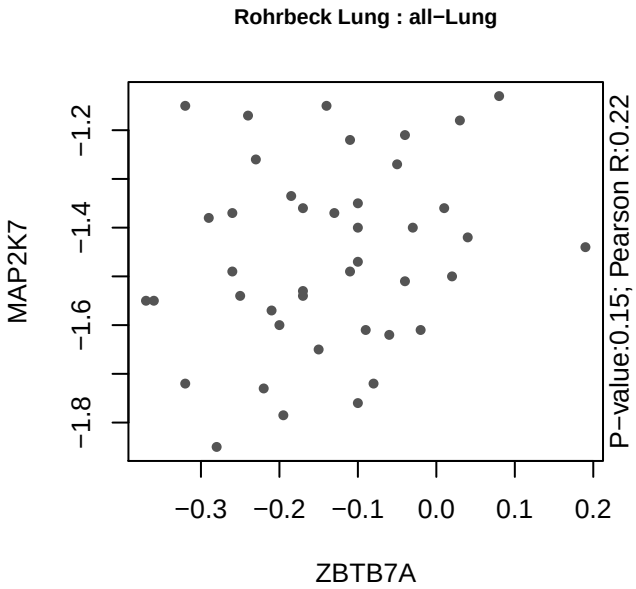

Rohrbeck Lung : all−Lung
LLGL1
ZBTB7A
P−value:0.22; Pearson R:0.19

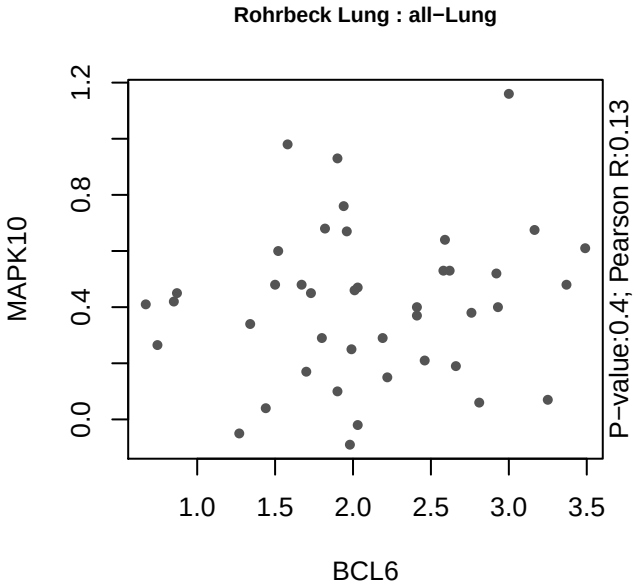

Rohrbeck Lung : all−Lung
LLGL2
ZBTB7A
P−value:0.95; Pearson R:−0.0096

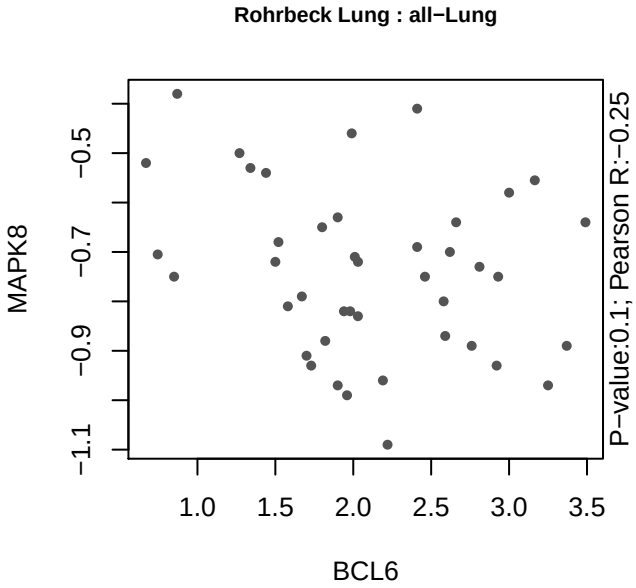

Rohrbeck Lung : all−Lung
MAP2K4
BCL6
P−value:0.0025; Pearson R:0.45

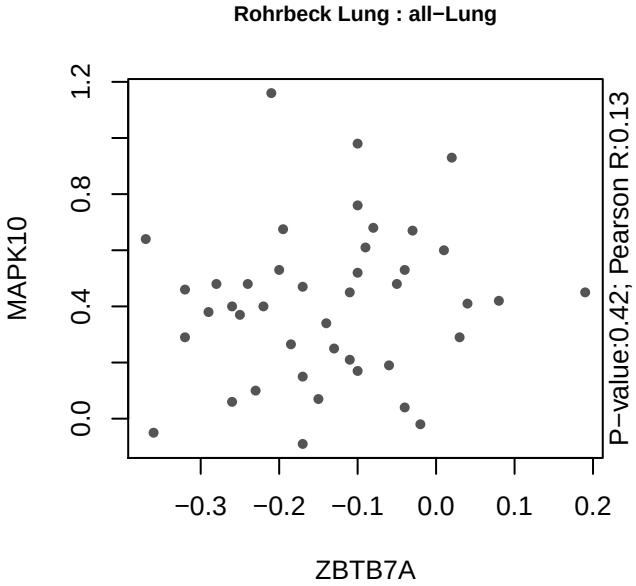

Rohrbeck Lung : all−Lung
MAP2K7
BCL6
P−value:0.00062; Pearson R:−0.51

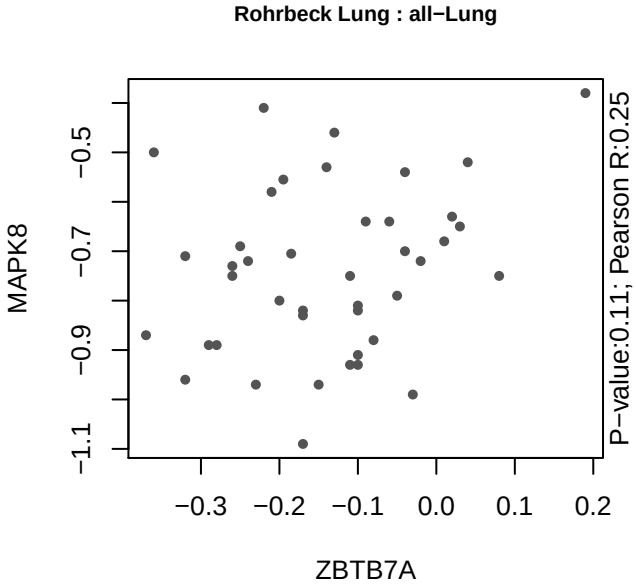

Rohrbeck Lung : all−Lung
MAP2K4
ZBTB7A
P−value:0.065; Pearson R:−0.29

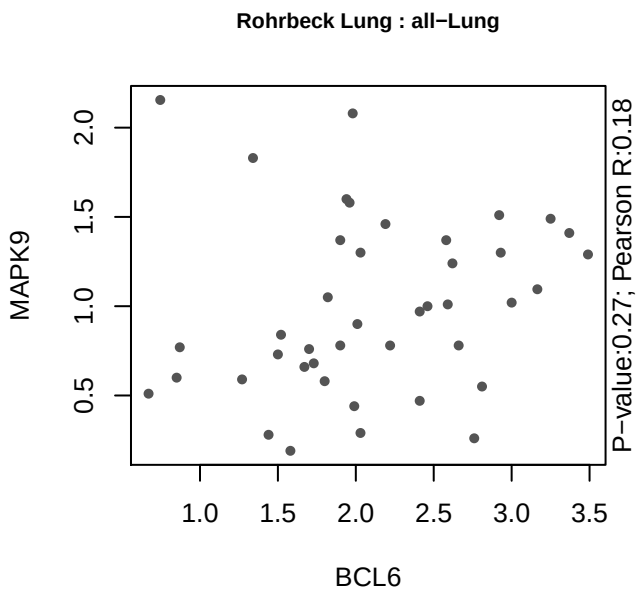

Rohrbeck Lung : all−Lung
MAP2K7
ZBTB7A
P−value:0.15; Pearson R:0.22

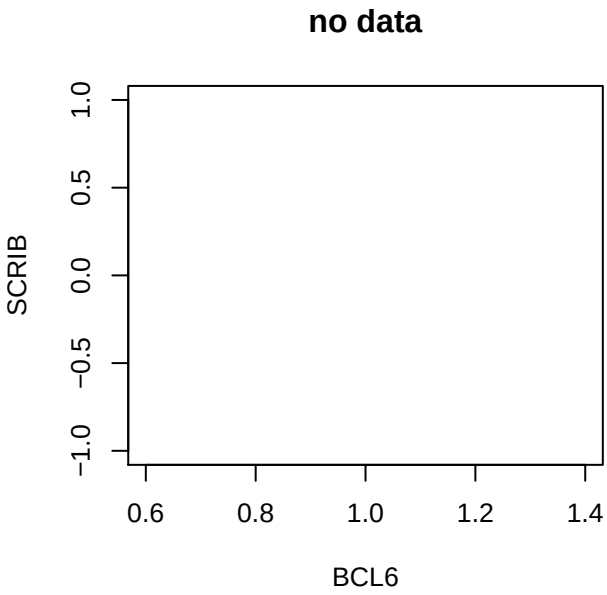

Rohrbeck Lung : all−Lung
MAPK10
BCL6
P−value:0.4; Pearson R:0.13

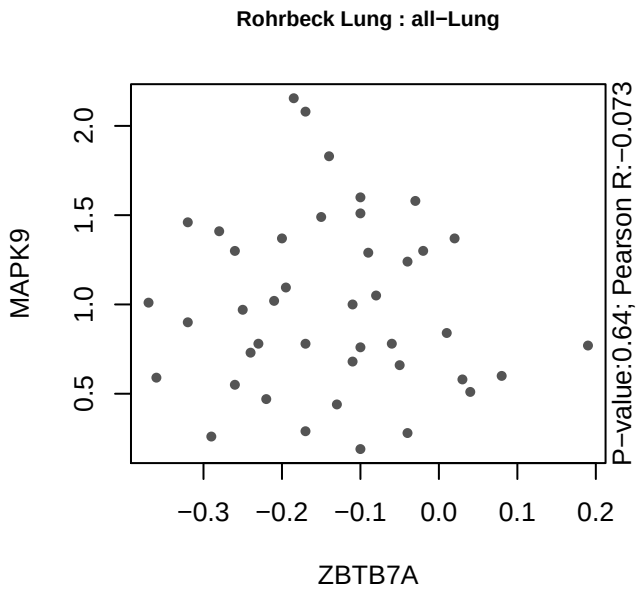

Rohrbeck Lung : all−Lung
MAPK8
BCL6
P−value:0.1; Pearson R:−0.25

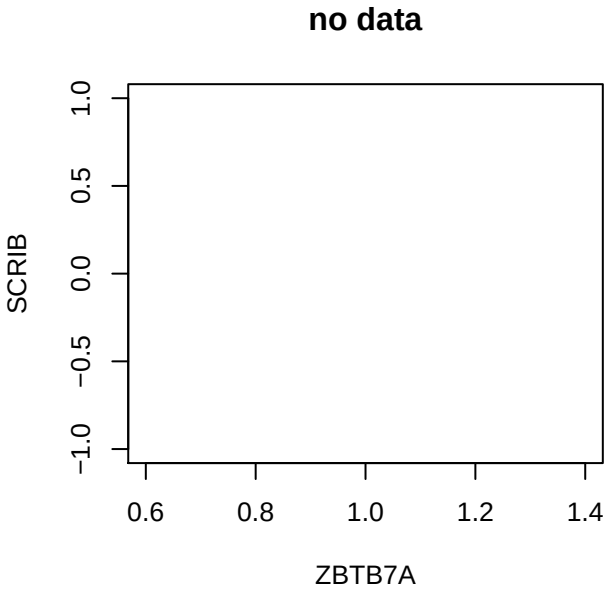

Rohrbeck Lung : all−Lung
MAPK10
ZBTB7A
P−value:0.42; Pearson R:0.13

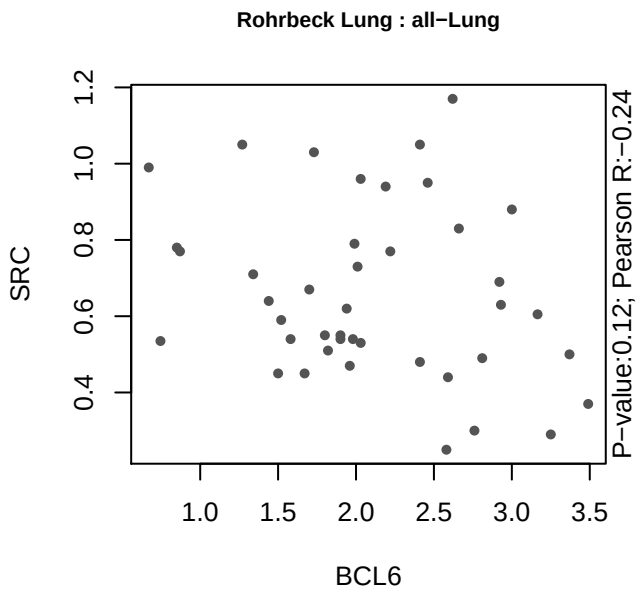

Rohrbeck Lung : all−Lung
MAPK8
ZBTB7A
P−value:0.11; Pearson R:0.25

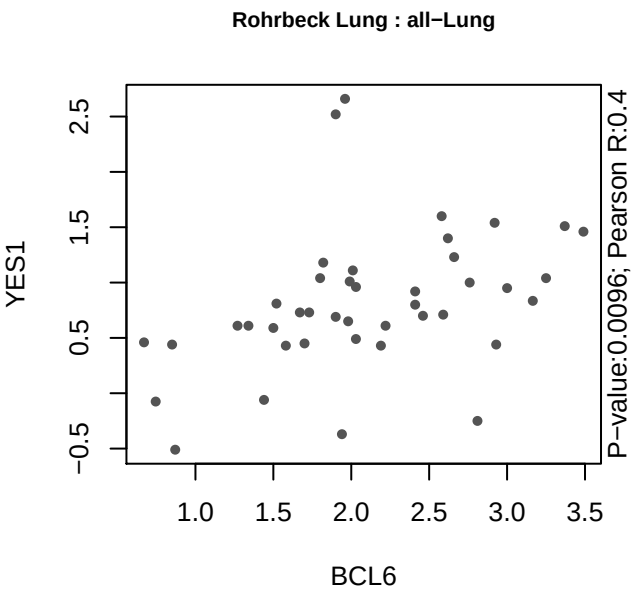

Rohrbeck Lung : all−Lung
MAPK9
BCL6
P−value:0.27; Pearson R:0.18

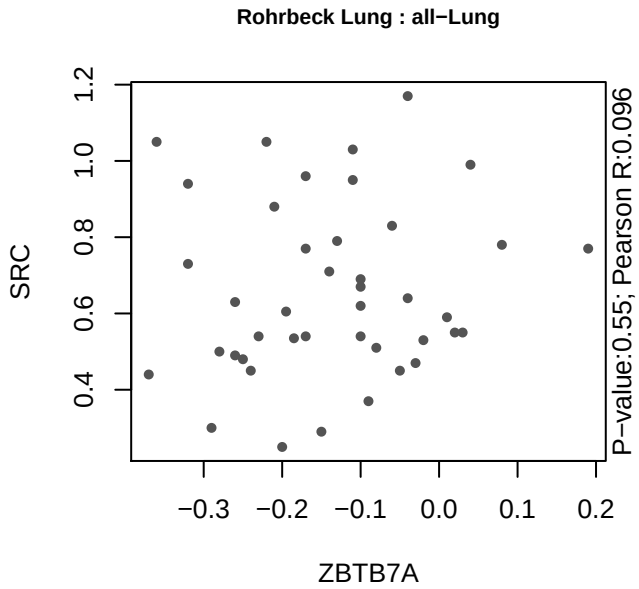

no data
SCRIB
BCL6

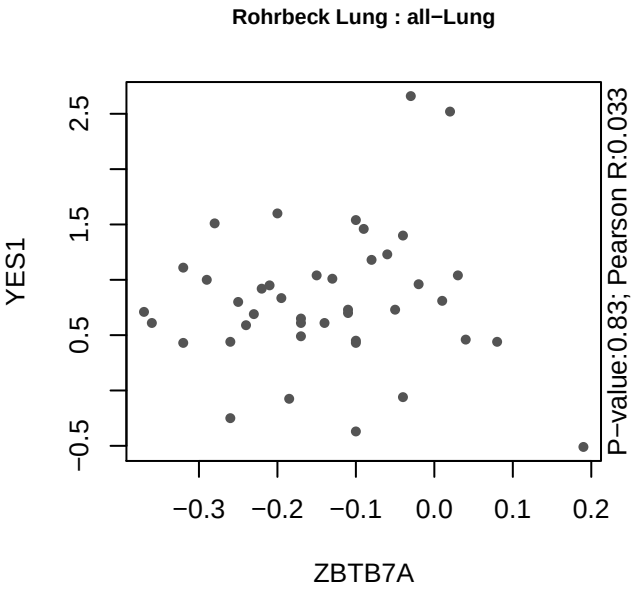

Rohrbeck Lung : all−Lung
MAPK9
ZBTB7A
P−value:0.64; Pearson R:−0.073

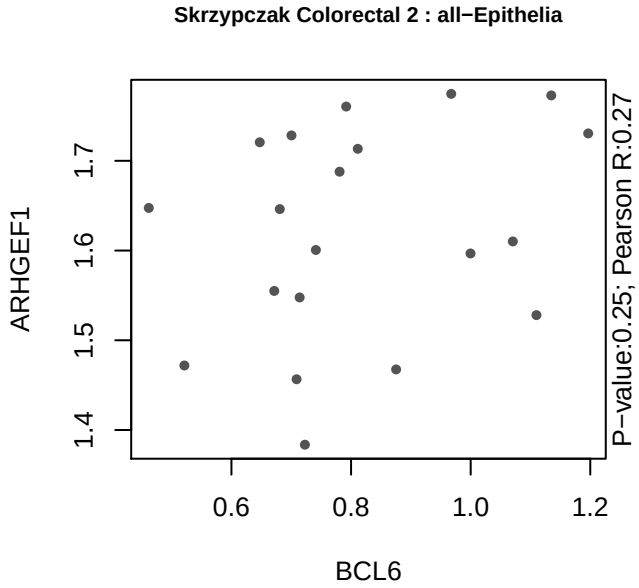

no data
SCRIB
ZBTB7A

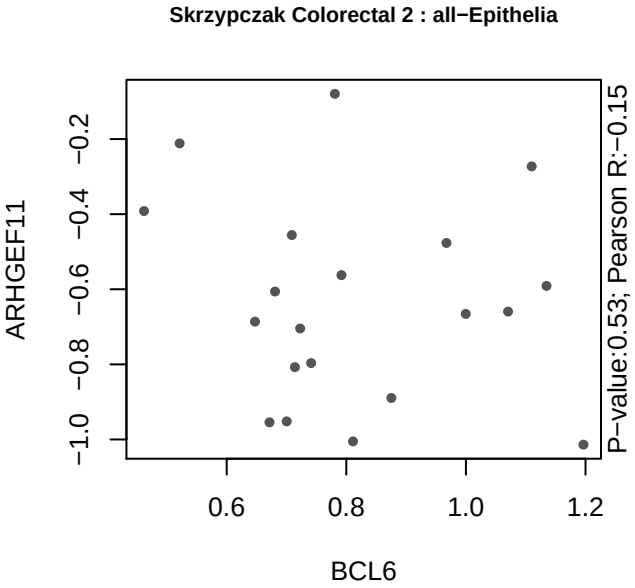

Rohrbeck Lung : all−Lung
SRC
BCL6
P−value:0.12; Pearson R:−0.24

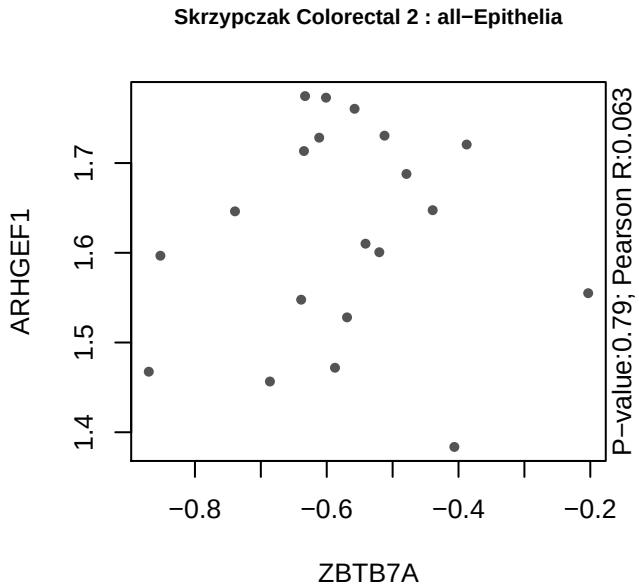

Rohrbeck Lung : all−Lung
YES1
BCL6
P−value:0.0096; Pearson R:0.4

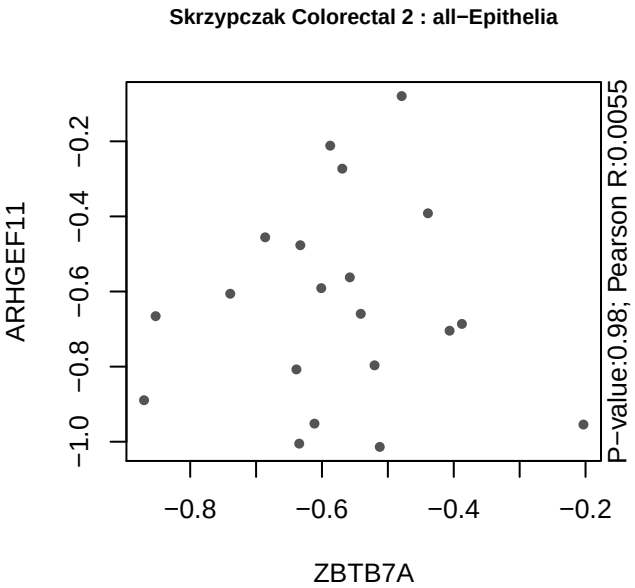

Rohrbeck Lung : all−Lung
SRC
ZBTB7A
P−value:0.55; Pearson R:0.096

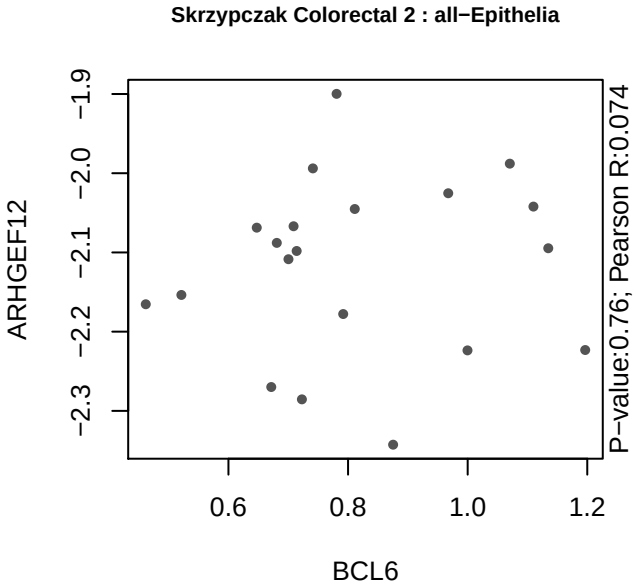

Rohrbeck Lung : all−Lung
YES1
ZBTB7A
P−value:0.83; Pearson R:0.033

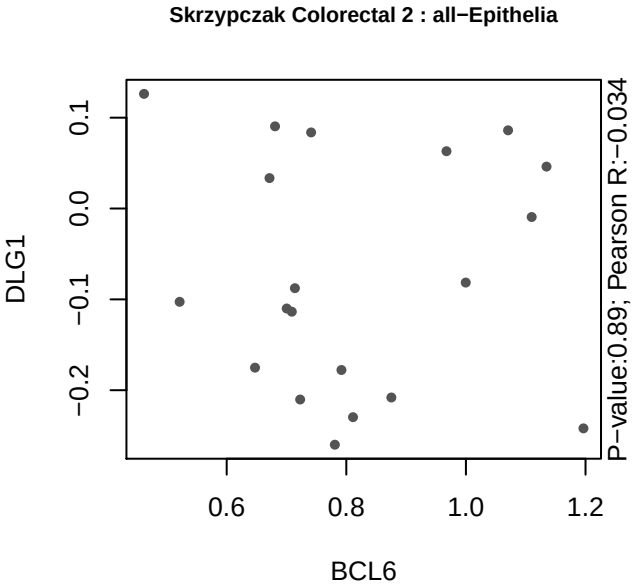

Skrzypczak Colorectal 2 : all−Epithelia
ARHGEF1
BCL6
P−value:0.25; Pearson R:0.27

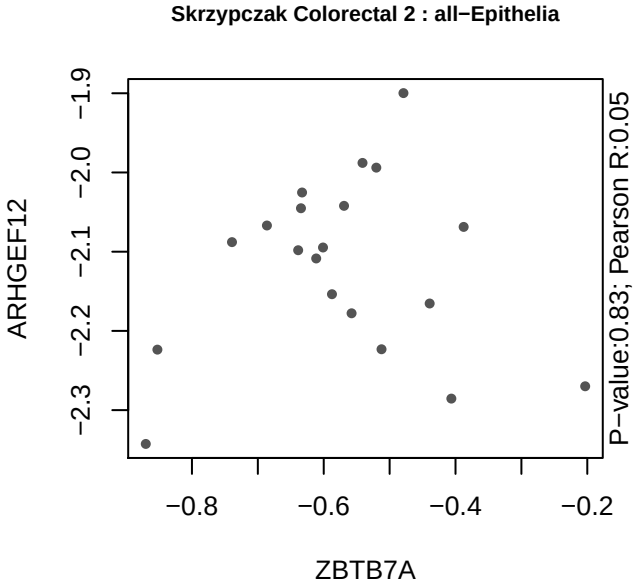

Skrzypczak Colorectal 2 : all−Epithelia
ARHGEF11
BCL6
P−value:0.53; Pearson R:−0.15

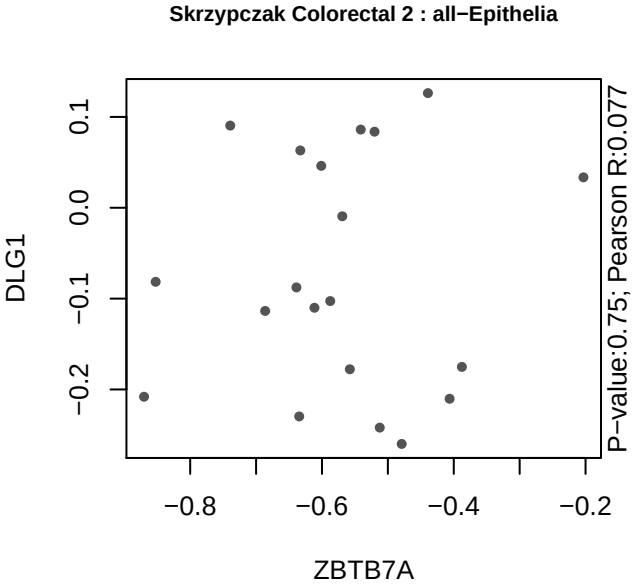

Skrzypczak Colorectal 2 : all−Epithelia
ARHGEF1
ZBTB7A
P−value:0.79; Pearson R:0.063

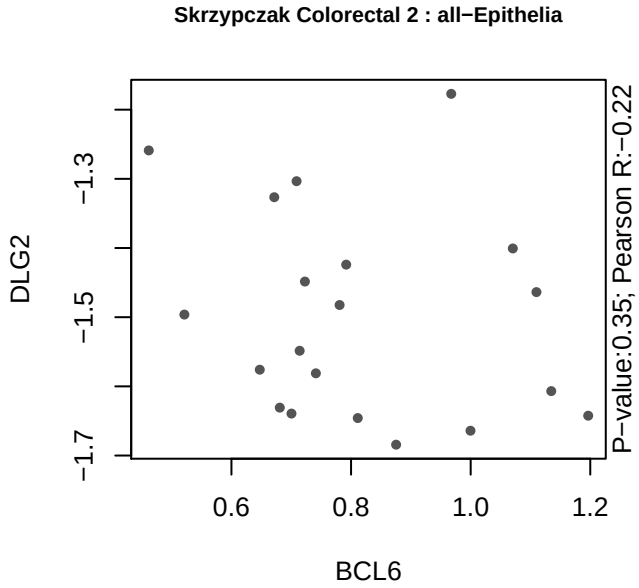

Skrzypczak Colorectal 2 : all−Epithelia
ARHGEF11
ZBTB7A
P−value:0.98; Pearson R:0.0055

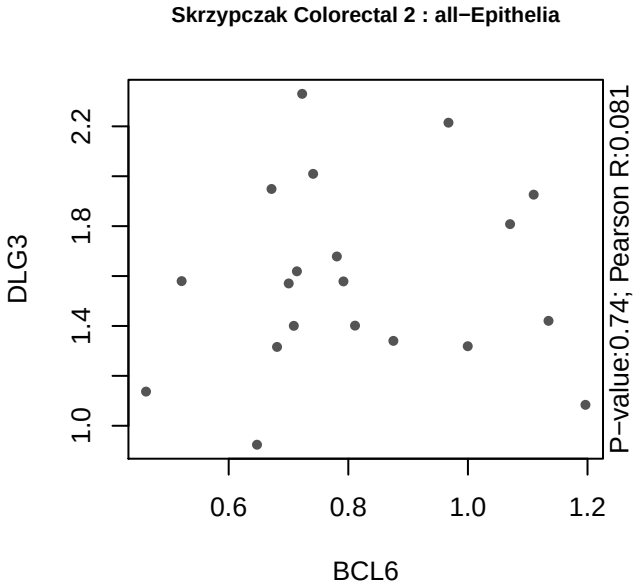

Skrzypczak Colorectal 2 : all−Epithelia
ARHGEF12
−1.9
−2.0
−2.1
−2.2
−2.3
0.6
0.8
1.0
1.2
BCL6
P−value:0.76; Pearson R:0.074

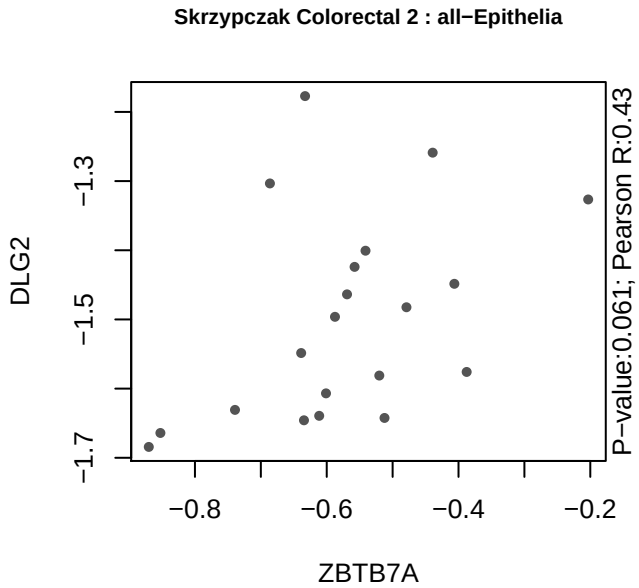

Skrzypczak Colorectal 2 : all−Epithelia
DLG1
0.1
0.0
−0.1
−0.2
0.6
0.8
1.0
1.2
BCL6
P−value:0.89; Pearson R:−0.034

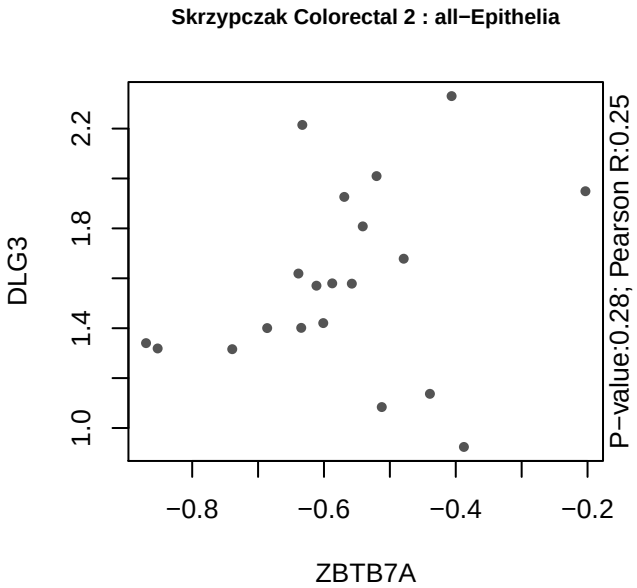

Skrzypczak Colorectal 2 : all−Epithelia
ARHGEF12
−1.9
−2.0
−2.1
−2.2
−2.3
−0.8
−0.6
−0.4
−0.2
ZBTB7A
P−value:0.83; Pearson R:0.05

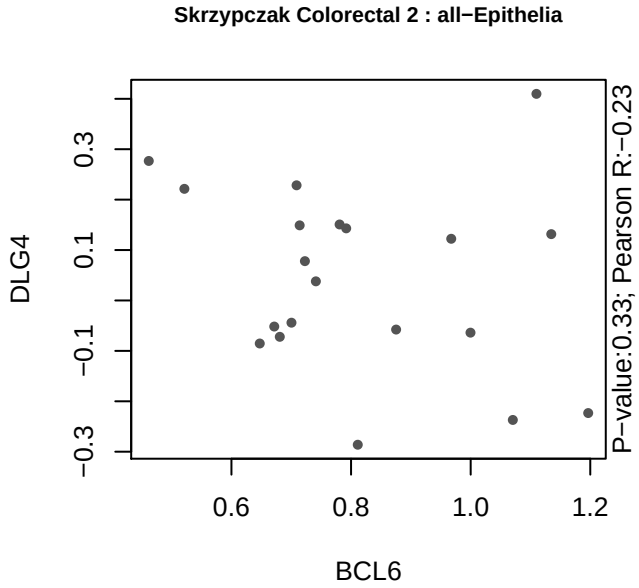

Skrzypczak Colorectal 2 : all−Epithelia
DLG1
0.1
0.0
−0.1
−0.2
−0.8
−0.6
−0.4
−0.2
ZBTB7A
P−value:0.75; Pearson R:0.077

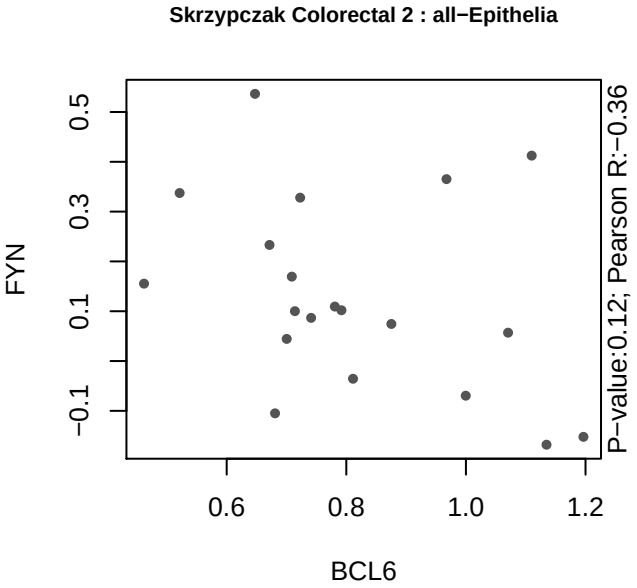

Skrzypczak Colorectal 2 : all−Epithelia
DLG2
BCL6
P−value:0.35; Pearson R:−0.22

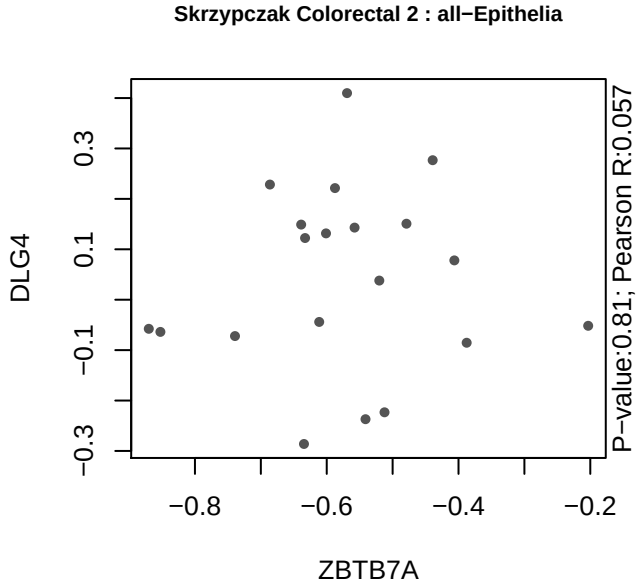

Skrzypczak Colorectal 2 : all−Epithelia
DLG3
BCL6
P−value:0.74; Pearson R:0.081

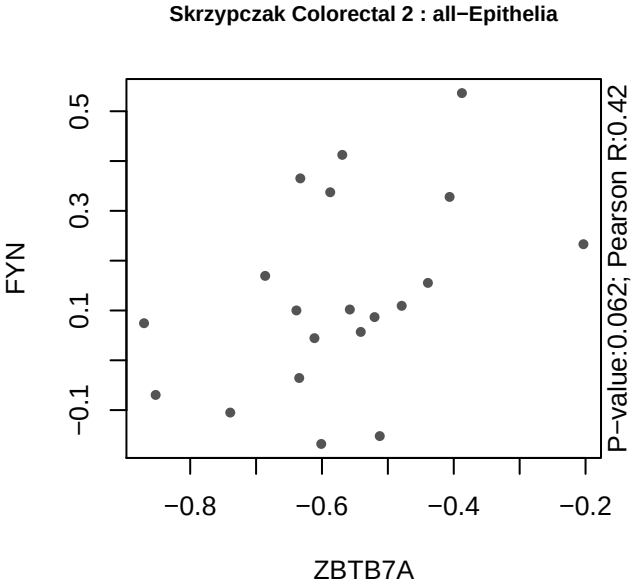

Skrzypczak Colorectal 2 : all−Epithelia
DLG2
ZBTB7A
P−value:0.061; Pearson R:0.43

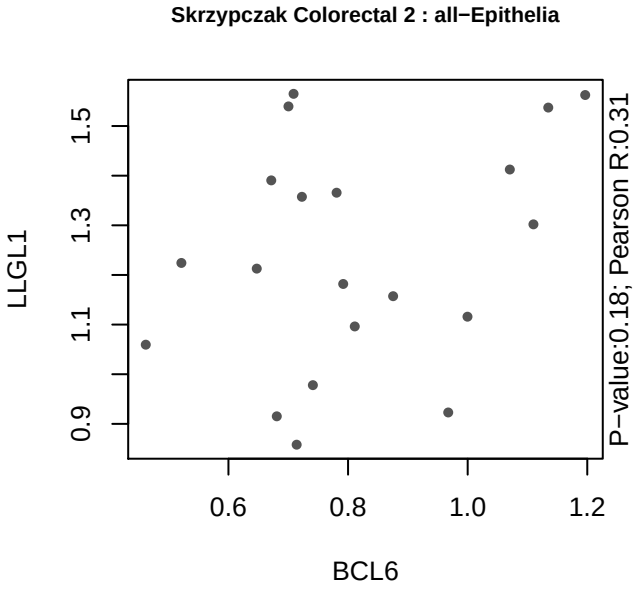

Skrzypczak Colorectal 2 : all−Epithelia
DLG3
ZBTB7A
P−value:0.28; Pearson R:0.25

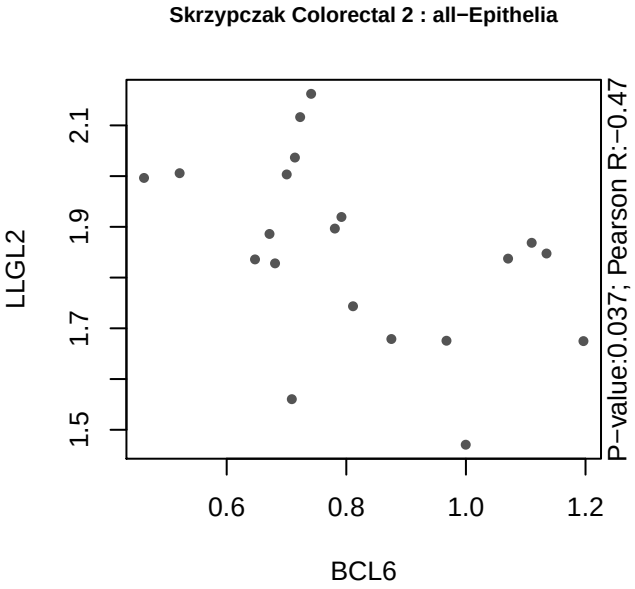

Skrzypczak Colorectal 2 : all−Epithelia
DLG4
BCL6
P−value:0.33; Pearson R:−0.23
−0.3
−0.1
0.1
0.3
0.6
0.8
1.0
1.2

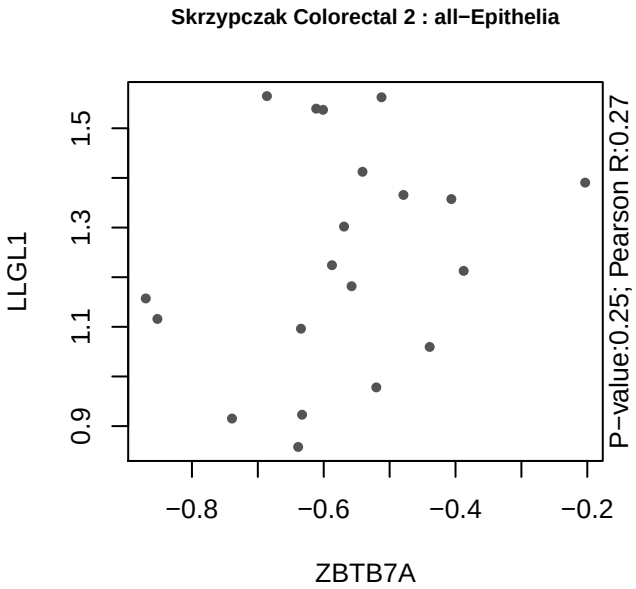

Skrzypczak Colorectal 2 : all−Epithelia
FYN
BCL6
P−value:0.12; Pearson R:−0.36
−0.1
0.1
0.3
0.5
0.6
0.8
1.0
1.2

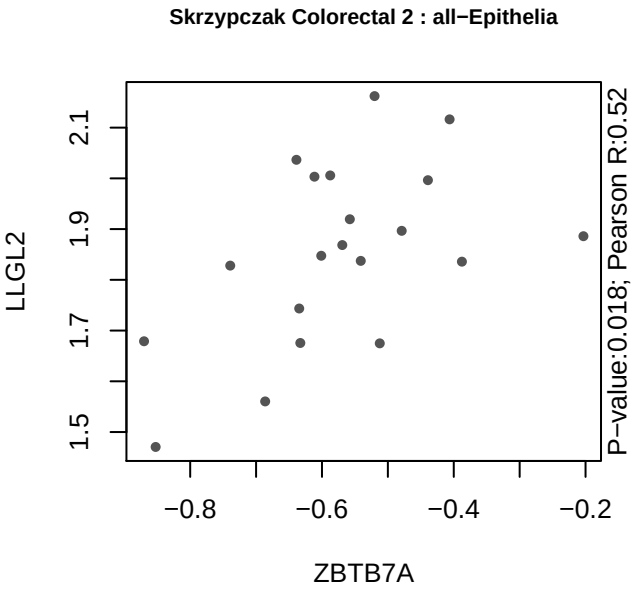

Skrzypczak Colorectal 2 : all−Epithelia
DLG4
ZBTB7A
P−value:0.81; Pearson R:0.057
−0.3
−0.1
0.1
0.3
−0.8
−0.6
−0.4
−0.2

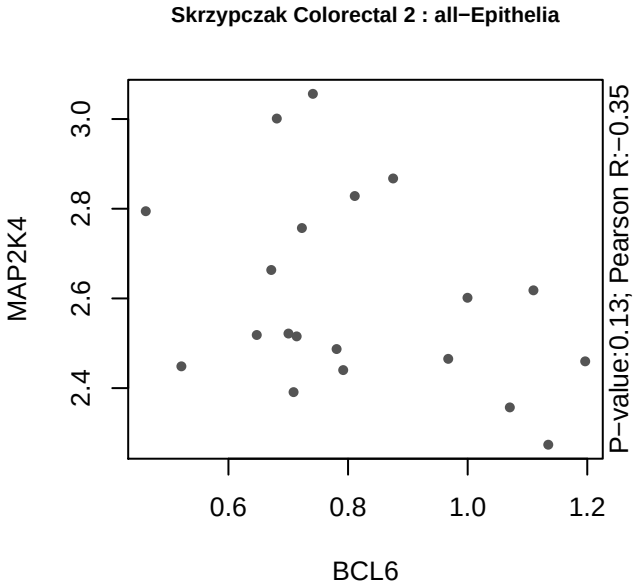

Skrzypczak Colorectal 2 : all−Epithelia
FYN
ZBTB7A
P−value:0.062; Pearson R:0.42
−0.1
0.1
0.3
0.5
−0.8
−0.6
−0.4
−0.2

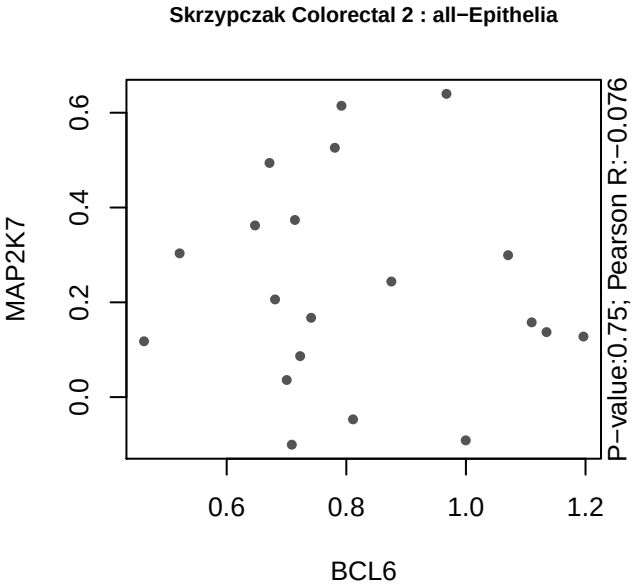

Skrzypczak Colorectal 2 : all−Epithelia
LLGL1
BCL6
P−value:0.18; Pearson R:0.31
0.9
1.1
1.3
1.5
0.6
0.8
1.0
1.2

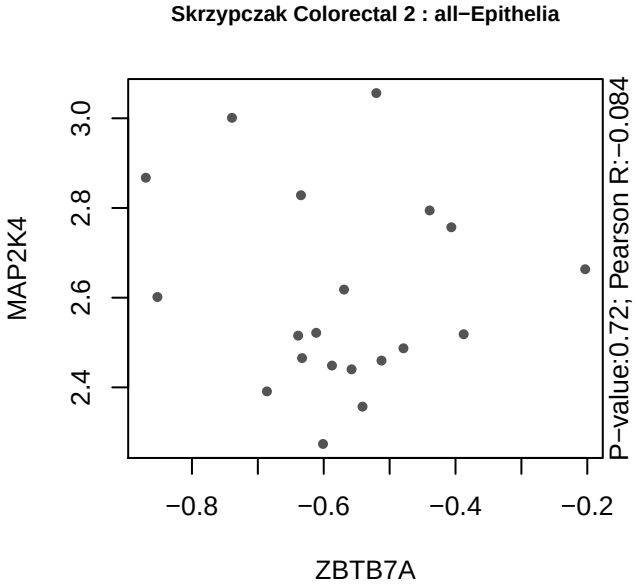

Skrzypczak Colorectal 2 : all−Epithelia
LLGL2
BCL6
P−value:0.037; Pearson R:−0.47
1.5
1.7
1.9
2.1
0.6
0.8
1.0
1.2

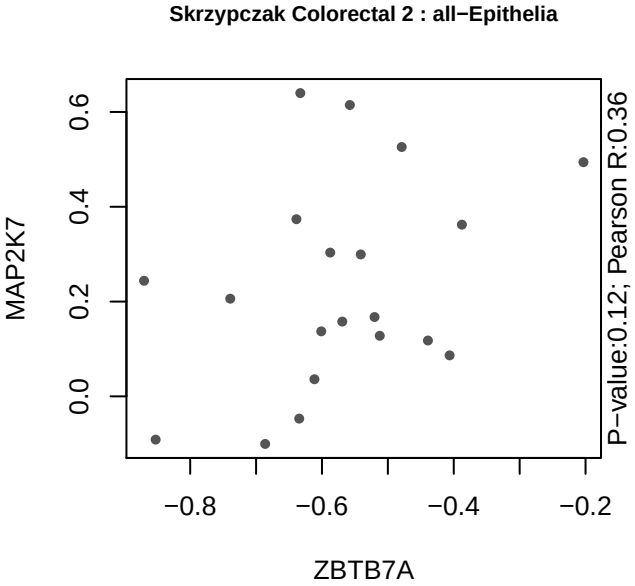

Skrzypczak Colorectal 2 : all−Epithelia
LLGL1
ZBTB7A
P−value:0.25; Pearson R:0.27
0.9
1.1
1.3
1.5
−0.8
−0.6
−0.4
−0.2

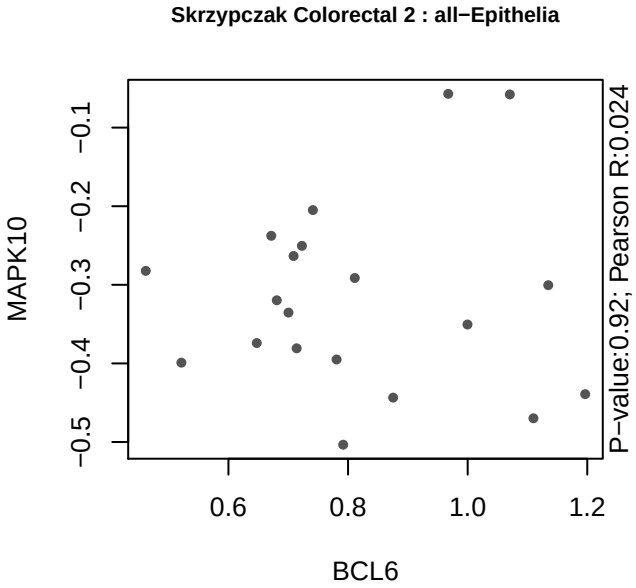

Skrzypczak Colorectal 2 : all−Epithelia
LLGL2
ZBTB7A
P−value:0.018; Pearson R:0.52
1.5
1.7
1.9
2.1
−0.8
−0.6
−0.4
−0.2

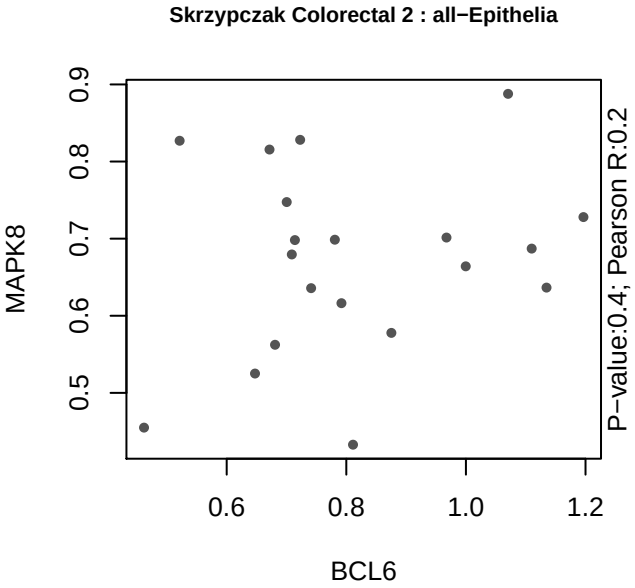

Skrzypczak Colorectal 2 : all−Epithelia
MAP2K4
BCL6
P−value:0.13; Pearson R:−0.35

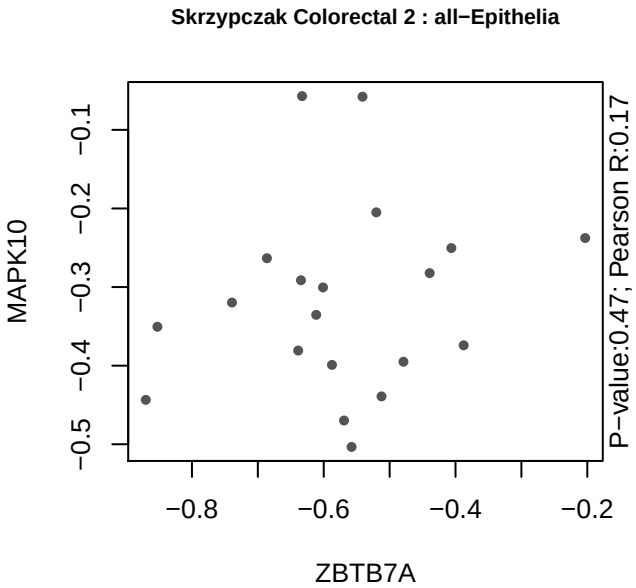

Skrzypczak Colorectal 2 : all−Epithelia
MAP2K7
BCL6
P−value:0.75; Pearson R:−0.076

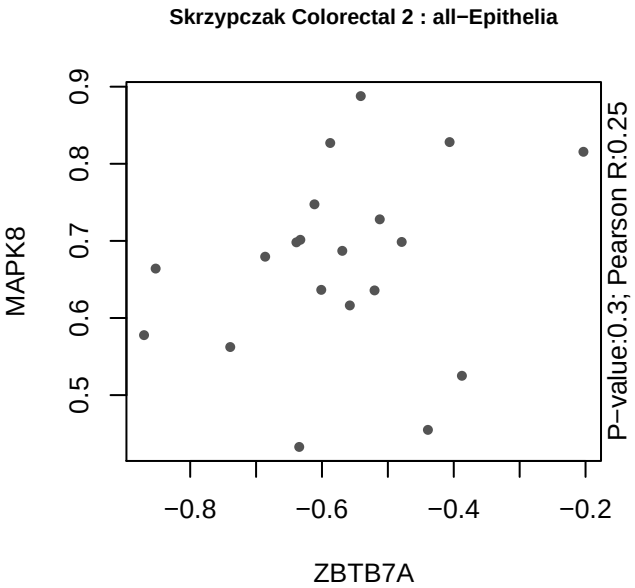

Skrzypczak Colorectal 2 : all−Epithelia
MAP2K4
ZBTB7A
P−value:0.72; Pearson R:−0.084

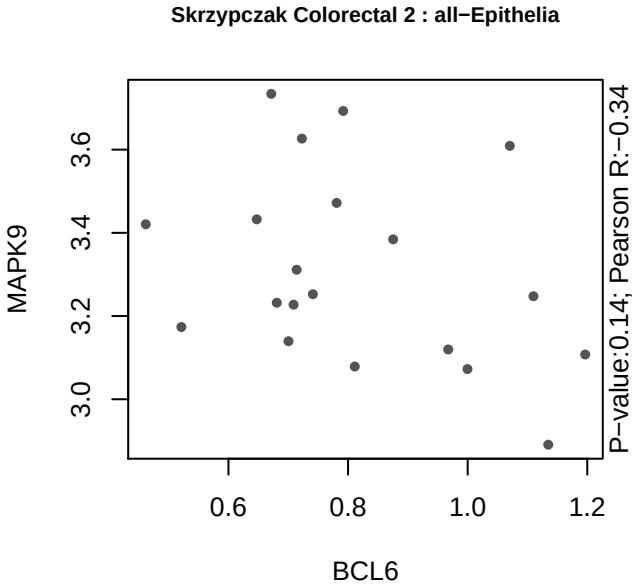

Skrzypczak Colorectal 2 : all−Epithelia
MAP2K7
ZBTB7A
P−value:0.12; Pearson R:0.36

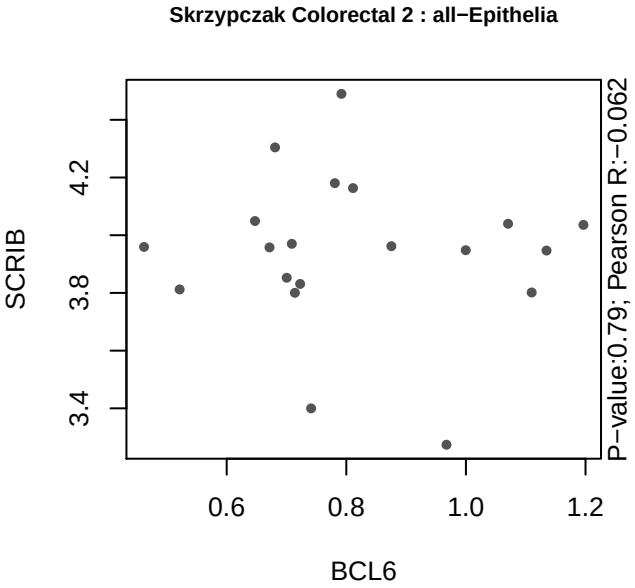

Skrzypczak Colorectal 2 : all−Epithelia
MAPK10
BCL6
P−value:0.92; Pearson R:0.024

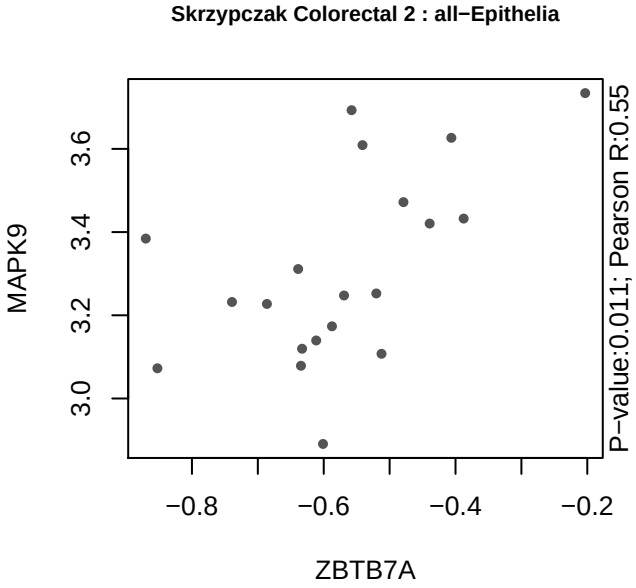

Skrzypczak Colorectal 2 : all−Epithelia
MAPK8
BCL6
P−value:0.4; Pearson R:0.2

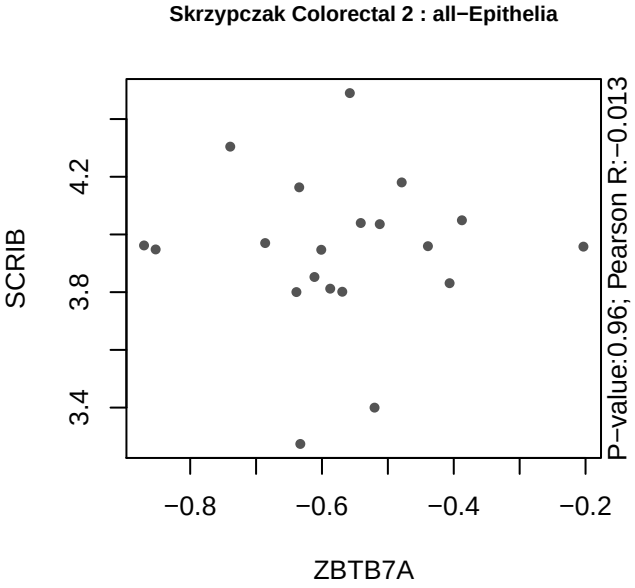

Skrzypczak Colorectal 2 : all−Epithelia
MAPK10
ZBTB7A
P−value:0.47; Pearson R:0.17

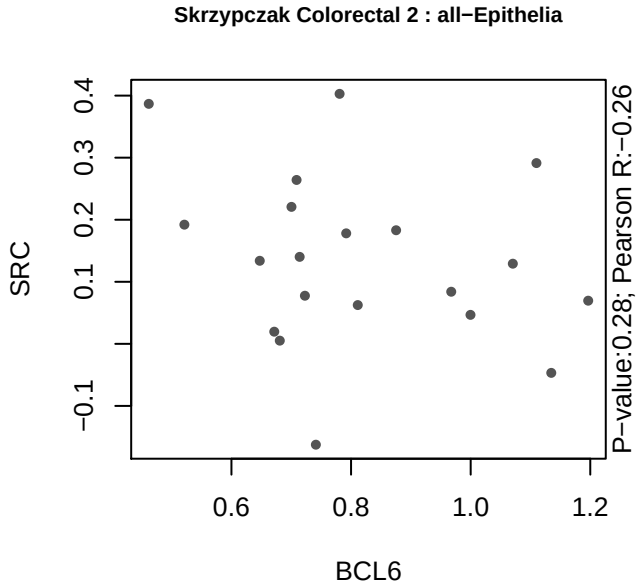

Skrzypczak Colorectal 2 : all−Epithelia
MAPK8
ZBTB7A
P−value:0.3; Pearson R:0.25

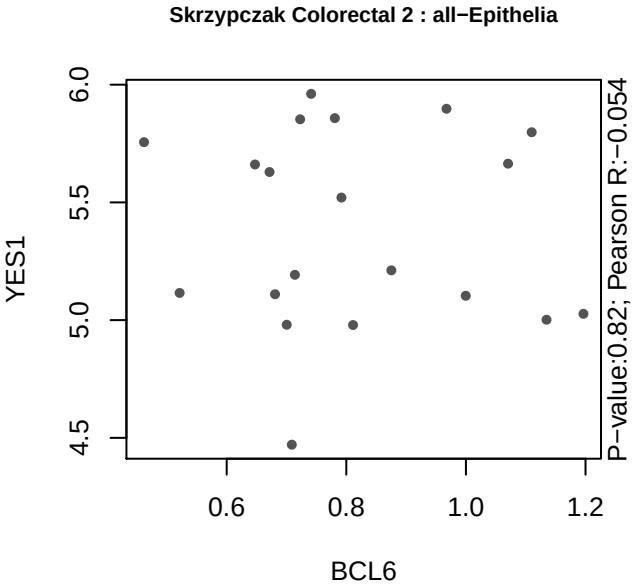

Skrzypczak Colorectal 2 : all−Epithelia
MAPK9
3.0
3.2
3.4
3.6
0.6
0.8
1.0
1.2
BCL6
P−value:0.14; Pearson R:−0.34

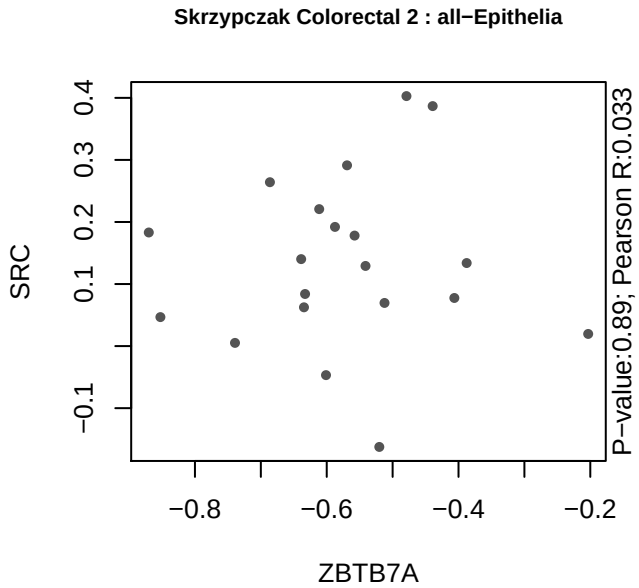

Skrzypczak Colorectal 2 : all−Epithelia
SCRIB
3.4
3.8
4.2
0.6
0.8
1.0
1.2
BCL6
P−value:0.79; Pearson R:−0.062

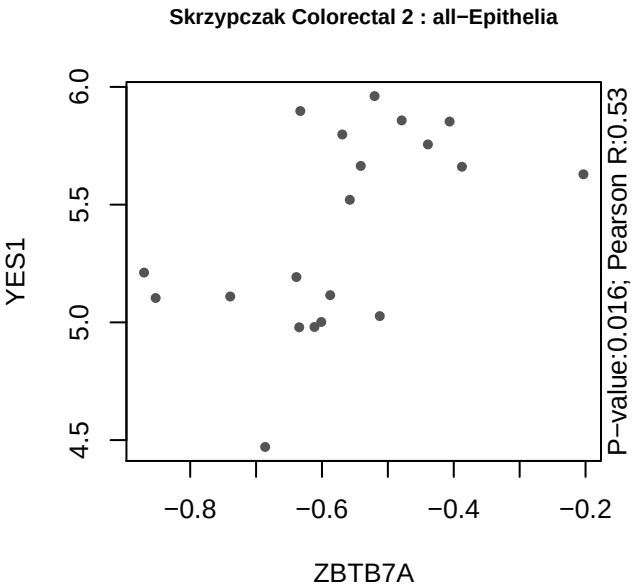

Skrzypczak Colorectal 2 : all−Epithelia
MAPK9
3.0
3.2
3.4
3.6
−0.8
−0.6
−0.4
−0.2
ZBTB7A
P−value:0.011; Pearson R:0.55

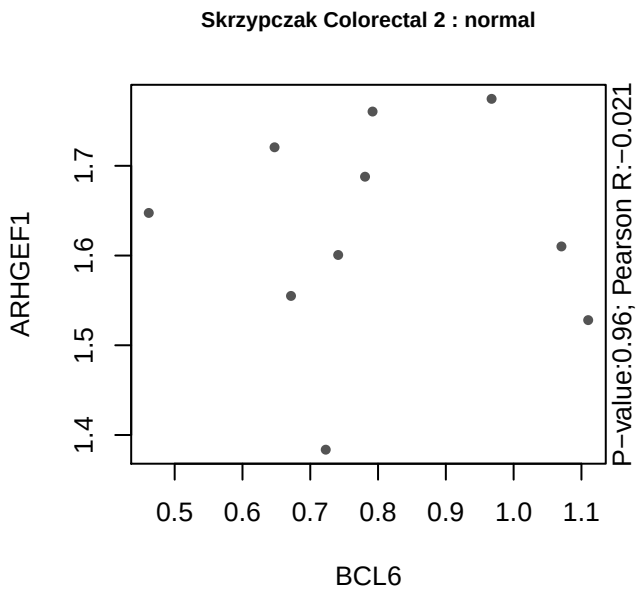

Skrzypczak Colorectal 2 : all−Epithelia
SCRIB
3.4
3.8
4.2
−0.8
−0.6
−0.4
−0.2
ZBTB7A
P−value:0.96; Pearson R:−0.013

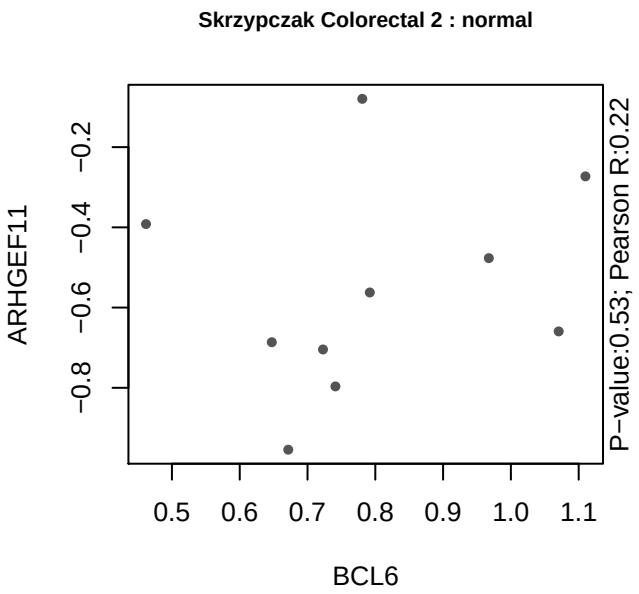

Skrzypczak Colorectal 2 : all−Epithelia
SRC
BCL6
P−value:0.28; Pearson R:−0.26
−0.1
0.1
0.2
0.3
0.4
0.6
0.8
1.0
1.2

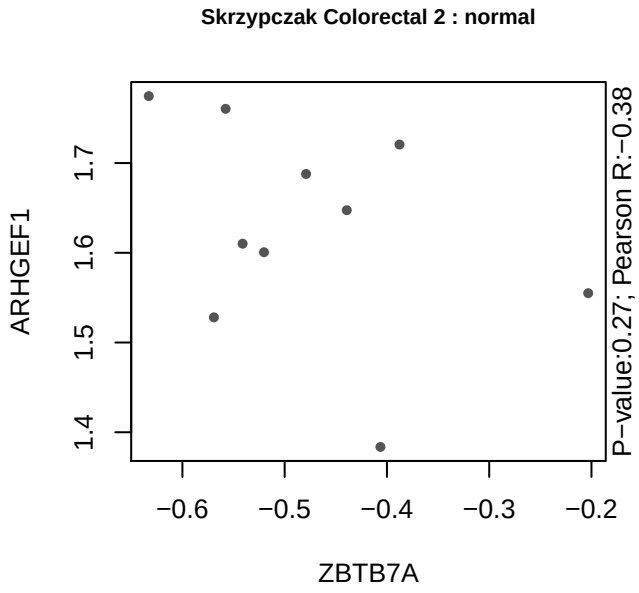

Skrzypczak Colorectal 2 : all−Epithelia
YES1
BCL6
P−value:0.82; Pearson R:−0.054
4.5
5.0
5.5
6.0
0.6
0.8
1.0
1.2

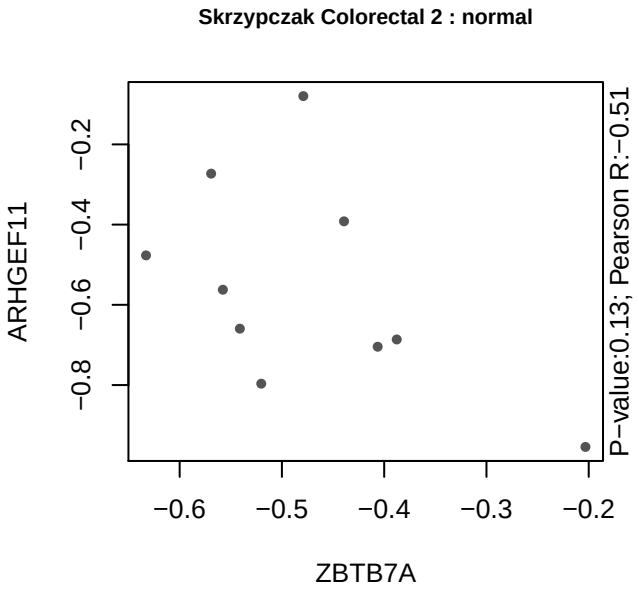

Skrzypczak Colorectal 2 : all−Epithelia
SRC
ZBTB7A
P−value:0.89; Pearson R:0.033
−0.1
0.1
0.2
0.3
0.4
−0.8
−0.6
−0.4
−0.2

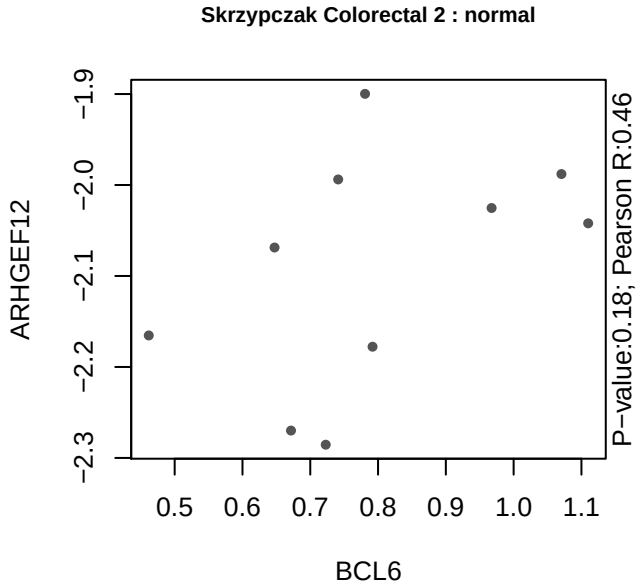

Skrzypczak Colorectal 2 : all−Epithelia
YES1
ZBTB7A
P−value:0.016; Pearson R:0.53
4.5
5.0
5.5
6.0
−0.8
−0.6
−0.4
−0.2

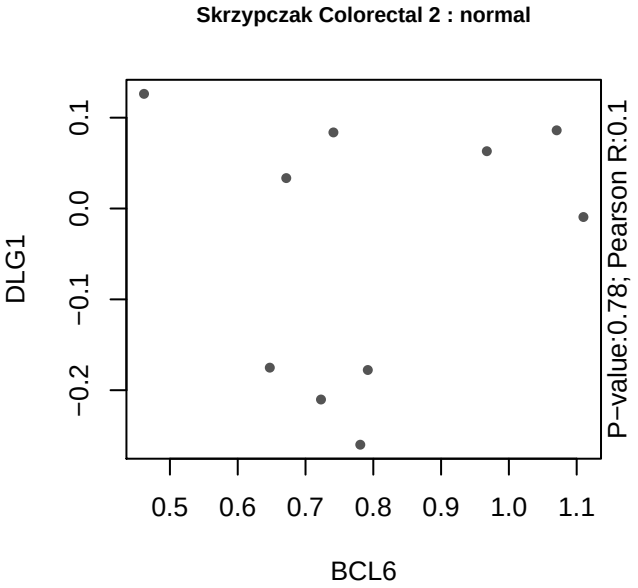

Skrzypczak Colorectal 2 : normal
ARHGEF1
BCL6
P−value:0.96; Pearson R:−0.021

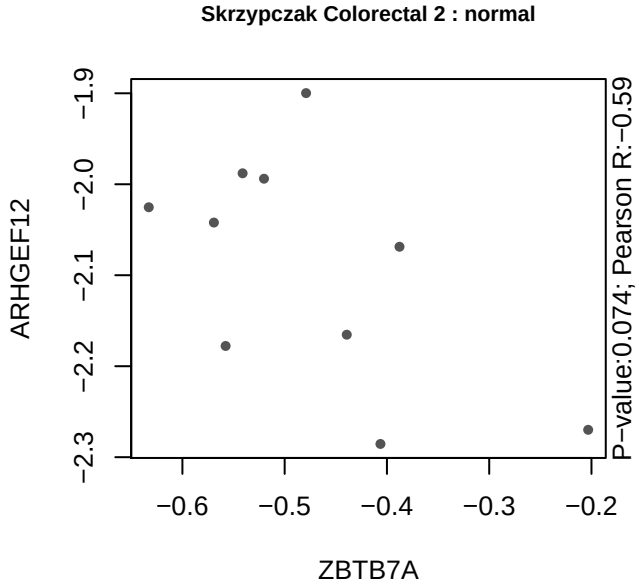

Skrzypczak Colorectal 2 : normal
ARHGEF11
BCL6
P−value:0.53; Pearson R:0.22

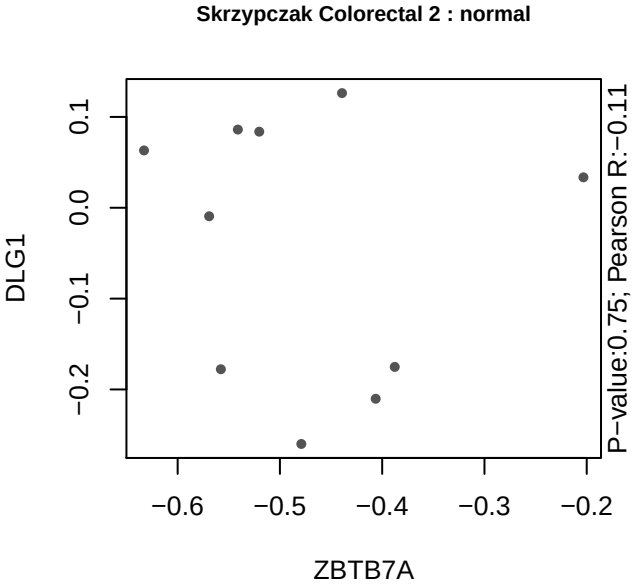

Skrzypczak Colorectal 2 : normal
ARHGEF1
ZBTB7A
P−value:0.27; Pearson R:−0.38

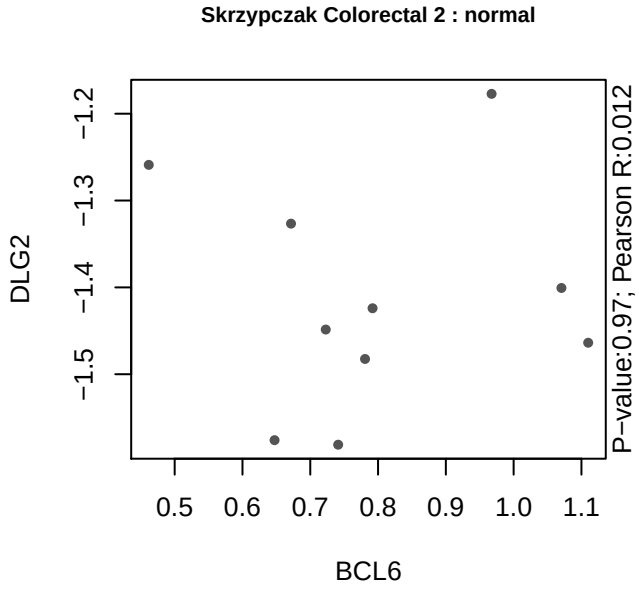

Skrzypczak Colorectal 2 : normal
ARHGEF11
ZBTB7A
P−value:0.13; Pearson R:−0.51

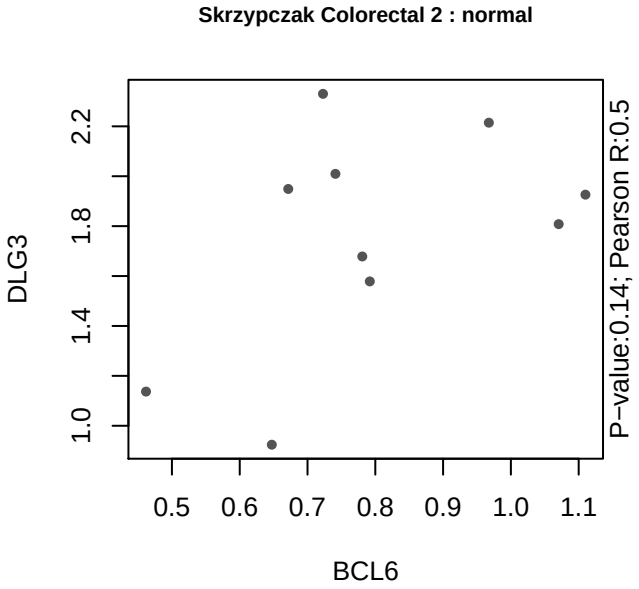

Skrzypczak Colorectal 2 : normal
ARHGEF12
BCL6
P−value:0.18; Pearson R:0.46

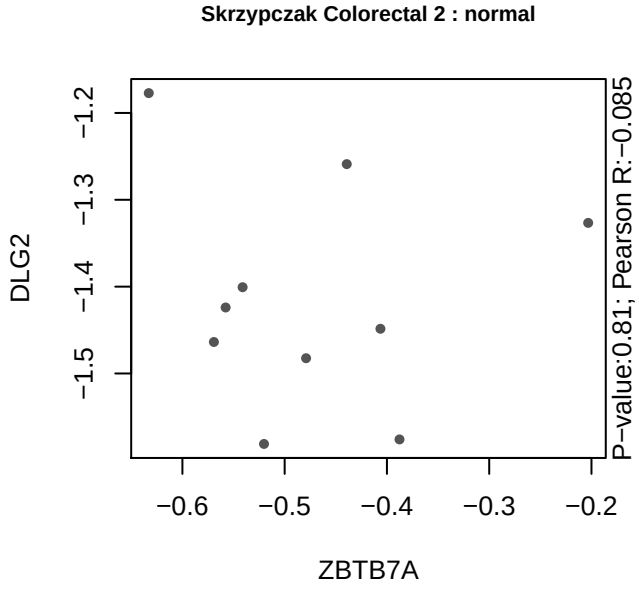

Skrzypczak Colorectal 2 : normal
DLG1
BCL6
P−value:0.78; Pearson R:0.1

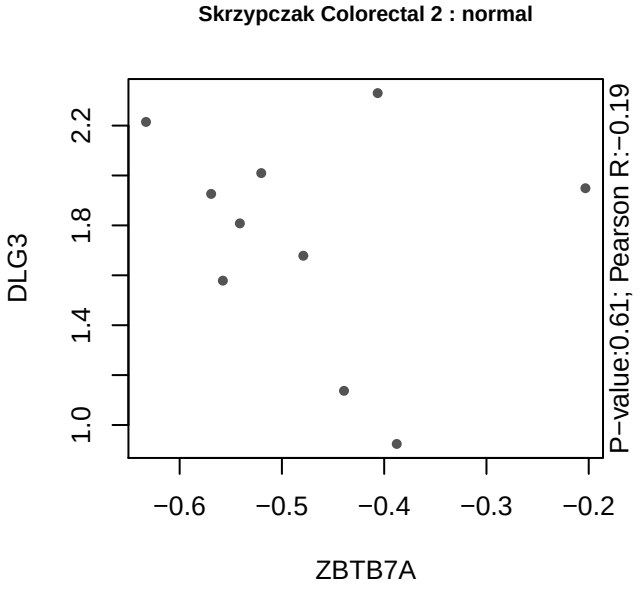

Skrzypczak Colorectal 2 : normal
ARHGEF12
ZBTB7A
P−value:0.074; Pearson R:−0.59

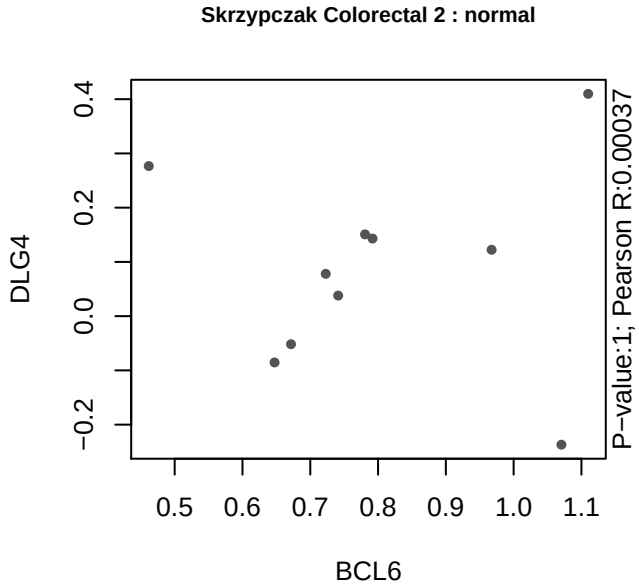

Skrzypczak Colorectal 2 : normal
DLG1
ZBTB7A
P−value:0.75; Pearson R:−0.11

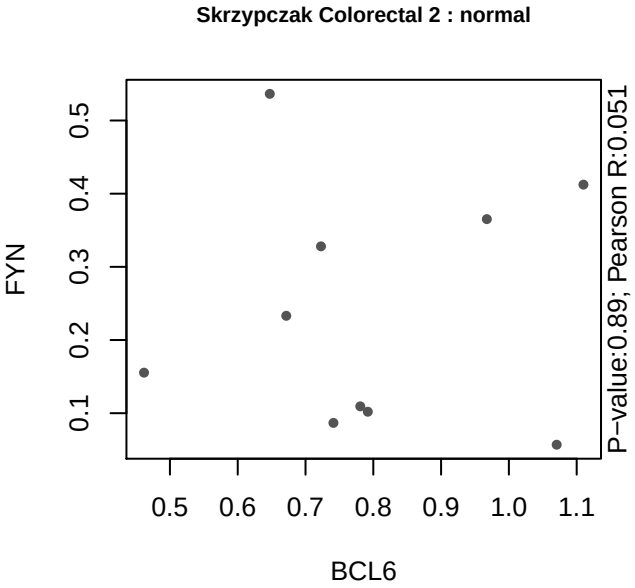

Skrzypczak Colorectal 2 : normal
DLG2
BCL6
P−value:0.97; Pearson R:0.012

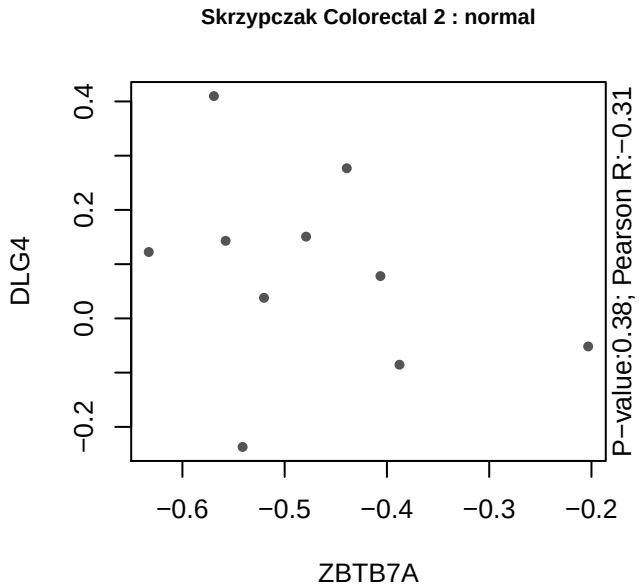

Skrzypczak Colorectal 2 : normal
DLG3
BCL6
P−value:0.14; Pearson R:0.5

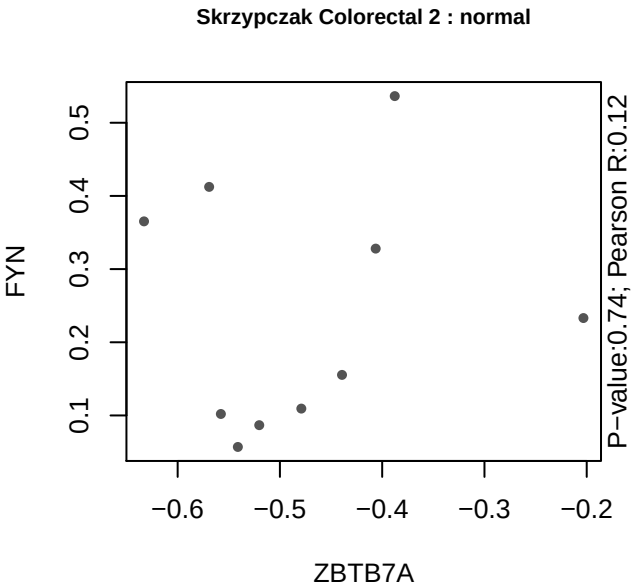

Skrzypczak Colorectal 2 : normal
DLG2
ZBTB7A
P−value:0.81; Pearson R:−0.085

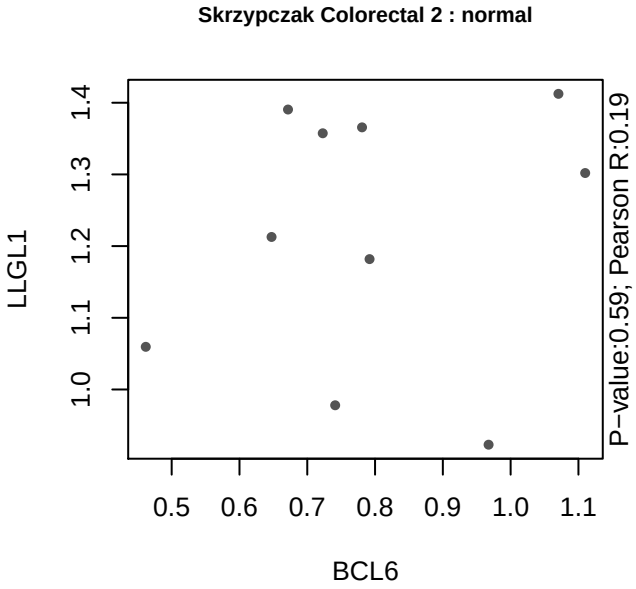

Skrzypczak Colorectal 2 : normal
DLG3
ZBTB7A
P−value:0.61; Pearson R:−0.19

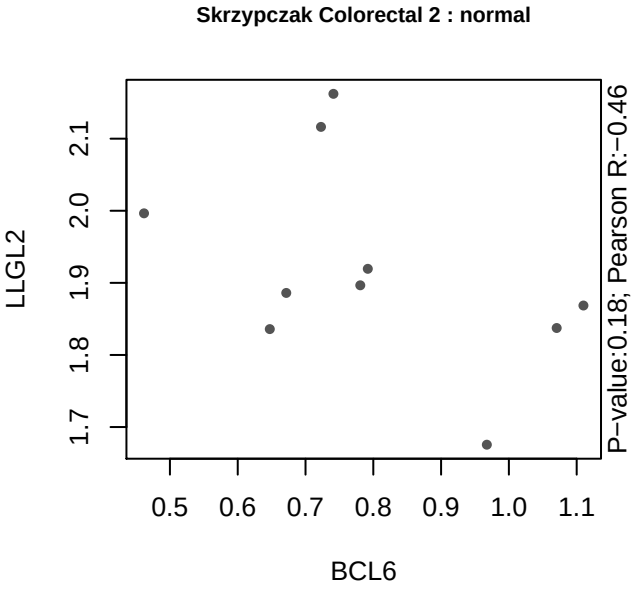

Skrzypczak Colorectal 2 : normal
DLG4
BCL6
P−value:1; Pearson R:0.00037

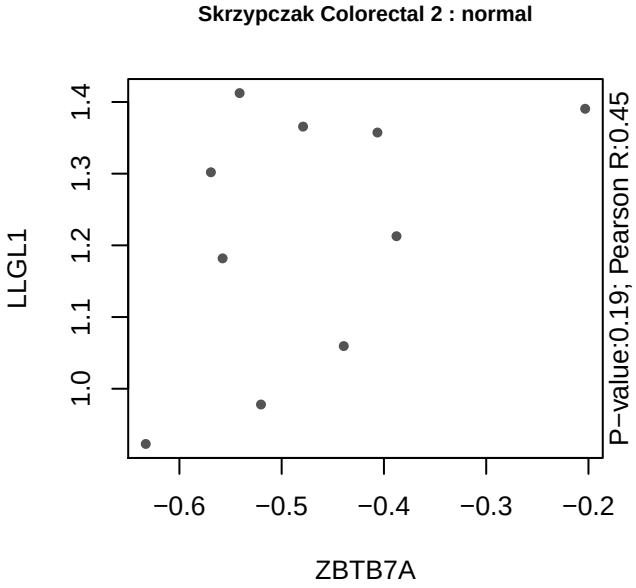

Skrzypczak Colorectal 2 : normal
FYN
BCL6
P−value:0.89; Pearson R:0.051

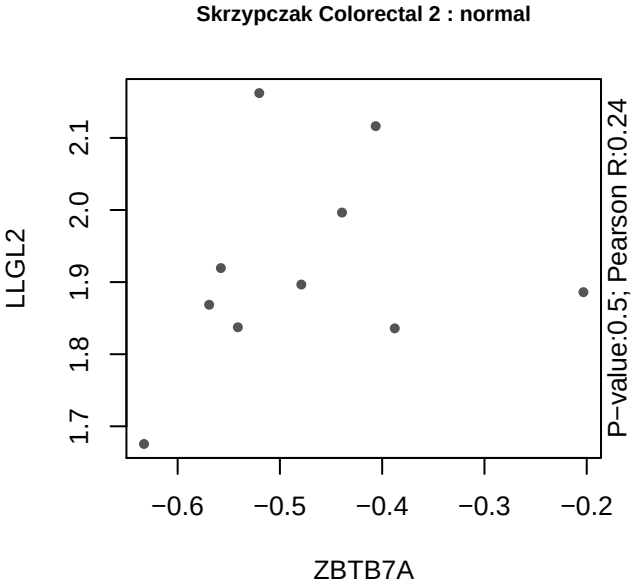

Skrzypczak Colorectal 2 : normal
DLG4
ZBTB7A
P−value:0.38; Pearson R:−0.31

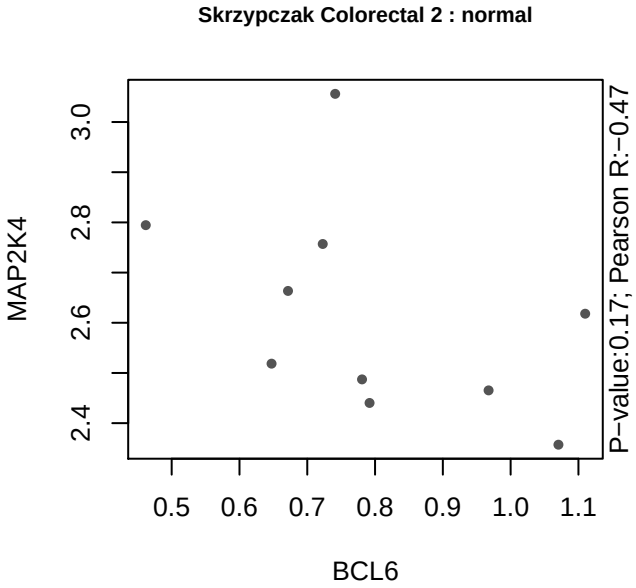

Skrzypczak Colorectal 2 : normal
FYN
ZBTB7A
P−value:0.74; Pearson R:0.12

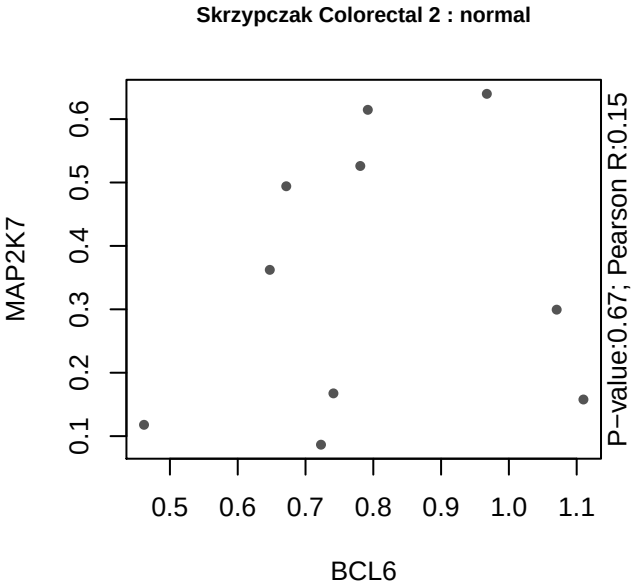

Skrzypczak Colorectal 2 : normal
LLGL1
BCL6
P−value:0.59; Pearson R:0.19

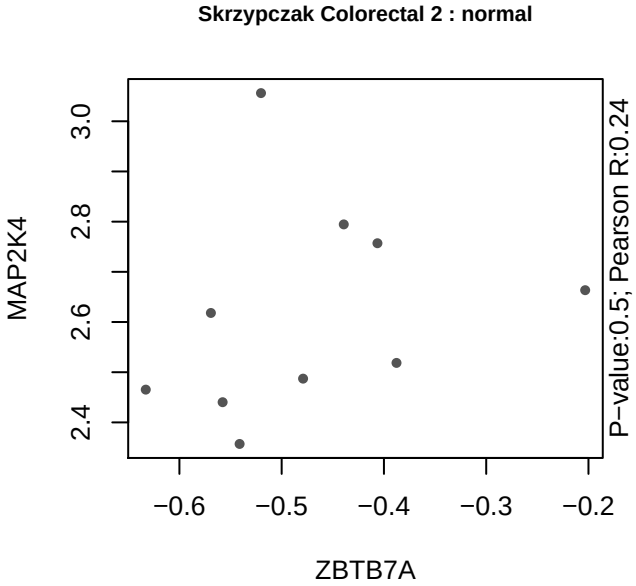

Skrzypczak Colorectal 2 : normal
LLGL2
BCL6
P−value:0.18; Pearson R:−0.46

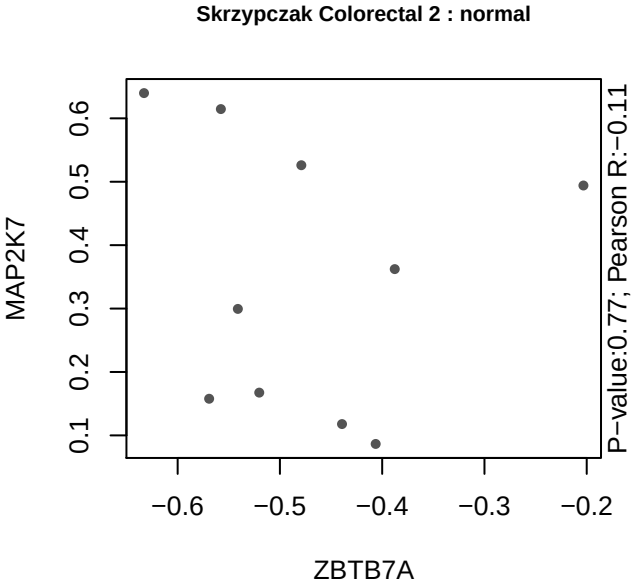

Skrzypczak Colorectal 2 : normal
LLGL1
ZBTB7A
P−value:0.19; Pearson R:0.45

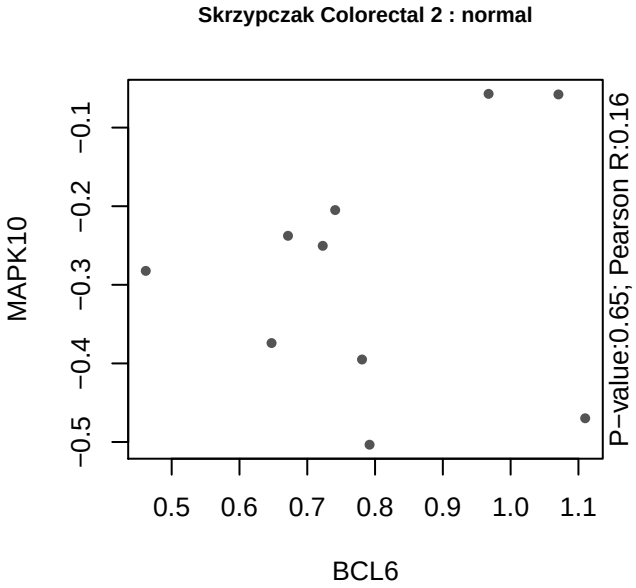

Skrzypczak Colorectal 2 : normal
LLGL2
ZBTB7A
P−value:0.5; Pearson R:0.24

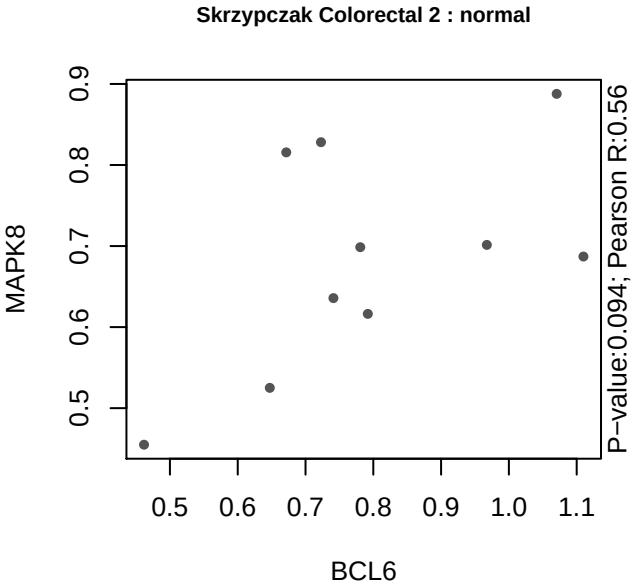

Skrzypczak Colorectal 2 : normal
MAP2K4
BCL6
P−value:0.17; Pearson R:−0.47

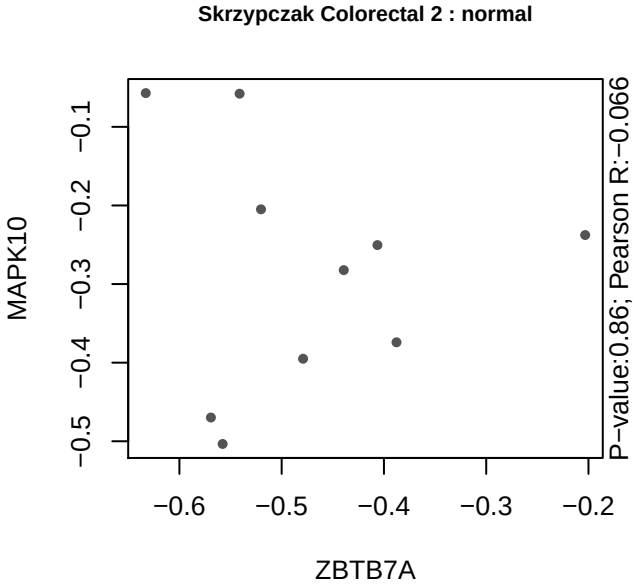

Skrzypczak Colorectal 2 : normal
MAP2K7
BCL6
P−value:0.67; Pearson R:0.15

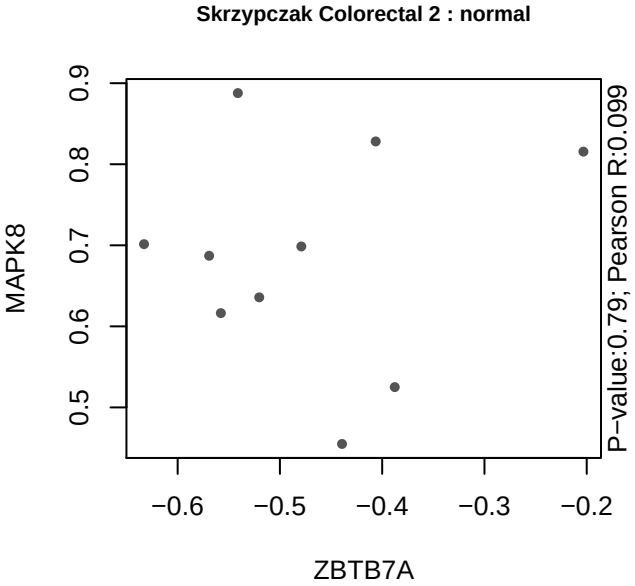

Skrzypczak Colorectal 2 : normal
MAP2K4
ZBTB7A
P−value:0.5; Pearson R:0.24

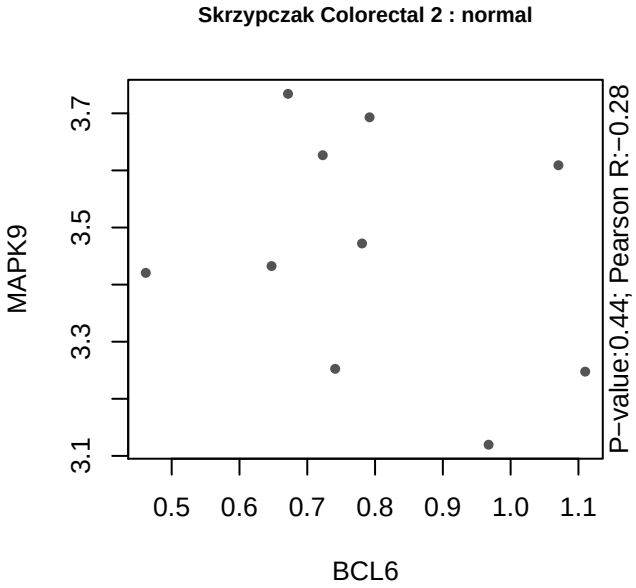

Skrzypczak Colorectal 2 : normal
MAP2K7
ZBTB7A
P−value:0.77; Pearson R:−0.11

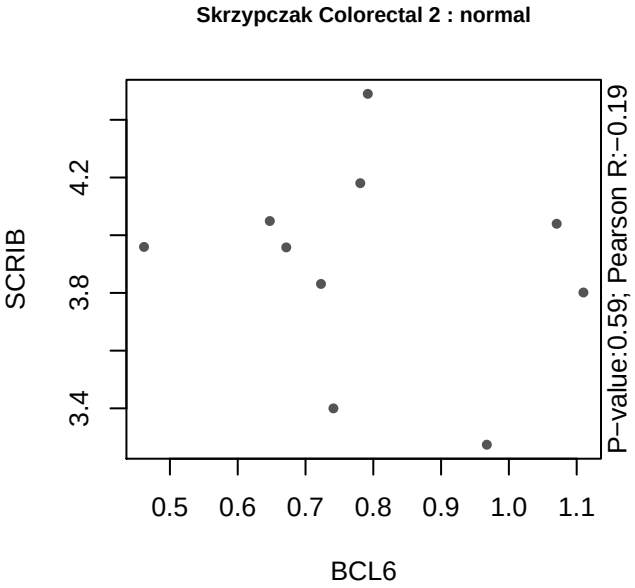

Skrzypczak Colorectal 2 : normal
MAPK10
BCL6
P−value:0.65; Pearson R:0.16

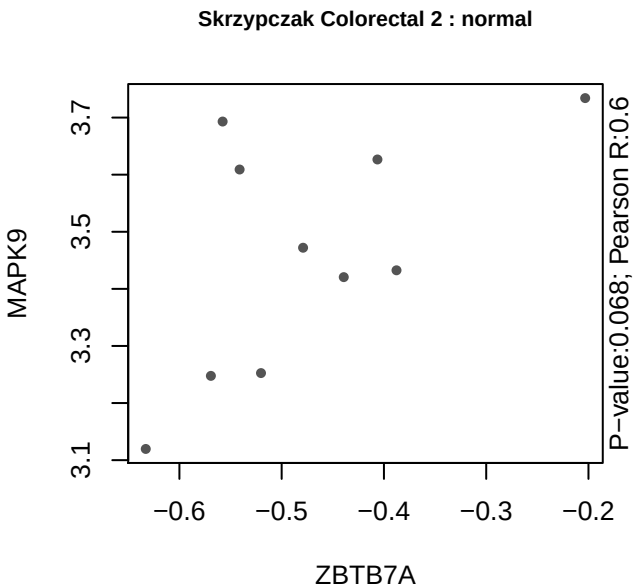

Skrzypczak Colorectal 2 : normal
MAPK8
BCL6
P−value:0.094; Pearson R:0.56

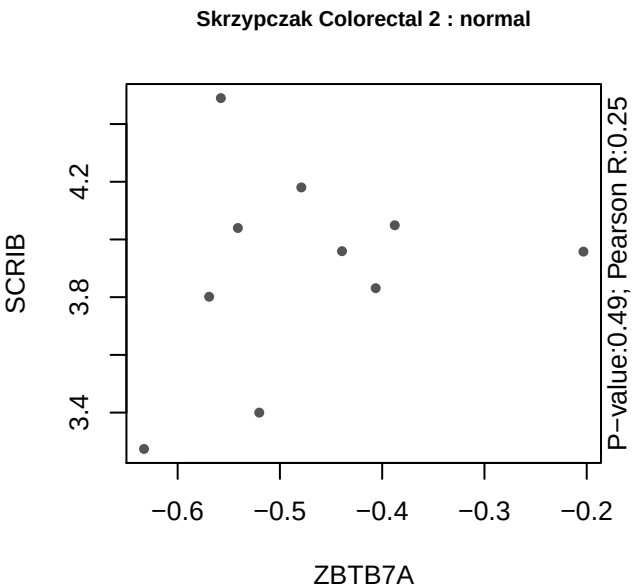

Skrzypczak Colorectal 2 : normal
MAPK10
ZBTB7A
P−value:0.86; Pearson R:−0.066

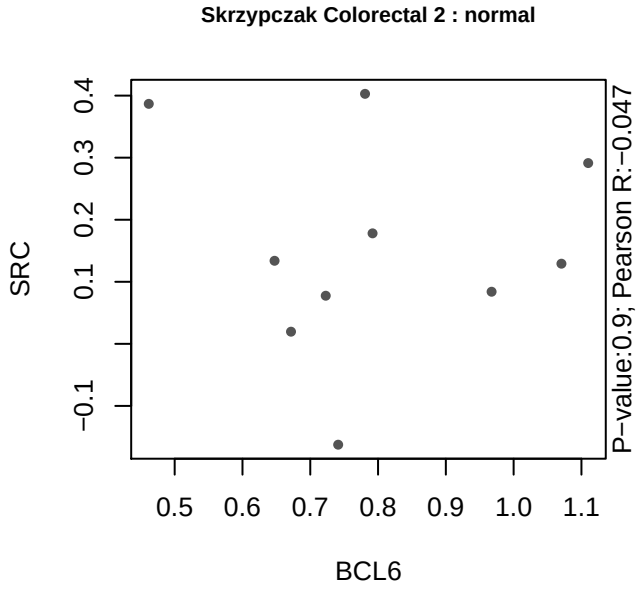

Skrzypczak Colorectal 2 : normal
MAPK8
ZBTB7A
P−value:0.79; Pearson R:0.099

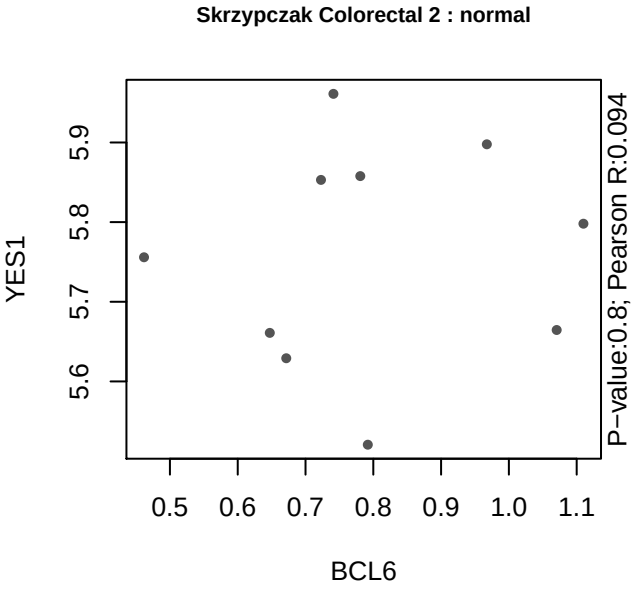

Skrzypczak Colorectal 2 : normal
MAPK9
BCL6
P−value:0.44; Pearson R:−0.28
3.1
3.3
3.5
3.7
0.5
0.6
0.7
0.8
0.9
1.0
1.1

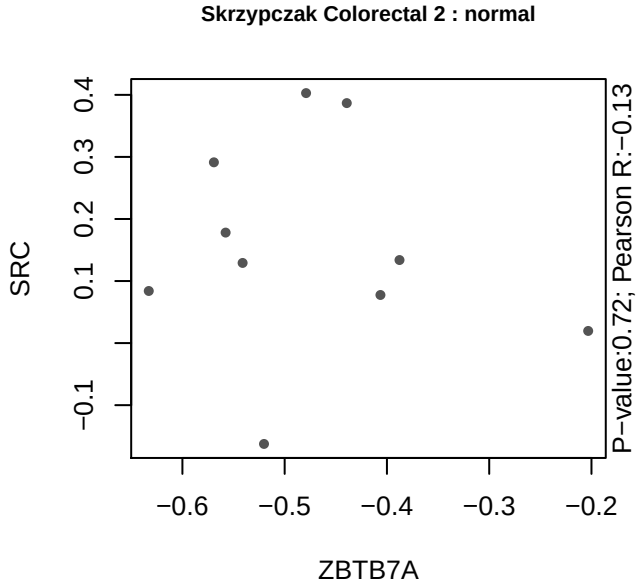

Skrzypczak Colorectal 2 : normal
SCRIB
BCL6
P−value:0.59; Pearson R:−0.19
3.4
3.8
4.2
0.5
0.6
0.7
0.8
0.9
1.0
1.1

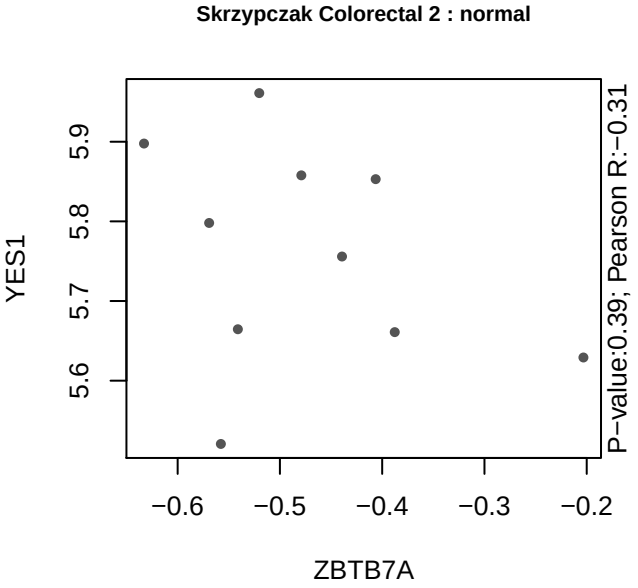

Skrzypczak Colorectal 2 : normal
MAPK9
ZBTB7A
P−value:0.068; Pearson R:0.6
3.1
3.3
3.5
3.7
−0.6
−0.5
−0.4
−0.3
−0.2

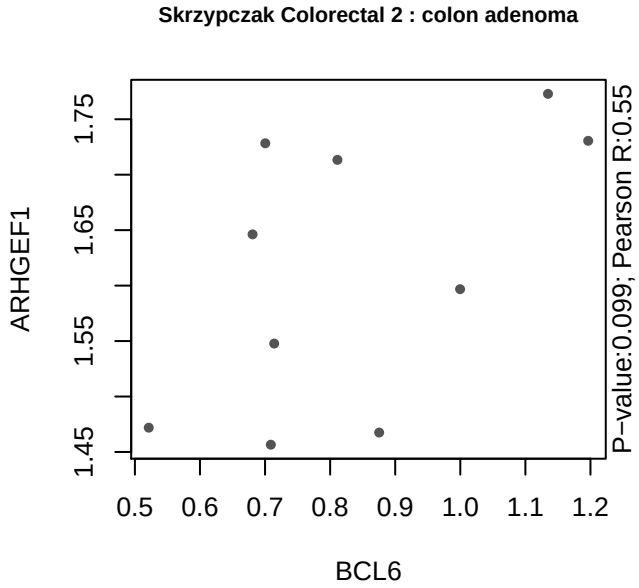

Skrzypczak Colorectal 2 : normal
SCRIB
ZBTB7A
P−value:0.49; Pearson R:0.25
3.4
3.8
4.2
−0.6
−0.5
−0.4
−0.3
−0.2

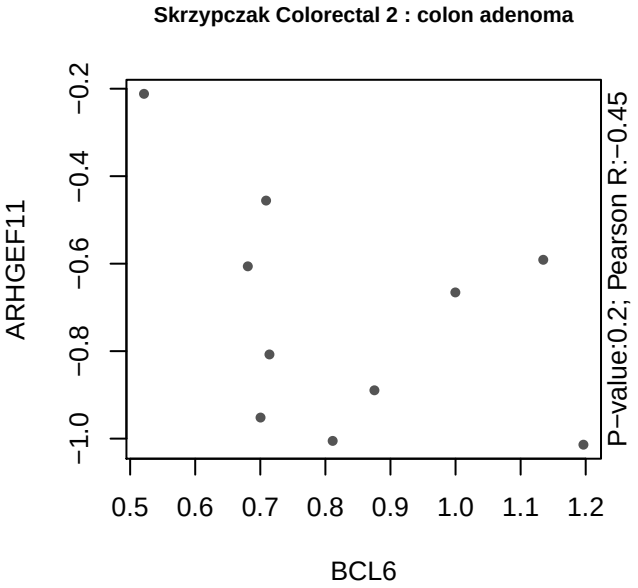

Skrzypczak Colorectal 2 : normal
SRC
BCL6
P−value:0.9; Pearson R:−0.047
−0.1
0.1
0.2
0.3
0.4
0.5
0.6
0.7
0.8
0.9
1.0
1.1

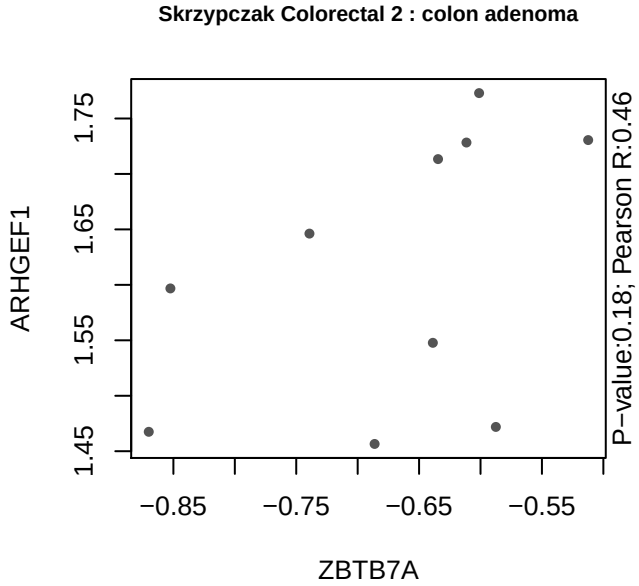

Skrzypczak Colorectal 2 : normal
YES1
BCL6
P−value:0.8; Pearson R:0.094
5.6
5.7
5.8
5.9
0.5
0.6
0.7
0.8
0.9
1.0
1.1

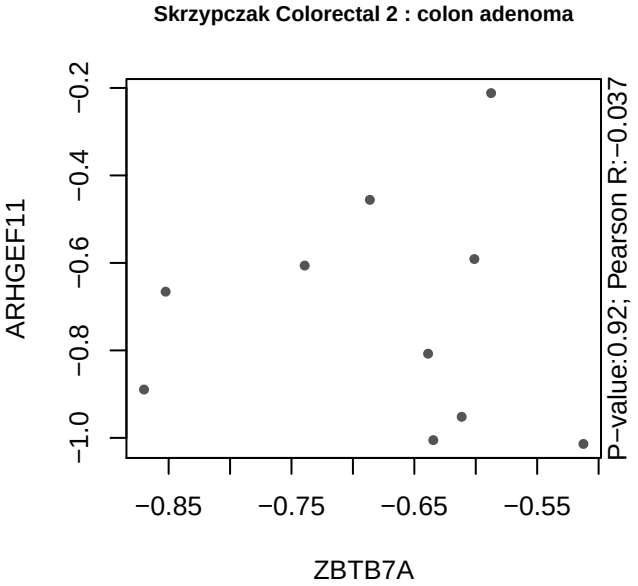

Skrzypczak Colorectal 2 : normal
SRC
ZBTB7A
P−value:0.72; Pearson R:−0.13
−0.1
0.1
0.2
0.3
0.4
−0.6
−0.5
−0.4
−0.3
−0.2

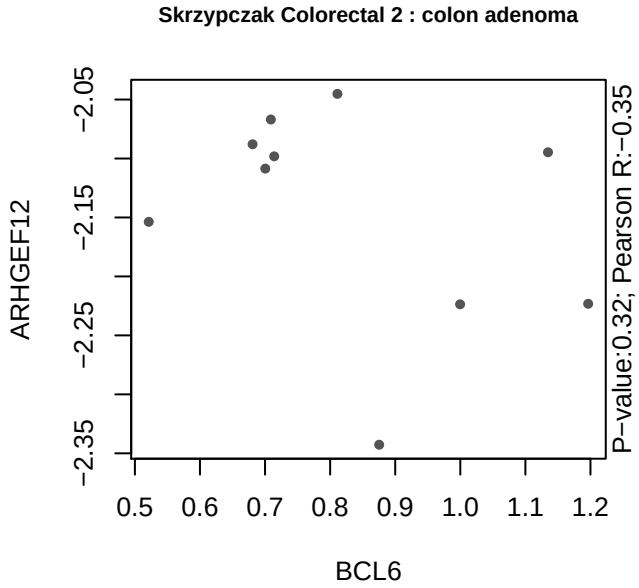

Skrzypczak Colorectal 2 : normal
YES1
ZBTB7A
P−value:0.39; Pearson R:−0.31
5.6
5.7
5.8
5.9
−0.6
−0.5
−0.4
−0.3
−0.2

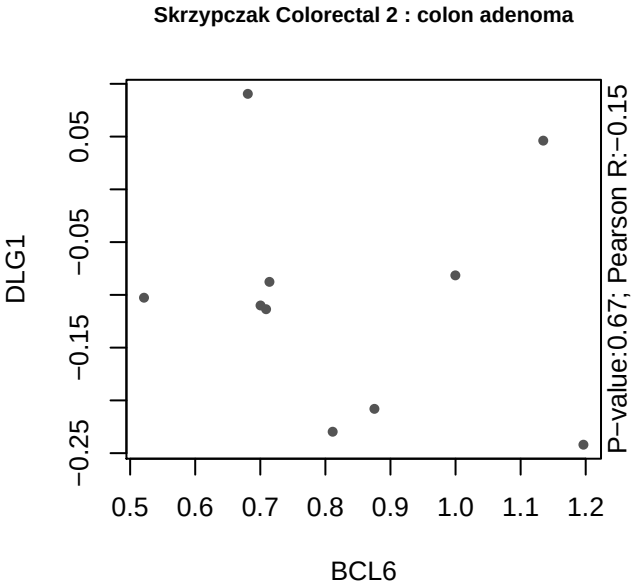

Skrzypczak Colorectal 2 : colon adenoma
ARHGEF1
BCL6
P−value:0.099; Pearson R:0.55
1.45
1.55
1.65
1.75
0.5
0.6
0.7
0.8
0.9
1.0
1.1
1.2

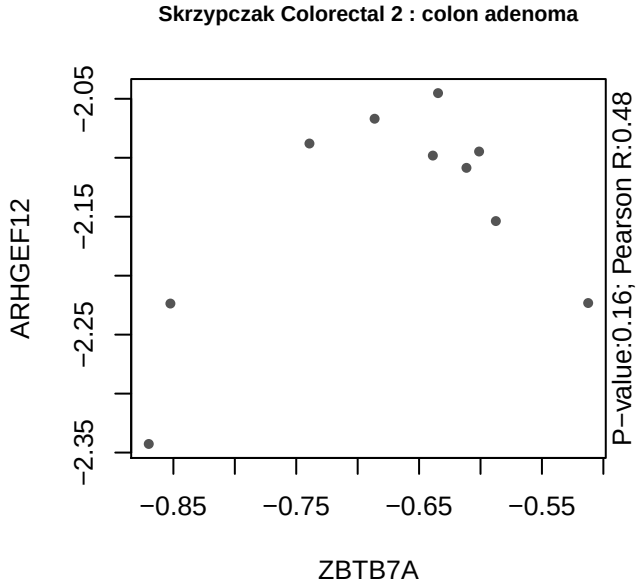

Skrzypczak Colorectal 2 : colon adenoma
ARHGEF11
BCL6
P−value:0.2; Pearson R:−0.45
−1.0
−0.8
−0.6
−0.4
−0.2
0.5
0.6
0.7
0.8
0.9
1.0
1.1
1.2

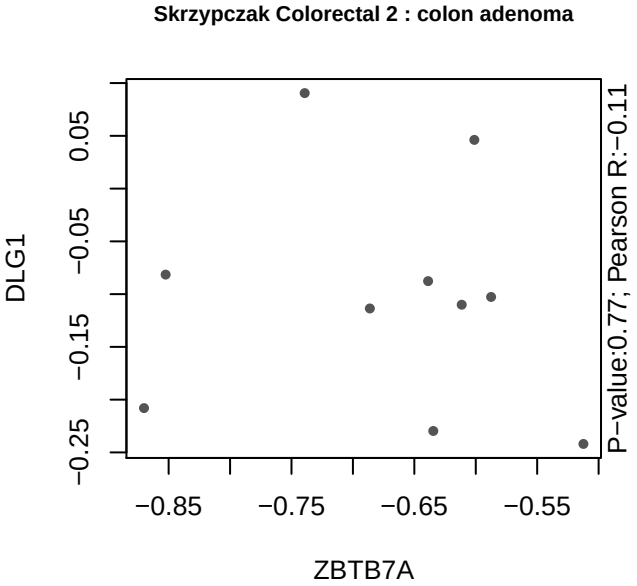

Skrzypczak Colorectal 2 : colon adenoma
ARHGEF1
ZBTB7A
P−value:0.18; Pearson R:0.46
1.45
1.55
1.65
1.75
−0.85
−0.75
−0.65
−0.55

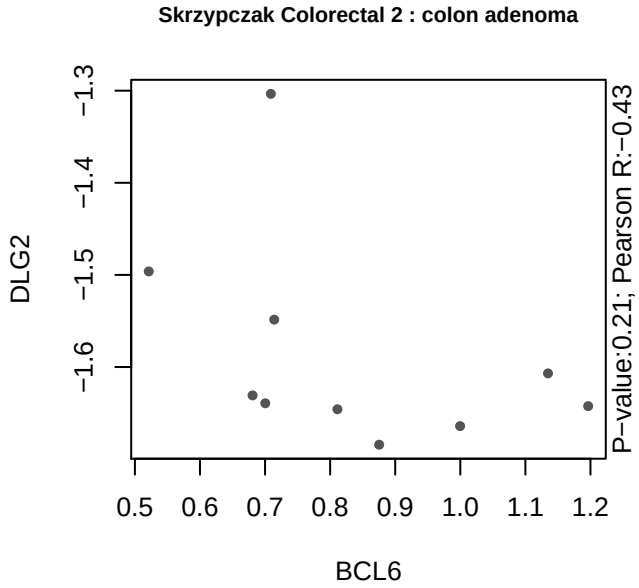

Skrzypczak Colorectal 2 : colon adenoma
ARHGEF11
ZBTB7A
P−value:0.92; Pearson R:−0.037
−1.0
−0.8
−0.6
−0.4
−0.2
−0.85
−0.75
−0.65
−0.55

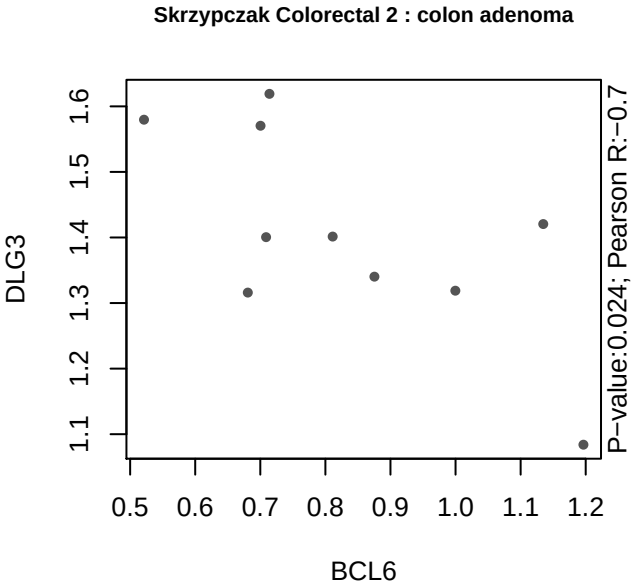

Skrzypczak Colorectal 2 : colon adenoma
ARHGEF12
BCL6
P−value:0.32; Pearson R:−0.35
−2.05
−2.15
−2.25
−2.35
0.5
0.6
0.7
0.8
0.9
1.0
1.1
1.2

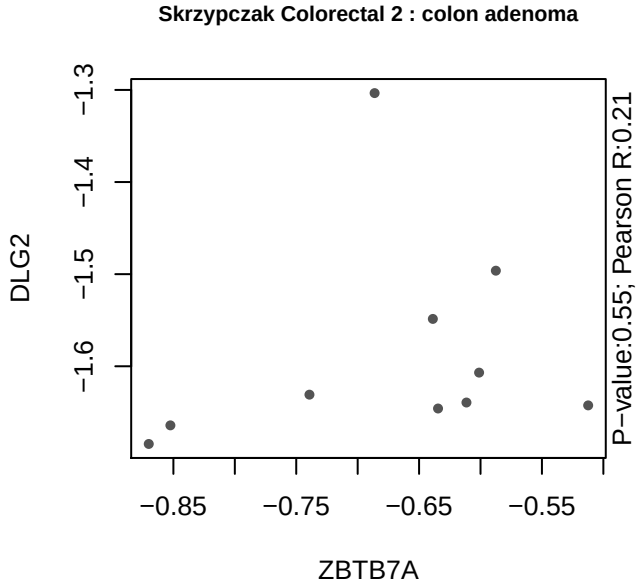

Skrzypczak Colorectal 2 : colon adenoma
DLG1
BCL6
P−value:0.67; Pearson R:−0.15
0.05
−0.05
−0.15
−0.25
0.5
0.6
0.7
0.8
0.9
1.0
1.1
1.2

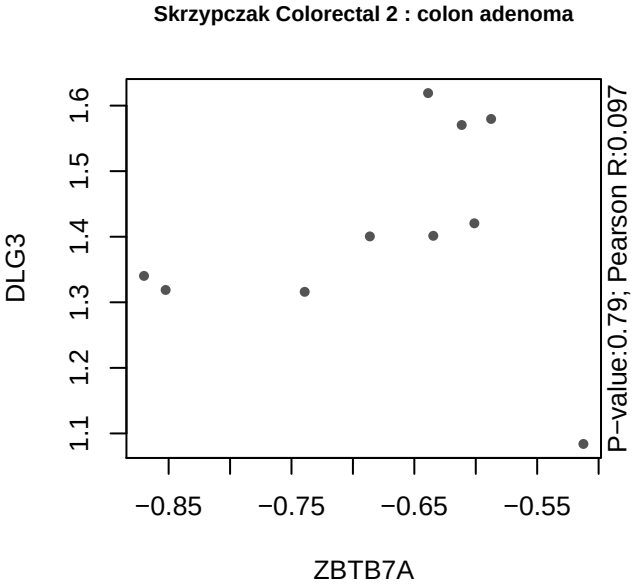

Skrzypczak Colorectal 2 : colon adenoma
ARHGEF12
ZBTB7A
P−value:0.16; Pearson R:0.48
−2.05
−2.15
−2.25
−2.35
−0.85
−0.75
−0.65
−0.55

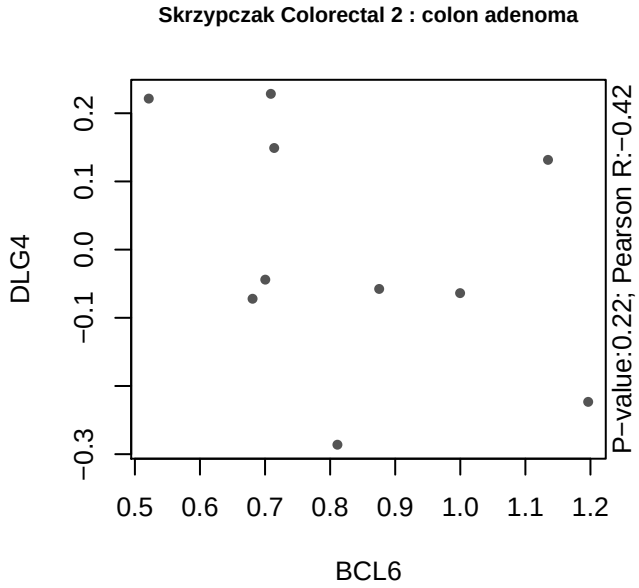

Skrzypczak Colorectal 2 : colon adenoma
DLG1
ZBTB7A
P−value:0.77; Pearson R:−0.11
0.05
−0.05
−0.15
−0.25
−0.85
−0.75
−0.65
−0.55

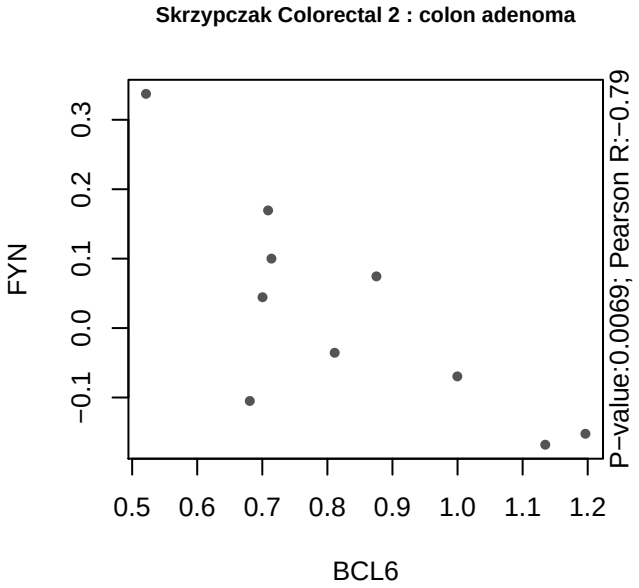

Skrzypczak Colorectal 2 : colon adenoma
DLG2
BCL6
P−value:0.21; Pearson R:−0.43
−1.3
−1.4
−1.5
−1.6
0.5
0.6
0.7
0.8
0.9
1.0
1.1
1.2

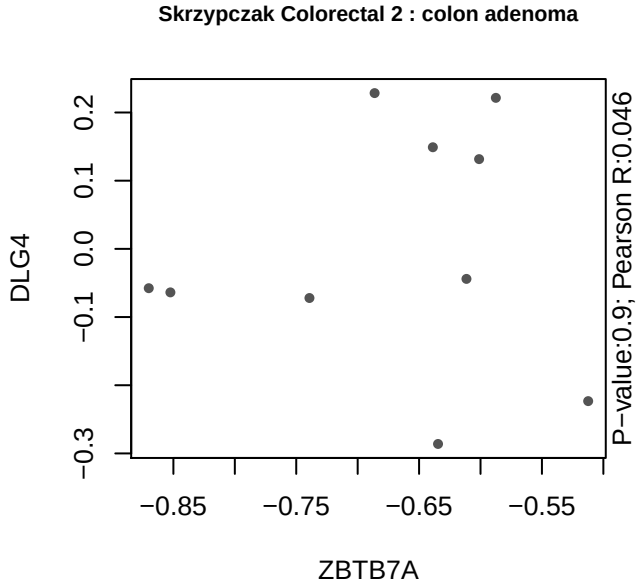

Skrzypczak Colorectal 2 : colon adenoma
DLG3
BCL6
P−value:0.024; Pearson R:−0.7
1.6
1.5
1.4
1.3
1.2
1.1
0.5
0.6
0.7
0.8
0.9
1.0
1.1
1.2

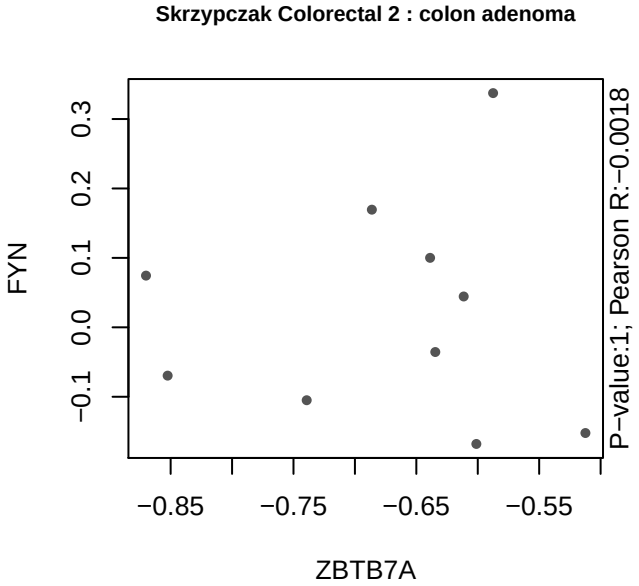

Skrzypczak Colorectal 2 : colon adenoma
DLG2
ZBTB7A
P−value:0.55; Pearson R:0.21
−1.3
−1.4
−1.5
−1.6
−0.85
−0.75
−0.65
−0.55

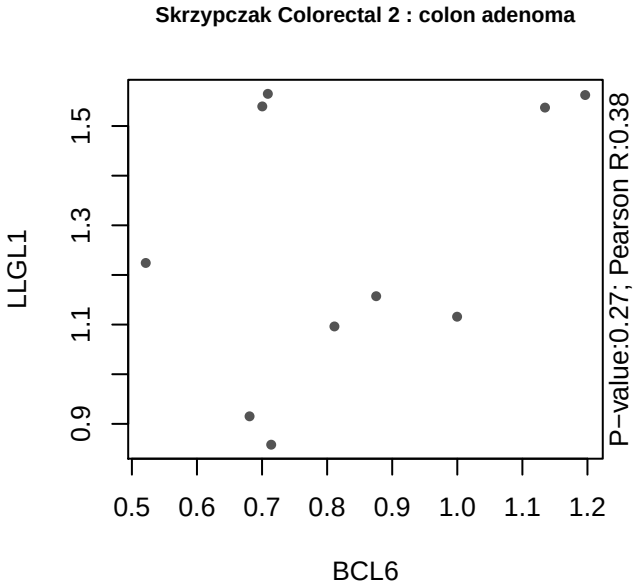

Skrzypczak Colorectal 2 : colon adenoma
DLG3
ZBTB7A
P−value:0.79; Pearson R:0.097
1.6
1.5
1.4
1.3
1.2
1.1
−0.85
−0.75
−0.65
−0.55

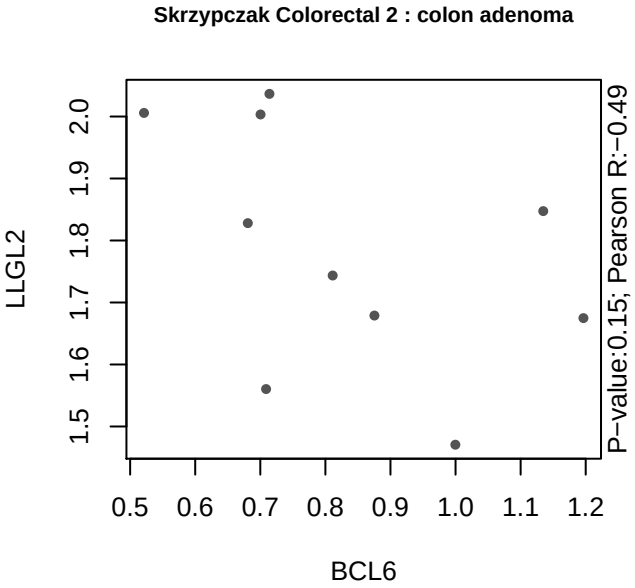

Skrzypczak Colorectal 2 : colon adenoma
DLG4
BCL6
P−value:0.22; Pearson R:−0.42

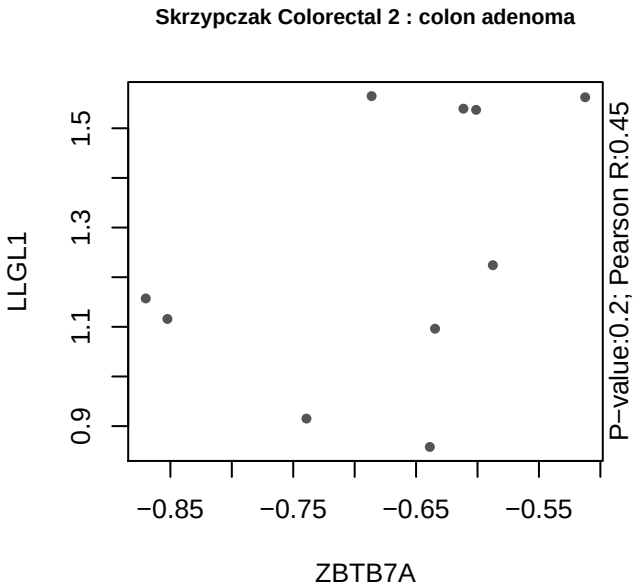

Skrzypczak Colorectal 2 : colon adenoma
FYN
BCL6
P−value:0.0069; Pearson R:−0.79

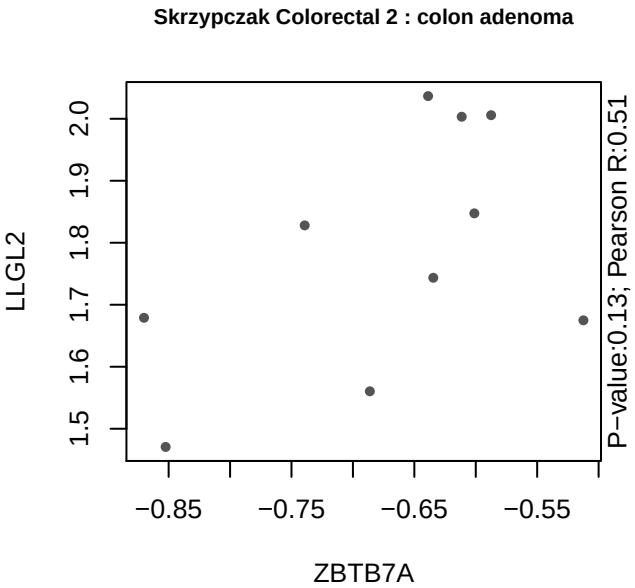

Skrzypczak Colorectal 2 : colon adenoma
DLG4
ZBTB7A
P−value:0.9; Pearson R:0.046

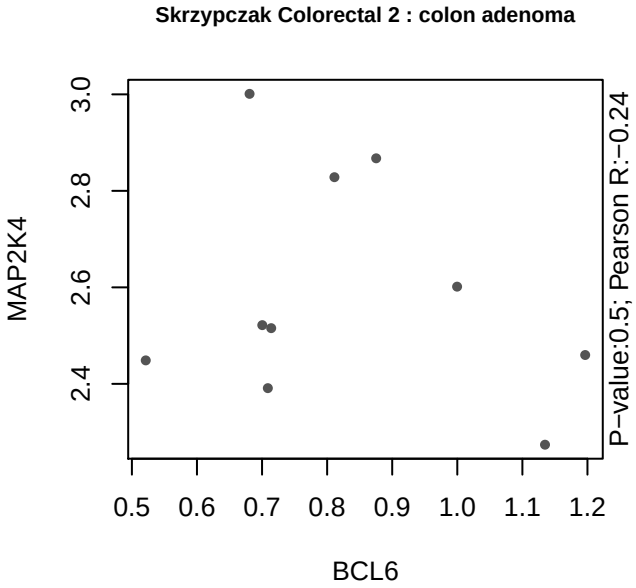

Skrzypczak Colorectal 2 : colon adenoma
FYN
ZBTB7A
P−value:1; Pearson R:−0.0018

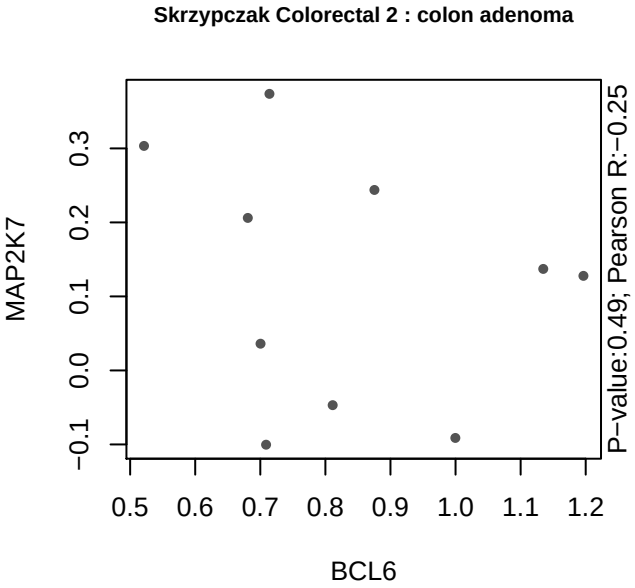

Skrzypczak Colorectal 2 : colon adenoma
LLGL1
BCL6
P−value:0.27; Pearson R:0.38

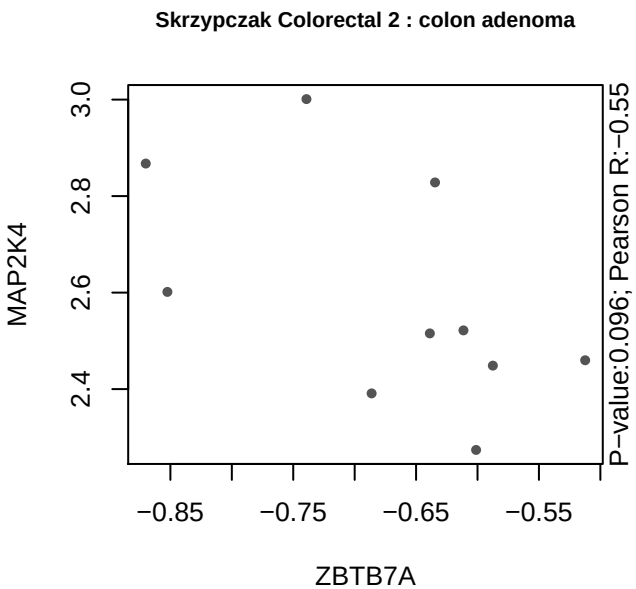

Skrzypczak Colorectal 2 : colon adenoma
LLGL2
BCL6
P−value:0.15; Pearson R:−0.49

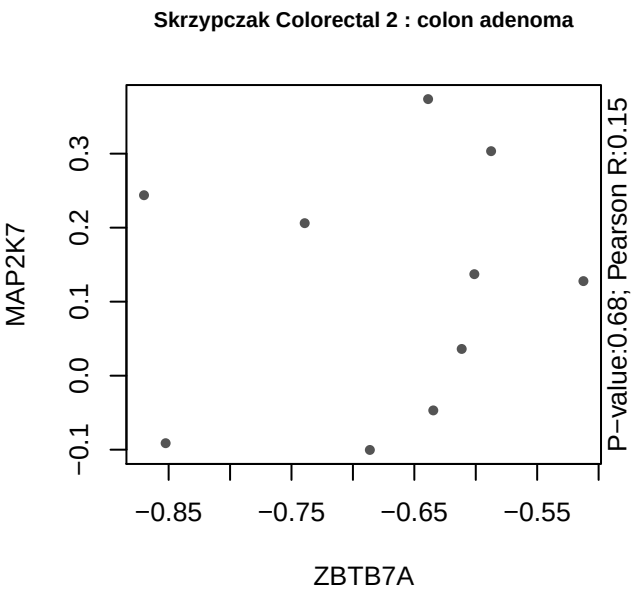

Skrzypczak Colorectal 2 : colon adenoma
LLGL1
ZBTB7A
P−value:0.2; Pearson R:0.45

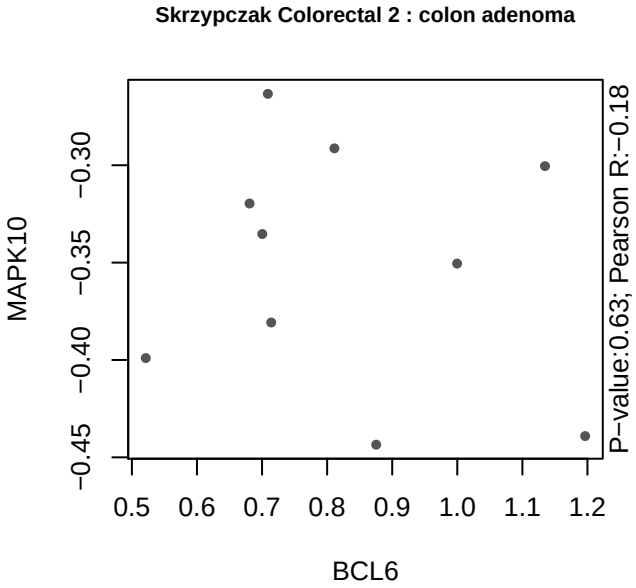

Skrzypczak Colorectal 2 : colon adenoma
LLGL2
ZBTB7A
P−value:0.13; Pearson R:0.51

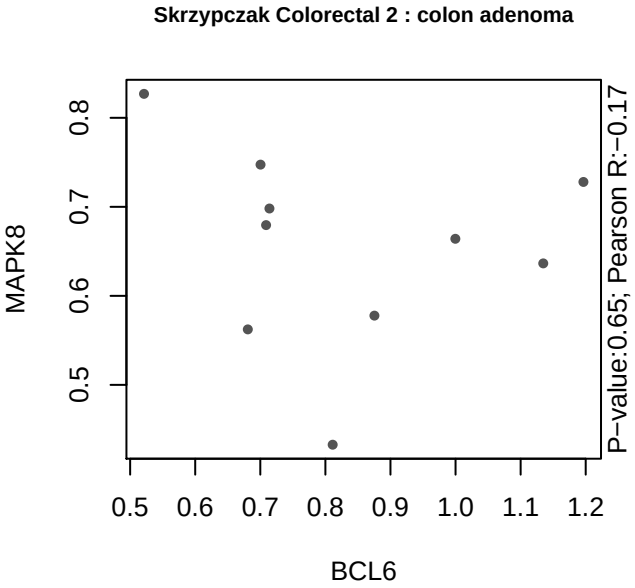

Skrzypczak Colorectal 2 : colon adenoma
MAP2K4
BCL6
P−value:0.5; Pearson R:−0.24
2.4
2.6
2.8
3.0
0.5
0.6
0.7
0.8
0.9
1.0
1.1
1.2

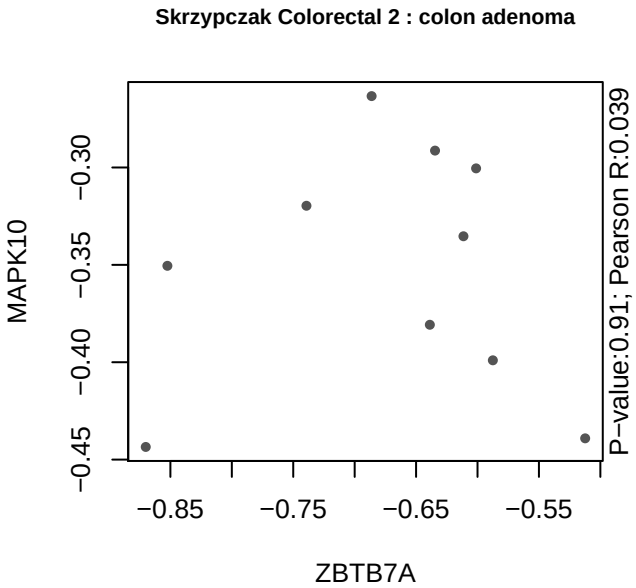

Skrzypczak Colorectal 2 : colon adenoma
MAP2K7
BCL6
P−value:0.49; Pearson R:−0.25
−0.1
0.0
0.1
0.2
0.3
0.5
0.6
0.7
0.8
0.9
1.0
1.1
1.2

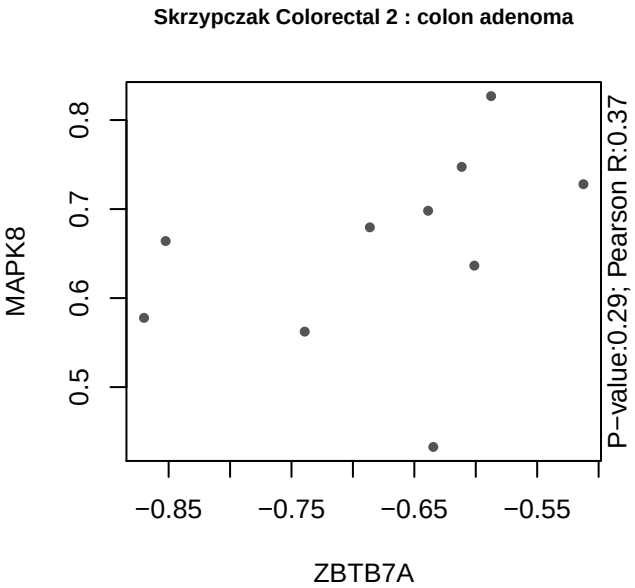

Skrzypczak Colorectal 2 : colon adenoma
MAP2K4
ZBTB7A
P−value:0.096; Pearson R:−0.55
2.4
2.6
2.8
3.0
−0.85
−0.75
−0.65
−0.55

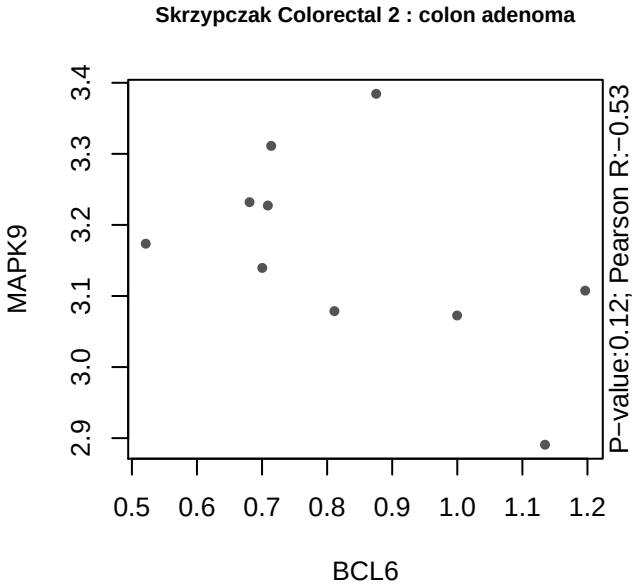

Skrzypczak Colorectal 2 : colon adenoma
MAP2K7
ZBTB7A
P−value:0.68; Pearson R:0.15
−0.1
0.0
0.1
0.2
0.3
−0.85
−0.75
−0.65
−0.55

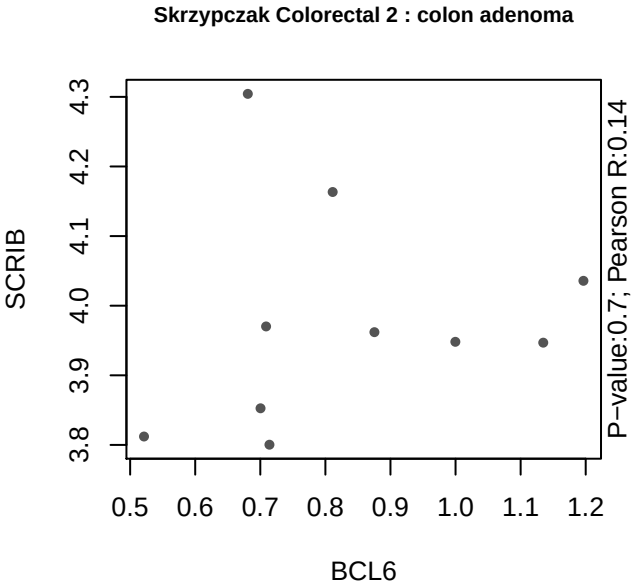

Skrzypczak Colorectal 2 : colon adenoma
MAPK10
−0.45
−0.40
−0.35
−0.30
0.5
0.6
0.7
0.8
0.9
1.0
1.1
1.2
BCL6
P−value:0.63; Pearson R:−0.18

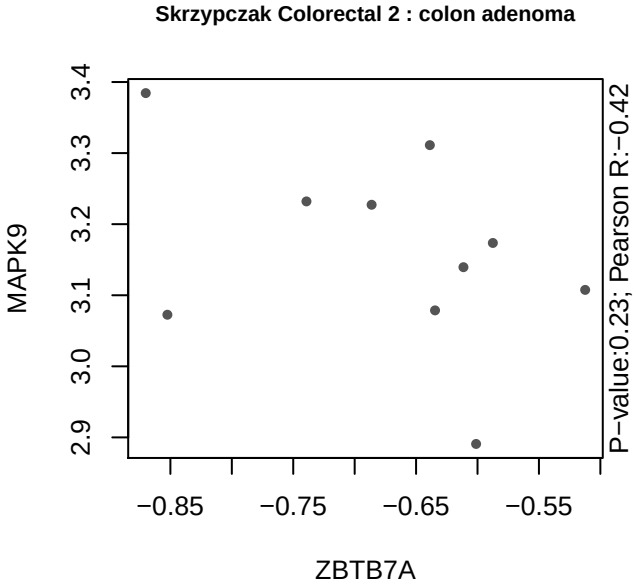

Skrzypczak Colorectal 2 : colon adenoma
MAPK8
0.5
0.6
0.7
0.8
0.5
0.6
0.7
0.8
0.9
1.0
1.1
1.2
BCL6
P−value:0.65; Pearson R:−0.17

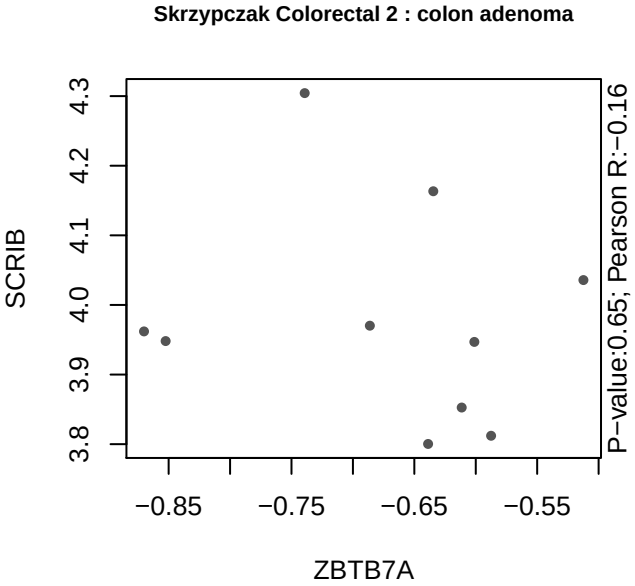

Skrzypczak Colorectal 2 : colon adenoma
MAPK10
−0.45
−0.40
−0.35
−0.30
−0.85
−0.75
−0.65
−0.55
ZBTB7A
P−value:0.91; Pearson R:0.039

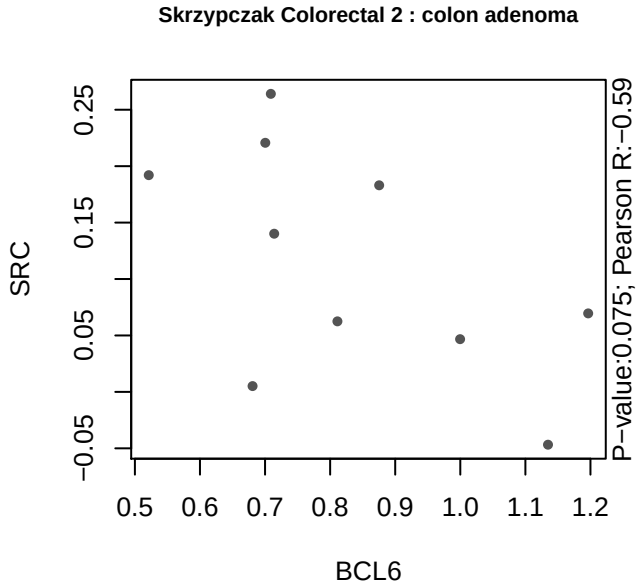

Skrzypczak Colorectal 2 : colon adenoma
MAPK8
0.5
0.6
0.7
0.8
−0.85
−0.75
−0.65
−0.55
ZBTB7A
P−value:0.29; Pearson R:0.37

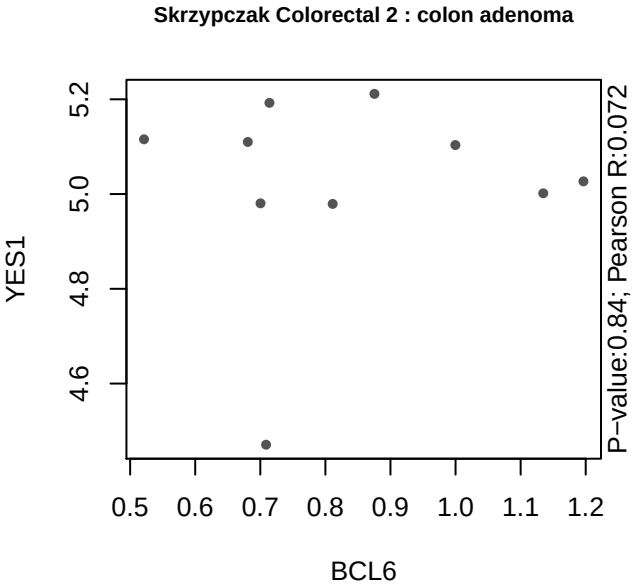

Skrzypczak Colorectal 2 : colon adenoma
MAPK9
BCL6
P−value:0.12; Pearson R:−0.53

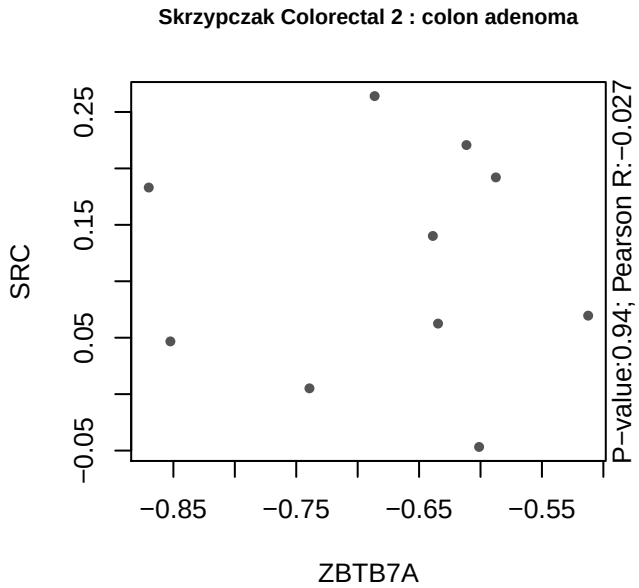

Skrzypczak Colorectal 2 : colon adenoma
SCRIB
BCL6
P−value:0.7; Pearson R:0.14

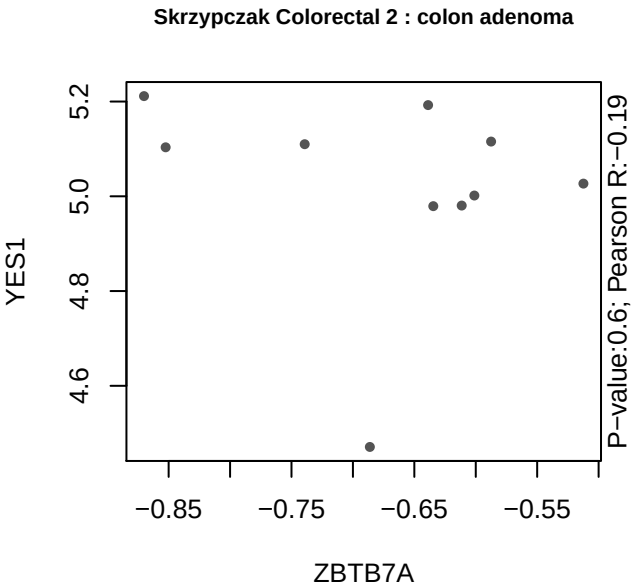

Skrzypczak Colorectal 2 : colon adenoma
MAPK9
ZBTB7A
P−value:0.23; Pearson R:−0.42

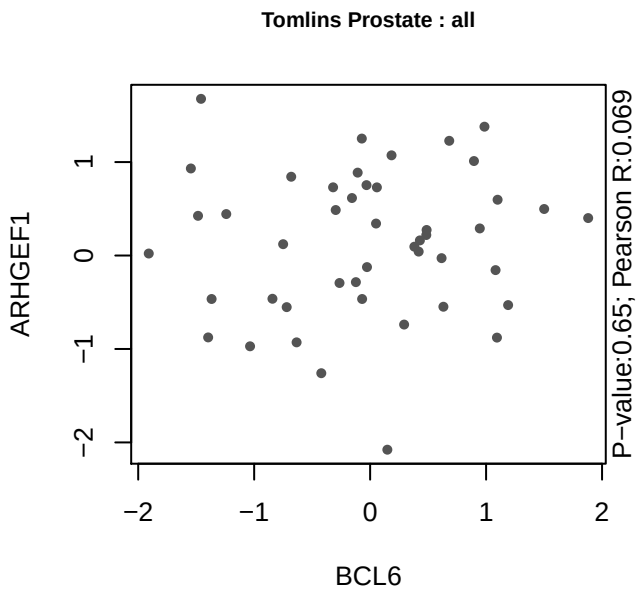

Skrzypczak Colorectal 2 : colon adenoma
SCRIB
ZBTB7A
P−value:0.65; Pearson R:−0.16

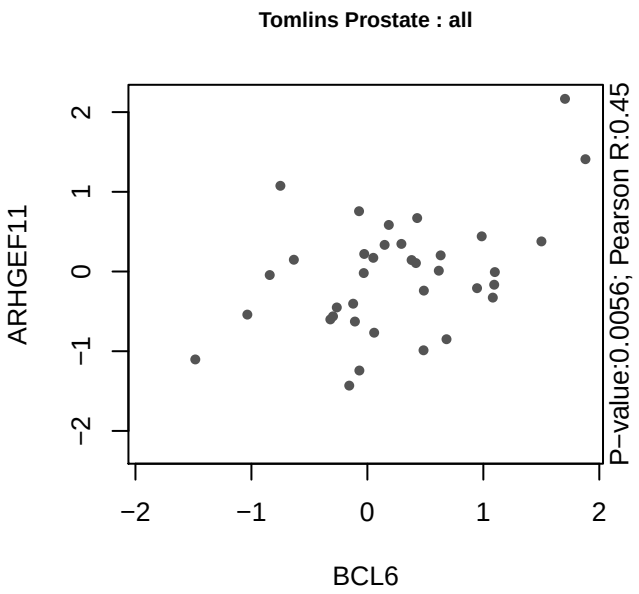

Skrzypczak Colorectal 2 : colon adenoma
SRC
BCL6
P−value:0.075; Pearson R:−0.59
−0.05
0.05
0.15
0.25
0.5
0.6
0.7
0.8
0.9
1.0
1.1
1.2

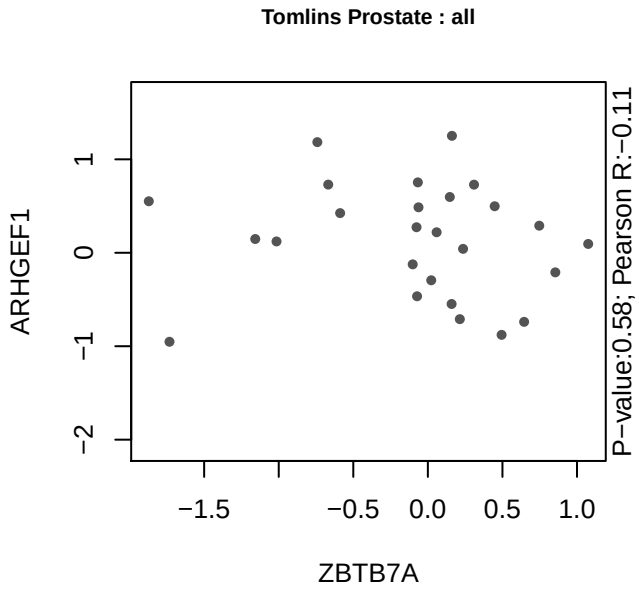

Skrzypczak Colorectal 2 : colon adenoma
YES1
BCL6
P−value:0.84; Pearson R:0.072
4.6
4.8
5.0
5.2
0.5
0.6
0.7
0.8
0.9
1.0
1.1
1.2

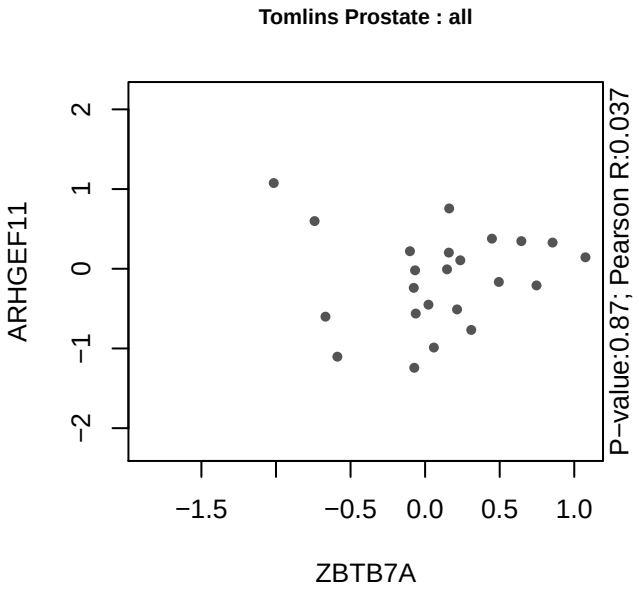

Skrzypczak Colorectal 2 : colon adenoma
SRC
ZBTB7A
P−value:0.94; Pearson R:−0.027
−0.05
0.05
0.15
0.25
−0.85
−0.75
−0.65
−0.55

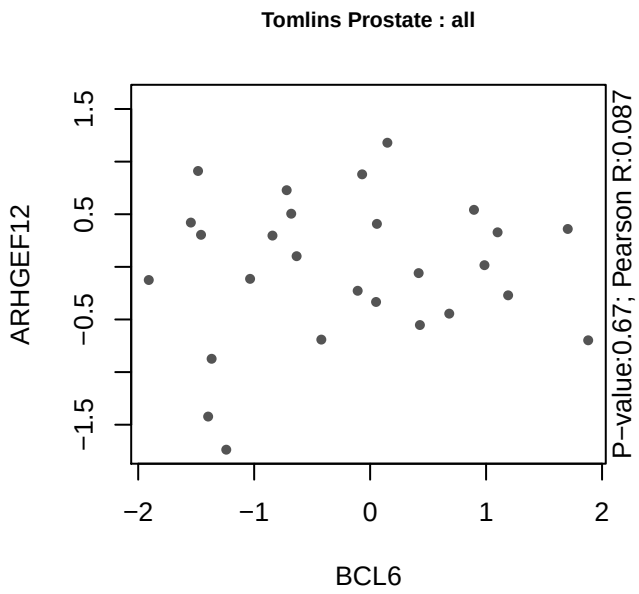

Skrzypczak Colorectal 2 : colon adenoma
YES1
ZBTB7A
P−value:0.6; Pearson R:−0.19
4.6
4.8
5.0
5.2
−0.85
−0.75
−0.65
−0.55

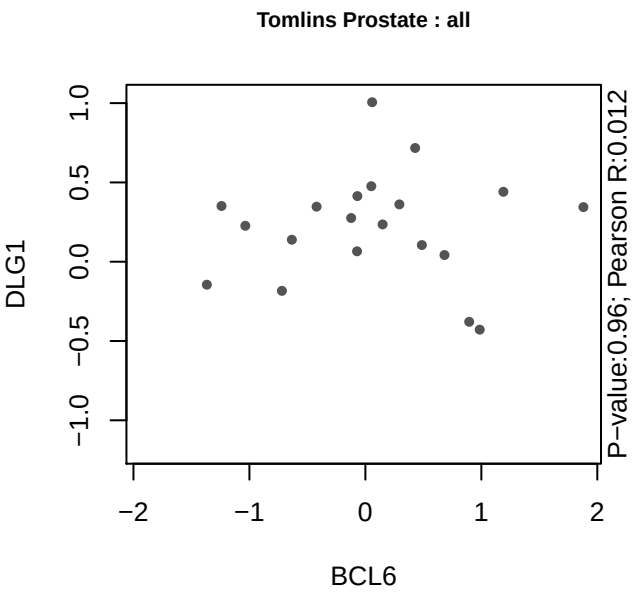

Tomlins Prostate : all
ARHGEF1
BCL6
P−value:0.65; Pearson R:0.069

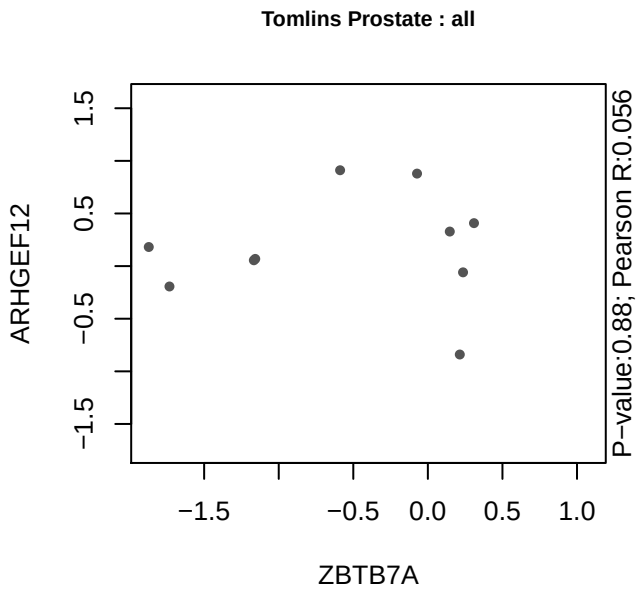

Tomlins Prostate : all
ARHGEF11
BCL6
P−value:0.0056; Pearson R:0.45

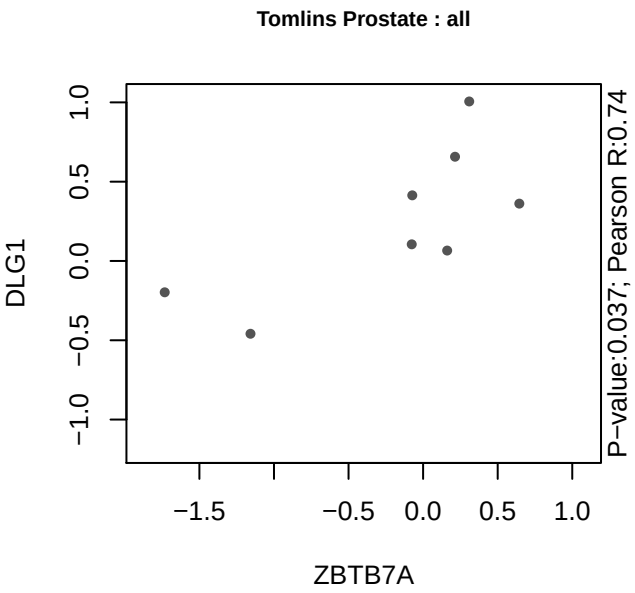

Tomlins Prostate : all
ARHGEF1
ZBTB7A
P−value:0.58; Pearson R:−0.11

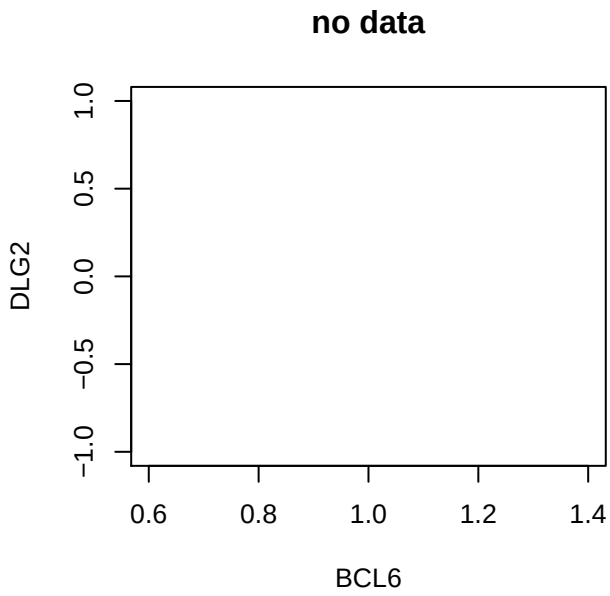

Tomlins Prostate : all
ARHGEF11
ZBTB7A
P−value:0.87; Pearson R:0.037

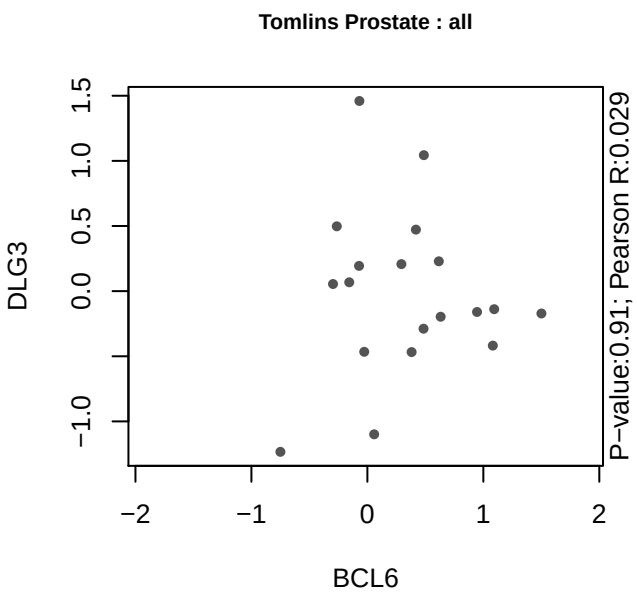

Tomlins Prostate : all
ARHGEF12
BCL6
P−value:0.67; Pearson R:0.087

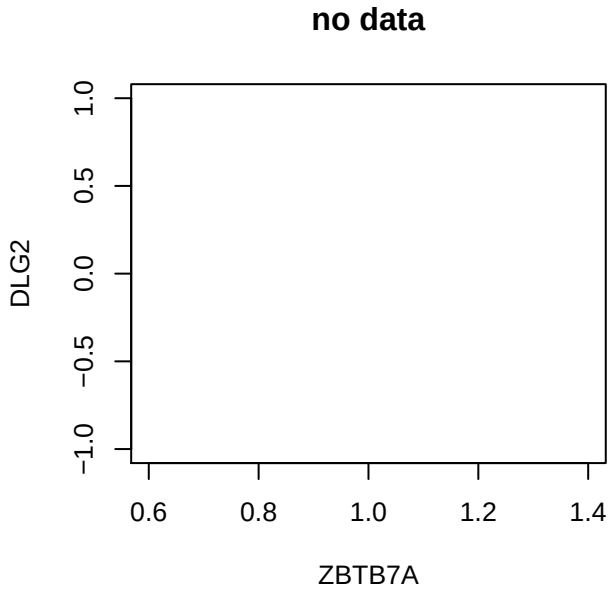

Tomlins Prostate : all
DLG1
BCL6
P−value:0.96; Pearson R:0.012

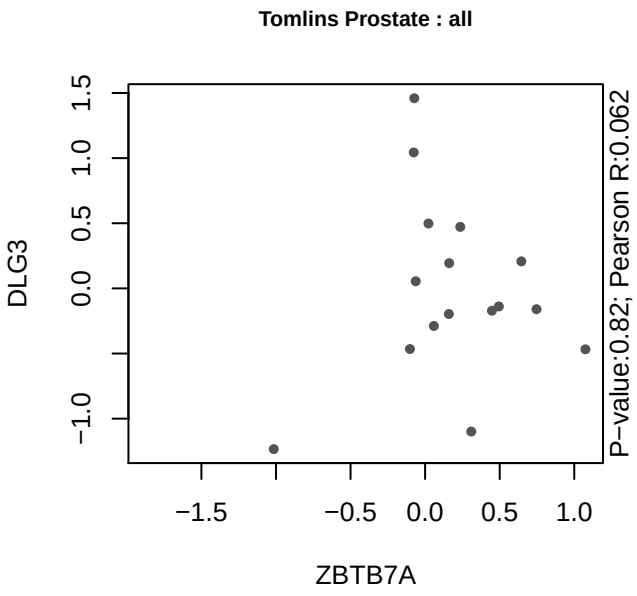

Tomlins Prostate : all
ARHGEF12
ZBTB7A
P−value:0.88; Pearson R:0.056

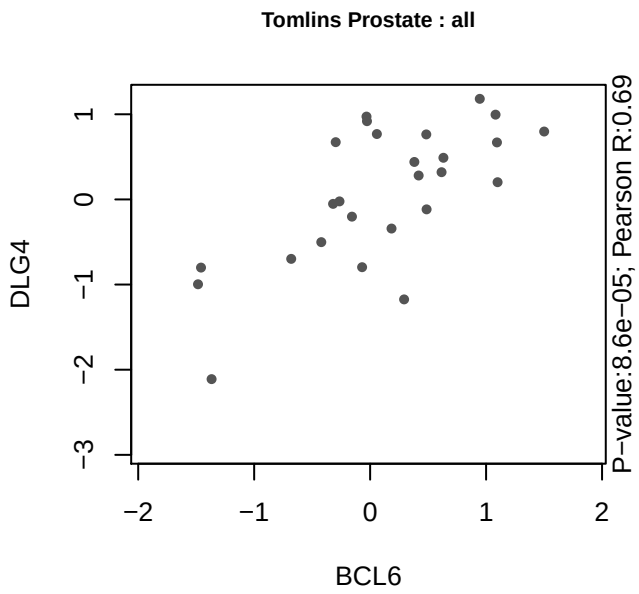

Tomlins Prostate : all
DLG1
ZBTB7A
P−value:0.037; Pearson R:0.74

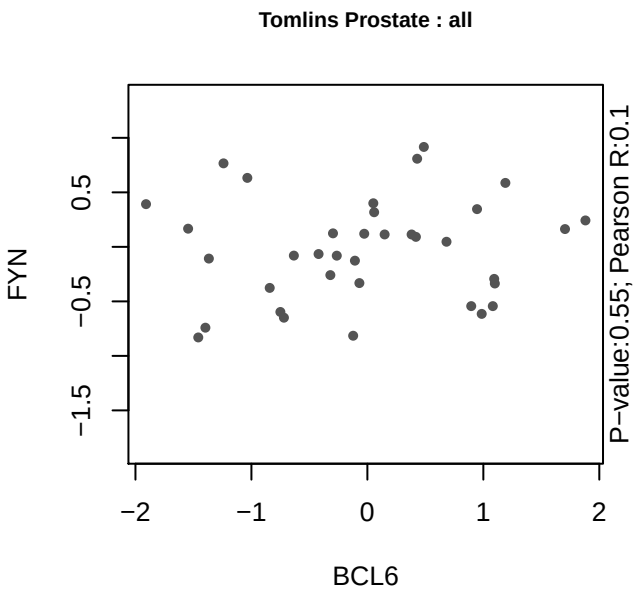

no data
DLG2
BCL6
−1.0
−0.5
0.0
0.5
1.0
0.6
0.8
1.0
1.2
1.4

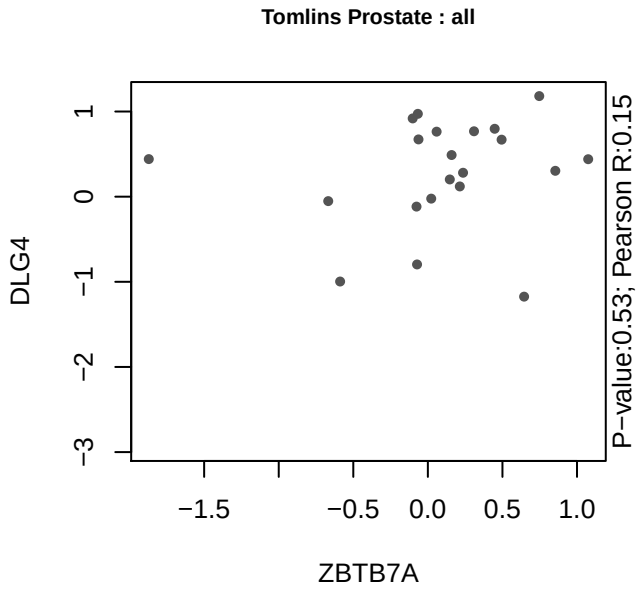

Tomlins Prostate : all
DLG3
BCL6
P−value:0.91; Pearson R:0.029
−1.0
0.0
0.5
1.0
1.5
−2
−1
0
1
2

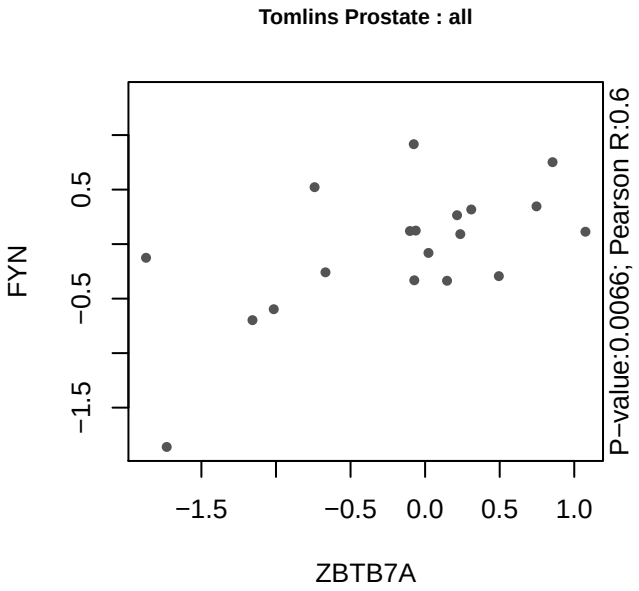

no data
DLG2
ZBTB7A
−1.0
−0.5
0.0
0.5
1.0
0.6
0.8
1.0
1.2
1.4

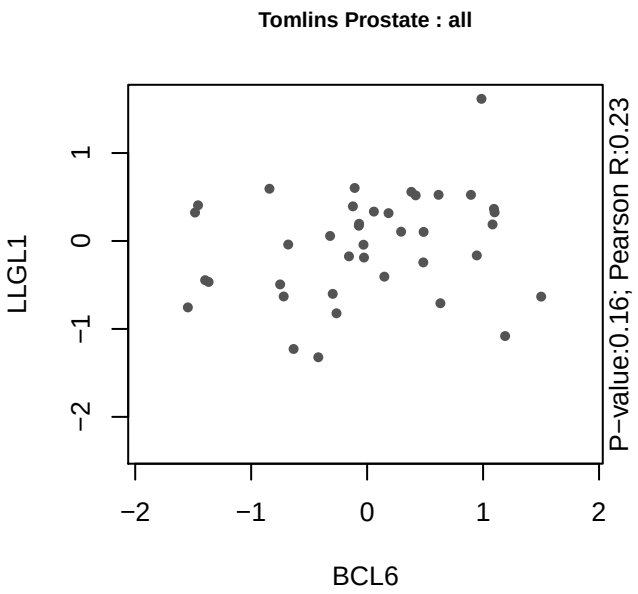

Tomlins Prostate : all
DLG3
ZBTB7A
P−value:0.82; Pearson R:0.062
−1.0
0.0
0.5
1.0
1.5
−1.5
−0.5
0.0
0.5
1.0

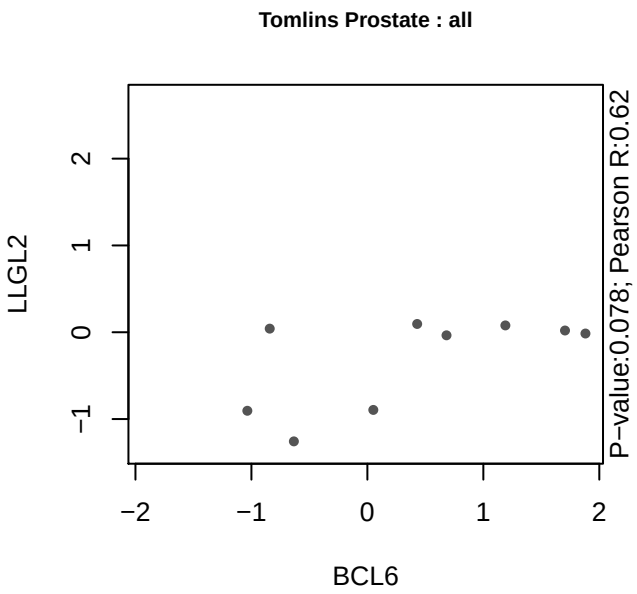

Tomlins Prostate : all
DLG4
BCL6
P−value:8.6e−05; Pearson R:0.69

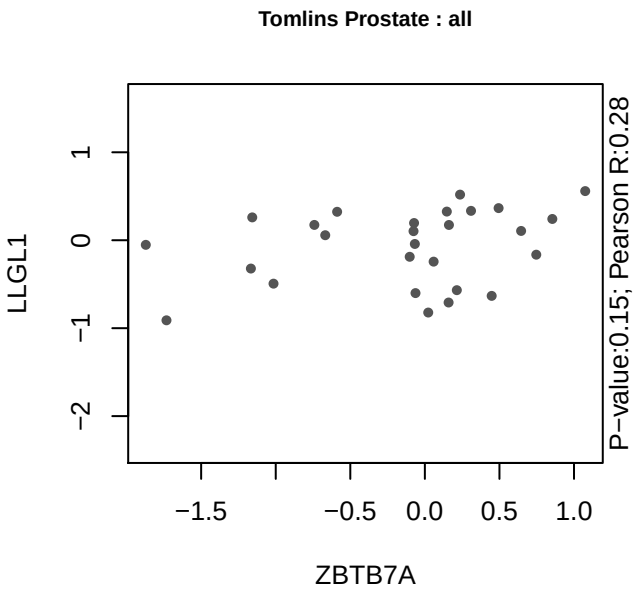

Tomlins Prostate : all
FYN
BCL6
P−value:0.55; Pearson R:0.1

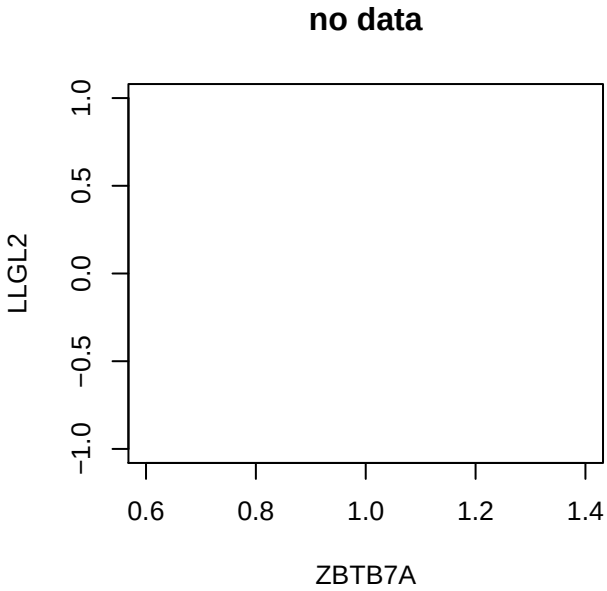

Tomlins Prostate : all
DLG4
ZBTB7A
P−value:0.53; Pearson R:0.15

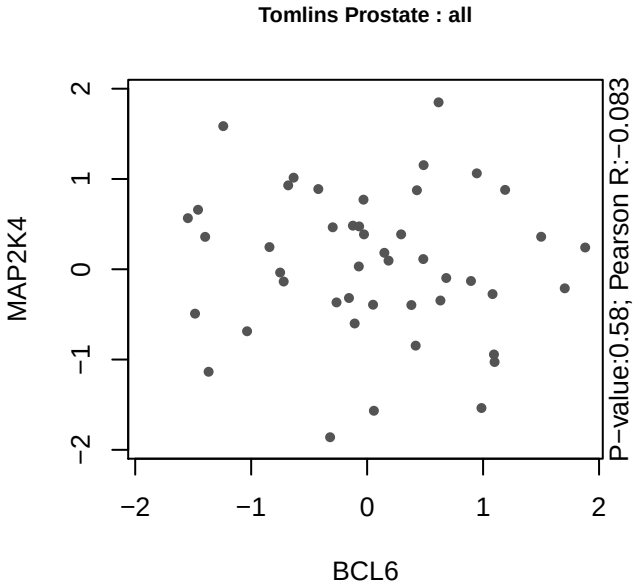

Tomlins Prostate : all
FYN
ZBTB7A
P−value:0.0066; Pearson R:0.6

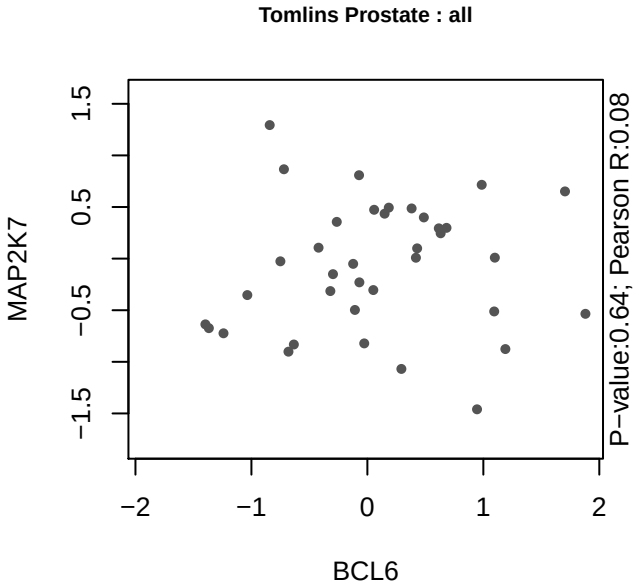

Tomlins Prostate : all
LLGL1
BCL6
P−value:0.16; Pearson R:0.23

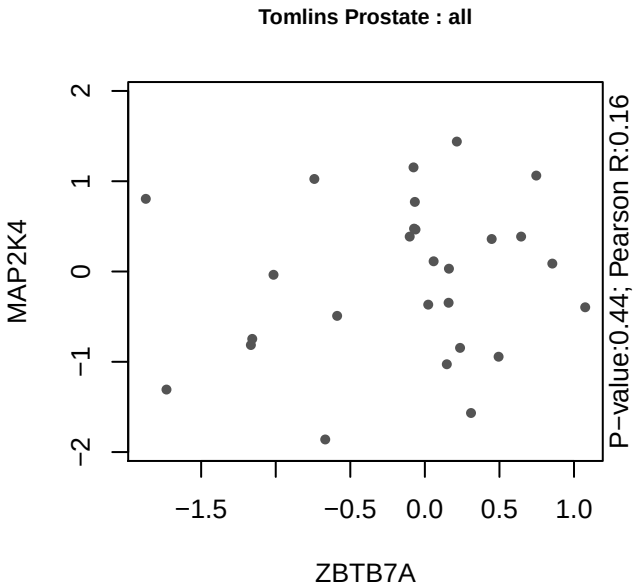

Tomlins Prostate : all
LLGL2
BCL6
P−value:0.078; Pearson R:0.62

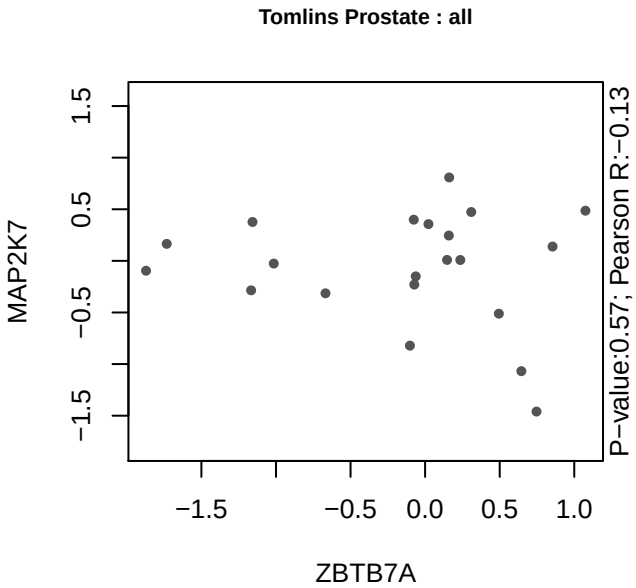

Tomlins Prostate : all
LLGL1
ZBTB7A
P−value:0.15; Pearson R:0.28

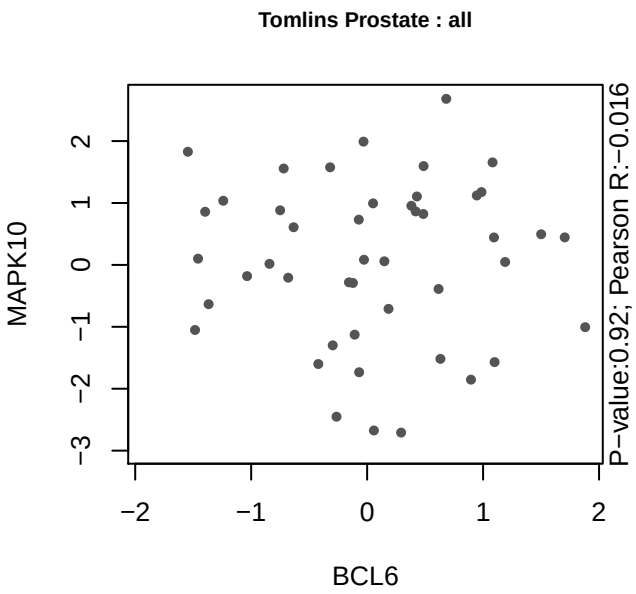

no data
LLGL2
ZBTB7A

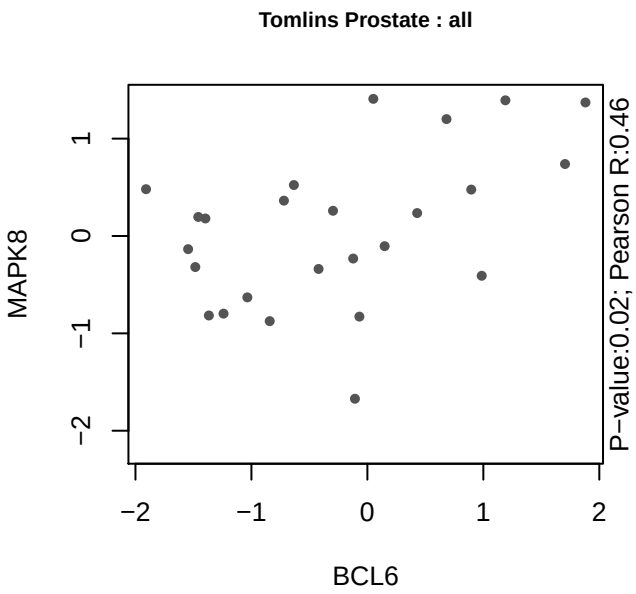

Tomlins Prostate : all
MAP2K4
BCL6
P−value:0.58; Pearson R:−0.083

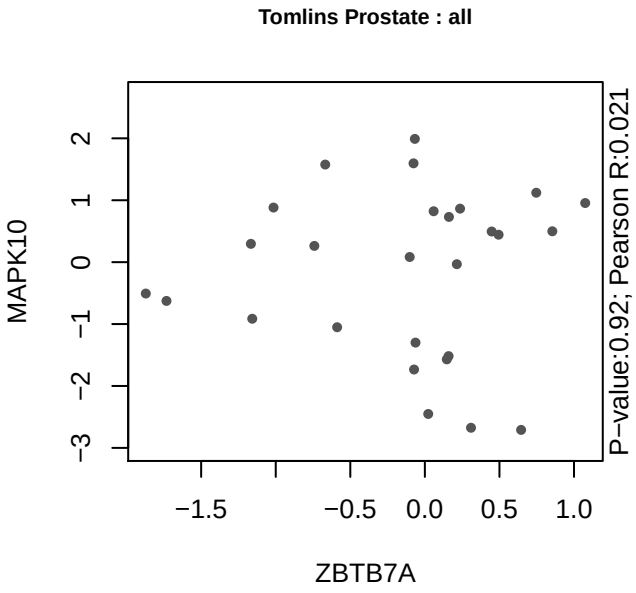

Tomlins Prostate : all
MAP2K7
BCL6
P−value:0.64; Pearson R:0.08

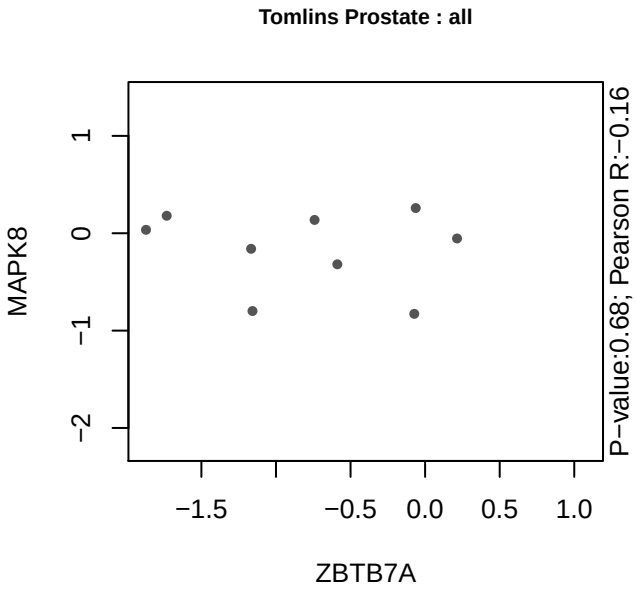

Tomlins Prostate : all
MAP2K4
ZBTB7A
P−value:0.44; Pearson R:0.16

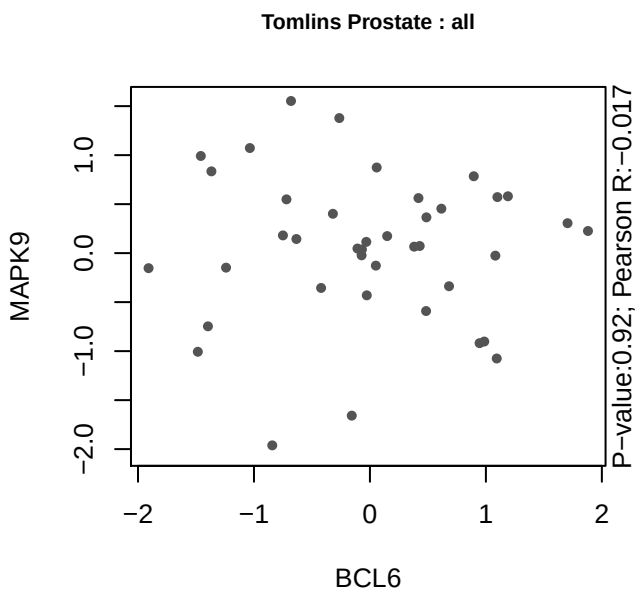

Tomlins Prostate : all
MAP2K7
ZBTB7A
P−value:0.57; Pearson R:−0.13

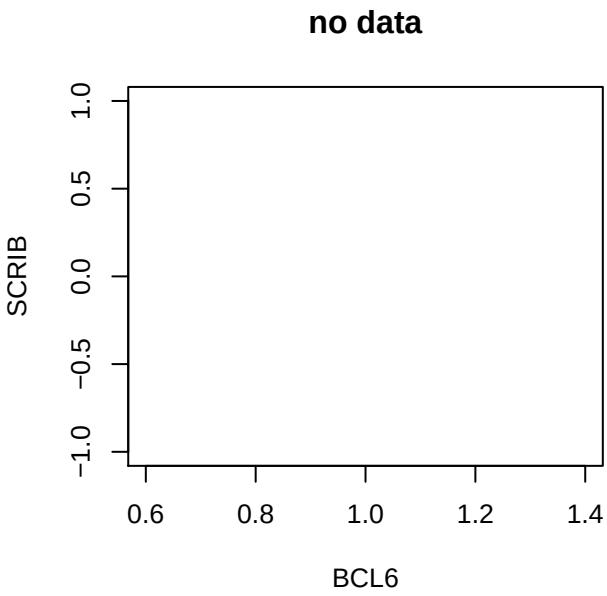

Tomlins Prostate : all
MAPK10
BCL6
P−value:0.92; Pearson R:−0.016

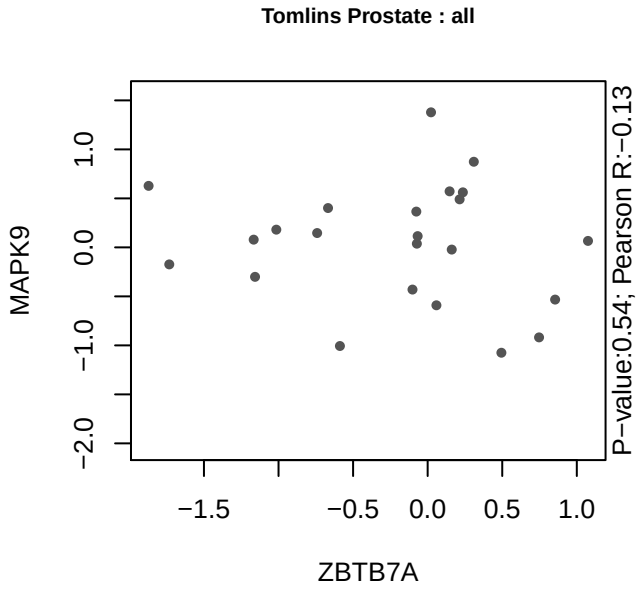

Tomlins Prostate : all
MAPK8
BCL6
P−value:0.02; Pearson R:0.46

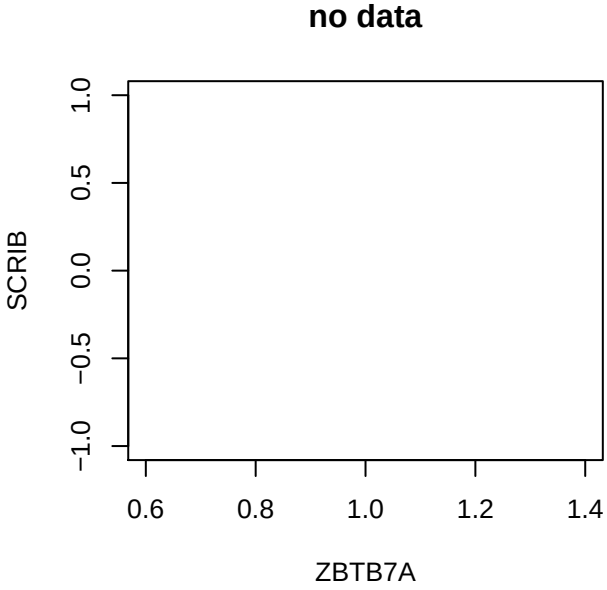

Tomlins Prostate : all
MAPK10
ZBTB7A
P−value:0.92; Pearson R:0.021

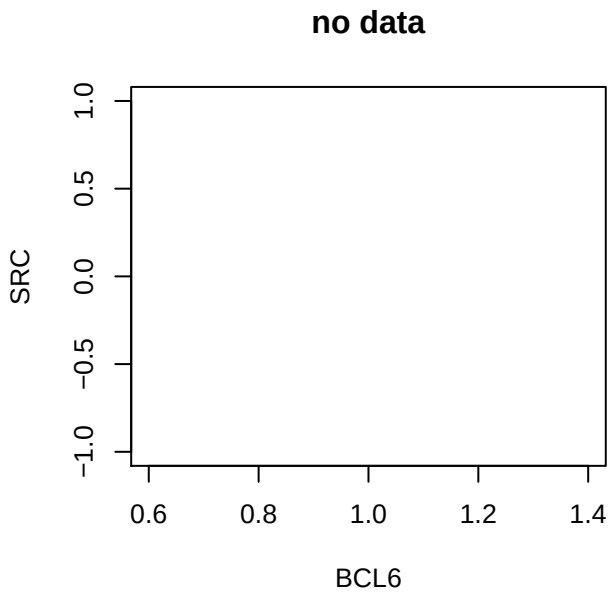

Tomlins Prostate : all
MAPK8
ZBTB7A
P−value:0.68; Pearson R:−0.16

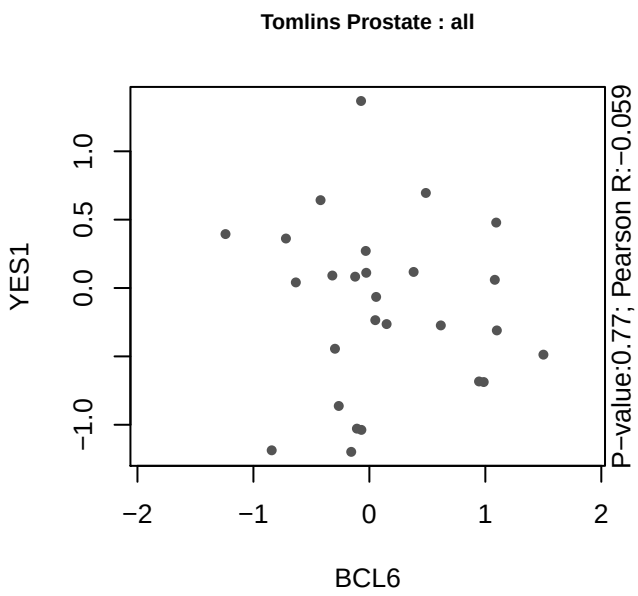

Tomlins Prostate : all
MAPK9
BCL6
P−value:0.92; Pearson R:−0.017
−2.0
−1.0
0.0
1.0
−2
−1
0
1
2

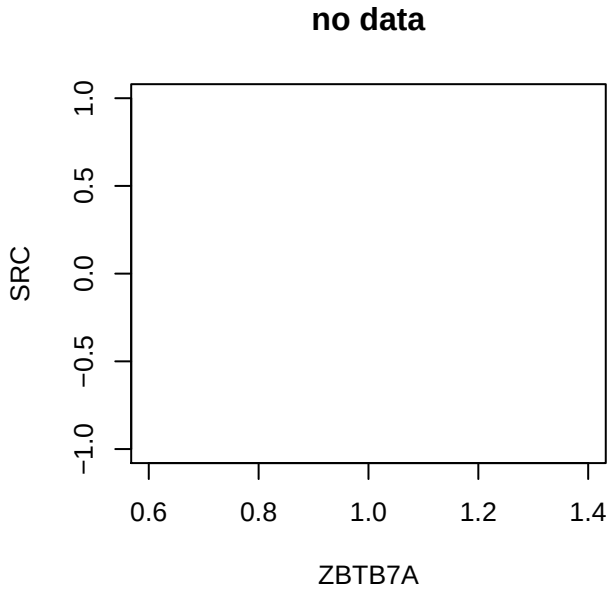

no data
SCRIB
BCL6
−1.0
−0.5
0.0
0.5
1.0
0.6
0.8
1.0
1.2
1.4

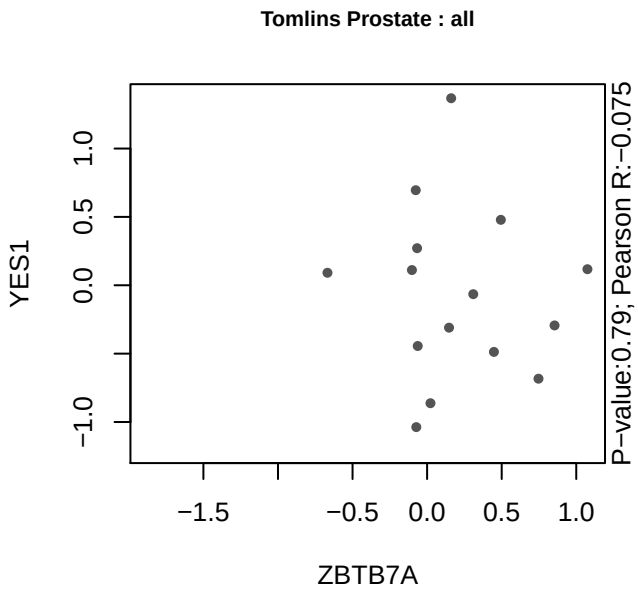

Tomlins Prostate : all
MAPK9
ZBTB7A
P−value:0.54; Pearson R:−0.13
−2.0
−1.0
0.0
1.0
−1.5
−0.5
0.0
0.5
1.0

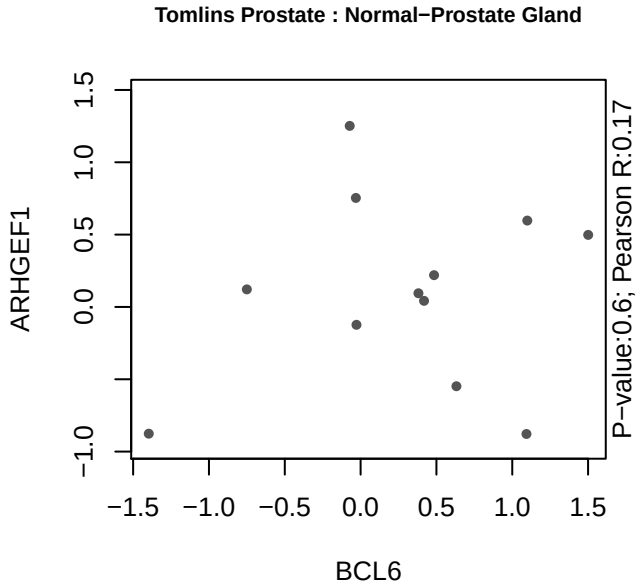

no data
SCRIB
ZBTB7A
−1.0
−0.5
0.0
0.5
1.0
0.6
0.8
1.0
1.2
1.4

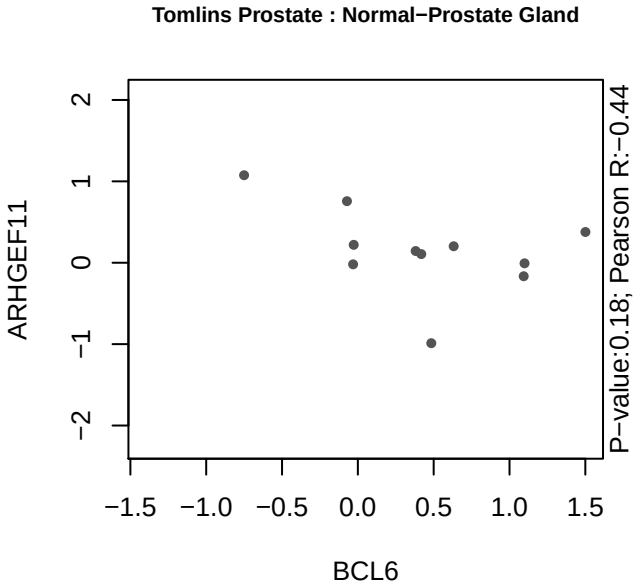

no data
SRC
BCL6
1.0
0.5
0.0
−0.5
−1.0
0.6
0.8
1.0
1.2
1.4

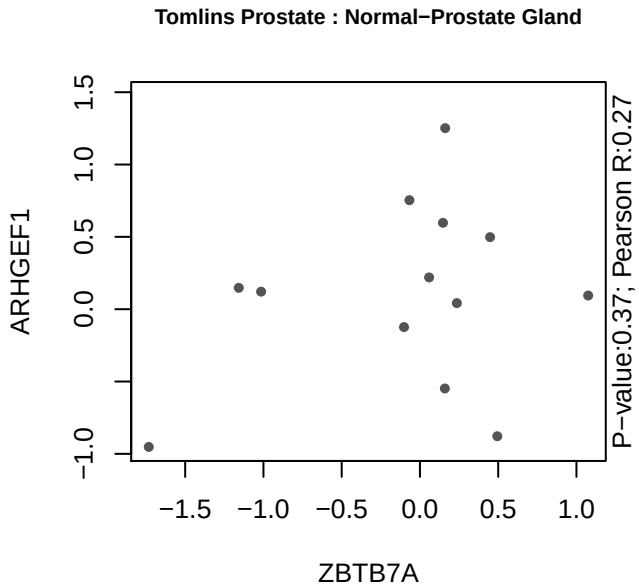

Tomlins Prostate : all
YES1
BCL6
P−value:0.77; Pearson R:−0.059
1.0
0.5
0.0
−1.0
−2
−1
0
1
2

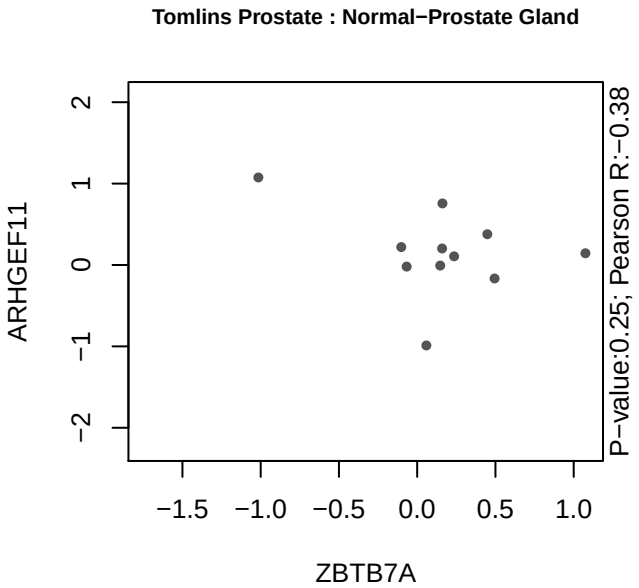

no data
SRC
ZBTB7A
1.0
0.5
0.0
−0.5
−1.0
0.6
0.8
1.0
1.2
1.4

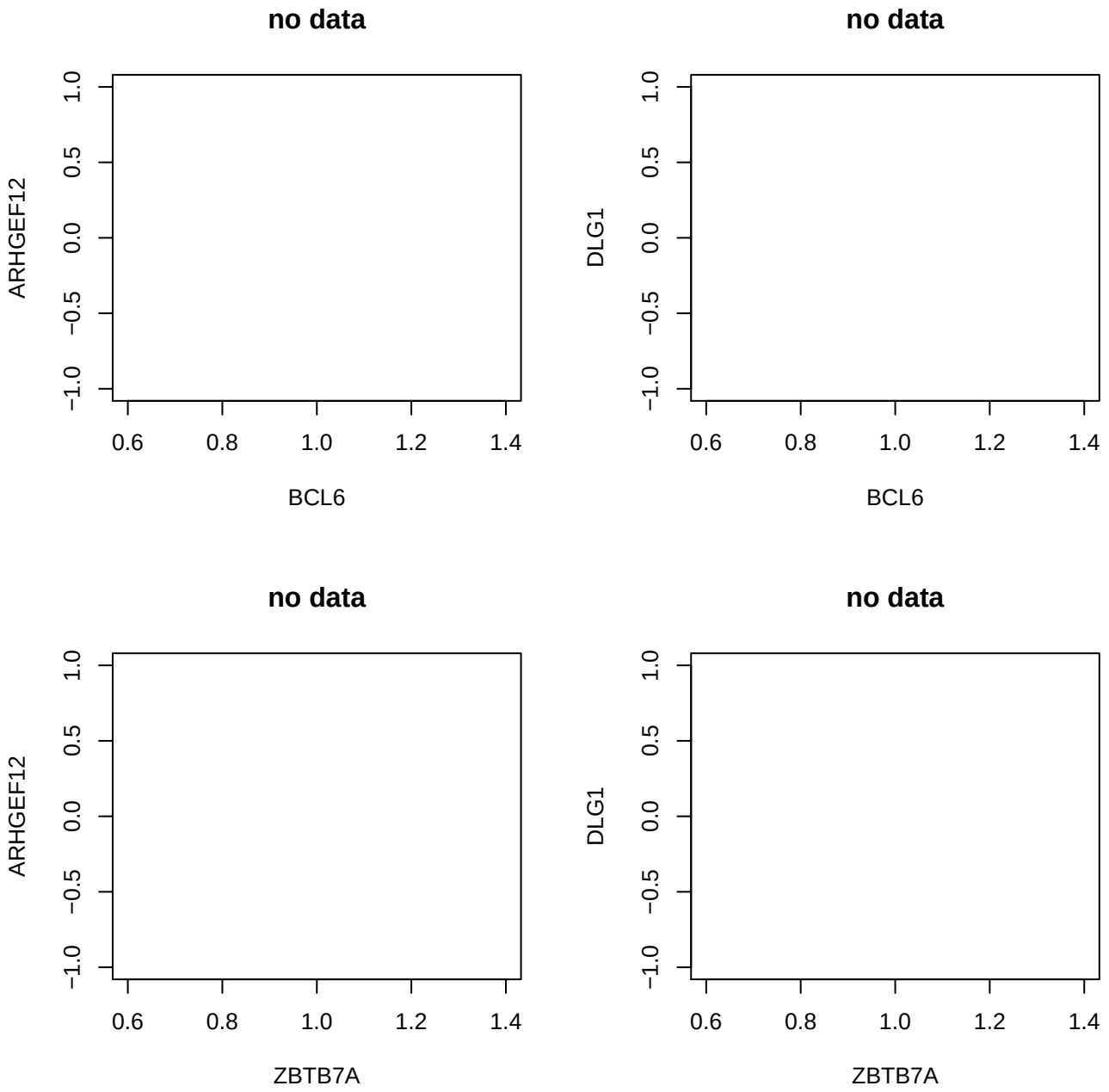

Tomlins Prostate : all
YES1
ZBTB7A
P−value:0.79; Pearson R:−0.075
1.0
0.5
0.0
−1.0
−1.5
−0.5
0.0
0.5
1.0

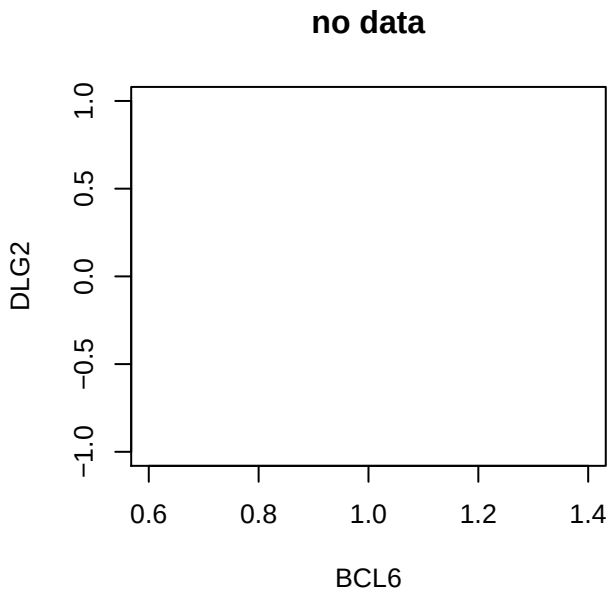

Tomlins Prostate : Normal−Prostate Gland
ARHGEF1
BCL6
P−value:0.6; Pearson R:0.17
−1.5
−1.0
−0.5
0.0
0.5
1.0
1.5

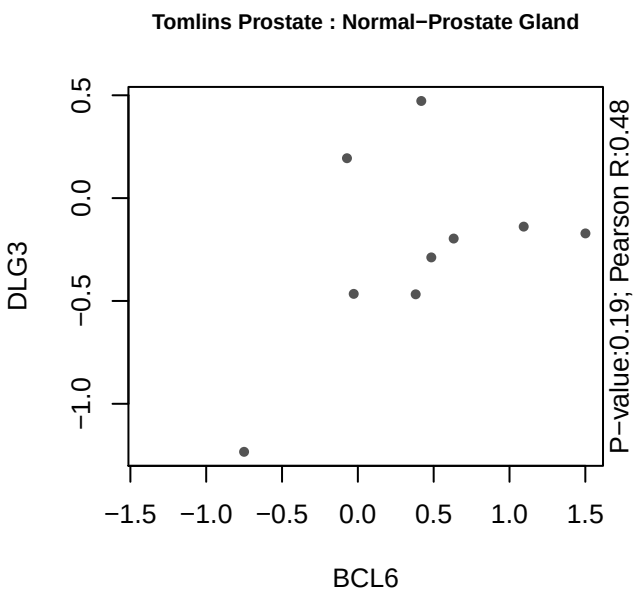

Tomlins Prostate : Normal−Prostate Gland
ARHGEF11
BCL6
P−value:0.18; Pearson R:−0.44
−2
−1
0
1
2

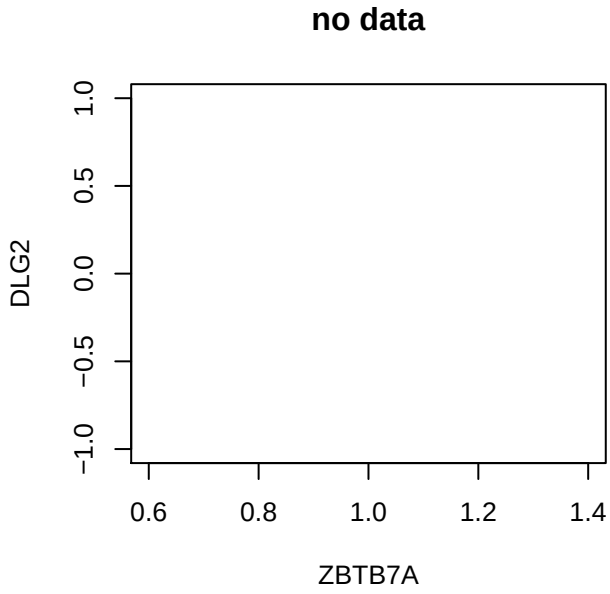

Tomlins Prostate : Normal−Prostate Gland
ARHGEF1
ZBTB7A
P−value:0.37; Pearson R:0.27

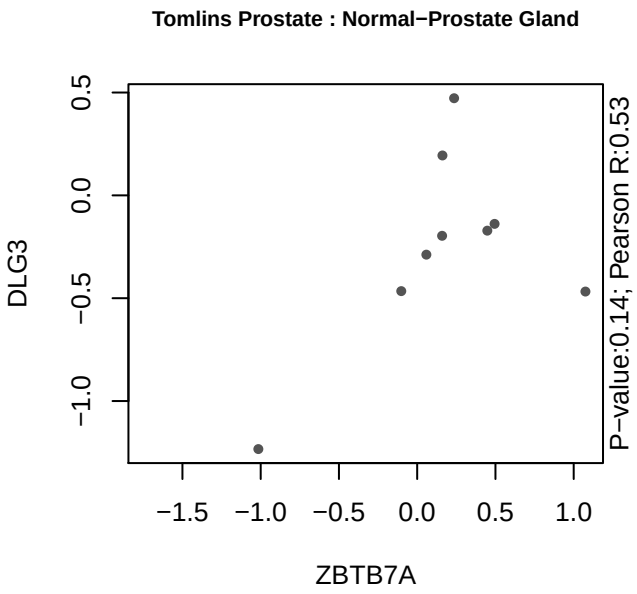

Tomlins Prostate : Normal−Prostate Gland
ARHGEF11
ZBTB7A
P−value:0.25; Pearson R:−0.38

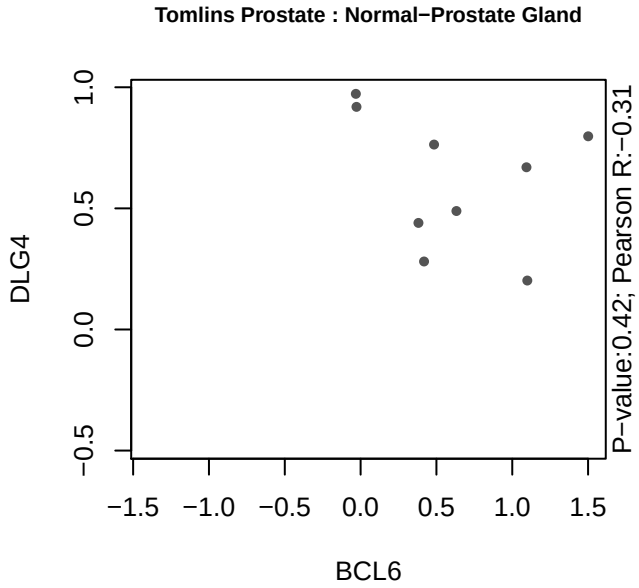

no data
ARHGEF12
BCL6
no data
DLG1
BCL6
no data
ARHGEF12
ZBTB7A
no data
DLG1
ZBTB7A
1.0
0.5
0.0
−0.5
−1.0
0.6
0.8
1.0
1.2
1.4

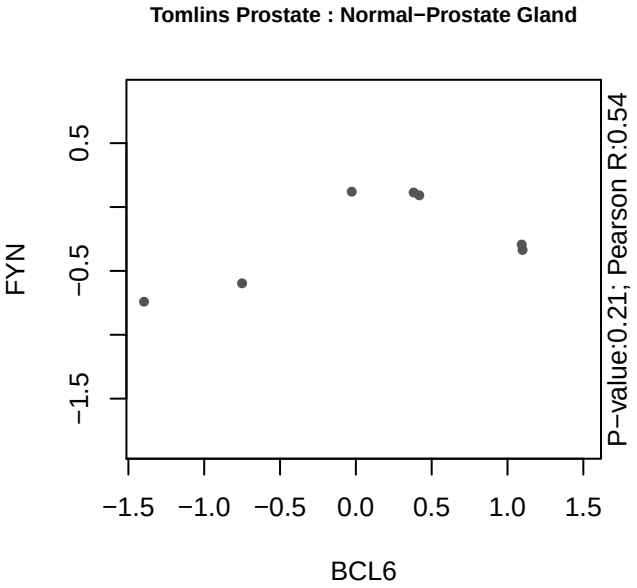

no data
DLG2
BCL6
1.0
0.5
0.0
−0.5
−1.0
0.6
0.8
1.0
1.2
1.4

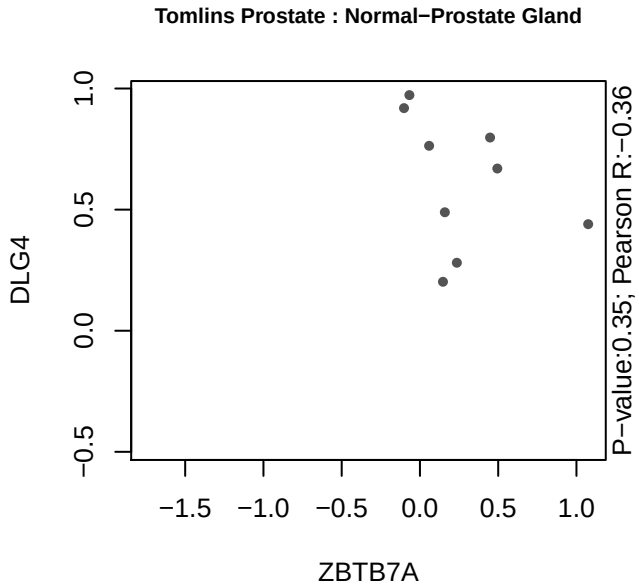

Tomlins Prostate : Normal−Prostate Gland
DLG3
BCL6
P−value:0.19; Pearson R:0.48
0.5
0.0
−0.5
−1.0
−1.5
−1.0
−0.5
0.0
0.5
1.0
1.5

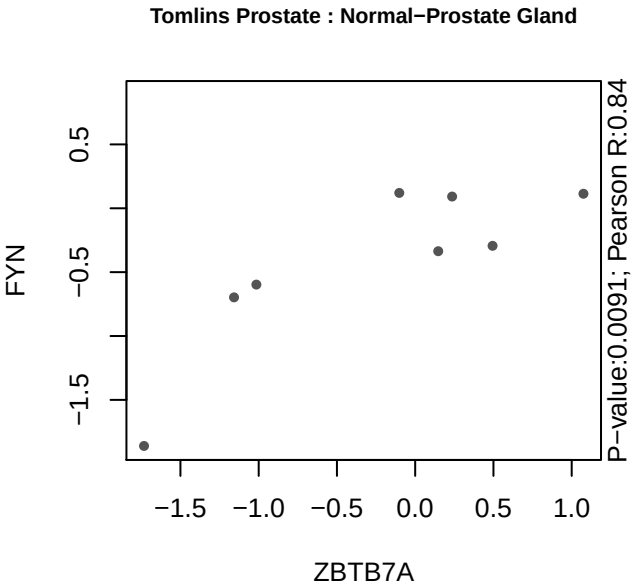

no data
DLG2
ZBTB7A
1.0
0.5
0.0
−0.5
−1.0
0.6
0.8
1.0
1.2
1.4

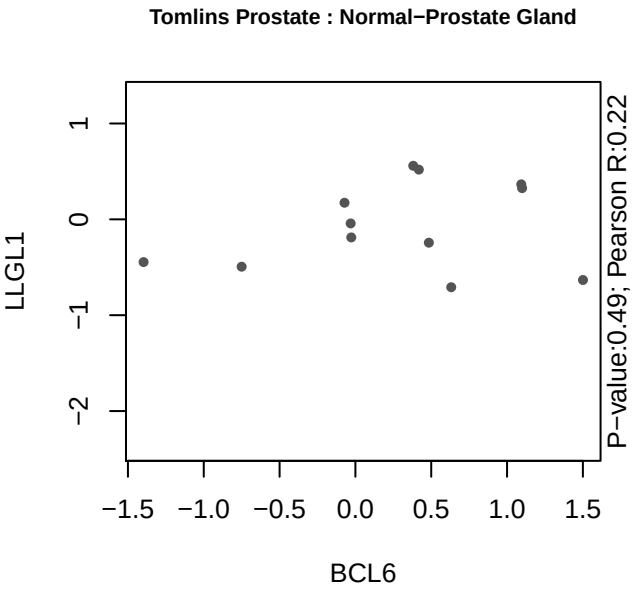

Tomlins Prostate : Normal−Prostate Gland
DLG3
ZBTB7A
P−value:0.14; Pearson R:0.53
0.5
0.0
−0.5
−1.0
−1.5
−1.0
−0.5
0.0
0.5
1.0

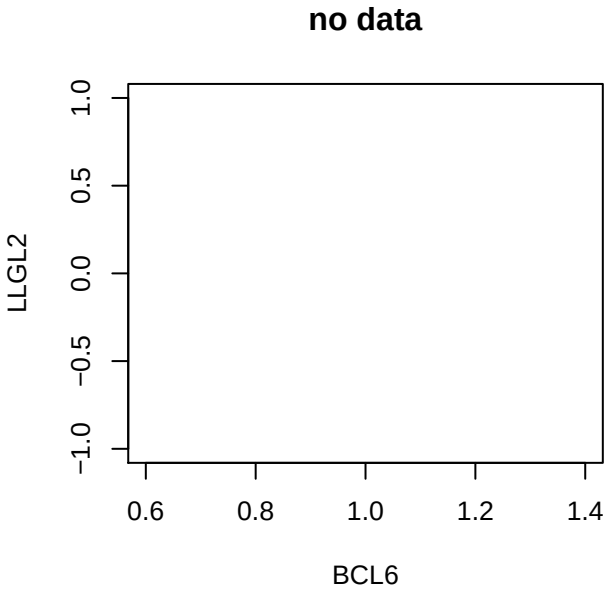

Tomlins Prostate : Normal−Prostate Gland
DLG4
BCL6
P−value:0.42; Pearson R:−0.31
1.0
0.5
0.0
−0.5
−1.5
−1.0
−0.5
0.0
0.5
1.0
1.5

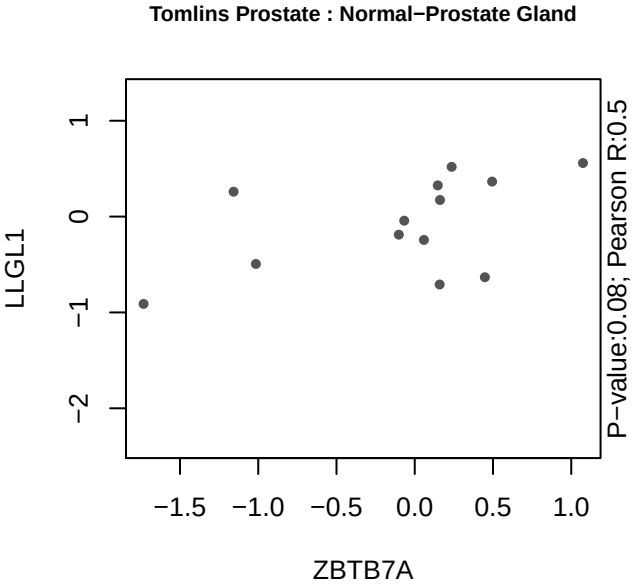

Tomlins Prostate : Normal−Prostate Gland
FYN
BCL6
P−value:0.21; Pearson R:0.54
0.5
−0.5
−1.5
−1.5
−1.0
−0.5
0.0
0.5
1.0
1.5

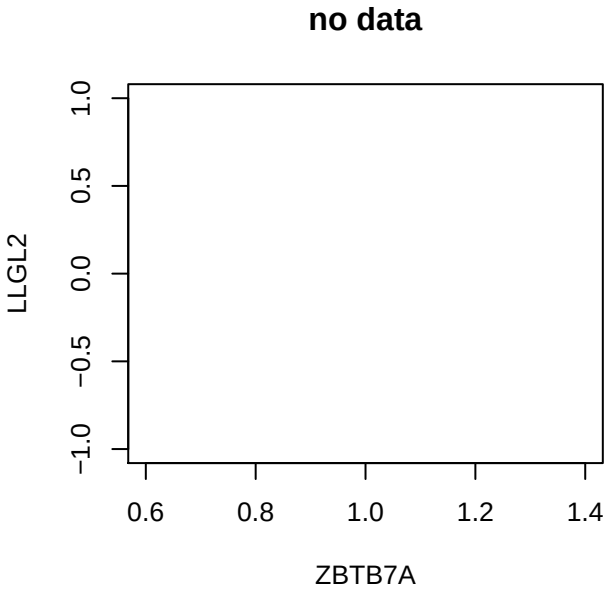

Tomlins Prostate : Normal−Prostate Gland
DLG4
ZBTB7A
P−value:0.35; Pearson R:−0.36
1.0
0.5
0.0
−0.5
−1.5
−1.0
−0.5
0.0
0.5
1.0

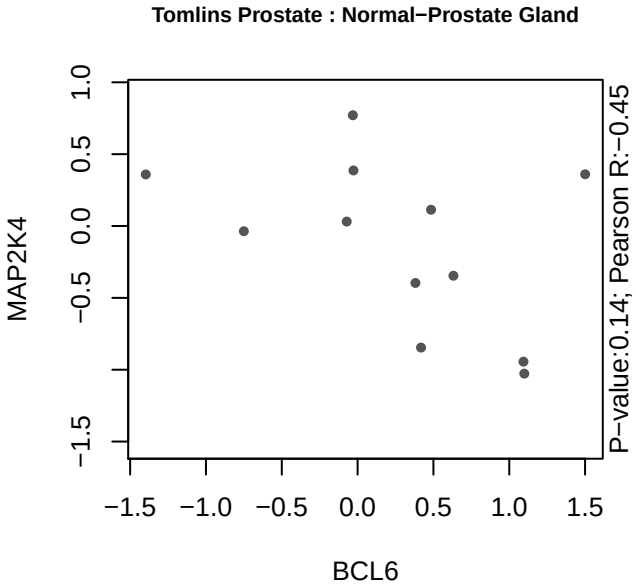

Tomlins Prostate : Normal−Prostate Gland
FYN
ZBTB7A
P−value:0.0091; Pearson R:0.84
0.5
−0.5
−1.5
−1.5
−1.0
−0.5
0.0
0.5
1.0

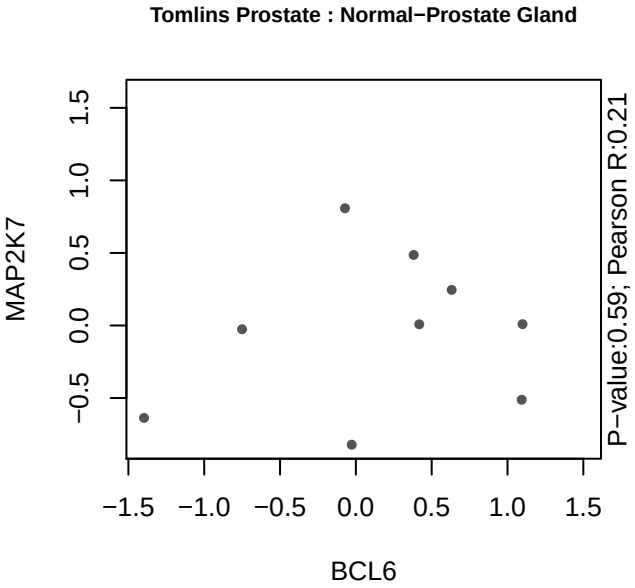

Tomlins Prostate : Normal−Prostate Gland
LLGL1
BCL6
P−value:0.49; Pearson R:0.22
−1.5
−1.0
−0.5
0.0
0.5
1.0
1.5
−2
−1
0
1

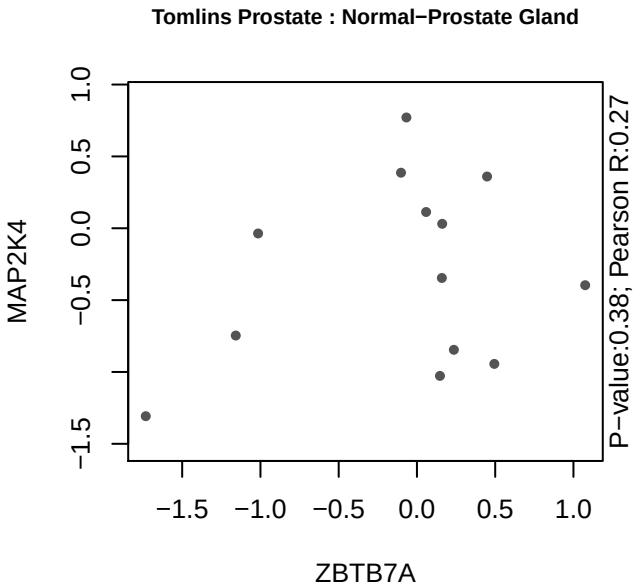

no data
LLGL2
BCL6
0.6
0.8
1.0
1.2
1.4
−1.0
−0.5
0.0
0.5
1.0

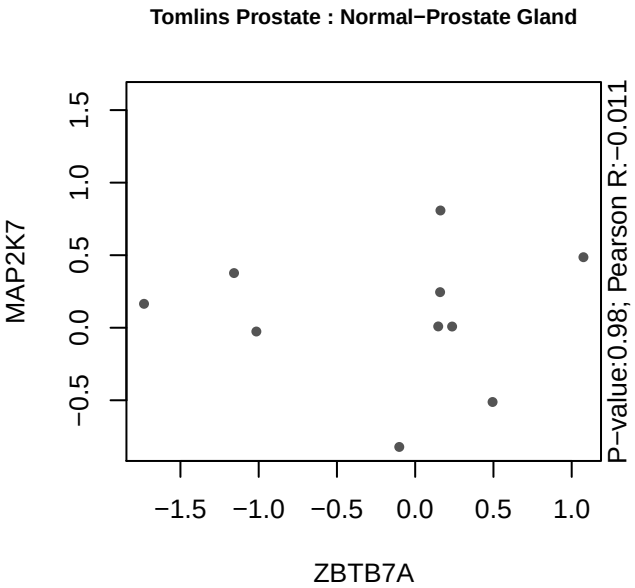

Tomlins Prostate : Normal−Prostate Gland
LLGL1
ZBTB7A
P−value:0.08; Pearson R:0.5
−1.5
−1.0
−0.5
0.0
0.5
1.0
−2
−1
0
1

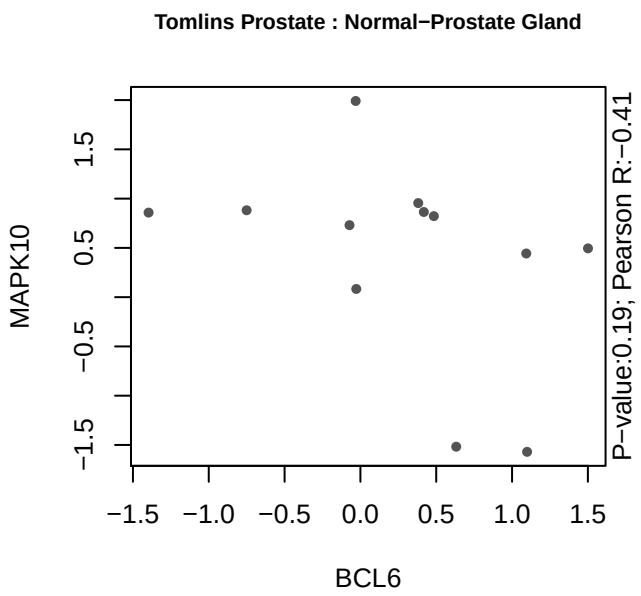

no data
LLGL2
ZBTB7A
0.6
0.8
1.0
1.2
1.4
−1.0
−0.5
0.0
0.5
1.0

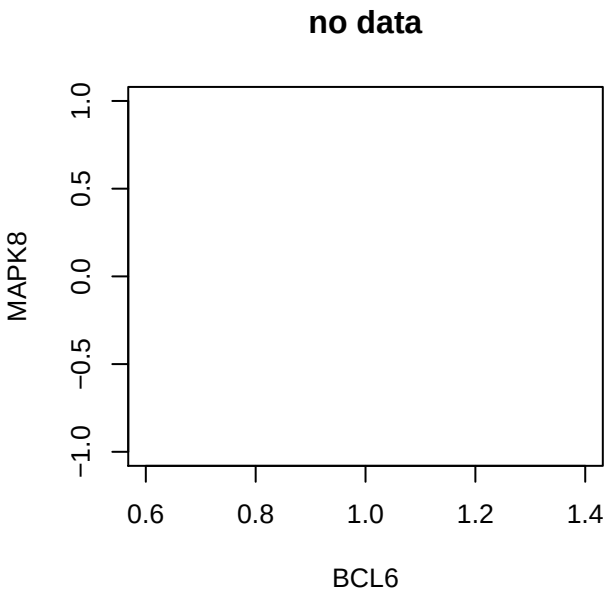

Tomlins Prostate : Normal−Prostate Gland
MAP2K4
BCL6
P−value:0.14; Pearson R:−0.45

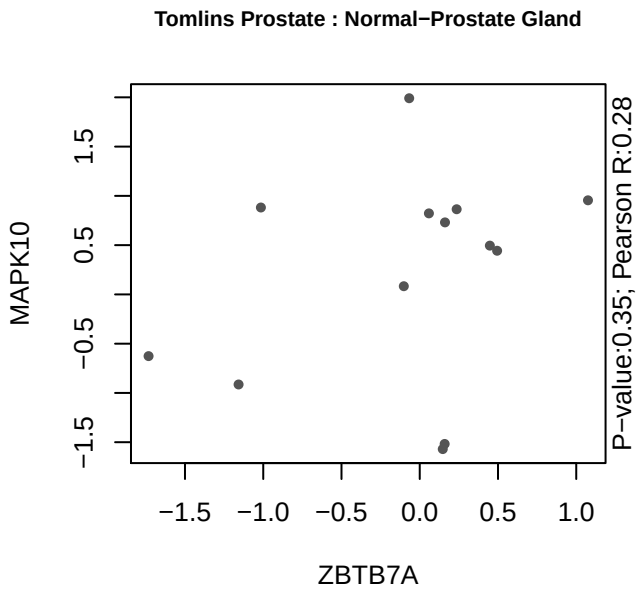

Tomlins Prostate : Normal−Prostate Gland
MAP2K7
BCL6
P−value:0.59; Pearson R:0.21

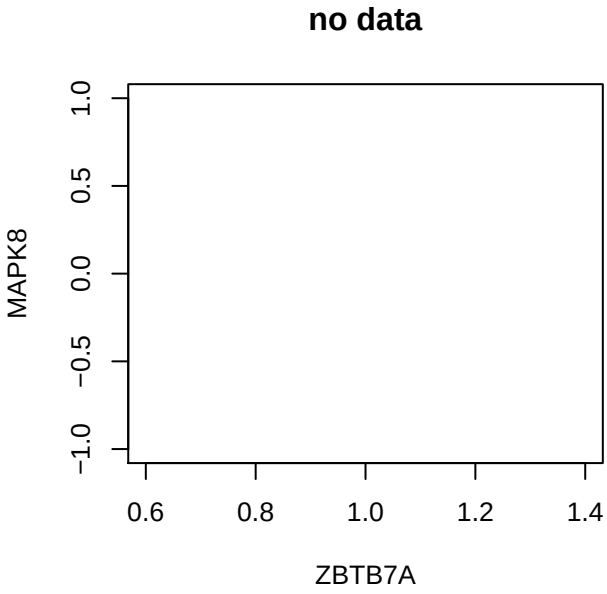

Tomlins Prostate : Normal−Prostate Gland
MAP2K4
ZBTB7A
P−value:0.38; Pearson R:0.27

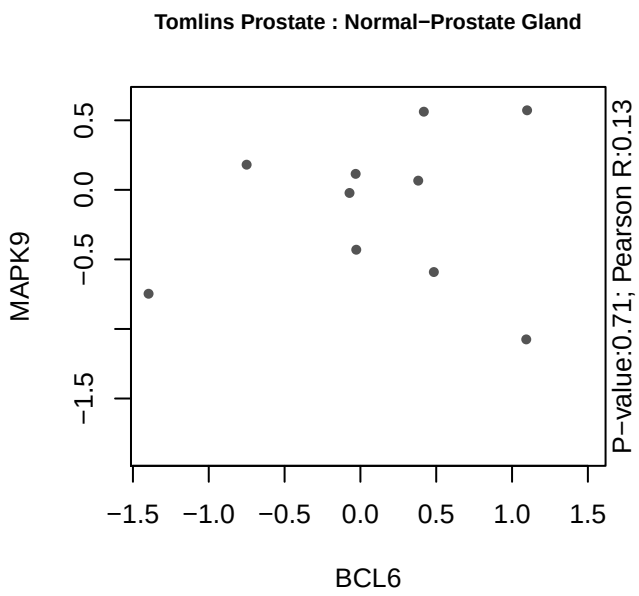

Tomlins Prostate : Normal−Prostate Gland
MAP2K7
ZBTB7A
P−value:0.98; Pearson R:−0.011

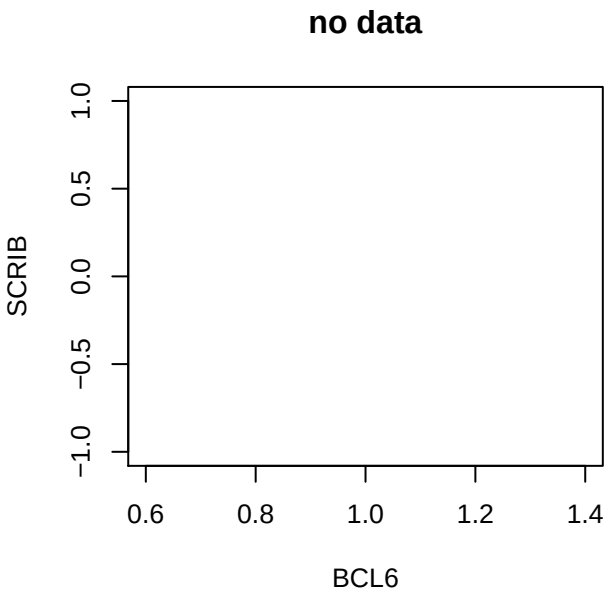

Tomlins Prostate : Normal−Prostate Gland
MAPK10
BCL6
P−value:0.19; Pearson R:−0.41
−1.5
−1.0
−0.5
0.0
0.5
1.0
1.5

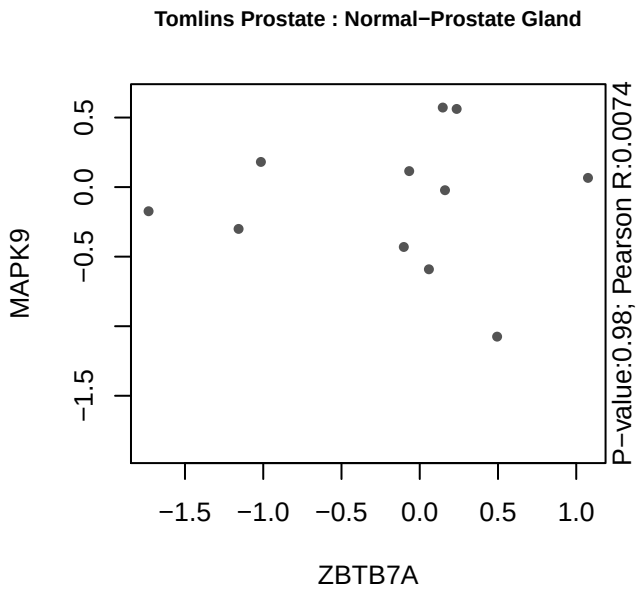

no data
MAPK8
BCL6
−1.0
−0.5
0.0
0.5
1.0
0.6
0.8
1.2
1.4

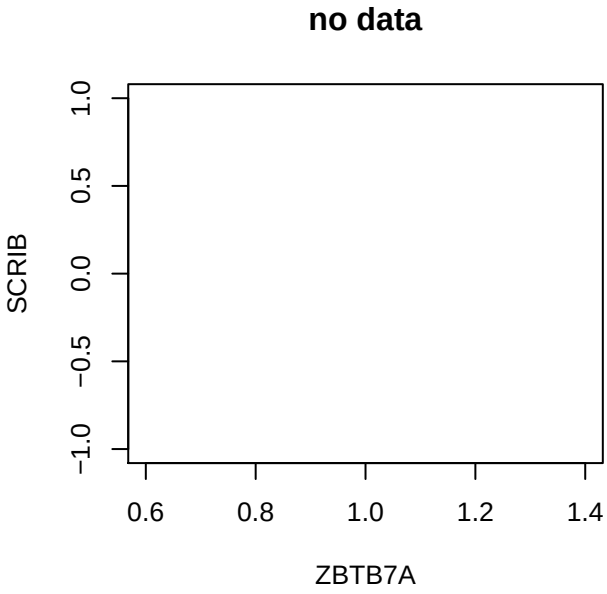

Tomlins Prostate : Normal−Prostate Gland
MAPK10
ZBTB7A
P−value:0.35; Pearson R:0.28
−1.5
−1.0
−0.5
0.0
0.5
1.0
1.5

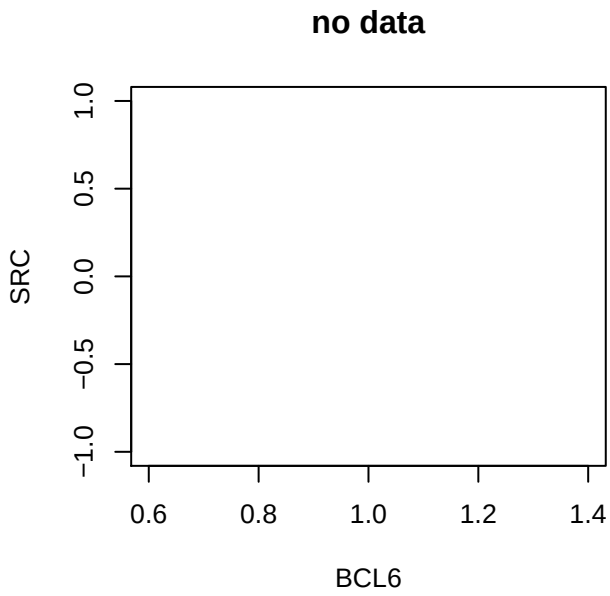

no data
MAPK8
ZBTB7A
−1.0
−0.5
0.0
0.5
1.0
0.6
0.8
1.2
1.4

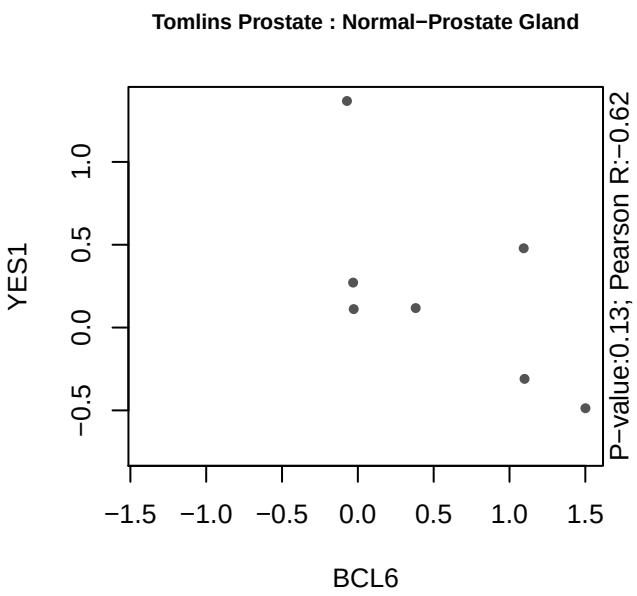

Tomlins Prostate : Normal−Prostate Gland
MAPK9
BCL6
P−value:0.71; Pearson R:0.13
−1.5
−1.0
−0.5
0.0
0.5
1.0
1.5

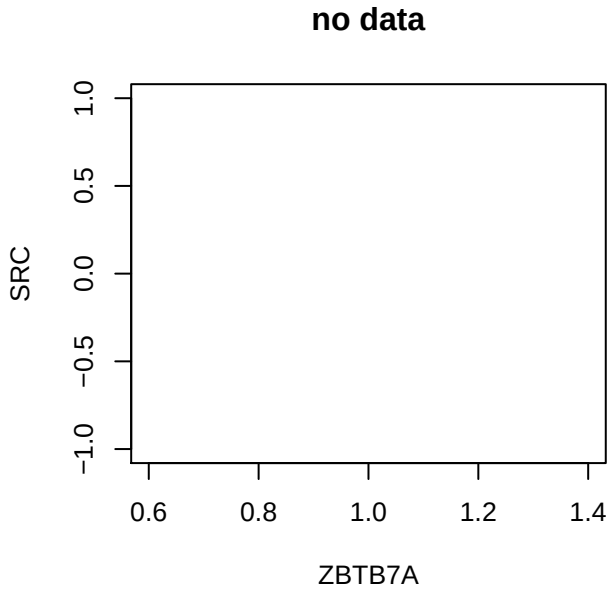

no data
SCRIB
BCL6
−1.0
−0.5
0.0
0.5
1.0
0.6
0.8
1.0
1.2
1.4

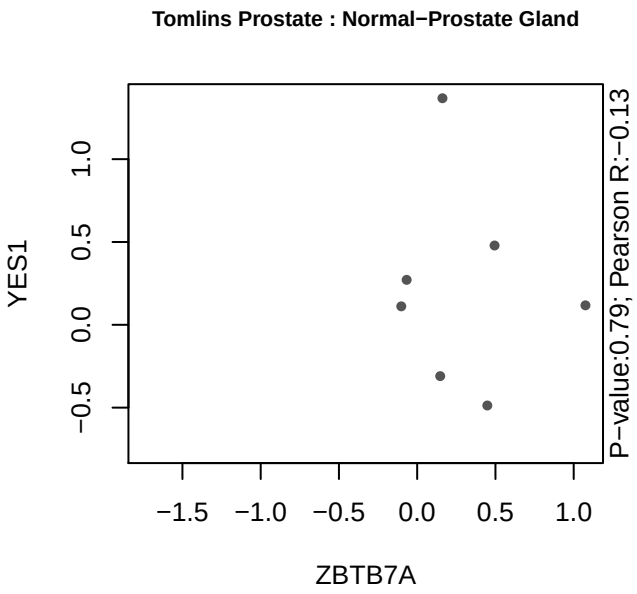

Tomlins Prostate : Normal−Prostate Gland
MAPK9
ZBTB7A
P−value:0.98; Pearson R:0.0074
−1.5
−1.0
−0.5
0.0
0.5
1.0

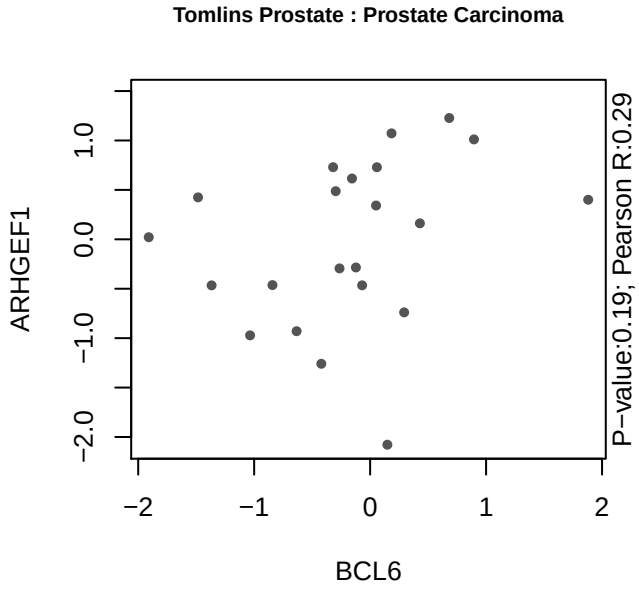

no data
SCRIB
ZBTB7A
−1.0
−0.5
0.0
0.5
1.0
0.6
0.8
1.0
1.2
1.4

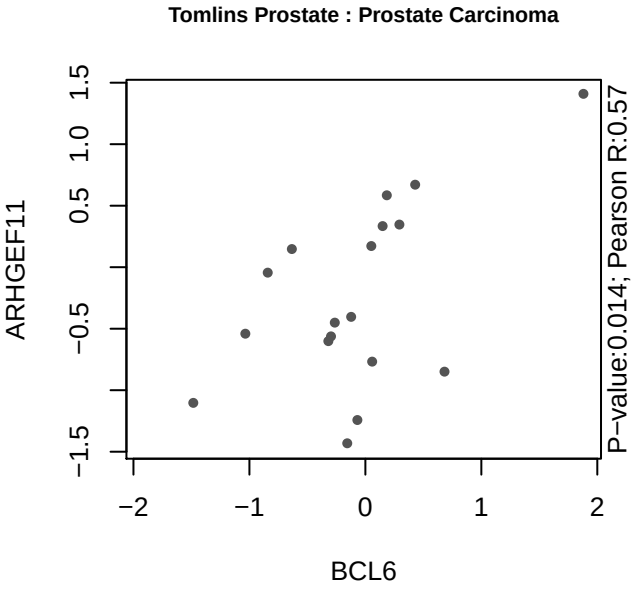

no data
SRC
BCL6
1.0
0.5
0.0
−0.5
−1.0
0.6
0.8
1.0
1.2
1.4

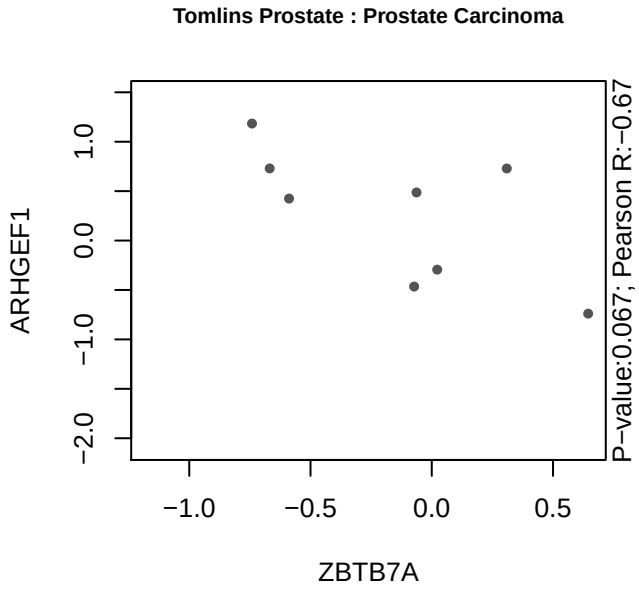

Tomlins Prostate : Normal−Prostate Gland
YES1
BCL6
P−value:0.13; Pearson R:−0.62
1.0
0.5
0.0
−0.5
−1.5
−1.0
−0.5
0.0
0.5
1.0
1.5

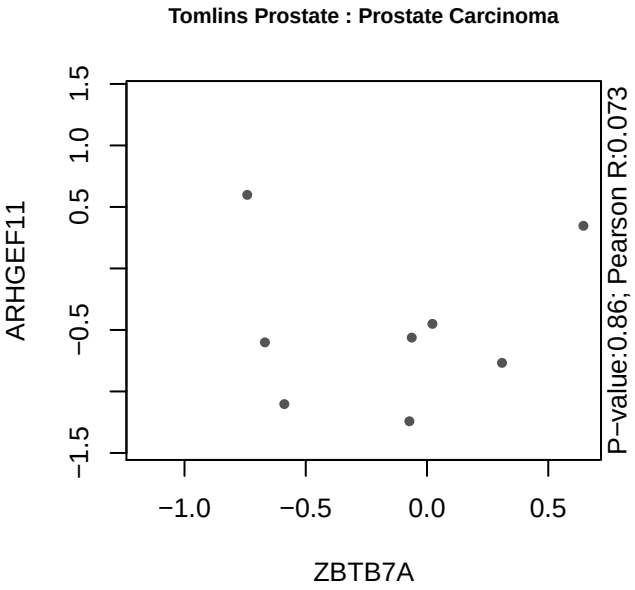

no data
SRC
ZBTB7A
1.0
0.5
0.0
−0.5
−1.0
0.6
0.8
1.0
1.2
1.4

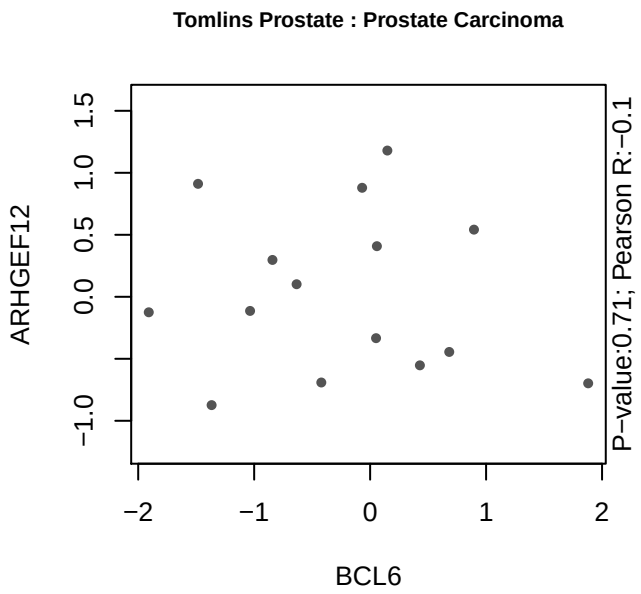

Tomlins Prostate : Normal−Prostate Gland
YES1
ZBTB7A
P−value:0.79; Pearson R:−0.13
1.0
0.5
0.0
−0.5
−1.5
−1.0
−0.5
0.0
0.5
1.0

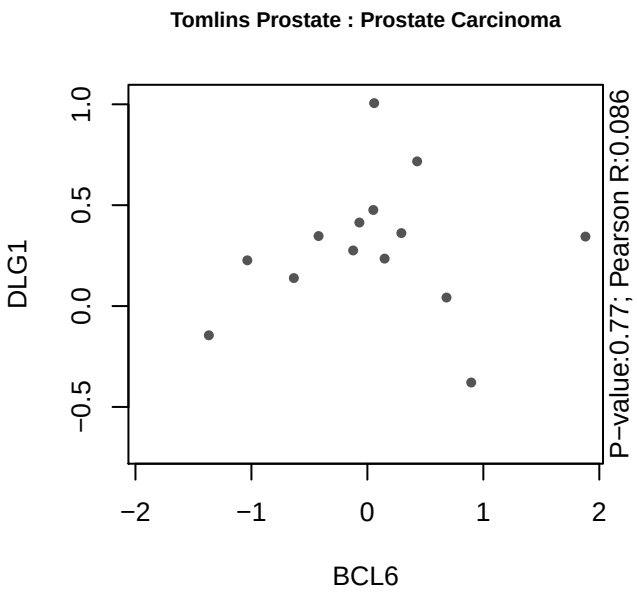

Tomlins Prostate : Prostate Carcinoma
ARHGEF1
BCL6
P−value:0.19; Pearson R:0.29

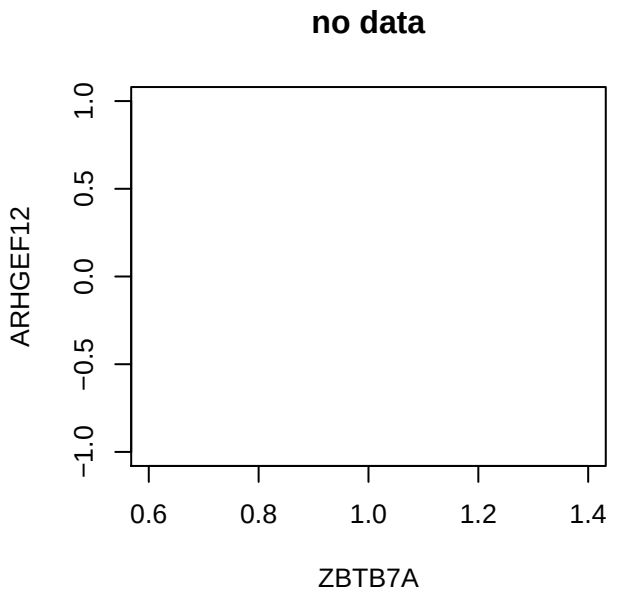

Tomlins Prostate : Prostate Carcinoma
ARHGEF11
BCL6
P−value:0.014; Pearson R:0.57

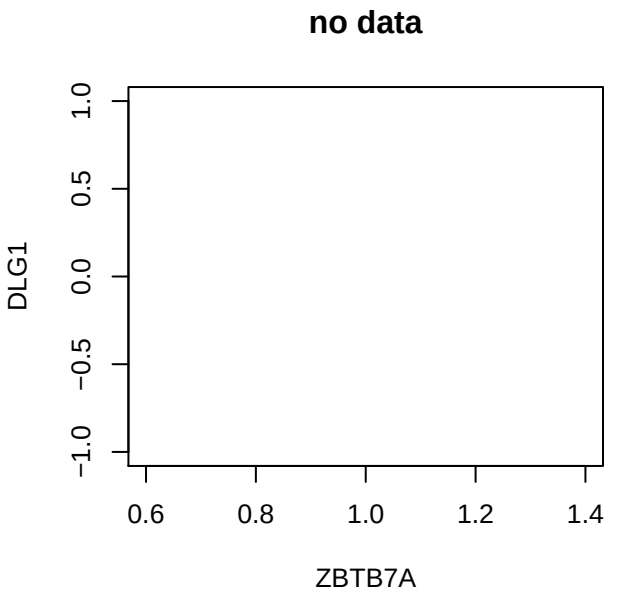

Tomlins Prostate : Prostate Carcinoma
ARHGEF1
ZBTB7A
P−value:0.067; Pearson R:−0.67

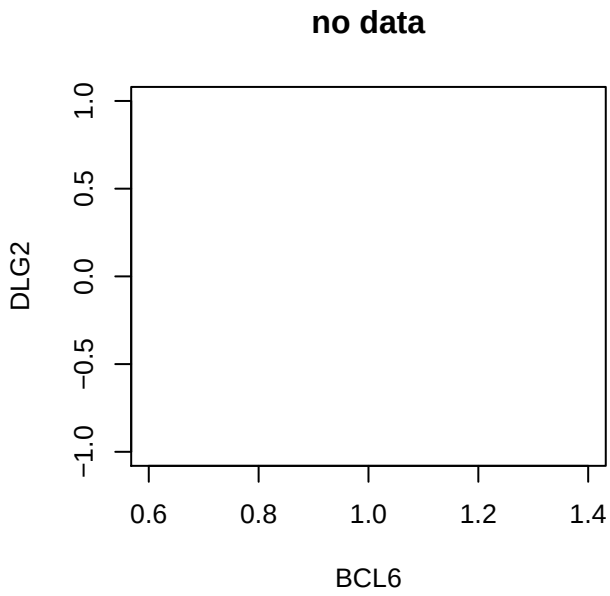

Tomlins Prostate : Prostate Carcinoma
ARHGEF11
ZBTB7A
P−value:0.86; Pearson R:0.073

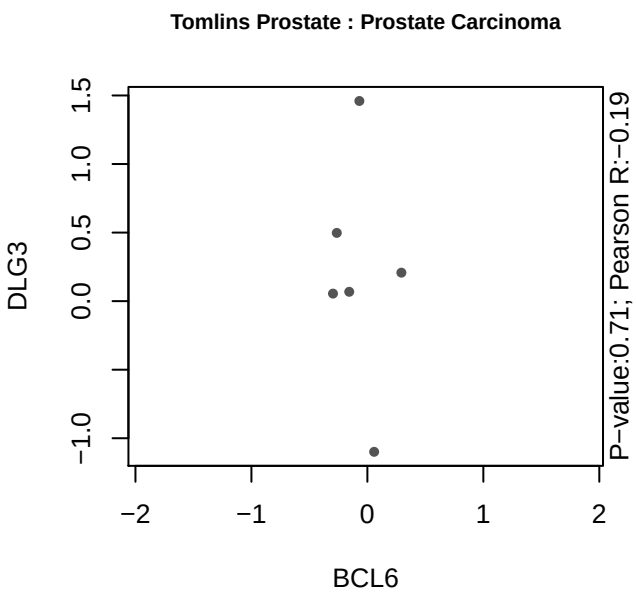

Tomlins Prostate : Prostate Carcinoma
ARHGEF12
BCL6
P−value:0.71; Pearson R:−0.1

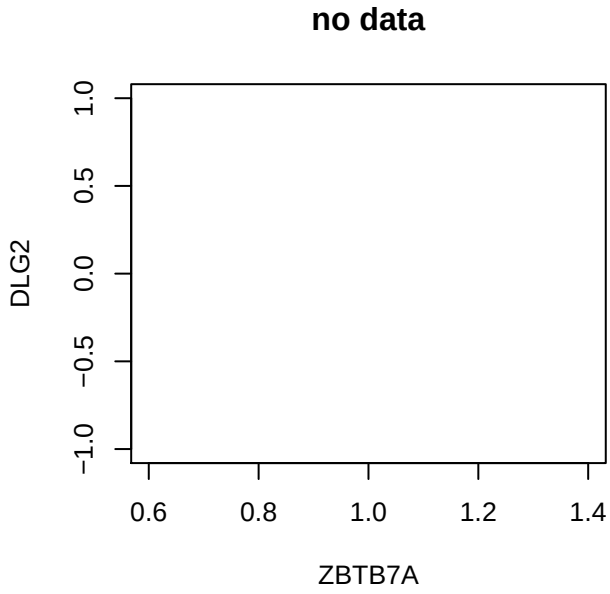

Tomlins Prostate : Prostate Carcinoma
DLG1
BCL6
P−value:0.77; Pearson R:0.086

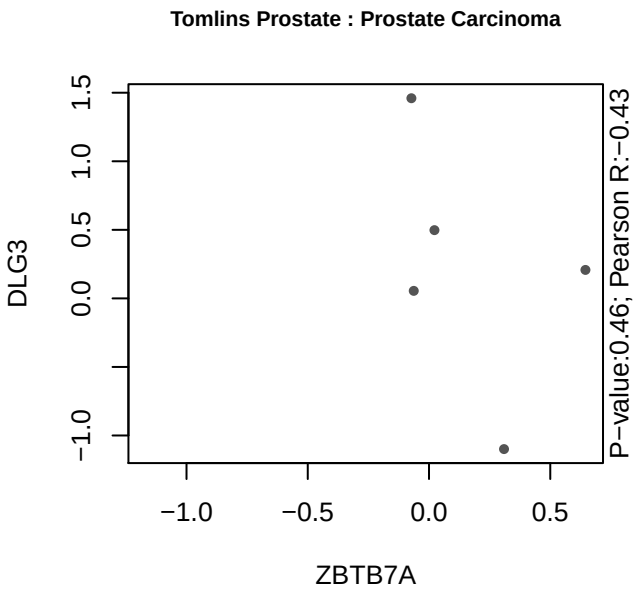

no data
ARHGEF12
ZBTB7A

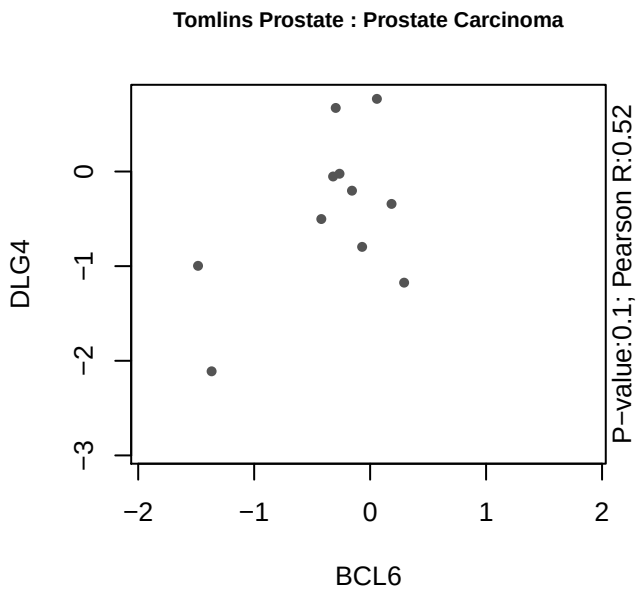

no data
DLG1
ZBTB7A

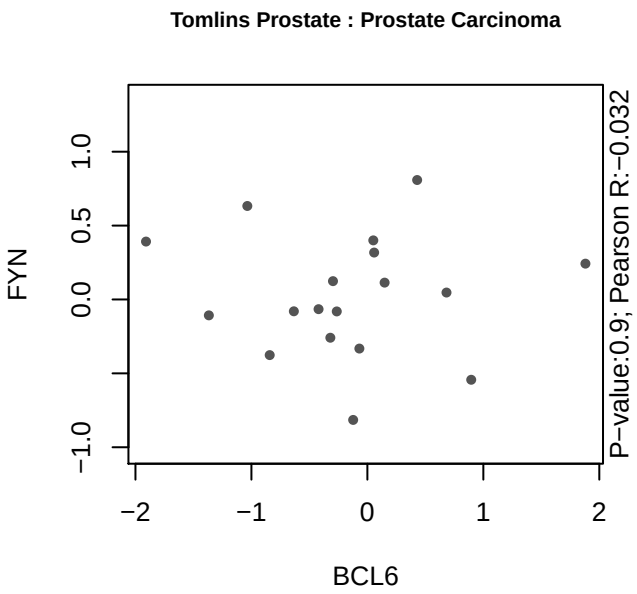

no data
DLG2
BCL6
−1.0
−0.5
0.0
0.5
1.0
0.6
0.8
1.0
1.2
1.4

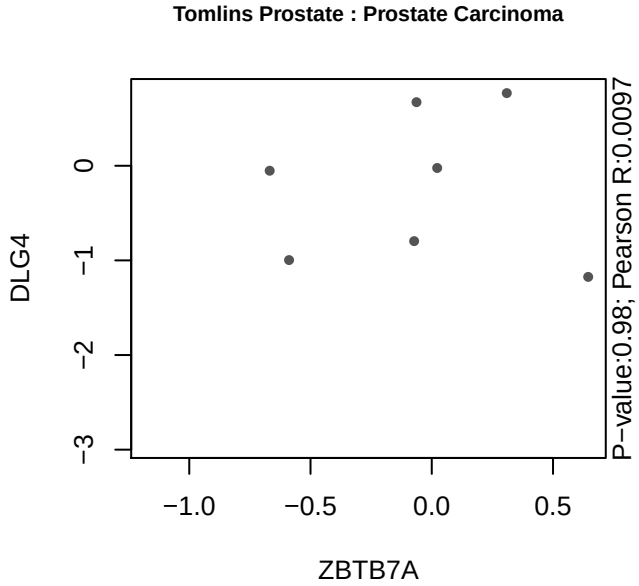

Tomlins Prostate : Prostate Carcinoma
DLG3
BCL6
P−value:0.71; Pearson R:−0.19
−1.0
0.0
0.5
1.0
1.5
−2
−1
0
1
2

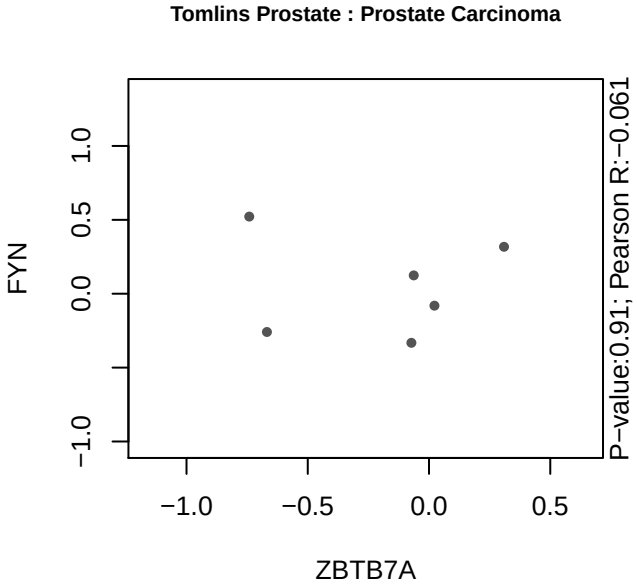

no data
DLG2
ZBTB7A
−1.0
−0.5
0.0
0.5
1.0
0.6
0.8
1.0
1.2
1.4

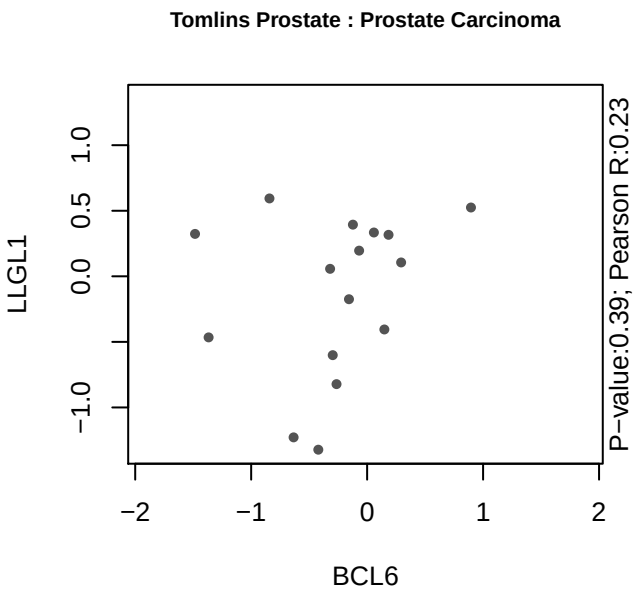

Tomlins Prostate : Prostate Carcinoma
DLG3
ZBTB7A
P−value:0.46; Pearson R:−0.43
−1.0
0.0
0.5
1.0
1.5
−1.0
−0.5
0.0
0.5

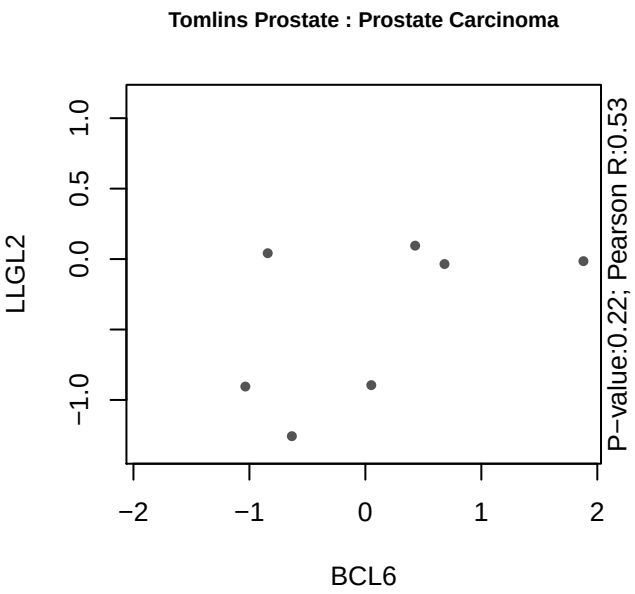

Tomlins Prostate : Prostate Carcinoma
DLG4
BCL6
P−value:0.1; Pearson R:0.52

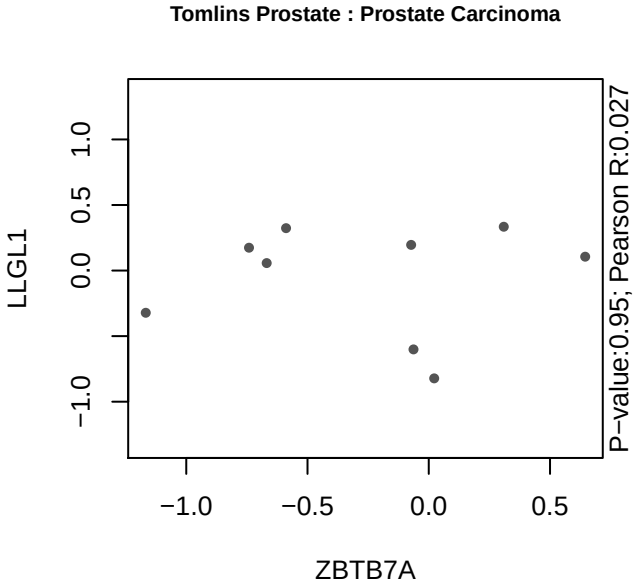

Tomlins Prostate : Prostate Carcinoma
FYN
BCL6
P−value:0.9; Pearson R:−0.032

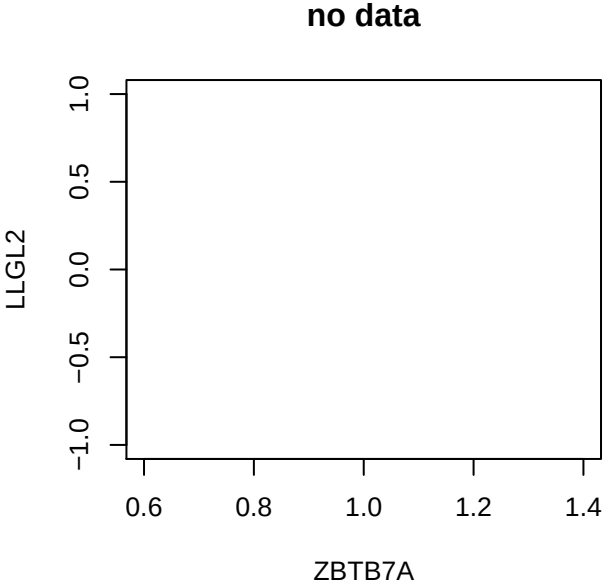

Tomlins Prostate : Prostate Carcinoma
DLG4
ZBTB7A
P−value:0.98; Pearson R:0.0097

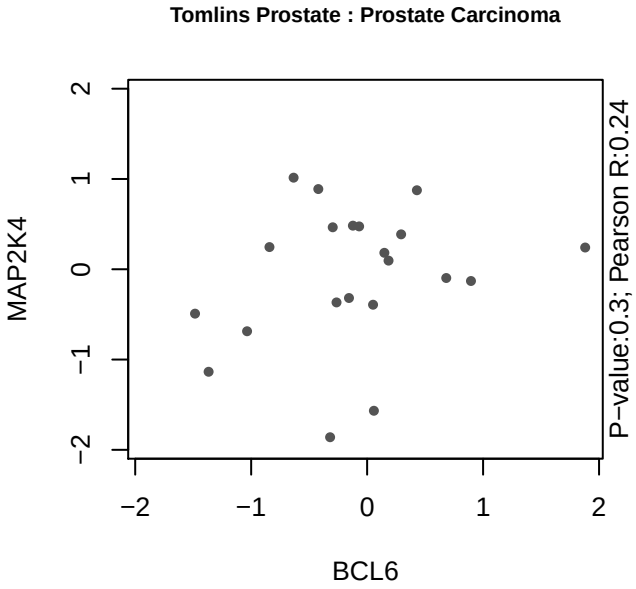

Tomlins Prostate : Prostate Carcinoma
FYN
ZBTB7A
P−value:0.91; Pearson R:−0.061

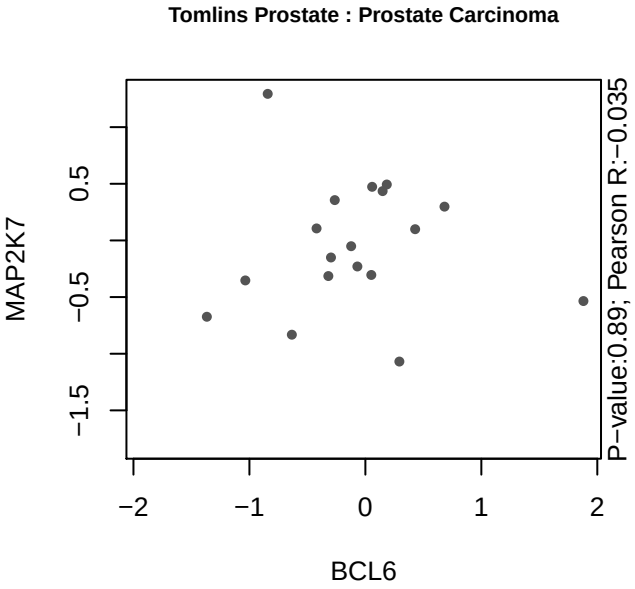

Tomlins Prostate : Prostate Carcinoma
LLGL1
BCL6
P−value:0.39; Pearson R:0.23

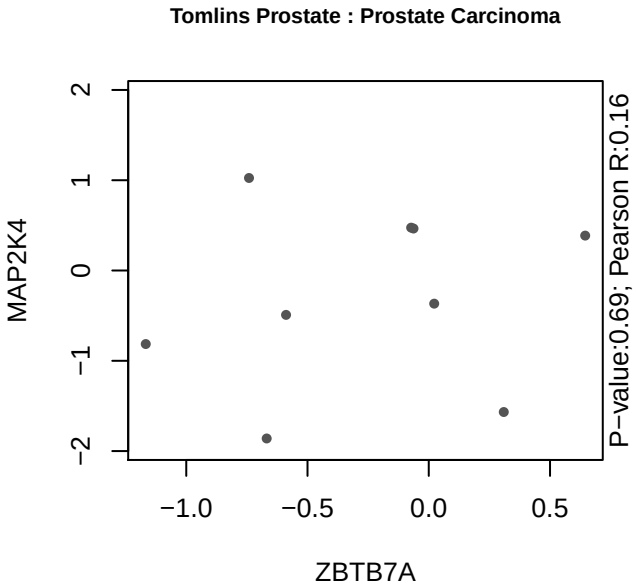

Tomlins Prostate : Prostate Carcinoma
LLGL2
BCL6
P−value:0.22; Pearson R:0.53

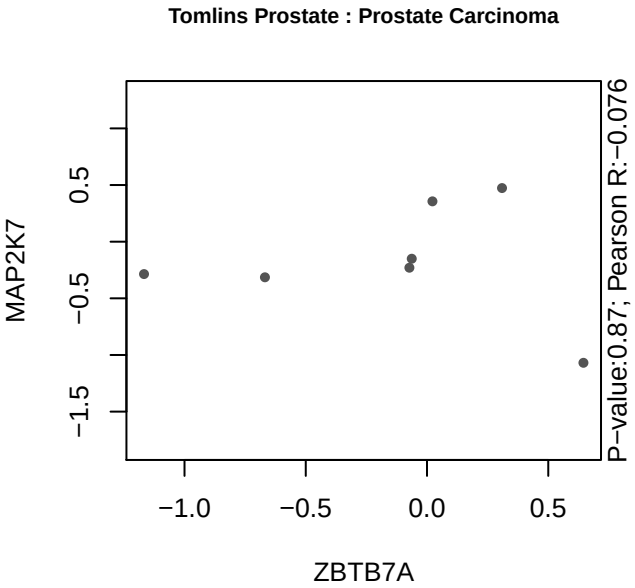

Tomlins Prostate : Prostate Carcinoma
LLGL1
ZBTB7A
P−value:0.95; Pearson R:0.027

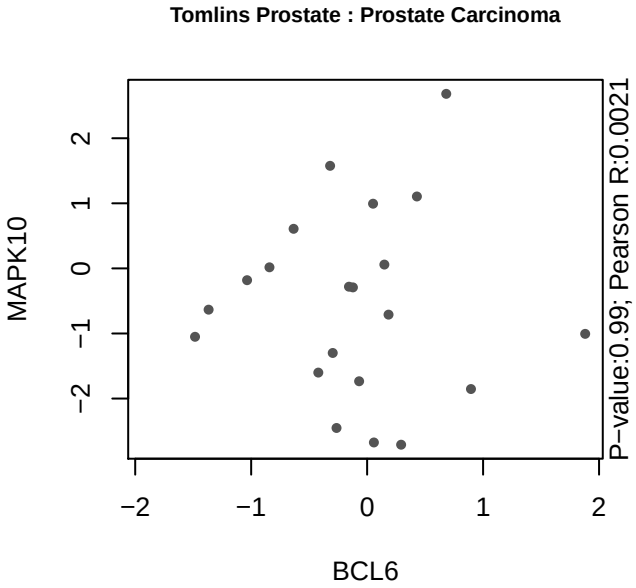

no data
LLGL2
ZBTB7A

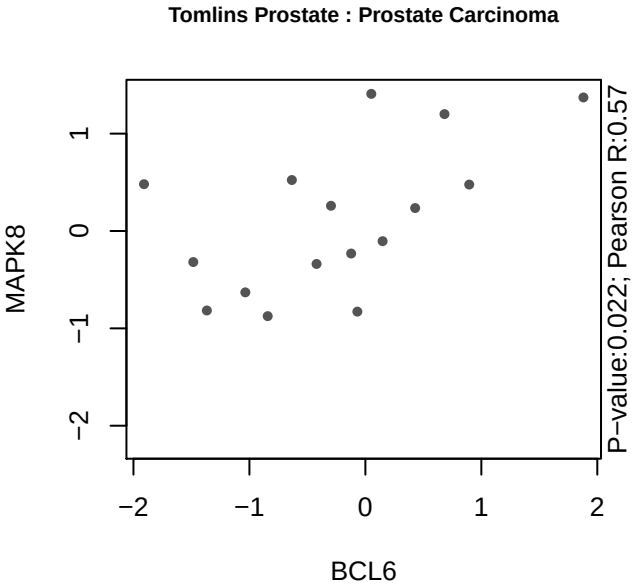

Tomlins Prostate : Prostate Carcinoma
MAP2K4
BCL6
P−value:0.3; Pearson R:0.24

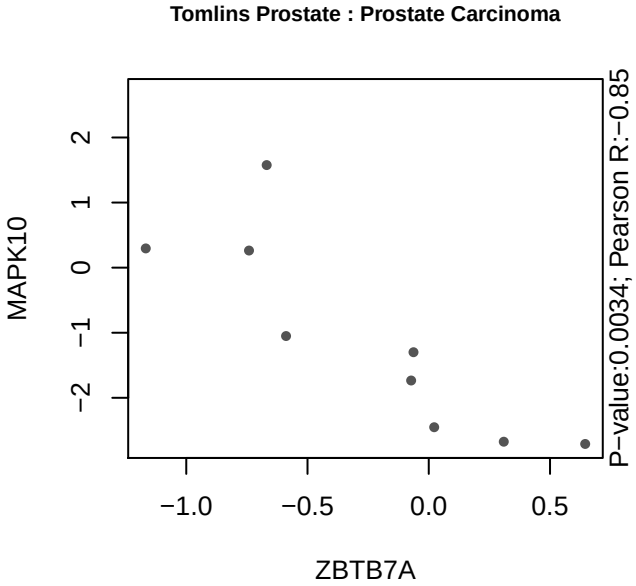

Tomlins Prostate : Prostate Carcinoma
MAP2K7
BCL6
P−value:0.89; Pearson R:−0.035

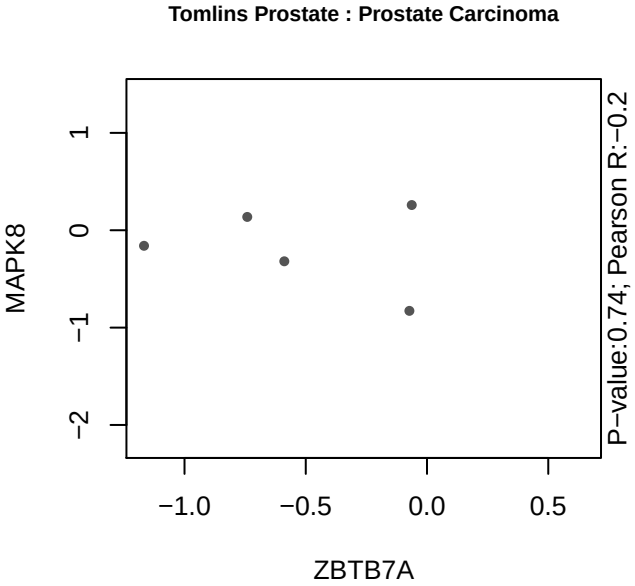

Tomlins Prostate : Prostate Carcinoma
MAP2K4
ZBTB7A
P−value:0.69; Pearson R:0.16

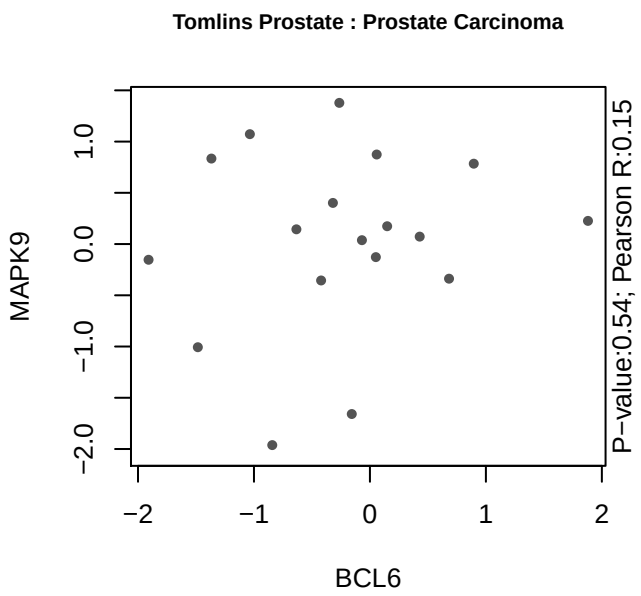

Tomlins Prostate : Prostate Carcinoma
MAP2K7
ZBTB7A
P−value:0.87; Pearson R:−0.076

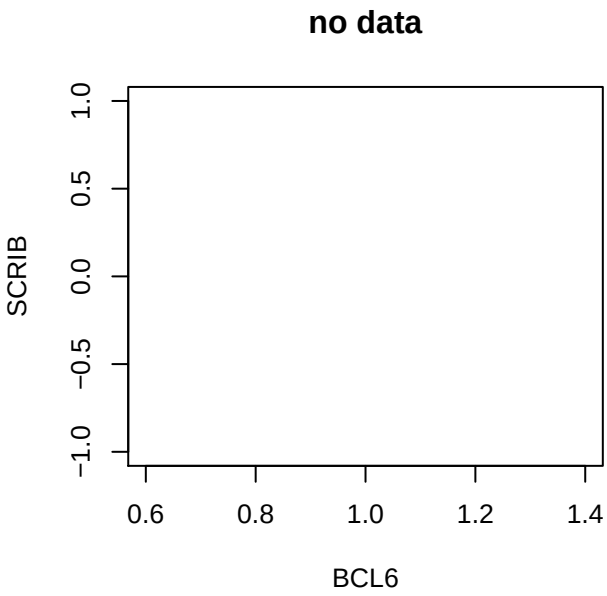

Tomlins Prostate : Prostate Carcinoma
MAPK10
BCL6
P−value:0.99; Pearson R:0.0021

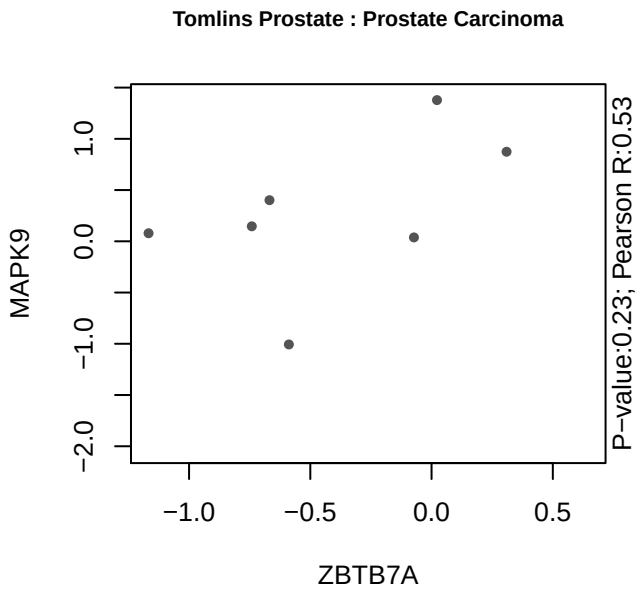

Tomlins Prostate : Prostate Carcinoma
MAPK8
BCL6
P−value:0.022; Pearson R:0.57

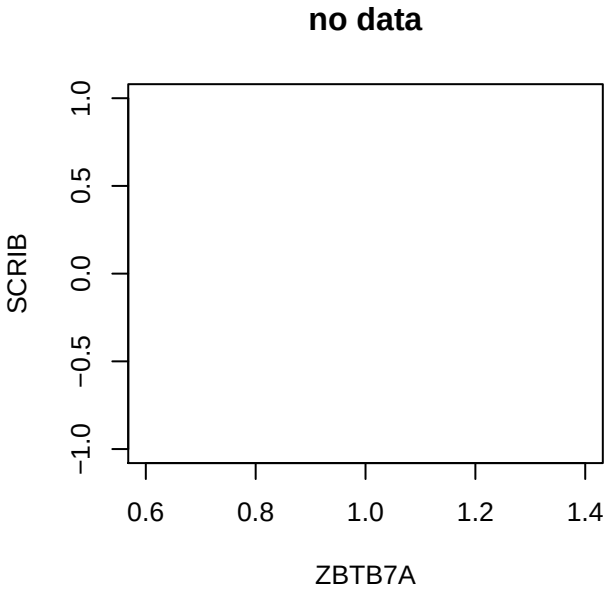

Tomlins Prostate : Prostate Carcinoma
MAPK10
ZBTB7A
P−value:0.0034; Pearson R:−0.85

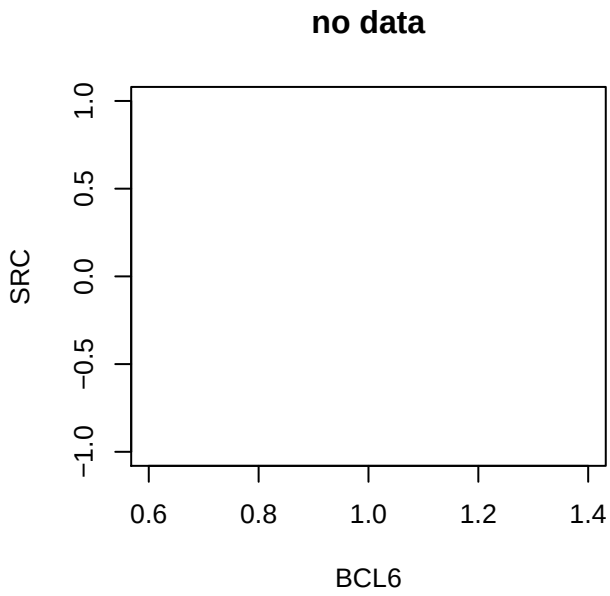

Tomlins Prostate : Prostate Carcinoma
MAPK8
ZBTB7A
P−value:0.74; Pearson R:−0.2

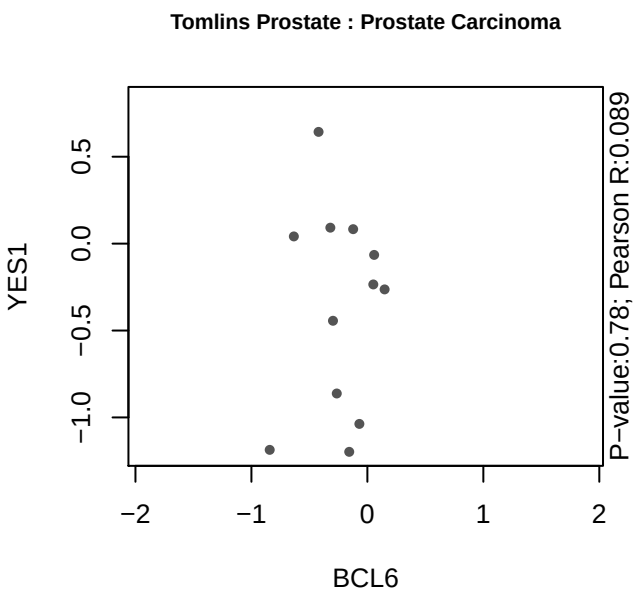

Tomlins Prostate : Prostate Carcinoma
MAPK9
BCL6
P−value:0.54; Pearson R:0.15
1.0
0.0
−1.0
−2.0
−2
−1
0
1
2

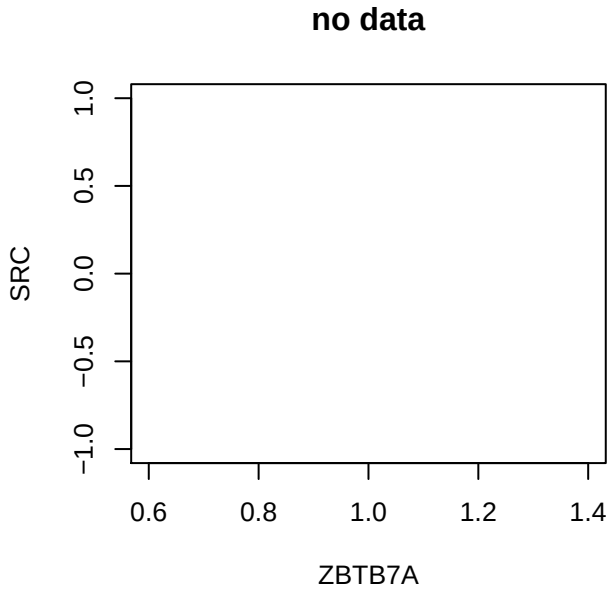

no data
SCRIB
BCL6
1.0
0.5
0.0
−0.5
−1.0
0.6
0.8
1.0
1.2
1.4

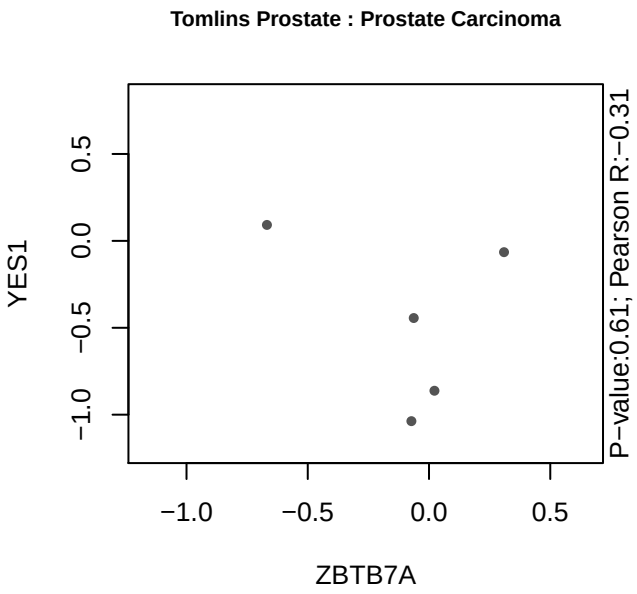

Tomlins Prostate : Prostate Carcinoma
MAPK9
ZBTB7A
P−value:0.23; Pearson R:0.53
1.0
0.0
−1.0
−2.0
−1.0
−0.5
0.0
0.5

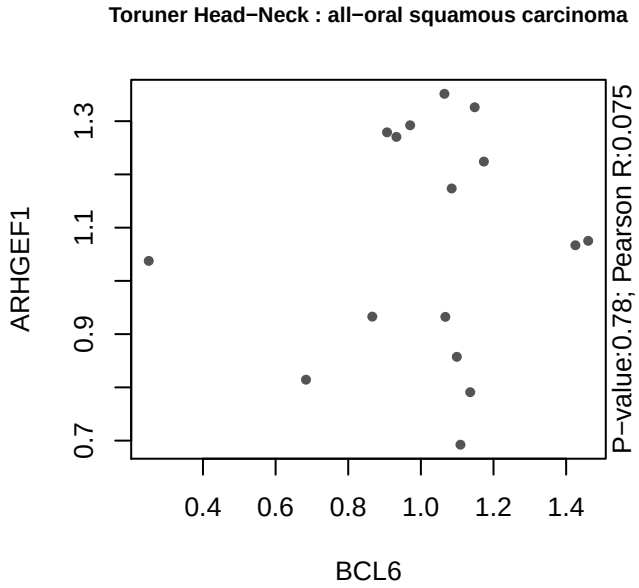

no data
SCRIB
ZBTB7A
1.0
0.5
0.0
−0.5
−1.0
0.6
0.8
1.0
1.2
1.4

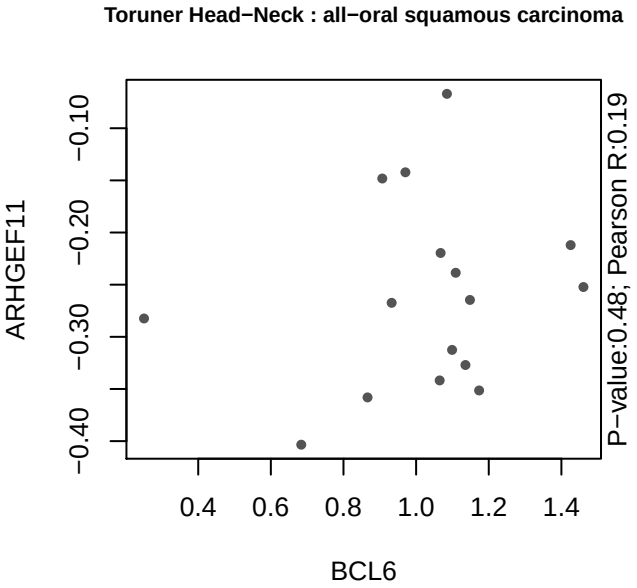

no data
SRC
BCL6
1.0
0.5
0.0
−0.5
−1.0
0.6
0.8
1.0
1.2
1.4

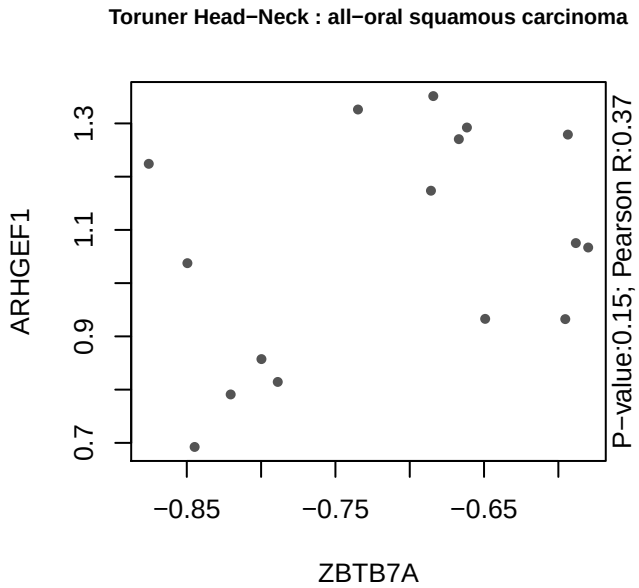

Tomlins Prostate : Prostate Carcinoma
YES1
BCL6
P−value:0.78; Pearson R:0.089
0.5
0.0
−0.5
−1.0
−2
−1
0
1
2

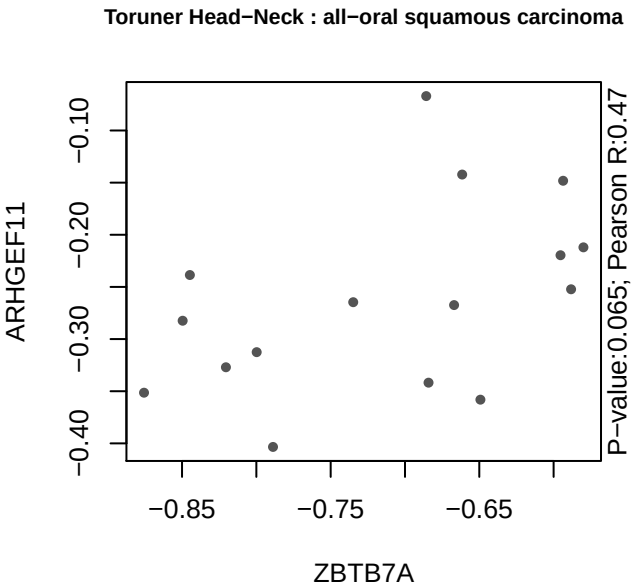

no data
SRC
ZBTB7A
1.0
0.5
0.0
−0.5
−1.0
0.6
0.8
1.0
1.2
1.4

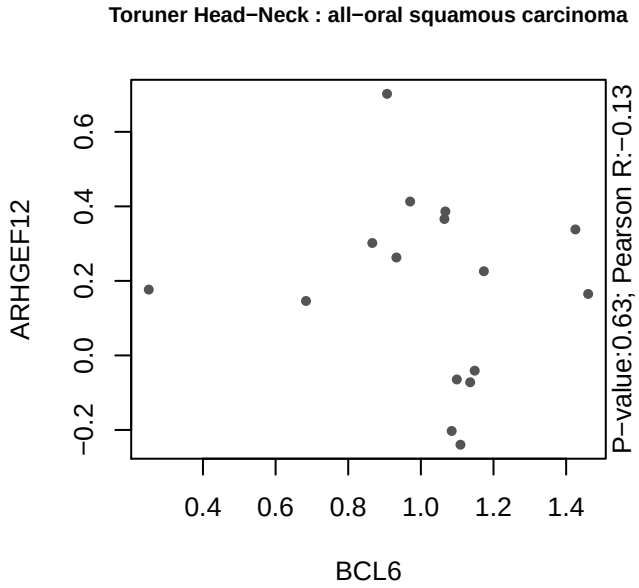

Tomlins Prostate : Prostate Carcinoma
YES1
ZBTB7A
P−value:0.61; Pearson R:−0.31
0.5
0.0
−0.5
−1.0
−1.0
−0.5
0.0
0.5

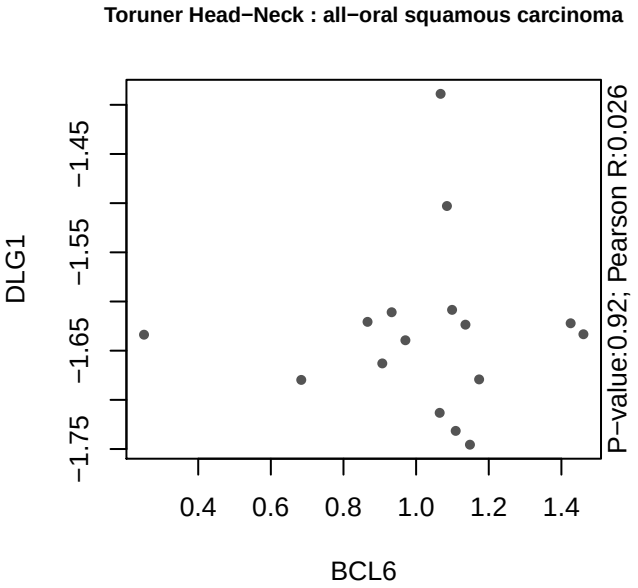

Toruner Head−Neck : all−oral squamous carcinoma
ARHGEF1
BCL6
P−value:0.78; Pearson R:0.075

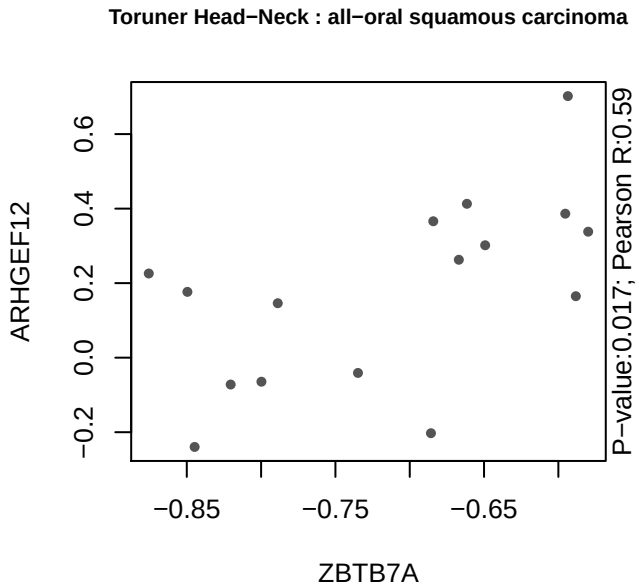

Toruner Head−Neck : all−oral squamous carcinoma
ARHGEF11
BCL6
P−value:0.48; Pearson R:0.19

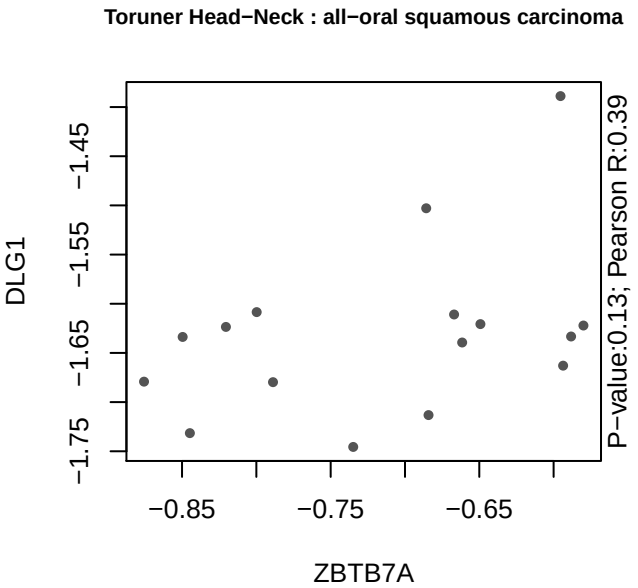

Toruner Head−Neck : all−oral squamous carcinoma
ARHGEF1
ZBTB7A
P−value:0.15; Pearson R:0.37

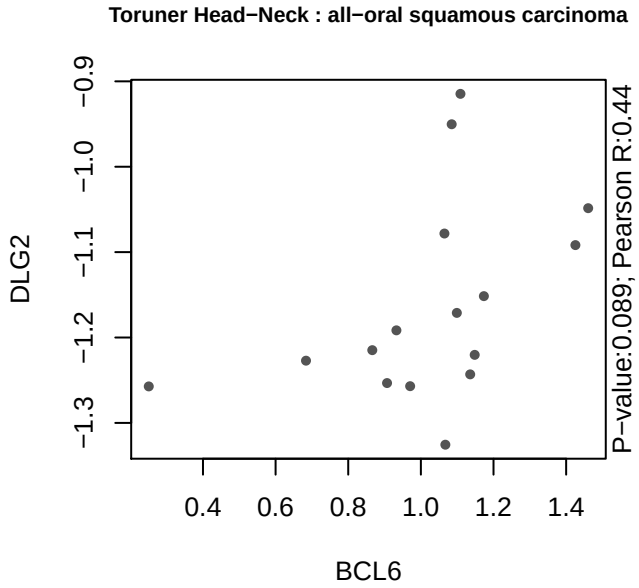

Toruner Head−Neck : all−oral squamous carcinoma
ARHGEF11
ZBTB7A
P−value:0.065; Pearson R:0.47

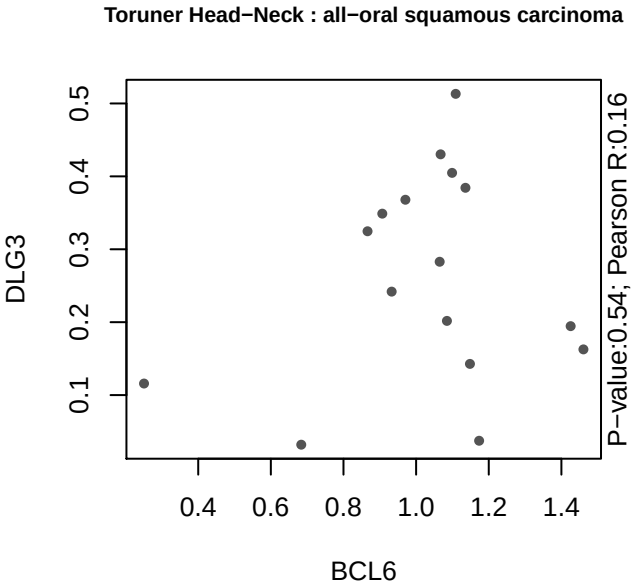

Toruner Head−Neck : all−oral squamous carcinoma
ARHGEF12
BCL6
P−value:0.63; Pearson R:−0.13

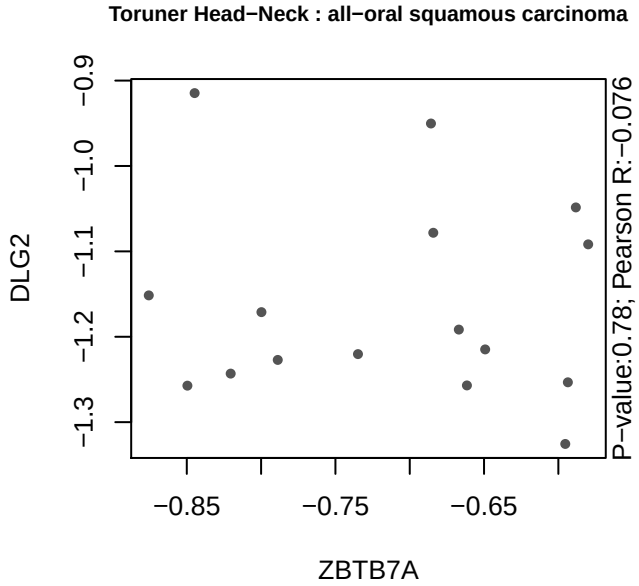

Toruner Head−Neck : all−oral squamous carcinoma
DLG1
BCL6
P−value:0.92; Pearson R:0.026

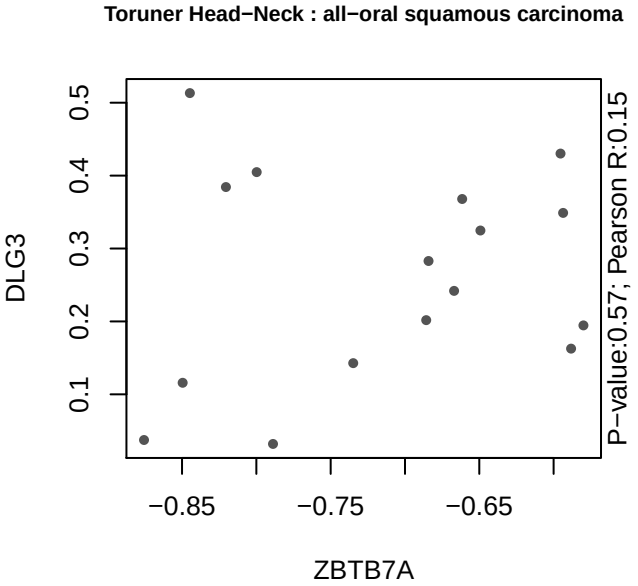

Toruner Head−Neck : all−oral squamous carcinoma
ARHGEF12
ZBTB7A
P−value:0.017; Pearson R:0.59

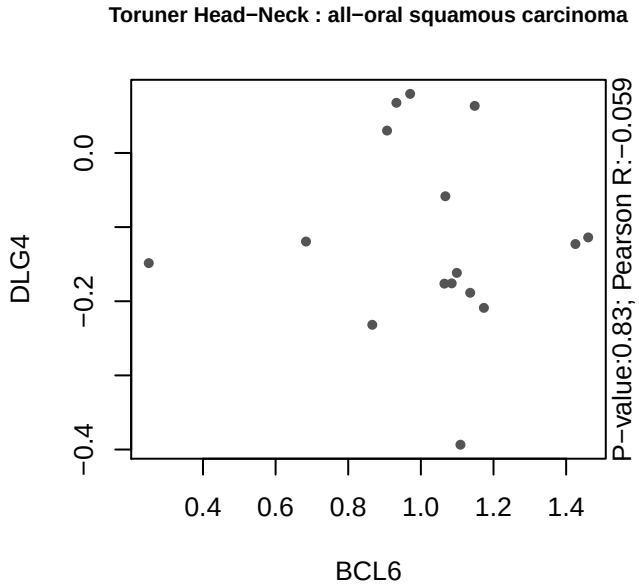

Toruner Head−Neck : all−oral squamous carcinoma
DLG1
ZBTB7A
P−value:0.13; Pearson R:0.39

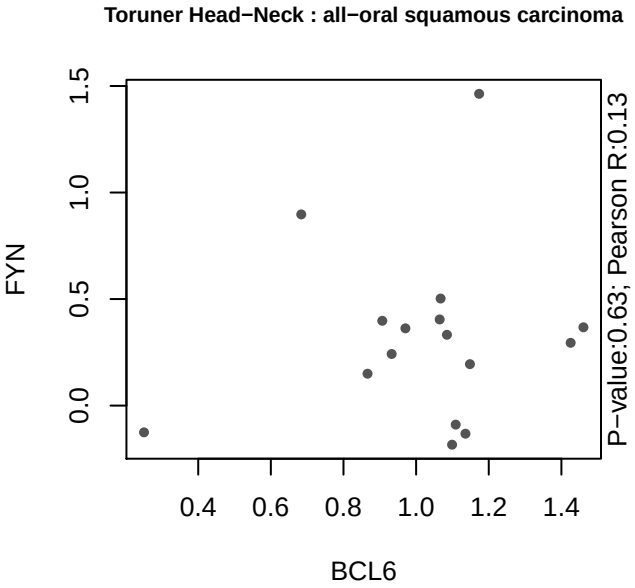

Toruner Head−Neck : all−oral squamous carcinoma
DLG2
BCL6
P−value:0.089; Pearson R:0.44
−0.9
−1.0
−1.1
−1.2
−1.3
0.4
0.6
0.8
1.0
1.2
1.4

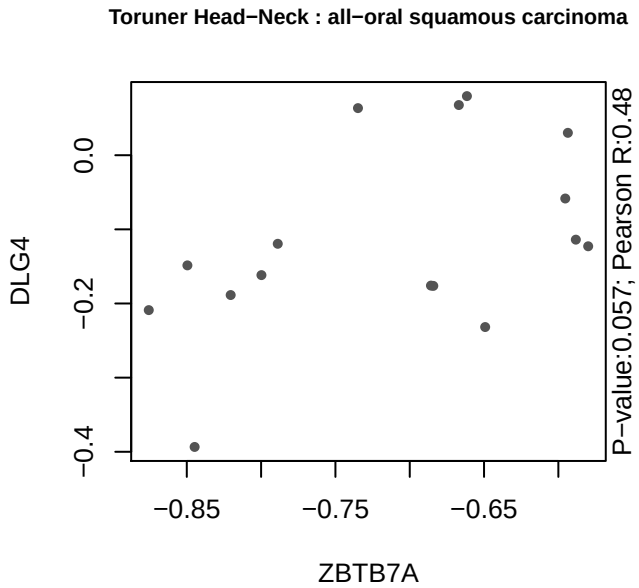

Toruner Head−Neck : all−oral squamous carcinoma
DLG3
BCL6
P−value:0.54; Pearson R:0.16
0.5
0.4
0.3
0.2
0.1
0.4
0.6
0.8
1.0
1.2
1.4

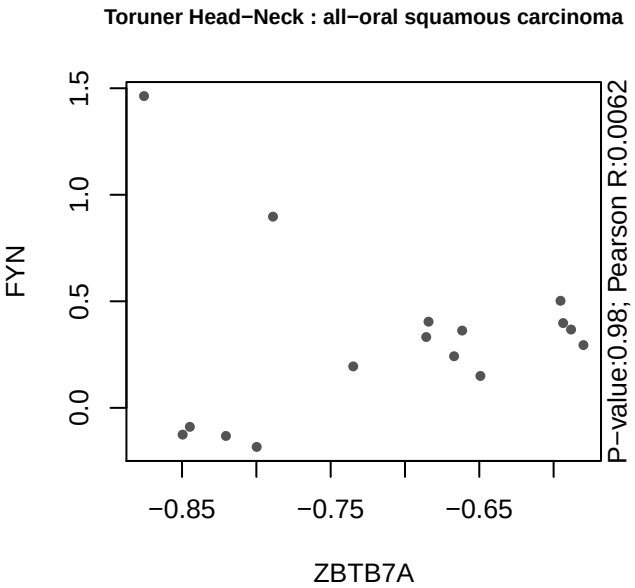

Toruner Head−Neck : all−oral squamous carcinoma
DLG2
ZBTB7A
P−value:0.78; Pearson R:−0.076
−0.9
−1.0
−1.1
−1.2
−1.3
−0.85
−0.75
−0.65

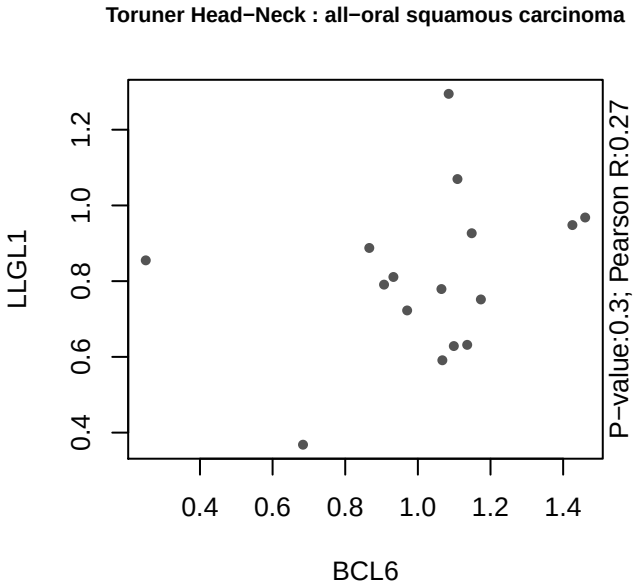

Toruner Head−Neck : all−oral squamous carcinoma
DLG3
ZBTB7A
P−value:0.57; Pearson R:0.15
0.5
0.4
0.3
0.2
0.1
−0.85
−0.75
−0.65

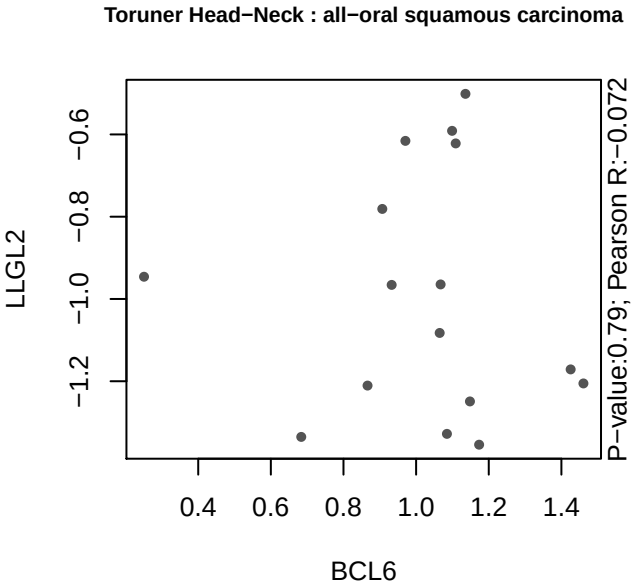

Toruner Head−Neck : all−oral squamous carcinoma
DLG4
BCL6
P−value:0.83; Pearson R:−0.059

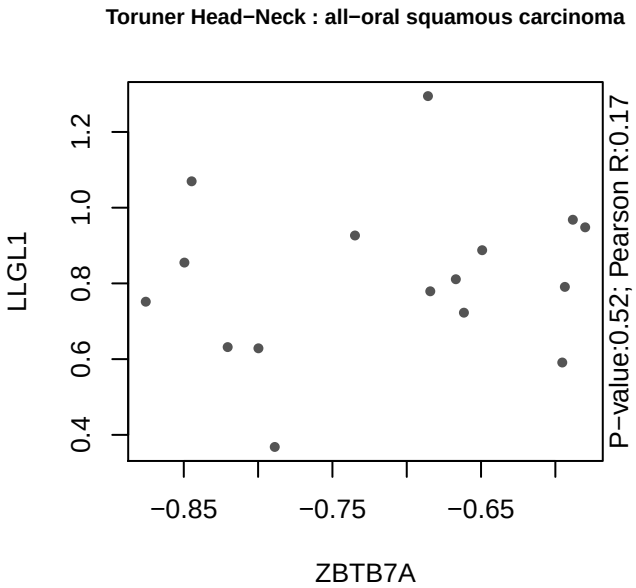

Toruner Head−Neck : all−oral squamous carcinoma
FYN
BCL6
P−value:0.63; Pearson R:0.13

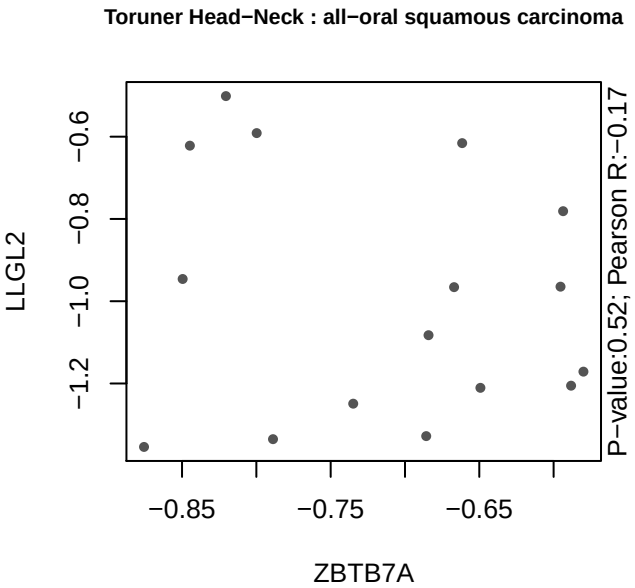

Toruner Head−Neck : all−oral squamous carcinoma
DLG4
ZBTB7A
P−value:0.057; Pearson R:0.48

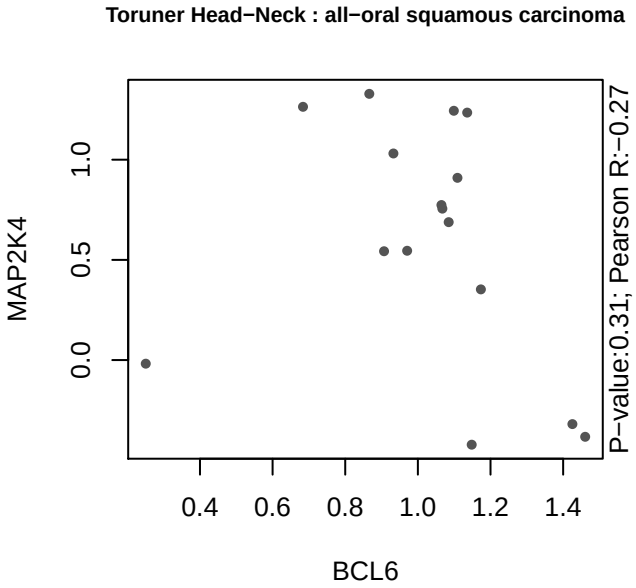

Toruner Head−Neck : all−oral squamous carcinoma
FYN
ZBTB7A
P−value:0.98; Pearson R:0.0062

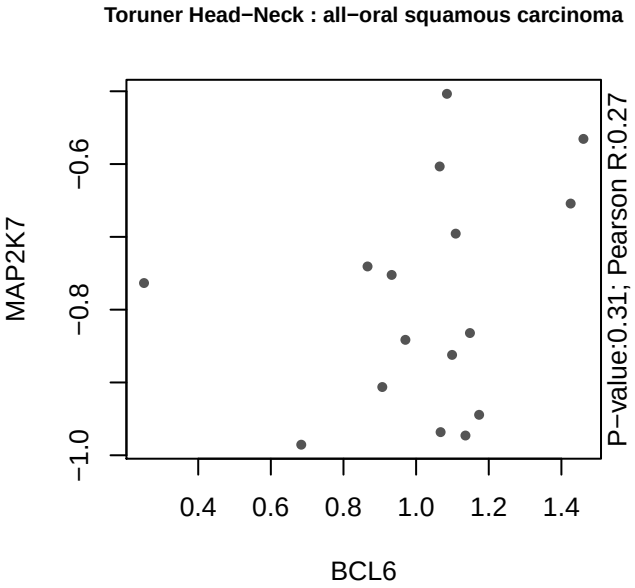

Toruner Head−Neck : all−oral squamous carcinoma
LLGL1
BCL6
P−value:0.3; Pearson R:0.27

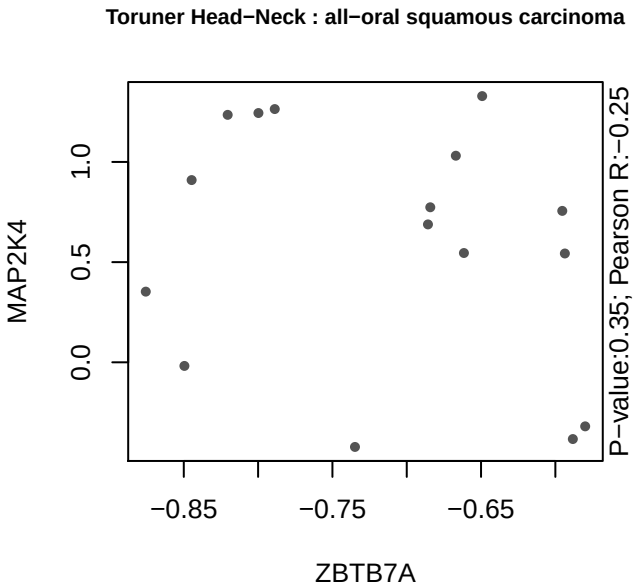

Toruner Head−Neck : all−oral squamous carcinoma
LLGL2
BCL6
P−value:0.79; Pearson R:−0.072

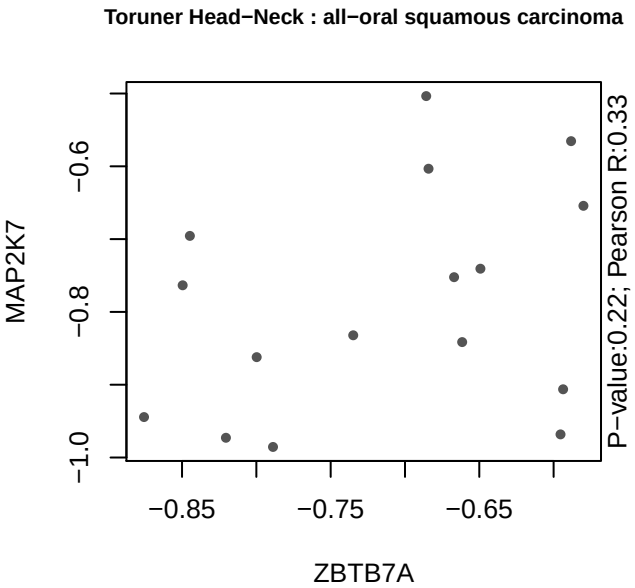

Toruner Head−Neck : all−oral squamous carcinoma
LLGL1
ZBTB7A
P−value:0.52; Pearson R:0.17

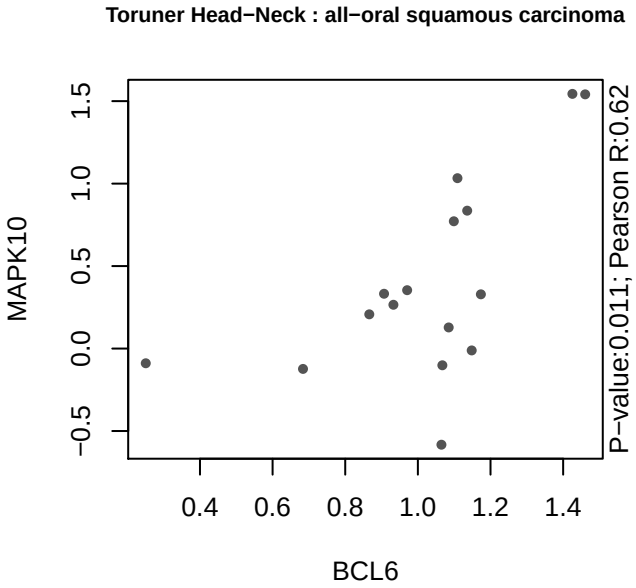

Toruner Head−Neck : all−oral squamous carcinoma
LLGL2
ZBTB7A
P−value:0.52; Pearson R:−0.17

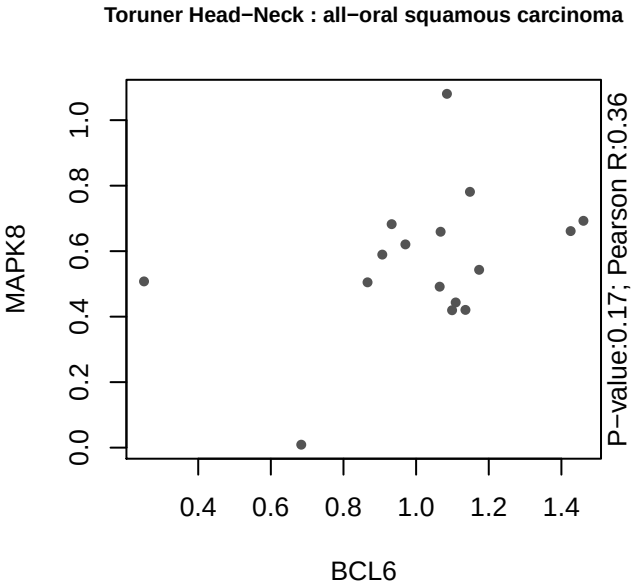

Toruner Head−Neck : all−oral squamous carcinoma
MAP2K4
BCL6
P−value:0.31; Pearson R:−0.27

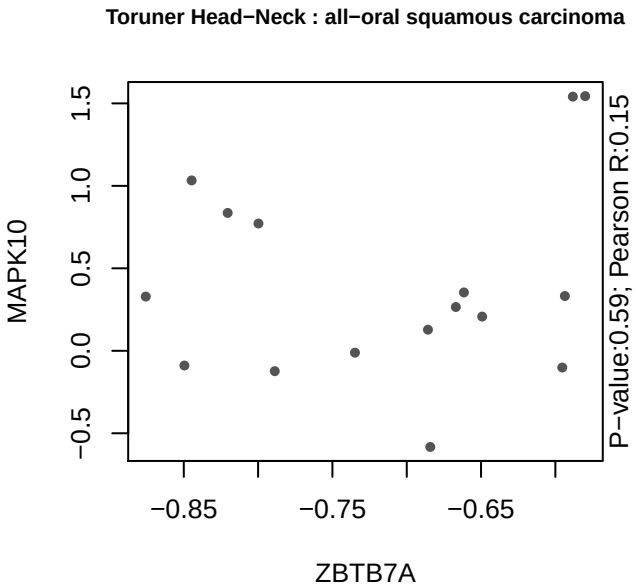

Toruner Head−Neck : all−oral squamous carcinoma
MAP2K7
BCL6
P−value:0.31; Pearson R:0.27

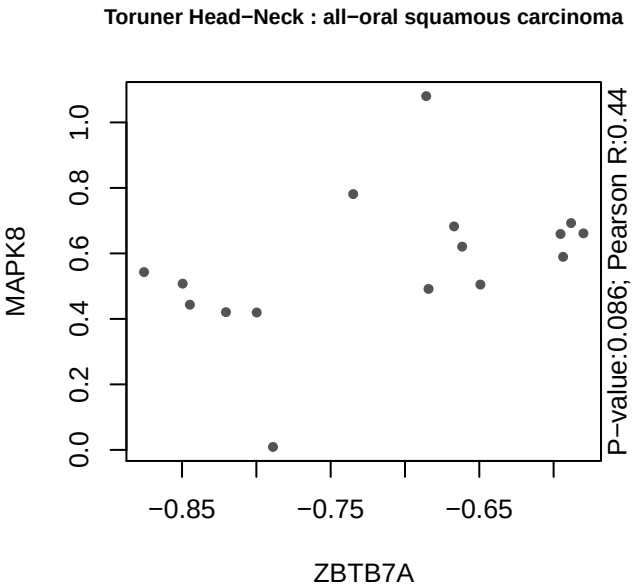

Toruner Head−Neck : all−oral squamous carcinoma
MAP2K4
ZBTB7A
P−value:0.35; Pearson R:−0.25

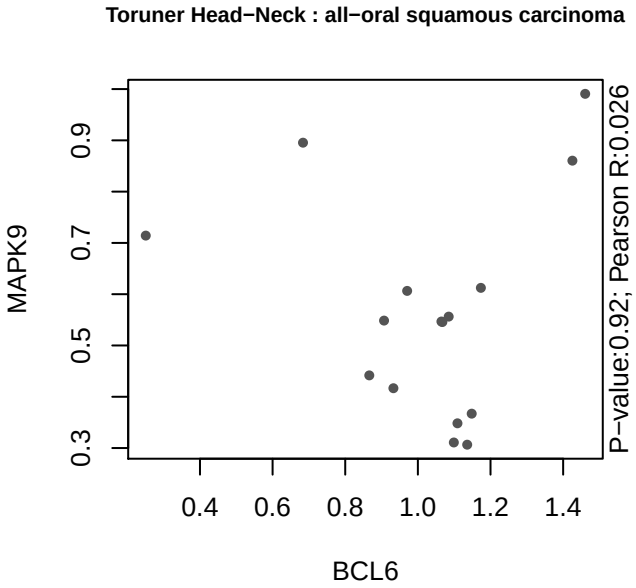

Toruner Head−Neck : all−oral squamous carcinoma
MAP2K7
ZBTB7A
P−value:0.22; Pearson R:0.33

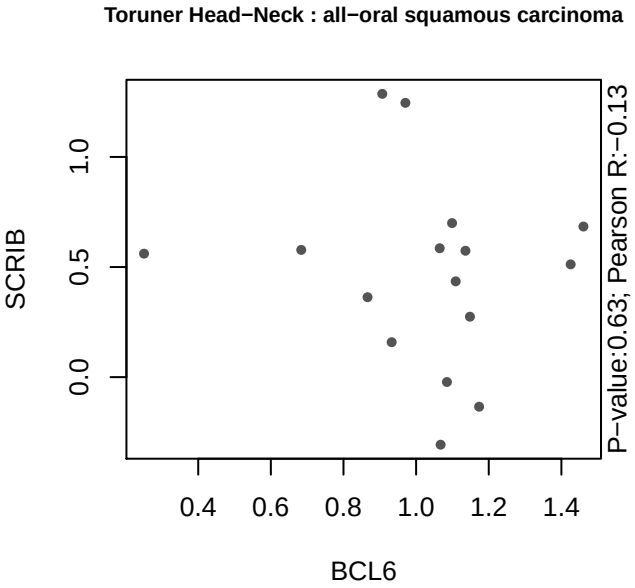

Toruner Head−Neck : all−oral squamous carcinoma
MAPK10
BCL6
P−value:0.011; Pearson R:0.62

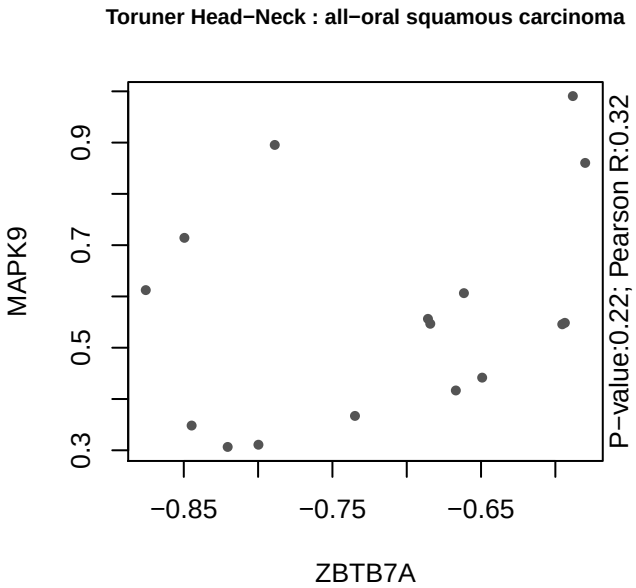

Toruner Head−Neck : all−oral squamous carcinoma
MAPK8
BCL6
P−value:0.17; Pearson R:0.36

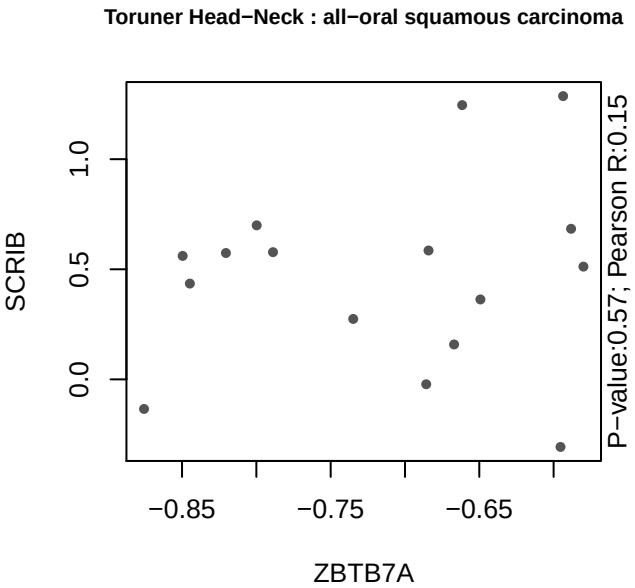

Toruner Head−Neck : all−oral squamous carcinoma
MAPK10
ZBTB7A
P−value:0.59; Pearson R:0.15

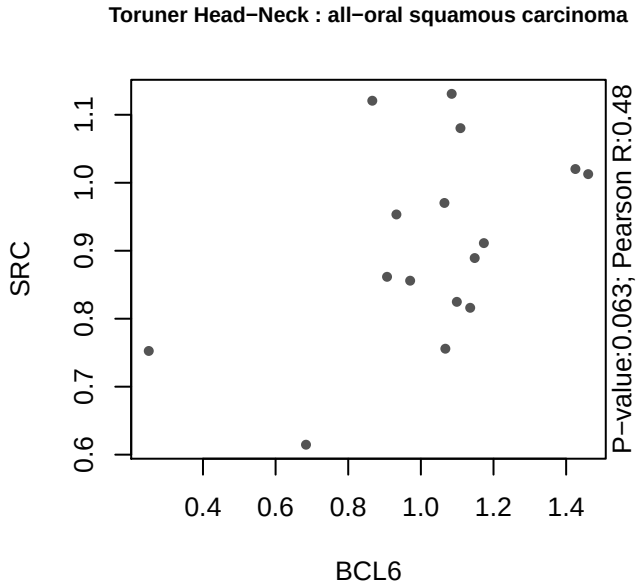

Toruner Head−Neck : all−oral squamous carcinoma
MAPK8
ZBTB7A
P−value:0.086; Pearson R:0.44

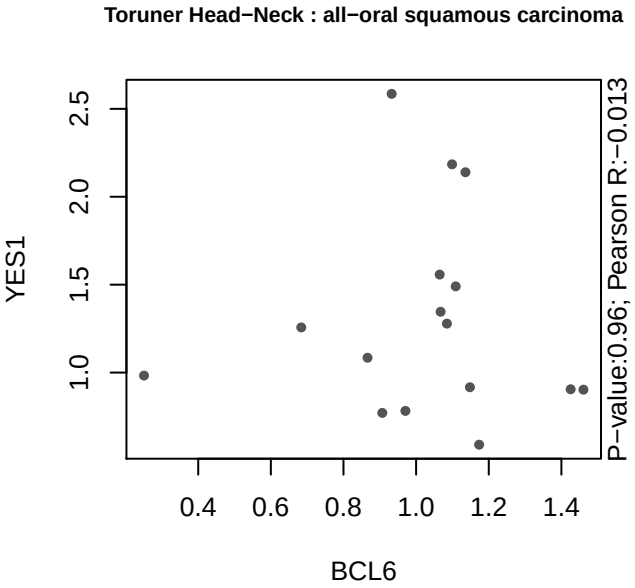

Toruner Head−Neck : all−oral squamous carcinoma
MAPK9
BCL6
P−value:0.92; Pearson R:0.026

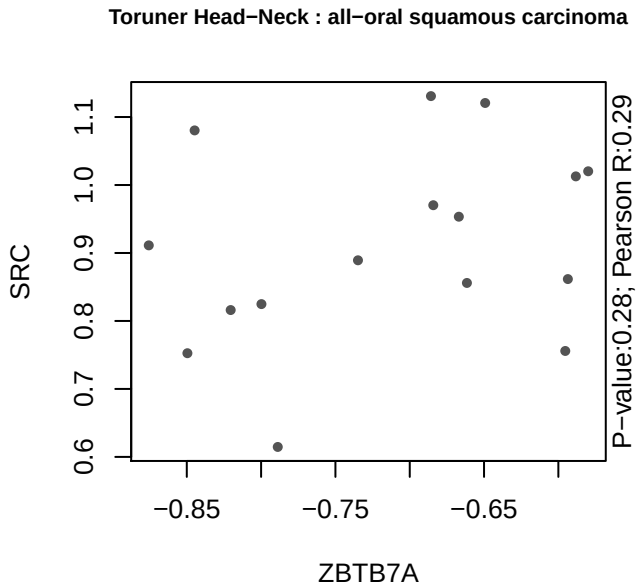

Toruner Head−Neck : all−oral squamous carcinoma
SCRIB
BCL6
P−value:0.63; Pearson R:−0.13

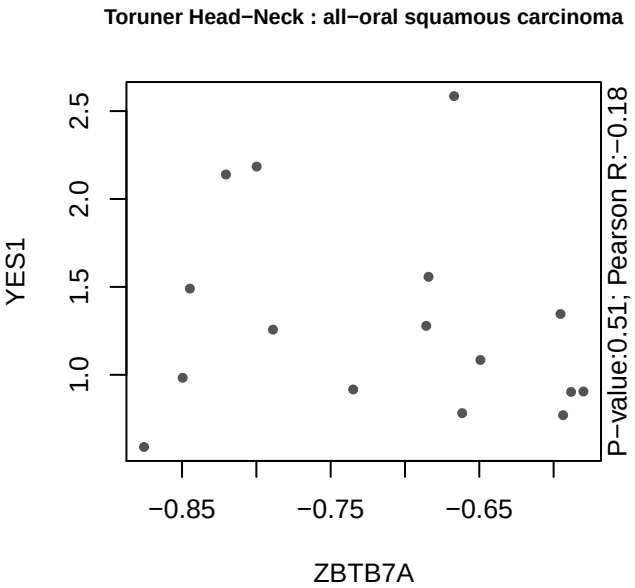

Toruner Head−Neck : all−oral squamous carcinoma
MAPK9
ZBTB7A
P−value:0.22; Pearson R:0.32

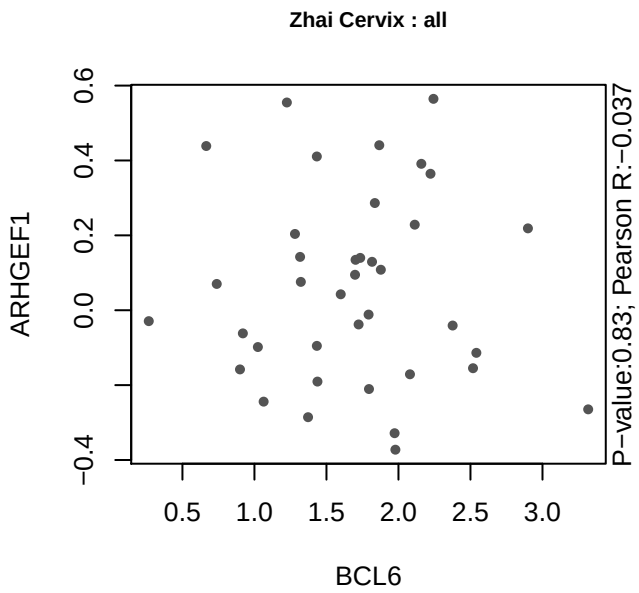

Toruner Head−Neck : all−oral squamous carcinoma
SCRIB
ZBTB7A
P−value:0.57; Pearson R:0.15

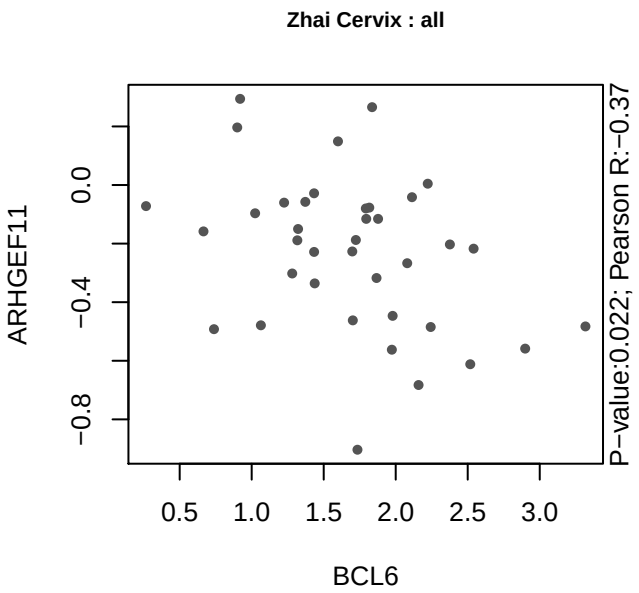

Toruner Head−Neck : all−oral squamous carcinoma
SRC
BCL6
P−value:0.063; Pearson R:0.48

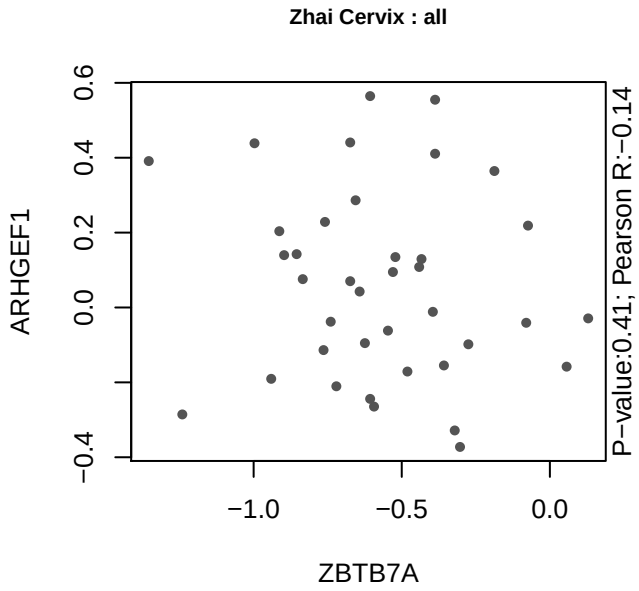

Toruner Head−Neck : all−oral squamous carcinoma
YES1
BCL6
P−value:0.96; Pearson R:−0.013

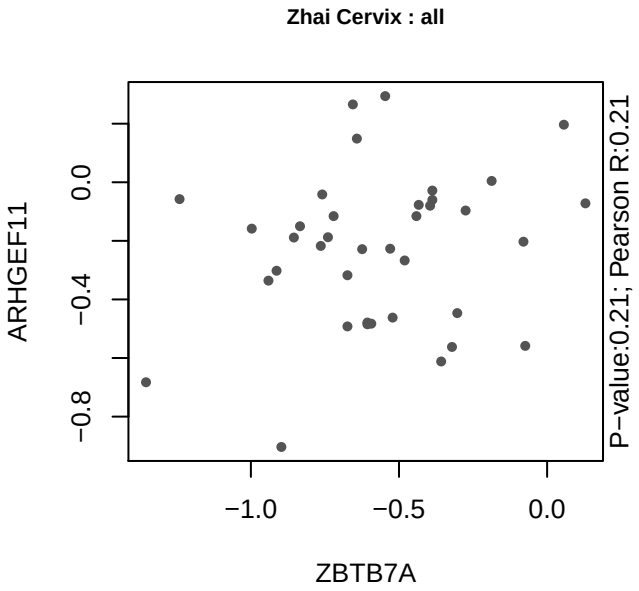

Toruner Head−Neck : all−oral squamous carcinoma
SRC
ZBTB7A
P−value:0.28; Pearson R:0.29

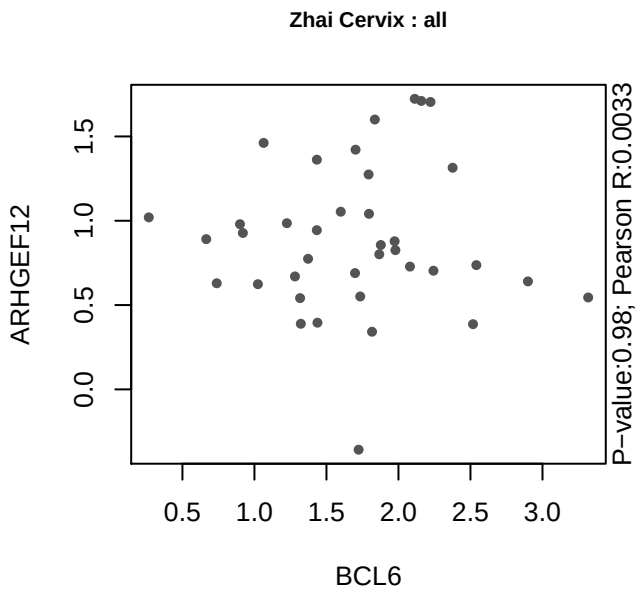

Toruner Head−Neck : all−oral squamous carcinoma
YES1
ZBTB7A
P−value:0.51; Pearson R:−0.18

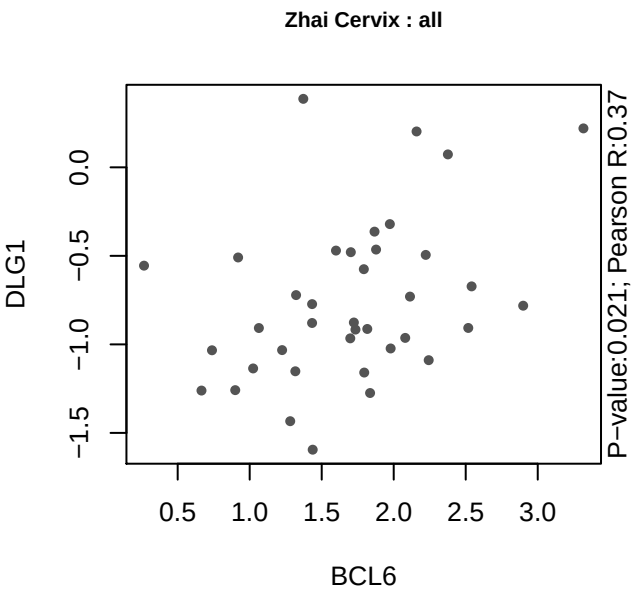

Zhai Cervix : all
ARHGEF1
BCL6
P−value:0.83; Pearson R:−0.037

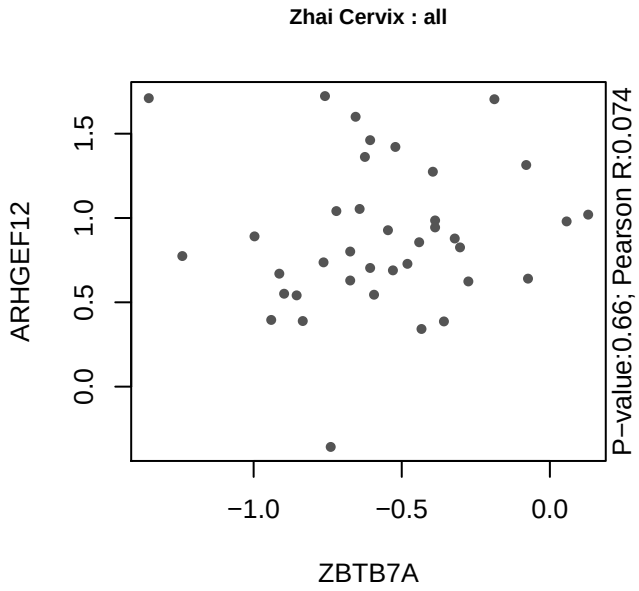

Zhai Cervix : all
ARHGEF11
BCL6
P−value:0.022; Pearson R:−0.37

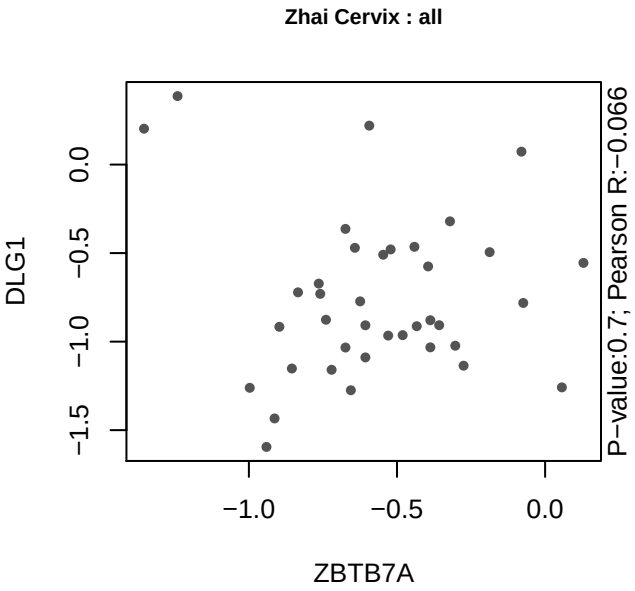

Zhai Cervix : all
ARHGEF1
ZBTB7A
P−value:0.41; Pearson R:−0.14

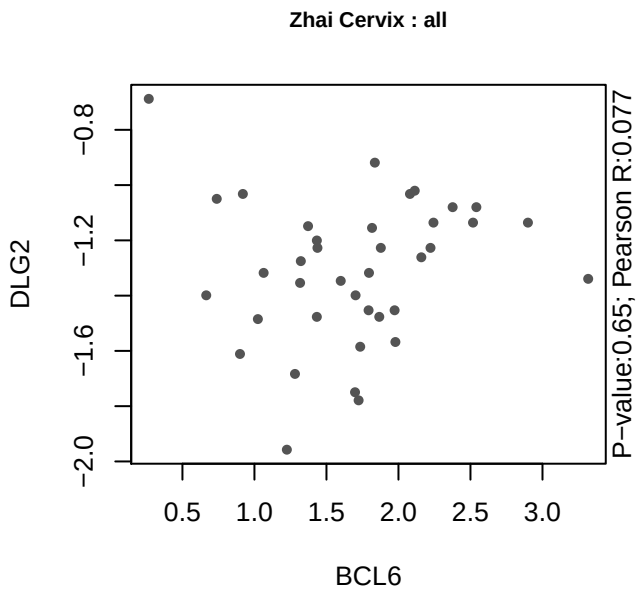

Zhai Cervix : all
ARHGEF11
ZBTB7A
P−value:0.21; Pearson R:0.21

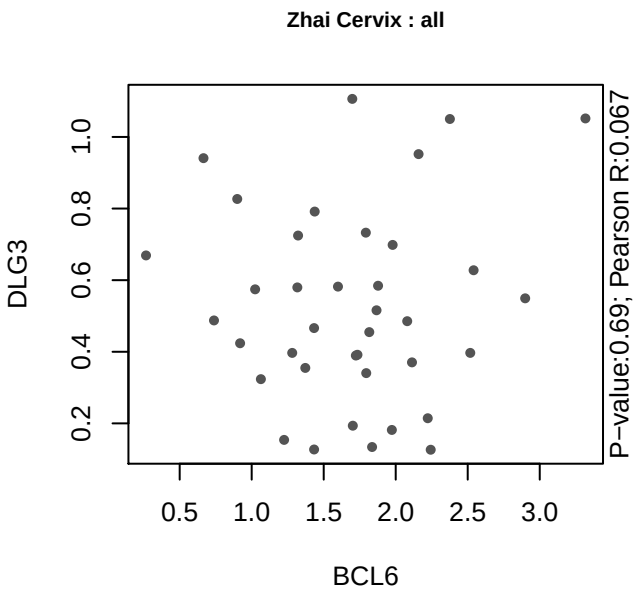

Zhai Cervix : all
ARHGEF12
BCL6
P−value:0.98; Pearson R:0.0033

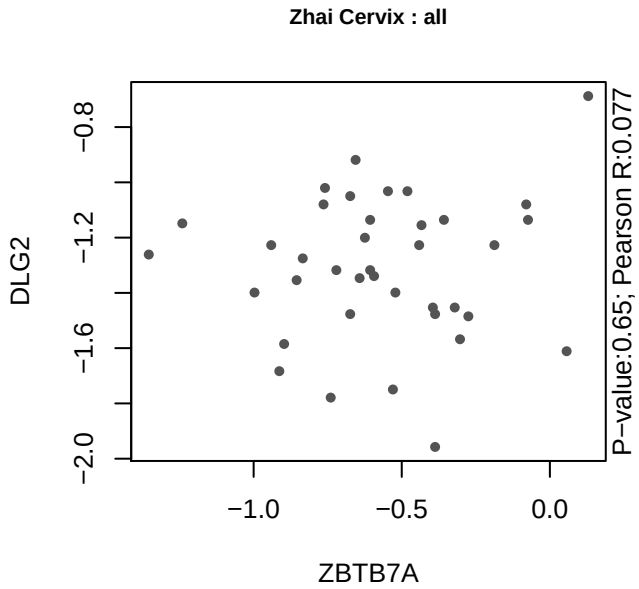

Zhai Cervix : all
DLG1
BCL6
P−value:0.021; Pearson R:0.37

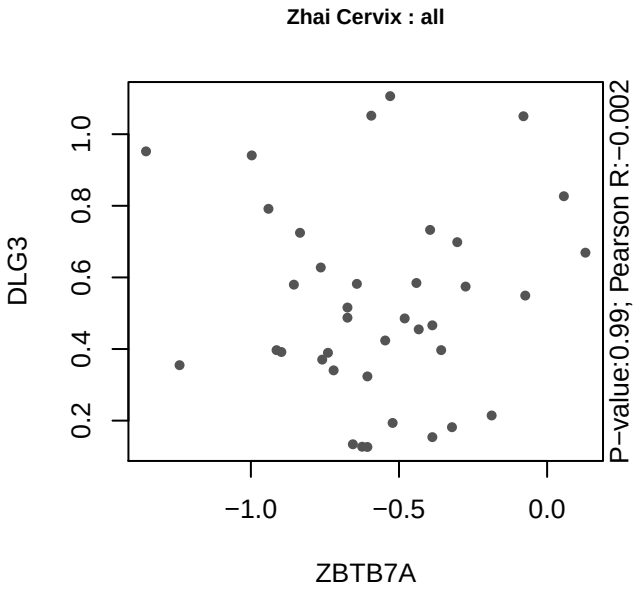

Zhai Cervix : all
ARHGEF12
ZBTB7A
P−value:0.66; Pearson R:0.074

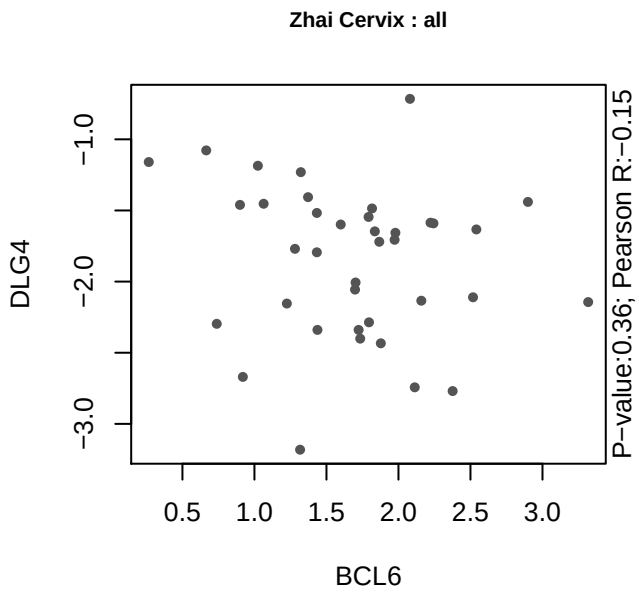

Zhai Cervix : all
DLG1
ZBTB7A
P−value:0.7; Pearson R:−0.066

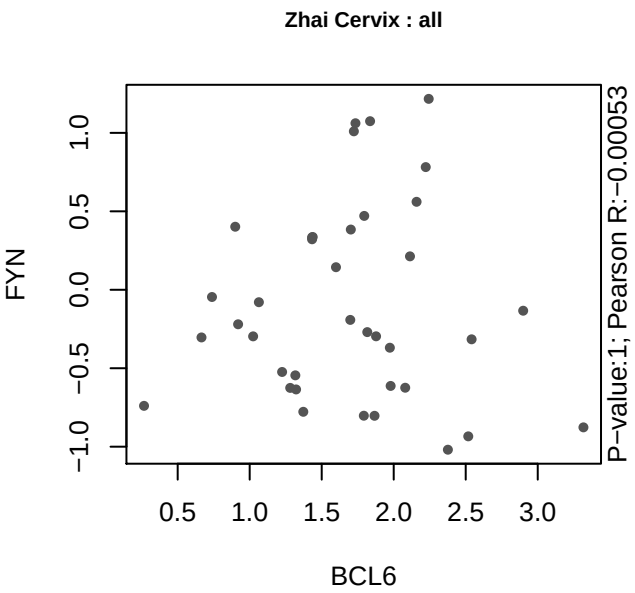

Zhai Cervix : all
DLG2
BCL6
P−value:0.65; Pearson R:0.077

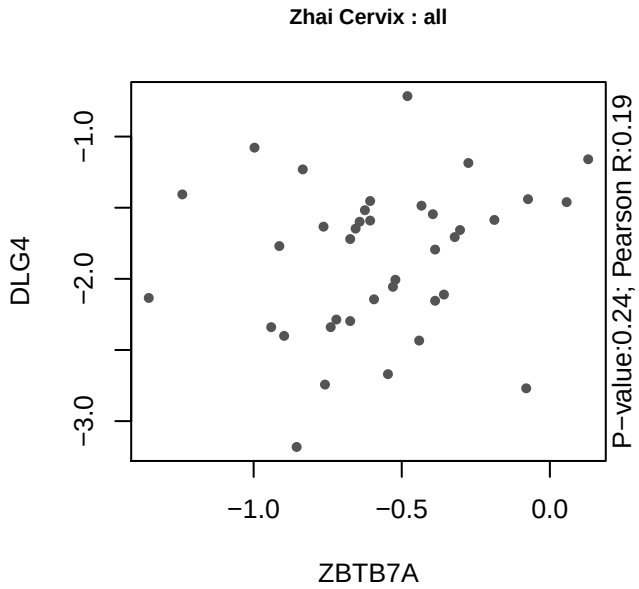

Zhai Cervix : all
DLG3
BCL6
P−value:0.69; Pearson R:0.067

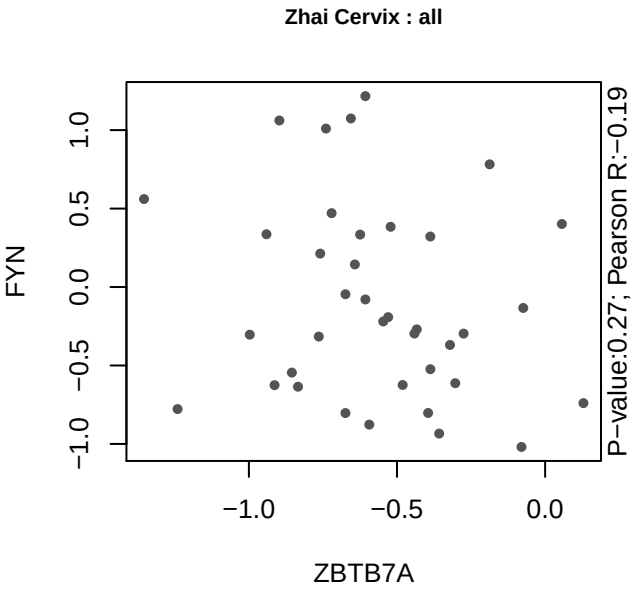

Zhai Cervix : all
DLG2
ZBTB7A
P−value:0.65; Pearson R:0.077

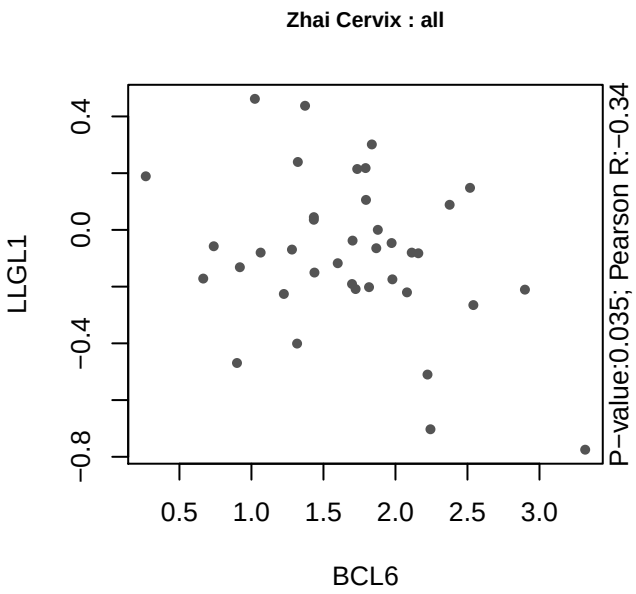

Zhai Cervix : all
DLG3
ZBTB7A
P−value:0.99; Pearson R:−0.002

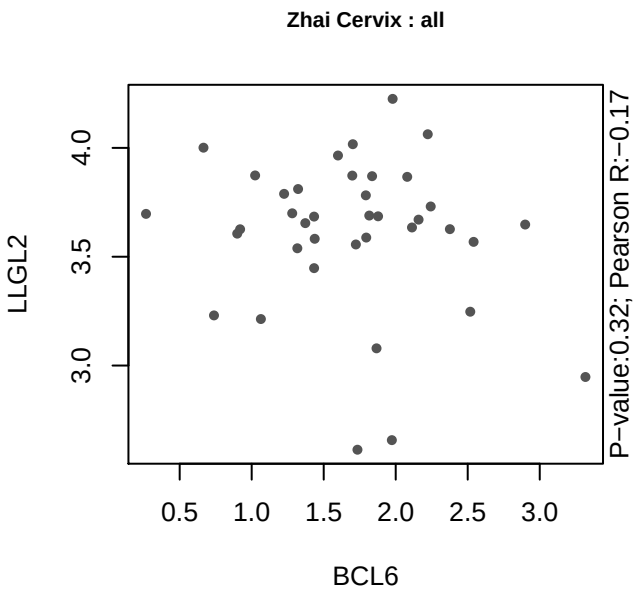

Zhai Cervix : all
DLG4
BCL6
P−value:0.36; Pearson R:−0.15

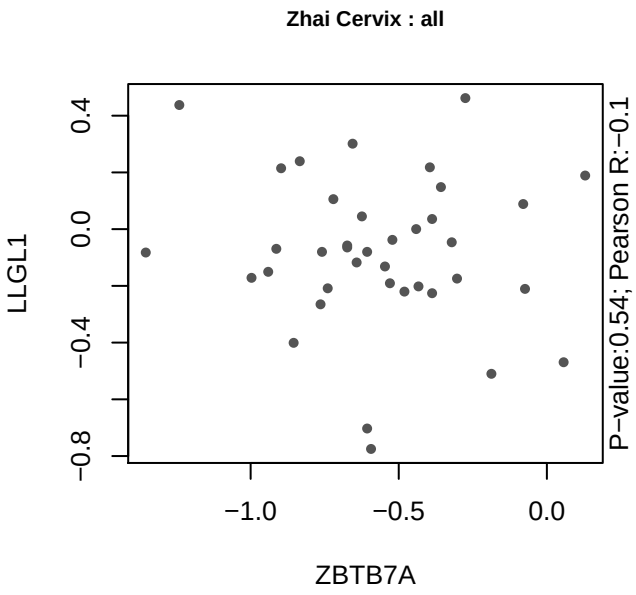

Zhai Cervix : all
FYN
BCL6
P−value:1; Pearson R:−0.00053

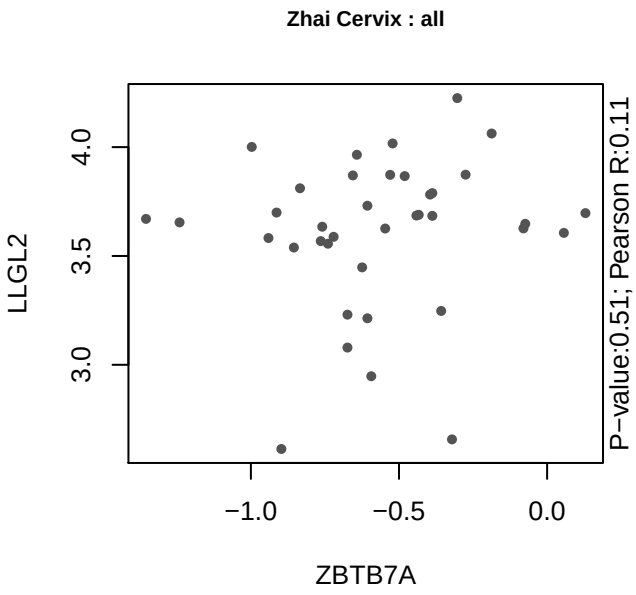

Zhai Cervix : all
DLG4
ZBTB7A
P−value:0.24; Pearson R:0.19

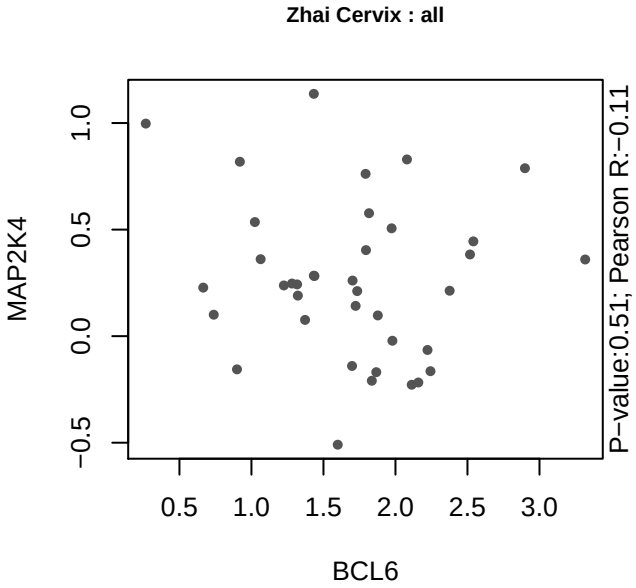

Zhai Cervix : all
FYN
ZBTB7A
P−value:0.27; Pearson R:−0.19

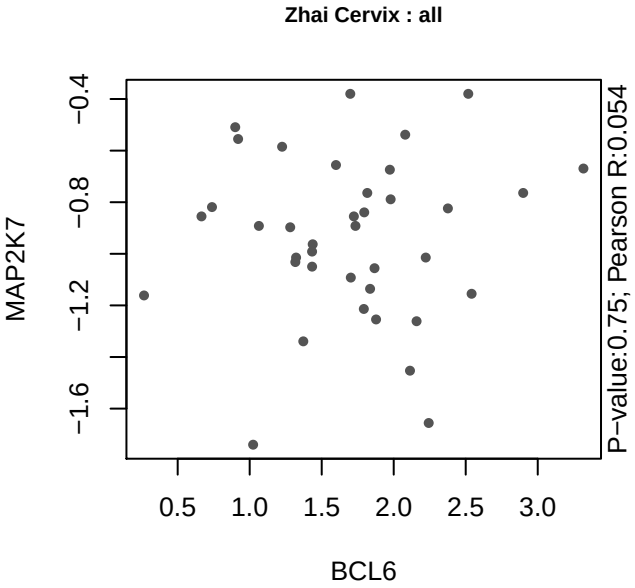

Zhai Cervix : all
LLGL1
BCL6
P−value:0.035; Pearson R:−0.34
0.4
0.0
−0.4
−0.8
0.5
1.0
1.5
2.0
2.5
3.0

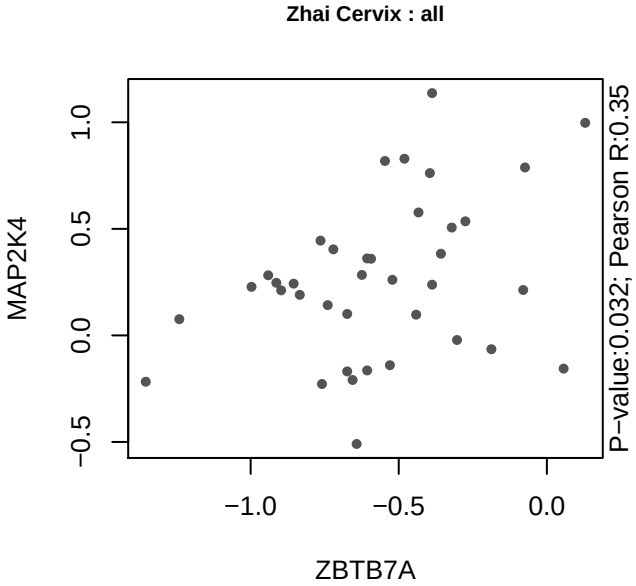

Zhai Cervix : all
LLGL2
BCL6
P−value:0.32; Pearson R:−0.17
4.0
3.5
3.0
0.5
1.0
1.5
2.0
2.5
3.0

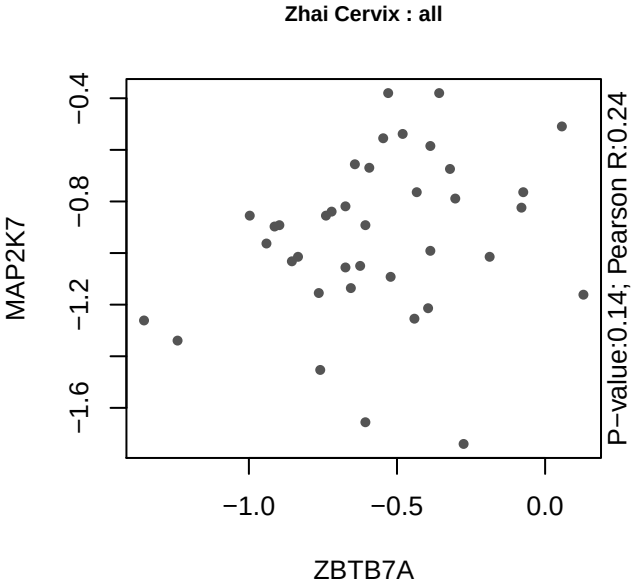

Zhai Cervix : all
LLGL1
ZBTB7A
P−value:0.54; Pearson R:−0.1
0.4
0.0
−0.4
−0.8
−1.0
−0.5
0.0

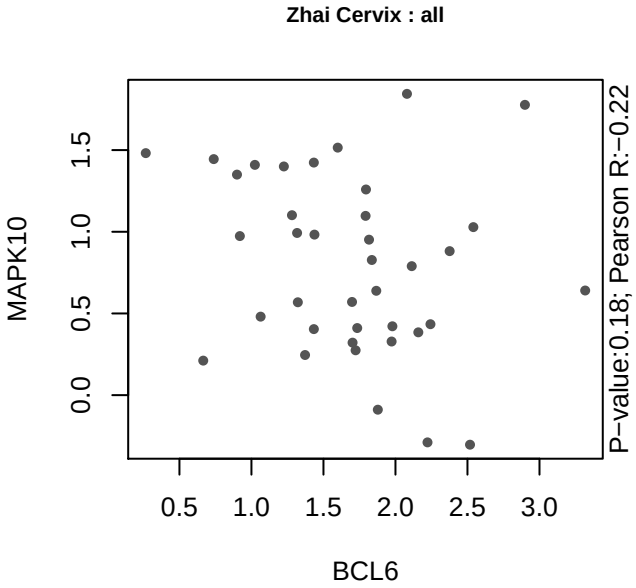

Zhai Cervix : all
LLGL2
ZBTB7A
P−value:0.51; Pearson R:0.11
4.0
3.5
3.0
−1.0
−0.5
0.0

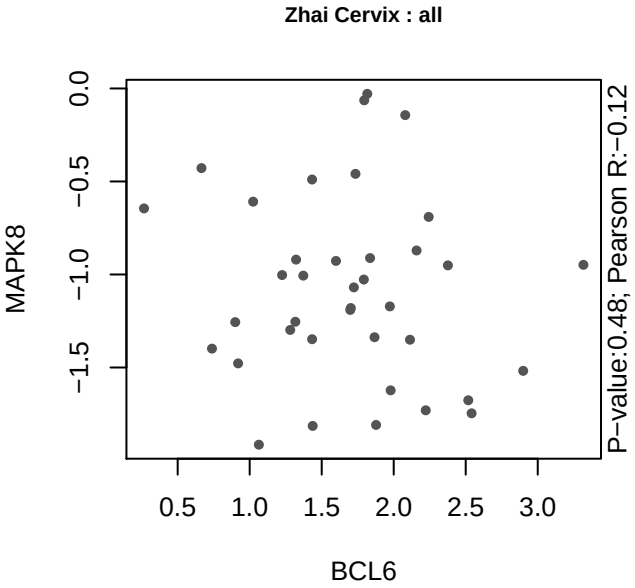

Zhai Cervix : all
MAP2K4
BCL6
P−value:0.51; Pearson R:−0.11

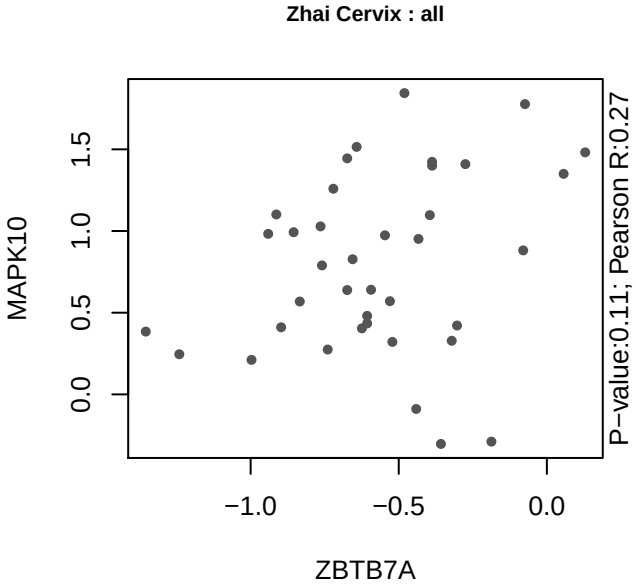

Zhai Cervix : all
MAP2K7
BCL6
P−value:0.75; Pearson R:0.054

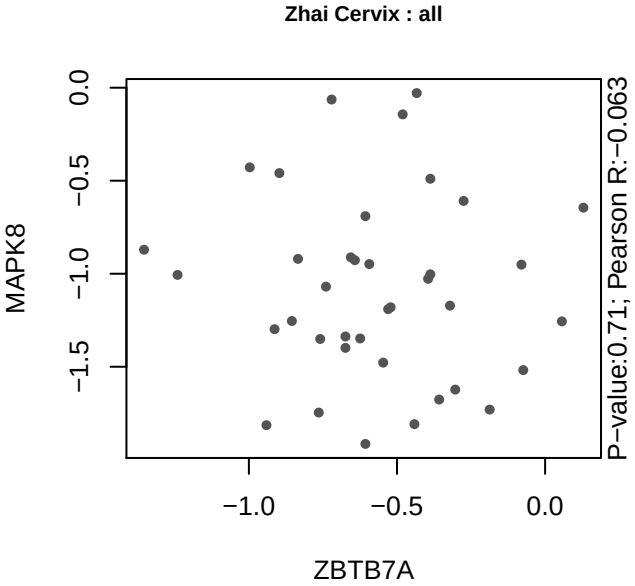

Zhai Cervix : all
MAP2K4
ZBTB7A
P−value:0.032; Pearson R:0.35

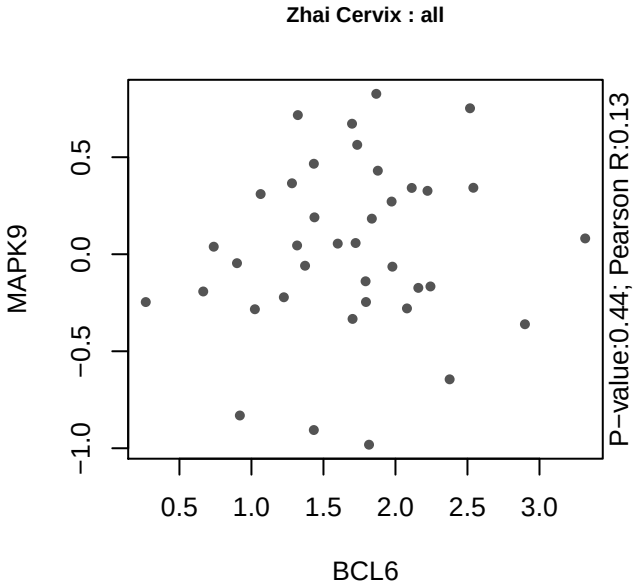

Zhai Cervix : all
MAP2K7
ZBTB7A
P−value:0.14; Pearson R:0.24

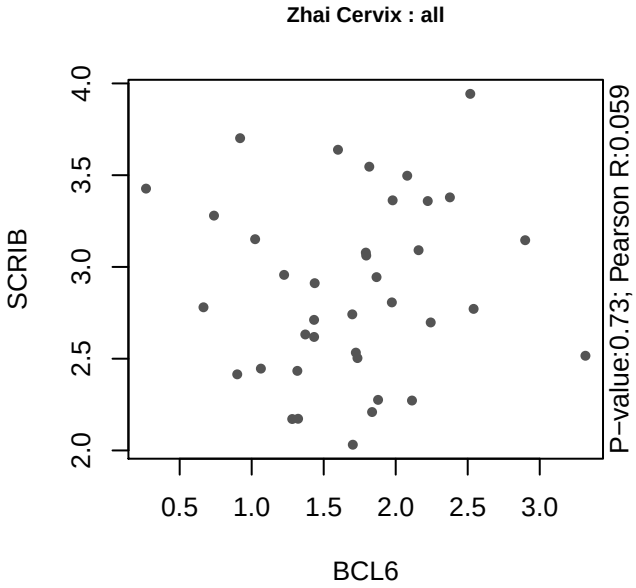

Zhai Cervix : all
MAPK10
BCL6
P−value:0.18; Pearson R:−0.22

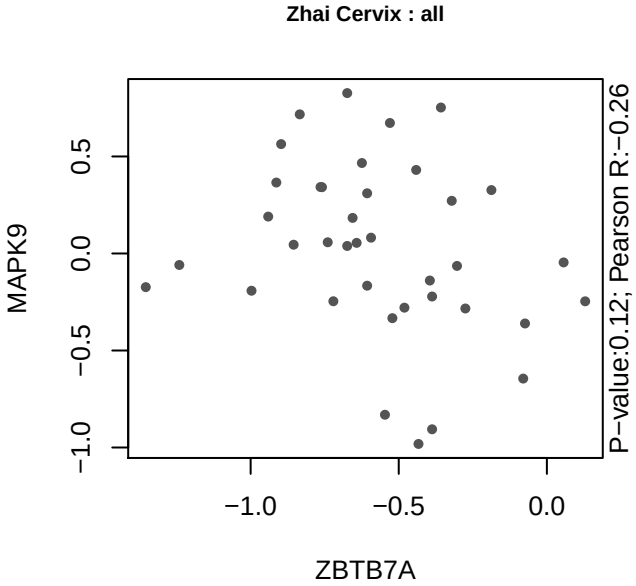

Zhai Cervix : all
MAPK8
BCL6
P−value:0.48; Pearson R:−0.12

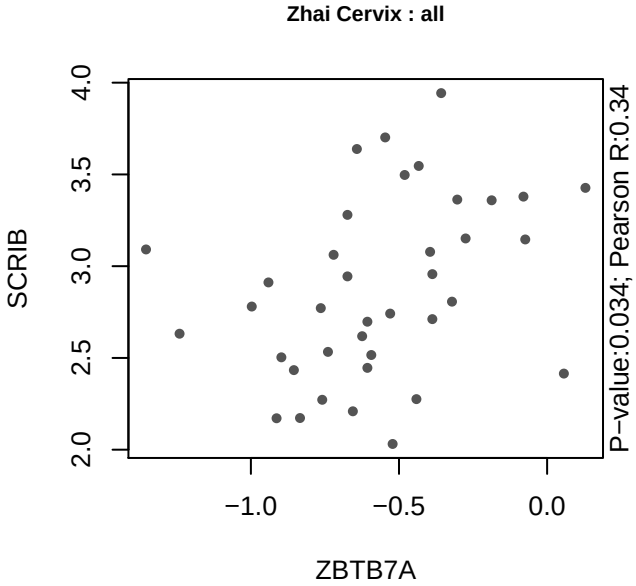

Zhai Cervix : all
MAPK10
ZBTB7A
P−value:0.11; Pearson R:0.27

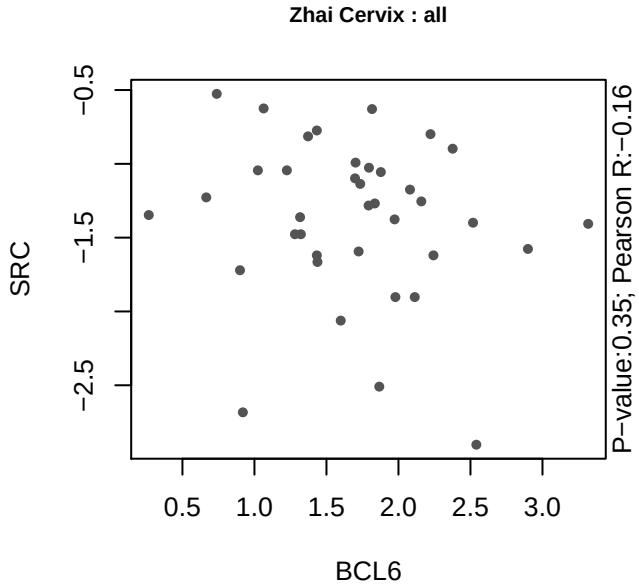

Zhai Cervix : all
MAPK8
ZBTB7A
P−value:0.71; Pearson R:−0.063

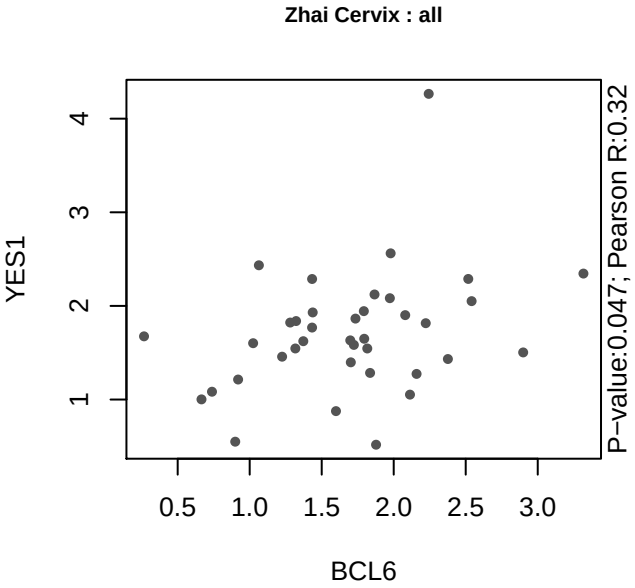

Zhai Cervix : all
MAPK9
BCL6
P−value:0.44; Pearson R:0.13

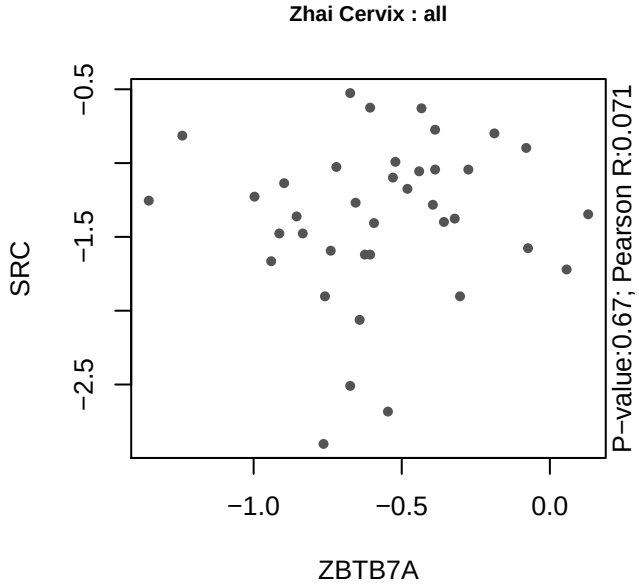

Zhai Cervix : all
SCRIB
BCL6
P−value:0.73; Pearson R:0.059

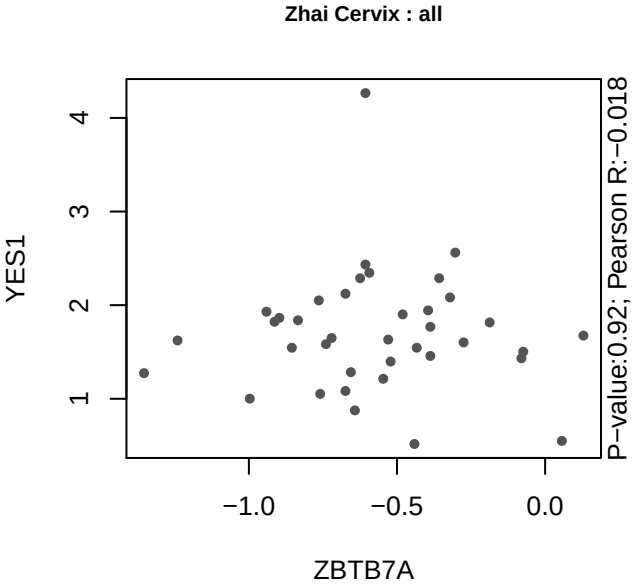

Zhai Cervix : all
MAPK9
ZBTB7A
P−value:0.12; Pearson R:−0.26

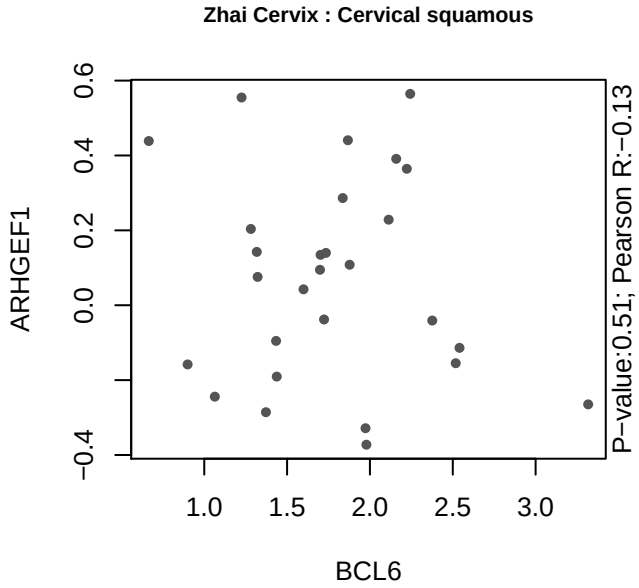

Zhai Cervix : all
SCRIB
ZBTB7A
P−value:0.034; Pearson R:0.34

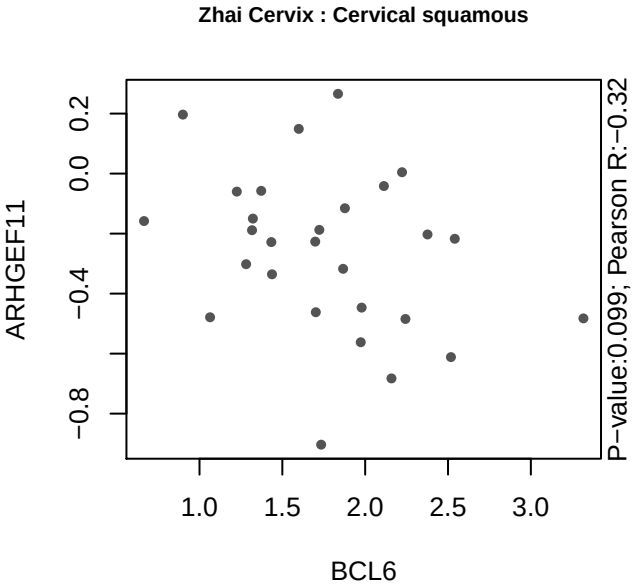

Zhai Cervix : all
SRC
BCL6
P−value:0.35; Pearson R:−0.16

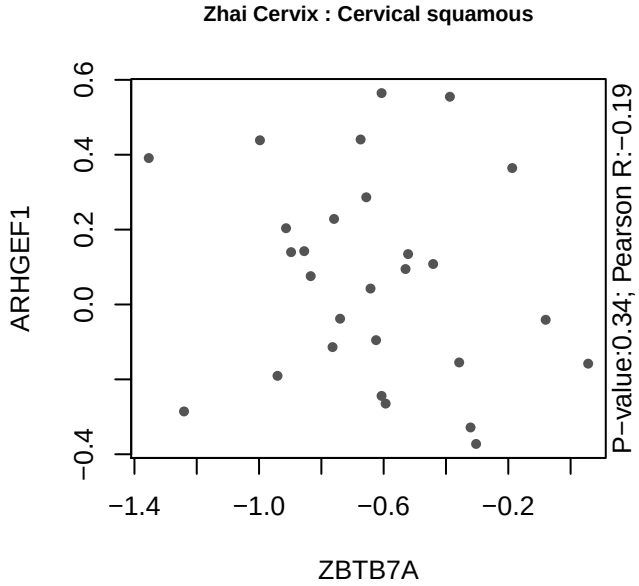

Zhai Cervix : all
YES1
BCL6
P−value:0.047; Pearson R:0.32

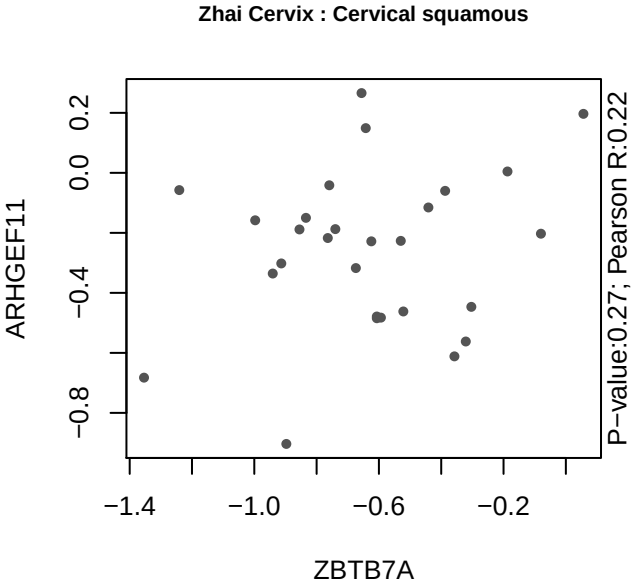

Zhai Cervix : all
SRC
ZBTB7A
P−value:0.67; Pearson R:0.071

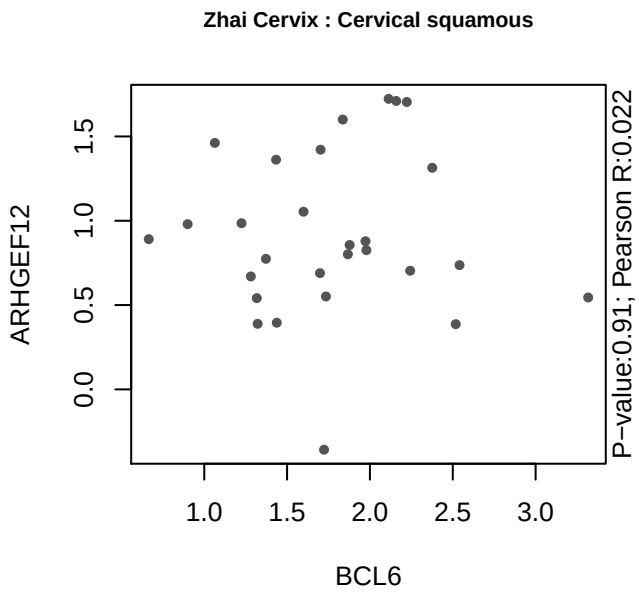

Zhai Cervix : all
YES1
ZBTB7A
P−value:0.92; Pearson R:−0.018

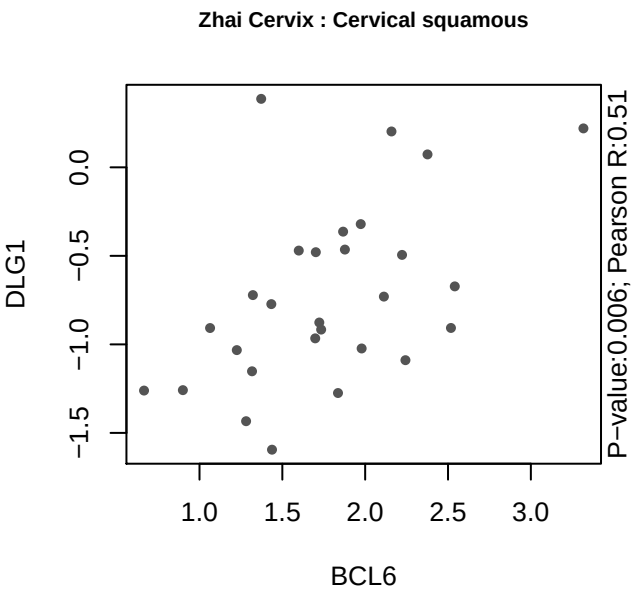

Zhai Cervix : Cervical squamous
ARHGEF1
BCL6
P−value:0.51; Pearson R:−0.13

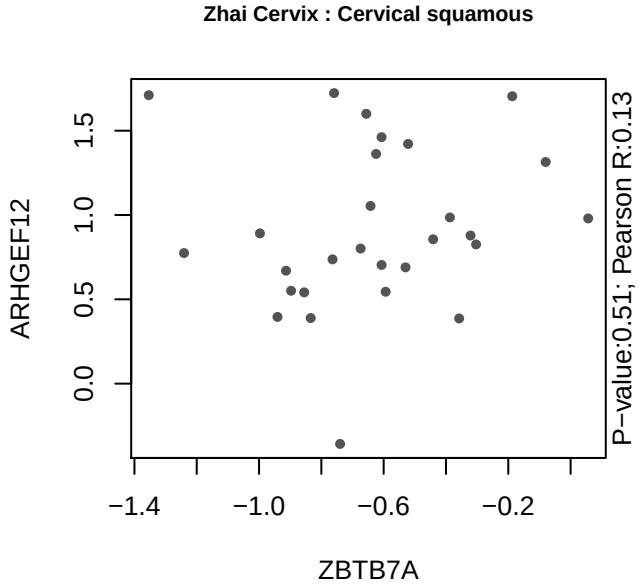

Zhai Cervix : Cervical squamous
ARHGEF11
BCL6
P−value:0.099; Pearson R:−0.32

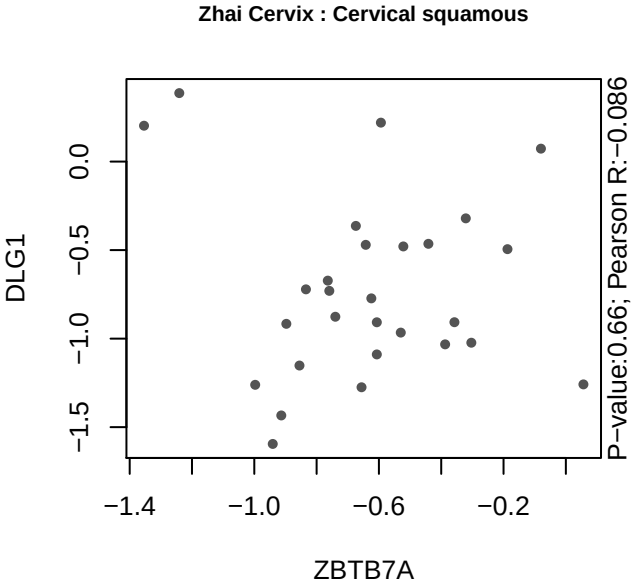

Zhai Cervix : Cervical squamous
ARHGEF1
ZBTB7A
P−value:0.34; Pearson R:−0.19

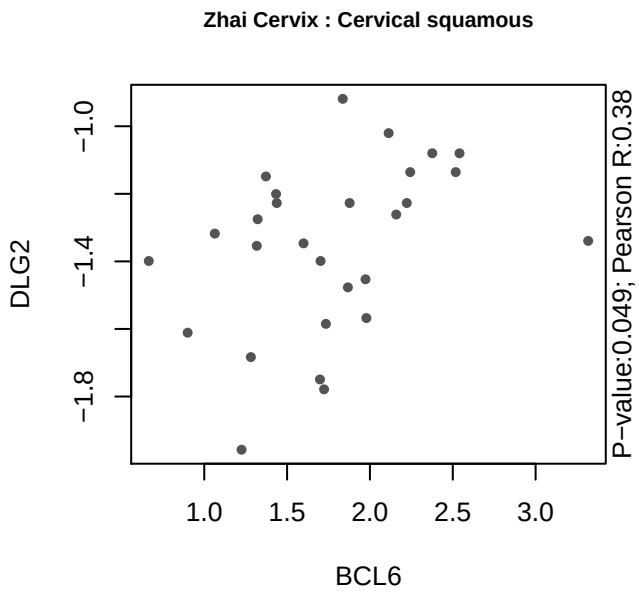

Zhai Cervix : Cervical squamous
ARHGEF11
ZBTB7A
P−value:0.27; Pearson R:0.22

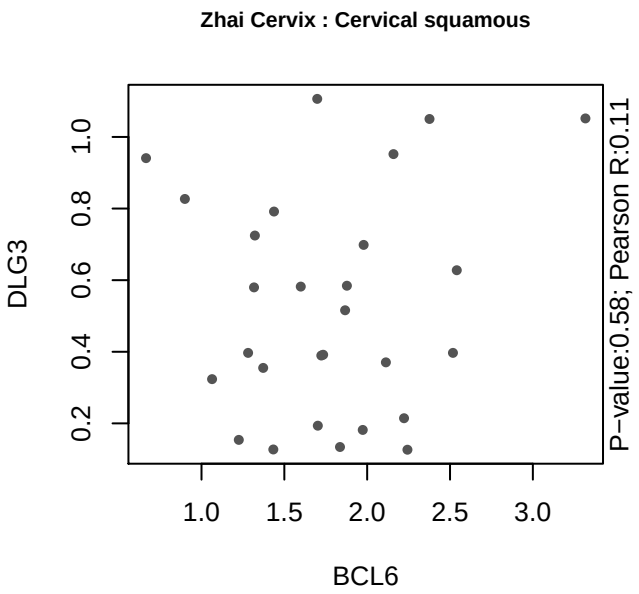

Zhai Cervix : Cervical squamous
ARHGEF12
BCL6
P−value:0.91; Pearson R:0.022

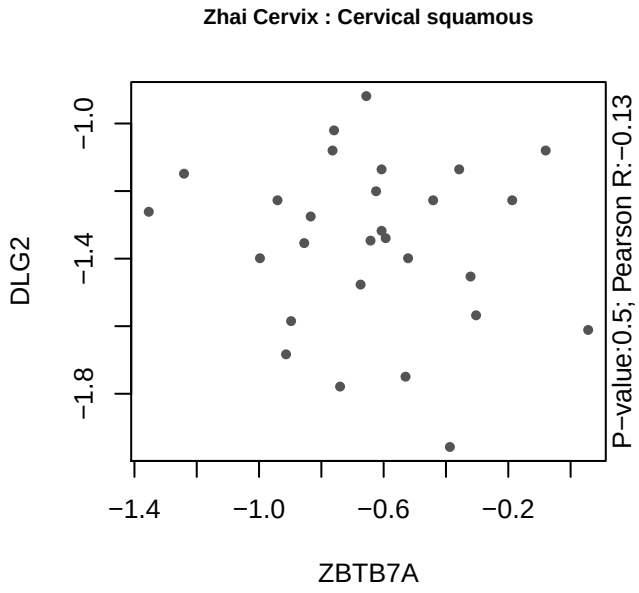

Zhai Cervix : Cervical squamous
DLG1
BCL6
P−value:0.006; Pearson R:0.51

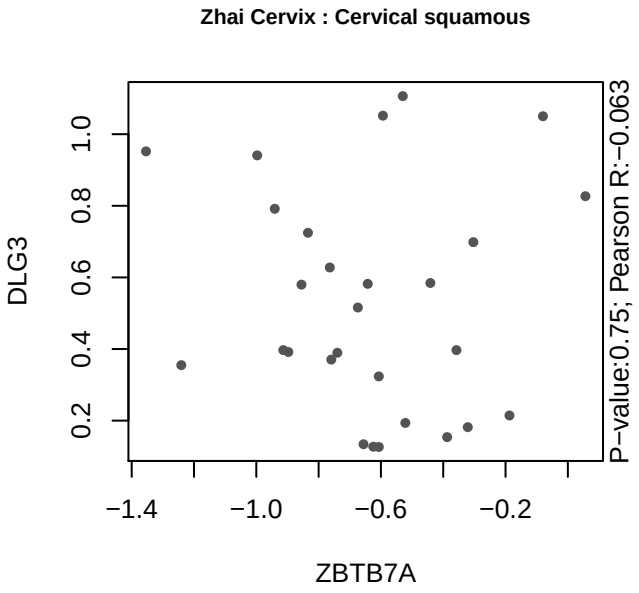

Zhai Cervix : Cervical squamous
ARHGEF12
ZBTB7A
P−value:0.51; Pearson R:0.13

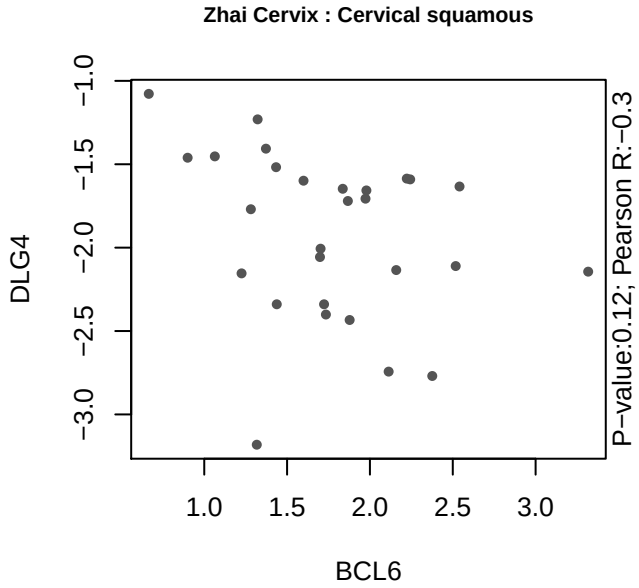

Zhai Cervix : Cervical squamous
DLG1
ZBTB7A
P−value:0.66; Pearson R:−0.086

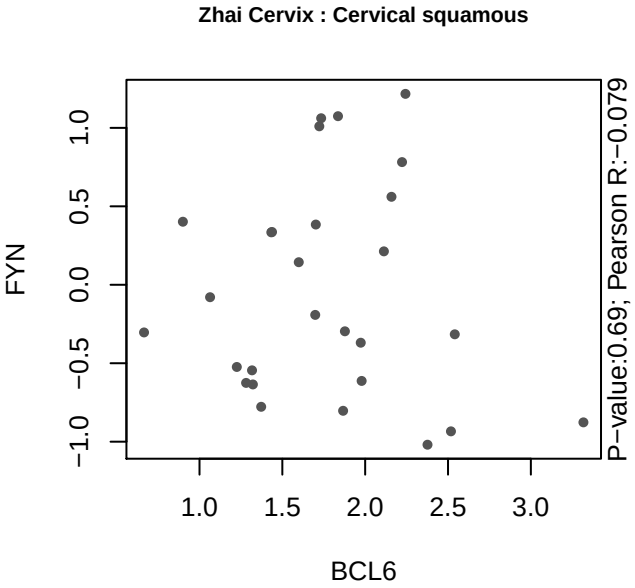

Zhai Cervix : Cervical squamous
DLG2
BCL6
P−value:0.049; Pearson R:0.38

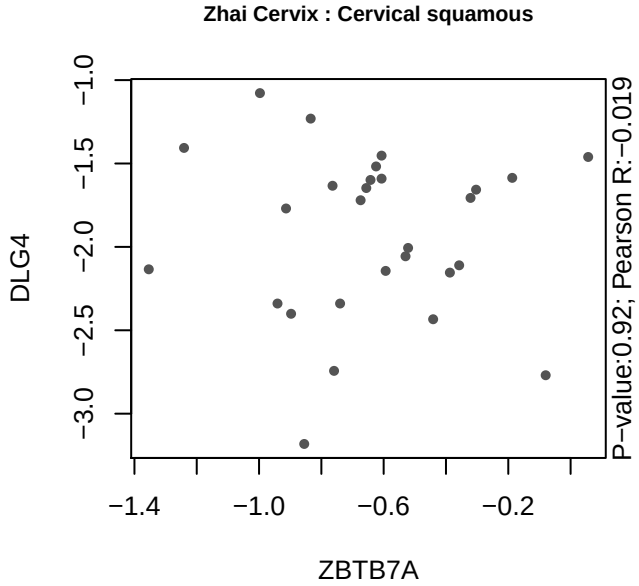

Zhai Cervix : Cervical squamous
DLG3
BCL6
P−value:0.58; Pearson R:0.11

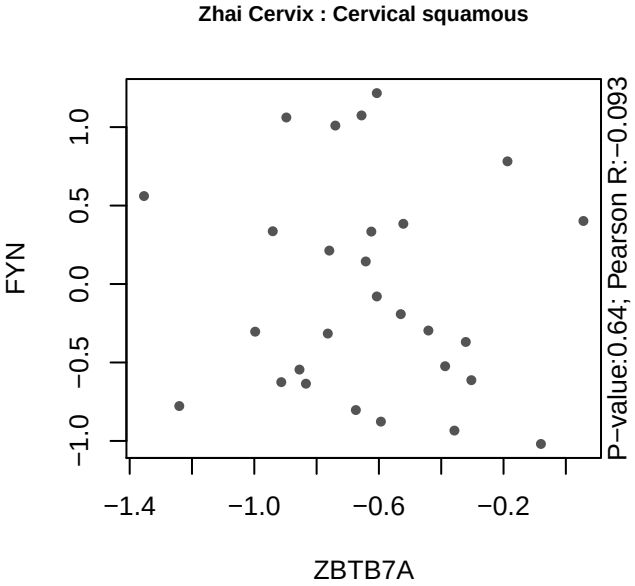

Zhai Cervix : Cervical squamous
DLG2
ZBTB7A
P−value:0.5; Pearson R:−0.13

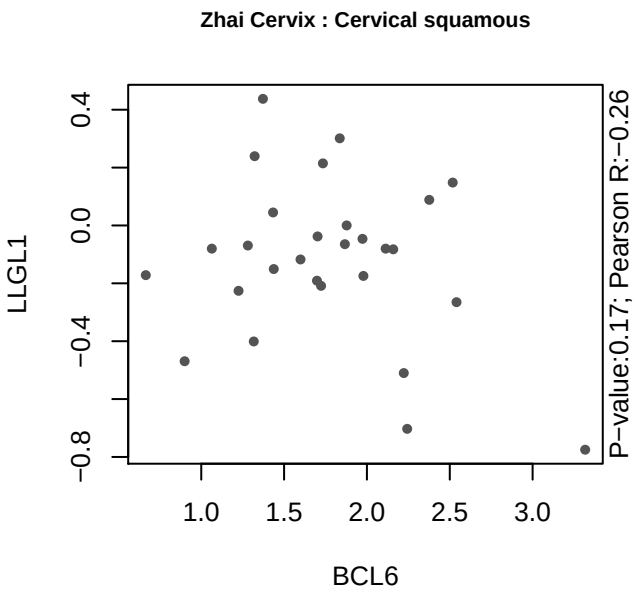

Zhai Cervix : Cervical squamous
DLG3
ZBTB7A
P−value:0.75; Pearson R:−0.063

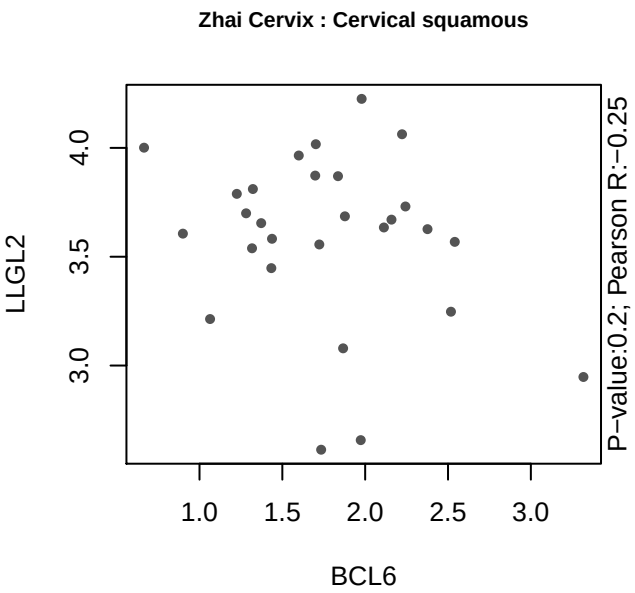

Zhai Cervix : Cervical squamous
DLG4
BCL6
P−value:0.12; Pearson R:−0.3

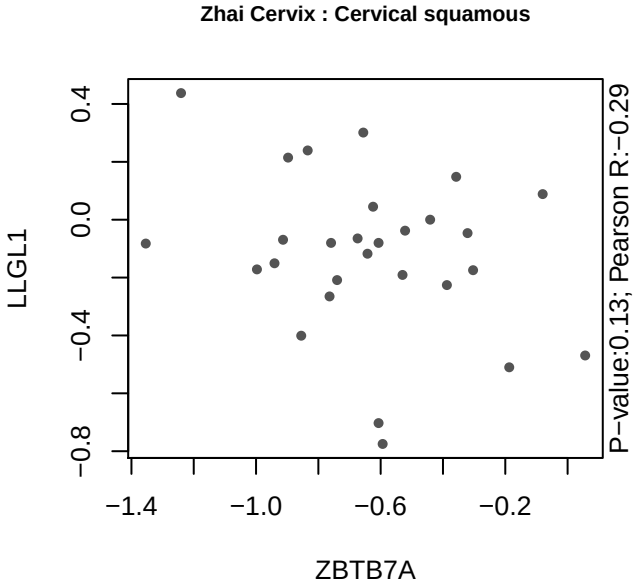

Zhai Cervix : Cervical squamous
FYN
BCL6
P−value:0.69; Pearson R:−0.079

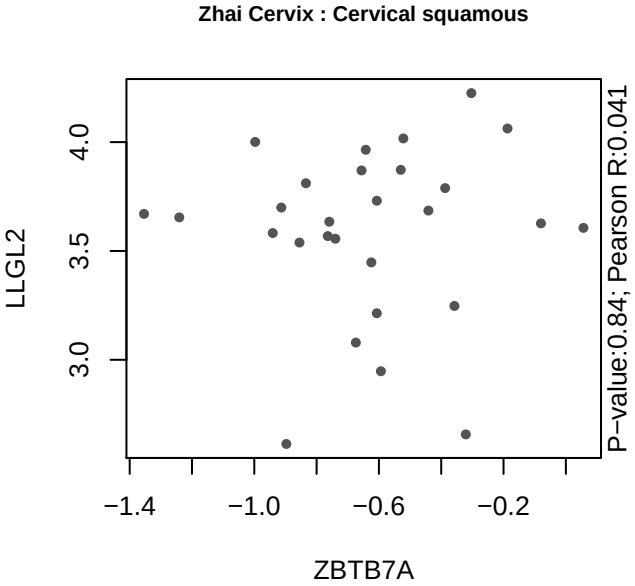

Zhai Cervix : Cervical squamous
DLG4
ZBTB7A
P−value:0.92; Pearson R:−0.019

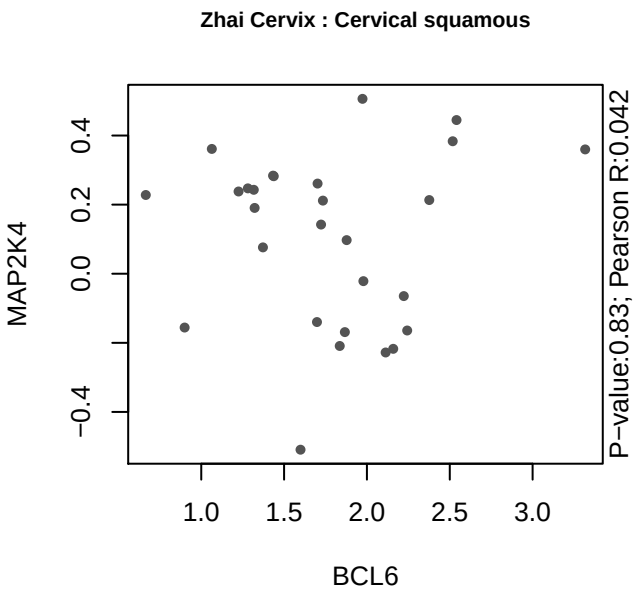

Zhai Cervix : Cervical squamous
FYN
ZBTB7A
P−value:0.64; Pearson R:−0.093

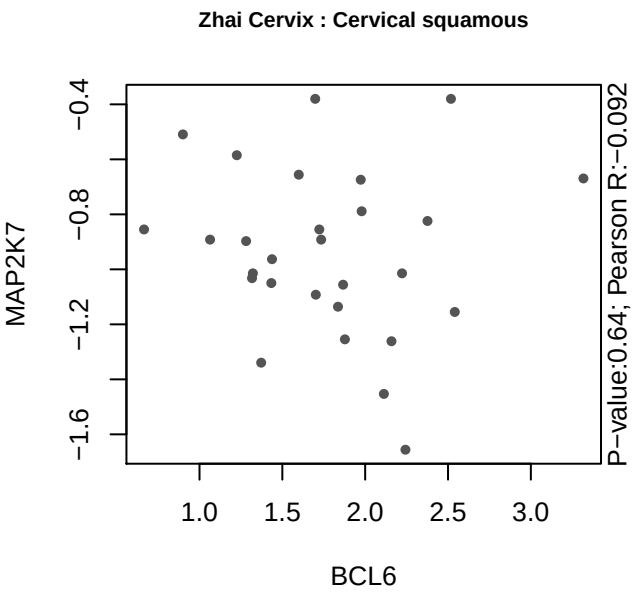

Zhai Cervix : Cervical squamous
LLGL1
BCL6
P−value:0.17; Pearson R:−0.26
0.4
0.0
−0.4
−0.8
1.0
1.5
2.0
2.5
3.0

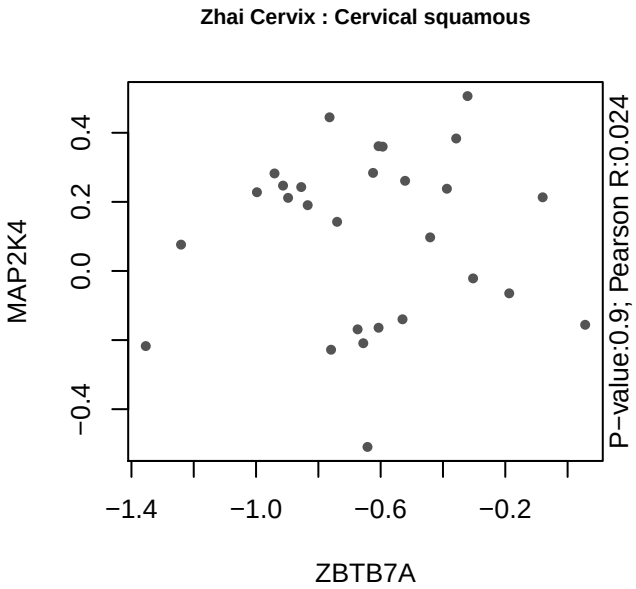

Zhai Cervix : Cervical squamous
LLGL2
BCL6
P−value:0.2; Pearson R:−0.25
4.0
3.5
3.0
1.0
1.5
2.0
2.5
3.0

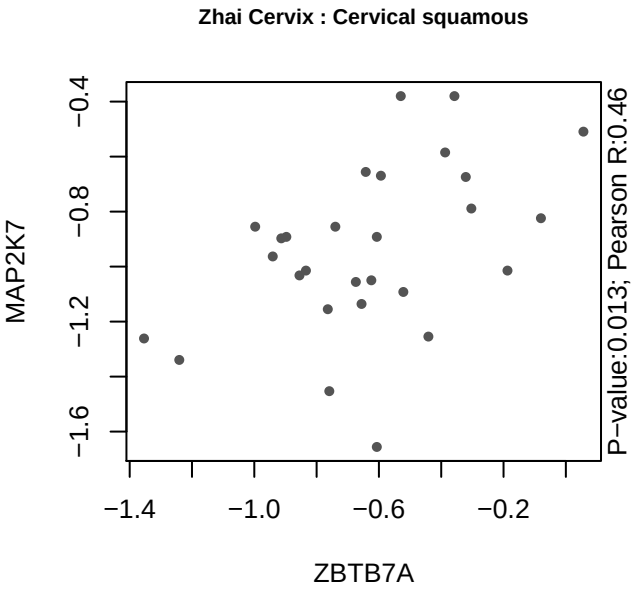

Zhai Cervix : Cervical squamous
LLGL1
ZBTB7A
P−value:0.13; Pearson R:−0.29
0.4
0.0
−0.4
−0.8
−1.4
−1.0
−0.6
−0.2

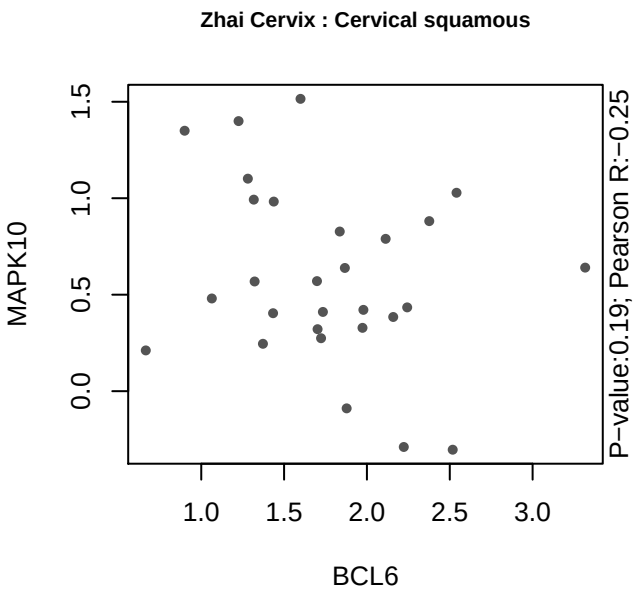

Zhai Cervix : Cervical squamous
LLGL2
ZBTB7A
P−value:0.84; Pearson R:0.041
4.0
3.5
3.0
−1.4
−1.0
−0.6
−0.2

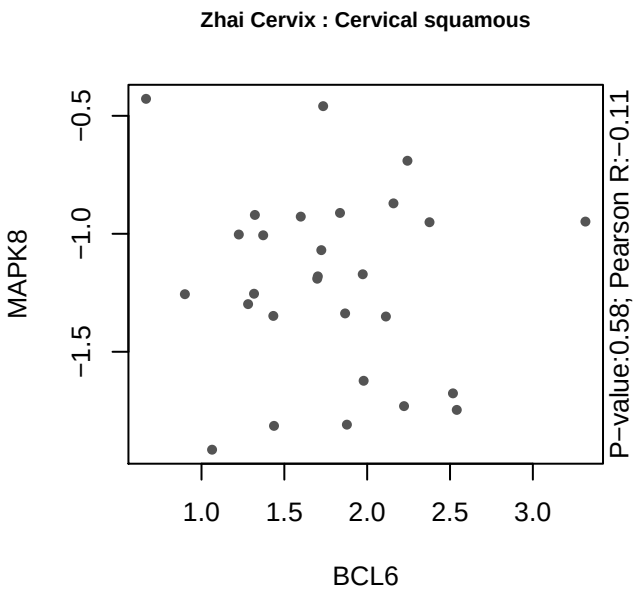

Zhai Cervix : Cervical squamous
MAP2K4
BCL6
P−value:0.83; Pearson R:0.042

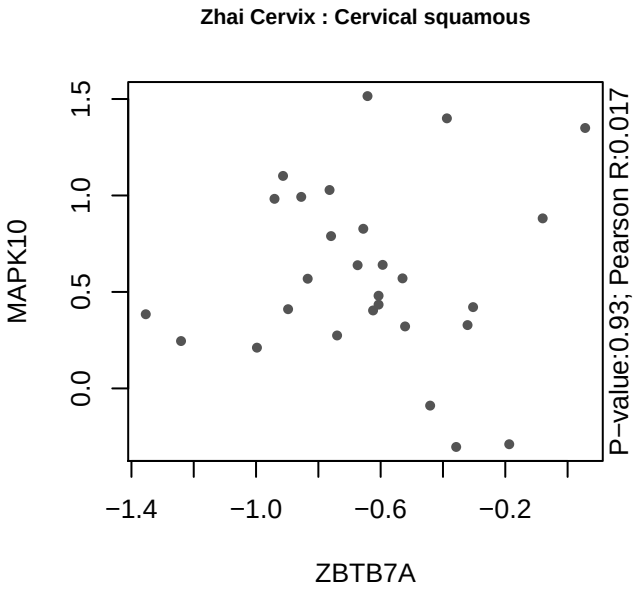

Zhai Cervix : Cervical squamous
MAP2K7
BCL6
P−value:0.64; Pearson R:−0.092

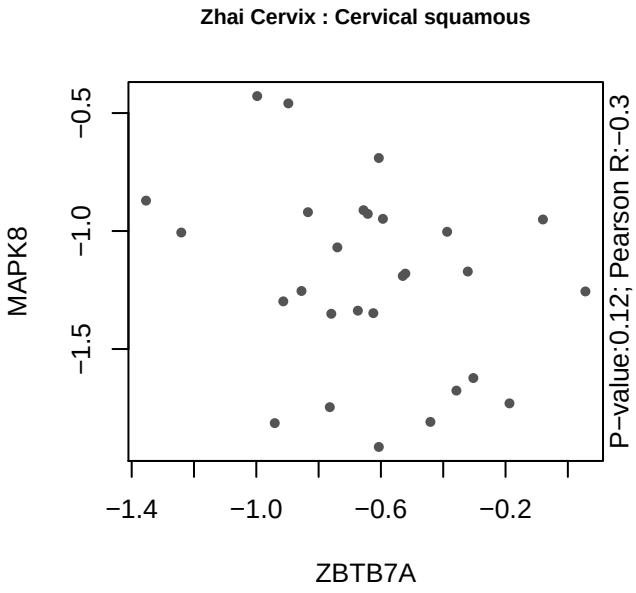

Zhai Cervix : Cervical squamous
MAP2K4
ZBTB7A
P−value:0.9; Pearson R:0.024

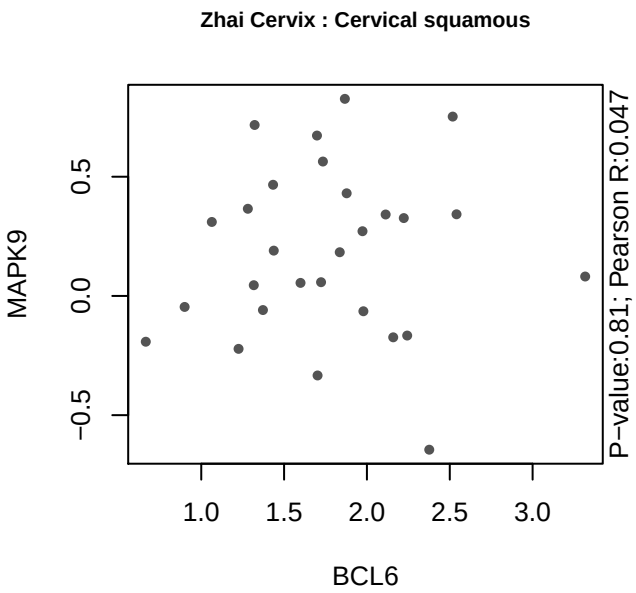

Zhai Cervix : Cervical squamous
MAP2K7
ZBTB7A
P−value:0.013; Pearson R:0.46

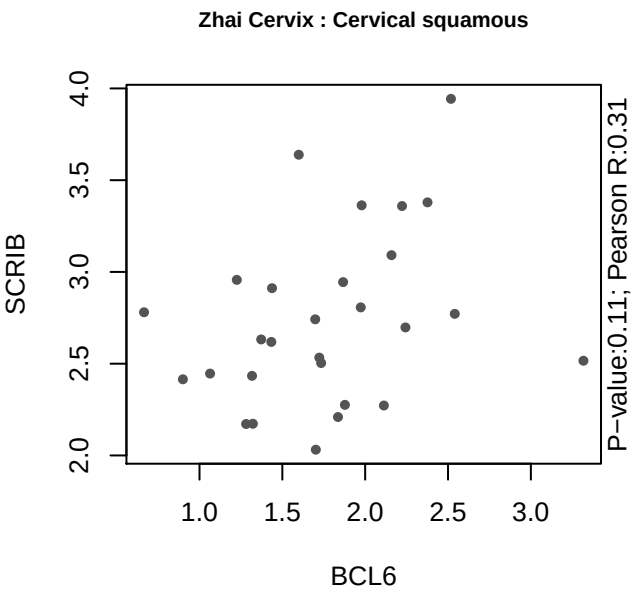

Zhai Cervix : Cervical squamous
MAPK10
BCL6
P−value:0.19; Pearson R:−0.25

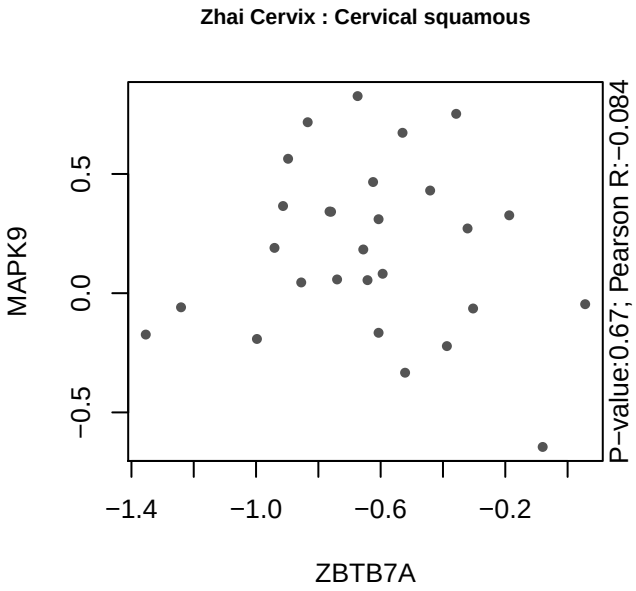

Zhai Cervix : Cervical squamous
MAPK8
BCL6
P−value:0.58; Pearson R:−0.11

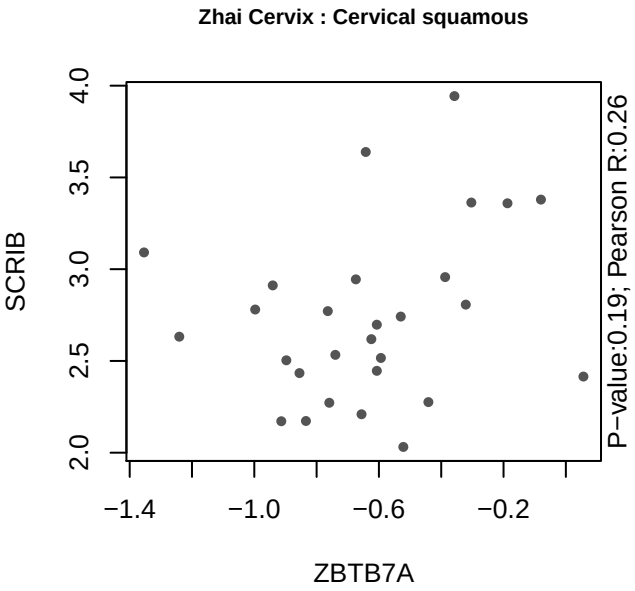

Zhai Cervix : Cervical squamous
MAPK10
ZBTB7A
P−value:0.93; Pearson R:0.017

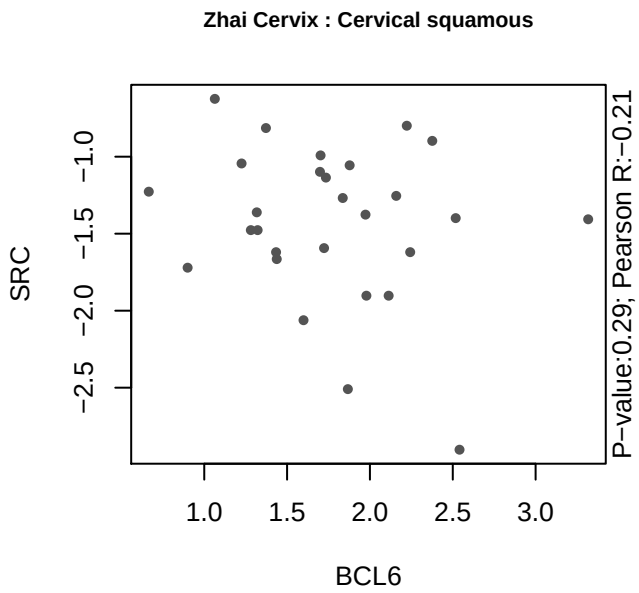

Zhai Cervix : Cervical squamous
MAPK8
ZBTB7A
P−value:0.12; Pearson R:−0.3

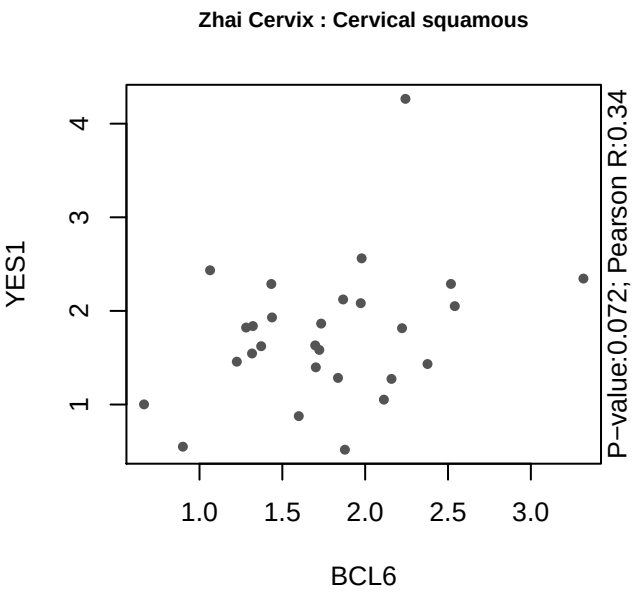

Zhai Cervix : Cervical squamous
MAPK9
BCL6
P−value:0.81; Pearson R:0.047

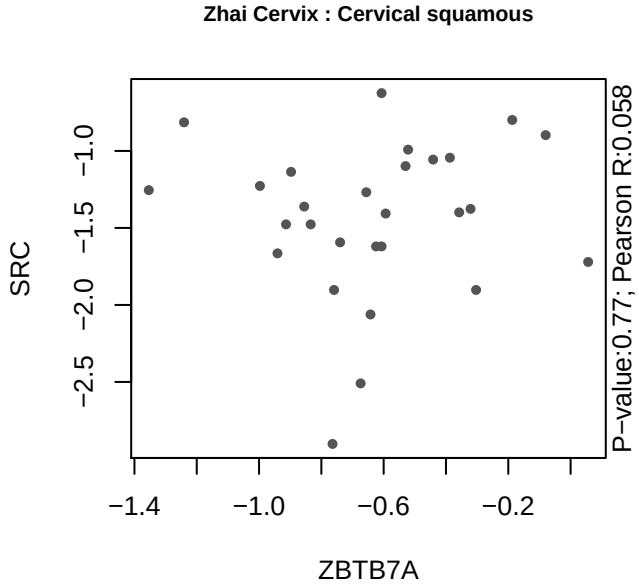

Zhai Cervix : Cervical squamous
SCRIB
BCL6
P−value:0.11; Pearson R:0.31

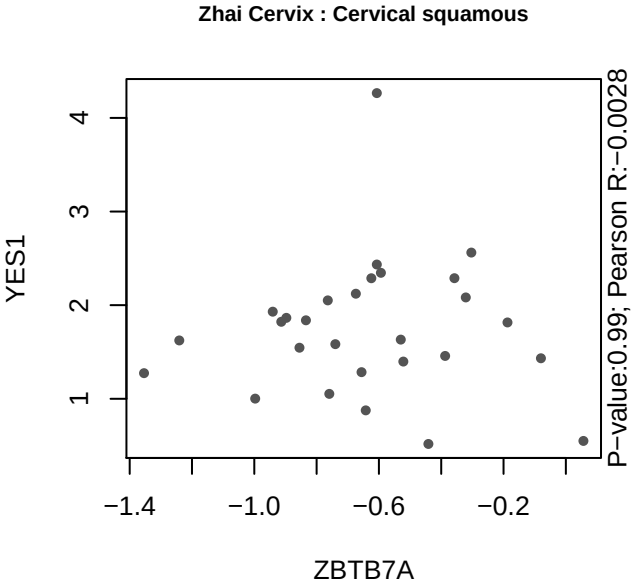

Zhai Cervix : Cervical squamous
MAPK9
ZBTB7A
P−value:0.67; Pearson R:−0.084

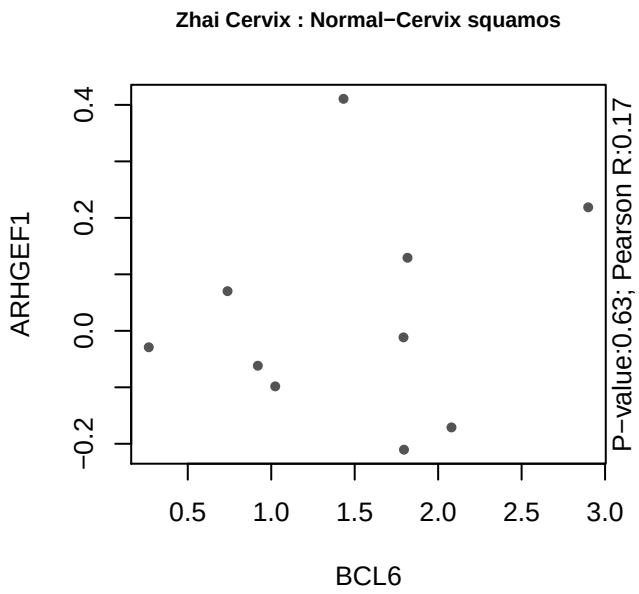

Zhai Cervix : Cervical squamous
SCRIB
ZBTB7A
P−value:0.19; Pearson R:0.26

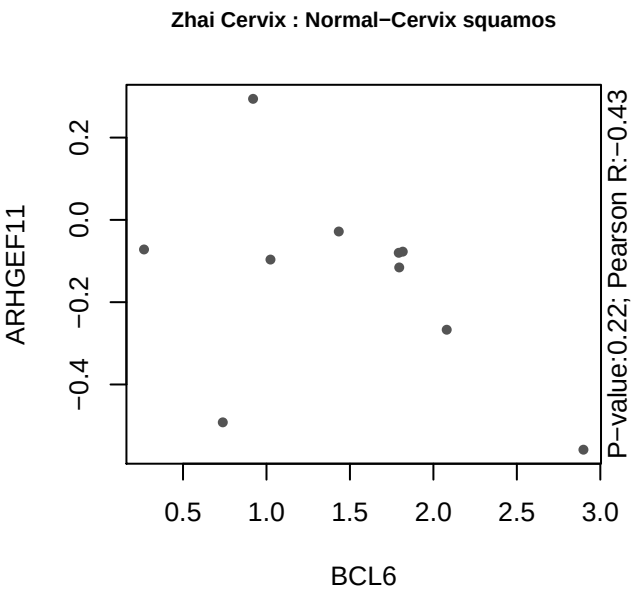

Zhai Cervix : Cervical squamous
SRC
BCL6
P−value:0.29; Pearson R:−0.21

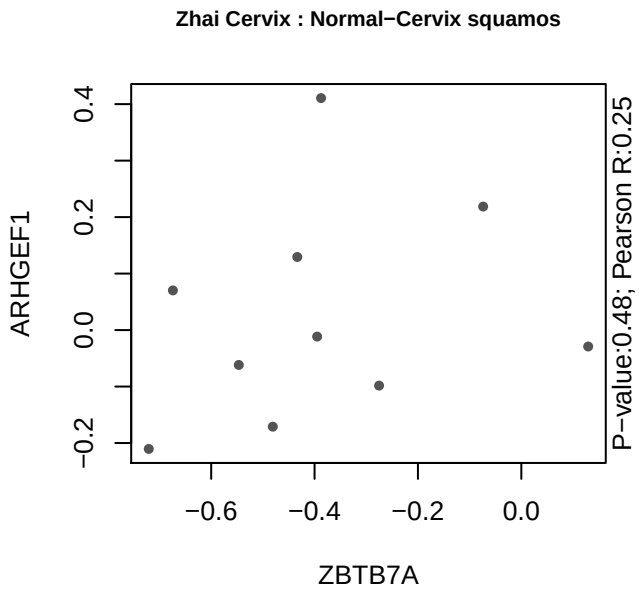

Zhai Cervix : Cervical squamous
YES1
BCL6
P−value:0.072; Pearson R:0.34

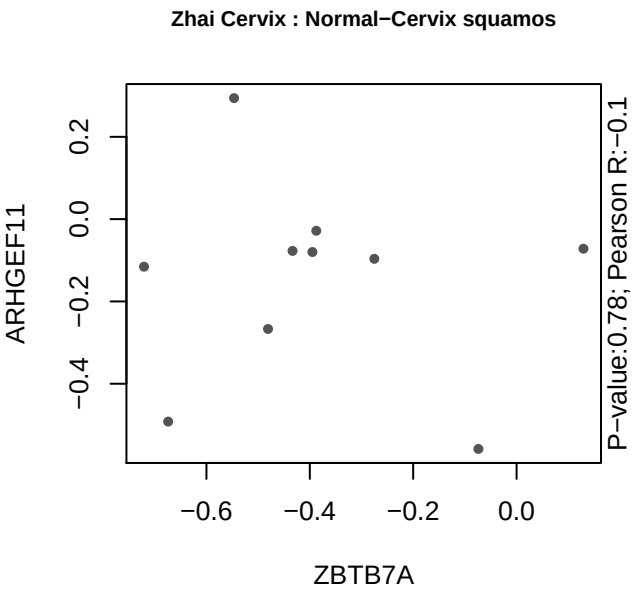

Zhai Cervix : Cervical squamous
SRC
ZBTB7A
P−value:0.77; Pearson R:0.058

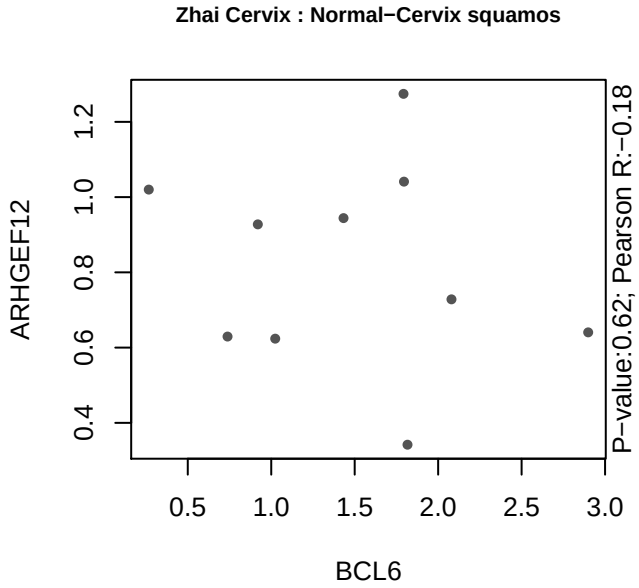

Zhai Cervix : Cervical squamous
YES1
ZBTB7A
P−value:0.99; Pearson R:−0.0028

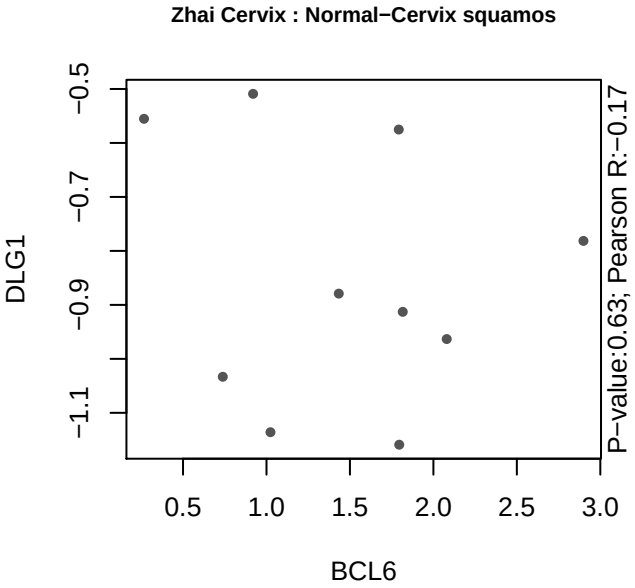

Zhai Cervix : Normal−Cervix squamos
ARHGEF1
BCL6
P−value:0.63; Pearson R:0.17

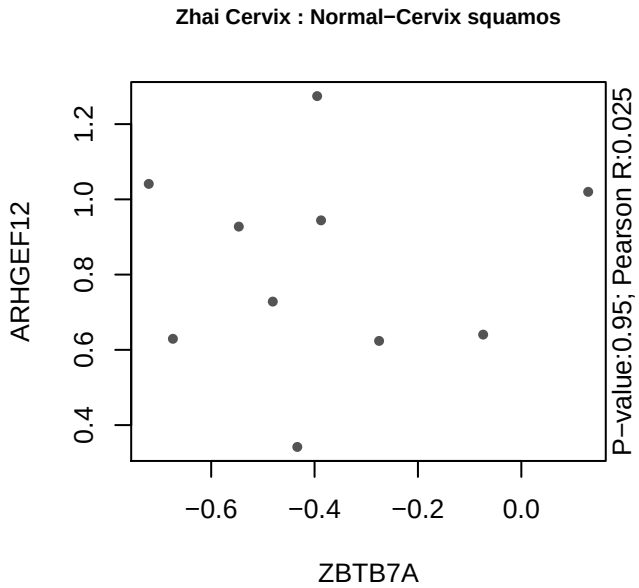

Zhai Cervix : Normal−Cervix squamos
ARHGEF11
BCL6
P−value:0.22; Pearson R:−0.43

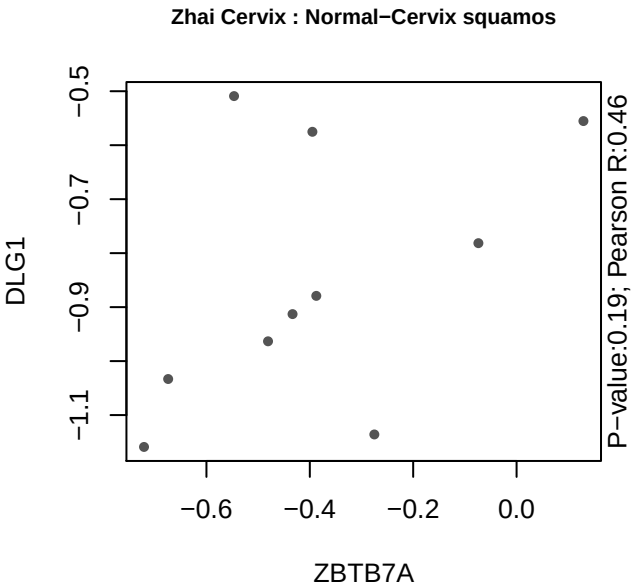

Zhai Cervix : Normal−Cervix squamos
ARHGEF1
ZBTB7A
P−value:0.48; Pearson R:0.25

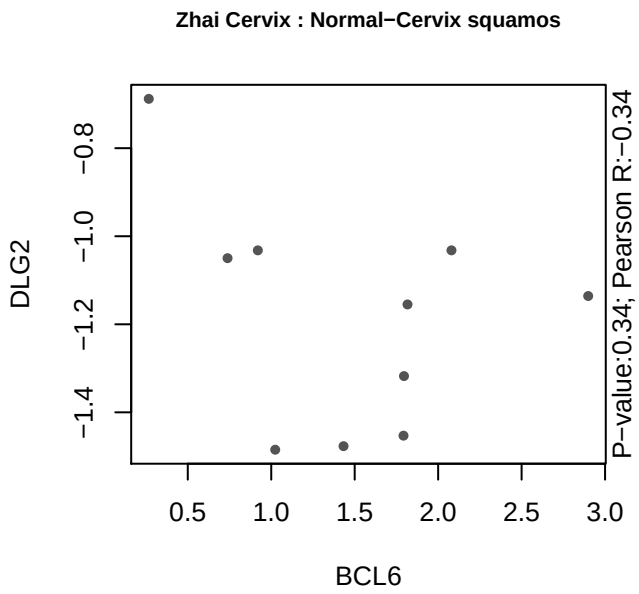

Zhai Cervix : Normal−Cervix squamos
ARHGEF11
ZBTB7A
P−value:0.78; Pearson R:−0.1

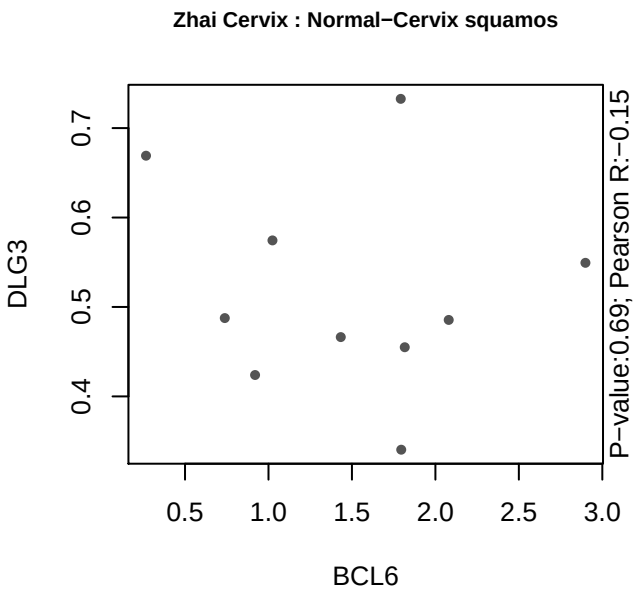

Zhai Cervix : Normal−Cervix squamos
ARHGEF12
BCL6
P−value:0.62; Pearson R:−0.18

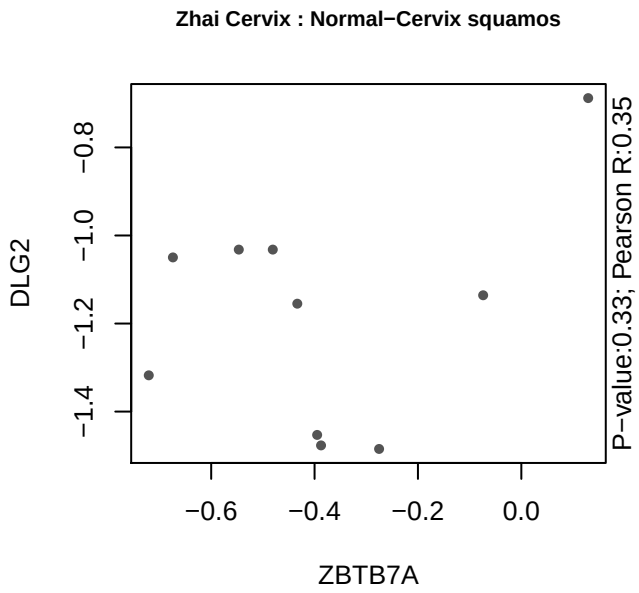

Zhai Cervix : Normal−Cervix squamos
DLG1
BCL6
P−value:0.63; Pearson R:−0.17

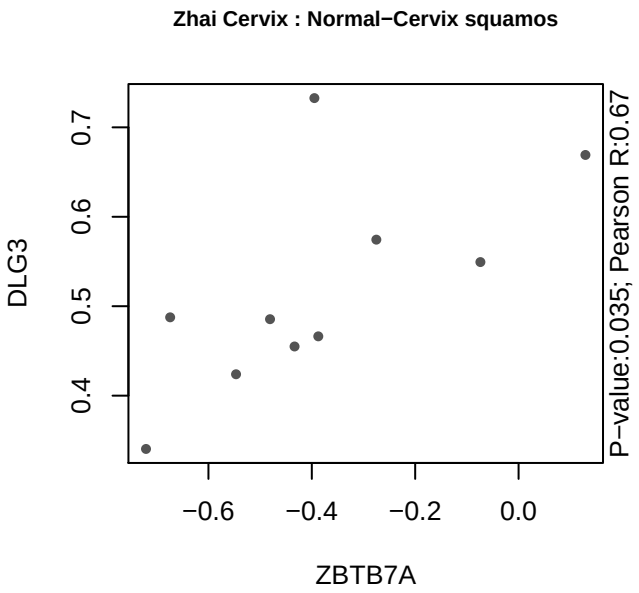

Zhai Cervix : Normal−Cervix squamos
ARHGEF12
ZBTB7A
P−value:0.95; Pearson R:0.025

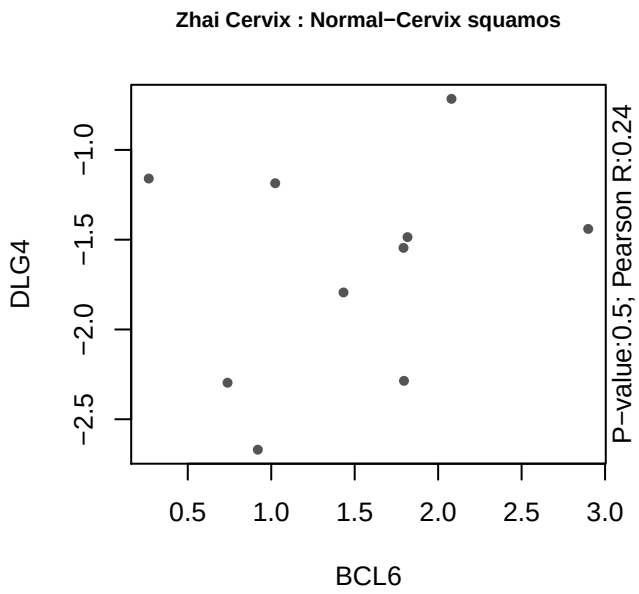

Zhai Cervix : Normal−Cervix squamos
DLG1
ZBTB7A
P−value:0.19; Pearson R:0.46

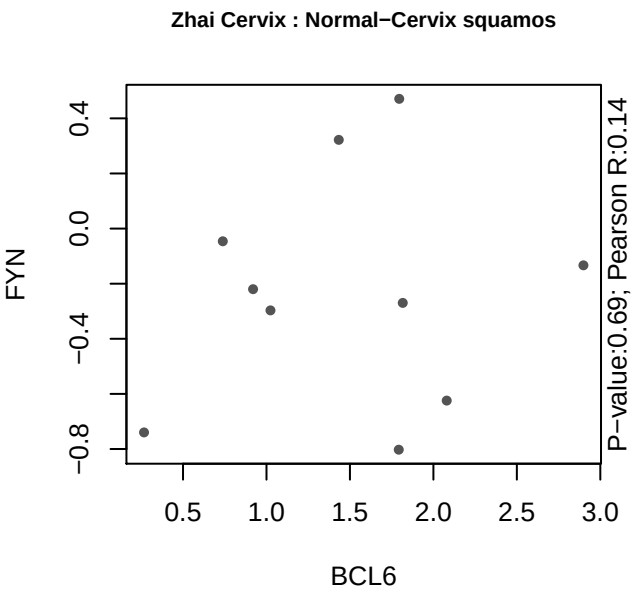

Zhai Cervix : Normal−Cervix squamos
DLG2
BCL6
P−value:0.34; Pearson R:−0.34

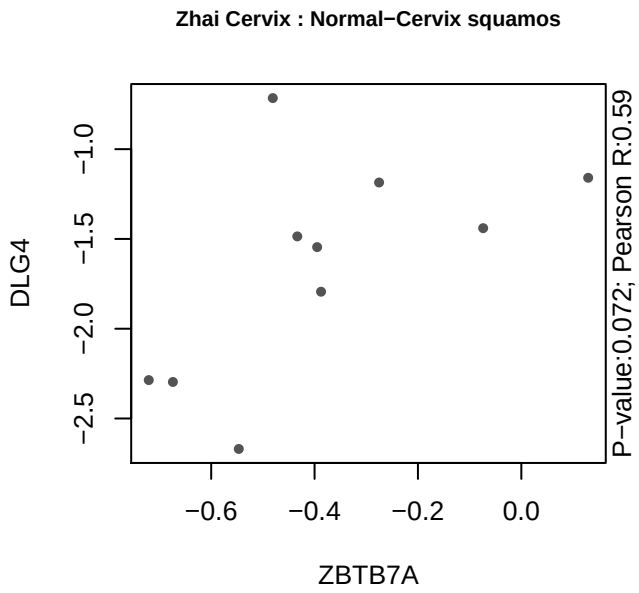

Zhai Cervix : Normal−Cervix squamos
DLG3
BCL6
P−value:0.69; Pearson R:−0.15

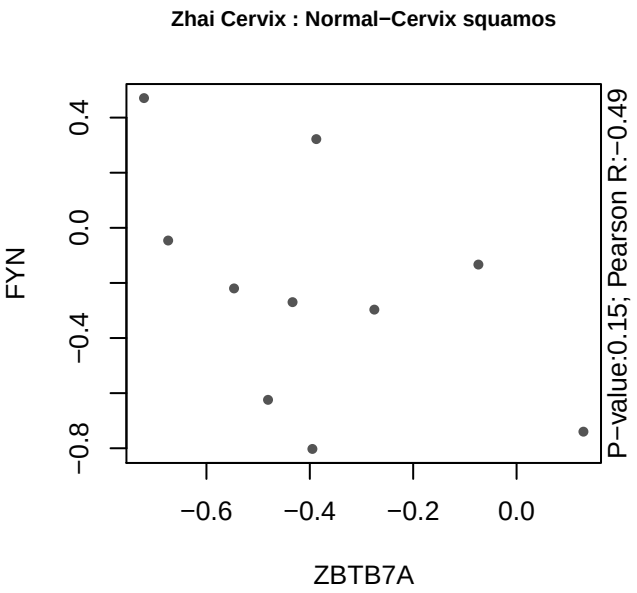

Zhai Cervix : Normal−Cervix squamos
DLG2
ZBTB7A
P−value:0.33; Pearson R:0.35

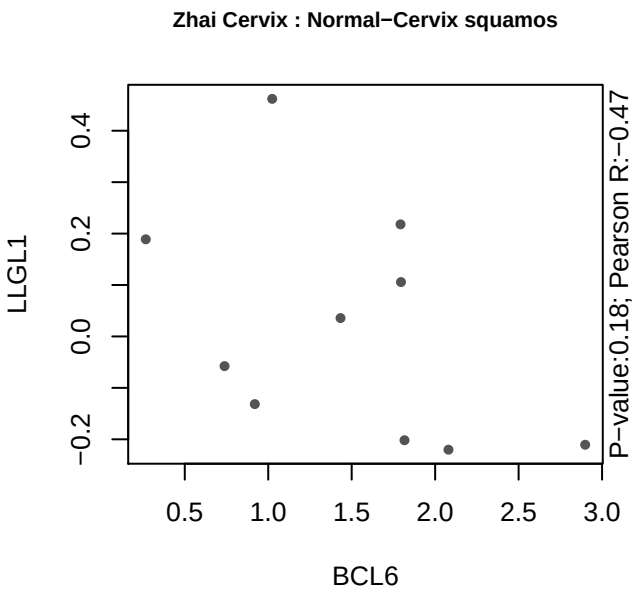

Zhai Cervix : Normal−Cervix squamos
DLG3
ZBTB7A
P−value:0.035; Pearson R:0.67

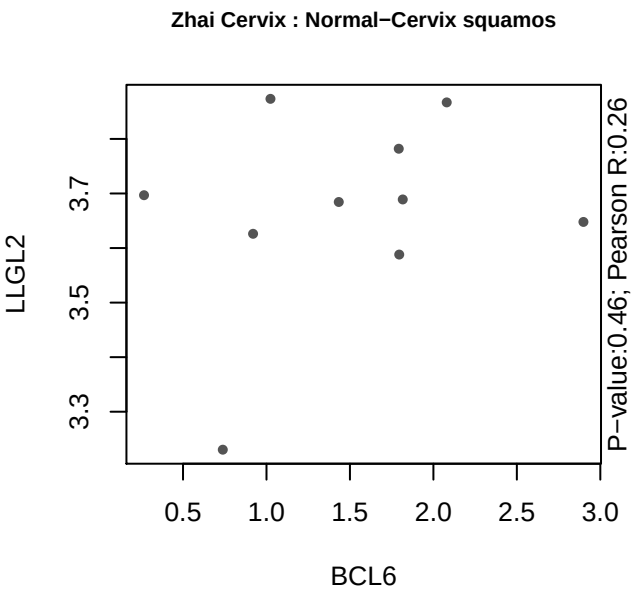

Zhai Cervix : Normal−Cervix squamos
DLG4
BCL6
P−value:0.5; Pearson R:0.24
−1.0
−1.5
−2.0
−2.5
0.5
1.0
1.5
2.0
2.5
3.0

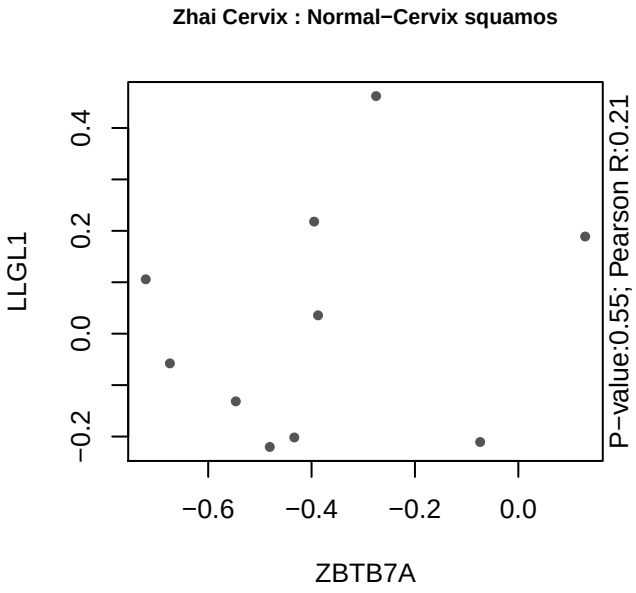

Zhai Cervix : Normal−Cervix squamos
FYN
BCL6
P−value:0.69; Pearson R:0.14
0.4
0.0
−0.4
−0.8
0.5
1.0
1.5
2.0
2.5
3.0

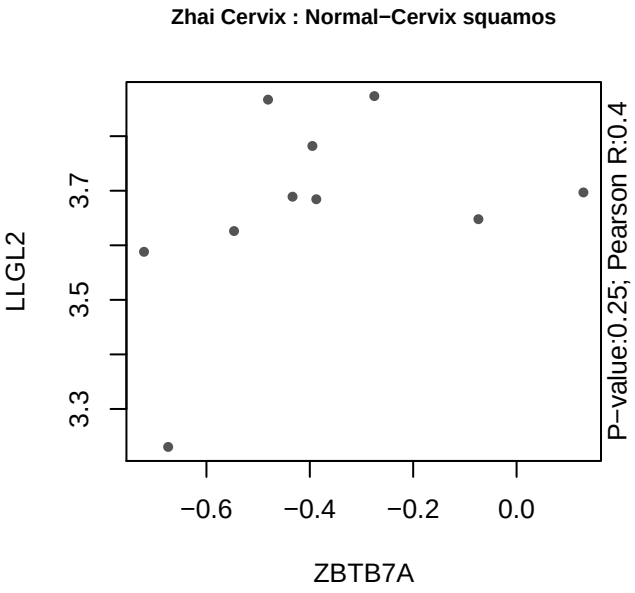

Zhai Cervix : Normal−Cervix squamos
DLG4
ZBTB7A
P−value:0.072; Pearson R:0.59
−1.0
−1.5
−2.0
−2.5
−0.6
−0.4
−0.2
0.0

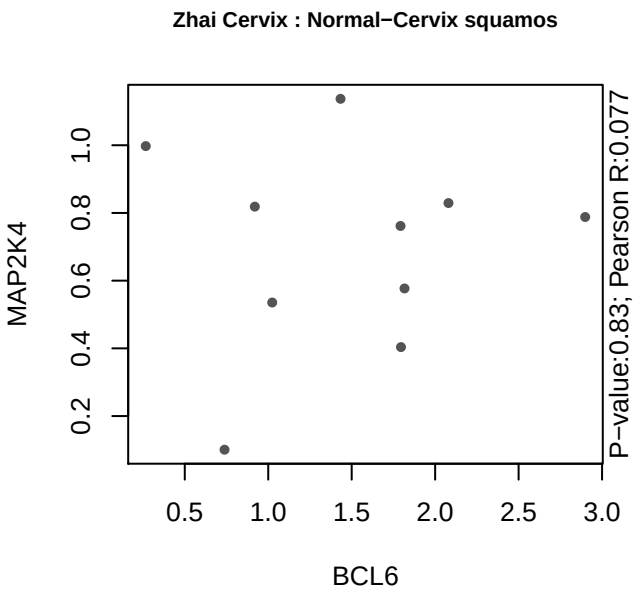

Zhai Cervix : Normal−Cervix squamos
FYN
ZBTB7A
P−value:0.15; Pearson R:−0.49
0.4
0.0
−0.4
−0.8
−0.6
−0.4
−0.2
0.0

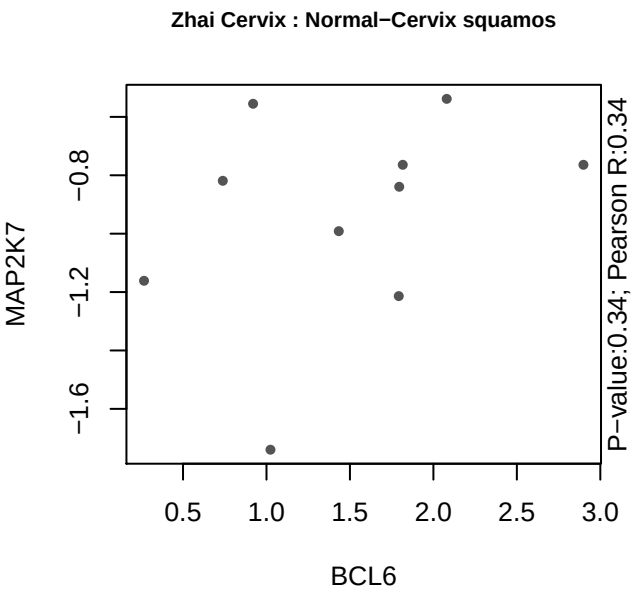

Zhai Cervix : Normal−Cervix squamos
LLGL1
BCL6
P−value:0.18; Pearson R:−0.47
−0.2
0.0
0.2
0.4
0.5
1.0
1.5
2.0
2.5
3.0

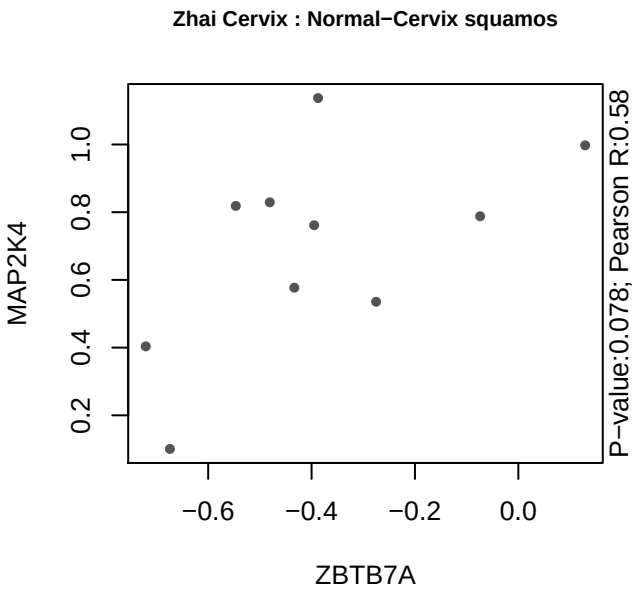

Zhai Cervix : Normal−Cervix squamos
LLGL2
BCL6
P−value:0.46; Pearson R:0.26
3.3
3.5
3.7
0.5
1.0
1.5
2.0
2.5
3.0

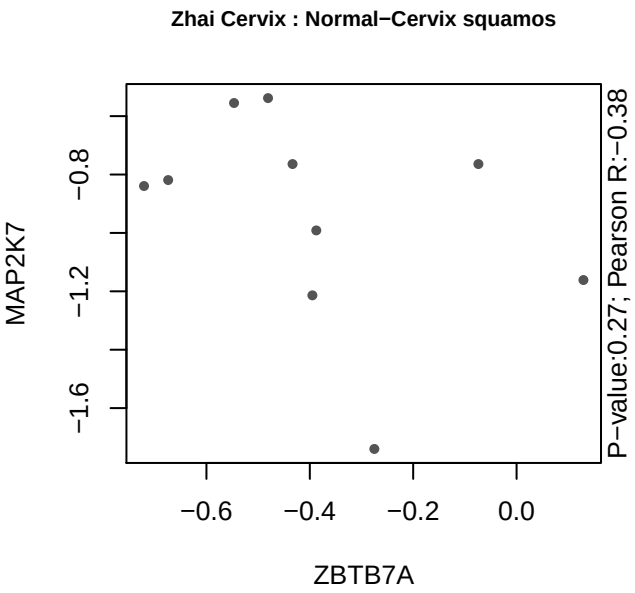

Zhai Cervix : Normal−Cervix squamos
LLGL1
ZBTB7A
P−value:0.55; Pearson R:0.21
−0.2
0.0
0.2
0.4
−0.6
−0.4
−0.2
0.0

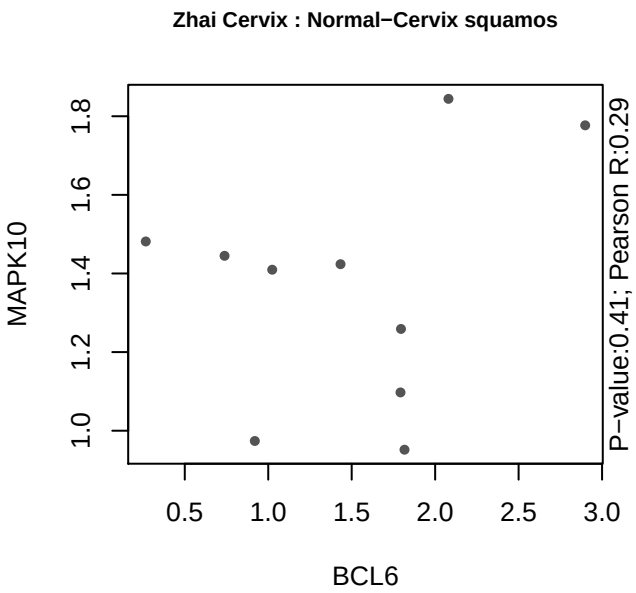

Zhai Cervix : Normal−Cervix squamos
LLGL2
ZBTB7A
P−value:0.25; Pearson R:0.4
3.3
3.5
3.7
−0.6
−0.4
−0.2
0.0

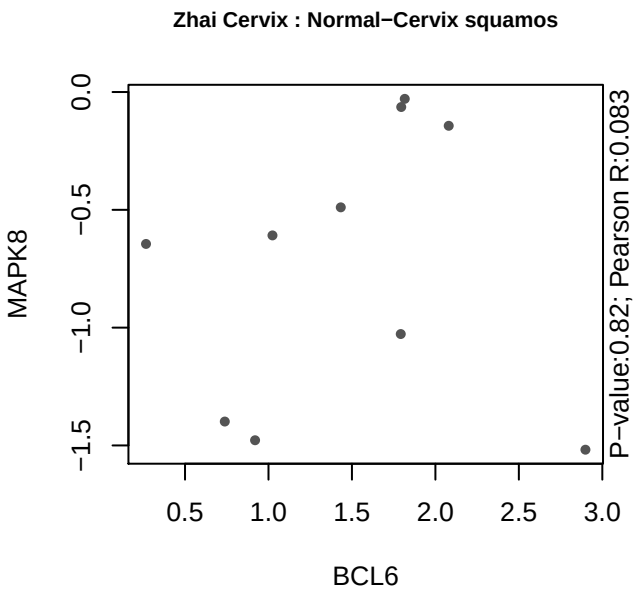

Zhai Cervix : Normal−Cervix squamos
MAP2K4
BCL6
P−value:0.83; Pearson R:0.077

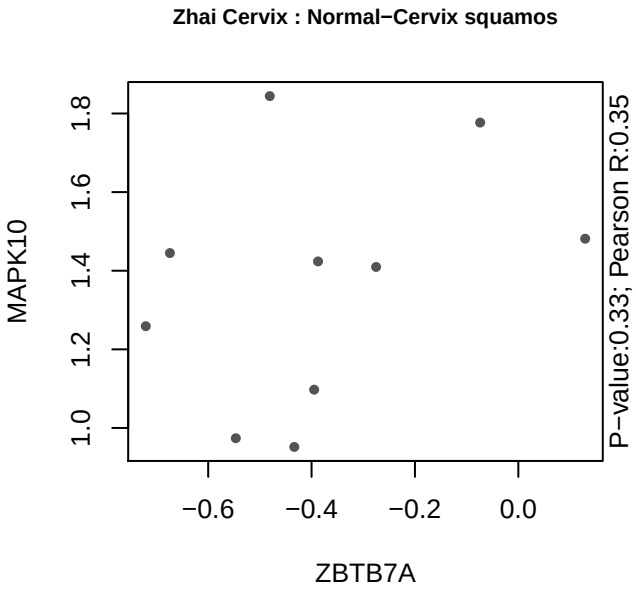

Zhai Cervix : Normal−Cervix squamos
MAP2K7
BCL6
P−value:0.34; Pearson R:0.34

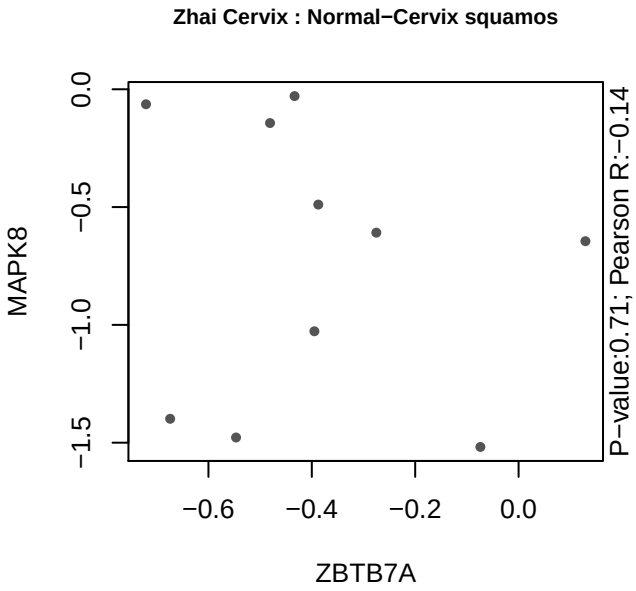

Zhai Cervix : Normal−Cervix squamos
MAP2K4
ZBTB7A
P−value:0.078; Pearson R:0.58

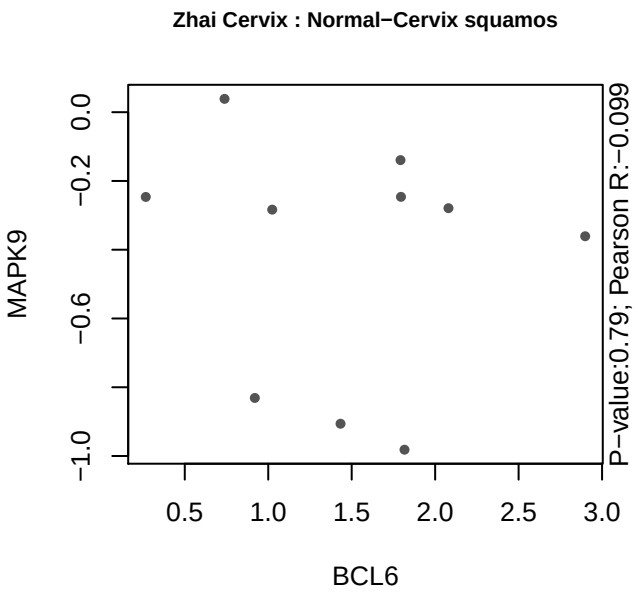

Zhai Cervix : Normal−Cervix squamos
MAP2K7
ZBTB7A
P−value:0.27; Pearson R:−0.38

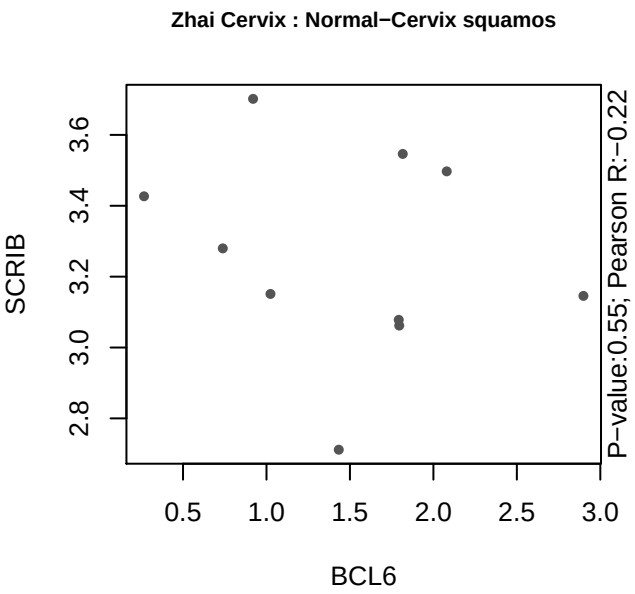

Zhai Cervix : Normal−Cervix squamos
MAPK10
BCL6
P−value:0.41; Pearson R:0.29

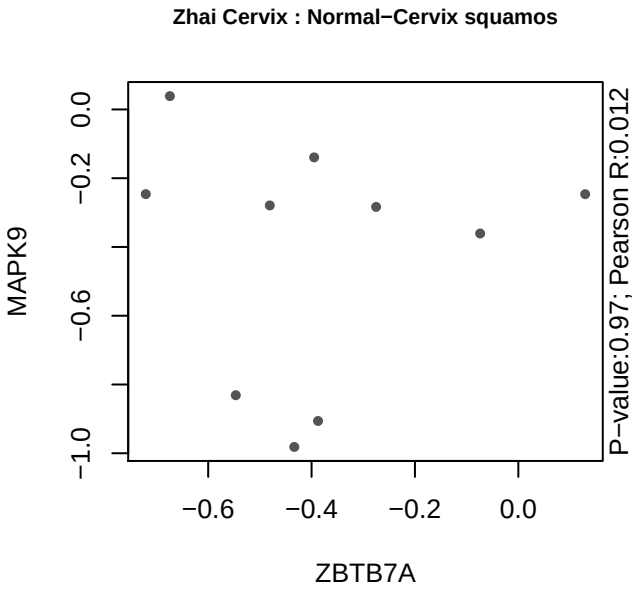

Zhai Cervix : Normal−Cervix squamos
MAPK8
BCL6
P−value:0.82; Pearson R:0.083

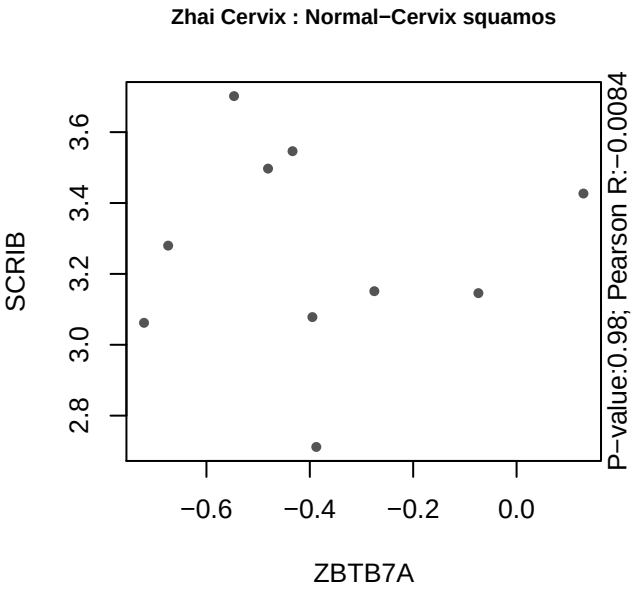

Zhai Cervix : Normal−Cervix squamos
MAPK10
ZBTB7A
P−value:0.33; Pearson R:0.35

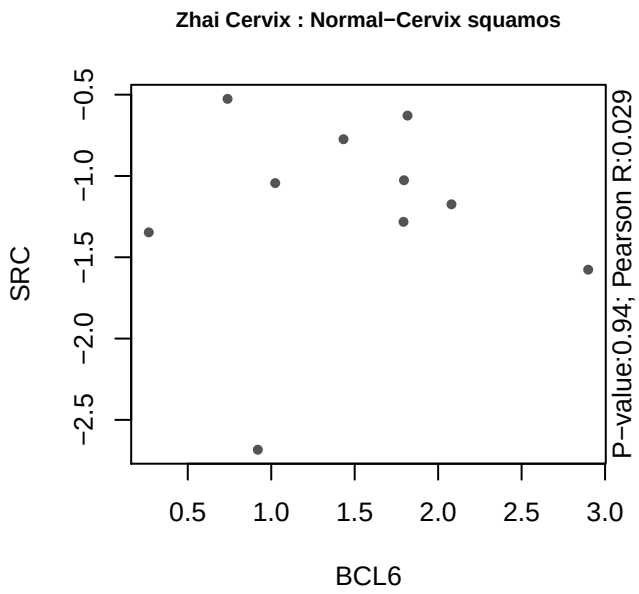

Zhai Cervix : Normal−Cervix squamos
MAPK8
ZBTB7A
P−value:0.71; Pearson R:−0.14

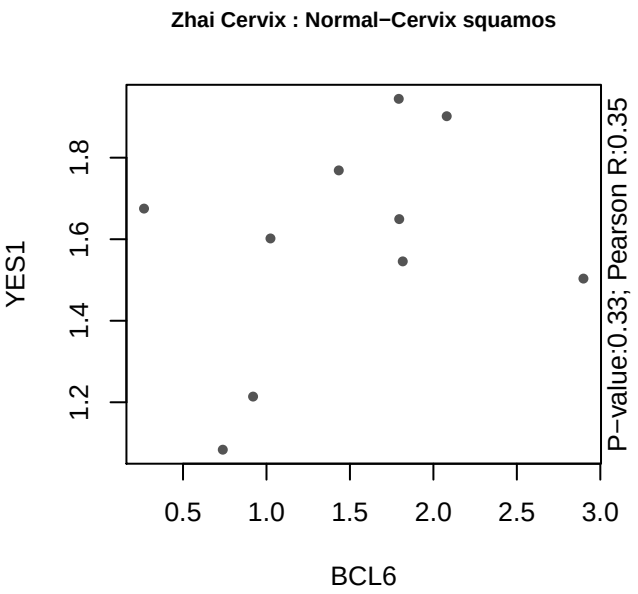

Zhai Cervix : Normal−Cervix squamos
MAPK9
BCL6
P−value:0.79; Pearson R:−0.099
−1.0
−0.6
−0.2
0.0
0.5
1.0
1.5
2.0
2.5
3.0

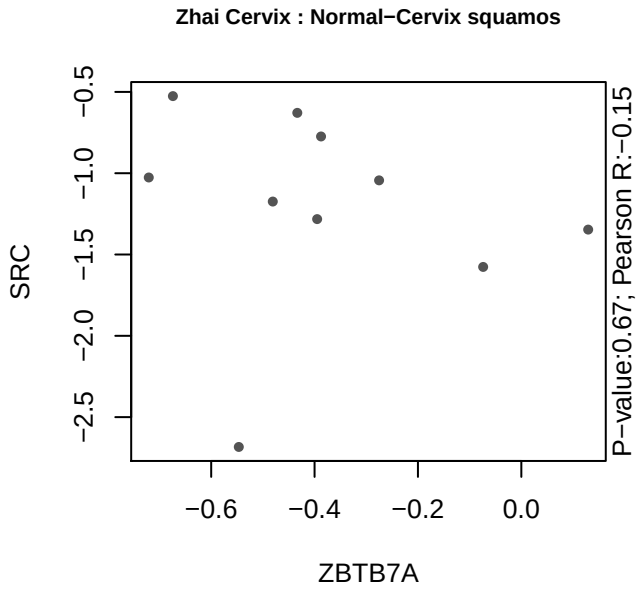

Zhai Cervix : Normal−Cervix squamos
SCRIB
BCL6
P−value:0.55; Pearson R:−0.22
2.8
3.0
3.2
3.4
3.6
0.5
1.0
1.5
2.0
2.5
3.0

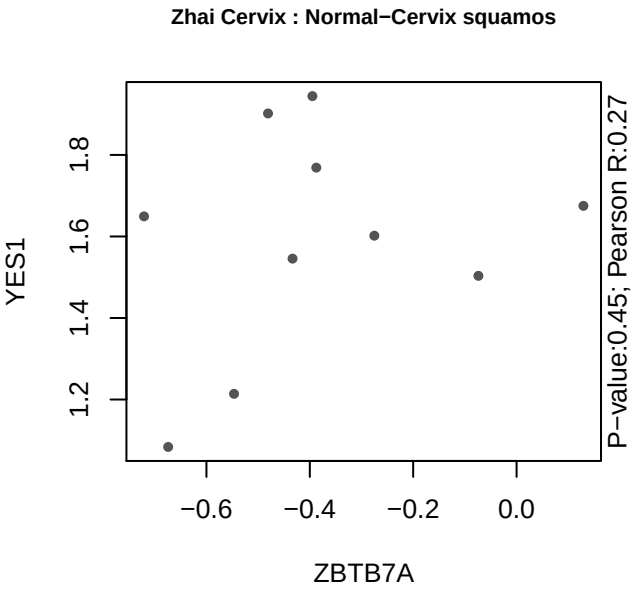

Zhai Cervix : Normal−Cervix squamos
MAPK9
ZBTB7A
P−value:0.97; Pearson R:0.012
−1.0
−0.6
−0.2
0.0
−0.6
−0.4
−0.2
0.0


Zhai Cervix : Normal−Cervix squamos
SCRIB
ZBTB7A
P−value:0.98; Pearson R:−0.0084
2.8
3.0
3.2
3.4
3.6
−0.6
−0.4
−0.2
0.0


Zhai Cervix : Normal−Cervix squamos
SRC
BCL6
P−value:0.94; Pearson R:0.029


Zhai Cervix : Normal−Cervix squamos
YES1
BCL6
P−value:0.33; Pearson R:0.35


Zhai Cervix : Normal−Cervix squamos
SRC
ZBTB7A
P−value:0.67; Pearson R:−0.15


Zhai Cervix : Normal−Cervix squamos
YES1
ZBTB7A
P−value:0.45; Pearson R:0.27

Supplementary Table 1:
All significant correlations in gene expression

Gene expression datasets	BTB-Zn gene	Polarity or cytoskeletal gene	P value	Pearson R	Notes
Gasper colon all	Bcl6	ARHGEF1	1,00E-06	-0,52	A
Gaspar colorectal adenoma	Bcl6	ARHGEF1	1,10E-05	-0,55	
Gaspar colon normal	Bcl6	ARHGEF1	1,60E-02	-0,51	N
Rohrbeck all-Lung (cancer only)	Bcl6	ARHGEF1	3,30E-02	-0,33	A
Boersma Breast all	ZBTB7A	ARHGEF1	1,00E-02	0,26	A
Tomlins Prostate all	Bcl6	ARHGEF11	5,60E-03	0,45	A
Tomlins Prostate Carcinoma	Bcl6	ARHGEF11	1,40E-02	0,57	*, #
Zhai Cervix all	Bcl6	ARHGEF11	2,20E-02	-0,37	A
Grutzmann Pancreas normal	Bcl6	ARHGEF11	3,70E-02	-0,63	N
Grutzmann Pancreas all (no met)	Bcl6	ARHGEF11	4,50E-02	-0,43	A
Boersma Breast all	ZBTB7A	ARHGEF11	2,80E-04	-0,37	A
Grutzmann Pancreas normal	Bcl6	ARHGEF12	4,90E-02	-0,6	N
Ma Breast 4 all	Bcl6	ARHGEF12	2,40E-02	0,28	A
Toruner Head-Neck all oral squamous carcinoma (cancer only)	ZBTB7A	ARHGEF12	1,70E-02	0,59	*
Grutzmann Pancreatic ductal adenocarcinoma	ZBTB7A	ARHGEF12	2,20E-02	-0,68	
Boersma Breast all	ZBTB7A	ARHGEF12	5,90E-10	0,58	A
Rohrbeck all-Lung (cancer only)	Bcl6	DLG1	1,10E-03	0,49	
Zhai Cervix all	Bcl6	DLG1	2,10E-02	0,37	A
Zhai Cervix Cervical squamous	Bcl6	DLG1	6,00E-03	0,51	
Collisson Pancreas all-adenocarcinoma	Bcl6	DLG1	4,60E-02	0,39	
Rohrbeck all-Lung (cancer only)	ZBTB7A	DLG1	4,70E-02	-0,31	
Tomlins Prostate all	ZBTB7A	DLG1	3,70E-02	0,74	A
Grutzmann Pancreas normal	ZBTB7A	DLG1	1,60E-02	0,7	N
Grutzmann Pancreas all (no met)	ZBTB7A	DLG1	1,30E-02	0,52	A
Gasper colon all	Bcl6	DLG2	2,20E-15	-0,75	A
Gaspar colorectal adenoma	Bcl6	DLG2	7,40E-13	-0,79	*, #
Gaspar colon normal	Bcl6	DLG2	8,40E-04	-0,66	N
Rohrbeck all-Lung (cancer only)	Bcl6	DLG2	2,00E-02	-0,36	*
Zhai Cervix Cervical squamous	Bcl6	DLG2	4,90E-02	0,38	
Boersma Breast all	Bcl6	DLG2	1,20E-02	0,26	A
Boersma Breast all	ZBTB7A	DLG2	7,90E-03	-0,27	A
Skrzypczak Colorectal 2 colon adenoma	Bcl6	DLG3	2,40E-02	-0,7	
Zhai Cervix Normal-Cervix squamous	ZBTB7A	DLG3	3,50E-02	0,67	N
Grutzmann Pancreas all (no met)	ZBTB7A	DLG3	1,90E-02	-0,5	A
Boersma Breast all	ZBTB7A	DLG3	5,10E-05	-0,4	A
Ma Breast 4 normal	ZBTB7A	DLG3	5,10E-04	0,61	N
Tomlins Prostate all	Bcl6	DLG4	8,60E-05	0,69	A
Toruner Head-Neck all oral squamous carcinoma (cancer only)	ZBTB7A	DLG4	5,70E-02	0,48	

Grutzmann Pancreas normal	ZBTB7A	DLG4	2,30E-02	0,67	N
Grutzmann Pancreas all (no met)	ZBTB7A	DLG4	2,20E-02	0,49	A
Gasper colon all	Bcl6	FYN	1,70E-06	-0,51	A
Gaspar colorectal adenoma	Bcl6	FYN	8,30E-07	-0,6	
Skrzypczak Colorectal 2 colon adenoma	Bcl6	FYN	6,90E-03	-0,79	
Tomlins Prostate all	ZBTB7A	FYN	6,60E-03	0,6	A
Tomlins Prostate Normal-Prostate Gland	ZBTB7A	FYN	9,10E-03	0,84	N
Boersma Breast all	ZBTB7A	FYN	2,50E-03	0,31	A
Gasper colon all	Bcl6	LLGL1	4,40E-15	0,75	A
Gaspar colorectal adenoma	Bcl6	LLGL1	2,60E-11	0,75	
Gaspar colon normal	Bcl6	LLGL1	4,60E-05	0,76	N
Rohrbeck all-Lung (cancer only)	Bcl6	LLGL1	3,80E-03	-0,44	*
Zhai Cervix all	Bcl6	LLGL1	3,50E-02	-0,34	A
Ma Breast 4 all	Bcl6	LLGL1	1,30E-03	0,39	A
Ma Breast 4 normal	Bcl6	LLGL1	1,80E-02	0,44	N
Ma Breast 4 primary ductal breast carcinoma	Bcl6	LLGL1	3,90E-02	0,34	
Ma Breast 2 all breast carcinoma	ZBTB7A	LLGL1	3,20E-02	0,34	
Gasper colon all	Bcl6	LLGL2	0,036	0,24	A
Gaspar colorectal adenoma	Bcl6	LLGL2	9,00E-04	0,43	
Skrzypczak Colorectal 2-all Epithelia	Bcl6	LLGL2	3,70E-02	-0,47	A
Skrzypczak Colorectal 2-all Epithelia	ZBTB7A	LLGL2	1,80E-02	0,52	A
Boersma Breast all	ZBTB7A	LLGL2	1,20E-04	-0,38	A
Ma Breast 4 normal	ZBTB7A	LLGL2	1,90E-02	0,44	N
Toruner Head-Neck all oral squamous carcinoma (cancer only)	Bcl6	MAPK10	1,10E-02	0,62	*
Boersma Breast normal	Bcl6	MAPK10	5,00E-02	0,29	N
Tomlins Prostate Carcinoma	ZBTB7A	MAPK10	3,40E-03	-0,85	
Gaspar colon normal	Bcl6	MAPK8	2,50E-02	-0,48	N
Tomlins Prostate all	Bcl6	MAPK8	2,00E-02	0,46	A
Tomlins Prostate Carcinoma	Bcl6	MAPK8	2,20E-02	0,57	*
Grutzmann Pancreas normal	Bcl6	MAPK8	2,10E-03	-0,82	N
Grutzmann Pancreas all (no met)	Bcl6	MAPK8	6,30E-03	-0,56	A
Grutzmann Pancreas all (no met)	ZBTB7A	MAPK8	1,10E-02	0,53	A
Gasper colon all	Bcl6	MAPK9	3,20E-13	0,71	A
Gaspar colorectal adenoma	Bcl6	MAPK9	4,40E-09	0,69	*, #
Gaspar colon normal	Bcl6	MAPK9	3,10E-06	0,82	N
Collisson Pancreas all-adenocarcinoma	Bcl6	MAPK9	8,00E-03	-0,5	
Grutzmann Pancreas normal	Bcl6	MAPK9	1,50E-02	0,71	N
Ma Breast 4 normal	Bcl6	MAPK9	6,30E-03	-0,5	N
Skrzypczak Colorectal 2-all Epithelia	ZBTB7A	MAPK9	1,10E-02	0,55	A
Boersma Breast all	ZBTB7A	MAPK9	9,90E-08	-0,51	A
Boersma Breast normal	ZBTB7A	MAPK9	1,10E-02	-0,37	N
Gaspar colorectal adenoma	Bcl6	MAP2K4	6,80E-03	0,36	*, #
Grutzmann Pancreas all (no met)	Bcl6	MAP2K4	8,50E-03	0,55	A
Grutzmann Pancreas normal	Bcl6	MAP2K4	4,00E-03	0,79	N
Ma Breast 4 all	Bcl6	MAP2K4	3,40E-03	-0,36	A

Ma Breast 4 normal	Bcl6	MAP2K4	1,20E-03	-0,58	N
Rohrbeck all-Lung (cancer only)	Bcl6	MAP2K4	2,50E-03	0,45	*
Zhai cervix all	ZBTB7A	MAP2K4	3,20E-02	0,35	A
Boersma Breast epithelial cancer	Bcl6	MAP2K7	2,30E-03	0,43	*, #
Gaspar colorectal adenoma	Bcl6	MAP2K7	2,20E-02	-0,31	
Rohrbeck all-Lung (cancer only)	Bcl6	MAP2K7	6,20E-04	-0,51	
Grutzmann Pancreas all (no met)	Bcl6	MAP2K7	2,40E-03	-0,61	A
Grutzmann Pancreas normal	Bcl6	MAP2K7	9,90E-03	-0,74	N
Grutzmann Pancreatic ductal adenocarcinoma	ZBTB7A	MAP2K7	5,10E-02	0,6	*, #
Grutzmann Pancreas all (no met)	ZBTB7A	MAP2K7	1,20E-02	0,52	A
Zhai Cervix Cervical squamous	ZBTB7A	MAP2K7	1,30E-02	0,46	*, #
Zhai Cervix all	ZBTB7A	SCRIB	3,40E-02	0,34	A
Ma Breast 4 all	ZBTB7A	SCRIB	1,10E-02	0,31	A
Ma Breast 4 normal	ZBTB7A	SCRIB	2,00E-02	0,44	N
Gasper colon all	Bcl6	SRC	1,70E-10	-0,65	A
Gaspar colorectal adenoma	Bcl6	SRC	5,30E-08	-0,65	
Gaspar colon normal	Bcl6	SRC	1,60E-03	-0,63	N
Grutzmann Pancreas normal	Bcl6	SRC	1,40E-02	-0,71	N
Grutzmann Pancreas all (no met)	Bcl6	SRC	3,00E-02	-0,46	A
Collisson Pancreas all-adenocarcinoma	ZBTB7A	SRC	3,10E-02	0,42	*
Grutzmann Pancreas normal	ZBTB7A	SRC	2,70E-03	0,81	N
Grutzmann Pancreas all (no met)	ZBTB7A	SRC	3,10E-04	0,7	A
Gasper colon all	Bcl6	YES1	1,60E-05	0,47	A
Gaspar colorectal adenoma	Bcl6	YES1	1,40E-04	0,49	*, #
Gaspar colon normal	Bcl6	YES1	3,40E-02	0,45	N
Rohrbeck all-Lung (cancer only)	Bcl6	YES1	9,60E-03	0,4	*
Zhai Cervix all	Bcl6	YES1	4,70E-02	0,32	A
Grutzmann Pancreas normal	Bcl6	YES1	5,60E-04	0,87	N
Grutzmann Pancreas all (no met)	Bcl6	YES1	8,40E-04	0,66	A
Boersma Breast all	Bcl6	YES1	5,00E-03	-0,29	A
Boersma Breast epithelial cancer	Bcl6	YES1	1,40E-02	-0,35	
Skrzypczak Colorectal 2-all Epithelia	ZBTB7A	YES1	1,60E-02	0,53	A

Red = positive correlation, Blue = negative correlation, Brown = borderline significance with positive correlation, A = All (normal & cancer), N= Normal, * Bcl6/ZBTB7 high and correlated as expected with the test gene (highlighted in green), # Trend is stronger in cancer compared with normal tissue (highlighted in yellow)